Modification of Azobenzene Based Switches

Dissertation

Towards the Academic Degree
Doctor Rerum Naturalium (Dr. rer. nat.)

Submitted to the
Department of Biology and Chemistry
of the University of Bremen

by

Melanie Walther

Bremen, September 2023

Reviewers:

1. Prof. Dr. Anne Staubitz (University of Bremen)
2. Prof. Dr. Peter Spiteller (University of Bremen)

Submitted in September 2023

Doctoral Colloquium: 23.10.2023

Versicherung an Eides statt

Ich, Melanie Walther, versichere an Eides Statt durch meine Unterschrift, dass ich die vorstehende Arbeit selbständig und ohne fremde Hilfe angefertigt und alle Stellen, die ich wörtlich dem Sinne nach aus Veröffentlichungen entnommen habe, als solche kenntlich gemacht habe, mich aus keiner anderen als der angegebenen Literatur oder sonstiger Hilfsmittel bedient habe.

Ich versichere an Eides statt, dass ich die vorgenannten Angaben nach bestem Wissen und Gewissen gemacht habe und dass die Angaben der Wahrheit entsprechen und ich nichts verschwiegen habe.

Die Strafbarkeit einer falschen eidesstattlichen Versicherung ist mir bekannt, namentlich die Strafandrohung gemäß §156 StGB bis zu drei Jahren Freiheitsstrafe oder Geldstrafe bei vorsätzlicher Begehung der Tat bzw. gemäß §161 Abs. 1 StGB bis zu einem Jahr Freiheitsstrafe oder Geldstrafe bei fahrlässiger Begehung.

Bremen, 20.09.2023

(Melanie Walther)

Erklärung zur elektronischen Version und Überprüfung einer Dissertation

Hiermit erkläre ich gemäß §7 Abs. 7, Punkt 4, dass die zu Prüfungszwecken beigelegte elektronische Version meiner Dissertation identisch ist mit der abgegebenen gedruckten Version.

Ich bin mit der Überprüfung meiner Dissertation gemäß §6 Abs. 2, Punkt 5 mit qualifizierter Software im Rahmen der Untersuchung von Plagiatsvorwürfen einverstanden.

Bremen, 20.09.2023

(Melanie Walther)

Publications

The present work was carried out under the supervision of Prof. Dr. Anne Staubitz from December 2018 to September 2023 at the Institute of Organic and Analytical Chemistry, Department of Biology and Chemistry of the University of Bremen.
This thesis is based on the following publications:

(I) **Modification of Azobenzenes by Cross-Coupling Reactions**
M. Walther, W. Kipke, S. Schultzke, S. Ghosh, A. Staubitz, *Synthesis* **2021**, *53*, 1213-1228.

(II) **Active Ester Functionalized Azobenzenes as Versatile Building Blocks**
S. Schultzke,‡ M. Walther,‡ A. Staubitz, *Molecules* **2021**, *26*, 3916.
‡ These authors contributed equally.

(III) ***ortho*-Functionalization of Azobenzenes via Hypervalent Iodine Reagents**
E. M. Di Tommaso, M. Walther, A. Staubitz, B. Olofsson, *Chem. Commun.* **2023**, *59*, 5047-5050.

(IV) **Stille vs. Suzuki - Cross-Coupling for the Functionalization of Diazocines**
M. Walther,‡ W. Kipke,‡ R. Renken, A. Staubitz, *RSC Adv.* **2023**, *13*, 15805-15809.
‡ These authors contributed equally.

All publications within this list are based on the collaboration of several researchers. The following overview is given for declaration regarding my own contribution to the multi-author publications included in this thesis.

(I) Modification of Azobenzenes by Cross-Coupling Reactions

Contribution in % of the total work load (up to 100% for each category):	
Concept and structure of the manuscript:	ca. 100%
Acquisition and structure of references:	ca. 90%
Preparation of figures and tables:	ca. 60%
Drafting of the manuscript:	ca. 65%
Proofreading of the manuscript:	ca. 70%

(II) Active Ester Functionalized Azobenzenes as Versatile Building Blocks

Contribution in % of the total work load (up to 100% for each category):	
Experimental concept and design:	ca. 45%
Experimental work and/or acquisition of (experimental) data:	ca. 50%
Data analysis and interpretation:	ca. 50%
Preparation of figures and tables:	ca. 50%
Drafting of the manuscript:	ca. 40%

(III) *ortho*-Functionalization of Azobenzenes via Hypervalent Iodine Reagents

Contribution in % of the total work load (up to 100% for each category):	
Experimental concept and design:	ca. 40%
Experimental work and/or acquisition of (experimental) data:	ca. 50%
Data analysis and interpretation:	ca. 50%
Preparation of figures and tables:	ca. 45%
Drafting of the manuscript:	ca. 40%

(IV) Stille vs. Suzuki - Cross-Coupling for the Functionalization of Diazocines

Contribution in % of the total work load (up to 100% for each category):	
Experimental concept and design:	ca. 50%
Experimental work and/or acquisition of (experimental) data:	ca. 45%
Data analysis and interpretation:	ca. 55%
Preparation of figures and tables:	ca. 50%
Drafting of the manuscript:	ca. 45%

Bremen, 20.09.2023

(Melanie Walther)

"All my life through, the new sights of nature made me rejoice like a child."

Marie Curie

Für Opa Kellerkuhle.

Acknowledgements

I am very grateful for all the support and help I have received during the creation of this thesis. I would like to express my sincere gratitude to all those without whom I would have not been able to complete this project:

First and foremost, I would like to express my deepest gratitude to my supervisor *Prof. Dr. Anne Staubitz* for accepting me as a doctoral student in her research group and for her invaluable guidance, support and mentorship not only throughout my doctoral thesis but also already back in Kiel during my years of study. Her expertise, passion for research and dedication to my academic development have been crucial in shaping this thesis. I am truly grateful for her continuous encouragement, insightful discussions, and unwavering belief in my abilities. She gave me the freedom to explore my own research ideas as a scientist, to continue my education in regards to my professional competencies and to grow overall as a human being.

I would like to extend my sincere appreciation to *Prof. Dr. Peter Spiteller* for generously devoting his time and expertise to review this thesis.

In addition, I want to thank all past and present members of the Staubitz group. I am thankful for the stimulating and inspiring environment that we created together. In particular, my thanks go to *Dr. Mathias Dowds* who laid the foundation for my interest in molecular switches in my master thesis and who continued to be a good friend and adviser for me. Also, I greatly appreciate *Sven Schultzke* and *Waldemar Kipke* for all the fruitful discussions about azobenzenes and diazocines and the valuable contributions during our collaborations. I want to thank *Yannik Appiarius* and *Philipp Gliese* for the insightful outside view on my research, for a great time in the lab and especially for making me feel welcome in Bremen from my first day on. I am very grateful that I can call so many of my colleagues my friends. The good souls of the research group, *Jasmin Richter*, *Petra Grundmann* and lately *Dr. Arne Wittstock*, deserve a special thank for all the organizational work in the background – from ordering chemicals over dealing with travel expense reports and coordinating the teaching duties to always having an open door for the problems of us PhD students. Additionally, I would like to thank *Dr. Shuo Li* for answering my questions regarding the formal procedures for this thesis and *Christoph Eschen* for proofreading on short notice.

I owe particular thanks to my cooperation partners in Sweden *Prof. Berit Olofsson* and *Ester Maria Di Tommaso*. Even though we encountered some difficulties during the project, we managed to face them and I always appreciated our interesting discussions. The shared insights have greatly enriched my work, and I am grateful for the opportunity

to work alongside such accomplished researchers.

I want to thank the NMR department, namely *Johannes Stelten* and *Dr. Wieland Wilker*, for the maintenance of the NMR spectrometer and *Dorit Kemken* and *Dr. Thomas Dülcks* for measuring all the mass spectra. Special thanks also go to *Dr. Marian Olaru* for measuring my crystal structures and *Dr. Pim Puylaert* for eventually processing the data.

Within this thesis I supervised several talented students including the bachelor theses and work as research assistant of *Raul Renken* and *Dimitrij Bogdanov* as well as the research internship of *Philipp Diephaus* and the last weeks of the apprenticeship as chemical laboratory assistant of *Amelie Sprengel*. I am thankful for their interest in my research and trust to work with me.

I would also like to acknowledge the financial support provided by *The Central Research Development Fund* of the University that enabled me to present my research at an international conference overseas.

Additionally, I would like to express my heartfelt appreciation to all my friends who have accompanied me on this academic and personal odyssey. Your friendship, encouragement, and moments of respite have been invaluable during this challenging period. I am especially obliged to *Phil*, *David*, *Sven* and *Isi* as well as *Yannik* and *Stivi* for making me feel home in Bremen; to *Basti*, *Helge*, *Silvia* and *Thorben* for their constant support and critical questioning from afar; to *Hanna* for the immense trust and freedom with *Fünkchen* and of course to *Pascal* and *Tim* for everything we could accomplish so far and will accomplish in the future with *BionicFuel*.

Finally, I am deeply indebted to my family for their unwavering love, encouragement, and support throughout this journey. Their belief in my abilities and their constant motivation have been the driving force behind my achievements. I am grateful for their understanding during the long hours of work, their patience during challenging times, and their celebration of every milestone reached. Particularly, I am thankful for having my sister *Mimi* by my side who has been a source of strength and inspiration for me in the last couple of years.

To everyone who has contributed to this thesis in one way or another, I extend my deepest gratitude. Your support has been integral to the completion of this work, and I am truly grateful for the positive impact you have had on my academic and personal growth.

Thank you.

Abstract

Photoswitchable molecules have gained significant interest, as their switching behavior on the molecular level can be exploited macroscopically by their incorporation into materials. Efficient and tailored synthetic strategies towards functionalized photoswitches are therefore needed. Due to their unique switching properties, azobenzene and its derivatives are among the most established and studied photoswitches. For applications in materials and life sciences, very specific substitution patterns are often necessary that have not been established even after more than a hundred years of azobenzene research.

In this work, methods were established by which iodinated precursors could be produced in good yields. Iodine substituents are highly versatile for further transformations like cross-coupling reactions or in oxidations to obtain iodine(III) compounds. Thus, there are ideal starting materials for generating a large library of photoswitchable molecules. The synthetic flexibility of this motif for late-stage functionalizations of azobenzenes was exploited in several chemical dimensions:

First, an efficient palladium catalyzed cross-coupling protocol for the synthesis of diverse *N*-hydroxysuccinimide functionalized azobenzenes and diazocines was developed. Its usefulness was demonstrated by condensation reactions of these active esters with primary amines.

In the second project, *ortho*-iodinated azobenzenes were successfully transformed into the corresponding hypervalent diaryliodonium salts. This new class of compounds was studied in terms of their structural and photoswitchable properties as well as their reactivity in transition metal-free arylation reactions. Here, the azobenzene moiety was selectively transferred to various nucleophiles under mild conditions granting access to a broad spectrum of *ortho*-functionalized azobenzenes.

In the third project, cross-coupling reactions of ethylene-bridged azobenzenes, diazocines, for late-stage functionalization were investigated. The iodinated precursors were efficiently converted into their stannylated and borylated derivatives and their utility in Stille as well as Suzuki cross-coupling reactions with a broad range of organic bromides proven.

With these methodological studies, different features regarding the photoswitch were explored: the *type* of the azobenzene (open and cyclic) and the *position* of the substitution (*meta*, *para* and especially *ortho*). Each azobenzene derivative contains its own challenges in synthesis and the later function because of these two aspects, among others.

The presented synthetic protocols enable the tailored implementation of azobenzene based switches into diverse materials.

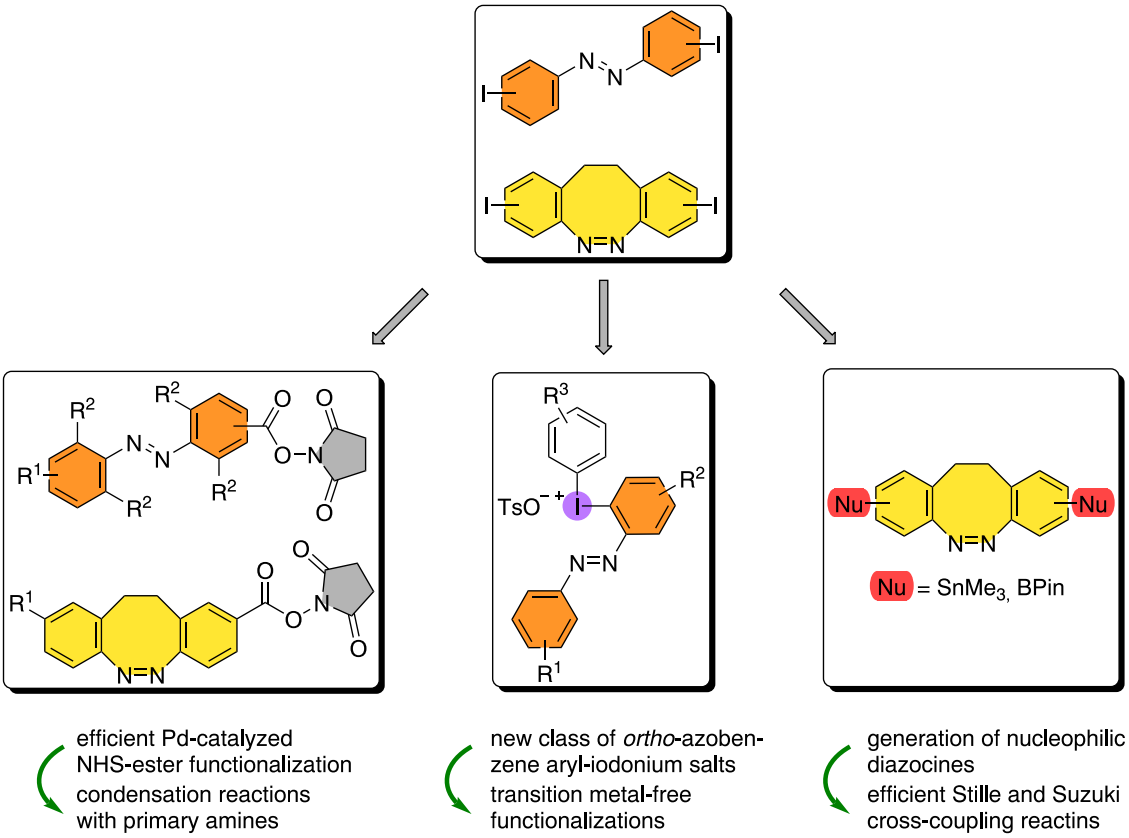
efficient Pd-catalyzed NHS-ester functionalization
condensation reactions with primary amines
new class of *ortho*-azobenzene aryl-iodonium salts
transition metal-free functionalizations
generation of nucleophilic diazocines
efficient Stille and Suzuki cross-coupling reactins
Nu = SnMe3, BPin

Kurzzusammenfassung

Photoschaltbare Moleküle haben großes Interesse erlangt, da ihr Schaltverhalten auf molekularer Ebene durch ihren Einbau in Materialien makroskopisch ausgenutzt werden kann. Dafür sind effiziente und maßgeschneiderte Synthesestrategien für funktionalisierte Photoschalter erforderlich. Aufgrund ihrer einzigartigen Schalteigenschaften gehören Azobenzol und seine Derivate zu den etabliertesten und meist untersuchten Photoschaltern. Für spezifische Anwendungen in den Material- und Lebenswissenschaften sind oft ganz spezielle Substitutionsmuster notwendig, die auch nach mehr als hundert Jahren Azobenzolforschung nicht etabliert sind.

In dieser Arbeit wurden Methoden entwickelt, mit denen iodierte Vorläuferverbindungen in guten Ausbeuten hergestellt werden können. Iodsubstituenten sind äußerst vielseitig für weitere Umwandlungen wie Kreuzkupplungsreaktionen oder bei Oxidationen zur Herstellung von Iod(III)-Verbindungen. Somit stehen ideale Ausgangsmaterialien für die Generierung einer großen Bibliothek photoschaltbarer Moleküle zur Verfügung. Die synthetische Flexibilität dieses Motivs für Funktionalisierungen von Azobenzolen im Spätstadium wurde in mehreren chemischen Dimensionen ausgenutzt:

Zunächst wurde ein effizientes Palladium-katalysiertes Kreuzkupplungsprotokoll für die Synthese verschiedener *N*-Hydroxysuccinimid-funktionalisierter Azobenzole und Diazocine entwickelt. Der Nutzen dieser Aktivester wurde durch Kondensationsreaktionen mit primären Aminen demonstriert.

Im zweiten Projekt wurden *ortho*-iodierte Azobenzole erfolgreich in die entsprechenden hypervalenten Diaryliodoniumsalze umgewandelt. Diese neue Verbindungsklasse wurde hinsichtlich ihrer strukturellen und photoschaltbaren Eigenschaften sowie ihrer Reaktivität in übergangsmetallfreien Arylierungsreaktionen untersucht. Dabei wurde die Azobenzoleinheit unter milden Bedingungen selektiv auf verschiedene Nukleophile übertragen, was den Zugang zu einem breiten Spektrum an *ortho*-funktionalisierten Azobenzolen ermöglichte.

Im dritten Projekt wurden Kreuzkupplungsreaktionen von ethylenverbrückten Azobenzolen (Diazocinen) zur Funktionalisierung in späten Synthesestadien untersucht. Die iodierten Vorläufer wurden effizient in ihre stannylierten und borylierten Derivate umgewandelt und ihre Nützlichkeit in Stille- und Suzuki-Kreuzkupplungsreaktionen mit einer breiten Palette organischer Bromide bewiesen.

Mit diesen methodischen Studien wurden verschiedene Besonderheiten des Photoschalters erforscht: die *Art* des Azobenzols (offen und zyklisch) und die *Position* der Substitution (*meta*, *para* und insbesondere *ortho*). Jedes Azobenzol-Derivat birgt unter anderem aufgrund dieser beiden Aspekte seine eigenen Herausforderungen bei der Synthese und der späteren Funktion.

Die vorgestellten Syntheseprotokolle ermöglichen die maßgeschneiderte Implementierung von Azobenzol-basierten Schaltern in verschiedene Materialien.

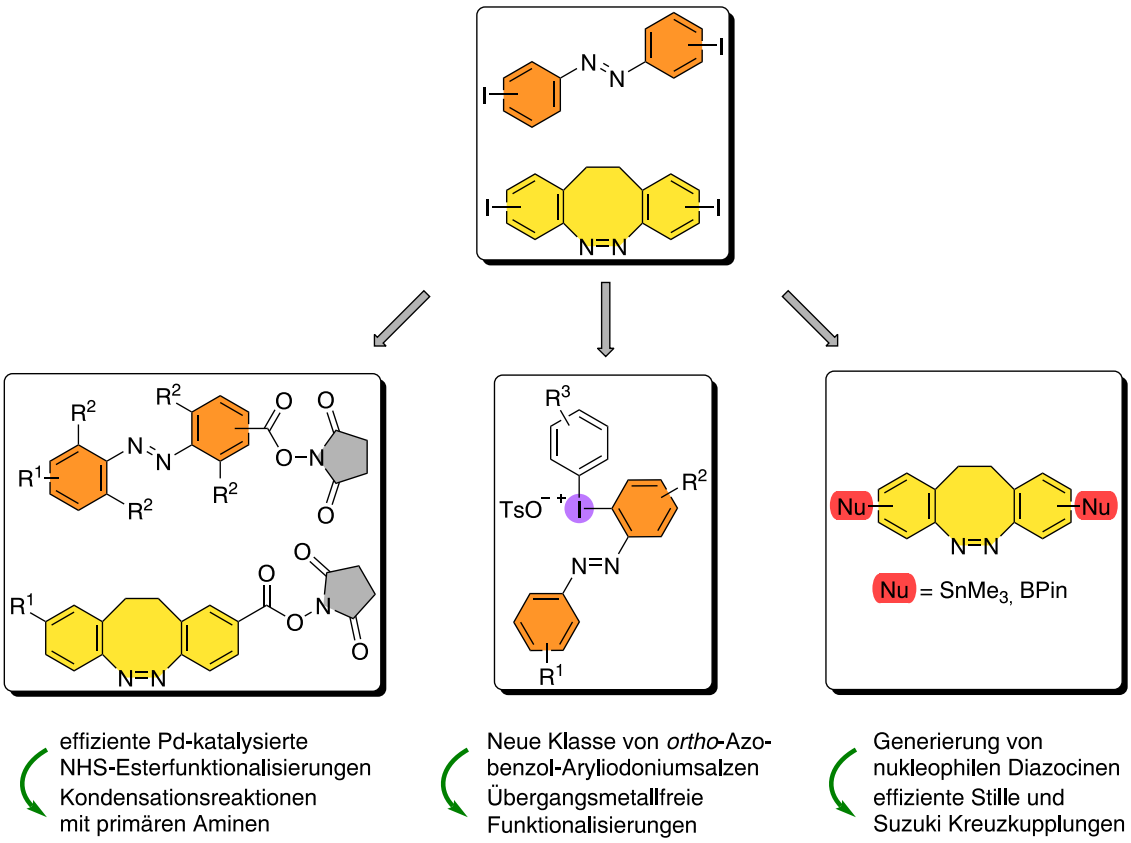

effiziente Pd-katalysierte NHS-Esterfunktionalisierungen Kondensationsreaktionen mit primären Aminen

Neue Klasse von *ortho*-Azobenzol-Aryliodoniumsalzen Übergangsmetallfreie Funktionalisierungen

Generierung von nukleophilen Diazocinen effiziente Stille und Suzuki Kreuzkupplungen

List of Abbreviations, Acronyms and Symbols

Abbreviations and acronyms are used in agreement with the standard of the subject.[1] Only nonstandard and unconventional abbreviations that appear in this thesis are listed here.

3c-4e	3-center-4-electron
***m*CPBA**	*meta*-chloroperoxybenzoic acid
ad	apparent doublet
APCI	atmospheric pressure chemical ionization
BBO	broadband observe
Boc	*tert*-butoxycarbonyl
CCDC	Cambridge Crystallographic Data Centre
CDI	1,1'-carbonyldiimidazol
CI	conical intersection
COD	cyclooctadiene
DBU	1,8-diazabicyclo[5.4.0]undec-7-ene
DCC	*N*,*N*'-dicyclohexylcarbodiimide
DCE	1,2-dichloroethane
DCM	dichloromethane
ddd	doublet of doublet of doublets
dd	doublet of doublets
DMAP	4-dimethylaminopyridine
DMEDA	1,2-dimethylethylenediamine
Dppf	1,1'-bis(diphenylphosphino)ferrocene
DSC	*N*,*N*'-disuccinimidyl carbonate
EDCl	1-ethyl-3-(3-dimethylaminopropyl)carbodiimide
EDG	electron donating group
FG	functional group
HATU	hexafluorophosphate azabenzotriazole tetramethyl uronium
Hex	hexyl
HMBC	heteronuclear multiple bond correlation
HSPyU	dipyrrolidino-(*N*-succinimidyloxy)-carbenium-hexafluorophosphat
HSQC	heteronuclear single quantum correlation
MOF	metal-organic framework
NCS	*N*-chlorosuccinimide
NHS	*N*-hydroxysuccinimide
NMP	*N*-methyl-2-pyrrolidone
Nu	nucleophile
OTf	triflate
PIDA	phenyliodine(III) diacetate

PIFA	(bis(trifluoroacetoxy)iodo)benzene
Pin	pinacolato
Porph	porphyrin
PSS	photostationary state
RG	reactive group
R	rest
TATA	triazatriangulenium
TBAB	tetrabutylammonium bromide
TBHP	*tert*-butyl hydroperoxide
TCBC	2,4,6-trichlorobenzoic acid
TFE	2,2,2-trifluoroethanol
TMP	trimethoxyphenyl
TON	turnover number
XantPhos Pd G3	[(4,5-bis(diphenylphosphino)-9,9-dimethylxanthene)-2-(2'-amino-1,1'-biphenyl)]palladium(II) methanesulfonate
Xantphos	4,5-bis-(diphenylphosphino)-9,9-dimethylxanthene
XPhos	dicyclohexyl[2',4',6'-tris(propan-2-yl)[1,1'-biphenyl]-2-yl]phosphane

Foreword

This thesis presents the synthesis and functionalization of various azobenzene and diazocine photoswitches. The research leading to this thesis was conducted at the University of Bremen. One project was performed in collaboration with the Department of Organic Chemistry, Stockholm University as different competencies of synthetic organic chemistry were needed.

The thesis is divided into five main chapters:

Chapter 1 - Introduction gives a general overview of the topics addressed by this thesis: the photoswitches azobenzenes and the related diazocines, the synthesis of functionalized derivatives and concepts for late-stage modification as well as hypervalent iodine compounds and *N*-hydroxysuccinimide esters. Parts of the section on the late-stage functionalization of azobenzenes and diazocines were published as a review article "Modification of Azobenzenes by Cross-Coupling Reactions". Thus, this part is less extensive in the remaining introduction.

Chapter 2 - Objectives covers the overall aims of this thesis.

Chapter 3 - Results and Discussion presents the three subprojects that have been published in peer-reviewed journals.

Chapter 4 - Conclusion and Outlook provides a summary of the presented work and potential future research aspects.

Chapter 5 - Experimental Section contains the Supporting Information of the research articles presented in Chapter 3.

In the **Appendix**, the reprinting permissions are collected.

Table of Contents

Versicherung an Eides statt I

Erklärung zur elektronischen Version und Überprüfung einer Dissertation II

Publications III

Acknowledgements VII

Abstract IX

Kurzzusammenfassung XI

List of Abbreviations, Acronyms and Symbols XIII

Foreword XV

1 Introduction 1

1.1 Azobenzene . . . 1

1.1.1 Properties and Isomerization . . . 1

1.1.2 Synthetic Procedures towards Functionalized Azobenzenes . . . 6

1.1.3 Late-Stage Functionalization . . . 8

1.2 Diazocines . . . 9

1.2.1 Properties and Isomerization . . . 9

1.2.2 Synthetic Procedures towards Functionalized Diazocines . . . 11

1.2.3 Late-Stage Functionalization . . . 13

1.3 *N*-Hydroxysuccinimide Ester . . . 14

1.4 Diaryliodonium Salts . . . 14

1.5 Modification of Azobenzenes by Cross-Coupling Reactions . . . 17

2 Objectives 35

3 Results and Discussion 37

3.1 Active Ester Functionalized Azobenzenes as Versatile Building Blocks . . . 37

3.2 *ortho*-Functionalization of Azobenzenes via Hypervalent Iodine Reagents . . . 52

3.3 Stille vs. Suzuki - Cross-Coupling for the Functionalization of Diazocines . . . 58

4 Conclusion and Outlook 65

5 Experimental Section 68

5.1 Active Ester Functionalized Azobenzenes as Versatile Building Blocks . . . 68

5.2 *ortho*-Functionalization of Azobenzenes via Hypervalent Iodine Reagents . . . 126

5.3 Stille vs. Suzuki - Cross-Coupling for the Functionalization of Diazocines . . . 168

References **208**

Permissions to Reprint **218**

M. Gao, D. Kwaria, Y. Norikane, Y. Yue, *Nat. Sci.* **2023**, 3, 1–45. 218

F. A. Jerca, et al., *Nat. Chem. Rev.* **2022**, *6*, 51–69. 219

R. Siewertsen, et al., *J. Am. Chem. Soc.* **2009**, *131*, 15594–15595. 220

1 Introduction

Molecular switches have witnessed significant progress in recent years due to the increasing demand for controlling molecular functions and properties in multiple scientific disciplines.[2–4] In 2016, the increasing importance of this research field was confirmed by the Nobel Prize in Chemistry awarded to Sauvage, Stoddart and Feringa for the design and synthesis of molecular maschines.[3] In general, a molecular switch can reversibly interconvert between at least two distinct states by an external stimulus such as light, mechanical stress or electrical stimulation; one of these states is thermodynamically stable whereas the others are metastable.[5] Among the broad range of molecular switches, azobenzene (**1**) and its derivatives have emerged as highly promising.[6] Due to their high thermal stability and photofatigue-resistant switching,[7,8] they have been employed in numerous applications, including photopharmacology,[9,10] molecular electronics[11,12] or thermal fuel storage.[13–16]

1.1 Azobenzene

Although azobenzene (**1**) has already been synthesized in 1834 by E. Mitscherlich,[17] it took more than a hundred years to discover the second isomer of azobenzene **(*Z*)-1**.[18] Owing to its chromophoric group, azobenzenes have not only become one of the largest class of synthetic dyes[19] but also one of the most studied photoswitches.[6]

1.1.1 Properties and Isomerization

Azobenzene (**1**) consists of two phenyl rings that are linked by a N=N unit. Due to the azo group, azobenzene (**1**) can reversibly undergo (*E*)- (*Z*)-isomerization (Scheme 1.1).[18] Upon illumination with ultraviolet (UV) light (320 - 365 nm), the (*E*)-isomer **(*E*)-1** can isomerize to the (*Z*)-form **(*Z*)-1**. The re-isomerization can either occur upon irradiation with visible (vis) light (400 - 450 nm) or thermally, owing to the thermodynamic stability of **(*E*)-1**.[20,21] The thermal relaxation takes place without degradation or side products.[7,8]

The physical properties of azobenzene (**1**) change tremendously upon isomerization, e.g., the geometry,[22,23] the dipole moment[21] or the absorption.[24] While the (*E*)-isomer **(*E*)-1** is planar[22] and shows no dipole moment,[21] the (*Z*)-form **(*Z*)-1** is bent[23] and has a dipole moment of 3.0 D.[21] The end-to-end distance, i.e., the span between the carbons at *para*-position, is reduced from 9 Å to 5.5 Å upon (*Z*)-(*E*)-isomerization.[6]

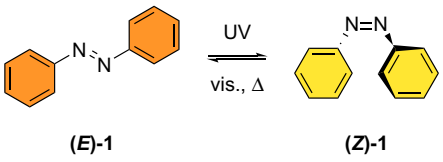

Scheme 1.1 Azobenzene (**1**) can reversibly isomerize photochemically and thermally between its (*E*)- **(*E*)-1** and (*Z*)-form **(*Z*)-1**.[18]

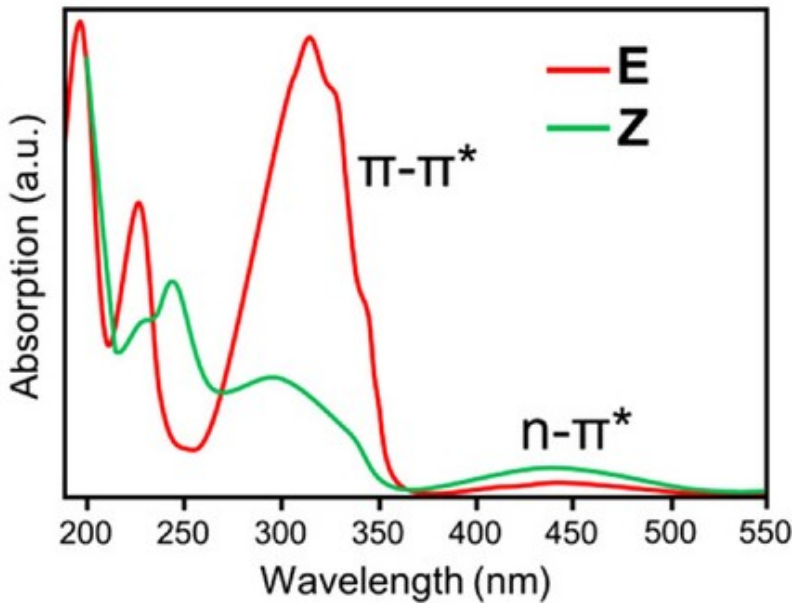

Figure 1.1 UV/vis absorption spectrum of **(*E*)-1** and **(*Z*)-1** in *n*-hexane.[25] © 2022 M. Gao, D. Kwaria, Y. Norikane, Y. Yue. Natural Sciences published by Wiley-VCH GmbH.

The UV/vis absorption spectrum of azobenzene (**1**) displays two characteristic absorption bands which correspond to $\pi\pi^*$ and $n\pi^*$ electronic transitions (Figure 1.1).[24] The first one occurs typically in the near UV region and the second one in the visible area.[6] For the (*E*)-isomer **(*E*)-1**, the $\pi\pi^*$ band is very intense but the $n\pi^*$ band is significantly weaker as it is symmetry-forbidden. In contrast, the $n\pi^*$ transition is allowed in the (*Z*)-isomer **(*Z*)-1** so that the intensity of this band is increased. The $\pi\pi^*$ band is now shifted to shorter wavelengths and much lower in intensity compared to the (*E*)-isomer **(*E*)-1**.[6,24]

The photoisomerization process of azobenzene (**1**) along with the pathways regarding the geometrical changes are still under discussion and have not been clarified in every detail.[24,26–33] The most widely accepted pathways are the torsion, inversion and inversion assisted torsion (hula-twist) mechanisms (Scheme 1.2).[20,29,34–37] In the torsion pathway, a torsional rotation around the N-N bond occurs. Consequently, the N-N-C angle remains constant but the C-N-N-C dihedral angle changes (Scheme 1.2 a). The opposite is the case in the inversion mechanism. Here, the C-N-N-C angle remains at 0 ° but one N-N-C angle enlarges to 180 ° whereas one azo-nitrogen atom is transitioned from sp^2 to sp hybridization (Scheme 1.2 b).[20,29,31] Combinations of the torsion and inversion mechanism like an inversion-assisted torsion are also discussed:[38] Due to the large amplitude motion of one phenyl ring in both mechanisms, the hula-twist pathway was assigned as predominant in constrained surroundings. The phenyl rings remain almost in place because the nitrogen atoms and the phenyl rings accomplish a concerted pedal-like movement (Scheme 1.2 c).[34–36]

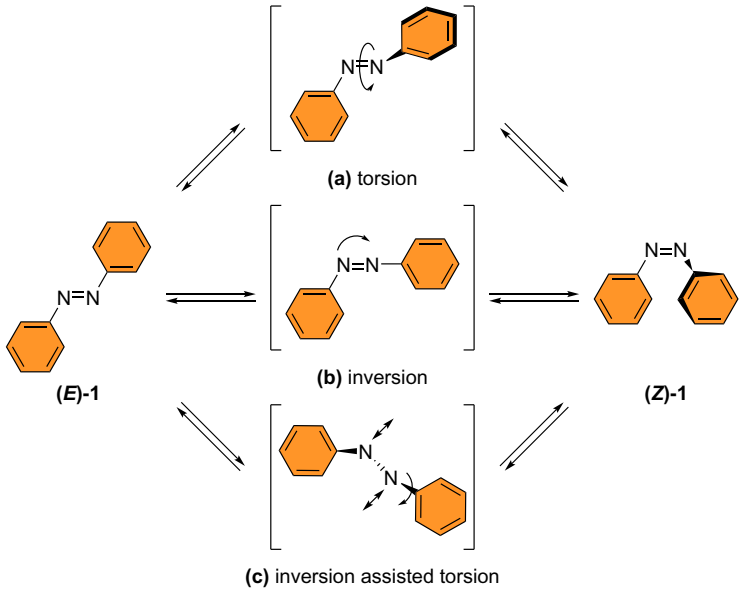

Scheme 1.2 Possible photoisomerization pathways of azobenzene (**1**). **(a)** Torsion around the central double bond. **(b)** Inversion on one of the two nitrogen atoms. **(c)** Inversion assisted torsion (hula-twist) of the three central bonds.[24]

The isomerization of azobenzene (**1**) proceeds photochemically either via $S_0 \rightarrow S_1$ (irradiation into $n\pi^*$, **S_1 entry point**) or via $S_0 \rightarrow S_2$ (irradiation into $\pi\pi^*$, **S_2 entry point**) excitations (Figure 1.2).[24,26–33] Upon photoisomerization, the two isomers enter the same excited state surfaces but the relaxation to **(*Z*)-1** occurs via a different conical intersection (CI).[24,39,40] The quantum yield of the S_2 excitation (0.12) is for azobenzenes lower than the one from S_1 excitation (0.40) as different mechanisms are followed (Figure 1.2).[39] Hence, the Kasha-Vavilov rule is violated, which implies that the quantum yield of luminescence is typically independent of the excitation wavelength. This can be explained as a result of the tendency for molecules in higher energy states to relax non-radiatively to the lowest excited state.[40–44]

Upon $n\pi^*$ excitation of **(*E*)-1** (**S_1 entry point**), the decay to S_0 arises via a CI reached through an inversion-assisted torsion ($S_1 \rightarrow CI(S_1/S_0) \rightarrow S_0$; **$S_1/S_0$ reactive CI**).[40,41,43,45] The reactive intersections (**S_1/S_0 reactive CI**) during excited state decay result in either **(*Z*)-1** or **(*E*)-1**, depending on whether the isomerization process succeeds or fails (Figure 1.2).[39,46]

The **S_1/S_0 unreactive CIs** encompass nearly planar geometries with symmetric $\alpha_{CNN} = \alpha_{NNC}$ bending (widening). This pathway is for $n\pi^*$ as well as for $\pi\pi^*$ excitations accessible and recovers exclusively (*E*)-azobenzene **(*E*)-1**. Both classes of the intersections (**reactive and unreactive CI**) concilitate all $S_1 \rightarrow S_0$ excited state decay events with the excitation wavelength determining the frequency at which each is accessed. For the $n\pi^*$ excitation, the S_1 population decay proceeds with 40% through the unreactive section and with 60% through the reactive CI, which yields **(*Z*)-1** in 24% and recovers **(*E*)-1** in 36%. This mirrors the overall $n\pi^*$ quantum yield (Figure 1.2).[39,46]

Upon $\pi\pi^*$ excitation of **(*E*)-1** (**S_2 entry point**), relaxation to the ground state S_0 proceeds with higher probability through the unreactive decay channel $S_2 \rightarrow CI(S_2/S_1) \rightarrow S_1 \rightarrow CI(S_1/S_0$ unreactive$) \rightarrow S_0$. This additional $S_1 \rightarrow S_0$ CI state is of high-energy, planar and non-productive and counts for 60% of the total energy decay revealing the overall decline of the quantum yield. Only 12% of the remaining population decay that pass through the reactive CI yields **(*Z*)-1** (Figure 1.2).[39,46]

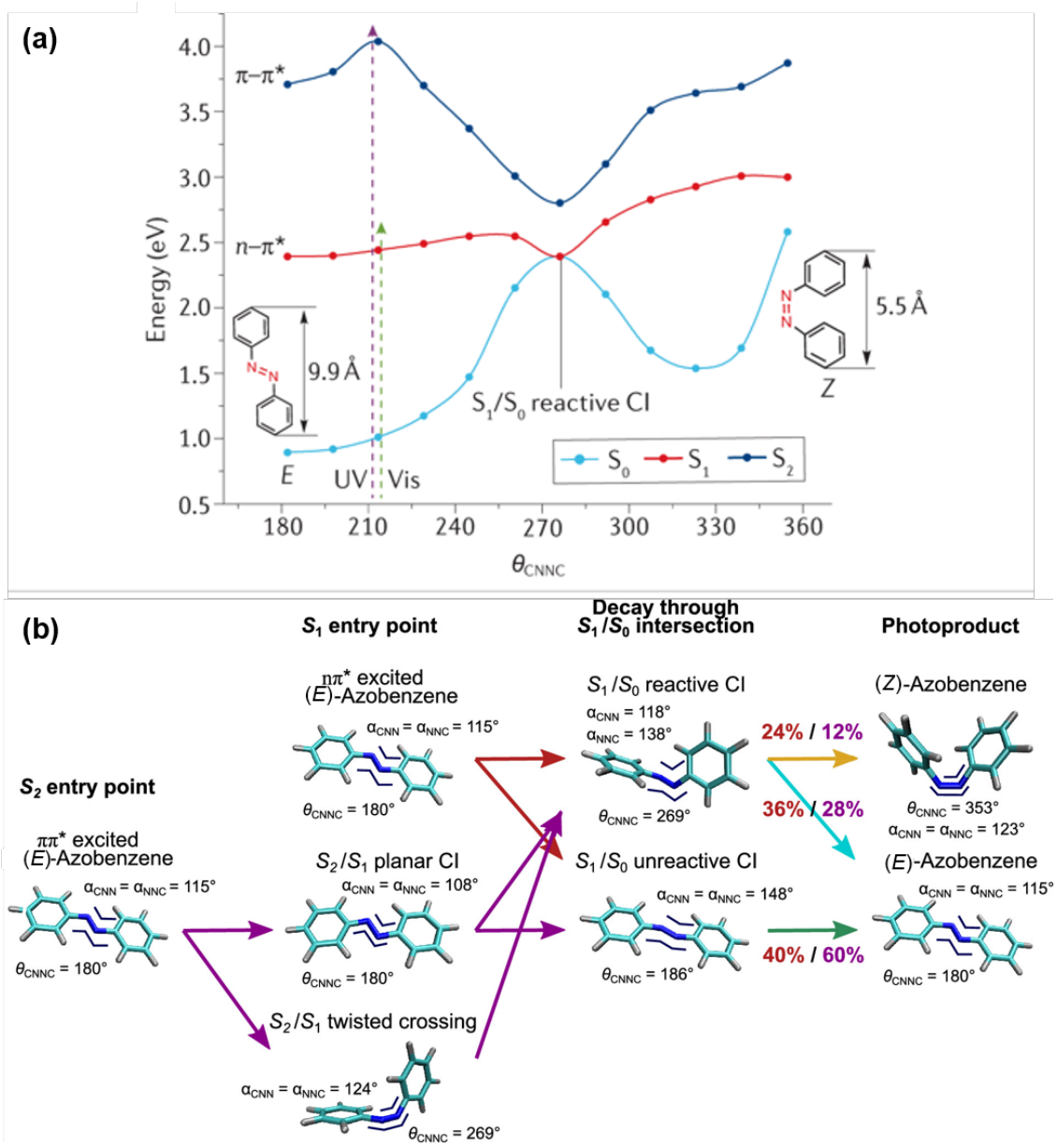

Figure 1.2 **(a)** Potential energy surface scans of azobenzene **1** along fixed values of the torsion coordinated with remaining degrees of freedom allowed to relax. **(b)** Graphical overview of the wavelength-dependent photochemistry of azobenzene **1**. The photoreaction followed from direct $n\pi^*$ excitation is marked by red arrows, the reaction following from $\pi\pi^*$ excitation first by purple arrows. Corresponding to the excitation type, the percentage of photoproducts obtained by each pathway is listed in red and purple. Adapted with permission.[46] © 2021, Springer Nature Unlimited.

The $S_2 \rightarrow S_1$ relaxation process also follows two distinct routes: The **S_2/S_1 twisted crossing** involves S_2/S_1 twisted intersection geometries by twisting in the θ_{CNNC} coordinate and symmetric widening of the $\alpha_{CNN} = \alpha_{NNC}$ angles. The **S_2/S_1 planar CI** bears S_2/S_1 planar intersections accessed through symmetric compression of the $\alpha_{CNN}/\alpha_{NNC}$ angles (Figure 1.2).[39,46]

The **$S_2 \rightarrow S_1$ twisted intersection** introduces a novel reactive pathway on S_1, where torsional motion occurs on S_2 rather than S_1 and a barrier of approximately 0.33 eV on S_2 is surmounted. This allows entry onto S_1 at a substantially twisted geometry. Through this new entry point, the wavepacket rapidly accesses the **$S_1 \rightarrow S_0$ reactive CI**, leading to a short delay time between the $S_2 \rightarrow S_1$ twisted and the $S_1 \rightarrow S_0$ reactive decay events. Although this high-energy decay pathway involving torsional dynamics on S_2 constitutes only a small fraction (12%) of the overall reaction yield, it is noteworthy that the $S_1 \rightarrow S_0$ reactive pathway becomes significantly more efficient when directed through this route. In this pathway, **(*Z*)-1** is produced with an efficiency of 67% (8 out of 12) compared to 40% (24 out of 60) in the case of nπ^* excitation (Figure 1.2).[39,46]

The process of the *thermal* relaxation of **(*Z*)-1** is dependent on the temperature, viscosity and polarity of the medium and can occur via in-plane inversion or rotation or hula-twist.[20,24,31,47–50] Recently, an involvement of triplet states has been discussed.[38,51]

Based on the order of their energetic electronic states $\pi\pi^*$ and nπ^*, azobenzenes are classified in three types: azobenzene type, aminoazobenzene type and pseudo-stilbene type.[52] For the azobenzene type, the $\pi\pi^*$ band in the UV region is strong while the nπ^* band in the visible range is weak. Aminoazobenzenes contain an electron-donating-group (EDG), such as hydroxy or amino, in *ortho*- or *para*-position resulting in very close or collapsed $\pi\pi^*$ and nπ^* bands in the UV/vis range. Pseudo-stilbenes bear an EDG and an electron-withdrawing group (EWG), such as cyano or nitro groups, at the *para*-positions resulting in a push/pull system with a large dipole moment. Thus, the $\pi\pi^*$ transition band is shifted drastically to red so that both bands appear with reversed order in the visible range. However, the nπ^* band is overlaid by the more intense $\pi\pi^*$ band.[6,53,54] Moreover, they often show intermolecular charge-transfer bands affecting their photophysical properties. In addition to the substituents on the azobenzene, the distortion of the azobenzene rings from planarity also influences the switching characteristics by increasing the absorption maxima of the nπ^* transition towards the range of visible light.[55]

The (*Z*)-isomer of azobenzene type derivatives demonstrates increased thermal stability with relaxation times ranging from hours to days at ambient conditions,[20,48,49] while the (*Z*)-aminoazobenzenes and -pseudo-stilbenes show higher relaxation rates with half-lifes of seconds to minutes or microseconds to milliseconds, respectively, at ambient conditions.[20,50] The thermal relaxation of azobenzene-type derivatives proceeds via inversion[20,48,49] and for the two other types via rotation.[20,50]

If azobenzenes are incorporated into cyclic structures, not only the distortion but also the ring strain influences the thermal stability leading to examples where the (*Z*)-isomer is thermodynamically stable. Here, the thermal relaxation via a hula-twist is favored.[24,55–57]

By introducing distinct subsituents and control of the substitution pattern of the two phenyl rings azobenzenes with tunable photochemical and photophysical properties can be synthesized.[46]

1.1.2 Synthetic Procedures towards Functionalized Azobenzenes

In order to obtain functionalized azobenzene derivatives **1b**, usually prefunctionalized starting materials **2a** or **2b** are reacted to form the azo group. The substituent on the starting material can either be a reactive functional group that is further transformed after generating the azo group (Scheme 1.3 a), or it can be first modified to the desired functionality and subsequently reacted to the azobenzene derivative **1b** (Scheme 1.3 b). These approaches highly depend on the availability of the respective precursors **2a** and **2b**, which might even not always be accessible and sensitive functional groups can sometimes not be obtained as they may react under the conditions required for azobenzene formation.[58,59]

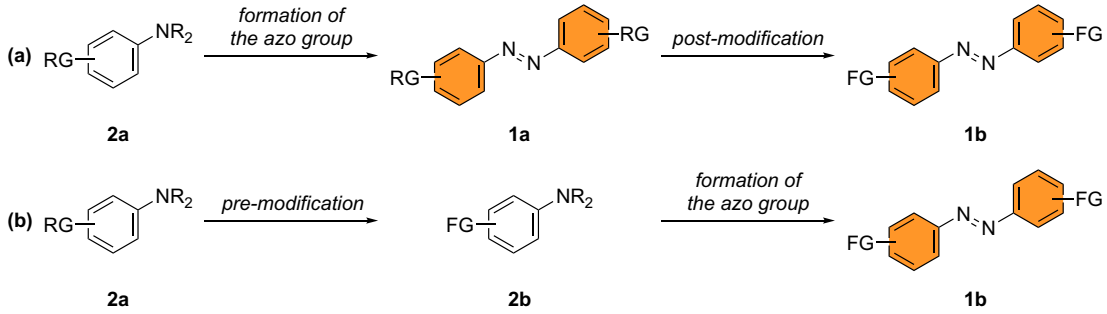

Scheme 1.3 Synthetic strategies towards functionalized azobenzenes **1a**. **(a)** A starting material decorated with a reactive group (RG) **2a** is transformed to the corresponding azobenzene **1b**, which is subsequently further modified to **1a**. **(b)** The starting material **3** is first altered and subsequently reacted to the azobenzene **1a**, which contains the desired end functionalization.

Several routes for the synthesis of functionalized azobenzenes **1c** and **1d** have been established depending on the desired substitution and availability of precursors (Scheme 1.4).[59]

Symmetric azobenzenes **1c** are mostly synthesized via oxidative coupling from the corresponding functionalized anilines **3** (Scheme 1.4 a)[60–63] or via reductive coupling based on prefunctionalized nitrobenzenes **4** (Scheme 1.4 b).[64,65] Over time, a large number of oxidizing or reducing agents, respectively, have been introduced. In a stoichiometric amount, MnO_2,[66] permanganates,[67,68] hypervalent iodines such as phenyliodine(III) diacetate (PIDA)[62] or AgO[69] were used as oxidant. Cu(I) compounds with O_2[61,63] or gold nanoparticles on Tio_2 with O_2[70] have been applied catalytically. As reducing agents, $LiAlH_4$[64,71] or $NaBH_4$[72,73] have been used among others.[74] Catalytic reductions using gold nanoparticles on TiO_2 and H_2[70] or a photocatalytic system of gold nanoparticles on ZrO_2[75] were also reported. Upon over-reduction to the hydrazobenzene, benzidine rearrangements occur.[76]

For the synthesis of asymmetric azobenzenes **1d** and **1e**, mainly azo couplings via the generation of a diazonium salt **4** (Scheme 1.4 c)[77,78] or the Mills reaction, a coupling of a nitrosoarene **7** with an aniline **3** (Scheme 1.4 d),[79–81] are utilized. In the azo coupling,

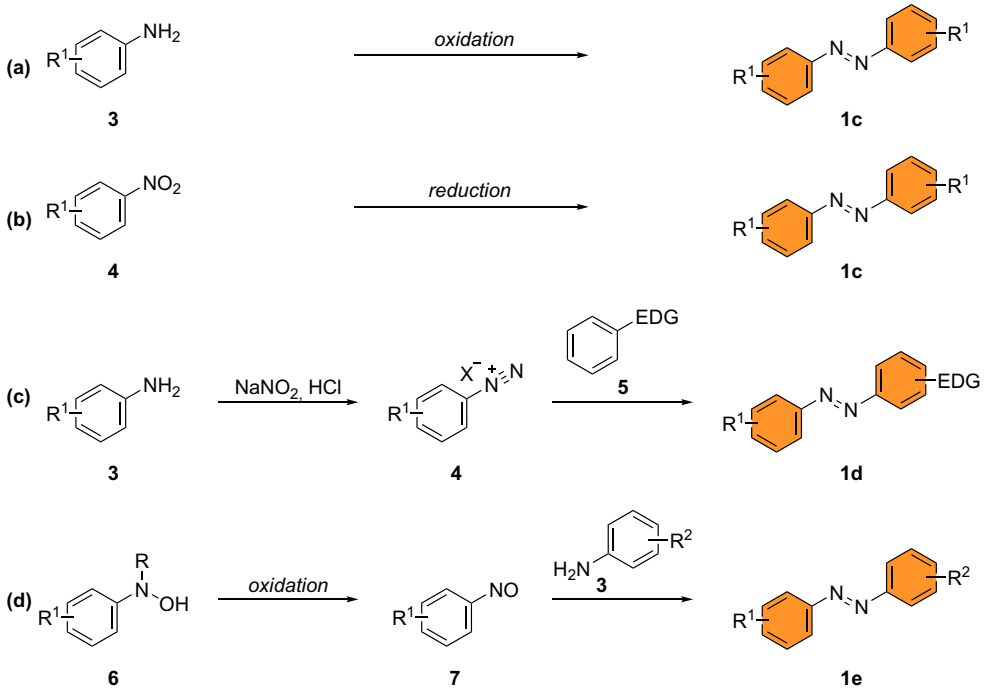

Scheme 1.4 Common synthetic routes towards functionalized azobenzenes **1c**, **1d** and **1e**. **(a)** Oxidative coupling of anilines **3**. **(b)** Reductive coupling of nitrobenzenes **4**. **(c)** Azocoupling via diazotation of anilines **3**. The formed diazonium salt **4** reacts with electron rich aromatic systems **5** in an elctrophilic aromatic substitution. **(d)** Mills reaction. Hydroxyanilines **6** are oxidized to nitrosobenzenes **7**, which subsequently undergo a condensation with anilines **3**.[59]

the diazonium salt **4** is obtained by diazotation of a primary amine **3** and reacts in an electrophilic aromatic substitution with an activated aromatic system **5** such as substituted arenes bearing a hydroxyl or amino group. This step is very pH sensitive and the stability of diazonium salts **4** is strongly influenced by the counterion. Thus, the diazotation is typically performed *in situ* under temperature control.[77,78,82] In the Mills reaction, hydroxyanilines **6** are oxidized to the corresponding nitrosobenzene **7** using various oxidizing agents, e.g., Oxone®,[81] *meta*-chloroperoxybenzoic acid (*m*CPBA),[83] or $KMnO_4$.[84] The oxidation is also possible by electrocatalysis.[85] The unsymmetrical azobenzene **1e** is generated by the condensation of **7** with an aniline **3**. The critical step in the Mills reaction, is the synthesis of the nitrosoarenes **7**, which can easily be overoxidized to the corresponding nitroarenes.[81,85]

In addition to these general methods, several others exist that can be used in very particular circumstances. One such reaction is the Wallach reaction, which converts azoxy derivatives into 4-hydroxyazobenzenes.[86] Another one are metal catalyzed couplings of *N*-*tert*-butoxycarbonyl (BOC) aryl hydrazines with aryl halide[87] or dehydrogenations of *N,N'*-diarylhydrazinces.[88] However, they have only limited synthetic relevance as, for example, unwanted side reactions occur due to rearrangements in the case of the Wallach reaction.[86]

1.1.3 Late-Stage Functionalization

Late-stage functionalization seeks to diminish the number of synthetic steps required to introduce specific functional groups or structural modifications by allowing the preparation of advanced intermediates that can be diversified as needed. Chemo- and site-selectivity as well as tolerance towards a wide range of functional groups are key elements of late-stage diversification. Thus, it has become a powerful and versatile tool in synthetic chemistry providing more efficient and practical routes to complex materials.[89]

Metal catalyzed cross-coupling reactions and C-H activation have proven to be potent and adaptable instruments in late-stage functionalizations. This also applies to azobenzene chemistry (see Section 1.5). As the review *Modification of Azobenzenes by Cross-Coupling Reactions*[90] already provides a broad overview, only a summary of the findings is given here:[1]

A manifold range of azobenzene derivatives for diverse applications have been synthesized by different types of cross-coupling reactions with Suzuki-Miyaura and Sonogashira being the most prevalent ones. Electrophilic and nucleophilic azobenzene derivatives have been employed in cross-coupling reactions although the number of examples is significantly higher for electrophilic azobenzenes. Regarding the catalytic system, palladium catalyses were dominant, but first examples using other transition metals such as nickel or cobalt exist. Cross-coupling reactions have been reported mainly for the diversification of the *para*-position but only a few for the *meta*- and even fewer for the *ortho*-position. Due to the adjacent lone electron pair of the nitrogen atoms, the reaction behavior of the *ortho*-position differs to the one for the *meta*- and *para*-position. C-H activation has been an alternative for altering the *ortho*-position. In this case, it has to be considered that the diazenyl group might not remain intact.

Only a few methods to functionalize azobenzenes without transforming a functional group have been reported. Selective halogenation of C-H bonds in the *meta*-position of asymmetric azobenzenes via electrophilic aromatic substitution using *N*-halosuccinimides and mechanochemistry[91] as well as mercuration using mercury trifluoroacetate in anhydrous trifluoroacetic acid[92] could be achieved. *para*-Aminated azobenzenes were synthesized by a cobalt catalyzed nucleophilic aromatic substitution of a hydrogen atom allowing the use of aliphatic amines and anilines as aminating reagents.[93]

Another way of modifying azobenzenes in a later synthesis stage is lithiation of the aryl group followed by quenching with an electrophile. *ortho*-Halogenated azobenzenes can directly be lithiated using standard procedures due to a stabilization of the *ortho*-lithiated species by N→Li coordination.[66,94–96] For lithiations in *meta*- and *para*-position, the reaction conditions have to be altered as organo-alkali reagents can reduce the diazene group to hydrazine derivatives **8a** and **8b** or even completely to amines reducing the yield drastically (Scheme 1.5 a).[11,97–99] By transmetalation of stannylated azobenzenes **1h** with methyllithium in THF, a selective lithiation in *para*, *meta* and *ortho* position without any

[1] For detailed references see publication M. Walther et al., *Synthesis* **2021**, *53*, 1213–1228 (Section 1.5).

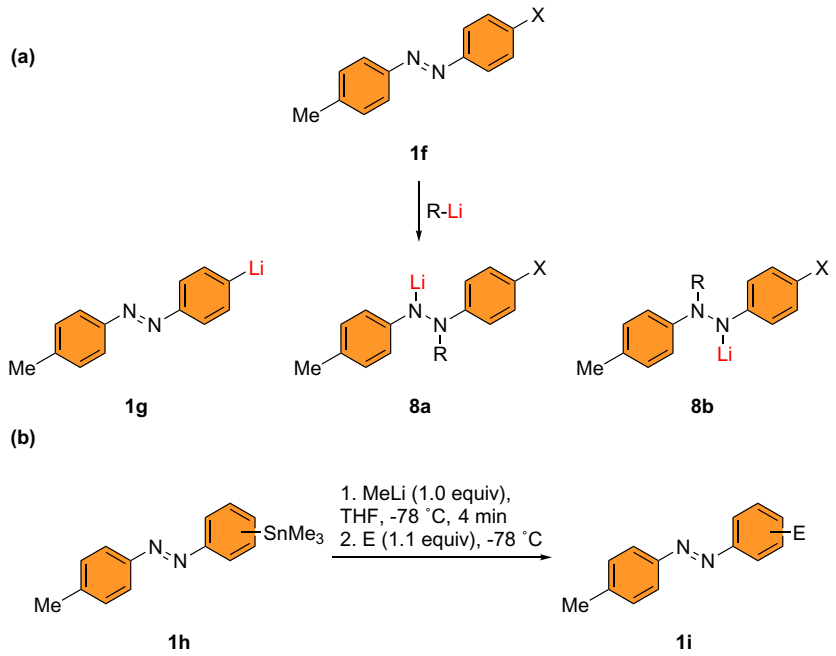

Scheme 1.5 (a) Possible lithiation products **1g**, **8a** and **8b** of *para*-iodoazobenzene. **(b)** Selective lithiation of stannylated azobenzenes **1h** via tin-lithium exchange and subsequent quenching with an electrophile (E).[100]

decomposition of the azo group could be achieved (Scheme 1.5 b). The intermediate aryl lithium species **1g** is less reactive towards electrophiles than alkyl lithium compounds hindering the attack of the azo group and thus, the functionalized azobenzenes **1i** were obtained in high yields.[100]

1.2 Diazocines

In recent years, 11,12-dihydrodibenzo[*c*,*g*][1,2]diazocines ethylene-bridged azobenzenes (**9**) or in short "diazocines" have gained significant attention because the relative stability of its (***E***)- **(*E*)-9** and (***Z***)-isomer **(*Z*)-9** is opposite to the one of linear azobenzenes due to its ring strain.[55]

1.2.1 Properties and Isomerization

Already synthesized in 1910,[101] photochromism of diazocine (**9**) was not discovered until 1995.[102] In contrast to linear azobenzenes **1**, the thermodynamically stable form is the boat-shaped (*Z*)-isomer **(*Z*)-9** which can reversibly interconvert to the metastable (*E*)-isomer **(*E*)-9** upon irradiation with blue light (370 - 400 nm) with over 90% efficiency. The re-isomerization takes places upon illumination with green light (480 - 550 nm) or through thermal relaxation (Scheme 1.6).[55,102] resulting in a better resolution of the nπ absorption bands of the isomeric states (Figure 1.3).[55] However, the thermal half-life time of (*E*)-diazocine **(*E*)-9**, measured in *n*-hexane, is considerably lower than that of azobenzene **1** owing to the ring strain (4.5 h at 28.5 °C[55] vs. 2 d at 20 °C[20]). In general,

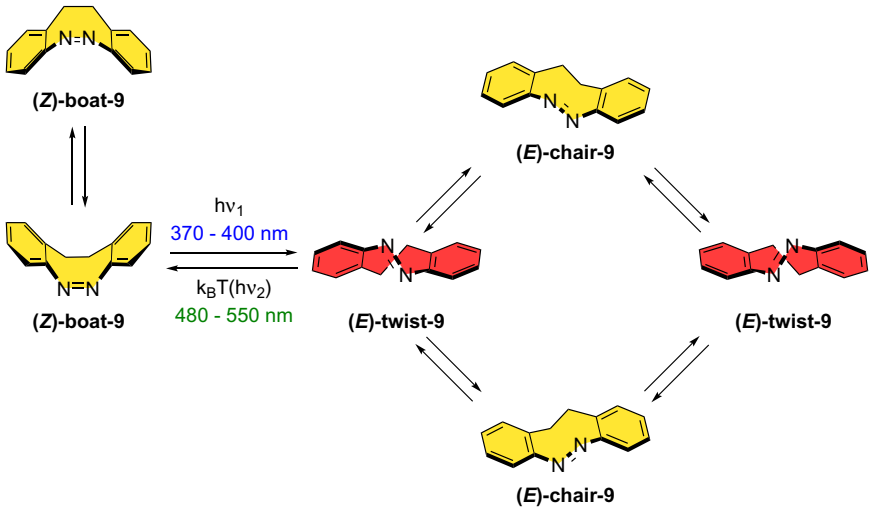

Scheme 1.6 Diazocine (**9**) can reversibly isomerize photochemically and thermally between its different configurations.[104]

diazocines **9** show a high photostability: Over repeated switching cycles, they did not reveal fatigue or photobleaching, i.e., some examples were measured over 5000 cycles.[103]

Since the nπ^* bands of **(*Z*)-9** and **(*E*)-9** are well separated, photoisomerization in both directions is possible addressing the $S_0 \rightarrow S_1$-transitions.[55] Diazocines **9** can not only undergo (*Z*)-(*E*)-isomerization but also conformational transitions, i.e., inversion of the **(*Z*)-boat-9** as well as twist- and twist-chair inversion of the (*E*)-isomer **(*E*)-9** (Scheme 1.6).[103,104] The conformational change of diazocine **9** as [6,8,6] condensed ring system are mainly attributed to the central heterocycle acting as a semi-rigid hinge between the two rigid phenyl rings. Hence, the $S_0 \rightarrow S_1$ photoexcitation (irradition into the nπ^*) induces a pedal-like hula-twist motion of the CNNC-moiety and great changes to the orientation of the benzene ring.[105] The favorable orientation of these rings and the steric blockade of the deactivation path promote a fast escape from the Franck-Condon region in the S_1 state (ca. 79 fs). Yet, the rotational rearrangement of the ethylene bridge, which is triggered by vibrational excitations decelerates the electronic relaxation to the S_0 state (270±60 fs). The relaxation dynamics of (*E*)-diazocine **(*E*)-9** in the S_1-state are much faster than those of (*Z*)-diazocine **(*Z*)-9**. While the short duration of the S_1 phase, an out-of-plane distortion of the benzene rings occurs before the guaranteed relaxation to S_0 takes place.[33,34,103,106–108]

As for azobenzenes **1**, the substituents and the substitution pattern play a crucial role in adjusting the photoswitchable properties of diazocines **9**. For example, EWG at the benzene rings or high strain in the ring system destabilizes the **(*E*)-9**, and thus, its thermal half-life.[103,109]

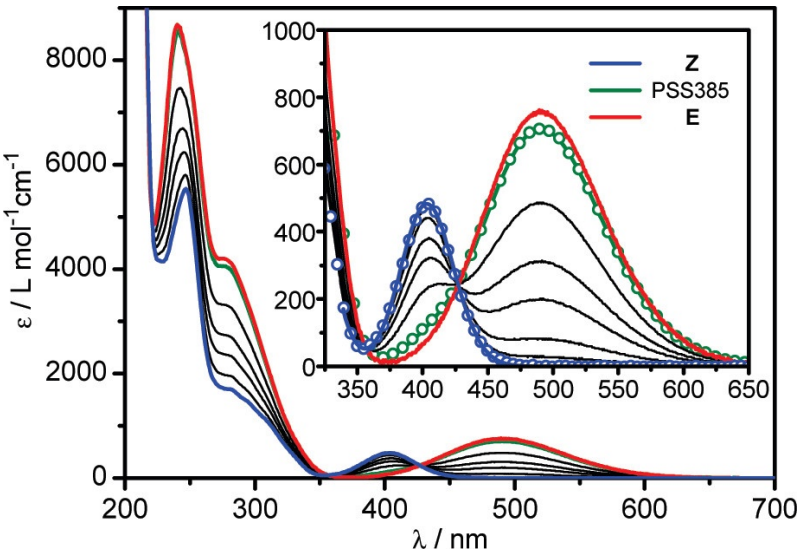

Figure 1.3 UV/vis absorption spectrum of **(*Z*)-9** (blue) and **(*E*)-9** (red) and the PSS385 (green) in *n*-hexane. The inset displays the S_1 ($n\pi^*$) region on an enlarged scale. Adapted with permission.[55] © 2014, American Chemical Society.

1.2.2 Synthetic Procedures towards Functionalized Diazocines

From a synthetic perspective, diazocine (**9**) can be conceptualized as a combination of two inflexible benzene rings connected by a diazo and an ethylene group. Compared to azobenzenes **1**, its synthesis is much more demanding because a medium sized ring has to be established. The ethylene bridge of the dibenzene moiety is generated mostly before forming the N=N bond because it tends to be less susceptible towards oxidation and reduction than the diazenyl group.[110–112]

The most common syntheses to obtain diazocines **9** involve the intramolecular reduction of 2,2'-ethylenedinitrodibenzenes **11** (Scheme 1.7 a)[111,113–115] or the intramolecular oxidation of 2,2'-ethylenedianilines **14a** (Scheme 1.7 b).[116–118] Both synthetic strategies can also be merged: If this strategy is followed, the 2,2'-ethylenedinitrodibenzenes **11** are first reduced to the corresponding 2,2'-ethylenedianilines **14b** and subsequently oxidized to form the N=N bond ((Scheme 1.7 c).[119–127]

The required functionalized ethylenedinitrodibenzene **11** can be synthesized via different routes, e.g., an oxidative coupling of nitrotoluenes **10** using bromine and potassium *tert*-butoxide (Scheme 1.7 a).[111,115] If two distinct toluene derivatives are used, a statistical mixture of difficult to separate products will be obtained due to the radical reaction mechanism of the first step.[121] A Wittig reaction of a benzylphosphonium halide with a benzaldehyde followed by a reduction of the formed stilbene yielded unsymmetric 2,2'-ethylenedinitrodibenzenes.[128] Asymmetric functionalized 2,2'-ethylenedianilines **14a** were obtained via Sonogashira cross-coupling of alkynes **12** with aryl halides **13** and a subsequent reduction of the corresponding tolane (Scheme 1.7 b).[117] A Wurtz-type coupling of benzyl halides with benzyllithium derivatives also delivered functionalized dibenzenes. However, the scope of tolerated functional groups was limited due to the harsh reaction conditions.[129]

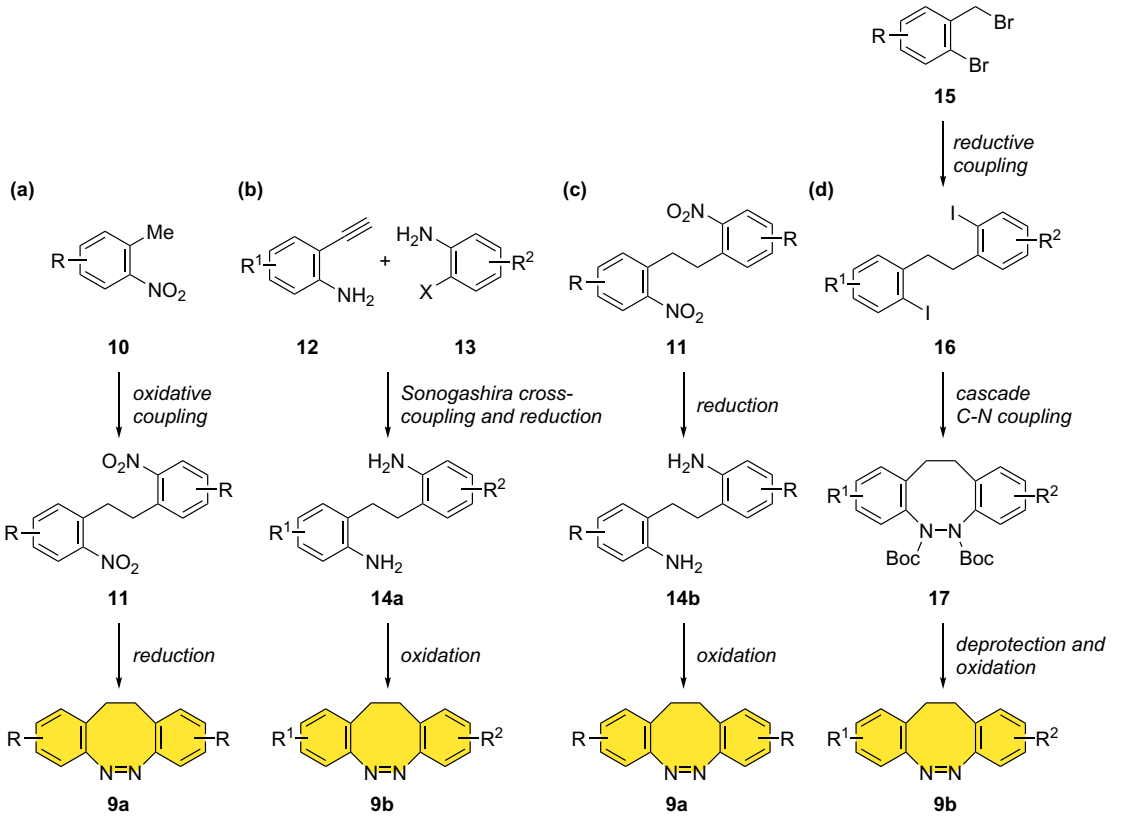

Scheme 1.7 Synthetic routes towards functionalized diazocines **9**. **(a)** Reduction of 2,2'-ethylenedinitrodibenzenes **11**.[111] **(b)** Oxidation of 2,2'-ethylenedianilines **14a**. **(c)** Reduction of 2,2'-ethylenedinitrodibenzenes **11**, followed by oxidation of 2,2'-ethylenedianilines **14b**.[130] **(d)** Cascade C-N coupling.[112]

As reducing agents in the reduction of 2,2'-ethylenedinitrodibenzenes **11**, a combination of Zn and $Ba(OH)_2$[113–115,119,122,124,126] or NH_4Cl,[125] $LiAlH_4$,[123] $NaNO_3$ with H_2SO_4,[120] $SnCl_2$,[121] Na_2S or a solvent-free approach with lead powder in a ball mill[111] were used (Scheme 1.7 a). For the oxidation of dianilines **14**, various systems can be employed: $CuCl_2/O_2$,[111,123,126] HgO,[119,122] glucose/NaOH,[120,131] *t*-BuOCl/NaI,[124] Oxone®,[127] peracetic acid,[118] *m*CPBA[117,121,125] or red copper/NH_4Br/pyridine (Scheme 1.7 b).[116]

Due to the redox nature of these reactions, the reductive pathway is prone to over- or under-reduction. Analogously, the oxidative pathway is susceptible towards over- or under-oxidation. Thus, the corresponding azoxy-, diazo dioxide- or hydrazo-derivatives can occur as side products.[109–111,117,132] In addition, the intramolecular reaction competes with the intermolecular redox reaction.[110,111] Hence, to obtain a sufficient yield, the amount of oxidant or reductant as well as the reaction conditions have to be chosen carefully.[111,117]

As an alternative, a cascade C-N coupling strategy has been developed where the diazocine bond is built by consecutive cross-coupling reactions between a 2,2'-ethanedihalodibenzene **16** and di-*tert*-butyl hydrazodicarboxylate (Scheme 1.7 d). 2-Bromobenzyl bromides **15** were reduced by *n*-butyllithium to form the ethylene bridge. Further lithiation and nucleophilic substitution with iodine delivered the corresponding diaryl diiodides **16**. Cu catalyzed cascade amidations of **16** with a dinucleophilic hydrazine derivative

yielded the BOC-protected diazocine heterocycle **17**. In a last step, the protecting group was cleaved via Lewis acid promoted hydrolysis and hydrazo group oxidized to the final diazocine **9b**.[112]

With those synthetic methodologies in hand, various *meta*- and *para*-functionalized diazocines **9** were obtained bearing functional groups such as halogens,[112,115,117,127] -OH,[112] -NH_2,[119,126] -CN,[112,117] or -vinyl.[126]

1.2.3 Late-Stage Functionalization

For the covalent incorporation of diazocines **9** into materials, functional groups attached to the aromatic rings are needed. Synthetic modifications to the ethylene bridge have also been described,[103,110,113,121,122,125,133,136–138,134,135] but they are not a focus of this thesis. If the substituents are not introduced by prefunctionalized starting materials (see Subsection 1.2.2), they can be inserted afterwards in late-stage diversification.

Bromine substituents were introduced *para* to the azo group under acidic conditions using *N*-bromosuccinimide (NBS) via electrophilic aromatic substitution (Scheme 1.8).[139]

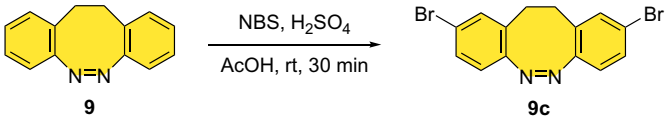

9 **9c**

Scheme 1.8 Electrophilic aromatic substitution of diazocine **9**.[139]

Halogenated diazocines like **9c** can be transformed into more complex derivatives, e.g., in cross-coupling reactions[115,127] (see Section 1.5). Since the publication of the review Modification of Azobenzenes by Cross-Coupling Reactions[90] the use of diazocines in cross-coupling reactions has increased. Buchwald-Hartwig couplings remained the most prominent type of cross-couplings with either halogenated or amine-substituted diazocines.[10,109,112,115,117,118] For example, chloride substituents on the diazocine were reacted in a Buchwald-Hartwig amination with lithium bis(trimethylsilyl)amide yielding the corresponding amines in 51-58% yield.[112] The Stille cross-coupling of diazocines[115,140] was expanded to nucleophilic derivatives, even though with a relatively low yield.[121] Moreover, the first examples of Sonogashira[141,142] and Negishi[124,143] cross-coupling reactions were reported and a copper(I) catalyzed Ullmann-type reaction was employed in the synthesis of azide funcionalized diazocines.[144]

Besides metal catalyzed cross-coupling reactions, brominated diazocines were converted into the corresponding cyano derivatives under standard Rosenmund-von Braun conditions, hydrolyzed to the free acid under basic conditions[109,127,145,146] and further transformed in carbodiimide coupling reactions.[127,145,146] For biological applications, diazocines with amine groups were used in carbodiimide or peptide couplings.[10,131,140,147] Diazocine based ligands for the usage in photoswitchable cages were synthesized by a copper catalyzed azide-alkyne cycloaddition "click reaction".[144] Alkyne substituted diazocines were incorporated

onto triazatriangulenium (TATA) platforms[113,114] and the first examples of diazocine-containing polymers have been reported.[148–151]

1.3 *N*-Hydroxysuccinimide Ester

N-hydroxysuccinimide (NHS) esters **21** are activated esters widely used in different areas of synthetic chemistry, such as bioconjugate chemistry,[152–156] peptide synthesis[157–159] or functionalized materials and polymers.[160–163] These bench-stable active esters **21** react under mild conditions with primary amines in a condensation reaction to form a stable amide bond. During this reaction, water-soluble NHS[159] is released enabling a straight-forward purification of the condensation product.[164]

The common way to synthesize NHS esters **21** is the coupling reaction of a carboxylic acid **20** with NHS in the presence of a carbodiimide coupling agent, e.g., *N,N'*-dicyclohexylcarbodiimide (DCC) (Scheme 1.9).[165,166] As a byproduct, an urea derivative is formed, which complicates the purification of the reaction mixture. Moreover, DCC is known to have an allergenic potential.[164]

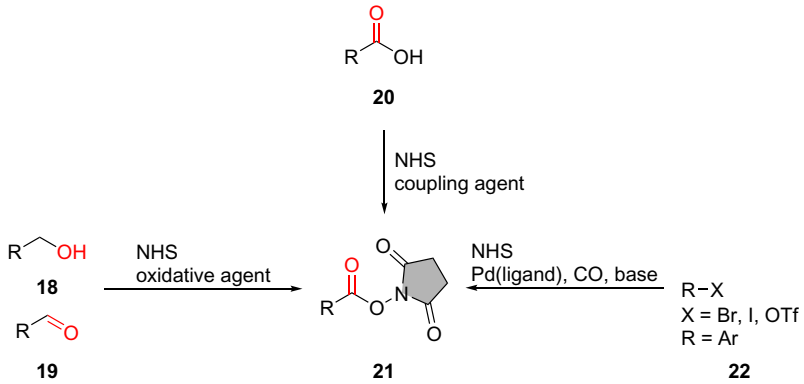

Scheme 1.9 Synthetic procedures to generate NHS esters **21**.[165–170]

Several alternatives for the activation of a carboxylic acid **20** have emerged: Anhydrides and their analogues[167] as well as alcohols[168] **18** and aldehydes[171] **19** were reacted with NHS under oxidizing conditions. Aryl halides and triflates **22** were employed in palladium catalyzed carbonylative cross-coupling reactions with NHS under a CO atmosphere.[169,170] The use of NHS formate as a CO surrogate has been reported to facilitate the practicability of the cross-coupling approach.[169]

As primary amines are ubiquitous in materials and life sciences, NHS esters **21** are much sought after compounds for further transformations.[156]

1.4 Diaryliodonium Salts

Due to their low toxicity and high selectivity, hypervalent iodine(III) compounds are efficient reagents for transition metal-free transformations under mild conditions.[172–174] The hypervalent bond can be described by a 3-center-4-electron (3c-4e) bond, which is

formed by the twofold occupied 5p orbital of the iodine with donation of one electron by each ligand. Thus, the central iodine atom bears a partial positive charge and is therefore electrophilic, while the apical ligands carry a partial negative charge (Figure 1.4).[175,176] Diaryliodonium salts **23** are composed of a hypervalent iodine(III) center and two carbon ligands, consisting of two aryl moieties and one heteroatom ligand.[174,177] X-ray experiments have proven a T-shaped form for iodine(III) reagents where the more electronegative ligand is in the apical position participating in the hypervalent X-I-C bond. As the diaryliodonium salts **23** are configurationally instable, Berry pseudorotation occurs and the apical and equatorial ligands can alter their position. Hence, for unsymmetric diaryliodonium salts **23b** it is difficult to predict, which carbon ligand donates an electron into the hypervalent bond. This uncertainty is depicted in an ionic form of the respective diaryliodonium salt **23** (Figure 1.4).[176]

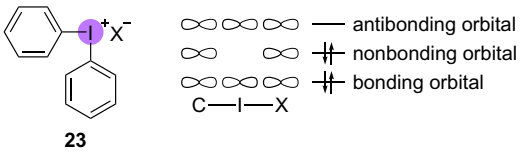

Figure 1.4 T-shaped ionic structure of a diaryliodonium salt **23** and molecular orbital of the 3c-4e bond.[175,176]

Since the first synthesis of a diaryliodonium salt **23** in 1894,[178] several synthetic procedures including one-pot protocols have been developed.[179–181] Using *m*CPBA as oxidant and trifluoromethanesulfonic acid (TfOH), symmetric diaryliodonium salts **23a** were obtained directly from iodine (**24**) and arenes **25a**. For more electron-rich arenes, the weaker *para*-toluenesulfonic acid (TsOH) was used, determining the counterion of the salt (Scheme 1.10 a). Unsymmetric salts **23b** were synthesized by similar reaction conditions, starting from the corresponding iodoarene **26** (Scheme 1.10 b).[179,180]

Diaryliodonium salts **23** are highly reactive electrophilic arylating agents due to the node in the nonbonding orbital of the hypervalent bond (see Figure 1.4). Initially, the counterion is replaced by an external nucleophile leading to the formation of a Nu-I bond.

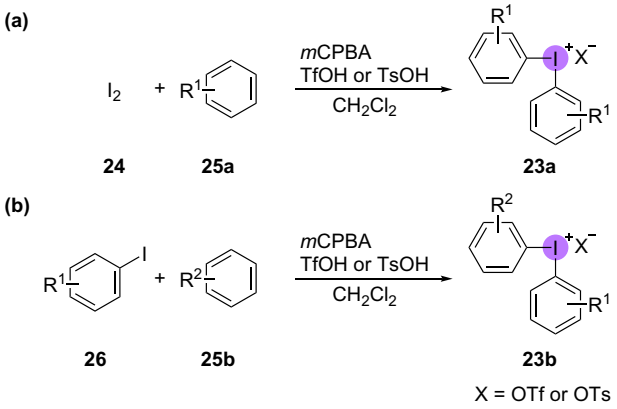

Scheme 1.10 One-pot synthesis of symmetric **23a** and asymmetric diaryliodonium salts **23b**.[179,180]

A subsequent reductive elimination provides the product and releases the aryl iodide **26a** (Scheme 1.11 a).[173] If unsymmetric salts **23b** are used, problems regarding chemoselectivity may arise. Preferably, the more electron-deficient aryl group is transferred as the transition state of the ligand coupling is better stabilized with an electron-deficient aryl group in the equatorial position.[176,182–187] This is in contrast to steric effects as *ortho*-substituted aryl groups are preferably transferred because of steric repulsions.[176,188,189] Thus, a prediction which ligand will be transferred can be difficult.[184]

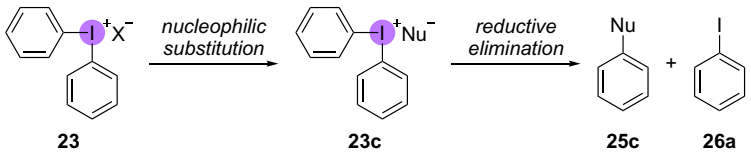

Scheme 1.11 General reactivity of diaryliodonium salts **23** with nucleophiles.

Nevertheless, diaryliodonium salts **23** have found application as efficient arylation reagents with a variety of nucleophiles, such as oxygen,[190–197] nitrogen,[198,199] carbon[200–205] or sulfur nucleophiles.[206,207]

1.5 Modification of Azobenzenes by Cross-Coupling Reactions

Title of Publication:

"Modification of Azobenzenes by Cross-Coupling Reactions"
M. Walther, W. Kipke, S. Schultzke, S. Ghosh, A. Staubitz, *Synthesis* **2021**, *53*, 1213–1228.
DOI: 10.1055/s-0040-1705999.

Abstract:

Azobenzenes are among the most extensively used molecular switches for many different applications. The need to tailor them to the required task often requires further functionalization. Cross-coupling reactions are ideally suited for late-stage modifications. This review provides an overview of recent developments in the modification of azobenzene and its derivatives by cross-coupling reactions.

Author Contribution to this Publication:

In this publication, I (M. Walther) conducted the literature research and compiled the structure of the review. I wrote most parts of the manuscript: abstract, introduction, azobenzenes as formally electrophilic and nucleophilic components, palladium catalysis (except Suzuki-Miyaura cross-coupling reactions), nickel catalysis, copper catalysis (except Ullmann reactions), cobalt catalysis, azobenzenes as ligands in catalysts, conclusions. For those parts, I also created the schemes (14 in total); for the other parts I updated the schemes according to the template. W. Kipke wrote the part about C-H activation reactions and diazocines, S. Schultzke the Suzuki-Miyaura cross-coupling reactions and S. Ghosh the Ullmann reactions. A. Staubitz was the principal investigator. She provided the idea for this short review and edited the article in the end.

Synthesis
Reviews and Full Papers in Chemical Synthesis
April 1, 2021 • Vol. 53, 1181–1378

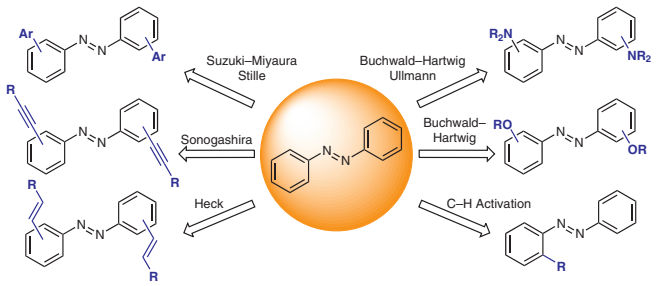

Modification of Azobenzenes by Cross-Coupling Reactions

M. Walther, W. Kipke, S. Schultzke, S. Ghosh, A. Staubitz

7

Thieme

1213

Synthesis M. Walther et al. THIEME OPEN ACCESS Short Review

Modification of Azobenzenes by Cross-Coupling Reactions

Melanie Walther[a,b]
Waldemar Kipke[a,b]
Sven Schultzke[a,b]
Souvik Ghosh[a,b]
Anne Staubitz*[a,b]

[a] University of Bremen, Institute for Analytical and Organic Chemistry, Leobener Straße 7, 28359 Bremen, Germany
staubitz@uni-bremen.de
[b] MAPEX Center for Materials and Processes, Bibliothekstraße 1, 28359 Bremen, Germany

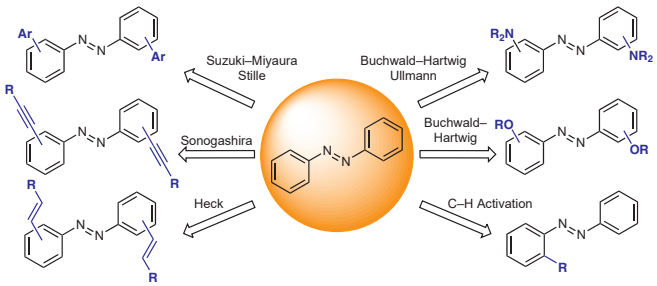

Received: 07.10.2020
Accepted after revision: 19.11.2020
Published online: 28.01.2021
DOI: 10.1055/s-0040-1705999; Art ID: ss-2020-z0528-sr

Abstract Azobenzenes are among the most extensively used molecular switches for many different applications. The need to tailor them to the required task often requires further functionalization. Cross-coupling reactions are ideally suited for late-stage modifications. This review provides an overview of recent developments in the modification of azobenzene and its derivatives by cross-coupling reactions.

1 Introduction
2 Azobenzenes as Formally Electrophilic Components
2.1 Palladium Catalysis
2.2 Nickel Catalysis
2.3 Copper Catalysis
2.4 Cobalt Catalysis
3 Azobenzenes as Formally Nucleophilic Components
3.1 Palladium Catalysis
3.2 Copper Catalysis
3.3 C–H Activation Reactions
4 Azobenzenes as Ligands in Catalysts
5 Diazocines
5.1 Synthesis
5.2 Cross-Coupling Reactions
6 Conclusion

Key words azobenzene, diazocine, molecular switches, cross-coupling reactions, C–H activation, metal-catalyzed

1 Introduction

Azobenzene and its derivatives are among the most investigated molecular switches.[1] They can interconvert photochemically and thermally between their metastable (*E*)- and (*Z*)-isomers (Figure 1).[2]

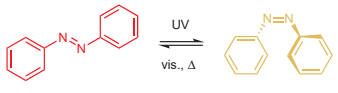

Figure 1 Reversible isomerization of azobenzene[2]

Several physicochemical characteristics are affected by this photoisomerization, e.g. geometry and end-to end distance,[3] electronic properties,[4] and polarity.[2] Whereas (*E*)-azobenzene is planar[3a] and without a dipole moment,[4] (*Z*)-azobenzene shows a non-planar geometry[3b] and a dipole moment of 3.0 D.[4] Consequently, azobenzene derivatives have gained great interest, for example for applications in data storage materials,[5] dynamic molecular devices,[1] or in photonics.[6]

Thus, manifold synthetic procedures have been developed for the preparation of azobenzene derivatives,[7] most with the formation of the diazenyl group as the key step. Methods to obtain symmetric azobenzenes range from reductive coupling of nitrobenzenes[8] or oxidative coupling of anilines.[9] The Mills reaction[10] or azo-coupling reactions[11] can be used to prepare asymmetric azobenzene derivatives. However, functionalized azobenzenes obtained in this way usually require prefunctionalized starting materials[7] which limits the synthetic modification possibilities. An additional problem is the susceptibility of the diazenyl group towards oxidizing[11b,12] and reducing[13] agents. Therefore, late-stage modification through cross-coupling reactions provides a valuable alternative to access a wider variety of azobenzene derivatives. This short review aims to give a broad, but not exhaustive, overview of the synthetic possibilities offered by cross-coupling reactions on azobenzenes and diazocines. In this short review, we distinguish between azobenzenes as formally electrophilic and formally nucleo-

(from left to right) **Melanie Walther** studied chemistry and business administration at the University of Kiel. After research stays at Cardiff University as well as at Stockholm University, she joined the Staubitz group for her master's thesis, dealing with photoswitchable polysiloxanes. During her following doctoral study at the University of Bremen she wants to expand the synthetic scope of molecular switches and their application into materials.
Waldemar Kipke studied biochemistry at Leibniz University in Hannover and obtained his bachelor's degree in 2016. He wrote his master's thesis about new ethylene-bridged molecular switches and obtained his master's degree in October 2018. During his Ph.D., he continues to work on molecular switches and new heterocycles containing B, Zr, and Sn.
Sven Schultzke studied chemistry at the University of Kiel and joined the Staubitz group for his bachelor's thesis about organogold(I) cross-coupling reactions. His upcoming research has been based on photoswitchable molecules, starting with a research exchange to the University of British Columbia in Vancouver for his master thesis and now his doctoral study, where he designs smart materials for 'soft grippers'.
Souvik Ghosh completed his M.Sc. from SVNIT, India. During his studies, he was a DAAD scholar at KIT, Germany and a OIST research scholar at OIST, Japan. In 2018, he joined the Staubitz group as Ph.D. student focusing on the synthesis of novel switchable molecules and their application in materials and polymer sciences.
Anne Staubitz was an assistant professor at the University of Kiel, before moving to the University of Bremen in 2015, where she has a full professorship for organic functional materials. Her main interests are light and force sensitive materials. The primary research focus is on their syntheses and properties, as well as applications. The second large research area in the group is comprised of compounds and materials that contain unusual combinations of main group elements and heavier elements.

philic components because of the different requirements and the corresponding difficulties in the synthesis of the azobenzene precursors, especially for nucleophilic derivatives.

2 Azobenzenes as Formally Electrophilic Components

(Pseudo)halogenated azobenzenes are used as an electrophilic component in cross-coupling reactions with a large variety of organometallic (nucleophilic) coupling partners. These (pseudo)halogenated species are usually obtained by employing prefunctionalized building blocks.[7] There are very few reported examples of the direct halogenation of azobenzene derivatives.[14] The relatively low reactivity of azobenzenes towards electrophilic halogenation reactions results from the electronic properties of the diazenyl group, which can form adducts with halogen halides leading to low yields.[14a,b] The use of elemental halogens often results in inseparable mixtures of mono-, di-, tri-, and tetrahalogenated products.[14a,c,d] Due to the lone-electron pairs on the nitrogen atoms, the diazenyl group can coordinate to metal catalysts facilitating substitution in the *ortho*-position.[14e] *ortho*-Halogenation is thus possible via metal-catalyzed C–H activation.[14c,e,f] However, different coordination patterns of the metal catalyst on the azobenzene moiety have been detected.[14d] Thus, selective halogenation remains challenging.[14e]

2.1 Palladium Catalysis

Palladium catalysts are the most frequently used catalysts in cross-coupling reactions. Therefore, the high number of palladium-catalyzed cross-coupling reactions of azobenzene derivatives that serve as a formally electrophilic component is no surprise.

2.1.1 Suzuki–Miyaura Cross-Coupling Reactions

The Suzuki–Miyaura cross-coupling reaction of (pseudo)-halogenated azobenzenes with boronic acids or esters is one of the most frequently used cross-coupling reactions for the modification of azobenzenes. Due to its convenience, reliability, and high yields, it is often used as the final synthetic step to combine large building blocks.[15] Of the many available examples, in this review we place a certain focus on polymers or molecules that self-assemble: such larger molecules are often not easy to prepare and this is where the benefits of the Suzuki–Miyaura cross-coupling are most relevant. Consequently, the Suzuki–Miyaura cross-coupling reaction gives access to many azobenzene derivatives with new applications in self-assembled materials[15a] or many liquid crystals,[15b–d,16] compounds that show tunable fluorescence,[17] photoswitchable porphyrin systems,[15e–g] dendrimers,[15h] polymers,[15i–o] metal-organic frameworks (MOFs),[15p] as well as molecular machines such as rotaxanes.[15q,r]

The first successful Suzuki–Miyaura cross-coupling reaction of an azobenzene derivative was described in a polymerization reaction (Scheme 1);[15i] different conjugated polymers were synthesized with molecular weights up to M_n = 9700 (in yields of 80–99%).

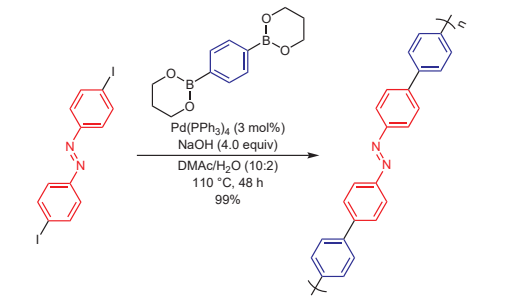

Scheme 1 Suzuki–Miyaura cross-coupling reaction for polymerization of an azobenzene derivative[15i]

Besides a benzene ring,[15i] more complex motifs such as a fluorene ring[15j,l,n,o] or a carbazole ring[15l,m,o] were successfully integrated in the conjugated main chain.

For the synthesis of rotaxanes, azobenzene derivatives were connected with two α-cyclodextrin units resulting in a [3]-rotaxane,[18] and later on a [1]-rotaxane.[15q,r] The azobenzene motif was either trapped in or bonded directly to the α-cyclodextrin units and subsequently capped by benzo[*de*]isoquinoline derivatives via cross-coupling.[15q,r,18]

Further possibilities are demonstrated by the implementation of two consecutive Suzuki cross-coupling reactions. Starting from a 4,4′-diiodoazobenzene, initial coupling with 4-bromophenylboronic acid gave a 4,4′-bis(4-bromophenyl)azobenzene that underwent a second cross-coupling reaction with a 4-substituted phenylboronic acid to give an azoterphenyl derivative (37–54% over 2 steps).[19]

Since 2016, several cross-coupling reactions have been performed using asymmetric azobenzene derivatives; in this way, molecules capable of precise self-assembly with additional non-covalent interactions were prepared in yields ranging from 26% to 94% (Scheme 2, A–C).[15c,16,17] Suzuki–Miyaura cross-coupling was also applied to functionalize nickel porphyrin systems with azobenzene moieties in excellent overall yields (Scheme 2, D).[15f] $Pd(PPh_3)_4$ served as Pd(0) catalyst with K_2CO_3 as base and the reaction was carried out in a toluene/EtOH/water mixture at 90 °C leading to good and sometimes excellent yields. The coupling was even successful with an azopyridine and with adjusted conditions for an azoimidazole unit. For the latter, the free amine of the imidazole was N-methylated to prevent a possible side reaction with $PdCl_2$(dppf) as the Pd(II) catalyst.[15f]

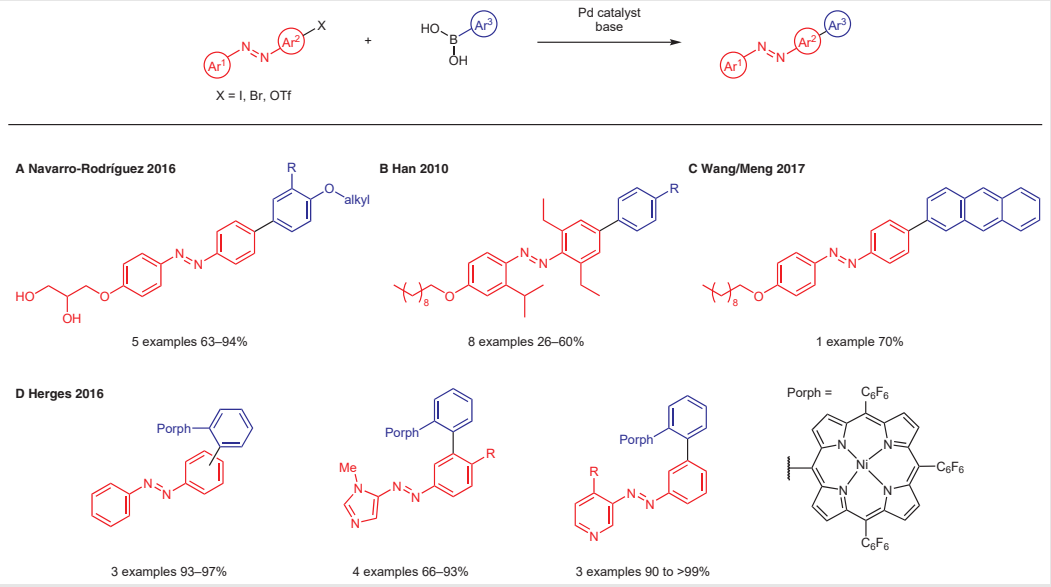

Scheme 2 Pd-catalyzed Suzuki–Miyaura cross-coupling reactions for enlarging a planar system (A–C)[15c,16,17] and for the functionalization of porphyrin systems (D)[15f]

2.1.2 Sonogashira Cross-Coupling Reactions

The palladium-catalyzed cross-coupling reaction of a terminal alkyne with halogenated azobenzenes represents another widely used functionalization possibility. In this way, an azobenzene unit can be connected with relatively long, rigid, and π-conjugated linkers in good to excellent yields.[20] The incorporated linkers then serve a specific function in the molecule: For example, the functionalization of ethynyl-1,6-methano[10]annulenes with azobenzene demonstrated the synthesis of electron-donor/acceptor systems that are suitable substrates for nonlinear optics or liquid crystals (Scheme 3, A).[20a] In different azobenzene systems for the synthesis of photochromic self-assembled monolayers, the rigid linker ensures sufficient control over the distance from the headgroup to the surface and features a cooperative switching behavior of the azobenzene units.[20b–d]

Hydrophobic fluorescent azobenzenes were transformed into water-soluble fluorescent 2-borylazobenzenes by incorporating ionic functional groups via Sonogashira coupling.[20e] Employing 4,4′-diiodoazobenzene as the starting material enabled a double cross-coupling; in this way, an azobenzene moiety containing two paramagnetic nitroxide spin labels was synthesized in which the ethynyl groups supported the formation of spin exchange coupling (Scheme 3, B left).[20f] Low-molecular organogelators were obtained by double cross-coupling of 3,3′-diiodoazobenzene with acetylene derivatives (Scheme 3, B right).[20g] The two urethane moieties were required for strong hydrogen bonding, whereas the two cholesterol units led to relatively weak van der Waals interactions.[20g] Moreover, an azobenzene bisporphyrin system[20d] as well as different *para*-alkynylazobenzene ligands and their corresponding organometallic cobalt complexes were obtained.[20h] As azotolanes usually show liquid crystallinity as well as highly birefringent features, this method was utilized for the synthesis of several azotolane monomers[20i,j] or polymers with azobenzene in the side chain[20k] or main chain[20l–n] (Scheme 3, C), respectively. Additionally, photoresponsive and fluorescent co-polymers (Scheme 3, D),[20o] polyamide-phenyleneethynylenes[20p] or a semiconducting colloidal porous organic polymer[20q] were obtained. The scope of electrophilic azobenzene cross-coupling partners was successfully broadened to bistriflates for the synthesis of rigid dendrimers in an acceptable yield.[20s,t]

2-Iodoazobenzene reacted with (trimethylsilyl)acetylene under Sonogashira conditions, but even after optimization of the reaction conditions the yield of 2-[(trimethylsilyl)ethynyl]azobenzene remained 50%.[21] Additionally, the product decomposed during workup because of the lability of the protecting group and the instability of the deprotected diazene. Coupling with more robust (triisopropylsilyl)- and (triethylsilyl)acetylene solved both problems and the product 2-[(trialkylsilyl)ethynyl]azobenzenes were obtained in 97% and 87% yield, respectively.[21]

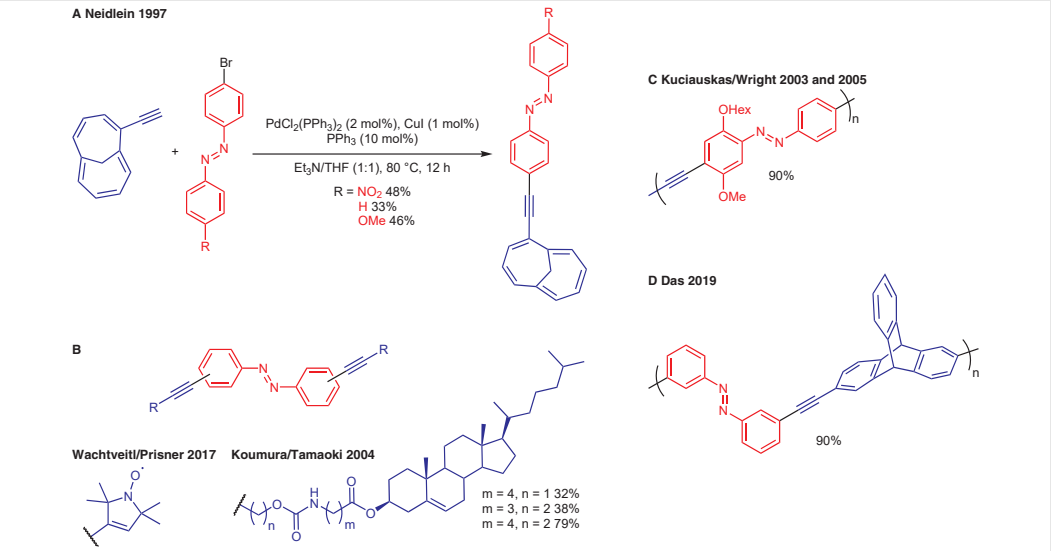

Scheme 3 Pd-catalyzed Sonogashira cross-coupling reactions of halogenated azobenzenes[20a,f,g,l,m,o]

2.1.3 Buchwald–Hartwig Cross-Coupling Reactions

This type of cross-coupling reaction is used to form C–N bonds. In 2020, the coupling of 3,5-dibromoazobenzene with *N*-Boc-*N*-(4-methoxyphenyl)hydrazide to give 3,5-bis[*N*′-Boc-*N*′-(4-methoxyphenyl)hydrazino]azobenzene in 58% yield was reported (Scheme 4).[22] The obtained product was then oxidized to yield a C_2-symmetric 3,5-bis(4-methoxyphenylazo)azobenzene. Unsymmetric tris(arylazo)-benzenes were accessible by sequential coupling.[22]

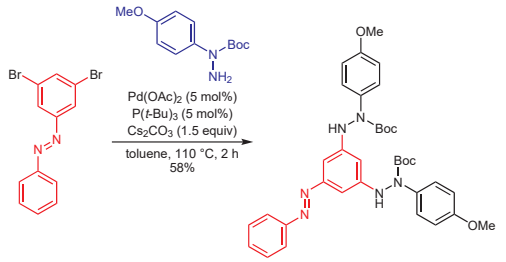

Scheme 4 Pd-catalyzed Buchwald–Hartwig cross-coupling reaction of 3,5-dibromoazobenzene[22]

2.1.4 Heck Reactions

The Heck reaction can be employed in order to preserve double bonds within the starting material for later functionalization. As with the Suzuki–Miyaura cross-coupling, we mainly discuss reports of larger functional polymers and assemblies. One interesting example is the functionalization of cage silsesquioxanes with azobenzene units via the Heck reaction (Scheme 5).[23] The synthesis of new azobenzene-doped hybrid porous polymers was thus possible.[24]

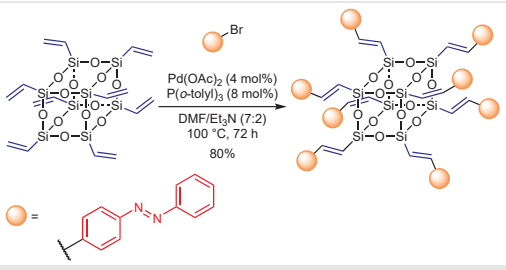

Scheme 5 Pd-catalyzed Heck reaction of 4-bromoazobenzene[23]

Poly(phenylenevinylene)-based conjugated polymers with azobenzene derivatives incorporated directly in the π-conjugative building units were prepared in quantitative yield and with a high molecular weight (M_n >10000) by coupling polymerization of divinylbenzenes with 4,4′-dihaloazobenzenes.[25] The Heck reaction of nipecotic acid (piperidine-3-carboxylic acid) derivatives with azobenzene triflates and iodides yielded vinyl ethers in good yields. However, the coupling was not possible for *ortho*-substituted azobenzenes. In this case, the Heck reaction needed to be performed with 1-iodo-2-nitrobenzene with the formation of the azobenzene by an azo coupling in a later step.[26]

2.1.5 Stille Reactions

In a Stille cross-coupling reaction, an organotin compound is reacted with a halide. Organostannanes are easy accessible and stable in air and moisture so that a broad range of functional groups can be used under mild conditions.[20l,25,27] In this way, 4,4′-dibromoazobenzene was coupled with tributylvinyltin to yield 4,4′-divinylazobenzene in 70% yield.[25] It was also possible to introduce heteroaromatic compounds into a polymer backbone via a Stille cross-coupling: The monomer 4,4′-diiodoazobenzene was reacted with four different bis(trimethylstannyl)-substituted heteroaromatic compounds to give poly(phenylene)based-polymers that were soluble in common organic solvents in moderate to excellent yields (Scheme 6).[27] Due to the extended main-chain conjugation, the thiophene-, furan-, and *N*-methylpyrrole-containing poly(phenylenes) showed strongly red-shifted absorptions in the visible region. Only the pyridine-containing poly(phenylene) had a low degree of main-chain conjugation, but contrary to other examples, it showed in solution reversible photoisomerization of azobenzene units with an accompanied change of the electrochemical properties. The (*Z*)-enhanced polymer was less susceptible to oxidation.[27]

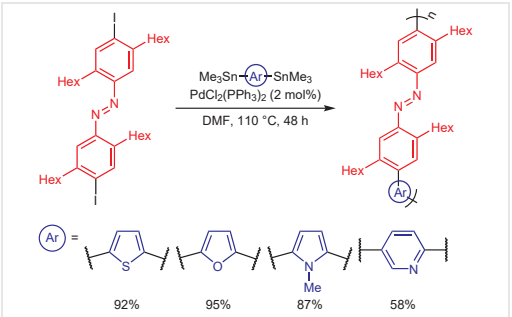

Scheme 6 Pd-catalyzed Stille cross-coupling reactions of diiodoazobenzenes[27]

2.2 Nickel Catalysis

Although palladium complexes are the most common catalysts in cross-coupling reactions, attempts have been made to replace palladium by less expensive metals such as nickel. For example, a nickel-catalyzed Heck reaction of aryl

triflates with vinyl ethers proceeded under mild reaction conditions, using a catalytic system consisting of bis(cyclooctadiene)nickel(0), 1,1′-bis(diphenylphosphino)ferrocene (DPPF), and tertiary amine Cy_2NMe, followed by hydrolysis to give the corresponding acetyl-substituted products with good functional group tolerance. It was also possible to incorporate a photoswitchable unit by the olefination of an azobenzene triflate followed by hydrolysis to give the corresponding acetyl derivative (Scheme 7).[28]

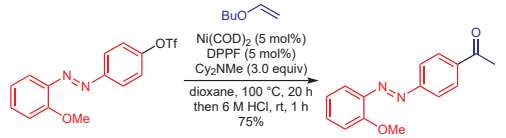

Scheme 7 Ni-catalyzed Heck reaction of an azobenzene triflate derivative[28]

2.3 Copper Catalysis

Copper catalysts are another alternative to palladium catalysts in cross-coupling reactions to obtain substrates otherwise not accessible.

2.3.1 Cadiot–Chodkiewicz Reactions

The copper-catalyzed Cadiot–Chodkiewicz reaction enables the formation of conjugated dienes. A synthetic route towards large-scale highly ordered porous structures from organometallic precursors via spontaneous self-assembly was established by using a two-step Cadiot–Chodkiewicz cross-coupling. Several neutral platinum–acetylide complexes with azobenzene groups in the center and long alkyl chains on both ends of the molecule were obtained in excellent to quantitative yields (Scheme 8).[29] In a similar fashion, poly(platinaynes) were synthesized with both *meta*- or *para*-substituted azobenzene spacers to compare their optoelectronic properties. In these complexes, the acetylide-functionalized azobenzene ligands could still undergo photoisomerization reversibly, although the switching process appeared to be more facile for *para*-substituted systems and with lower photoisomerization in solution in comparison to smaller systems.[30]

2.3.2 Ullmann Reactions

The Ullmann reaction is a powerful tool for C–N bond formation. The Ullmann coupling of 4,4′-dibromoazobenzene with 3,6-bis(9*H*-carbazol-9-yl)-9*H*-carbazole gave a bis(tercarbazole)azobenzene derivative in 46% yield that was used as a precursor for the fabrication of photoresponsive microporous films (Scheme 9).[31]

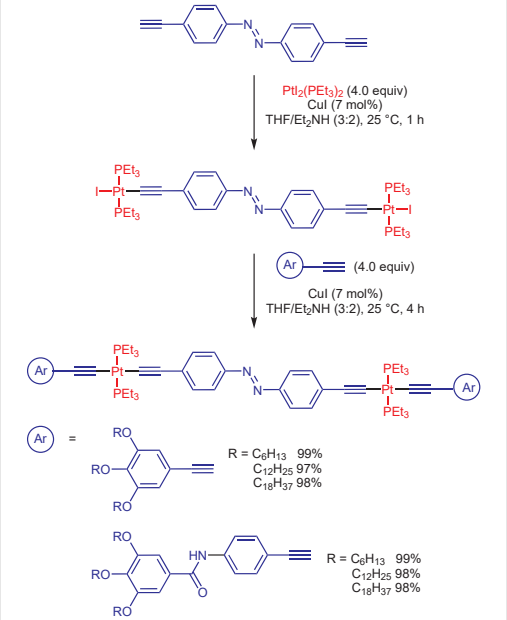

Scheme 8 Cu-catalyzed two-step Cadiot–Chodkiewicz cross-coupling reaction of alkynyl-functionalized azobenzenes[29]

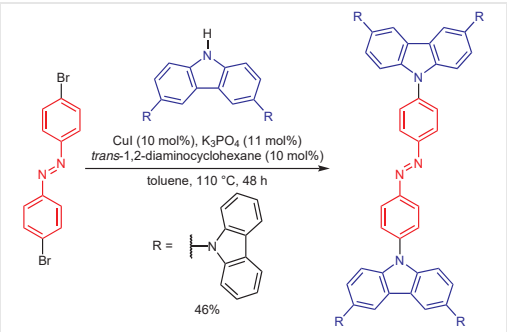

Scheme 9 Cu-catalyzed Ullmann coupling of dibrominated azobenzene[31]

2.4 Cobalt Catalysis

Another alternative to palladium catalysis is the use of cobalt as an inexpensive metal. For example, the C(sp^2)–P cross-coupling of vinyl, styryl, and aryl halides with diphenyl phosphine oxide and dialkyl phosphinate using a unique Co/Cu catalytic system gave the corresponding

phosphoryl-substituted products. This protocol showed robust functional group tolerance that enabled the coupling of 4,4′-diiodoazobenzene with diisopropyl phosphite to give 4,4′-bis(diisopropoxyphosphoryl)azobenzene in 76% yield (Scheme 10).[32]

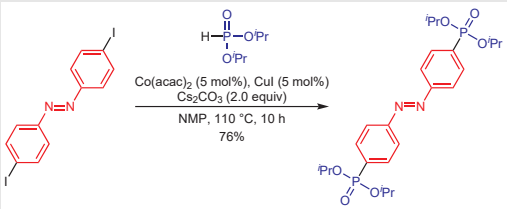

Scheme 10 Co/Cu-catalyzed C(sp^2)–P cross-coupling reaction of 4,4′-diiodoazobenzene[32]

3 Azobenzenes as Formally Nucleophilic Components

In cross-coupling reactions, the formal nucleophile is an (organo)metallic species. Organometallic, nucleophilic azobenzene derivatives can be obtained either by halogen–metal exchange of the (pseudo)halogenated azobenzene or by applying an appropriate cross-coupling reaction with a dimetallic reagent (Scheme 11, A) (see later for C–H activation).[7b,33] However, in the case of azobenzenes, halogen–metal exchange can lead to the reduction of the azo group as a dominating side reaction (Scheme 11, B).[34] From the perspective of the formally nucleophilic azobenzene, the main limitation is access to the azobenzene starting material. There has been very little research performed in this area in terms of systematic investigations and thus, it is difficult to distill common principles or indeed select the most seminal papers.

3.1 Palladium Catalysis

Palladium catalysts are also most commonly used in cross-coupling reactions involving azobenzene derivatives as the formally nucleophilic component. In terms of the obtained product structure, the same criteria apply for the selection of the specific cross-coupling reaction as are utilized for electrophilic azobenzene derivatives. However, a key consideration is the availability of the metalated azobenzene.

3.1.1 Suzuki–Miyaura Cross-Coupling Reactions

The first use of an azobenzene derivative as a nucleophile in a Suzuki–Miyaura cross-coupling reaction was reported in 2007;[36] the coupling of a boronic acid pinacol ester functionalized azobenzene with diverse iodoarenes gave arylate azobenzenes in 41–72% yields.[36] While the cross-coupling reactions themselves are relatively unremarkable, the importance is in the synthesis of the starting material by cross-coupling of a (pseudo)halogenated azobenzene with the boronic ester.[36,37] A second approach is the condensation of a nitrosobenzene and aniline boronic acid ester; the boronic acid ester is unaffected by the condensation reaction.[36] Due to the efficiency of this method, a number of synthetic targets[38] were assessed. Moreover, an azobenzene-4-boronic acid pinacol ester derivative was used as the nucleophile and 4-bromo-2,2,2′,2′-tetrafluoroazobenzene derivatives as the electrophile, which enabled the use of azobenzene as both cross-coupling components. The resulting product undergoes orthogonal switching, where the azobenzene units are switched separately to give 4 different isomers by green, blue, or ultraviolet light or electrocatalytic isomerization (Scheme 12).[37]

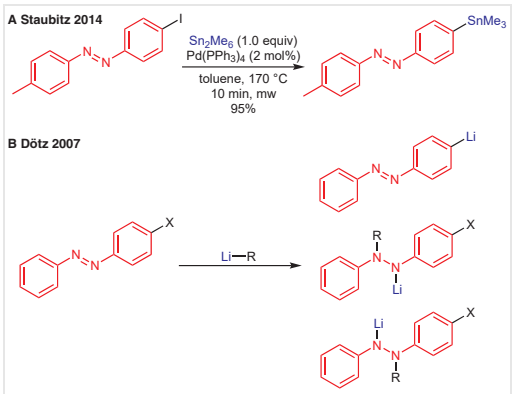

Scheme 11 (A) Stille–Kelly cross-coupling reaction of 4-iodo-4′-methylazobenzene with hexamethyldistannane;[33] (B) halogen–metal exchange of a halogenated azobenzene with the possible reduction of the diazenyl group[35]

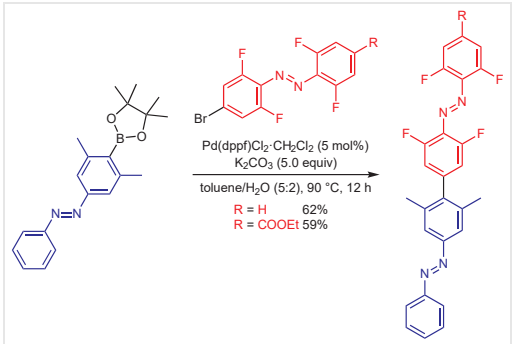

Scheme 12 Pd-catalyzed Suzuki–Miyaura cross-coupling reaction of an azobenzene-4-boronic acid pinacol ester and 4-bromo-2,2,2′,2′-tetrafluoroazobenzene derivatives[37]

3.1.2 Sonogashira Cross-Coupling Reactions

In 2014, the preparation of an azobenzene liquid crystal was reported by the Sonogashira cross-coupling reaction of an ethynyl-substituted azobenzene with 1-bromooctane.[39] This protocol was utilized in 2017 for the coupling of an azobenzene derivative with aryl bromides (Scheme 13, A).[15d] The Sonogashira cross-coupling reaction has also been used for the synthesis of artificial helical oligomers[40] or polymers[41] in which the photoisomerization of the azobenzene moieties triggers a geometric change. Novel azobenzene-containing hydroxyphenylglycine-derived poly(*m*-phenyleneethynylene)s were synthesized by polymerization through the Sonogashira couplings (thus formally a polycondensation) of 3,5-diethynylazobenzenes with various diiodinated amides (Scheme 13, B).[41a]

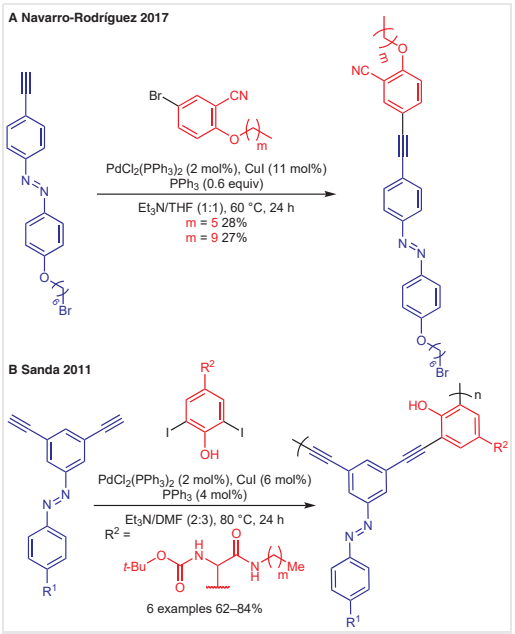

Scheme 13 Pd-catalyzed Sonogashira cross-coupling reactions of alkynyl-functionalized azobenzenes[15d,41a]

Furthermore, the Sonogashira reaction was used to prepare a hairy-rod like π-conjugated polymer with a fluorene unit in the backbone.[42] The late-stage functionalization of poly(aryl ethers) with azobenzene moieties was feasible, in which polymer bromo side groups react with 4-(dimethylamino)-3′-ethynylazobenzene.[43]

3.1.3 Buchwald–Hartwig Cross-Coupling Reactions

The Buchwald–Hartwig cross-coupling reaction can be used to form C–N bonds. The Buchwald–Hartwig amination of various polystyrene and poly(iminoarylene) derivatives was reported to give the corresponding products with aminoazobenzene groups in the side chain (Scheme 14).[44] The absence of characteristic stretching vibrations of the starting materials in the IR spectrum indicated a full loading of the obtained polymer.[44]

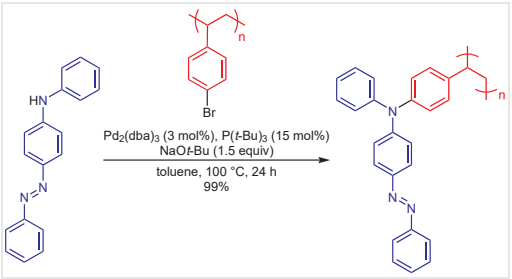

Scheme 14 Pd-catalyzed Buchwald–Hartwig amination of 4-(phenylamino)azobenzene[44]

This methodology was applied to the synthesis of amorphous materials such as branched triarylamine derivatives,[45] a spiro-linked bifluorene[46] as well as a perfluorocyclobutane (PFCB) aryl ether polymer[47] or a poly(arylimino) derivative.[48] It was even possible to prepare ferrocenophanes with azobenzene derivatives in the ligand and to use them as a redox-active and chromophore site showing potential as electron- or acid-responsive organic materials.[49]

3.1.4 Heck Reactions

The Heck reaction of dihaloazobenzenes with divinylarenes as well as the reverse case, the coupling of 4,4′-divinylazobenzene with dihaloarenes, to produce photoresponsive poly(phenylenevinylene)s was investigated. However, the obtained polymers were largely insoluble in common organic solvents, hence this route was discarded.[25]

3.1.5 Stille Reactions

An efficient microwave-assisted method to prepare stannylated azobenzenes was developed to circumvent the possible reduction of the diazenyl group during halogen–metal exchange. These organostannyl-substituted azobenzenes subsequently served as nucleophiles in high-yielding Stille cross-coupling reactions (Scheme 15).[33]

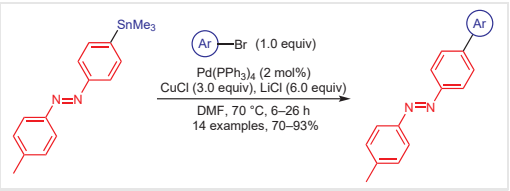

Scheme 15 Pd-catalyzed Stille cross-coupling reaction using stannylated azobenzene as nucleophile[33]

3.2 Copper Catalysis

A copper-catalyzed Ullmann cross-coupling reaction was the method of choice for the synthesis of bis[4-(phenyldiazenyl)phenyl]amine and tris[4-(phenyldiazenyl)phenyl]amine by varying the stoichiometric quantities of the electrophilic component (Scheme 16).[50]

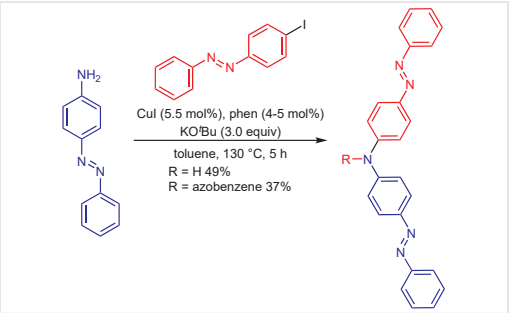

Scheme 16 Cu-catalyzed Ullmann cross-coupling reaction of 4-iodoazobenzene with amino-azobenzene[50]

The Ullmann cross-coupling reaction is also useful for generating phenol ethers through C–O bond formation. In this way, a series of azobenzene-functionalized poly(ether sulfone)s were prepared, using a catalyst system of CuI and 2,2,6,6-tetramethylheptane-3,5-dione (TMHD), that had high glass transition temperatures (T_g >199 °C) (Scheme 17).[51] Irradiation and writing/erasing experiments indicated a large photoinduced birefringence and good stability of the photoinduced orientation of the polymers. This makes them interesting for applications in reversible optical storage.[51]

This synthetic procedure was expanded to the synthesis of an azobenzene-containing poly(aryl ether) with carboxyl side groups capable of coordination to rare earth complexes.[43]

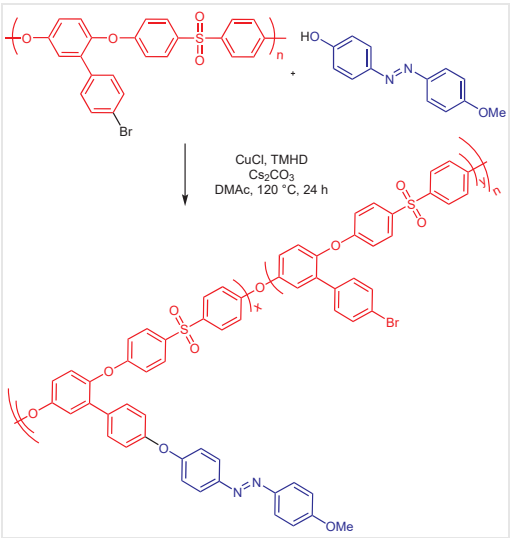

Scheme 17 Cu-catalyzed Ullmann cross-coupling reaction of poly(ether sulfone)s with bromine side groups and 4-[(4-methoxyphenyl)diazenyl]phenol with different functionalization degrees (x = 20, 45, 100)[51]

3.3 C–H Activation Reactions

C–H Activation reactions catalyzed by different transition metals have played an important role especially in the functionalization of azobenzene derivatives in the *ortho*-position.

3.3.1 Palladium-Catalyzed C–H Activation Reactions

The *ortho*-directing property of the azo group has been exploited in palladium-catalyzed C–H activation reactions.[14e,52] In many such reactions, the azobenzene is transformed by reaction with the diazenyl group. For example, azobenzenes were used for the synthesis of indazole backbones through palladium-catalyzed C–H functionalization and subsequent intramolecular cyclization.[52a] In a similar approach, 3*H*-indazol-3-ones were prepared from azobenzene derivatives using formic acid as carbon monoxide source (Scheme 18, A).[52g] *ortho*-C–H Amination of azoarenes with trimethylsilyl azide yielded 2-aryl-2*H*-benzotriazoles (Scheme 18, B).[52b] In this reaction, electron-donating substituents (alkyl, alkoxy) give higher product yields (58–87%) than electron-withdrawing groups, such as CF_3 (8%).

Late-stage functionalization of azobenzenes in the *ortho*-position was reported by the Trauner group (Scheme 19, A).[14e] These tetra-*ortho*-chlorinated azobenzenes are of

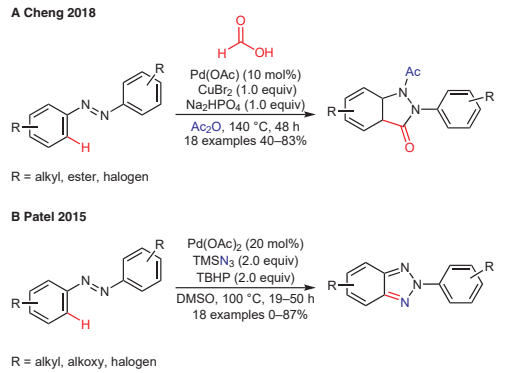

Scheme 18 Pd-catalyzed C–H activation reactions of azobenzene derivatives yielding heteroaromatic compounds[52b,g]

special interest because of their redshifted isomerization to *cis* at λ ≈ 560 nm. Azoarenes were functionalized with phenylhydrazine using a Pd(II) catalyst with atmospheric oxygen as the oxidant (Scheme 19, B).[52c] Wu, Wang, and coworkers reported the acylation of azobenzene derivatives with benzylic ethers (Scheme 19, C).[52d]

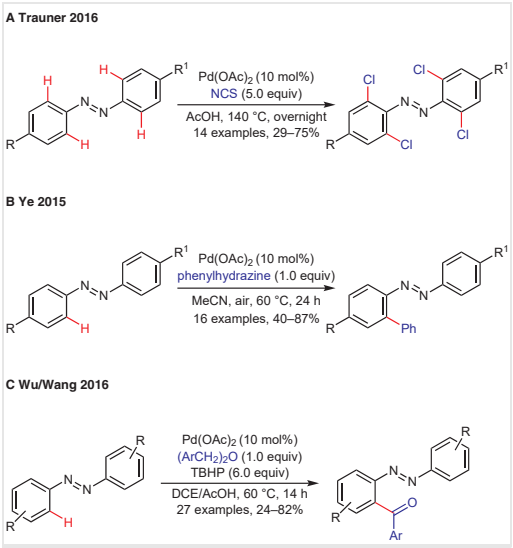

Scheme 19 Pd-catalyzed C–H activation reactions of azobenzene derivatives[14e,52c,d]

3.3.2 Rhodium-Catalyzed C–H Activation Reactions

Rhodium has been shown to be a potent *ortho* C–H activator of azobenzene derivatives. There are several reported examples of the formation of C–N bonds,[53] 2-aryl-2*H*-benzotriazoles,[54] and indazoles and indoles[55] similar in yields to the palladium-catalyzed reactions. A very useful reaction is the *ortho*-heteroarylation of azobenzenes by rhodium-catalyzed cross-dehydrogenative coupling (Scheme 20).[56] Such conjugated biaryls might be of special interest for luminous materials.

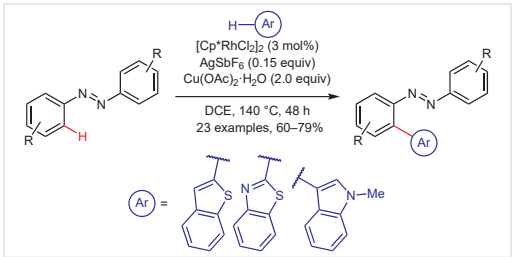

Scheme 20 Rh-catalyzed C–H activation reactions of azobenzene derivatives[56]

3.3.3 Ruthenium-Catalyzed C–H Activation Reactions

Ruthenium-catalyzed C–H activation reactions of azobenzene derivatives have been reported.[57] Of particular interest is the *meta*/*ortho*-selective C–H alkylation of azoarenes. Using a carboxylic acid promoted Ru(II)-catalyzed C_{Ar}–H alkylation reaction of 4,4′-substituted azobenzenes with secondary and tertiary alkyl bromides gave selectively the *meta*-product (Scheme 21),[58] while under the same reaction conditions, primary alkyl groups gave the *ortho*-product. To our knowledge this is the only reported reaction so far which allows C–H activation in the *meta* position. Coupling with alkyl chlorides was unsuccessful. Furthermore, bulky groups, such as *tert*-butyl (Y = *t*-Bu), on the azobenzene, prevented the reaction.[58]

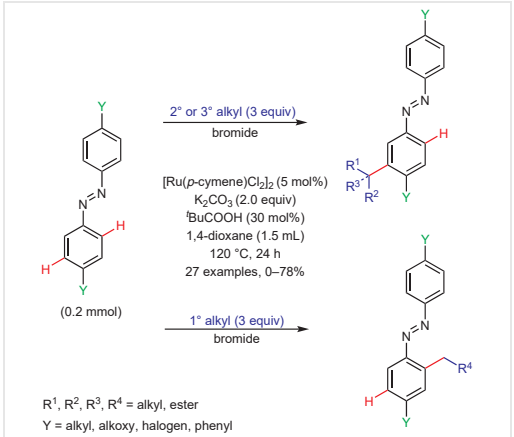

Scheme 21 Ru-catalyzed C–H activation reactions of azobenzenes[58]

3.3.4 Cobalt-Catalyzed C–H Activation Reactions

Cobalt-catalyzed C–H activation reactions are largely unknown on azobenzene derivatives and only a few examples exist.[59] A synthetic procedure for the azo-directed selective 1,4-addition of maleimides by Co(III)-catalyzed C–H activation was reported (Scheme 22).[59c] Worth noting is the use of low amounts of additives, as well as the fact that it does not require the use of a copper source.[59c]

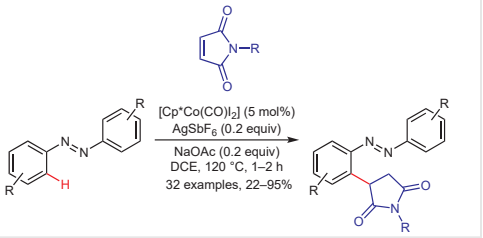

Scheme 22 Co-catalyzed C–H activation reactions of azobenzene derivatives[59c]

3.3.5 Iridium-Catalyzed C–H Activation Reactions

The Ir(III)-catalyzed [4+2] cyclization of azobenzenes with diazotized Meldrum's acid via a two-step reaction with an initial C–H alkylation, followed by intramolecular annulation gave 3-oxo-2,3-dihydrocinnoline-4-carboxylic acids or esters depending on the solvent used (Scheme 23).[60]

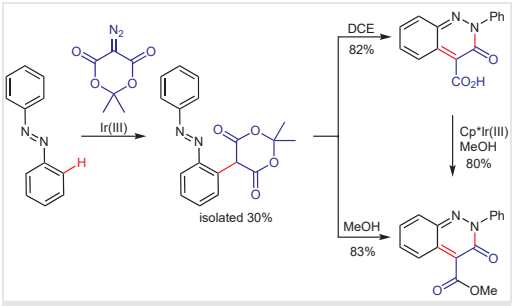

Scheme 23 Ir-catalyzed C–H activation reaction of azobenzene[60]

3.3.6 Copper-Catalyzed C–H Activation Reactions

Azobenzenes can be functionalized by a Cu(II)-catalyzed aerobic oxidative amidation with amides yielding the corresponding 2-(acylamino)azobenzenes in moderate to excellent yields (Scheme 24).[61]

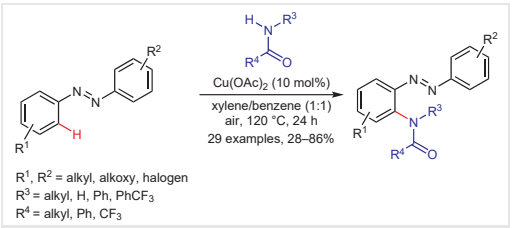

Scheme 24 Cu-catalyzed C–H activation reactions of azobenzene derivatives[61]

3.3.7 Iron-Catalyzed C–H Activation Reactions

To date only one example of an iron-catalyzed C–H activation reaction has been reported. An iron hydride complex bearing a 2,5-bis(di-*tert*-butylphosphinomethyl)pyrrolide ligand reacted with azobenzene. However, further functionalization was unsuccessful since the pentacoordinated aryl–iron complex was inert toward various reagents (Scheme 25).[62]

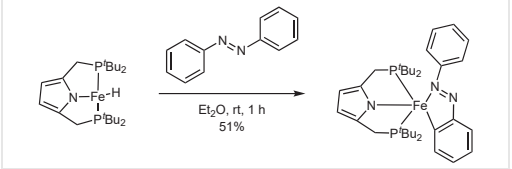

Scheme 25 Fe-catalyzed C–H activation of azobenzene[62]

4 Azobenzenes as Ligands in Catalysts

In addition to their use as a reactant in cross-coupling reactions, azobenzene derivatives can be also employed as ligands for catalysts in cross-coupling reactions.[63] Here, the N-donor capability of the diazenyl group (due to the lone electron pair on the nitrogen atoms) is used to form transition metal complexes. The incorporation of azo chromophores has enabled the synthesis of complexes with interesting physicochemical properties such as photoluminescence. Complexes with multidentate azoaromatic ligands are significantly stabilized because of the enhanced π-acceptor behavior compared to monocyclopalladated azobenzenes.[63e] Although the synthesis of azo-containing phosphine Pd(II) and Pt(II) complexes was reported in 1999, and the first results of their catalytic use were demonstrated in Heck reactions,[64] it took a further decade before this possibility was explored in more detail.[63]

In 2010, the synthesis of a polystyrene-anchored Pd(II) azo complex (Figure 2, A) and its application in the Suzuki–Miyaura as well as Sonogashira cross-coupling reactions was reported; various aryl halides were reacted with phen-

ylboronic acids or terminal alkynes in excellent yields (68–100% yield, 27 examples) under phosphine-free and aerobic reaction conditions in aqueous medium.[63b] A similar catalytic system showed comparable recyclability, but, in addition, it could even be employed in Heck reactions (89–96% yield, 5 examples).[63d]

A single core palladacyclic azobenzene catalyst with *CNCN* chelation was successfully synthesized (Figure 2, B) and used successfully in Suzuki–Miyaura and Heck reactions. However, it was only moderately active (27–70% yield, 4 examples) and required high temperatures that led to decomposition of the catalyst.[63c]

A symmetric bisazobenzene derivative was used as chelating ligand to obtain unsymmetric *CNN* pincer palladacycles (Figure 2, C) that showed high turnover numbers (TONs) even under the harsh conditions of the Heck reaction (60–93% yield, 9 examples, TONs up to 93000).[63e]

Phosphine-free Pd(II) complexes with 2,2′-bis(alkylamino)-azobenzene ligands were obtained in good yields by reaction of the ligands with sodium tetrachloropalladate. In this work, the benzyl derivative (Figure 2, D) showed high catalytic activity in Suzuki–Miyaura and Heck reactions under mild conditions in the presence of air and moisture (65–93% yield, 22 examples).[63f]

It should be noted that the photoswitchability of the azobenzenes in Figure 2 was not exploited.

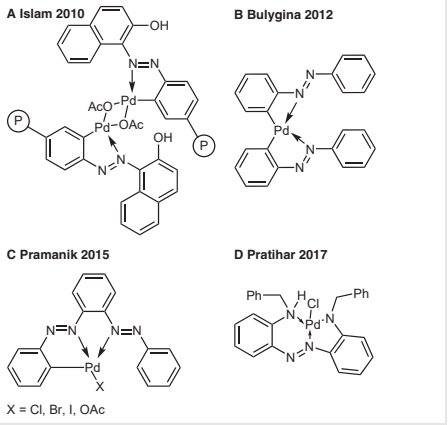

Figure 2 Evolution of palladium azo catalysts used in different cross-coupling reactions[63b,c,e,f]

5 Diazocines

(*Z*)-11,12-Dihydrodibenzo[*c*,*g*][1,2]diazocines (diazocines) are ethylene-bridged azobenzenes that can be switched from their thermodynamic stable (*Z*)- to the metastable (*E*)-isomer by using blue light at λ ≈ 370–400 nm and back from the (*E*)- to the (*Z*)-isomer by green light at λ ≈ 480–550 nm (Figure 3).[65]

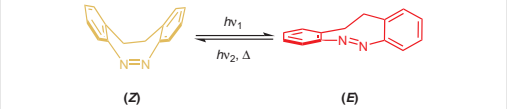

Figure 3 Structure and isomerization of diazocine

The switching properties of unsubstituted diazocines are different to unsubstituted azobenzenes. Diazocines show better resolution of absorption bands between the two isomeric states and switching is possible with light in the visible range.[65] However, the substituents have a great impact on the switching properties of both azobenzenes and diazocines. For example, tetra-*ortho*-chlorinated azobenzenes can be switched to (*Z*) at λ ≈ 560 nm, which exceeds the redshift of regular diazocines. Amino substituents on diazocines have also been shown to reduce the separation of the absorption bands yielding low amounts of (*E*)-isomers (25–30%).[66] The synthesis of diazocines is more demanding compared to azobenzenes, which is why only few applications have been reported to date.[65,67]

5.1 Synthesis

The key step in any diazocine synthesis is the cyclization to form the diazene moiety. This has been performed by reduction of 2,2′-dinitrobibenzyls,[65,67,68] or the oxidation of 2,2′-ethylenedianilines (Figure 4).[69]

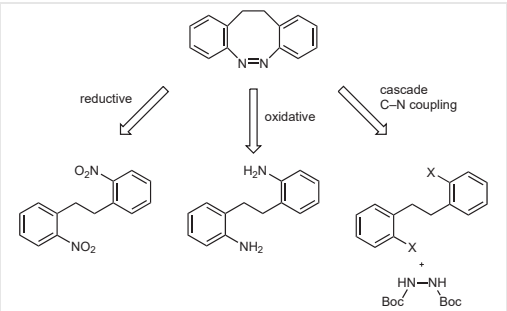

Figure 4 Retrosynthetic approach towards diazocines[65,67–70]

A novel route involving a cross-coupling reaction has been introduced by connecting the C–N bond instead of the N–N bond (Scheme 26).[70] The diazocine ring in this route is formed via consecutive cross-coupling reactions between a 2,2′-dihalobibenzyl and di-*tert*-butyl hydrazodicarboxylate.[70]

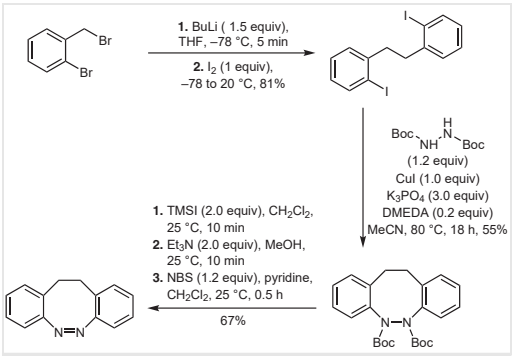

Scheme 26 Synthesis of diazocine through cross-coupling reaction[70]

5.2 Cross-Coupling Reactions

To date there are only a few reports of palladium-catalyzed cross-coupling reactions of diazocines. Therefore, a comparison with cross-coupling reactions of azobenzenes is, at present, of little informative value. Due to the different electronic and geometric structures of azobenzenes and diazocines, a different reactivity can be expected (as the lone pairs in diazocine are not aligned with the π-systems of the aromatic rings). At first glance the yields seem to be lower for cross-coupling reactions on diazocines, but this might be misleading since it is unknown if the reaction conditions were optimized. The Heck reaction of an 8-substituted 3-bromodiazocine with a glutamate derivative yielded diazocine ligands capable of light-controlling neural receptors (Scheme 27).[67c]

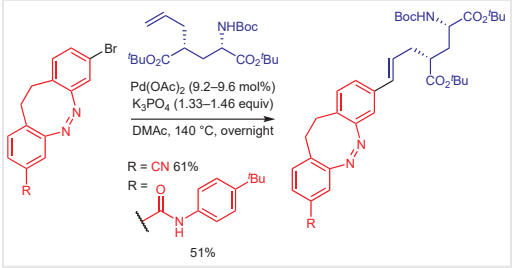

Scheme 27 Pd-catalyzed Heck coupling of diazocine derivatives[67c]

A Buchwald–Hartwig coupling on 3-bromodiazocines with *tert*-butyl carbamates was successfully performed (Scheme 28, A).[69b] Furthermore, the coupling of benzophenone imine with bromodiazocines was reported (Scheme 28, B).[71] The synthesis of a diazocine with turn-on fluorescence was achieved by the coupling of 3,8-dibromodiazocine with diphenylamine (Scheme 28, C).[72]

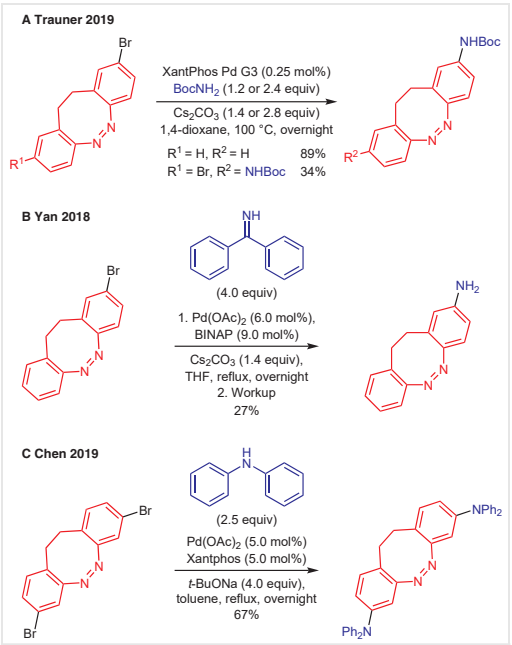

Scheme 28 Buchwald–Hartwig cross-coupling reactions of diazocine derivatives[69b,71,72]

Turn-on fluorescence diazocines were prepared by a Stille cross-coupling reaction (Scheme 29, A).[72] Furthermore, it was possible to obtain a pyroglutamate diazocine derivative via the Stille cross-coupling reaction (Scheme 29, B).[67e]

6 Conclusion

Cross-coupling reactions have proved to be a powerful tool for the late-stage modification of both electrophilic and nucleophilic azobenzene derivatives, with palladium catalysis being most prevalent. The Suzuki–Miyaura and Sonogashira cross-coupling reactions are the most widely used. First examples of cross-coupling reactions catalyzed by other transition metals than palladium, such as nickel or cobalt, have been published thus broadening the scope of cross-coupling reactions towards new bond formations that are not possible with palladium catalysts. At present, the number of examples of the use of azobenzenes as formally electrophilic reactants is much greater than that for their use as formally nucleophilic reactants. Most likely, this does not reflect intrinsic problems with nucleophilic azobenzenes, but rather that their accessibility is limited at present

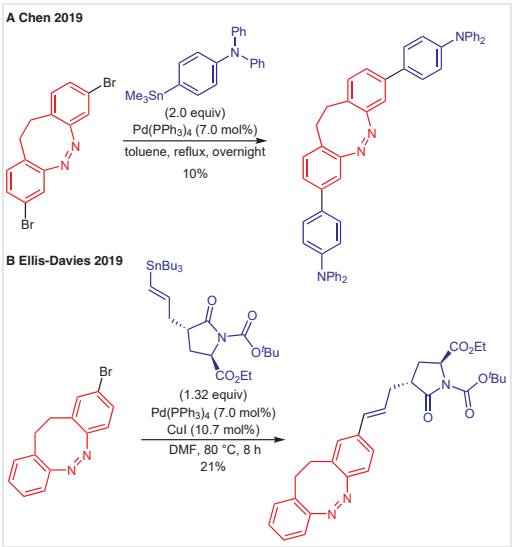

Scheme 29 Pd-catalyzed Stille cross-coupling reactions of diazocine derivatives[67e,72]

and requires more research. The reported yields do not significantly differ for cross-coupling reactions with azobenzene as formally the electrophilic or as nucleophilic component. However, due to the difficulties in the synthesis of nucleophilic azobenzene derivatives, cross-coupling reactions involving formally electrophilic azobenzene derivatives are favored. Normally, cross-coupling reactions with formally nucleophilic azobenzene derivatives are only used if the as nucleophilic coupling partner in the reaction of electrophilic azobenzene derivative cannot be synthesized. Most reported examples of cross-coupling reactions involving azobenzene derivatives employ the *para*-isomer; there are few examples of the use of the *meta*- or even the *ortho*-isomer. In fact, some groups specifically pointed out that cross-coupling reactions on *ortho*-azobenzene derivatives were unsuccessful. So cross-coupling reactions in the *ortho*-position of azobenzenes are almost, but not completely, unknown. The different reaction behavior of *ortho*-azobenzene derivatives in comparison to their corresponding *meta*- and *para*-isomers can be attributed to the nature of the diazenyl group; due to the adjacent lone electron pair on the nitrogen atoms, the diazenyl group can interact with substituents in the *ortho*-position. For example, *ortho*-halogenated precursors that are easily accessible can be directly lithiated because the *ortho*-lithiated species is significant stabilized by N→Li coordination. Although the diazenyl group has this directing and stabilizing effect also for transition metal insertions, only very few examples of metalated *ortho*-azobenzenes exist. C–H Activation is, therefore, a valuable alternative especially for the modification of *ortho*-azobenzenes. In almost all examples of C–H activation on azobenzenes, the *ortho*-position was functionalized. Here, the use of palladium complexes as catalysts was not as dominant as for the cross-coupling reactions. Another promising field is the use of complexed azobenzene derivatives acting as ligands or promotors for catalysts. New synthetic procedures for the preparation of diazocines means that they are accessible in good yields. Therefore, further functionalization possibilities through cross-coupling reactions can now be explored.

Funding Information

A.S. and S.S. thank the German Research Foundation (DFG) for the financial support within the priority program SPP 2100 'Soft Material Robotic Systems', Subproject STA1195/5-1, 'Insect feet inspired concepts soft touch grippers with dynamically adjustable grip strength'.

Acknowledgment

The authors would like to thank Dr. Anne Heitmann for proofreading.

References

(1) Merino, E.; Ribagorda, M. *Beilstein J. Org. Chem.* **2012**, *8*, 1071.
(2) Hartley, G. S. *Nature* **1937**, *140*, 281.
(3) (a) Brown, C. J. *Acta Crystallogr.* **1966**, *21*, 146. (b) Mostad, A.; Rømming, C. *Acta Chem. Scand.* **1971**, *25*, 3561.
(4) Hartley, G. S.; Le Fèvre, R. J. W. *J. Chem. Soc.* **1939**, 531.
(5) Åstrand, P.-O.; Ramanujam, P. S.; Hvilsted, S.; Bak, K. L.; Sauer, S. P. A. *J. Am. Chem. Soc.* **2000**, *122*, 3482.
(6) (a) Cheben, P.; del Monte, F.; Worsfold, D. J.; Carlsson, D. J.; Grover, C. P.; Mackenzie, J. D. *Nature* **2000**, *408*, 64. (b) Ikeda, T.; Sasaki, T.; Ichimura, K. *Nature* **1993**, *361*, 428.
(7) (a) Merino, E. *Chem. Soc. Rev.* **2011**, *40*, 3835. (b) Léonard, E.; Mangin, F.; Villette, C.; Billamboz, M.; Len, C. *Catal. Sci. Technol.* **2016**, *6*, 379.
(8) (a) Nystrom, R. F.; Brown, W. G. *J. Am. Chem. Soc.* **1948**, *70*, 3738. (b) Khan, A.; Hecht, S. *Chem. Commun.* **2006**, 4764.
(9) (a) Pausacker, K. H. *J. Chem. Soc.* **1953**, 1989. (b) Lu, W.; Xi, C. *Tetrahedron Lett.* **2008**, *49*, 4011. (c) Ma, H.; Li, W.; Wang, J.; Xiao, G.; Gong, Y.; Qi, C.; Feng, Y.; Li, X.; Bao, Z.; Cao, W.; Sun, Q.; Veaceslav, C.; Wang, F.; Lei, Z. *Tetrahedron* **2012**, *68*, 8358. (d) Zhang, C.; Jiao, N. *Angew. Chem. Int. Ed.* **2010**, *49*, 6174.
(10) (a) Ibne-Rasa, K. M.; Lauro, C. G.; Edwards, J. O. *J. Am. Chem. Soc.* **1963**, *85*, 1165. (b) Davey, M. H.; Lee, V. Y.; Miller, R. D.; Marks, T. J. *J. Org. Chem.* **1999**, *64*, 4976.
(11) (a) Cohen, T.; Lewarchik, R. J.; Tarino, J. Z. *J. Am. Chem. Soc.* **1974**, *96*, 7753. (b) Shine, H. J.; Zmuda, H.; Kwart, H.; Horgan, A. G.; Brechbiel, M. *J. Am. Chem. Soc.* **1982**, *104*, 5181.
(12) Matsui, M.; Iwata, Y.; Kato, T.; Shibata, K. *Dyes Pigm.* **1988**, *9*, 109.
(13) (a) Katritzky, A. R.; Wu, J.; Verin, S. V. *Synthesis* **1995**, 651. (b) Farhadi, S.; Sepahvand, S. *J. Mol. Catal. A: Chem.* **2010**, *318*, 75. (c) Alberti, A.; Bedogni, N.; Benaglia, M.; Leardini, R.; Nanni, D.; Pedulli, G. F.; Tundo, A.; Zanardi, G. *J. Org. Chem.* **1992**, *57*, 607.

(14) (a) Burns, J.; McCombie, H.; Scarborough, H. A. *J. Chem. Soc.* **1928**, 2928. (b) Robertson, P. W.; Hitchings, T. R.; Will, G. M. *J. Chem. Soc.* **1950**, 808. (c) Fahey, D. R. *J. Organomet. Chem.* **1971**, *27*, 283. (d) Fahey, D. R. *J. Chem. Soc. D* **1970**, 417. (e) Konrad, D. B.; Frank, J. A.; Trauner, D. *Chem. Eur. J.* **2016**, *22*, 4364. (f) Li, J.; Cong, W.; Gao, Z.; Zhang, J.; Yang, H.; Jiang, G. *Org. Biomol. Chem.* **2018**, *16*, 3479.
(15) (a) Han, M. R.; Hashizume, D.; Hara, M. *Acta Crystallogr., Sect. E* **2006**, *62*, o3001. (b) Bléger, D.; Ciesielski, A.; Samorì, P.; Hecht, S. *Chem. Eur. J.* **2010**, *16*, 14256. (c) De Jesús, M.; Larios-López, L.; Rodríguez-González, R. J.; Navarro-Rodríguez, D. *J. Mol. Liq.* **2016**, *222*, 1031. (d) Torres-Rocha, O. L.; Larios-López, L.; Rodríguez-González, R. J.; Felix-Serrano, I.; Navarro-Rodríguez, D. *J. Mol. Liq.* **2017**, *225*, 251. (e) Huang, W.; Lee, S.-K.; Sung, Y. M.; Peng, F.; Yin, B.; Ma, M.; Chen, B.; Liu, S.; Kirk, S. R.; Kim, D.; Song, J. *Chem. Eur. J.* **2015**, *21*, 15328. (f) Heitmann, G.; Dommaschk, M.; Löw, R.; Herges, R. *Org. Lett.* **2016**, *18*, 5228. (g) Yin, B.; Kim, T.; Zhou, M.; Huang, W.; Kim, D.; Song, J. *Org. Lett.* **2017**, *19*, 2654. (h) Nguyen, T.-T.-T.; Turp, D.; Wang, D.; Nolscher, B.; Laquai, F.; Mullen, K. *J. Am. Chem. Soc.* **2011**, *133*, 11194. (i) Izumi, A.; Teraguchi, M.; Nomura, R.; Masuda, T. *Macromolecules* **2000**, *33*, 5347. (j) Li, L.; He, F.; Wang, X.; Ma, N.; Li, L. *ACS Appl. Mater. Interfaces* **2012**, *4*, 4927. (k) Cheng, H. L.; Tang, M. T.; Tuchinda, W.; Enomoto, K.; Chiba, A.; Saito, Y.; Kamiya, T.; Sugimoto, M.; Saeki, A.; Sakurai, T.; Omichi, M.; Sakamaki, D.; Seki, S. *Adv. Mater. Interfaces* **2015**, *2*, 1400450. (l) Zhao, R.; Zhan, X.; Yao, L.; Chen, Q.; Xie, Z.; Ma, Y. *Macromol. Rapid Commun.* **2016**, *37*, 610. (m) Huang, C.-W.; Ji, W.-Y.; Kuo, S.-W. *Polym. Chem.* **2018**, *9*, 2813. (n) Wang, K.; Yin, L.; Miu, T.; Liu, M.; Zhao, Y.; Chen, Y.; Zhou, N.; Zhang, W.; Zhu, X. *Mater. Chem. Front.* **2018**, *2*, 1112. (o) Otaki, M.; Kumai, R.; Goto, H. *J. Polym. Sci., Part A: Polym. Chem.* **2019**, *57*, 1756. (p) Wang, Z.; Müller, K.; Valášek, M.; Grosjean, S.; Bräse, S.; Wöll, C.; Mayor, M.; Heinke, L. *J. Phys. Chem. C* **2018**, *122*, 19044. (q) Ma, X.; Qu, D.; Ji, F.; Wang, Q.; Zhu, L.; Xu, Y.; Tian, H. *Chem. Commun.* **2007**, 1409. (r) Ma, X.; Wang, Q.; Tian, H. *Tetrahedron Lett.* **2007**, *48*, 7112. (s) Reuter, R.; Wegner, H. A. *Beilstein J. Org. Chem.* **2012**, *8*, 877.
(16) Chen, Y.; Li, C.; Xu, X.; Liu, M.; He, Y.; Murtaza, I.; Zhang, D.; Yao, C.; Wang, Y.; Meng, H. *ACS Appl. Mater. Interfaces* **2017**, *9*, 7305.
(17) Han, M.; Norikane, Y.; Onda, K.; Matsuzawa, Y.; Yoshida, M.; Hara, M. *New J. Chem.* **2010**, *34*, 2892.
(18) Qu, D. H.; Wang, Q. C.; Ma, X.; Tian, H. *Chem. Eur. J.* **2005**, *11*, 5929.
(19) Köhl, I.; Lüning, U. *Synthesis* **2014**, *46*, 2376.
(20) (a) Bryant-Friedrich, A. C.; Neidlein, R. *Helv. Chim. Acta* **1997**, *80*, 1639. (b) Yu, B.-C.; Shirai, Y.; Tour, J. M. *Tetrahedron* **2006**, *62*, 10303. (c) Zarwell, S.; Rück-Braun, K. *Tetrahedron Lett.* **2008**, *49*, 4020. (d) Zeitouny, J.; Aurisicchio, C.; Bonifazi, D.; De Zorzi, R.; Geremia, S.; Bonini, M.; Palma, C. A.; Samorì, P.; Listorti, A.; Belbakra, A.; Armaroli, N. *J. Mater. Chem.* **2009**, *19*, 4715. (e) Itoi, H.; Kambe, T.; Kano, N.; Kawashima, T. *Inorg. Chim. Acta* **2012**, *381*, 117. (f) Jaumann, E. A.; Steinwand, S.; Klenik, S.; Plackmeyer, J.; Bats, J. W.; Wachtveitl, J.; Prisner, T. F. *Phys. Chem. Chem. Phys.* **2017**, *19*, 17263. (g) Koumura, N.; Kudo, M.; Tamaoki, N. *Langmuir* **2004**, *20*, 9897. (h) Moreno, C.; Arnanz, A.; Medina, R.-M.; Macazaga, M.-J.; Pascual, M.; García-Frutos, E. M.; Martínez-Gimeno, E.; Marcos, M.-L. *Organometallics* **2015**, *34*, 2971. (i) Zhao, Y.; Li, K.; Zhang, Y.; Zhao, Y.; Miao, Z. *Mol. Cryst. Liq. Cryst.* **2017**, *650*, 7. (j) Huo, X.; Xu, Q. P.; Miao, Z. *Appl. Mech. Mater.* **2014**, *584-586*, 1705. (k) Okano, K.; Tsutsumi, O.; Shishido, A.; Ikeda, T. *J. Am. Chem. Soc.* **2006**, *128*, 15368. (l) Kuciauskas, D.; Porsch, M. J.; Pakalnis, S.; Lott, K. M.; Wright, M. E. *J. Phys. Chem. B* **2003**, *107*, 1559. (m) Humphrey, J. L.; Lott, K. M.; Wright, M. E.; Kuciauskas, D. *J. Phys. Chem. B* **2005**, *109*, 21496. (n) Shen, D.; Pan, Z.; Xu, H.; Cheng, S.; Zhu, X.; Fan, L. *Chin. J. Chem.* **2010**, *28*, 1279. (o) Ansari, M.; Bera, R.; Mondal, S.; Das, N. *ACS Omega* **2019**, *4*, 9383. (p) Iba, S.; Ishida, T.; Sanda, F. *Polym. Bull.* **2020**, *77*, 1121. (q) Nath, I.; Chakraborty, J.; Khan, A.; Arshad, M. N.; Azum, N.; Rab, M. A.; Asiri, A. M.; Alamry, K. A.; Verpoort, F. *J. Catal.* **2019**, *377*, 183. (r) Mohamed Ahmed, M. S.; Mori, A. *Tetrahedron* **2004**, *60*, 9977. (s) Liao, L.-X.; Stellacci, F.; McGrath, D. V. *J. Am. Chem. Soc.* **2004**, *126*, 2181. (t) Casas-Solvas, J. M.; Vargas-Berenguel, A. *Tetrahedron Lett.* **2008**, *49*, 6778.
(21) Shirtcliff, L. D.; Weakley, T. J. R.; Haley, M. M.; Köhler, F.; Herges, R. *J. Org. Chem.* **2004**, *69*, 6979.
(22) Heindl, A. H.; Wegner, H. A. *Beilstein J. Org. Chem.* **2020**, *16*, 22.
(23) Liu, Y.; Yang, W.; Liu, H. *Chem. Eur. J.* **2015**, *21*, 4731.
(24) Jiang, C.; Yang, W.; Liu, H. *Russ. Chem. Bull.* **2016**, *65*, 1076.
(25) Izumi, A.; Teraguchi, M.; Nomura, R.; Masuda, T. *J. Polym. Sci., Part A: Polym. Chem.* **2000**, *38*, 1057.
(26) Quandt, G.; Höfner, G.; Pabel, J.; Dine, J.; Eder, M.; Wanner, K. T. *J. Med. Chem.* **2014**, *57*, 6809.
(27) Izumi, A.; Nomura, R.; Masuda, T. *Macromolecules* **2001**, *34*, 4342.
(28) Gøgsig, T. M.; Kleimark, J.; Nilsson Lill, S. O.; Korsager, S.; Lindhardt, A. T.; Norrby, P. O.; Skrydstrup, T. *J. Am. Chem. Soc.* **2012**, *134*, 443.
(29) Xu, X.-D.; Zhang, J.; Chen, L.-J.; Zhao, X.-L.; Wang, D.-X.; Yang, H.-B. *Chem. Eur. J.* **2012**, *18*, 1659.
(30) Al-Balushi, R. A.; Haque, A.; Jayapal, M.; Al-Suti, M. K.; Husband, J.; Khan, M. S.; Skelton, J. M.; Molloy, K. C.; Raithby, P. R. *Inorg. Chem.* **2016**, *55*, 10955.
(31) Zhao, R.; Han, J.; Huang, M.; Liu, F.; Wang, L.; Ma, Y. *Macromol. Rapid Commun.* **2017**, *38*, 1700274.
(32) Ghosh, T.; Maity, P.; Kundu, D.; Ranu, B. C. *New J. Chem.* **2016**, *40*, 9556.
(33) Strueben, J.; Gates, P. J.; Staubitz, A. *J. Org. Chem.* **2014**, *79*, 1719.
(34) Strueben, J.; Lipfert, M.; Springer, J.-O.; Gould, C. A.; Gates, P. J.; Sönnichsen, F. D.; Staubitz, A. *Chem. Eur. J.* **2015**, *21*, 11165.
(35) Garlichs-Zschoche, F. A.; Dötz, K. H. *Organometallics* **2007**, *26*, 4535.
(36) Harvey, J. H.; Butler, B. K.; Trauner, D. *Tetrahedron Lett.* **2007**, *48*, 1661.
(37) Zhao, F.; Grubert, L.; Hecht, S.; Bléger, D. *Chem. Commun.* **2017**, *53*, 3323.
(38) (a) Hansen, M. J.; Lerch, M. M.; Szymanski, W.; Feringa, B. L. *Angew. Chem. Int. Ed.* **2016**, *55*, 13514. (b) Hierrezuelo, J.; Rico, R.; Valpuesta, M.; Díaz, A.; López-Romero, J. M.; Rutkis, M.; Kreigberga, J.; Kampars, V.; Algarra, M. *Tetrahedron* **2013**, *69*, 3465.
(39) Miao, Z.; Li, Y.; Zhang, X. *Appl. Mech. Mater.* **2014**, *584-586*, 1673.
(40) (a) Yu, Z.; Hecht, S. *Angew. Chem. Int. Ed.* **2011**, *50*, 1640. (b) Yu, Z.; Hecht, S. *Chem. Eur. J.* **2012**, *18*, 10519.
(41) (a) Sogawa, H.; Shiotsuki, M.; Matsuoka, H.; Sanda, F. *Macromolecules* **2011**, *44*, 3338. (b) Sogawa, H.; Shiotsuki, M.; Sanda, F. *Macromolecules* **2013**, *46*, 4378. (c) Okano, K.; Shishido, A.; Ikeda, T. *Adv. Mater.* **2006**, *18*, 523.
(42) Gerstel, P.; Klumpp, S.; Hennrich, F.; Poschlad, A.; Meded, V.; Blasco, E.; Wenzel, W.; Kappes, M. M.; Barner-Kowollik, C. *ACS Macro Lett.* **2014**, *3*, 10.
(43) Zhang, Y.; Chen, S. *RSC Adv.* **2018**, *8*, 37348.
(44) Kanbara, T.; Oshima, M.; Imayasu, T.; Hasegawa, K. *Macromolecules* **1998**, *31*, 8725.

(45) Honma, A.; Kanbara, T.; Hasegawa, K. *Mol. Cryst. Liq. Cryst.* **2000**, *345*, 125.
(46) Chun, C.; Kim, M.-J.; Vak, D.; Kim, D. Y. *J. Mater. Chem.* **2003**, *13*, 2904.
(47) Chun, C.; Ghim, J.; Kim, M.-J.; Kim, D. Y. *J. Polym. Sci., Part A: Polym. Chem.* **2005**, *43*, 3525.
(48) Chen, X.; Chang, G. *Chin. J. Chem.* **2009**, *27*, 2093.
(49) Sakano, T.; Horie, M.; Osakada, K.; Nakao, H. *Eur. J. Inorg. Chem.* **2005**, 644.
(50) Bahrenburg, J.; Sievers, C. M.; Schönborn, J. B.; Hartke, B.; Renth, F.; Temps, F.; Näther, C.; Sönnichsen, F. D. *Photochem. Photobiol. Sci.* **2013**, *12*, 511.
(51) Zhang, Y.; Zhang, Q.; Pei, S.; Wang, Y.; Zhang, H.; Jiang, Z. *High Perform. Polym.* **2014**, *26*, 946.
(52) (a) Li, H.; Li, P.; Wang, L. *Org. Lett.* **2013**, *15*, 620. (b) Khatun, N.; Modi, A.; Ali, W.; Patel, B. K. *J. Org. Chem.* **2015**, *80*, 9662. (c) Li, M.; Ye, Y. *ChemCatChem* **2015**, *7*, 4137. (d) Hong, G.; Aruma, A. N.; Zhu, X.; Wu, S.; Wang, L. *Synthesis* **2016**, *48*, 1147. (e) Yong, W. S.; Park, S.; Yun, H.; Lee, P. H. *Adv. Synth. Catal.* **2016**, *358*, 1958. (f) Fu, X.; Wei, Z.; Xia, C.; Shen, C.; Xu, J.; Yang, Y.; Wang, K.; Zhang, P. *Catal. Lett.* **2017**, *147*, 400. (g) Gu, N.; Sun, S.; Cheng, J. *Tetrahedron Lett.* **2018**, *59*, 1069.
(53) (a) Wang, H.; Yu, Y.; Hong, X.; Tan, Q.; Xu, B. *J. Org. Chem.* **2014**, *79*, 3279. (b) Fu, T.; Yang, J.; Sun, H.; Zhang, C.; Xiang, H.; Zhou, X. *Asian J. Org. Chem.* **2018**, *7*, 1844.
(54) Li, J.; Zhou, H.; Zhang, J.; Yang, H.; Jiang, G. *Chem. Commun.* **2016**, *52*, 9589.
(55) (a) Cai, S.; Lin, S.; Yi, X.; Xi, C. *J. Org. Chem.* **2017**, *82*, 512. (b) Oh, Y.; Han, S. H.; Mishra, N. K.; De, U.; Lee, J.; Kim, H. S.; Jung, Y. H.; Kim, I. S. *Eur. J. Org. Chem.* **2017**, 6265. (c) Zhu, J.; Sun, S.; Cheng, J. *Tetrahedron Lett.* **2018**, *59*, 2284.
(56) Deng, H.; Li, H.; Wang, L. *Org. Lett.* **2016**, *18*, 3110.
(57) Bruce, M. I.; Iqbal, M. Z.; Stone, F. G. A. *Chem. Commun.* **1970**, 1325.
(58) Li, G.; Ma, X.; Jia, C.; Han, Q.; Wang, Y.; Wang, J.; Yu, L.; Yang, S. *Chem. Commun.* **2017**, *53*, 1261.
(59) (a) Borah, G.; Borah, P.; Patel, P. *Org. Biomol. Chem.* **2017**, *15*, 3854. (b) Hande, A. E.; Muniraj, N.; Prabhu, K. R. *ChemistrySelect* **2017**, *2*, 5965. (c) Muniraj, N.; Prabhu, K. R. *J. Org. Chem.* **2017**, *82*, 6913.
(60) Borah, G.; Patel, P. *Org. Biomol. Chem.* **2019**, *17*, 2554.
(61) Li, G.; Chen, X.; Lv, X.; Jia, C.; Gao, P.; Wang, Y.; Yang, S. *Sci. China: Chem.* **2018**, *61*, 660.
(62) Kato, T.; Kuriyama, S.; Nakajima, K.; Nishibayashi, Y. *Chem. Asian J.* **2019**, *14*, 2097.
(63) (a) Lee, K.-E.; Jeon, H.-T.; Han, S.-Y.; Ham, J.; Kim, Y.-J.; Lee, S. W. *Dalton Trans.* **2009**, 6578. (b) Islam, S. M.; Mondal, P.; Roy, A. S.; Mondal, S.; Hossain, D. *Tetrahedron Lett.* **2010**, *51*, 2067. (c) Bulygina, L. A.; Khrushcheva, N. S.; Peregudova, S. M.; Sokolov, V. I. *Russ. Chem. Bull.* **2012**, *61*, 1998. (d) Priyadarshani, N.; Suriboot, J.; Bergbreiter, D. E. *Green Chem.* **2013**, *15*, 1361. (e) Roy, S.; Pramanik, S.; Ghorui, T.; Pramanik, K. *RSC Adv.* **2015**, *5*, 22544. (f) Pratihar, J. L.; Mandal, P.; Lin, C.-H.; Lai, C. K.; Mal, D. *Polyhedron* **2017**, *135*, 224.
(64) Alder, M. J.; Cross, W. I.; Flower, K. R.; Pritchard, R. G. *J. Organomet. Chem.* **1999**, *590*, 123.
(65) Siewertsen, R.; Neumann, H.; Buchheim-Stehn, B.; Herges, R.; Näther, C.; Renth, F.; Temps, F. *J. Am. Chem. Soc.* **2009**, *131*, 15594.
(66) Moormann, W.; Langbehn, D.; Herges, R. *Beilstein J. Org. Chem.* **2019**, *15*, 727.
(67) (a) Joshi, D. K.; Mitchell, M. J.; Bruce, D.; Lough, A. J.; Yan, H. *Tetrahedron* **2012**, *68*, 8670. (b) Eljabu, F.; Dhruval, J.; Yan, H. *Bioorg. Med. Chem. Lett.* **2015**, *25*, 5594. (c) Cabré, G.; Garrido-Charles, A.; González-Lafont, À.; Moormann, W.; Langbehn, D.; Egea, D.; Lluch, J. M.; Herges, R.; Alibés, R.; Busqué, F.; Gorostiza, P.; Hernando, J. *Org. Lett.* **2019**, *21*, 3780. (d) Trads, J. B.; Hüll, K.; Matsuura, B. S.; Laprell, L.; Fehrentz, T.; Görldt, N.; Kozek, K. A.; Weaver, C. D.; Klöcker, N.; Barber, D. M.; Trauner, D. *Angew. Chem. Int. Ed.* **2019**, *58*, 15421. (e) Thapaliya, E. R.; Zhao, J.; Ellis-Davies, G. C. R. *ACS Chem. Neurosci.* **2019**, *10*, 2481.
(68) (a) Tellkamp, T.; Shen, J.; Okamoto, Y.; Herges, R. *Eur. J. Org. Chem.* **2014**, 5456. (b) Moormann, W.; Langbehn, D.; Herges, R. *Synthesis* **2017**, *49*, 3471. (c) Samanta, S.; Qin, C.; Lough, A. J.; Woolley, G. A. *Angew. Chem. Int. Ed.* **2012**, *51*, 6452. (d) Li, S.; Han, G.; Zhang, W. *Macromolecules* **2018**, *51*, 4290. (e) Deo, C.; Bogliotti, N.; Métivier, R.; Retailleau, P.; Xie, J. *Chem. Eur. J.* **2016**, *22*, 9092.
(69) (a) Wang, J.; He, J.; Zhi, C.; Luo, B.; Li, X.; Pan, Y.; Cao, X.; Gu, H. *RSC Adv.* **2014**, *4*, 16607. (b) Maier, M. S.; Hüll, K.; Reynders, M.; Matsuura, B. S.; Leippe, P.; Ko, T.; Schäffer, L.; Trauner, D. *J. Am. Chem. Soc.* **2019**, *141*, 17295.
(70) Li, S.; Eleya, N.; Staubitz, A. *Org. Lett.* **2020**, *22*, 1624.
(71) Jun, M.; Joshi, D. K.; Yalagala, R. S.; Vanloon, J.; Simionescu, R.; Lough, A. J.; Gordon, H. L.; Yan, H. *ChemistrySelect* **2018**, *3*, 2697.
(72) Zhu, Q.; Wang, S.; Chen, P. *Org. Lett.* **2019**, *21*, 4025.

2 Objectives

The work presented in this thesis focuses on the late-stage functionalization of azobenzene based switches aiming to overcome synthetic limitations caused by the use of prefunctionalized starting materials. Therefore, efficient methodologies for the synthesis of key intermediates starting from iodinated precursors were to be developed and subsequently their usefulness in organic syntheses was to be proven. To obtain those central building blocks, three general approaches were to be pursued: two different types of transition metal catalyzed cross-coupling reactions and the oxidation to a hypervalent species.

Cross-Coupling Protocol for Photoswitchable NHS Esters. In the first subproject (Section 3.1), a robust Pd catalyzed synthetic procedure for the formation of photoswitchable active esters, more precisely NHS functionalized azobenzene **1k** and diazocine derivatives **9e**, was to be developed. The potential of these active ester was to be tested in condensation reactions with primary amines, which are often highly relevant in a biological context (Scheme 2.1). Emphasis also was to be placed on the synthesis of previously unaddressed or even inaccessible derivatives.

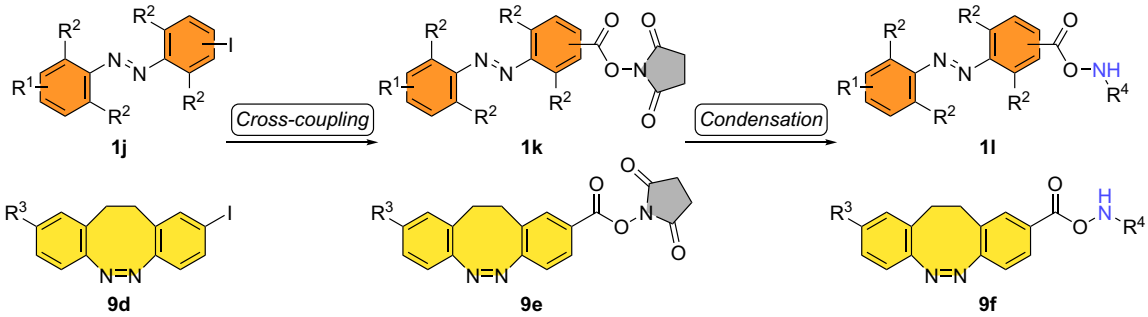

Scheme 2.1 Synthetic strategy towards NHS ester functionalized azobenzenes **1k** and diazocines **9e** for subsequent condensation reactions with primary amines.

Hypervalent Iodine(III) Azobenzene Derivatives. Moreover, a new synthetic pathway for the generation of *ortho*-functionalized azobenzenes **1n** was to be examined (Section 3.2). Therefore, hypervalent iodine(III) chemistry was to be employed in conjunction with *ortho*-azobenzenes **1m** leading to the formation of a new compound class that could be used in transition metal-free arylation reactions with different types of nucleophiles (Scheme 2.2).

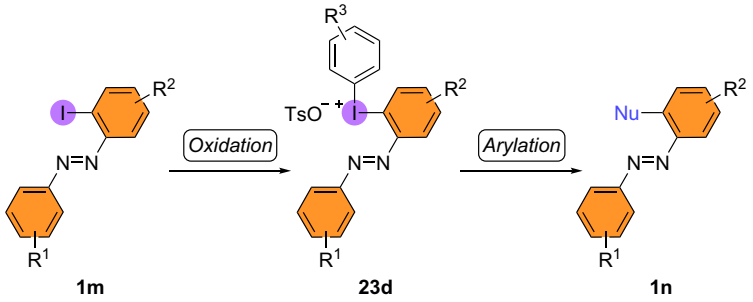

Scheme 2.2 Synthetic strategy towards *ortho*-azobenzene(aryl)iodonium salts for subsequent transition metal-free arylations with nucleophiles.

Cross-Coupling Reactions of Metalated Diazocines. Finally, cross-coupling reactions of diazocines **9** were to be investigated (Section 3.3). Hereby, the iodinated diazocines **9d** should be first converted into the formally nucleophilic cross-coupling partner **9e** and **9f** and then reacted with organic bromides in Stille and Suzuki cross-coupling reactions to obtain a wide range of functionalized diazocine derivatives **9g** (Scheme 2.3).

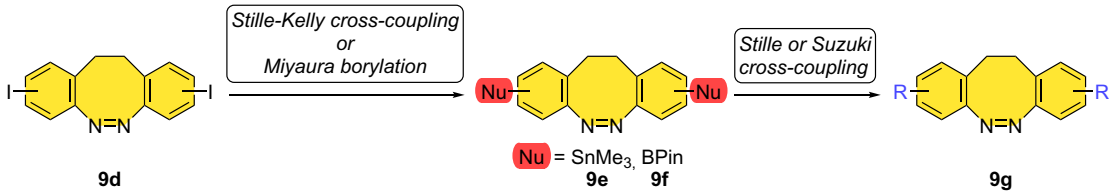

Scheme 2.3 Synthetic strategy towards stannylated **9e** and borylated diazocines **9f** for subsequent Stille and Suzuki cross-coupling reactions.

3 Results and Discussion

3.1 Active Ester Functionalized Azobenzenes as Versatile Building Blocks

Aim:

NHS esters belong to the group of active esters which are highly susceptible to nucleophilic attacks. In contrast to other active esters, they can be isolated and stored. As they react selectively under mild conditions with primary amines, which are ubiquitous, NHS esters have found usage in many applications, from biology to material science. Combining NHS ester with photoswitches enables photoresponsiveness to the materials. Thus, a synthetic methodology was established to obtain a broad range of NHS active ester functionalized azobenzene based photoswitches starting from iodinated precursors. Subsequently, their utilization in condensation reactions with primary amines was investigated in order to show the further application potential. Especially, derivatives that can be switched using visible light were of high interest.

Title of Publication:

"Active Ester Functionalized Azobenzenes as Versatile Building Blocks"
S. Schultzke,[‡] M. Walther,[‡] A. Staubitz, *Molecules* **2021**, *26*, 3916.
DOI: 10.3390/molecules26133916.
[‡] These authors contributed equally.

 The manuscript and the supporting information including detailed experimental procedures, characterization data and copies of NMR spectra are available free of charge on the journal's website.

Abstract:

Azobenzenes are important molecular switches that can still be difficult to functionalize selectively. A high yielding Pd-catalyzed cross-coupling method under mild conditions for the introduction of NHS esters to azobenzenes and diazocines has been established. Yields were consistently high with very few exceptions. The NHS functionalized azobenzenes react with primary amines quantitatively. These amines are ubiquitous in biological systems and in material science.

Author Contribution to this Publication:

In this project, S. Schultzke and I (M. Walther) contributed equally. Together we specified the project and its scope. The iodinated precursor and NHS ester were prepared and characterized by S. Schultzke (23 compounds) and me (18 compounds). I performed the screening of the catalytic system for the Pd catalyzed carbonylation. Additionally, I was responsible for the two application examples of the NHS ester. Here, I prepared and characterized the two amino acid derivatives. The Supporting Information was written by S. Schultzke and me for our respective experimental contributions. The manuscript was conceptualized and written by S. Schultzke and me in close cooperation with A. Staubitz, the principal investigator of this project.

molecules

MDPI

Article

Active Ester Functionalized Azobenzenes as Versatile Building Blocks

Sven Schultzke [1,2,†], Melanie Walther [1,2,†] and Anne Staubitz [1,2,*]

[1] Institute for Analytical and Organic Chemistry, University of Bremen, Leobener Straße 7, D-28359 Bremen, Germany; schultzke@uni-bremen.de (S.S.); melanie.walther@uni-bremen.de (M.W.)
[2] MAPEX Center for Materials and Processes, University of Bremen, Bibliothekstraße 1, D-28359 Bremen, Germany
* Correspondence: staubitz@uni-bremen.de; Tel.: +49-421-218-63210
† These authors contributed equally to this work.

Abstract: Azobenzenes are important molecular switches that can still be difficult to functionalize selectively. A high yielding Pd-catalyzed cross-coupling method under mild conditions for the introduction of NHS esters to azobenzenes and diazocines has been established. Yields were consistently high with very few exceptions. The NHS functionalized azobenzenes react with primary amines quantitatively. These amines are ubiquitous in biological systems and in material science.

Keywords: azobenzene; diazocine; molecular switches; palladium-catalyzed carbonylation; photoswitchable NHS ester; *N*-hydroxysuccinimide; chemical biology

Citation: Schultzke, S.; Walther, M.; Staubitz, A. Active Ester Functionalized Azobenzenes as Versatile Building Blocks. *Molecules* **2021**, *26*, 3916. https://doi.org/10.3390/molecules26133916

Academic Editors: Estelle Léonard and Muriel Billamboz

Received: 31 May 2021
Accepted: 23 June 2021
Published: 26 June 2021

1. Introduction

Photoswitchable molecules add photoresponsiveness to diverse materials such as polymers [1–6], dendrimers [7,8] or biomolecules [9–23]. By precise adjustment of the synthetic strategy the switch can be incorporated into the target material and its switching properties can be utilized. However, in many cases, it is exactly this tailored functionalization of the photoswitch that is the major challenge and the bottleneck in a successful project.

Due to its fast and efficient photoswitching characteristics, as well as its high fatigue-resistance [24], azobenzene is widely used in versatile applications such as molecular machines [3,25–28], data storage materials [29–32], or photopharmacology [9–23]. Upon irradiation with UV-light, typical azobenzenes undergo isomerization from the thermodynamically favored (*E*)-isomer to the less stable (*Z*)-isomer (Figure 1, left). The re-isomerization can occur either by irradiation with light or by thermal relaxation [24,33]. The half-lives of the latter strongly depend on the azobenzenes' substitution pattern and are therefore tunable for the specific application [34]. The isomerization is accompanied by a change of several physicochemical characteristics: the geometry [35,36], the end-to end-distance [35,36], and the electronic properties [37] (e.g., absorption and dipole moment). The thermodynamically favored (*E*)-form is planar [35] and without a dipole moment [37]. The (*Z*)-isomer on the other hand has a bent geometry where the phenyl rings are twisted ~55° out of plane to the azo group [36]. Moreover, the (*Z*)-isomer shows a dipole moment of 3.0 Debye [37]. The end-to-end distance of the (*E*)- and (*Z*)-isomer differs by ~3.5 Å [35,36]. In biological systems, azobenzenes bind typically in an elongated confirmation; its biological activity is controllable via the switching process [9]. The isomerization to the (*Z*)-isomer occurs by irradiation with UV-light, which might harm cells and tissues [38–40]. Therefore, a red-shifting of the absorption wavelength is desirable and in biological applications may be even necessary [9]. In addition, a separation of the absorption spectra of both isomers is important to avoid mixtures of isomers. Starting from 2009, *ortho*-substituted azobenzenes [41–50] and ethylene-bridged azobenzenes, the so-called diazocines [51,52], have been discovered to be promising candidates to overcome the two limitations of a typical

Molecules **2021**, *26*, 3916

azobenzene. Depending on the substituents in *ortho*-position, not only the absorption is shifted towards longer wavelength but also the thermal half-life may be drastically extended due to steric and electronic interactions [48]. Diazocines are also a particularly important class of azobenzenes, because the bent (*Z*)-isomer is thermodynamically favored due to the ring strain of the eight-membered ring (Figure 1, right). The isomerization of diazocines is in both directions possible using visible light; the isomerization to the elongated (*E*)-form occurs upon irradiation with light in the range of 400 nm, the re-isomerization to (*Z*) with 530 nm [51].

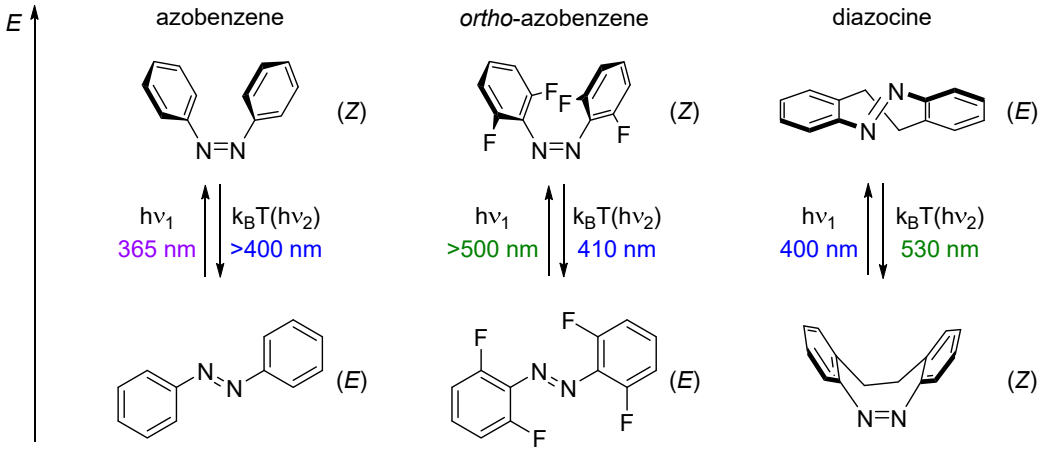

Figure 1. Isomerization of azobenzene [24], tetra-ortho-fluorinated azobenzene [48] and diazocine [51].

To incorporate such azobenzenes into a larger system, a suitable functional group is necessary that reacts selectively with the specific target position of the material. *N*-Hydroxysuccinimide (NHS) esters react selectively under mild conditions with primary amines, which can be found for example in commercially available polymers but of course also in all proteins and peptides as well as in nucleic acids. Due to the ubiquity of primary amines, NHS esters are versatile building blocks for instance in peptide synthesis [53–55], bioconjugate chemistry [56–60] as well as functionalized materials and polymers [61–71]. The use of NHS esters for the formation of amides has several advantages: NHS esters are comparatively easy to prepare. They are the only active esters that can be isolated [72]. In comparison to the coupling reaction of a primary amine with a carboxylic acid using a carbodiimide coupling agent such as *N*,*N*′-dicyclohexylcarbodiimide (DCC), NHS esters are less toxic. They can be used under physiologic or slightly basic conditions [72]. Moreover, the products of their transformations are easier to purify as water-soluble NHS is released during the amide formation [53].

Traditionally, NHS esters are synthesized by a coupling reaction of the carboxylic acid with NHS in the presence of a carbodiimide coupling agent [73,74], which is known to have an allergenic potential and to form urea as byproduct. Thus, the product purification might be challenging [72]. The carboxylic acid can also be activated by using anhydrides and their analogues for example *N*,*N*′-disuccinimidyl carbonate (DSC) [75]. More recently, coupling reactions of alcohols [76] and aldehydes [77] with NHS under oxidizing conditions have been investigated. Carbonylative cross-coupling reactions represents another synthetic strategy towards NHS esters [78,79]. Until recently, a carbon monoxide atmosphere was needed for this type of reaction prohibiting a safe and easy-to-handle implementation of the reaction. By using NHS formate as CO surrogate this drawback could be avoided and an efficient protocol on Pd-catalyzed carbonylation reactions under mild conditions developed [78].

The synthesis of NHS functionalized azobenzenes has been, so far, mainly performed via the traditional coupling approach of the corresponding carboxylic acid with NHS and a carbodiimide coupling agent [80–84] (Scheme 1a). Unsymmetric azobenzenes with a carboxylic acid moiety can be obtained via Mills reaction [85,86] or azo coupling [68,81–84], symmetric ones via a reductive coupling of nitrobenzoic acid [70,84,87–89]. Only a few examples exist with the NHS ester in *meta*-position and even fewer are reported for the *ortho*-position [80]. However, NHS functionalized azobenzenes with other *ortho*-substituents that shift the absorption wavelength in the region of visible light have not been reported so far. In case of the diazocines, their incorporation into materials is often performed via peptide coupling of an amine functionalized diazocine [90–92]. Only one example of a diazocine with an NHS ester in *meta*-position to the azo group has been reported (Scheme 1b) [93]. Here, the final diazocine was obtained in an overall yield of 3% after five steps. The carbonyl function was connected to the phenyl rings of the diazocine with a methylene bridge allowing more rotational degrees of freedom compared to a direct linkage [93].

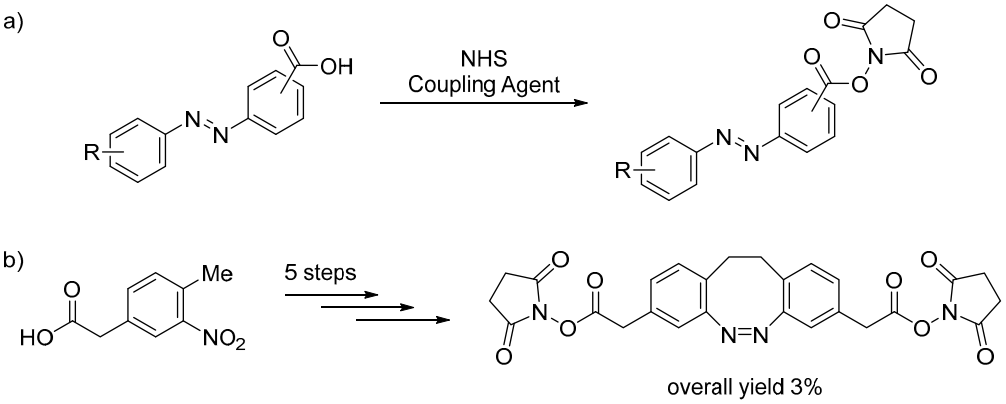

Scheme 1. Synthetic approach towards NHS functionalized azobenzenes [80] (**a**) and diazocine [93] (**b**).

We could recently show that cross-coupling reactions are a versatile tool for late-stage functionalization of *para*-substituted azobenzene derivatives [94]. For diazocines, only few examples on cross-coupling reactions with differing yields have been reported, mainly Buchwald-Hartwig cross-coupling [95] or Stille reactions [11,96].

We report an efficient Pd-catalyzed carbonylation protocol, based on previously work of Barré et al. [78], to transform iodinated azobenzenes into the corresponding active NHS ester under mild conditions with NHS formate as CO surrogate. The iodinated precursors are easily accessible and a high tolerance of functional groups was achieved, including other halogen substituents. The usefulness of the obtained NHS functionalized azobenzenes was demonstrated in two examples by coupling the NHS esters with an amino acid.

2. Results

The combination of palladium acetate as catalyst and Xantphos as ligand was demonstrated to be a high yielding synthetic method in the literature for Pd-catalyzed carbonylation reactions [78,79]. Therefore, we started our investigation with this catalytic system for the functionalization of mono-iodinated azobenzenes **1** (Scheme 2). Although other possible ligands were screened, the combination of palladium acetate with Xantphos was shown to be the best condition for the catalytic carbonylation of iodinated azobenzenes. In this way, mono-iodinated azobenzenes, at first without further substituents were reacted with NHS formate (**2**). ^{1}H NMR analysis with an internal reference revealed a quantitative conversion to the desired *para*- **3a** and *meta*-derivative **3b**. Unfortunately, no conversion

Molecules **2021**, *26*, 3916

to the *ortho*-functionalized azobenzene **3c** was detected; and the starting material was completely recovered. It is very common that the functionalization of azobenzenes by cross-coupling is low yielding or entirely unsuccessful. It also aligns with our own findings that cross-coupling reactions at *ortho*-position of azobenzenes are rarely possible [94]. Next, azobenzene derivatives with further substitutions were tested (**3d**–**3n**). A wide range of functional groups was tolerated: Starting with a hydroxy group in *para*-position, **3d** was obtained in an isolated yield of 95%. Also, an amine function on the azobenzene did not cause problems even though it might have been possible that the formed NHS ester directly reacts with this aromatic primary amine; **3e** could be isolated in 92%. The acetamide functionalized azobenzene **3f** was isolated in a yield of 86%. However, the conversion was determined by ^{1}H NMR analysis to be over 95%. Moreover, azobenzene derivatives containing an electron withdrawing group, such as 4-nitro-4′-iodoazobenzene (**1g**), were converted to the corresponding NHS ester in quantitative yield. Even the vinylated species **1h** was successfully transformed to **3h** and isolated in a yield of 60%. Moreover, the functionalization of three additional azobenzene derivatives proofs the versatility of the demonstrated reaction: In particular, an azobenzene with both an ether and a primary hydroxyl group (**3i**, 79%), an alkoxylated tetra-*ortho*-azobenzene (**3j**, 94%) and a unique sterically hindered azobenzene with a naphthalene motif (**3k**, 74%) were all successfully synthesized.

The coupling reaction proceeded chemo-selectively in excellent yields when azobenzene derivatives were used that had both, an iodine and a bromine substituent. Thus, the obtained NHS functionalized azobenzene derivatives **3l**–**n** enable potential further functionalization reactions by cross-coupling strategies.

Considering the latest research trends to use azobenzene derivatives that can be switched with visible light and to incorporate these into different types of applications, we were interested to transfer our results for mono-iodinated azobenzenes to di-iodinated azobenzenes (Scheme 3). This posed no problems for **5a** and **5b** (Scheme 3), which were synthesized in excellent yields. The synthesis of **5a** was additionally performed on a 2.00 mmol scale leading to a comparable yield as the 100 µmol batch (96%). Here, the reaction setup was slightly modified: A pressure tube was used as a reaction vessel which was closed quickly after the addition of triethylamine. However, difficulties occurred for **5c** and **5d**. For **5c,** we initially observed that the reaction was incomplete. A mixture of mono-substituted NHS ester-azobenzene and di-substituted NHS ester-azobenzene was detected. We hypothesized that the solubility of the iodinated azobenzene **4c** might be too low. Therefore, we changed the solvent to the more polar DMF, as this solvent was reported to lead to comparable yields as THF [78]. However, DMF is slightly basic [97] and thus initializes the decomposition of the NHS formate (**2**). Traces of dimethylamine, a common impurity in DMF [98], can enhance this decomposition. The concomitant release of carbon dioxide increased the pressure inside the vial so much that a subsequent addition of triethyl amine via syringe was difficult. Without the additional base, however, the decomposition of **2** was not sufficient for a full conversion. Changing the solvent to DMSO instead, resolved this problem. The conversion of **4c** increased drastically for the tetra-*ortho*-methoxylated-azobenzene; **5c** was synthesized in a yield of 91%.

Unfortunately, the tetra-*ortho*-fluorinated azobenzene **4d** was only converted in traces to **5d** as detected by ^{1}H NMR analysis. Even the change to a more polar solvent did not increase the yield. Instead, there were so many reaction products that they could not be further analyzed. In these rare cases, in which the cross-coupling approach fails, alternative strategies need to be developed. In this instance, we were able to synthesize the fluorinated target molecule **5d** by the coupling of the carboxylic acid **6** with NHS (**7**) using 1-ethyl-3-(3-dimethylaminopropyl)carbodiimide (EDCl) and 4-dimethylaminopyridine (DMAP) as coupling agent (Scheme 4). The yield could not be improved by using other coupling agents such as DCC, HATU, HSPyU, 1,1′-carbonyldiimidazol (CDI) or 2,4,6-trichlorobenzoic acid (TCBC).

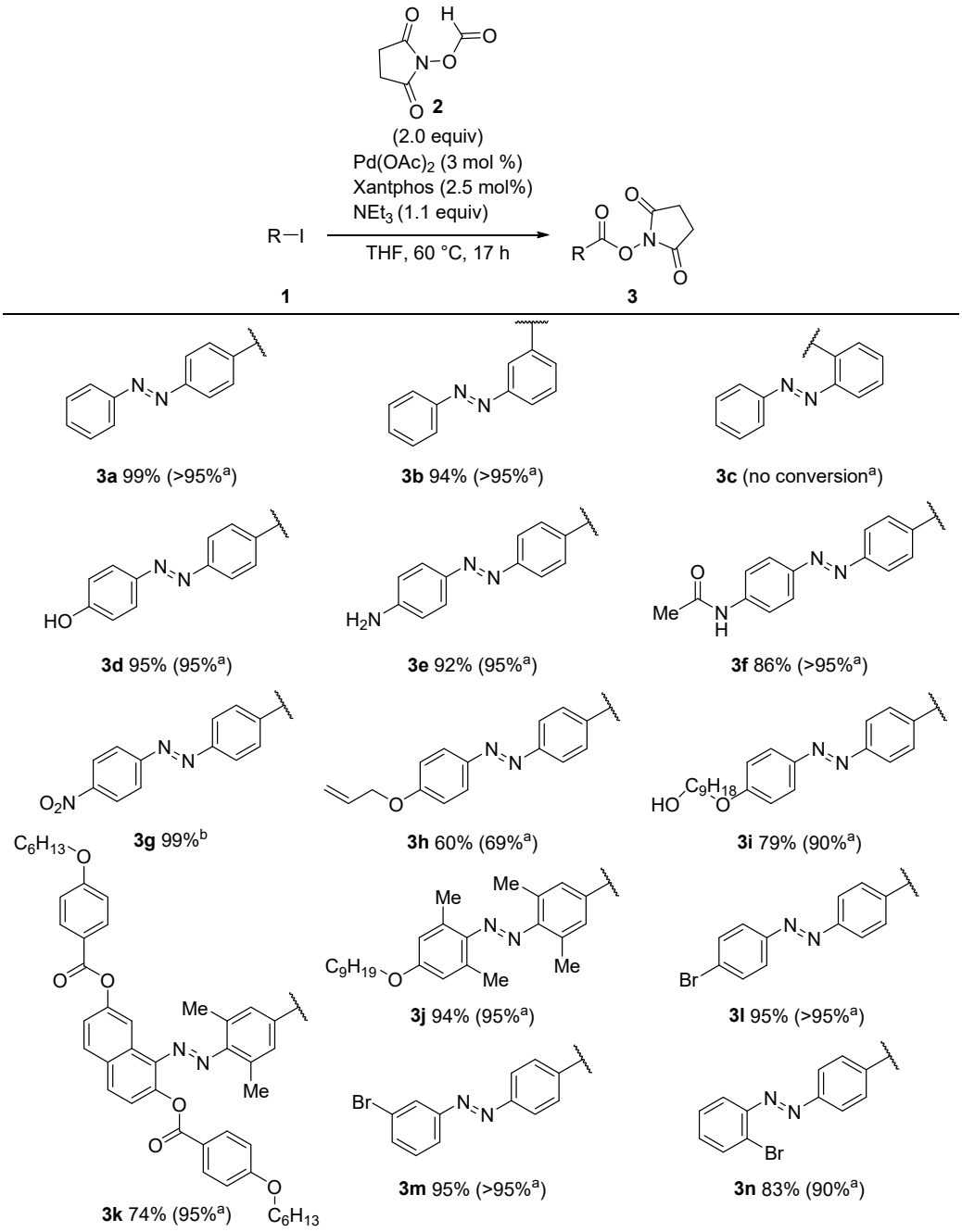

Scheme 2. Scope of the Pd-catalyzed NHS functionalization of mono-iodinated azobenzenes. [a] Yields in brackets were determined by using 1,3,5-trimethoxybenzene as internal reference for ^{1}H NMR analysis; all other yields are isolated yields. [b] In DMSO.

Molecules **2021**, *26*, 3916

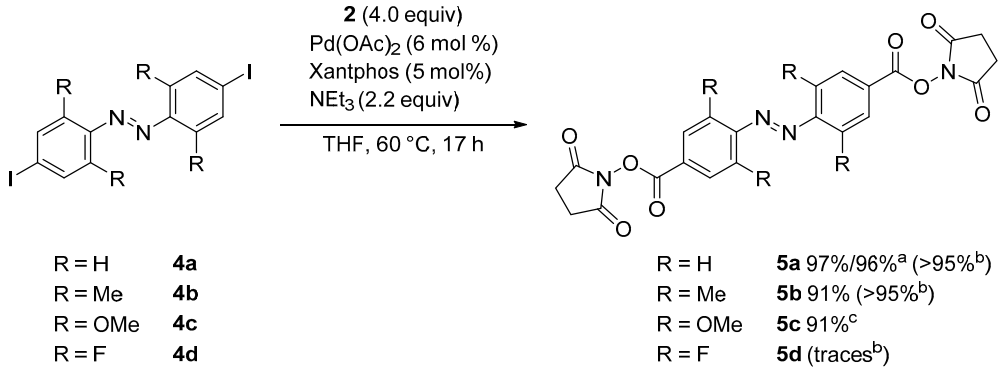

Scheme 3. Scope of the Pd-catalyzed NHS functionalization of di-iodinated azobenzenes. [a] 2.00 mmol scale. [b] Yields in brackets were determined by using 1,3,5-trimethoxybenzene as internal reference for ^{1}H NMR analysis; all other yields are isolated yields. [c] In DMSO.

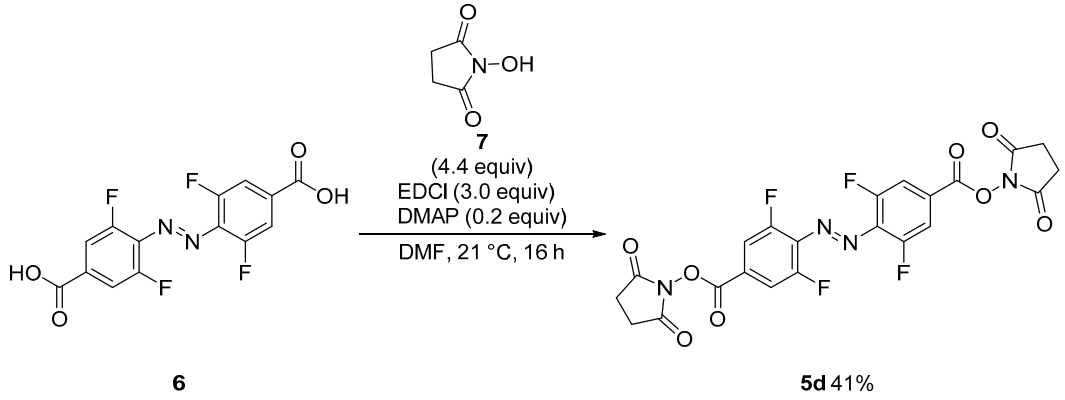

Scheme 4. Alternative synthetic route to obtain the NHS functionalized tetra-*ortho*-fluorinated azobenzene.

In contrast to typical azobenzenes, the (*Z*)-isomer is thermodynamically favored in diazocines making them a desirable molecule for applications. Moreover, the switching is possible with visible light. Diazocines bearing a carboxyl group are demanding to synthesize with moderate overall yields [99,100]. As iodinated diazocines can be easily obtained [95], we were interested to transfer our method to diazocines. Analogously to the difficulties for di-iodinated azobenzenes, the use of THF as solvent led only to a partial conversion; in case of the di-iodinated diazocine, a mixture of mono- and di-functionalized derivatives was obtained. Again, these problems were resolved by using DMSO as solvent and diazocines **6a** and **6b** were obtained in near-quantitative yields (Scheme 5).

To demonstrate the usefulness of the obtained NHS ester derivatives for reactions with a primary amine, azobenzene **2a** and diazocine **8b** were reacted with L-alanine *tert*-butyl ester hydrochloride under slightly basic conditions yielding the corresponding amino acid derivatives **9a** and **9b** in excellent to quantitative yield (Scheme 6).

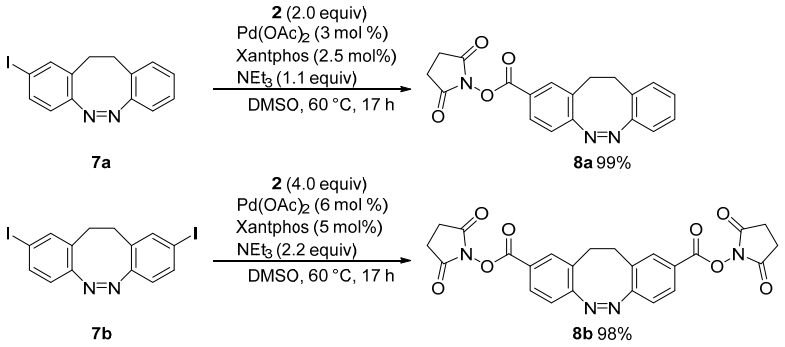

Scheme 5. Pd-catalyzed NHS functionalization of iodinated diazocines.

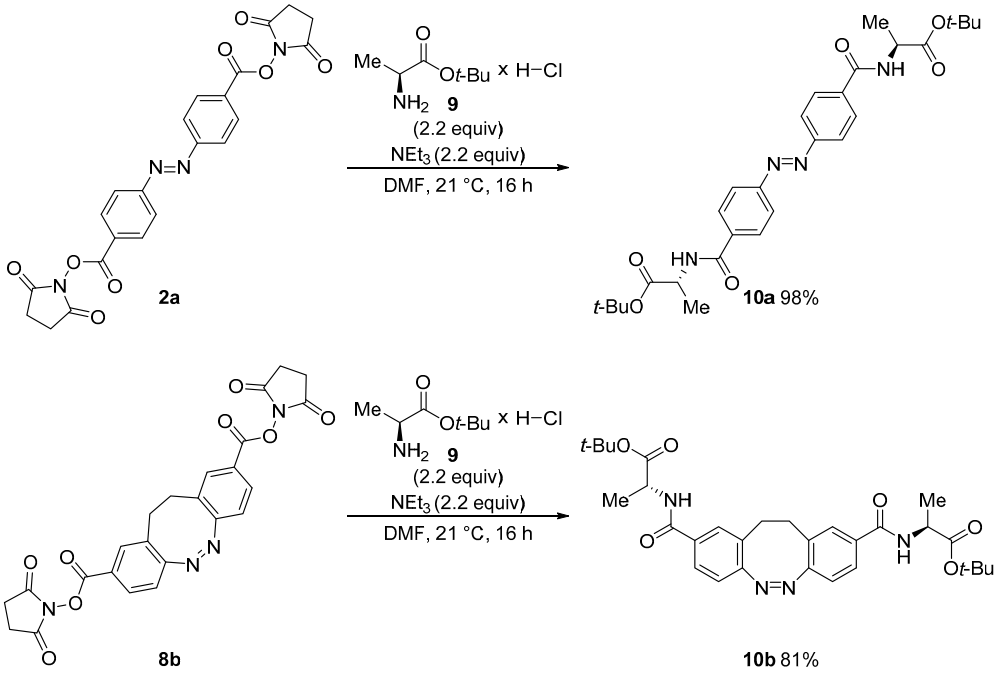

Scheme 6. Condensation reaction of NHS derivatives with L-alanine *tert*-butyl ester hydrochloride.

3. Discussion

This robust and high-yielding protocol enables new possibilities for the molecular design of azobenzene and diazocines derivatives. A large scope of 14 mono-functionalized and 5 di-functionalized azobenzenes and diazocines were prepared in high to excellent yields. Iodinated azobenzenes are fairly easy to synthesize and a vast number of protocols are available. In contrast to this, the traditional synthetic route requires a carboxyl group on the azobenzene for the esterification to yield the NHS functionality. This is a severe synthetic limitation. Indeed, the carboxylated analogous of **3g**, **3k–l** have not been reported, but the corresponding NHS derivatives can now be synthesized via our synthetic approach. These advantages are even more important considering that the solubility of di-carboxylated azobenzenes in organic solvents is low. Furthermore, the synthesis of more

complex azobenzenes with a carboxyl-functionality requires many synthetical steps or are unknown until today. The practicality of the approach was shown by the condensation of two di-functionalized NHS esters with a protected amino acid.

4. Materials and Methods

4.1. General Information

For reactions under inert conditions, a nitrogen filled glovebox (Pure Lab^{HE} from Inert, Amesbury, MA USA) and standard Schlenk techniques were used (Supplementary Materials). All carbonylation reactions were performed in microwave reaction vials sealed with a septum cap from Biotage (Biotage, Uppsala, Sweden). All glassware was dried in an oven at 200 °C for several hours prior to use. NMR tubes were dried in an oven at 110 °C for several hours prior to use. NMR spectra were recorded on a Bruker Avance Neo 600 (Bruker BioSpin, Rheinstetten, Germany) (600 MHz (^{1}H), 151 MHz (^{13}C{^{1}H}), 565 MHz (^{19}F) at 298 K. All ^{1}H NMR and ^{13}C{^{1}H} NMR spectra were referenced to the residual proton signals of the solvent (^{1}H) or the solvent itself (^{13}C{^{1}H}). ^{19}F NMR spectra were referenced internally against trichlorofluoromethane. The exact assignment of the peaks was performed by two-dimensional NMR spectroscopy such as ^{1}H COSY, ^{13}C{^{1}H} HSQC and ^{1}H/^{13}C{^{1}H} HMBC when possible. High-resolution EI mass spectra were recorded on a MAT 95XL double-focusing mass spectrometer from Finnigan MAT (Thermo Fisher Scientific, Waltham, MA, USA) at an ionization energy of 70 eV. Samples were measured by a direct or indirect inlet method with a source temperature of 200 °C. High-resolution ESI and APCI mass spectra were measured by a direct inlet method on an Impact II mass spectrometer from Bruker Daltonics (Bruker Daltonics, Bremen, Germany). ESI mass spectra were recorded in the positive ion collection mode.

IR spectra were recorded on a Nicolet i510 FT-IR spectrometer from Thermo Fisher Scientific (Thermo Fisher Scientific, Waltham, MA, USA) with a diamond window in an area from 500–4000 cm^{-1} with a resolution of 4 cm^{-1}. All samples were measured 16 times against a background scan. Melting points were recorded on a Büchi Melting Point M-560 (Büchi, Essen, Germany) and are reported corrected. Thin layer chromatography (TLC) was performed using TLC Silica gel 60 F_{254} from Merck (Merck, Darmstadt, Germany) and compounds were visualized by exposure to UV light at a wavelength of 254 nm. Column chromatography was performed either manually using silica gel 60 (0.015–0.040 mm) from Merck (Merck, Darmstadt, Germany) or by using a PuriFlash 4250 column machine (Interchim, Mannheim, Germany). Silica gel columns of the type CHROMABOND Flash RS 15 SPHERE SiOH 15 µm (Macherey-Nagel, Düren, Germany) were used. The sample was applied via dry load with Celite® 503 (Macherey-Nagel, Düren, Germany) as column material. If stated, Celite® 503 (Macherey-Nagel, Düren, Germany) was used as filtration aid. The use of abbreviations follows the conventions from the ACS Style guide [101].

4.2. General Procedures

4.2.1. General Procedure 1 Carbonylation

(a) Mono-iodinated molecular switch

Under inert conditions, the corresponding mono-iodinated molecular switch (200 µmol, 2.00 equiv), $Pd(OAc)_2$ (1.35 mg, 6.00 µmol, 3 mol%), Xantphos (2.89 mg, 5.00 µmol, 2.5 mol%) and 2,5-dioxopyrrolidin-1-yl formate (57.2 mg, 400 µmol, 4.00 equiv) were dissolved in dry THF (3 mL) in a pressure reaction vial. A solution of 1,3,5-trimethoxybenzene (16.8 mg, 100 µmol) as an internal standard in dry THF (1 mL) was added. The vial was sealed and heated to 60 °C. A solution of triethyl amine (22.2 mg, 220 µmol, 2.20 equiv) in dry THF (1 mL) was quickly added. Fast gas evolution was observed and the reaction was stirred for 17 h at 60 °C. After cooling to 21 °C, the solvent was removed under reduced pressure. The residue was re-dissolved in DCM (10 mL), filtered through Celite® and the solvent removed under reduced pressure.

(b) Di-iodinated molecular switch

Under inert conditions, the corresponding di-iodinated molecular switch (100 μmol, 1.00 equiv), $Pd(OAc)_2$ (1.35 mg, 6.00 μmol, 6 mol%), Xantphos (2.89 mg, 5.00 μmol, 5 mol%) and 2,5-dioxopyrrolidin-1-yl formate (57.2 mg, 400 μmol, 4.00 equiv) were dissolved in dry THF (3 mL) in a pressure reaction vial. A solution of 1,3,5-trimethoxybenzene (16.8 mg, 100 μmol) as an internal standard in dry THF (1 mL) was added. The vial was sealed and heated to 60 °C. A solution of triethyl amine (22.2 mg, 220 μmol, 2.20 equiv) in dry THF (1 mL) was quickly added. Fast gas evolution was observed and the reaction was stirred for 17 h at 60 °C. After cooling to 21 °C, the solvent was removed under reduced pressure. The residue was re-dissolved in DCM (10 mL), filtered through Celite® and the solvent removed under reduced pressure.

4.2.2. General Procedure 2 Carbonylation

(a) Mono-iodinated molecular switch

Under inert conditions, the corresponding mono-iodinated switch (200 μmol, 2.00 equiv), $Pd(OAc)_2$ (1.35 mg, 6.00 μmol, 3 mol%), Xantphos (2.89 mg, 5.00 μmol, 2.5 mol%) and 2,5-dioxopyrrolidin-1-yl formate (57.2 mg, 400 μmol, 4.00 equiv) were dissolved in dry THF (4 mL) in a pressure reaction vial. The vial was sealed and heated to 60 °C. A solution of triethyl amine (22.2 mg, 220 μmol, 2.20 equiv) in dry THF (1 mL) was quickly added. Fast gas evolution was observed and the reaction was stirred for 17 h at 60 °C. After cooling to 21 °C, the solvent was removed under reduced pressure. The residue was re-dissolved in DCM (10 mL) and extracted with water (20 mL) and brine (20 mL). The combined organic layers were dried over magnesium sulfate, filtered and the solvent removed under reduced pressure.

(b) Di-iodinated molecular switch

Under inert conditions, the corresponding di-iodinated switch (100 μmol, 1.00 equiv), $Pd(OAc)_2$ (1.35 mg, 6.00 μmol, 6 mol%), Xantphos (2.89 mg, 5.00 μmol, 5 mol%) and 2,5-dioxopyrrolidin-1-yl formate (57.2 mg, 400 μmol, 4.00 equiv) were dissolved in dry THF (4 mL) in a pressure reaction vial. The vial was sealed and heated to 60 °C. A solution of triethyl amine (22.2 mg, 220 μmol, 2.20 equiv) in dry THF (1 mL) was quickly added. Fast gas evolution was observed and the reaction was stirred for 17 h at 60 °C. After cooling to 21 °C, the solvent was removed under reduced pressure. The residue was re-dissolved in DCM (10 mL) and extracted with water (20 mL) and brine (20 mL). The combined organic layers were dried over magnesium sulfate, filtered and the solvent removed under reduced pressure.

4.2.3. General Procedure Condensation Reaction

Triethyl amine (2.20 equiv) was added to a solution of L-alanine *tert*-butyl ester hydrochloride (2.20 equiv) in dry DMF. A solution of the corresponding di-NHS functionalized molecular switch (1.00 equiv) in dry DMF was added and the resulting mixture was stirred at 21 °C for 16 h. Water and ethyl acetate were added, and the mixture was washed with brine (3×). The combined organic phases were dried over magnesium sulfate, filtered and the solvent removed under reduced pressure yielding the product.

Supplementary Materials: The following are available online: general information, a list of all reagents and solvents, experimental procedures and analytical data, determination of ^{1}H NMR yield, images of all NMR spectra.

Author Contributions: Conceptualization, S.S. and M.W.; methodology, S.S. and M.W.; validation, S.S., M.W. and A.S.; formal analysis, S.S. and M.W.; investigation, S.S., M.W. and A.S.; resources, A.S.; data curation, S.S. and M.W.; writing—original draft preparation, S.S., M.W. and A.S.; writing—review and editing, S.S, M.W. and A.S.; visualization, S.S. and M.W.; supervision, A.S.; project administration, A.S.; funding acquisition, A.S. All authors have read and agreed to the published version of the manuscript.

Funding: This research was funded by the GERMAN RESEARCH FOUNDATION (DFG) within the priority program SPP 2100 "Soft Material Robotic Systems", Subproject STA1195/5-1, "Insect feet inspired concepts soft touch grippers with dynamically adjustable grip strength".

Conflicts of Interest: The authors declare no conflict of interest.

Sample Availability: Samples of the compounds may be available from the authors. Please contact the authors for further details.

References

1. Zhou, H.; Xue, C.; Weis, P.; Suzuki, Y.; Huang, S.; Koynov, K.; Auernhammer, G.K.; Berger, R.; Butt, H.-J.; Wu, S. Photoswitching of Glass Transition Temperatures of Azobenzene-Containing Polymers Induces Reversible Solid-to-Liquid Transitions. *Nat. Chem.* **2017**, *9*, 145–151. [CrossRef] [PubMed]
2. Ikeda, T.; Sasaki, T.; Ichimura, K. Photochemical switching of polarization in ferroelectric liquid-crystal films. *Nature* **1993**, *361*, 428–430. [CrossRef]
3. Yamada, M.; Kondo, M.; Mamiya, J.-I.; Yu, Y.; Kinoshita, M.; Barrett, C.J.; Ikeda, T. Photomobile Polymer Materials: Towards Light-Driven Plastic Motors. *Angew. Chem. Int. Ed.* **2008**, *47*, 4986–4988. [CrossRef] [PubMed]
4. Kizilkan, E.; Strueben, J.; Jin, X.; Schaber, C.F.; Adelung, R.; Staubitz, A.; Gorb, S.N. Influence of the Porosity on the Photoresponse of a Liquid Crystal Elastomer. *R. Soc. Open. Sci.* **2016**, *3*, 150700. [CrossRef] [PubMed]
5. Kizilkan, E.; Strueben, J.; Staubitz, A.; Gorb, S.N. Bioinspired Photocontrollable Microstructured Transport Device. *Sci. Robot.* **2017**, *2*, eaak9454. [CrossRef]
6. Dowds, M.; Bank, D.; Strueben, J.; Soto, D.P.; Sönnichsen, F.D.; Renth, F.; Temps, F.; Staubitz, A. Efficient Reversible Photoisomerisation with Large Solvodynamic Size-Switching of a Main Chain poly(azobenzene-alt-trisiloxane). *J. Mater. Chem. C* **2020**, *8*, 1835–1845. [CrossRef]
7. Archut, A.; Vögtle, F.; De Cola, L.; Azzelini, G.C.; Balzani, V.; Ramanujam, P.S.; Berg, R.H. Azobenzene-Functionalized Cascade Molecules: Photoswitchable Supramolecular Systems. *Chem. Eur. J.* **1998**, *4*, 699–706. [CrossRef]
8. Pötschke, D.; Ballauff, M.; Lindner, P.; Fischer, M.; Vögtle, F. Analysis of the Structure of Dendrimers in Solution by Small-Angle Neutron Scattering Including Contrast Variation. *Macromolecules* **1999**, *32*, 4079–4087. [CrossRef]
9. Beharry, A.A.; Woolley, G.A. Azobenzene Photoswitches for Biomolecules. *Chem. Soc. Rev.* **2011**, *40*, 4422–4437. [CrossRef]
10. Schehr, M.; Ianes, C.; Weisner, J.; Heintze, L.; Muller, M.P.; Pichlo, C.; Charl, J.; Brunstein, E.; Ewert, J.; Lehr, M.; et al. 2-Azo-, 2-Diazocine-thiazols and 2-Azo-imidazoles as Photoswitchable Kinase Inhibitors: Limitations and Pitfalls of the Photoswitchable Inhibitor Approach. *Photochem. Photobiol. Sci.* **2019**, *18*, 1398–1407. [CrossRef] [PubMed]
11. Heintze, L.; Schmidt, D.; Rodat, T.; Witt, L.; Ewert, J.; Kriegs, M.; Herges, R.; Peifer, C. Photoswitchable Azo- and Diazocine-Functionalized Derivatives of the VEGFR-2 Inhibitor Axitinib. *Int. J. Mol. Sci.* **2020**, *21*, 8961. [CrossRef]
12. Wegener, M.; Hansen, M.J.; Driessen, A.J.M.; Szymanski, W.; Feringa, B.L. Photocontrol of Antibacterial Activity: Shifting from UV to Red Light Activation. *J. Am. Chem. Soc.* **2017**, *139*, 17979–17986. [CrossRef]
13. Hoorens, M.W.H.; Ourailidou, M.E.; Rodat, T.; van der Wouden, P.E.; Kobauri, P.; Kriegs, M.; Peifer, C.; Feringa, B.L.; Dekker, F.J.; Szymanski, W. Light-Controlled Inhibition of BRAFV600E Kinase. *Eur. J. Med. Chem.* **2019**, *179*, 133–146. [CrossRef] [PubMed]
14. Hull, K.; Morstein, J.; Trauner, D. In Vivo Photopharmacology. *Chem. Rev.* **2018**, *118*, 10710–10747. [CrossRef]
15. Stein, M.; Middendorp, S.J.; Carta, V.; Pejo, E.; Raines, D.E.; Forman, S.A.; Sigel, E.; Trauner, D. Azo-Propofols: Photochromic Potentiators of GABA(A) Receptors. *Angew. Chem. Int. Ed.* **2012**, *51*, 10500–10504. [CrossRef] [PubMed]
16. Velema, W.A.; Szymanski, W.; Feringa, B.L. Photopharmacology: Beyond Proof of Principle. *J. Am. Chem. Soc.* **2014**, *136*, 2178–2191. [CrossRef] [PubMed]
17. Arkhipova, V.; Fu, H.; Hoorens, M.W.H.; Trinco, G.; Lameijer, L.N.; Marin, E.; Feringa, B.L.; Poelarends, G.J.; Szymanski, W.; Slotboom, D.J.; et al. Structural Aspects of Photopharmacology: Insight into the Binding of Photoswitchable and Photocaged Inhibitors to the Glutamate Transporter Homologue. *J. Am. Chem. Soc.* **2021**, *143*, 1513–1520. [CrossRef] [PubMed]
18. Kolarski, D.; Miller, S.; Oshima, T.; Nagai, Y.; Aoki, Y.; Kobauri, P.; Srivastava, A.; Sugiyama, A.; Amaike, K.; Sato, A.; et al. Photopharmacological Manipulation of Mammalian CRY1 for Regulation of the Circadian Clock. *J. Am. Chem. Soc.* **2021**, *143*, 2078–2087. [CrossRef]
19. Hansen, M.J.; Hille, J.I.C.; Szymanski, W.; Driessen, A.J.M.; Feringa, B.L. Easily Accessible, Highly Potent, Photocontrolled Modulators of Bacterial Communication. *Chem* **2019**, *5*, 1293–1301. [CrossRef]
20. Volgraf, M.; Gorostiza, P.; Numano, R.; Kramer, R.H.; Isacoff, E.Y.; Trauner, D. Allosteric Control of an Ionotropic Glutamate Receptor with an Optical Switch. *Nat. Chem. Biol.* **2006**, *2*, 47–52. [CrossRef]
21. Banghart, M.; Borges, K.; Isacoff, E.; Trauner, D.; Kramer, R.H. Light-Activated Ion Channels for Remote Control of Neuronal Firing. *Nat. Neurosci.* **2004**, *7*, 1381–1386. [CrossRef] [PubMed]
22. Velema, W.A.; van der Berg, J.P.; Hansen, M.J.; Szymanski, W.; Driessen, A.J.; Feringa, B.L. Optical Control of Antibacterial Activity. *Nat. Chem.* **2013**, *5*, 924–928. [CrossRef]
23. Zhang, Y.; Erdmann, F.; Fischer, G. Augmented Photoswitching Modulates Immune Signaling. *Nat. Chem. Biol.* **2009**, *5*, 724–726. [CrossRef] [PubMed]

24. Yager, K.G.; Barrett, C.J. Novel Photo-Switching using Azobenzene Functional Materials. *J. Photochem. Photobiol. A* **2006**, *182*, 250–261. [CrossRef]
25. Lancia, F.; Ryabchun, A.; Katsonis, N. Life-Like Motion Driven by Artificial Molecular Machines. *Nat. Rev. Chem.* **2019**, *3*, 536–551. [CrossRef]
26. Iamsaard, S.; Asshoff, S.J.; Matt, B.; Kudernac, T.; Cornelissen, J.J.; Fletcher, S.P.; Katsonis, N. Conversion of Light into Macroscopic Helical Motion. *Nat. Chem.* **2014**, *6*, 229–235. [CrossRef] [PubMed]
27. Koshima, H.; Ojima, N.; Uchimoto, H. Mechanical Motion of Azobenzene Crystals upon Photoirradiation. *J. Am. Chem. Soc.* **2009**, *131*, 6890–6891. [CrossRef]
28. Gelebart, A.H.; Mulder, D.J.; Varga, M.; Konya, A.; Vantomme, G.; Meijer, E.W.; Selinger, R.L.B.; Broer, D.J. Making Waves in a Photoactive Polymer Film. *Nature* **2017**, *546*, 632–636. [CrossRef]
29. Ikeda, T.; Tsutsumi, O. Optical Switching and Image Storage by Means of Azobenzene Liquid-Crystal Films. *Science* **1995**, *268*. [CrossRef] [PubMed]
30. Liu, Z.F.; Hashimoto, K.; Fujishima, A. Photoelectrochemical Information Storage Using an Azobenzene Derivative. *Nature* **1990**, *347*, 658–660. [CrossRef]
31. Yamamoto, T.; Hasegawa, M.; Kanazawa, A.; Sihiono, T.; Ikeda, T. Holographic Gratings and Holographic Image Storage via Photochemical Phase Transitions of Polymer Azobenzene Liquid-Crystal Films. *J. Mater. Chem.* **2000**, *10*, 337–342. [CrossRef]
32. Åstrand, P.-O.; Ramanujam, P.S.; Hvilsted, S.; Bak, K.L.; Sauer, S.P.A. Ab Initio Calculation of the Electronic Spectrum of Azobenzene Dyes and Its Impact on the Design of Optical Data Storage Materials. *J. Am. Chem. Soc.* **2000**, *122*, 3482–3487. [CrossRef]
33. Hartley, G.S. The Cis-form of Azobenzene. *Nature* **1937**, *140*, 281. [CrossRef]
34. Bandara, H.M.; Burdette, S.C. Photoisomerization in Different Classes of Azobenzene. *Chem. Soc. Rev.* **2012**, *41*, 1809–1825. [CrossRef] [PubMed]
35. Brown, C.J. A Refinement of the Crystal Structure of Azobenzene. *Acta Cryst.* **1966**, *21*, 146–152. [CrossRef]
36. Mostad, A.; Rømming, C. A Refinement of the Crystal Structure of cis-Azobenzene. *Acta Chem. Scand.* **1971**, *25*, 3561–3568. [CrossRef]
37. Monti, S.; Orlandi, G.; Palmieri, P. Features of the Photochemically Active State Surfaces of Azobenzenes. *Chem. Phys.* **1982**, *71*, 87–99. [CrossRef]
38. Brash, D.E.; Rudolph, J.A.; Simon, J.A.; Lin, A.; McKenna, G.J.; Baden, H.P.; Halperin, A.J.; Pontén, J. A role for sunlight in skin cancer: UV-induced p53 mutations in squamous cell carcinoma. *Proc. Natl. Acad. Sci. USA* **1991**, *88*, 10124–10128. [CrossRef] [PubMed]
39. Forman, J.; Dietrich, M.; Todd Monroe, W. Photobiological and Thermal Effects of Photoactivating UVA Light Doses on Cell Cultures. *Photochem. Photobiol. Sci.* **2007**, *6*, 649–658. [CrossRef]
40. Dong, Q.; Svoboda, K.; Tiersch, T.R.; Todd Monroe, W. Photobiological effects of UVA and UVB light in zebrafish embryos: Evidence for a competent photorepair system. *J. Photochem. Photobiol. B* **2007**, *88*, 137–146. [CrossRef]
41. Beharry, A.A.; Sadovski, O.; Woolley, G.A. Azobenzene Photoswitching without Ultraviolet Light. *J. Am. Chem. Soc.* **2011**, *133*, 19684–19687. [CrossRef] [PubMed]
42. Samanta, S.; McCormick, T.M.; Schmidt, S.K.; Seferos, D.S.; Woolley, G.A. Robust visible light photoswitching with ortho-thiol substituted azobenzenes. *Chem. Commun.* **2013**, *49*, 10314–10316. [CrossRef] [PubMed]
43. Samanta, S.; Beharry, A.A.; Sadovski, O.; McCormick, T.M.; Babalhavaeji, A.; Tropepe, V.; Woolley, G.A. Photoswitching Azo Compounds in Vivo with Red Light. *J. Am. Chem. Soc.* **2013**, *135*, 9777–9784. [CrossRef]
44. Rullo, A.; Reiner, A.; Reiter, A.; Trauner, D.; Isacoff, E.Y.; Woolley, G.A. Long wavelength optical control of glutamate receptor ion channels using a tetra-ortho-substituted azobenzene derivative. *Chem. Commun.* **2014**, *50*, 14613–14615. [CrossRef]
45. Konrad, D.B.; Frank, J.A.; Trauner, D. Synthesis of Redshifted Azobenzene Photoswitches by Late-Stage Functionalization. *Chem. Eur. J.* **2016**, *22*, 4364–4368. [CrossRef]
46. Hansen, M.J.; Lerch, M.M.; Szymanski, W.; Feringa, B.L. Direct and Versatile Synthesis of Red-Shifted Azobenzenes. *Angew. Chem. Int. Ed.* **2016**, *55*, 13514–13518. [CrossRef]
47. Dong, M.; Babalhavaeji, A.; Collins, C.V.; Jarrah, K.; Sadovski, O.; Dai, Q.; Woolley, G.A. Near-Infrared Photoswitching of Azobenzenes under Physiological Conditions. *J. Am. Chem. Soc.* **2017**, *139*, 13483–13486. [CrossRef] [PubMed]
48. Bléger, D.; Schwarz, J.; Brouwer, A.M.; Hecht, S. o-Fluoroazobenzenes as Readily Synthesized Photoswitches Offering Nearly Quantitative Two-Way Isomerization with Visible Light. *J. Am. Chem. Soc.* **2012**, *134*, 20597–20600. [CrossRef] [PubMed]
49. Lameijer, L.N.; Budzak, S.; Simeth, N.A.; Hansen, M.J.; Feringa, B.L.; Jacquemin, D.; Szymanski, W. General Principles for the Design of Visible-Light-Responsive Photoswitches: Tetra-ortho-Chloro-Azobenzenes. *Angew. Chem. Int. Ed.* **2020**, *59*, 21663–21670. [CrossRef]
50. Yang, Y.; Hughes, R.P.; Aprahamian, I. Near-Infrared Light Activated Azo-BF2 Switches. *J. Am. Chem. Soc.* **2014**, *136*, 13190–13193. [CrossRef]
51. Siewertsen, R.; Neumann, H.; Buchheim-Stehn, B.; Herges, R.; Näther, C.; Renth, F.; Temps, F. Highly Efficient Reversible Z-E Photoisomerization of a Bridged Azobenzene with Visible Light through Resolved S1(nπ*) Absorption Bands. *J. Am. Chem. Soc.* **2009**, *131*, 15594–15595. [CrossRef]

52. Lentes, P.; Stadler, E.; Röhricht, F.; Brahms, A.; Gröbner, J.; Sönnichsen, F.D.; Gescheidt, G.; Herges, R. Nitrogen Bridged Diazocines: Photochromes Switching within the Near-Infrared Region with High Quantum Yields in Organic Solvents and in Water. *J. Am. Chem. Soc.* **2019**, *141*, 13592–13600. [CrossRef]
53. Anderson, G.W.; Zimmerman, J.E.; Callahan, F.M. N-Hydroxysuccinimide Esters in Peptide Synthesis. *J. Am. Chem. Soc.* **1963**, *85*, 3039. [CrossRef]
54. Anderson, G.W.; Zimmerman, J.E.; Callahan, F.M. The Use of Esters of N-Hydroxysuccinimide in Peptide Synthesis. *J. Am. Chem. Soc.* **1964**, *86*, 1839–1842. [CrossRef]
55. Anderson, G.W.; Callahan, F.M.; Zimmerman, J.E. Synthesis of N-Hydroxysuccinimide Esters of Acyl Peptides by the Mixed Anhydride Method. *J. Am. Chem. Soc.* **1967**, *89*, 178. [CrossRef] [PubMed]
56. Nicolas, J.; Khoshdel, E.; Haddleton, D.M. Bioconjugation onto Biological Surfaces with Fluorescently Labeled Polymers. *Chem. Commun.* **2007**, 1722–1724. [CrossRef]
57. Koniev, O.; Wagner, A. Developments and Recent Advancements in the Field of Endogenous Amino Acid Selective Bond Forming Reactions for Bioconjugation. *Chem. Soc. Rev.* **2015**, *44*, 5495–5551. [CrossRef]
58. A, S.; Xu, Q.; Zhou, D.; Gao, Y.; Vasquez, J.M.; Greiser, U.; Wang, W.; Liu, W.; Wang, W. Hyperbranched PEG-Based Multi-NHS Polymer and Bioconjugation with BSA. *Polym. Chem.* **2017**, *8*, 1283–1287. [CrossRef]
59. Stephanopoulos, N.; Francis, M.B. Choosing an Effective Protein Bioconjugation Strategy. *Nat. Chem. Biol.* **2011**, *7*, 876–884. [CrossRef]
60. Luo, Y.; Prestwich, G.D. Hyaluronic Acid-N-hydroxysuccinimide: A Useful Intermediate for Bioconjugation. *Bioconjugate Chem.* **2001**, *12*, 1085–1088. [CrossRef]
61. Fissi, A.; Ciardelli, F. Photoresponsive Polymers: Azobenzene-Containg Poly-(L-Lysine). *Biopolymers* **1987**, *26*, 1993–2007. [CrossRef]
62. Fang, L.; Han, G.; Zhang, J.; Zhang, H.; Zhang, H. Synthesis of Well-Defined Easily Crosslinkable Azobenzene Side-Chain Liquid Crystalline Polymers via Reversible Addition–Fragmentation Chain Transfer Polymerization and Photomechanical Properties of their Post-Crosslinked Fibers. *Eur. Polym. J.* **2015**, *69*, 592–604. [CrossRef]
63. Gallot, B.; Fafiotte, M. Poly(L-lysine) Containing Azobenzene Units in the Side Chains: Influence of the Degree of Substitution on Liquid Crystalline Structure and Thermotropic Behaviour. *Liq. Cryst.* **1997**, *23*, 137–146. [CrossRef]
64. Guo, C.; Gao, J.; Ma, S.; Zhang, H. Efficient Preparation of Chemically Crosslinked Recyclable Photodeformable Azobenzene Polymer Fibers with High Processability and Reconstruction Ability via a Facile Post-Crosslinking Method. *Eur. Polym. J.* **2020**, *139*, 109998. [CrossRef]
65. Han, G.; Zhang, H.; Chen, J.; Sun, Q.; Zhang, Y.; Zhang, H. Easily Crosslinkable Side-Chain Azobenzene Polymers for Fast and Persistent Fixation of Surface Relief Gratings. *New J. Chem.* **2015**, *39*, 1410–1420. [CrossRef]
66. Li, X.; Gao, Y.; Kuang, Y.; Xu, B. Enzymatic Formation of a Photoresponsive Supramolecular Hydrogel. *Chem. Commun.* **2010**, *46*, 5364–5366. [CrossRef]
67. Li, X.; Wen, R.; Zhang, Y.; Zhu, L.; Zhang, B.; Zhang, H. Photoresponsive Side-Chain Liquid Crystalline Polymers with an Easily Cross-Linkable Azobenzene Mesogen. *J. Mater. Chem.* **2009**, *19*, 236–245. [CrossRef]
68. Lv, J.-a.; Wang, W.; Wu, W.; Yu, Y. A Reactive Azobenzene Liquid-Crystalline Block Copolymer as a Promising Material for Practical Application of Light-Driven Soft Actuators. *J. Mater. Chem. C* **2015**, *3*, 6621–6626. [CrossRef]
69. Pang, X.; Xu, B.; Qing, X.; Wei, J.; Yu, Y. Photo-Induced Bending Behavior of Post-Crosslinked Liquid Crystalline Polymer/Polyurethane Blend Films. *Macromol. Rapid. Commun.* **2018**, *39*, 1700237. [CrossRef]
70. Rastogi, S.K.; Anderson, H.E.; Lamas, J.; Barret, S.; Cantu, T.; Zauscher, S.; Brittain, W.J.; Betancourt, T. Enhanced Release of Molecules upon Ultraviolet (UV) Light Irradiation from Photoresponsive Hydrogels Prepared from Bifunctional Azobenzene and Four-Arm Poly(ethylene glycol). *ACS Appl. Mater. Interfaces* **2018**, *10*, 30071–30080. [CrossRef]
71. Wang, C.; Fadeev, M.; Zhang, J.; Vazquez-Gonzalez, M.; Davidson-Rozenfeld, G.; Tian, H.; Willner, I. Shape-Memory and Self-Healing Functions of DNA-Based Carboxymethyl Cellulose Hydrogels Driven by Chemical or Light Triggers. *Chem. Sci.* **2018**, *9*, 7145–7152. [CrossRef] [PubMed]
72. Barré, A.; Ţînţaş, M.-L.; Levacher, V.; Papamicaël, C.; Gembus, V. An Overview of the Synthesis of Highly Versatile N-Hydroxysuccinimide Esters. *Synthesis* **2016**, *49*, 472–483. [CrossRef]
73. Patel, N.; Davies, M.C.; Hartshorne, M.; Heaton, R.J.; Roberts, C.J.; Tendler, S.J.B.; Williams, P.M. Immobilization of Protein Molecules onto Homogeneous and Mixed Carboxylate-Terminated Self-Assembled Monolayers. *Langmuir* **1997**, *13*, 6485–6490. [CrossRef]
74. Zhan, N.; Palui, G.; Merkl, J.-P.; Mattoussi, H. Bio-Orthogonal Coupling as a Means of Quantifying the Ligand Density on Hydrophilic Quantum Dots. *J. Am. Chem. Soc.* **2016**, *138*, 3190–3201. [CrossRef]
75. Ghosh, A.K.; Doung, T.T.; McKee, S.P.; Thompson, W.J. N,N′-Dissuccinimidyl Carbonate: A Useful Reagent for Alkoxycarbonylation of Amines. *Tetrahedron Lett.* **1992**, *33*, 2781–2784. [CrossRef]
76. Schulze, A.; Giannis, A. IBX-Mediated Conversion of Primary Alcohols and Aldehydes to N-Hydroxysuccinimide Esters. *Adv. Synth. Catal.* **2004**, *346*, 252–256. [CrossRef]
77. Tan, B.; Toda, N.; Barbas, C.F., 3rd. Organocatalytic Amidation and Esterification of Aldehydes with Activating Reagents by a Cross-Coupling Strategy. *Angew. Chem. Int. Ed.* **2012**, *51*, 12538–12541. [CrossRef]

78. Barré, A.; Ţînţaş, M.-L.; Alix, F.; Gembus, V.; Papamicaël, C.; Levacher, V. Palladium-Catalyzed Carbonylation of (Hetero)Aryl, Alkenyl and Allyl Halides by Means of N-Hydroxysuccinimidyl Formate as CO Surrogate. *J. Org. Chem.* **2015**, *80*, 6537–6544. [CrossRef]
79. Ueda, T.; Konishi, H.; Manabe, K. Trichlorophenyl Formate: Highly Reactive and Easily Accessible Crystalline CO Surrogate for Palladium-Catalyzed Carbonylation of Aryl/Alkenyl Halides and Triflates. *Org. Lett.* **2012**, *14*, 5370–5373. [CrossRef]
80. Keiper, S.; Vyle, J.S. Reversible Photocontrol of Deoxyribozyme-Catalyzed RNA Cleavage under Multiple-Turnover Conditions. *Angew. Chem. Int. Ed.* **2006**, *45*, 3306–3309. [CrossRef]
81. Zhou, M.; Haldar, S.; Franses, J.; Kim, J.-M.; Thompson, D.H. Synthesis and Self-assembly Properties of Acylated Cyclodextrins and Nitrilotriacetic Acid (NTA)-modified Inclusion Ligands for Interfacial Protein Crystallization. *Supramol. Chem.* **2006**, *17*, 101–111. [CrossRef]
82. Hu, M.; Li, L.; Wu, H.; Su, Y.; Yang, P.Y.; Uttamchandani, M.; Xu, Q.H.; Yao, S.Q. Multicolor, one- and two-photon imaging of enzymatic activities in live cells with fluorescently Quenched Activity-Based Probes (qABPs). *J. Am. Chem Soc.* **2011**, *133*, 12009–12020. [CrossRef]
83. Tuuttila, T.; Lipsonen, J.; Huuskonen, J.; Rissanen, K. Chiral Donor–π-Acceptor Azobenzene Dyes. *Dyes Pigm.* **2009**, *80*, 34–40. [CrossRef]
84. Zhao, D.; Ouyang, D.; Jiang, M.; Liao, Y.; Peng, H.; Xie, X. Photomodulated Electro-optical Response in Self-Supporting Liquid Crystalline Physical Gels. *Langmuir* **2018**, *34*, 7519–7526. [CrossRef] [PubMed]
85. Fatas, P.; Longo, E.; Rastrelli, F.; Crisma, M.; Toniolo, C.; Jimenez, A.I.; Cativiela, C.; Moretto, A. Bis(azobenzene)-Based Photoswitchable, Prochiral, Calpha-Tetrasubstituted Alpha-Amino Acids for Nanomaterials Applications. *Chem. Eur. J.* **2011**, *17*, 12606–12611. [CrossRef] [PubMed]
86. Velema, W.A.; Hansen, M.J.; Lerch, M.M.; Driessen, A.J.; Szymanski, W.; Feringa, B.L. Ciprofloxacin-Photoswitch Conjugates: A Facile Strategy for Photopharmacology. *Bioconjug. Chem.* **2015**, *26*, 2592–2597. [CrossRef] [PubMed]
87. Liu, D.; Xie, Y.; Shao, H.; Jiang, X. Using Azobenzene-Embedded Self-Assembled Monolayers to Photochemically Control Cell Adhesion Reversibly. *Angew. Chem. Int. Ed.* **2009**, *48*, 4406–4408. [CrossRef] [PubMed]
88. Tarn, D.; Ferris, D.P.; Barnes, J.C.; Ambrogio, M.W.; Stoddart, J.F.; Zink, J.I. A reversible light-operated nanovalve on mesoporous silica nanoparticles. *Nanoscale* **2014**, *6*, 3335–3343. [CrossRef]
89. Hamon, F.; Blaszkiewicz, C.; Buchotte, M.; Banaszak-Léonard, E.; Bricout, H.; Tilloy, S.; Monflier, E.; Cézard, C.; Bouteiller, L.; Len, C.; et al. Synthesis and characterization of a new photoinduced switchable beta-cyclodextrin dimer. *Beilstein J. Org. Chem.* **2014**, *10*, 2874–2885. [CrossRef]
90. Samanta, S.; Qin, C.; Lough, A.J.; Woolley, G.A. Bidirectional Photocontrol of Peptide Conformation with a Bridged Azobenzene Derivative. *Angew. Chem. Int. Ed.* **2012**, *51*, 6452–6455. [CrossRef] [PubMed]
91. Trads, J.B.; Hull, K.; Matsuura, B.S.; Laprell, L.; Fehrentz, T.; Gorldt, N.; Kozek, K.A.; Weaver, C.D.; Klocker, N.; Barber, D.M.; et al. Sign Inversion in Photopharmacology: Incorporation of Cyclic Azobenzenes in Photoswitchable Potassium Channel Blockers and Openers. *Angew. Chem. Int. Ed.* **2019**, *58*, 15421–15428. [CrossRef]
92. Reynders, M.; Matsuura, B.S.; Bérouti, M.; Simoneschi, D.; Marzio, A.; Pagano, M.; Trauner, D. PHOTACs Enable Optical Control of Protein Degradation. *Sci. Adv.* **2020**, *6*, eaay5064. [CrossRef] [PubMed]
93. Preußke, N.; Moormann, W.; Bamberg, K.; Lipfert, M.; Herges, R.; Sönnichsen, F.D. Visible-Light-Driven Photocontrol of the Trp-Cage Protein Fold by a Diazocine Cross-Linker. *Org. Biomol. Chem.* **2020**, *18*, 2650–2660. [CrossRef] [PubMed]
94. Walther, M.; Kipke, W.; Schultzke, S.; Ghosh, S.; Staubitz, A. Modification of Azobenzenes by Cross-Coupling Reactions. *Synthesis* **2021**, *53*, 1213–1228. [CrossRef]
95. Maier, M.S.; Hüll, K.; Reynders, M.; Matsuura, B.S.; Leippe, P.; Ko, T.; Schäffer, L.; Trauner, D. Oxidative Approach Enables Efficient Access to Cyclic Azobenzenes. *J. Am. Chem. Soc.* **2019**, *141*, 17295–17304. [CrossRef] [PubMed]
96. Thapaliya, E.R.; Zhao, J.; Ellis-Davies, G.C.R. Locked-Azobenzene: Testing the Scope of a Unique Photoswitchable Scaffold for Cell Physiology. *ACS Chem. Neurosci.* **2019**, *10*, 2481–2488. [CrossRef]
97. Fawcett, W.R. Acidity and Basicity Scales for Polar Solvents. *J. Phys. Chem.* **1993**, *97*, 9540–9546. [CrossRef]
98. Magtaan, J.K.; Devocelle, M.; Kelleher, F. Regeneration of Aged DMF for Use in Solid-Phase Peptide Synthesis. *J. Pep. Sci.* **2019**, *25*, e3139. [CrossRef] [PubMed]
99. Li, S.; Eleya, N.; Staubitz, A. Cross-coupling strategy for the synthesis of diazocines. *Org. Lett.* **2020**, *22*, 1624–1627. [CrossRef] [PubMed]
100. Joshi, D.K.; Mitchell, M.J.; Bruce, D.; Lough, A.J.; Yan, H. Synthesis of cyclic azobenzene analogues. *Tetrahedron* **2012**, *68*, 8670–8676. [CrossRef]
101. A.M.; Garson, L.R. (Eds.) *The ACS Style Guide: Effective Communication of Scientific Information*, 3rd ed.; Coghill, American Chemical Society: Washington, DC, USA, 2006.

3.2 *ortho*-Functionalization of Azobenzenes via Hypervalent Iodine Reagents

Aim:

Cross-coupling reactions are a powerful tool for late-stage functionalization of azobenzenes in *meta*- and *para*-position. Although *ortho*-halogenated and -metalated azobenzenes are accessible, there is a lack of literature on cross-coupling methods for this specific position. As an alternative, C-H activations are used which also require a transition metal catalyst and often the diazenyl group is not retained. Currently, *ortho*-substituted azobenzenes are much sought after photoswitches to reach absorption in the visible range of light or thermally stable (*Z*)-isomers. Hypervalent iodine(III) compounds are known to be efficient reagents in transition metal free syntheses under mild conditions. Particularly, diaryliodonium salts have shown great potential as electrophilic arylating reagents with various carbon and heteroatom nucleophiles. The combination of azobenzenes with iodine(III) chemistry was envisioned to address the challenges associated with the synthesis of *ortho*-functionalized azobenzenes.

Title of Publication:

"*ortho*-Functionalization of azobenzenes via hypervalent iodine reagents"
E. M. Di Tommaso, M. Walther, A. Staubitz, B. Olofsson, *Chem. Commun.* **2023**, *59*, 5047–5050.
DOI: 10.1039/D3CC01060K.

Abstract:

ortho-Functionalized azobenzenes are much sought after molecular switches, as they may be turned to absorb in the visible range of light and the (*Z*)-isomers can have high thermal half-lives. To enable straightforward access to these targets, we have developed a synthetic route via novel *ortho*-substituted azobenzene-functionalized diaryliodonium salts. Selective transfer of the azobenzene moiety to O-, N-, C- and S-nucleophiles under mild, transition metal-free conditions gives access to an unprecedented range of *ortho*-substituted azobenzenes. The photoswitching properties of the reagents were investigated and the structure was determined by X-ray crystallography.

Author Contribution to this Publication:

A. Staubitz and B. Olofsson conceived the initial project. E. M. Di Tommaso and I (M. Walther) performed the experiments and analyzed the data. More precisely, I synthesized and characterized the iodinated azobenzene precursors (7 compounds). I performed the investigation of the photoswitchable properties via ^{1}H NMR and UV/Vis spectroscopy and compared the normal valent azobenzene with the corresponding hypervalent derivative. I isolated the crystal of the *ortho*-azobenzene derived diaryliodonium salt suitable for X-ray crystallography. M. Olaru performed the single crystal X-ray diffraction measurement and structure refinement. I analyzed the crystal structure. E. M. Di Tommaso developed the synthetic route to the *ortho*-azobenzene(aryl)iodonium salts, investigated its scope (7 compounds) and performed the arylation reactions using the hypervalent azobenzene (15 compounds). E. M. Di Tommaso and I wrote the Supporting Information for our respective experimental contributions. The manuscript was written and edited by all authors. I was mainly responsible for the part about azobenzenes in the introduction, the discussion about the crystal structure and the photoswitchable properties. A. Staubitz and B. Olofsson were the principal investigators in this project.

ChemComm

ROYAL SOCIETY OF CHEMISTRY

COMMUNICATION

View Article Online
View Journal | View Issue

Cite this: *Chem. Commun.*, 2023, **59**, 5047

Received 3rd March 2023,
Accepted 29th March 2023

DOI: 10.1039/d3cc01060k

rsc.li/chemcomm

ortho-Functionalization of azobenzenes *via* hypervalent iodine reagents†

Ester Maria Di Tommaso, [a] Melanie Walther, [bc] Anne Staubitz *[bc] and Berit Olofsson *[a]

***ortho*-Functionalized azobenzenes are much sought after molecular switches, as they may be tuned to absorb in the visible range of light and the (*Z*)-isomers can have high thermal half-lives. To enable straightforward access to these targets, we have developed a synthetic route *via* novel *ortho*-substituted azobenzene-functionalized diaryliodonium salts. Selective transfer of the azobenzene moiety to O-, N-, C- and S-nucleophiles under mild, transition metal-free conditions gives access to an unprecedented range of *ortho*-substituted azobenzenes. The photoswitching properties of the reagents were investigated and the structure was determined by X-ray crystallography.**

Azobenzenes are important molecular switches that can be photochemically switched between the thermodynamically stable (*E*)-isomer and the metastable (*Z*)-isomer.[1] Exceptions exist, in which the stabilities are reversed.[2] They show a high thermal[3] and photochemical stability,[1] and the switching mechanisms are well understood.[4] Using targeted syntheses, it is often possible to obtain certain properties. Hence, there is an increasing number of applications, *e.g.* in switchable polymers with diverse purposes,[5] biomedical applications,[6] or as solar thermal fuels.[7] For each task, the azobenzene has to be finely adjusted due to two main issues.[8] The thermal stability of the less stable isomer can cause an unavoidable background isomerization[9] and the overlap of the isomers' absorption spectra results in photostationary states (PSSs) of low selectivity for either isomer at a particular wavelength.[10]

Current research focuses on *ortho*-substituted azobenzenes to reach thermally stable (*Z*)-isomers or an absorption in the visible range of light.[11] Switching occurs with wavelengths as long as 720 nm,[12] and highly selective PSS (tetra-*ortho*-fluorinated azobenzene: $PSS_{(Z)}$ 91%/$PSS_{(E)}$ 86%).[10] However, there are few synthetic methods available for their synthesis (Scheme 1a).[3,13] They can be prepared from appropriately substituted anilines[11a,14] and further functionalized *via* nucleophilic substitution,[15] or through transition metal-catalyzed C–H activation.[16] While azobenzenes decorated with carbon,[17] oxygen,[17a,18] nitrogen[19] and halide[16,19b] substituents in the *ortho*-position have been synthesized, synthetic drawbacks include the need for transition metal catalysts, long reaction times at elevated temperatures and scope limitations. Surprisingly, the literature is void of cross-coupling methods in the *ortho*-position, irrespective of whether the azobenzene moiety serves as an organometallic nucleophilic component or as an electrophilic halogenated cross-coupling partner,[13] despite access to *ortho*-metalated azobenzenes.[20]

Hypervalent iodine(III) compounds are efficient reagents for a wide range of transformations under mild reaction conditions.[21] Diaryliodonium salts have been recognized as highly reactive electrophilic arylating reagents with a variety

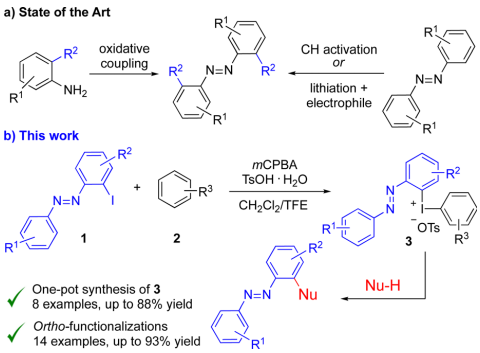

Scheme 1 Synthesis of *ortho*-substituted azobenzenes. (a) State of the art. (b) This work.

[a] *Department of Organic Chemistry, Arrhenius Laboratory, Stockholm University, Stockholm, Sweden. E-mail: berit.olofsson@su.se*
[b] *University of Bremen, Institute for Analytical and Organic Chemistry, Bremen, Germany. E-mail: staubitz@uni-bremen.de*
[c] *University of Bremen, MAPEX Center for Materials and Processes, Bremen, Germany*

† Electronic supplementary information (ESI) available. CCDC 2215795. For ESI and crystallographic data in CIF or other electronic format see DOI: https://doi.org/10.1039/d3cc01060k

of carbon and heteroatom nucleophiles under both metal-free and metal-catalyzed conditions.[22] Furthermore, they are relatively non-toxic, bench-stable and easily synthesized through one-pot reactions of iodoarenes and arenes or arylboronic acids.[23]

We envisioned that the combination of azobenzenes with iodine(III) chemistry could overcome the limitations in the synthesis of *ortho*-functionalized azobenzenes. Herein, we showcase the successful synthesis and applications of *ortho*-azobenzene diaryliodonium salts in metal-free arylations to access hitherto unobtainable products (Scheme 1b).

The study commenced by investigating suitable conditions for the synthesis of diaryliodonium salts **3** from the corresponding *ortho*-iodoazobenzenes **1**.[24] Our standard one-pot conditions with *m*CPBA and triflic or tosic acid and a suitable arene failed,[23b,d] as did one-pot reactions of **1** with arylboronic acids.[23c] To our delight, a sequential one-pot reaction[25] with oxidation of iodoarene **1** using *m*CPBA and tosic acid at 40 °C, followed by the addition of arene **2** at room temperature was successful for the synthesis of the novel iodonium salts **3** (Scheme 2). In this way, the otherwise unsubstituted *ortho*-azobenzene iodonium salt **3a** was obtained in 84% isolated yield from **1a**. A stepwise synthesis of **3a** with isolation of the corresponding [hydroxy(tosyloxy)iodo]arene before treatment with anisole gave **3a** in 78% overall yield.[24] Anion exchange to the corresponding triflate salt **3a′** could be performed by *in situ* treatment with triflic acid or workup with NaOTf.[24,25b]

The scope investigations were focused on the synthesis of unsymmetric diaryliodonium salts (Ar^1Ar^2IX) to avoid wasting a precious azobenzene moiety in subsequent arylations. The anisyl moiety is often an efficient "dummy group" in chemoselective arylations with Ar^1Ar^2IX under metal-free conditions.[26] Anisole

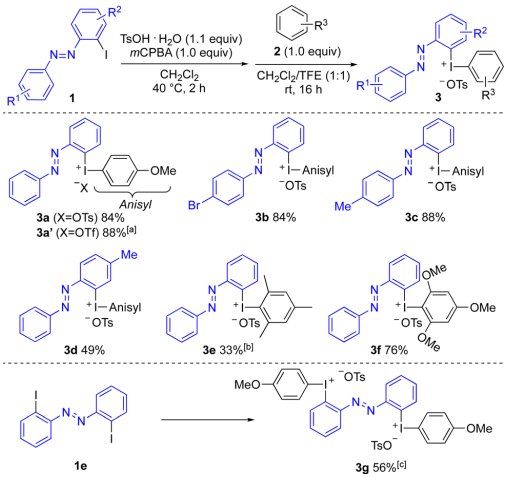

Scheme 2 Scope of *ortho*-azobenzene(aryl)iodonium salts **3** (isolated yields after precipitation). [a] After workup with NaOTf. [b] TFE as the only solvent. [c] TsOH·H_2O (2.2 equiv.), *m*CPBA (2.0 equiv.) and anisole (2.0 equiv.).

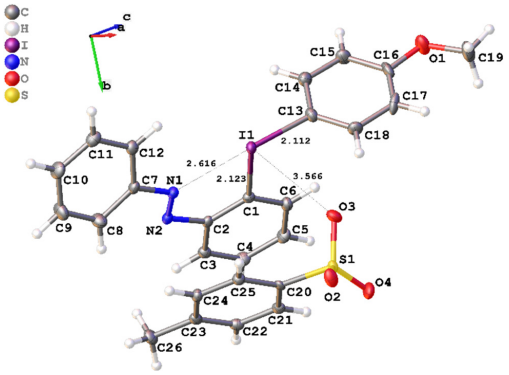

Fig. 1 X-ray crystal structure of the (*E*)-isomer of **3a** with selected bond lengths. Selected angles: C(13)–I(1)–O(3) 81.84(10)°; O(3)–I(1)–C(1) 90.45(9)°; N(1)–I(1)–O(3) 107.47°; C(1)–I(1)–N(1) 69.2(1)°; C(13)–I(1)–C(1) 94.56(12)°; N(1)–I(1)–C(13) 8.54(5).

was hence utilized as the standard arene in reactions with substituted *ortho*-iodoazobenzenes **1b–d** to provide iodonium salts **3a–d** in good to high yields. Substituents were well tolerated on the *para*-azo aryl moiety, with bromo-substituted salt **3b** well positioned for further late-stage functionalizations. Further substituents on the iodo-substituted aryl group were also tolerated, as shown by methyl-substituted product **3d**. Mesitylene and trimethoxybenzene could be utilized to provide iodonium salts **3e** and **3f** bearing a mesityl or trimethoxyphenyl (TMP) dummy group, which are reported to give chemoselective arylations with certain nucleophiles.[26] Bis(diaryliodonium) salt **3g** was obtained in good yield through difunctionalization of the corresponding diiodo-azobenzene **1e**.

It was possible to grow single crystals of the (*E*)-isomer of salt **3a**, suitable for X-ray diffraction analysis (Fig. 1, CCDC number: 2215795). Diaryliodonium salts generally have the typical T-shape of iodine(III) compounds, where one aryl group and the counterion reside in the hypervalent bond.[21] Interestingly, the X-ray structure of **3a** displays an N–I-aryl hypervalent bond with an N–I interaction of 2.616 Å, whereas the tosylate anion coordinates perpendicular to the hypervalent bond (bond angles: C(13)–I(1)–O(3) 81.84(10)°; O(3)–I(1)–C(1) 90.45(9)°). While azo-coordination to iodine(III) is unknown, Nachtsheim and coworkers have recently reported on related N–I interactions in iodine(III) reagents.[27] Preliminary calculations indicate that the pseudocyclic structure is favored for the (*E*)-isomer, whereas the (*Z*)-isomer lacks the N–I stabilizing interaction and the expected I–OTs coordination is favored.[24]

The influence of the hypervalent iodine moiety on the photoswitching behavior of the azobenzene was examined by ^{1}H NMR and UV/vis spectroscopy in $CDCl_3/CHCl_3$, comparing iodonium salt **3a** and the parent azobenzene **1a**. Under ambient conditions, both molecules existed exclusively as the (*E*)-isomer. Upon irradiation with UV light (340 nm), both molecules switched to the corresponding (*Z*)-isomer ((*E*)/(*Z*) ratio: 32/68 (**1a**), 29/71 (**3a**)). Re-isomerization occurred upon irradiation

View Article Online
ChemComm Communication

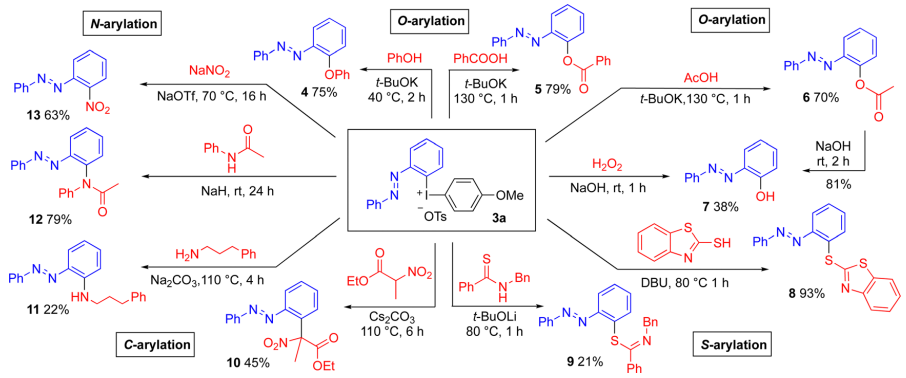

Scheme 3 Metal-free arylations of C, N, O and S-nucleophiles with reagent **3a**.

with visible light (450 nm) ((*E*)/(*Z*) ratio: 90/10 (**1a**), 72/28 (**3a**)). A complete conversion to the (*E*)-isomer could not be achieved photochemically but no significant photodegradation was detected for **1a** and **3a** upon repeated switching. The incorporation of the hypervalent moiety had almost no influence on the absorption maxima of the azobenzene switch: (π–π*: 325 nm (**1a**), 338 nm (**3a**); n–π*: 434 nm (**1a**), 436 nm (**3a**)). However, the thermal half-life was significantly decreased ($t_{1/2}$: 124.6 h (**1a**), 5.83 h (**3a**)). This can be attributed to the strong electron acceptor character of the iodine(III) moiety, and the N–I stabilizing interaction in the (*E*)-isomer of **3a**.

To demonstrate the utility of the novel reagents, well-established methods for transition metal-free arylation of various nucleophiles with diaryliodonium salt **3a** were utilized to provide a range of *ortho*-substituted azobenzene products. The transformations proceeded with complete chemoselectivity and retained (*E*)-configuration (Scheme 3). *O*-Arylation of phenol and carboxylic acids[28] delivered the azobenzene-functionalized diaryl ether **4** and aryl esters **5** and **6** in good yields. The aryl ester **6** could be hydrolyzed under mild conditions into 2-hydroxyazobenzene **7** in 81% yield, which has excellent features as a structural motif in pharmaceutical and materials science.[18b] The synthesis of product **7** was also feasible through the hydroxylation of **3a** with hydrogen peroxide[29] in a moderate yield. As Pd-catalyzed *ortho*-acyloxylation and hydroxylation of azobenzenes is reported,[17a,18] we were eager to evaluate the reactivity of **3a** with other types of nucleophiles.

To our delight, *S*-arylation with a mercaptothiazole[30] delivered the novel, heterocyclic azobenzene product **8** in excellent yield (93%). The arylation of thioamide[31] to thioimidates **9** was more difficult. Even the *C*-arylation of a substituted nitroester[32] could be performed to provide the sterically congested product **10**. Methods for *N*-arylation were next explored, and the arylation of a primary amine[33] proved to be challenging. The novel, amino-substituted product **11** was obtained in 22% yield due to partial decomposition of **3a** under the reaction conditions. On the other hand, the arylation of acetanilide[34] proceeded smoothly to give the tertiary amide **12** in 79% yield. Furthermore, arylation of sodium nitrite[35] delivered *ortho*-nitro azobenzene (**13**) in 63% yield.

The *O*-arylation methodology[28] was subsequently employed to achieve more advanced *ortho*-functionalized azobenzene products that should be relevant in supramolecular chemistry, materials science[14,36] and biological chemistry[37] (Scheme 4). The reaction of bis(diaryl)iodonium salt **3g** with phenol gave the *ortho*-diphenoxylated azobenzene **14** and the steroid estrone was arylated with reagent **3a** to diaryl ether **15** in 60% yield. Moreover, the *O*-arylation of protected ribose[38] delivered the arylated derivative **16**. Arylation of acetyl-protected cholic acid produced ester **17** in moderate yield, as the basic conditions caused partial hydrolysis of the acetate groups, with

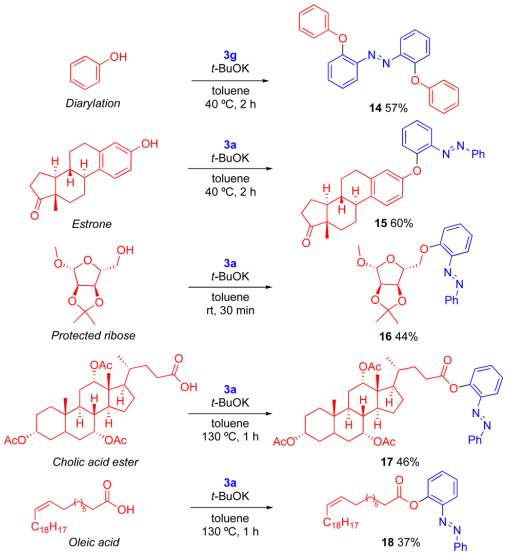

Scheme 4 *O*-Arylations to provide complex *ortho*-substituted azobenzenes. Conditions: **3** (1.0 equiv.), nucleophile and *t*BuOK (1.2–2.1 equiv.), in toluene.

competing arylation to give byproduct **6** in 20% yield.[24] Finally, the *O*-arylation of oleic acid produced the functionalized ester **18**. It should be noted that **8–11** and **15–18** are novel *ortho*-azobenzenes, illustrating the utility of the method to quickly reach a variety of targets. In comparison with literature methods to reach the known products **4–7** and **12–14**, our method often has milder conditions and shorter reaction times.[24]

In conclusion, the synthesis of *ortho*-azobenzene-derived diaryliodonium salts was achieved in high yields. The novel iodonium reagents were demonstrated as chemoselective arylation reagents with a range of C, N, O and S-nucleophiles under mild and metal-free conditions. The X-ray crystal structure revealed that the nitrogen is involved in hypervalent bonding with the iodine(III) center. The photoswitching properties of the azobenzene were retained in the hypervalent azobenzene derivatives but the incorporation of the hypervalent iodine bond influenced the position of the absorption maxima and drastically reduced the half-life time.

Financial support for this study was provided through the Swedish Research Council (2015-04404 and 2019–04232). Dr Marian Olaru is acknowledged for measuring the crystal structure and Malte Pankau for initial contributions to the project.

A.S. and B.O. conceived the project; E.M.D.T. and M.W. performed the experiments and analyzed the data; all authors contributed to writing the manuscript; A.S. and B.O. supervised the project and acquired the funding. All authors have read and agreed to the published version of the manuscript.

Conflicts of interest

There are no conflicts to declare.

Notes and references

1 H. M. Bandara and S. C. Burdette, *Chem. Soc. Rev.*, 2012, **41**, 1809–1825.
2 R. Siewertsen, H. Neumann, B. Buchheim-Stehn, R. Herges, C. Näther, F. Renth and F. Temps, *J. Am. Chem. Soc.*, 2009, **131**, 15594–15595.
3 E. Merino, *Chem. Soc. Rev.*, 2011, **40**, 3835–3853.
4 T. Kumpulainen, B. Lang, A. Rosspeintner and E. Vauthey, *Chem. Rev.*, 2017, **117**, 10826–10939.
5 (*a*) K. M. Herbert, H. E. Fowler, J. M. McCracken, K. R. Schlafmann, J. A. Koch and T. J. White, *Nat. Rev. Mater.*, 2022, **7**, 23–38; (*b*) A. Natansohn and P. Rochon, *Chem. Rev.*, 2002, **102**, 4139–4175; (*c*) T. Ikeda and O. Tsutsumi, *Science*, 1995, **268**, 1873–1875.
6 (*a*) N. Yasuike, K. M. Blacklock, H. Lu, A. S. I. Jaikaran, S. McDonald, M. Uppalapati, S. D. Khare and G. A. Woolley, *ChemPhotoChem*, 2019, **3**, 431–440; (*b*) A. C. Impastato, A. Shemet, N. A. Veprek, G. Saper, H. Hess, L. Rao, A. Gennerich and D. Trauner, *Angew. Chem., Int. Ed.*, 2022, **61**, e202115846.
7 (*a*) A. Kunz, A. H. Heindl, A. Dreos, Z. Wang, K. Moth-Poulsen, J. Becker and H. A. Wegner, *ChemPlusChem*, 2019, **84**, 1145–1148; (*b*) Z. Wang, P. Erhart, T. Li, Z.-Y. Zhang, D. Sampedro, Z. Hu, H. A. Wegner, O. Brummel, J. Libuda, M. B. Nielsen and K. Moth-Poulsen, *Joule*, 2021, **5**, 3116–3136.
8 L. N. Lameijer, S. Budzak, N. A. Simeth, M. J. Hansen, B. L. Feringa, D. Jacquemin and W. Szymanski, *Angew. Chem., Int. Ed.*, 2020, **59**, 21663–21670.
9 H. A. Wegner, *Angew. Chem., Int. Ed.*, 2012, **51**, 4787–4788.
10 D. Bléger, J. Schwarz, A. M. Brouwer and S. Hecht, *J. Am. Chem. Soc.*, 2012, **134**, 20597–20600.
11 (*a*) C. Knie, M. Utecht, F. Zhao, H. Kulla, S. Kovalenko, A. M. Brouwer, P. Saalfrank, S. Hecht and D. Bleger, *Chem. – Eur. J.*, 2014, **20**, 16492–16501; (*b*) A. A. Beharry, O. Sadovski and G. A. Woolley, *J. Am. Chem. Soc.*, 2011, **133**, 19684–19687; (*c*) M. J. Hansen, M. M. Lerch, W. Szymanski and B. L. Feringa, *Angew. Chem., Int. Ed.*, 2016, **128**, 13713–13716.
12 M. Dong, A. Babalhavaeji, C. V. Collins, K. Jarrah, O. Sadovski, Q. Dai and G. A. Woolley, *J. Am. Chem. Soc.*, 2017, **139**, 13483–13486.
13 M. Walther, W. Kipke, S. Schultzke, S. Ghosh and A. Staubitz, *Synthesis*, 2021, 1213–1228.
14 S. Mehrparvar, Z. N. Scheller, C. Wölper and G. Haberhauer, *J. Am. Chem. Soc.*, 2021, **143**, 19856–19864.
15 K. Kuntze, J. Viljakka, E. Titov, Z. Ahmed, E. Kalenius, P. Saalfrank and A. Priimagi, *Photochem. Photobiol. Sci.*, 2022, **21**, 159–173.
16 D. B. Konrad, J. A. Frank and D. Trauner, *Chem. – Eur. J.*, 2016, **22**, 4364–4368.
17 (*a*) C. Qian, D. Lin, Y. Deng, X.-Q. Zhang, H. Jiang, G. Miao, X. Tang and W. Zeng, *Org. Biomol. Chem.*, 2014, **12**, 5866–5875; (*b*) M. Li and Y. Ye, *ChemCatChem*, 2015, **7**, 4137–4142; (*c*) Z. Liu, Y. Xian, J. Lan, Y. Luo, W. Ma and J. You, *Org. Lett.*, 2019, **21**, 1037–1041.
18 (*a*) T. H. L. Nguyen, N. Gigant, S. Delarue-Cochin and D. Joseph, *J. Org. Chem.*, 2016, **81**, 1850–1857; (*b*) X. Fu, Z. Wei, C. Xia, C. Shen, J. Xu, Y. Yang, K. Wang and P. Zhang, *Catal. Lett.*, 2017, **147**, 400–406.
19 (*a*) Y.-F. Liang, X. Li, X. Wang, Y. Yan, P. Feng and N. Jiao, *ACS Catal.*, 2015, **5**, 1956–1963; (*b*) Z. Ahmed, A. Siiskonen, M. Virkki and A. Priimagi, *Chem. Commun.*, 2017, **53**, 12520–12523.
20 (*a*) J. Hoffmann, T. J. Kuczmera, E. Lork and A. Staubitz, *Molecules*, 2019, **24**, 303; (*b*) M. Juribašić, I. Halasz, D. Babić, D. Cinčić, J. Plavec and M. Ćurić, *Organometallics*, 2014, **33**, 1227–1234.
21 (*a*) A. Yoshimura and V. V. Zhdankin, *Chem. Rev.*, 2016, **116**, 3328–3435; (*b*) *Patai's Chemistry of Functional Groups: The Chemistry of Hypervalent Halogen Compounds*, Wiley, ed. B. Olofsson, I. Marek and Z. Rappoport, Chichester, 2019; (*c*) *Hypervalent Iodine Chemistry*, ed. T. Wirth, Springer International Publishing, Cham, 2016.
22 (*a*) E. A. Merritt and B. Olofsson, *Angew. Chem., Int. Ed.*, 2009, **48**, 9052–9070; (*b*) K. Aradi, B. L. Tóth, G. L. Tolnai and Z. Novák, *Synlett*, 2016, 1456–1485; (*c*) P. Villo and B. Olofsson, *Patai's Chemistry of Functional Groups*, Wiley, Chichester, 2019, pp. 461–522.
23 (*a*) M. D. Hossain, Y. Ikegami and T. Kitamura, *J. Org. Chem.*, 2006, **71**, 9903–9905; (*b*) M. Bielawski, M. Zhu and B. Olofsson, *Adv. Synth. Catal.*, 2007, **349**, 2610–2618; (*c*) M. Bielawski, D. Aili and B. Olofsson, *J. Org. Chem.*, 2008, **73**, 4602–4607; (*d*) M. Zhu, N. Jalalian and B. Olofsson, *Synlett*, 2008, 592–596.
24 See the ESI† for details.
25 (*a*) T. L. Seidl, S. K. Sundalam, B. McCullough and D. R. Stuart, *J. Org. Chem.*, 2016, **81**, 1998–2009; (*b*) M. D. Hossain and T. Kitamura, *Tetrahedron*, 2006, **62**, 6955–6960; (*c*) E. Lindstedt, M. Reitti and B. Olofsson, *J. Org. Chem.*, 2017, **82**, 11909–11914.
26 (*a*) C. H. Oh, J. S. Kim and H. H. Jung, *J. Org. Chem.*, 1999, **64**, 1338–1340; (*b*) J. Malmgren, S. Santoro, N. Jalalian, F. Himo and B. Olofsson, *Chem. – Eur. J.*, 2013, **19**, 10334–10342; (*c*) D. R. Stuart, *Chem. – Eur. J.*, 2017, **23**, 15852–15863.
27 (*a*) K. Aertker, R. J. Rama, J. Opalach and K. Muñiz, *Adv. Synth. Catal.*, 2017, **359**, 1290–1294; (*b*) A. Boelke, E. Lork and B. J. Nachtsheim, *Chem. – Eur. J.*, 2018, **24**, 18653–18657; (*c*) A. Boelke, S. Sadat, E. Lork and B. J. Nachtsheim, *Chem. Commun.*, 2021, **57**, 7434–7437.
28 N. Jalalian, T. B. Petersen and B. Olofsson, *Chem. – Eur. J.*, 2012, **18**, 14140–14149.
29 M. Reitti, R. Gurubrahamam, M. Walther, E. Lindstedt and B. Olofsson, *Org. Lett.*, 2018, **20**, 1785–1788.
30 S. Sarkar, N. Wojciechowska, A. A. Rajkiewicz and M. Kalek, *Eur. J. Org. Chem.*, 2022, e202101408.
31 P. Villo, G. Kervefors and B. Olofsson, *Chem. Commun.*, 2018, **54**, 8810–8813.
32 C. Dey, E. Lindstedt and B. Olofsson, *Org. Lett.*, 2015, **17**, 4554–4557.
33 N. Purkait, G. Kervefors, E. Linde and B. Olofsson, *Angew. Chem., Int. Ed.*, 2018, **57**, 11427–11431.
34 F. Tinnis, E. Stridfeldt, H. Lundberg, H. Adolfsson and B. Olofsson, *Org. Lett.*, 2015, **17**, 2688–2691.
35 M. Reitti, P. Villo and B. Olofsson, *Angew. Chem., Int. Ed.*, 2016, **55**, 8928–8932.
36 (*a*) X. Yao, T. Li, J. Wang, X. Ma and H. Tian, *Adv. Opt. Mater.*, 2016, **4**, 1322–1349; (*b*) E. Fuentes, M. Gerth, J. A. Berrocal, C. Matera, P. Gorostiza, I. K. Voets, S. Pujals and L. Albertazzi, *J. Am. Chem. Soc.*, 2020, **142**, 10069–10078.
37 Y. M. Osornio, P. Uebelhart, S. Bosshard, F. Konrad, J. S. Siegel and E. M. Landau, *J. Org. Chem.*, 2012, **77**, 10583–10595.
38 G. L. Tolnai, U. J. Nilsson and B. Olofsson, *Angew. Chem., Int. Ed.*, 2016, **55**, 11226–11230.

3.3 Stille vs. Suzuki - Cross-Coupling for the Functionalization of Diazocines

Aim:

Until recently (see Section 1.5), cross-coupling reactions of diazocines were hardly investigated and the few reported examples suffered from low yields and no general approach. As the possibilities for the synthesis of diazocines have significantly improved, cross-coupling reactions as a tool for late-stage functionalization of diazocines gained more interest, mostly with the diazocine as the formally electrophilic component. Here, a more holistic cross-coupling approach was developed with the diazocine being the formally nucleophilic component. Via the following coupling with organic bromides, the access to functionalized diazocines was expanded.

Title of Publication:

"Stille vs. Suzuki – Cross-Coupling for the Functionalization of Diazocines"
M. Walther,[‡] W. Kipke,[‡] R. Renken, A. Staubitz, *RSC Adv.* **2023**, *13*, 15805–15809.
DOI: 10.1039/D3RA02988C.
[‡] These authors contributed equally.

Abstract:

Diazocines are fairly new molecular switches and only few examples of cross-coupling reactions have been reported. In this work, we systematically compare the Stille cross-coupling of 2,9-bis-stannylated diazocines and Suzuki cross-coupling of 2,9-bis-borylated diazocines with organic bromides. It was found that a catalyst system of $Pd(OAc)_2$/XPhos was most suitable for a wide variety of coupling partners for both cross-coupling types yielding 47 - 94% (Stille cross-coupling) and 0 - 95% (Suzuki cross-coupling), respectively. Furthermore, three coupling reactions were performed exemplary on 3,8-bis-stannylated (71 - 84%) and 3,8-bis-borylated (77 - 83%) diazocines giving similarly good results. In general, the Stille cross-coupling produced better results in terms of isolated yield.

Author Contribution to this Publication:

For this publication, W. Kipke and I (M. Walther) contributed equally. Together we developed the idea of the project. The *para*-iodinated diazocine was prepared and characterized by W. Kipke and me both, and I performed the synthesis and characterization of the *meta*-iodinated diazocine. W. Kipke established the synthesis route towards the borylated diazocines and the subsequent Suzuki cross-coupling. He performed the scope of the Suzuki coupling for the *para*-borylated diazocine, while the scope of the *meta*-derivative was accomplished by the both of us. I was responsible for the stannylated diazocines and the following Stille reaction. Here, I conducted the couplings with the *meta*-derivative and the majority of the couplings with the *para*-substituted diazocine (16 compounds) as well as characterized the products. The other Stille reactions (8 compounds) of the *para*-stannylated diazocine were performed by R. Renken as part of his Bachelor thesis under my guidance. The optimization of the Stille reaction was performed by myself and R. Renken under my guidance. The Supporting Information and the manuscript were written by W. Kipke and me, edited by A. Staubitz, the principal investigator of the project.

RSC Advances

ROYAL SOCIETY OF CHEMISTRY

PAPER

View Article Online
View Journal | View Issue

Check for updates

Cite this: *RSC Adv.*, 2023, **13**, 15805

Stille *vs.* Suzuki – cross-coupling for the functionalization of diazocines†

Melanie Walther, ‡[ab] Waldemar Kipke, ‡[ab] Raul Renken[a] and Anne Staubitz *[ab]

Received 5th May 2023
Accepted 17th May 2023

DOI: 10.1039/d3ra02988c

rsc.li/rsc-advances

Diazocines are azobenzene derived macrocyclic photoswitches with well resolved photostationary states for the (*E*)- and (*Z*)-isomers, which improves their addressability by light. In this work, effective procedures for the stannylation and borylation of diazocines in different positions are reported. Their use in Stille cross-coupling and Suzuki cross-coupling reactions with organic bromides is demonstrated in yields of 47–94% (Stille cross-coupling) and 0–95% (Suzuki cross-coupling), respectively.

Introduction

In the last few years, ethylene-bridged azobenzenes, diazocines, have garnered interest because of their photochemical properties.[1] The bent (*Z*)-isomer is the thermodynamically favoured state, which can be switched to the stretched (*E*)-configuration using violet light (400 nm). The re-isomerization takes place upon irradiation with green light (520 nm) or thermally. The n–π^* absorption maxima of both isomers are well separated, which improves their specific addressability by light.[1a] Thus, diazocines are promising candidates for a wide range of applications, *e.g.* molecular imaging,[2] optical data storage[2b,3] and photodynamic therapy.[4] They also have been incorporated into functional polymers.[2a,c,3,5] However, the synthesis of functionalized diazocines is more demanding than of similarly substituted azobenzenes.[6] Since the discovery of photoswitchable properties of diazocine in 2009,[1a] the main focus has been on the development of efficient synthetic routes to obtain diazocines with various functional groups.[6] Several strategies with a broad substrate scope have been published, *e.g.* reduction of dinitro compounds,[7] oxidation of dianiline derivatives[4a,8] or a cross-coupling strategy.[9] With those in hand, the number of accessible diazocines was greatly enhanced: precursors with more complex substitution patterns were used and unsymmetrical diazocines could be obtained.[4b,10]

However, one common tool in organic chemistry for late-stage functionalization, namely cross-coupling reactions, has only been used sporadically, with diazocine as the formally electrophilic component.[4a,8a,11] and one single example with a stannylated diazocine.[12] In those examples, the cross-coupling reactions were not further investigated (Scheme 1a). We were interested in a more general cross-coupling protocol that tolerates a broad variety of functional groups, and which proceeds *via* easily accessible and storable diazocine precursors. They necessitated a high yielding synthesis of stannylated and borylated diazocines, which serve as new synthetic reagents in efficient protocols for Stille and Suzuki cross-coupling reactions. As with azobenzenes,[13] it is much rarer to be able to prepare the photoswitch as the formally nucleophilic reagent, because of the risk of reduction of the N=N double bond,[14] *e.g.* reductions of the azo group with bis(pinacolato)diboron have been reported.[15]. However, if organic bromides can be used as coupling partners, the range of accessible products is much broadened (Scheme 1b).

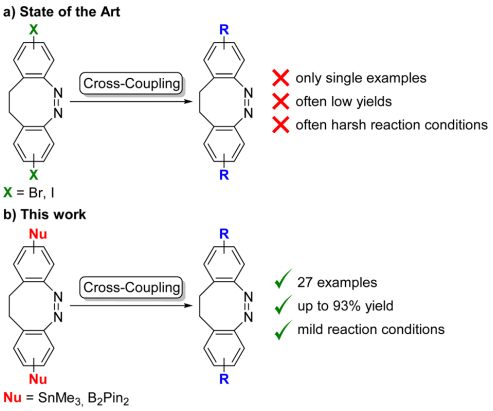

Scheme 1 Cross-coupling reaction of diazocines.

[a]University of Bremen, Institute for Analytical and Organic Chemistry, Leobener Straße 7, D-28359 Bremen, Germany. E-mail: staubitz@uni-bremen.de
[b]University of Bremen, MAPEX Center for Materials and Processes, Bibliothekstraße 1, D-28359 Bremen, Germany

† Electronic supplementary information (ESI) available. See DOI: https://doi.org/10.1039/d3ra02988c

‡ These authors contributed equally.

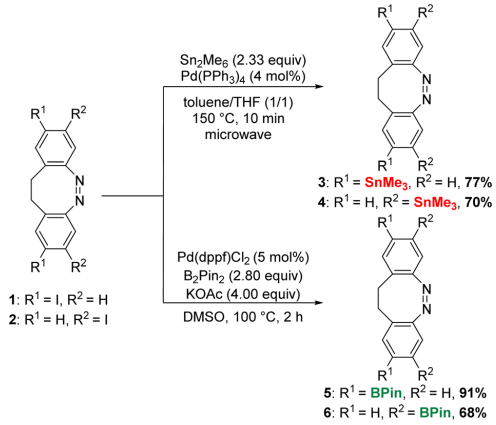

Scheme 2 Synthesis of stannylated **3**–**4** and borylated diazocines **5**–**6**.

Results and discussion

The iodinated diazocines **1** and **2** were synthesized according to optimized literature procedures in yields of 71% and 37%, respectively (see ESI†).[1a,11g,12] These were to serve as starting materials for the stannylated (**3**–**4**) or borylated diazocines (**5**–**6**) as key reagents (Scheme 2). We elected those two types of cross-coupling reaction because of the high bench stability of the corresponding metallated derivatives. Moreover, there was a high potential for the optimization of the Stille reaction as the reported examples led to very low yields of the cross-coupling (10–31%).[11b,c,12] To our knowledge, no Suzuki cross-coupling of diazocines has previously been reported.

The stannylated diazocines could be prepared by a microwave assisted Stille–Kelly cross-coupling:[13a] In this fashion, the coupling of **1** with hexamethyldistannane provided **3** in 77% and the *meta*-derivative **4** was obtained in a similar yield of 70%. In comparison to the previously published *meta*-monostannylated diazocine (51%),[12] the efficiency of the cross-coupling procedure was significantly higher.

However, the borylation was less straightforward: to synthesize the borylated precursors **5** and **6** Miyaura borylation was used as the starting point.[16] Unfortunately, this led to the formation of a reduced species in significant amounts (see ESI†). We attempted to suppress the reduction by applying a range of other catalysts, solvents or bases (see ESI†). However, it emerged that to obtain **5** in high yields up to 91%, the reaction time was the most important parameter (Scheme 2). Therefore, monitoring the reaction progress was crucial. Finally, the Miyaura borylation of **2** furnished **6** in a yield of 68%.

With the diazocine derivatives **3**–**6** in hand, we investigated their ability to serve as the formally nucleophilic coupling partner in Stille and Suzuki cross-coupling reactions (Scheme 3). The Stille reaction required significant optimization efforts regarding the catalytic systems, additives and reaction temperature (see ESI†). Eventually, a modified procedure by Buchwald[17] using a combination of $Pd(OAc)_2$ and XPhos as catalytic system and CsF as additive proved to be superior in the test reaction of **3** with 4-bromotoluene (92% yield after 4 h).

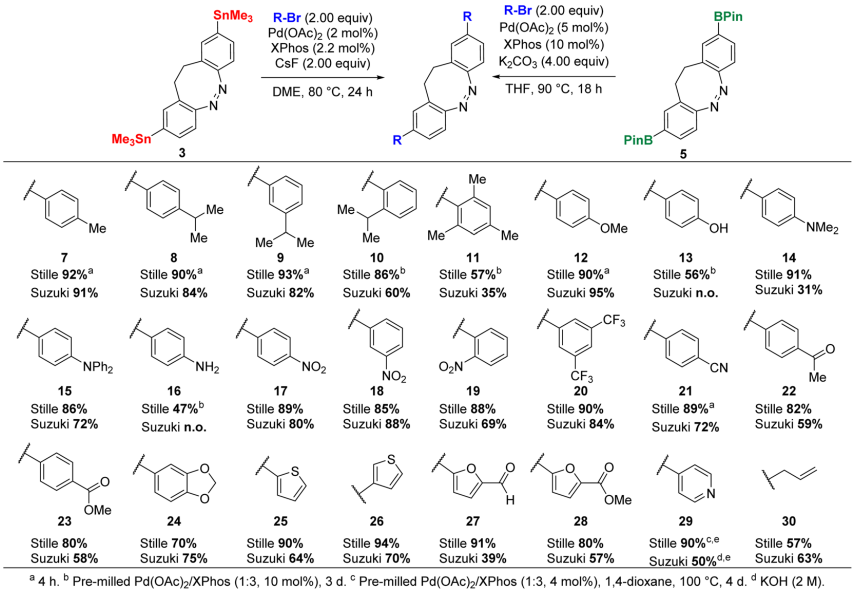

a 4 h. b Pre-milled $Pd(OAc)_2$/XPhos (1:3, 10 mol%), 3 d. c Pre-milled $Pd(OAc)_2$/XPhos (1:3, 4 mol%), 1,4-dioxane, 100 °C, 4 d. d KOH (2 M). e Used as hydrogen chloride. n.o. = not obtained.

Scheme 3 Scope of Stille and Suzuki cross-coupling reactions for *para*-substituted diazocines **3** and **5**.

For the Suzuki cross-coupling, several catalysts and ligands were investigated (see ESI†). We found that the catalytic system involving $Pd(OAc)_2$ and XPhos also yielded the best result for the Suzuki cross-coupling in the coupling reaction between **5** and 4-bromotoluene (91%).

Subsequently, this catalytic system was tested with an electron rich and an electron deficient aromatic electrophile: the coupling of the electron rich 4-bromoanisole performed in a yield of 90% for the Stille coupling and 95% for the Suzuki coupling. The reaction with the electron deficient 1-bromo-4-nitrobenzene yielded **17** in 89% (Stille) and 80% (Suzuki).

Attaching *para*-, *meta*- and *ortho*-isopropyl benzene to obtain **8**, **9** and **10** was possible in high yields except for the Suzuki coupling of 1-bromo-2-isopropylbenzene. In this case, the yield was significantly lower with 60% compared to the Stille coupling reaction with 86%. Steric hindrance seemed to influence the Suzuki cross-coupling more strongly than the Stille cross-coupling. This observation was supported by the synthesis of mesityl-diazocine **11** and *o*-nitrophenyl-diazocine **19**. However, to gain the sterically demanding di-functionalized diazocines **10** and **11** in a sufficient yield *via* the Stille reaction, the amount of catalyst needed to be increased: while the standard reaction conditions mainly led to the mono-coupled diazocines, using 10 mol% of a 1 : 3 mixture of $Pd(OAc)_2$/XPhos furnished **10** in 86% and **11** in 57% yield. Increasing the catalyst load (up to 20 mol%) for the Suzuki cross-coupling, did not improve the yield of **11**.

Further cross-coupling reactions of electron deficient compounds provided **18**, **20** and **21** in high yields for both cross-coupling types tolerating nitro, nitrile and trifluoromethyl groups. The coupling of stronger coordinating compounds with free electron pairs, *e.g.* aryl aldehyde (**22**), aryl ester (**23**) and furan heterocycles (**27** and **28**), proceeded in low to moderate yields (39–59%) for the Suzuki cross-coupling, while the Stille cross-coupling gave high yields (80–91%). The same trend became apparent upon the coupling of other heterocycles such as thiophenes (**25** and **26**) or pyridine (**29**): the Stille coupling yielded excellent results (90–94%), whereas moderate yields were obtained with the Suzuki coupling (57–66%). However, the functionalization with 4-bromopyridine proved to be challenging for both cross-coupling types.

For the Stille reaction of **3** with 4-bromopyridine it was necessary to increase the temperature to 100 °C and thus the solvent had to be changed to the higher boiling DMSO. For the Suzuki coupling no product could be isolated applying the standard conditions. The desired compound **29** was only obtained with potassium hydroxide a stronger base in aqueous mixture with THF instead of potassium carbonate.

Other electron rich aryl bromides were coupled with **3** and **5** yielding tertiary amines **14** and **15** as well as benzo-dioxole **24** in good to excellent yields. Only compound **14** was isolated in a lower yield of 31% for the Suzuki coupling. Moreover, it was possible to react the unprotected 4-bromophenol and aniline *via* the Stille reaction using 10 mol% of a 1 : 3 mixture of $Pd(OAc)_2$/XPhos. The corresponding diazocines 13 and 16 were obtained in 56% and 47% yield, respectively.

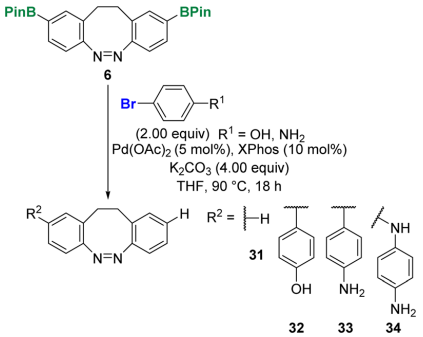

Scheme 4 Side reactions of Suzuki cross-coupling.

For the corresponding Suzuki cross-couplings a multitude of different species was observed (Scheme 4). In both cases, the unsubstituted diazocine **31** was obtained as the main product. Besides the monosubstituted side products **32** and **33**, we could also identify secondary amine **34** as a coupling product with 4-bromoaniline, which suggests a competing Buchwald–Hartwig cross-coupling reaction. In order to solve the problem, we increased the catalyst load to 20 mol% and changed the base (2 M KOH) but neither changing one condition nor changing both at the same time led to the desired products **13** and **16**.

Lastly, it was also possible to react diazocines **3** and **5** with a non-aromatic bromide. Allyl bromide was coupled to yield **30** in 57% (Stille) and 63% (Suzuki), which could be of use as crosslinker for polymerization reactions (Scheme 3).

It was also investigated if the substitution position of the diazocine influences the cross-coupling reactions. In line with the previous test reactions for *para*-substituted diazocines **3** and **5**, 4-bromotoluene, 4-bromoanisole and 1-bromo-4-nitrobenzene were therefore coupled as model substrates with **4** and **6** (Scheme 5). In all cases, good yields were obtained for the Stille (71–84%) and Suzuki coupling (77–83%). In comparison with the corresponding reactions with *para*-substituted diazocines **3** and **5**, the yields were generally lower; *e.g.* the coupling of 4-bromoanisole with *para*-substituted diazocines **3** and **5** proceeded in 90% (Stille) and 95% (Suzuki) but with *meta*-substituted diazocines **4** and **6** in 71% (Stille) and 78% (Suzuki).

Experimental

General procedure for the Stille–Kelly cross-coupling reaction

Under inert conditions, the corresponding di-iodinated diazocine (345 mg, 750 μmol, 1.00 equiv.), hexamethyldistannane (573 mg, 1.75 mmol, 2.33 equiv.) and $[Pd(PPh_3)_4]$ (34.8 mg, 30.0 μmol, 4 mol%) were dissolved in toluene (2.5 mL) and THF (2.5 mL) in a microwave reaction vessel. The reaction mixture was stirred for 10 min at 150 °C under microwave irradiation and subsequently filtered through Celite®. Then, the solvent and excess hexamethyldistannane were removed under reduced pressure (9.5 × 10–2 mbar, 80 °C). The residue was purified *via* column chromatography on silica.

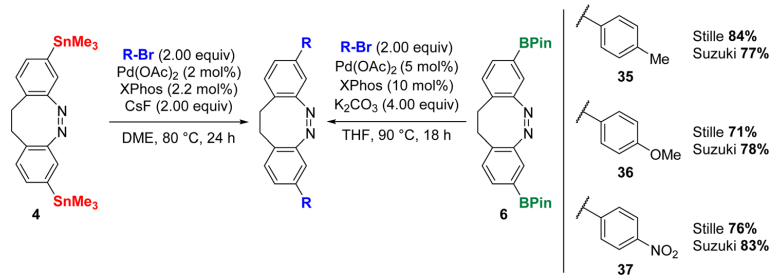

Scheme 5 Scope of Stille and Suzuki cross-coupling reactions for *meta*-substituted diazocines **4** and **6**.

General procedure for the Miyaura borylation

Under inert conditions, the corresponding di-iodinated diazocine (1.00 equiv.), $Pd(dppf)Cl_2$ (5 mol%), B_2Pin_2 (2.80 equiv.) and KOAc (4.00 equiv.) were dissolved in DMSO (10 mL $mmol^{-1}$). The mixture was stirred at 100 °C and the reaction progress was monitored by TLC (cyclohexane/DCM/ethyl acetate 55/40/5). After completion (approx. 2 h), the reaction mixture was diluted with ethyl acetate (20 mL $mmol^{-1}$) and washed with brine (4 × 50 mL $mmol^{-1}$). The organic phase was dried over sodium sulfate, filtered and the solvent removed *in vacuo*. The residue was purified by column chromatography on silica (eluent: cyclohexane/DCM/ethyl acetate 55/40/5) to obtain the corresponding diazocine as a yellow solid.

General procedure for Stille cross-coupling reaction

Under inert conditions, the corresponding di-stannylated diazocine (53.4 mg, 100 µmol, 1.00 equiv.), the corresponding brominated coupling partner (200 µmol, 2.00 equiv.), $Pd(OAc)_2$ (449 µg, 2.00 µmol, 2 mol%), XPhos (1.05 mg, 2.20 µmol, 2.2 mol%) and CsF (30.4 mg, 200 µmol, 2.00 equiv.) were dissolved in dry DME (2 mL) in a pressure reaction vial. The mixture was stirred at 80 °C for 24 h. After cooling to 23 °C, the reaction mixture was filtered through Celite® and the solvent was removed under reduced pressure.

General procedure for Suzuki cross-coupling

Under inert conditions, the corresponding di-borylated diazocine 5 (46.0 mg, 100 µmol, 1.00 equiv.), $Pd(OAc)_2$ (1.12 mg, 5 µmol, 5 mol%), XPhos (4.77 mg, 10.0 µmol, 10 mol%), K_2CO_3 (69.11 mg, 500 µmol, 5.00 equiv.) and the corresponding brominated coupling partner (200 µmol, 2.00 equiv.) were dissolved in THF (5 mL) and sealed in a pressure reaction vial. The mixture was stirred at 90 °C for 18 h. After cooling to 23 °C, the reaction mixture was filtered through Celite® and the solvent was removed under reduced pressure.

Conclusions

In summary, we developed a robust synthetic methodology to bench-stable bis-stannylated and bis-borylated diazocines in *meta*- and *para*-position to the azo group. These served precursors for Stille and Suzuki cross-coupling reactions with a broad scope of electrophiles. The catalytic system $Pd(OAc)_2$/XPhos yielded good to excellent results and tolerated a wide range of functional groups. In this way, functionalized diazocines that might be of interest in material science or biological applications were straight-forward synthesized. While steric hindrance and electron lone pairs lowered the yield, this was observed for the Stille reaction to a smaller extent. Here, the reaction conditions could be easily adapted in order to obtain the desired product in a satisfying yield. Moreover, the coupling of anilines or phenols was possible using the Stille cross-coupling, while Buchwald–Hartwig type side reactions were observed under the Suzuki conditions. Overall, the Stille reaction produced better results in terms of isolated yields and in most cases less catalyst was needed. Nevertheless, other factors besides the yield have to be considered when planning a reaction. In fact, the Stille coupling outperformed the Suzuki coupling applying the here described conditions but the higher potential health risk of the Stille coupling due to the involvement of tin compounds should be mentioned. Depending on the scientific question, the use of the borylated compound for Suzuki coupling reactions might be preferred.

Author contributions

Conceptualization, M. W., W. K. and A. S.; methodology, M. W. and W. K.; validation, M. W., W. K. and A. S.; formal analysis, M. W., W. K. and R. R.; investigation, M. W., W. K. and R. R.; resources, A. S.; data curation, M. W. and W. K.; writing—original draft preparation, M. W. and W. K.; writing—review and editing, M. W., W. K., R. R. and A. S.; visualization, M. W. and W. K.; supervision, A. S.; project administration, A. S.; funding acquisition, A. S. all authors have read and agreed to the published version of the manuscript.

Conflicts of interest

There are no conflicts to declare.

Acknowledgements

The authors are grateful to Amelie Sprengel for measuring IR spectra.

Notes and references

1 (*a*) R. Siewertsen, H. Neumann, B. Buchheim-Stehn, R. Herges, C. Näther, F. Renth and F. Temps, *J. Am. Chem. Soc.*, 2009, **131**, 15594–15595; (*b*) C. Deo, N. Bogliotti, R. Métivier, P. Retailleau and J. Xie, *Chem.–Eur. J.*, 2016, **22**, 9092–9096; (*c*) M. Hammerich, C. Schutt, C. Stahler, P. Lentes, F. Rohricht, R. Hoppner and R. Herges, *J. Am. Chem. Soc.*, 2016, **138**, 13111–13114.

2 (*a*) M. H. Burk, S. Schröder, W. Moormann, D. Langbehn, T. Strunskus, S. Rehders, R. Herges and F. Faupel, *Macromolecules*, 2020, **53**, 1164–1170; (*b*) M. H. Burk, D. Langbehn, G. Hernández Rodríguez, W. Reichstein, J. Drewes, S. Schröder, S. Rehders, T. Strunskus, R. Herges and F. Faupel, *ACS Appl. Polym. Mater.*, 2021, **3**, 1445–1456; (*c*) S. Li, R. Colaco and A. Staubitz, *ACS Appl. Polym. Mater.*, 2022, **4**, 6825–6833.

3 S. Li, G. Han and W. Zhang, *Macromolecules*, 2018, **51**, 4290–4297.

4 (*a*) G. Cabré, A. Garrido-Charles, À. González-Lafont, W. Moormann, D. Langbehn, D. Egea, J. M. Lluch, R. Herges, R. Alibés, F. Busqué, P. Gorostiza and J. Hernando, *Org. Lett.*, 2019, **21**, 3780–3784; (*b*) J. Ewert, L. Heintze, M. Jorda-Redondo, J. S. von Glasenapp, S. Nonell, G. Bucher, C. Peifer and R. Herges, *J. Am. Chem. Soc.*, 2022, **144**, 15059–15071; (*c*) M. Reynders, B. S. Matsuura, M. Bérouti, D. Simoneschi, A. Marzio, M. Pagano and D. Trauner, *Sci. Adv.*, 2020, **6**, eaay5064; (*d*) S. Samanta, C. Qin, A. J. Lough and G. A. Woolley, *Angew. Chem., Int. Ed.*, 2012, **51**, 6452–6455.

5 S. Li, K. Bamberg, Y. Lu, F. D. Sönnichsen and A. Staubitz, *Polymers*, 2023, **15**, 1306.

6 M. Walther, W. Kipke, S. Schultzke, S. Ghosh and A. Staubitz, *Synthesis*, 2021, **53**, 1213–1228.

7 (*a*) W. Moormann, D. Langbehn and R. Herges, *Synthesis*, 2017, **49**, 3471–3475; (*b*) H. Sell, C. Nather and R. Herges, *Beilstein J. Org. Chem.*, 2013, **9**, 1–7; (*c*) F. Klockmann, C. Fangmann, E. Zender, T. Schanz, C. Catapano and A. Terfort, *ACS Omega*, 2021, **6**, 18434–18441; (*d*) W. Moormann, D. Langbehn and R. Herges, *Beilstein J. Org. Chem.*, 2019, **15**, 727–732; (*e*) D. K. Joshi, M. J. Mitchell, D. Bruce, A. J. Lough and H. Yan, *Tetrahedron*, 2012, **68**, 8670–8676.

8 (*a*) M. S. Maier, K. Hull, M. Reynders, B. S. Matsuura, P. Leippe, T. Ko, L. Schaffer and D. Trauner, *J. Am. Chem. Soc.*, 2019, **141**, 17295–17304; (*b*) J. Wang, J. He, C. Zhi, B. Luo, X. Li, Y. Pan, X. Cao and H. Gu, *RSC Adv.*, 2014, **4**, 16607–16611.

9 S. Li, N. Eleya and A. Staubitz, *Org. Lett.*, 2020, **22**, 1624–1627.

10 (*a*) J. B. Trads, K. Hull, B. S. Matsuura, L. Laprell, T. Fehrentz, N. Gorldt, K. A. Kozek, C. D. Weaver, N. Klocker, D. M. Barber and D. Trauner, *Angew. Chem., Int. Ed.*, 2019, **58**, 15421–15428; (*b*) N. Preußke, W. Moormann, K. Bamberg, M. Lipfert, R. Herges and F. D. Sönnichsen, *Org. Biomol. Chem.*, 2020, **18**, 2650–2660.

11 (*a*) M. Jun, D. K. Joshi, R. S. Yalagala, J. Vanloon, R. Simionescu, A. J. Lough, H. L. Gordon and H. Yan, *ChemistrySelect*, 2018, **3**, 2697–2701; (*b*) E. R. Thapaliya, J. Zhao and G. C. R. Ellis-Davies, *ACS Chem. Neurosci.*, 2019, **10**, 2481–2488; (*c*) Q. Zhu, S. Wang and P. Chen, *Org. Lett.*, 2019, **21**, 4025–4029; (*d*) M. Reynders, A. Chaikuad, B. T. Berger, K. Bauer, P. Koch, S. Laufer, S. Knapp and D. Trauner, *Angew. Chem., Int. Ed.*, 2021, **60**, 20178–20183; (*e*) T. Ko, M. M. Oliveira, J. M. Alapin, J. Morstein, E. Klann and D. Trauner, *J. Am. Chem. Soc.*, 2022, **144**, 21494–21501; (*f*) H. Lee, J. Tessarolo, D. Langbehn, A. Baksi, R. Herges and G. H. Clever, *J. Am. Chem. Soc.*, 2022, **144**, 3099–3105; (*g*) S. Schultzke, M. Walther and A. Staubitz, *Molecules*, 2021, **26**, 3916.

12 L. Heintze, D. Schmidt, T. Rodat, L. Witt, J. Ewert, M. Kriegs, R. Herges and C. Peifer, *Int. J. Mol. Sci.*, 2020, **21**, 8961.

13 (*a*) J. Strueben, P. J. Gates and A. Staubitz, *J. Org. Chem.*, 2014, **79**, 1719–1728; (*b*) J. Strueben, M. Lipfert, J.-O. Springer, C. A. Gould, P. J. Gates, F. D. Sönnichsen and A. Staubitz, *Chem.–Eur. J.*, 2015, **21**, 11165–11173.

14 A. R. Katritzky, J. Wu and S. V. Verin, *Synthesis*, 1995, **1995**, 651–653.

15 (*a*) G. Wang, H. Zhang, J. Zhao, W. Li, J. Cao, C. Zhu and S. Li, *Angew. Chem., Int. Ed.*, 2016, **55**, 5985–5989; (*b*) M. Song, H. Zhou, G. Wang, B. Ma, Y. Jiang, J. Yang, C. Huo and X. C. Wang, *J. Org. Chem.*, 2021, **86**, 4804–4811.

16 T. Ishiyama, M. Murata and N. Miyaura, *J. Org. Chem.*, 1995, **60**, 7508–7510.

17 J. R. Naber and S. L. Buchwald, *Adv. Synth. Catal.*, 2008, **350**, 957–961.

4 Conclusion and Outlook

This thesis aimed at enhancing the late-stage functionalization of azobenzenes to expand the access towards tailored azobenzene based photoswitches for future applications in materials and life sciences. Different chemical dimensions and several features of the azobenzene were examined. Therefore, efficient protocols for the synthesis of the iodinated precursors were installed and the flexibility of this motif was exploited in three distinct approaches:

Cross-Coupling Protocol for Photoswitchable NHS Esters. In the first subproject (Section 3.1), a robust and efficient cross-coupling procedure to yield mono- and di-NHS functionalized azobenzene **1k** and diazocine derivatives **9e** under mild conditions was established. For this purpose, the iodinated precursors **1j** and **9d** were reacted with NHS formate as CO surrogate in a palladium catalyzed carbonylation to the corresponding active esters **1k** and **9e** that were subsequently quantitatively converted in a condensation reaction using a carboxyl group protected amino acid (Scheme 4.1).

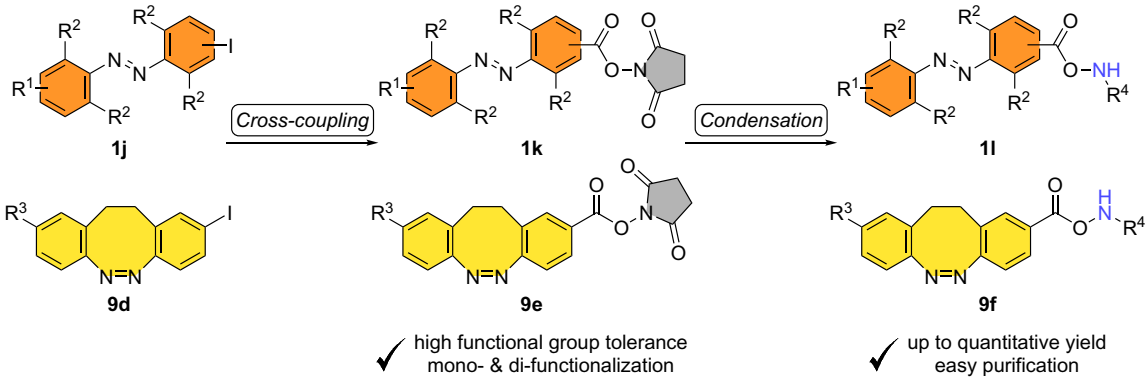

Scheme 4.1 The NHS functionalized azobenzenes **1k** and diazocines **9e** were obtained via a Pd catalyzed carbonylation reaction with NHS formate and subsequently reacted with a carboxyl group protected amino acid in a condensation.

With this newly developed procedure, it was possible to synthesize previously inaccessible photoswitches, which cannot be obtained by conventional syntheses for active esters, e.g., azobenzenes decorated with an ether or a primary hydroxyl group as well as a further bromine substituent. Moreover, tetra-*ortho*-functionalized azobenzenes and diazocines could be utilized. Thus, active esters with absorption in the visible range of light and separated absorption maxima were acquired, which are two main aims of current azobenzene research. As NHS esters react readily and in a quantitative manner with primary amines, this becomes even more relevant for biological applications[208] where UV light might harm cells and where primary amines are ubiquitous in all types of biomolecules. Hence, future research will focus on the integration of the obtained NHS esters **1k** and **9e** into materials and the investigation of the material properties for the desired application.

Hypervalent Iodine(III) Azobenzene Derivatives. By combining hypervalent iodine(III) chemistry with *ortho*-azobenzenes **1m**, a new class of compounds was created: *ortho*-azobenzene(aryl)iodonium salts **23d** (Section 3.2). These useful building blocks were obtained in high yields via oxidation of *ortho*-iodinated azobenzenes **1m** using *m*CPBA and their potential as chemoselective arylation agents was demonstrated upon reactions with different C, N, O and S-nucleophiles under mild and transition metal-free conditions (Scheme 4.2). The structural and photoswitchable properties of the hypervalent iodine(III) azobenzene **23d** were investigated revealing that the nitrogen of the azobenzene is involved in hypervalent bonding with the iodine(III) center in the (*E*)-isomer. The photoswitchable features were retained: While the incorporation of the hypervalent iodine bond influenced the position of the absorption maxima only slightly, the half-life time was significantly decreased, most likely due to N-I stabilizing interactions in the (*E*)-isomer and the strong electron acceptor character of the iodine(III) moiety.

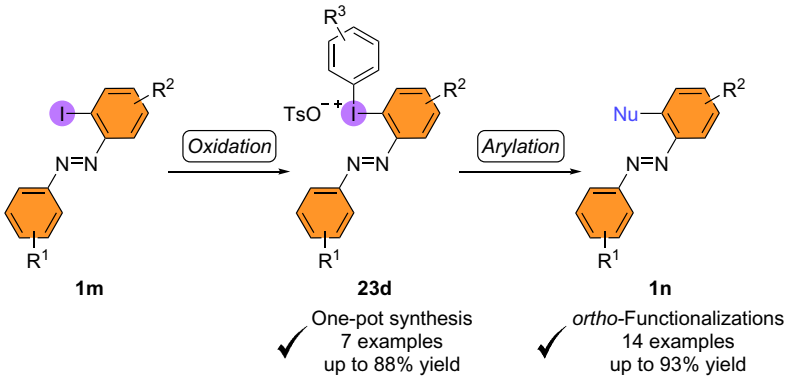

Scheme 4.2 The *ortho*-azobenzene(aryl)iodonium salts **23d** were obtained via oxidation using *m*CPBA in a one-pot synthesis and subsequently reacted with C, N, O and S-nucleophiles in mild transition metal-free arylations yielding a large scope of *ortho*-functionalized azobenzenes **1n**.

The photoswitchable properties of azobenzenes **1** are highly tunable via *ortho*-functionalization, i.e., not only the position of the absorption maxima can be altered drastically but also the half-life of the metastable (*Z*)-isomer **(*Z*)-1**. Hence, modification possibilities of the *ortho*-positon are in great demand. Especially, since cross-coupling reactions often fail *ortho* to the diazenyl group and C-H activation carries the risk that the azo bridge does not persist the reaction conditions. The oxidation to hypervalent iodine(III) azobenzene derivatives **23d** and following arylations expand significantly the toolbox for *ortho*-functionalization of azobenzenes **1**. Future research will therefore extend the possibilities of this methodolodgy even further. For example, different substitution patterns are conceivable to produce tetra-*ortho*-substituted azobenzenes switchable with visible light based on precursors such as 2,2'-diiodo-6,6'-dimethylazobenzene.

Cross-Coupling Reactions of Metalated Diazocines. Finally, cross-coupling reactions of *meta*- and *para*-difunctionalized diazocines **9e** and **9f** were investigated (Section 3.3). In a first step, the iodinated diazocines **9d** were either stannylated via Stille-Kelly cross-coupling using hexamethyldistannane or borylated via Miyaura borylation using bis(pinacolato)diboron. These served afterwards as formally nucleophilic component in Stille and Suzuki cross-coupling reactions with a wide range of organic bromides (Scheme 4.3).

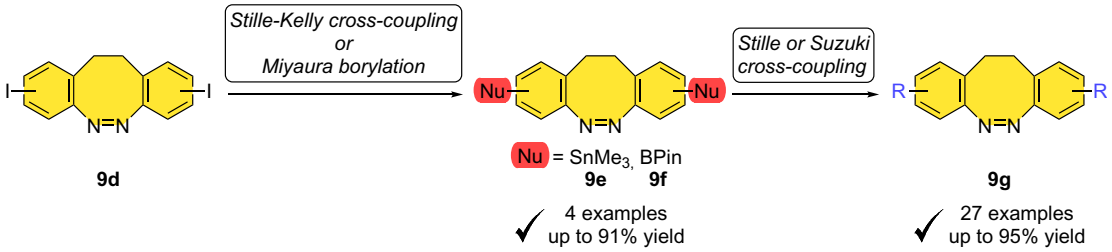

Scheme 4.3 Stannylated **9e** and borylated diazocines **9f** were obtained via Stille-Kelly cross-coupling or Miyaura borlyation, respectively. These molecules were then reacted in Stille and Suzuki cross-couplings with various organic bromides.

Not only were robust synthetic protocols for the generation of bis-stannylated **9e** and bis-borylated diazocines **9f** developed but also general cross-coupling conditions for nucleophilic diazocines established, showing a high tolerance to functional groups. This enabled the transition from single individual examples in literature to a more holistic approach in the late-stage functionalization of diazocines facilitating the use of this type of photoswitch in different fields of science. Especially for applications, where it is beneficial to have the (*E*)-isomer as the thermodynamically stable isomer, this synthesis strategy is of high value. Moreover, with the bis-stannylated diazocines **9e** in hand, a tin-lithium exchange will become feasible facilitating access to a new field of functionalizations for diazocines.

In summary, three efficient methodologies for late-stage functionalization of azobenzene based switches were established. Different chemical dimensions and characteristics of the photoswitch were investigated. For the latter, diverse substitution patterns were obtained for cyclic and open azobenzene derivatives enabling the tuning of the switching properties without using pre-functionalized starting materials. Current emphases of azobenzene research can be addressed by the developed synthetic procedures such as switching with visible light. Consequently, the next step will be the incorporation of the photoswitches into materials for various types of applications.

5 Experimental Section

5.1 Active Ester Functionalized Azobenzenes as Versatile Building Blocks

Supporting Information

Active Ester Functionalized Azobenzenes as Versatile Building Blocks

Sven Schultzke [1,2,†], Melanie Walther [1,2,†] and Anne Staubitz [1,2,*]

[1] University of Bremen, Institute for Analytical and Organic Chemistry, Leobener Straße 7, D-28359 Bremen, Germany

[2] University of Bremen, MAPEX Center for Materials and Processes, Bibliothekstraße 1, D-28359 Bremen, Germany

* Correspondence: staubitz@uni-bremen.de; Tel.: +49421/21863210

† Both authors contributed equally to this work.

Table of Contents

General Information ... 3
Reagents ... 4
Solvents ... 5
Syntheses ... 6
General procedure 1 ... 6
General procedure 2 ... 6
2,5-Dioxopyrrolidin-1-yl (*E*)-4-(phenyldiazenyl)benzoate[2] (**3a**) ... 7
2,5-Dioxopyrrolidin-1-yl (*E*)-3-(phenyldiazenyl)benzoate[2] (**3b**) ... 7
2,5-Dioxopyrrolidin-1-yl (*E*)-4-((4-hydroxyphenyl)diazenyl)benzoate[3] (**3d**) ... 8
2,5-Dioxopyrrolidin-1-yl (*E*)-4-((4-aminophenyl)diazenyl)benzoate (**3e**) ... 8
2,5-Dioxopyrrolidin-1-yl (*E*)-4-((4-acetamidophenyl)diazenyl)benzoate (**3f**) ... 9
2,5-Dioxopyrrolidin-1-yl (*E*)-4-((4-nitrophenyl)diazenyl)benzoate (**3g**) ... 9
2,5-Dioxopyrrolidin-1-yl (*E*)-4-((4-(allyloxy)phenyl)diazenyl)benzoate (**3h**) ... 10
2,5-Dioxopyrrolidin-1-yl (*E*)-4-((4-((9-hydroxynonyl)oxy)phenyl)diazenyl)benzoate (**3i**) ... 10
2,5-Dioxopyrrolidin-1-yl (*E*)-4-((2,6-dimethyl-4-(nonyloxy)phenyl)diazenyl)-3,5-dimethylbenzoate (**3j**) ... 11

2,5-Dioxopyrrolidin-1-yl (*E*)-4-((2,7-bis(4-(hexyloxy)phenoxy)naphthalen-1-yl)diazenyl)-3,5-dimethylbenzoate (**3k**) ... 12
2,5-Dioxopyrrolidin-1-yl (*E*)-4-((4-bromophenyl)diazenyl)benzoate (**3l**) ... 12
2,5-Dioxopyrrolidin-1-yl (*E*)-4-((3-bromophenyl)diazenyl)benzoate (**3m**) ... 13
2,5-Dioxopyrrolidin-1-yl (*E*)-4-((2-bromophenyl)diazenyl)benzoate (**3n**) ... 13
Bis(2,5-dioxopyrrolidin-1-yl)4,4´-(diazene-1,2-diyl)(*E*)-dibenzoate[5] (**5a**) ... 14
Bis(2,5-dioxopyrrolidin-1-yl) 4,4'-(diazene-1,2-diyl)(*E*)-bis(3,5-dimethoxybenzoate) (**5b**) ... 14
Bis(2,5-dioxopyrrolidin-1-yl) 4,4'-(diazene-1,2-diyl)(*E*)-bis(3,5-dimethylbenzoate) (**5c**) ... 15
Bis(2,5-dioxopyrrolidin-1-yl) 4,4'-(diazene-1,2-diyl)(*E*)-bis(3,5-difluorobenzoate) (**5d**) ... 15
2,5-Dioxopyrrolidin-1-yl (Z)-11,12-dihydrodibenzo[c,g][1,2]diazocine-2-carboxylate (**8a**) ... 16
Bis(2,5-dioxopyrrolidin-1-yl) (Z)-11,12-dihydrodibenzo[c,g][1,2]diazocine-2,9-dicarboxylate (**8b**) . 17
Di-*tert*-butyl 2,2'-((4,4'-(diazene-1,2-diyl)bis(benzoyl))bis(azanediyl))(*E*)-dipropionate (**10a**) ... 17
Di-*tert*-butyl 2,2'-((11,12-dihydrodibenzo[c,g][1,2]diazocine-2,9-dicarbonyl)bis(azane-diyl))(*Z*)-dipropionate (**10b**) ... 18
Determination of the ^{1}H NMR Yields ... 19
N-Hydroxysuccinimidyl formate[5] (**2**) ... 21
(*E*)-1-(4-Iodophenyl)-2-phenyldiazene[6] (**1a**) ... 21
(*E*)-1-(3-Iodophenyl)-2-phenyldiazene[6] (**1b**) ... 22
(*E*)-1-(2-Iodophenyl)-2-phenyldiazene[6] (**1c**) ... 22
(*E*)-4-((4-Iodophenyl)diazenyl)phenol[7] (**1d**) ... 23
(*E*)-4-((4-Iodophenyl)diazenyl)aniline (**1e**) ... 23
(*E*)-*N*-(4-((4-Iodophenyl)diazenyl)phenyl)acetamide (**1f**) ... 24
(*E*)-1-(4-Iodophenyl)-2-(4-nitrophenyl)diazene[8] (**1g**) ... 24
(*E*)-1-(4-(Allyloxy)phenyl)-2-(4-iodophenyl)diazene[9] (**1h**) ... 25
(*E*)-9-(4-((4-Iodophenyl)diazenyl)phenoxy)nonan-1-ol (**1i**) ... 26
(*E*)-4-((4-Iodo-2,6-dimethylphenyl)diazenyl)-3,5-dimethylphenol (**S1**) ... 26
(*E*)-1-(2,6-Dimethyl-4-(nonyloxy)phenyl)-2-(4-iodo-2,6-dimethylphenyl)diazene (**1j**) ... 27
(*E*)-1-((4-Iodo-2,6-dimethylphenyl)diazenyl)naphthalene-2,7-diol (**S2**) ... 27
(*E*)-1-((4-Iodo-2,6-dimethylphenyl)diazenyl)naphthalene-2,7-diyl bis(4-(hexyloxy)benzoate) (**1k**) . 28
(*E*)-1-(4-Bromophenyl)-2-(4-iodophenyl)diazene[10] (**1l**) ... 29
(*E*)-1-(3-Bromophenyl)-2-(4-iodophenyl)diazene (**1m**) ... 29
(*E*)-1-(2-Bromophenyl)-2-(4-iodophenyl)diazene (**1n**) ... 30
(*E*)-1,2-Bis(4-iodophenyl)diazene[11] (**4a**) ... 31
4-Iodo-2,6-dimethylaniline[12] (**S3**) ... 31
(*E*)-1,2-Bis(4-iodo-2,6-dimethylphenyl)diazene[13] (**4b**) ... 32
4-Bromo-2,6-dimethoxyaniline[14] (**S4**) ... 32
(*E*)-1,2-Bis(4-bromo-2,6-dimethoxyphenyl)diazene[15] (**S5**) ... 33

(*E*)-1,2-Bis(4-iodo-2,6-dimethoxyphenyl)diazene (**4c**) 33
4-Iodo-2,6-difluoro-aniline[16] (**S6**) 34
(*E*)-1,2-bis(2,6-difluoro-4-iodophenyl)diazene[17] (**4d**) 34
4-Bromo-2,6-difluoroaniline[18] (**S7**) 35
4-Amino-3,5-difluorobenzonitrile[19] (**S8**) 35
4-Amino-3,5-difluorobenzoic acid[20] (**S9**) 36
Ethyl 4-amino-3,5-difluorobenzoate[20] (**S10**) 36
(*E*)-4,4'-(Diazene-1,2-diyl)bis(3,5-difluorobenzoic acid)[17] (**S11**) 37
(*E*)-4,4'-(Diazene-1,2-diyl)bis(3,5-difluorobenzoic acid)[20] (**6**) 37
2-(2-(2-Aminophenethyl)phenyl)isoindoline-1,3-dione[21] (**S12**) 38
2-(2-Aminophenethyl)-4-iodoaniline[21] (**S13**) 39
(*Z*)-2-Iodo-11,12-dihydrodibenzo[c,g][1,2]diazocine[21] (**7a**) 39
2,2'-(Ethane-1,2-diyl)bis(4-iodoaniline)[21] (**S14**) 40
(*Z*)-2,9-Diiodo-11,12-dihydrodibenzo[c,g][1,2]diazocine[21] (**7b**) 40
References 41
^{1}H, ^{13}C{^{1}H} and ^{19}F NMR Spectra of the Purified Compounds 43
^{1}H NMR Spectra for the Determination of the ^{1}H NMR Yield 105

General Information

For reactions under inert conditions, a nitrogen filled glovebox (Pure Lab^{HE} from Inert, Amesbury, MA USA) and standard Schlenk techniques were used.

All carbonylation reactions were performed in microwave reaction vials sealed with a septum cap from Biotage (Biotage, Uppsala, Sweden).

All glassware was dried in an oven at 200 °C for several hours prior to use. NMR tubes were dried in an oven at 110 °C for several hours prior to use.

NMR spectra were recorded on a Bruker Avance Neo 600 (Bruker BioSpin, Rheinstetten, Germany) (600 MHz (^{1}H), 151 MHz (^{13}C{^{1}H}), 565 MHz (^{19}F) at 298 K. All ^{1}H NMR and ^{13}C{^{1}H} NMR spectra were referenced to the residual proton signals of the solvent (^{1}H) or the solvent itself (^{13}C{^{1}H}). ^{19}F NMR spectra were referenced internally against trichlorofluoromethane. The exact assignment of the peaks was performed by two-dimensional NMR spectroscopy such as ^{1}H COSY, ^{13}C{^{1}H} HSQC and ^{1}H/^{13}C{^{1}H} HMBC when possible.

High-resolution EI mass spectra were recorded on a MAT 95XL double-focusing mass spectrometer from Finnigan MAT (Thermo Fisher Scientific, Waltham, MA, USA) at an ionization energy of 70 eV. Samples were measured by a direct or indirect inlet method with a source temperature of 200 °C. High-resolution ESI and APCI mass spectra were measured by a direct inlet method on an Impact II mass spectrometer from Bruker Daltonics (Bruker Daltonics, Bremen, Germany). ESI mass spectra were recorded in the positive ion collection mode.

IR spectra were recorded on a Nicolet i510 FT-IR spectrometer from Thermo Fisher Scientific (Thermo Fisher Scientific, Waltham, MA, USA) with a diamond window in an area from 500 – 4000 cm^{-1} with a resolution of 4 cm^{-1}. All samples were measured 16 times against a background scan.

Melting points were recorded on a Büchi Melting Point M-560 (Büchi, Essen, Germany) and are reported corrected.

Thin layer chromatography (TLC) was performed using TLC Silica gel 60 F_{254} from Merck (Merck, Darmstadt, Germany) and compounds were visualized by exposure to UV light at a wavelength of 254 nm. Column chromatography was performed either manually using silica gel 60 (0.015-0.040 mm) from Merck (Merck, Darmstadt, Germany) or by using a PuriFlash 4250 column machine (Interchim, Mannheim, Germany). Silica gel columns of the type CHROMABOND Flash RS 15 SPHERE SiOH 15 µm (Macherey-Nagel, Düren, Germany) were used. The sample was applied via dry load with Celite® 503 (Macherey-Nagel, Düren, Germany) as column material. If stated, Celite® 503 (Macherey-Nagel, Düren, Germany) was used as filtration aid.

The use of abbreviations follows the conventions from the ACS Style guide[1].

Reagents

All chemicals were commercially available and used without purification unless stated otherwise.

Table S1. List of supplier and purity of used chemicals.

Reagent	Supplier	Purity	Comments
L-Alanine *tert*-butyl ester hydrochloride	Apollo Scientific		stored in a fridge in a glovebox
4-Aminoacetanilide	TCI	>98%	
2-Bromoaniline	Fluorochem	97%	
3-Bromoaniline	TCI	>98.0%	
4-Bromoaniline	Sigma Aldrich	97%	
9-Bromo-1-nonanol	Sigma Aldrich	95%	
N-Bromosuccinimide	Sigma Aldrich	98%	
1,8-Diazabicyclo[5.4.0]-undec-7-ene	Apollo	99.6%	
2,6-Difluoroanilin	chemPur	97%	
2,7-Dihydroxynapthalene	TCI	99%	
2,6-Dimethoxyanilin	BLDPharm	97%	
2,6-Dimethylaniline	TCI	99%	
3,5-Dimethylphenol	Sigma Aldrich	98%	
2,2'-Ethylenedianiline	TCI	>98%	
Hydrazine monohydrate	abcr	98%	
Hydrochloric acid	Sigma Aldrich		fuming, ≥37%
N-Hydroxysuccinimide	Apollo Scientific	>97%	
Iodine	abcr	99%	
4-Iodoaniline	Sigma Aldrich	98%	
N-Iodosuccinimide	Apollo Scientific	98%	
Magnesium sulfate	VWR		dried
Manganese dioxide	Merck		(precipitated active) for synthesis

meta-Chloroperoxybenzoic acid	Acros	70 – 75%[1]	
Nitrosobenzene	TCI	>98.0%	stored in a fridge
Oxone®	abcr		monopersulfate
Palladium acetate	Carbolution	98%	
Phenol	Sigma Aldrich	99%	
Phthalic anhydride	Acros	99%	
Potassium iodide	abcr	99%	
Sodium carbonate	Org Laborchemie	99.9%	
Sodium chloride	Th. Geyer	min 99.0%	
Sodium hydrogen carbonate	VWR	ACS, Reag. Ph. Eur.	
Sodium hydroxide	VWR	98%	
Sodium nitrite	Sigma Aldrich	97%	
Triethyl amine	Fluorochem	anhydrous	degassed, stored in a glovebox
1,3,5-Trimethoxybenzene	Sigma Aldrich	≥99%	
Xantphos	BLD Pharm	98%	

Solvents

All solvents for purification and extraction were used as received. All solvents used for synthesis under inert conditions were dried by a solvent purification system (SPS) from Inert Technologies.

Table S2. List of supplier and purity of used solvents.

Solvent	Supplier	Purity	Comments
Acetic Acid	Merck	≥99.8%	
Acetone	Sigma Aldrich	>99.5%	
Acetonitrile	Fisher Scientific	≥99.5%	
Cyclohexane	Merck	≥99.5%	
Chloroform	Sigma Aldrich	>99%	
Chloroform-d_1	Euroisotop	99.8%	
DCM	Merck	≥99.9%	
DMF	Acros Organics	99.8%	Extra dry, AcroSeal™
DMSO	VWR	technical grade	
DMSO	Acros Organics	99.7%	Extra dry, AcroSeal™
DMSO-d_6		>99.00%	
Ethanol	VWR	≥99.8%	absolute
Ethyl acetate	Merck	≥99.5%	
Formic acid	Sigma Aldrich	97%	
Methanol	VWR	≥99.8%	
1-Methyl-2-pyrrolidone	TCI	>99%	Low water content
Tetrahydrofuran	VWR	HPLC grade	anhydrous from SPS, stored in a glovebox
Tetrahydrofuran	Fisher Scientific	≥99.8%	
Toluene	Merck	≥99.7%	
Water		deionized	

[1] The exact concentration was determined by iodometric titration against sodium thiosulfate.

Syntheses

General procedure 1

a) Mono-iodinated molecular switch

Under inert conditions, the corresponding mono-iodinated switch (200 µmol, 2.00 equiv), $Pd(OAc)_2$ (1.35 mg, 6.00 µmol, 3 mol%), Xantphos (2.89 mg, 5.00 µmol, 2.5 mol%) and 2,5-dioxopyrrolidin-1-yl formate (**2**) (57.2 mg, 400 µmol, 4.00 equiv) were dissolved in dry THF (3 mL) in a pressure reaction vial. A solution of 1,3,5-trimethoxybenzene (16.8 mg, 100 µmol) as an internal standard in dry THF (1 mL) was added. The vial was sealed and heated to 60 °C. A solution of triethyl amine (22.2 mg, 220 µmol, 2.20 equiv) in dry THF (1 mL) was quickly added. Fast gas evolution was observed and the reaction was stirred for 17 h at 60 °C. After cooling to 21 °C, the solvent was removed under reduced pressure. The residue was re-dissolved in DCM (10 mL), filtered through Celite® and the solvent removed under reduced pressure.

b) Di-iodinated molecular switch

Under inert conditions, the corresponding di-iodinated molecular switch (100 µmol, 1.00 equiv), $Pd(OAc)_2$ (1.35 mg, 6.00 µmol, 6 mol%), Xantphos (2.89 mg, 5.00 µmol, 5 mol%) and 2,5-dioxopyrrolidin-1-yl formate (**2**) (57.2 mg, 400 µmol, 4.00 equiv) were dissolved in dry THF (3 mL) in a pressure reaction vial. A solution of 1,3,5-trimethoxybenzene (16.8 mg, 100 µmol) as an internal standard in dry THF (1 mL) was added. The vial was sealed and heated to 60 °C. A solution of triethyl amine (22.2 mg, 220 µmol, 2.20 equiv) in dry THF (1 mL) was quickly added. Fast gas evolution was observed and the reaction was stirred for 17 h at 60 °C. After cooling to 21 °C, the solvent was removed under reduced pressure. The residue was re-dissolved in DCM (10 mL), filtered through Celite® and the solvent removed under reduced pressure.

General procedure 2

a) Mono-iodinated molecular switch

Under inert conditions, the corresponding mono-iodinated switch (200 µmol, 2.00 equiv), $Pd(OAc)_2$ (1.35 mg, 6.00 µmol, 3 mol%), Xantphos (2.89 mg, 5.00 µmol, 2.5 mol%) and 2,5-dioxopyrrolidin-1-yl formate (**2**) (57.2 mg, 400 µmol, 4.00 equiv) were dissolved in dry THF (4 mL) in a pressure reaction vial. The vial was sealed and heated to 60 °C. A solution of triethyl amine (22.2 mg, 220 µmol, 2.20 equiv) in dry THF (1 mL) was quickly added. Fast gas evolution was observed and the reaction was stirred for 17 h at 60 °C. After cooling to 21 °C, the solvent was removed under reduced pressure. The residue was re-dissolved in DCM (10 mL) and extracted with water (20 mL) and brine (20 mL). The combined organic layers were dried over $MgSO_4$, filtered and the solvent removed under reduced pressure.

b) Di-iodinated molecular switch

Under inert conditions, the corresponding di-iodinated switch (100 µmol, 1.00 equiv), $Pd(OAc)_2$ (1.35 mg, 6.00 µmol, 6 mol%), Xantphos (2.89 mg, 5.00 µmol, 5 mol%) and 2,5-dioxopyrrolidin-1-yl formate (**2**) (57.2 mg, 400 µmol, 4.00 equiv) were dissolved in dry THF (4 mL) in a pressure reaction vial. The vial was sealed and heated to 60 °C. A solution of triethyl amine (22.2 mg, 220 µmol, 2.20 equiv) in dry THF (1 mL) was quickly added. Fast gas evolution was observed and the reaction was stirred for 17 h at 60 °C. After cooling to 21 °C, the solvent was removed under reduced pressure. The residue was re-dissolved in DCM (10 mL) and extracted with water (20 mL) and brine (20 mL). The combined organic layers were dried over $MgSO_4$, filtered and the solvent removed under reduced pressure.

2,5-Dioxopyrrolidin-1-yl (*E*)-4-(phenyldiazenyl)benzoate[2] (**3a**)

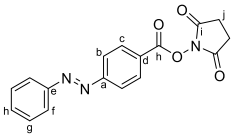

Compound **3a** was synthesized according to general procedure 2a from (*E*)-1-(4-iodophenyl)-2-phenyldiazene (**1a**) (61.6 mg, 200 µmol, 2.00 equiv). The product **3b** was obtained after crystallization from *n*-hexane/DCM (3:1) at -21 °C as a red solid (64.1 mg, 198 µmol, 99%, Lit.:[2] 84%[2]).

^{1}H NMR (600 MHz, $CDCl_3$) δ = 8.30 (d, ^3J = 8.5 Hz, 2H, *H*-c), 8.02 (d, ^3J = 8.5 Hz, 2H, *H*-b), 7.99 – 7.96 (m, 2H, *H*-f), 7.57 – 7.52 (m, 3H, *H*-g/h), 2.94 (s, br, 4H, *H*-j) ppm.
^{13}C{^{1}H} NMR (151 MHz, $CDCl_3$) δ = 169.3 (*C*-i), 161.6 (*C*-h), 156.3 (*C*-a), 152.6 (*C*-e), 132.3 (*C*-h), 131.9 (*C*-c), 129.4 (*C*-g), 126.7 (*C*-d), 123.5 (*C*-f), 123.2 (*C*-b), 25.9 (*C*-j) ppm.
IR (ATR): $\tilde{\nu}$ = 2999 (w), 2359 (w), 1790 (s), 1726 (s), 1600 (m), 1496 (w), 1427 (m), 1408 (m), 1366 (m), 1306 (w), 1256 (w), 1204 (s), 1151 (m), 1070 (s), 1019 (m), 999 (s), 928 (m), 867 (s), 849 (m), 812 (m), 771 (s) cm^{-1}.
HRMS (EI, 70 eV) *m/z* (%): $[M]^+$ calcd for $[C_{17}H_{13}N_3O_4]^+$ 323.09006; found 323.09003 (10), 209.2 (100).
Mp: 226 °C**.**
R$_f$: 0.65 (*n*-hexane/DCM 1:1).

2,5-Dioxopyrrolidin-1-yl (*E*)-3-(phenyldiazenyl)benzoate[2] (**3b**)

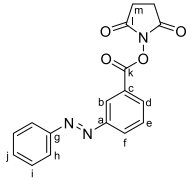

Compound **3b** was synthesized according to general procedure 1a from (*E*)-1-(4-iodophenyl)-2-phenyldiazene (**1b**) (61.6 mg, 200 µmol, 2.00 equiv). The compound was purified by column chromatography on silica (eluent: gradient *n*-hexane/ethyl acetate 1:0 → 0:1) yielding **3b** as an orange solid (60.5 mg, 188 µmol, 94%, Lit.:[2] 95%[3]).

^{1}H NMR (600 MHz, $CDCl_3$) δ = 8.68 (at, ^4J = 1.9 Hz, 1H, *H*-b), 8.25 – 8.22 (m, 2H, *H*-d/f), 7.97 – 7.94 (m, 2H, *H*-h), 7.69 (t, ^3J = 7.8 Hz, 1H, *H*-e), 7.57 – 7.50 (m, 3H, *H*-i/j), 2.94 (s, br, 4H, *H*-m) ppm.
^{13}C{^{1}H} NMR (151 MHz, $CDCl_3$) δ = 169.2 (*C*-l), 161.6 (*C*-k), 152.8 (*C*-a), 152.5 (*C*-g), 132.5 (*C*-d), 131.9 (*C*-j), 129.9 (*C*-e), 129.4 (*C*-i), 129.1 (*C*-f), 126.4 (*C*-d), 125.0 (*C*-b), 123.3 (*C*-h), 25.9 (*C*-m) ppm.
IR (ATR): $\tilde{\nu}$ = 2921 (w), 2359 (w), 1766 (m), 1727 (s), 1431 (m), 1371 (m), 1287 (w), 1257 (m), 1203 (s), 1149 (m), 1135 (m), 1070 (s), 1038 (m), 1014 (m), 923 (m), 867 (m), 812 (m), 765 (s), 740 (s) cm^{-1}.
HRMS (EI, 70 eV) *m/z* (%): $[M]^+$ calcd for $[C_{17}H_{13}N_3O_4]^+$ 323.09006; found 323.09006 (7), 77.0 (100).
Mp: 151 °C**.**
R$_f$: 0.59 (*n*-hexane/DCM 1:1).

[2] In this report, the product was prepared by coupling of the corresponding carboxylic acid with NHS using DCC.
[3] In this report, the product was prepared by coupling of the corresponding carboxylic acid with NHS using DCC.

2,5-Dioxopyrrolidin-1-yl (*E*)-4-((4-hydroxyphenyl)diazenyl)benzoate[3] (**3d**)

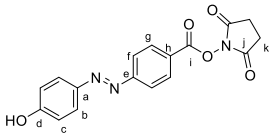

Compound **3d** was synthesized according to general procedure 1a from (*E*)-4-((4-iodophenyl)diazenyl)phenol (**1d**) (64.8 mg, 200 µmol, 2.00 equiv). The compound was purified by column chromatography on silica (eluent: gradient *n*-hexane/ethyl acetate 1:0 → 0:1) yielding **3d** as an orange powder (64.5 mg, 190 µmol, 95%, Lit.:[3] 90%[4]).

^{1}H NMR (600 MHz, DMSO-d_6) δ = 10.60 (s, 1H, O*H*-d), 8.27 (d, ^3J = 8.2 Hz, 2H, *H*-g), 8.01 (d, ^3J = 8.2 Hz, 2H, *H*-f), 7.89 (d, ^3J = 8.4 Hz, 2H, *H*-b), 6.99 (d, ^3J = 8.4 Hz, 2H, *H*-c), 2.92 (s, 4H, *H-k)* ppm.
^{13}C{^{1}H} NMR (151 MHz, DMSO-d_6) δ = 170.79 (C-j), 162.66 (C-a), 161.82 (C-i), 156.45 (C-e), 145.85 (C-d), 132.01 (*C*-g), 126.20 (*C*-b), 125.62 (C-h), 123.33 (*C*-f), 116.68 (*C*-c), 26.03 (*C*-k).
IR (ATR): $\tilde{\nu}$ = 3487 (w), 1764 (m), 1719 (s), 1601 (m), 1591 (w), 1431 (m), 1405 (m), 1275 (m), 1206 (s), 1156 (m), 1098 (m), 1015 (m), 1005 (s), 991 (m), 859 (w), 841 (s), 738 (m), 723 (m), 690 (m), 661 (m) cm^{-1}.
HRMS (EI, 70 eV) *m/z* (%): $[M]^+$ calcd for $[C_{17}H_{13}N_3O_5]^+$ 339.08497; found 339.08536 (15), 93.0 (100).
Mp: 241 °C.
R$_f$: 0.25 (*n*-hexane/ethyl acetate 1:1).

2,5-Dioxopyrrolidin-1-yl (*E*)-4-((4-aminophenyl)diazenyl)benzoate (**3e**)

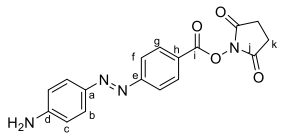

Compound **3e** was synthesized according to general procedure 1a from (*E*)-4-((4-iodophenyl)diazenyl)-aniline (**1e**) (64.8 mg, 200 µmol, 2.00 equiv). The solid was dissolved in ethyl acetate, washed with water (2 × 20 mL) and brine (20 mL). The combined organic phases were dried over $MgSO_4$, filtered and the solvent removed under reduced pressure. The crude product was crystalized from *n*-hexane/DCM (3:1) to obtain **3e** as an orange solid (65.6 mg, 172 µmol, 86%).

^{1}H NMR (600 MHz, DMSO-d_6) δ = 8.22 (d, ^3J = 8.6 Hz, 2H, *H*-g), 7.93 (d, ^3J = 8.6 Hz, 2H, *H*- f), 7.75 (d, ^3J = 8.9 Hz, 2H, *H*- b), 6.71 (d, ^3J = 8.9 Hz, 2H, *H*-c), 6.47 (s, 2H, NH_2-d) 2.91 (s, br, 4H, *H*-k) ppm.
^{13}C{^{1}H} NMR (151 MHz, DMSO-d_6) δ = 170.37 (*C*-j), 161.43 (*C*-i), 156.65 (*C*-e), 154.35 (*C*-a), 143.04 (*C*-d), 131.46 (*C*-g), 126.37 (*C*-b), 123.82 (*C*-h), 122.37 (*C*-f), 113.54 (*C*-c), 25.57 (*C*-k) ppm.
IR (ATR): $\tilde{\nu}$ = 3451 (w), 3366 (w), 1761 (s), 1725 (s), 1597 (m), 1456 (s), 1427 (m), 1401 (w), 1320 (w), 1255 (w), 1231 (w), 1205 (s), 1076 (m), 1046 (w), 1014 (m), 1014 (m), 861 (m), 835 (s), 726 (w), 690 (w) cm^{-1}.
HRMS (EI, 70 eV) *m/z* (%): $[M]^+$ calcd for $[C_{17}H_{14}N_4O_4]^+$ 338.10096; found 338.10115 (10), 92.1 (100).
Mp: 218 °C.
R$_f$: 0.25 (*n*-hexane/ethyl acetate 1:1).

[4] In this report, the product was prepared by coupling of the corresponding carboxylic acid with NHS using DCC.

2,5-Dioxopyrrolidin-1-yl (*E*)-4-((4-acetamidophenyl)diazenyl)benzoate (**3f**)

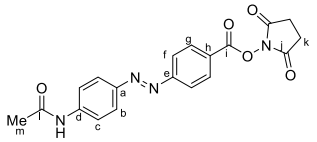

Compound **3f** was synthesized according to general procedure 1a from (*E*)*N*-(4-((4-iodophenyl)-diazenyl)phenyl)acetamide (**1f**) (64.8 mg, 200 µmol, 2.00 equiv). The solid was dissolved in ethyl acetate, washed with water (2 × 20 mL) and brine (20 mL). The combined organic phases were dried over $MgSO_4$, filtered and the solvent removed under reduced pressure. The crude product was crystalized from *n*-hexane/DCM (3:1) to obtain **3f** as an orange solid (65.6 mg, 172 µmol, 86%).

^{1}H NMR (600 MHz, DMSO- d_6) δ = 10.40 (s, 1H, N*H*-d) 8.29 (d, ^3J = 8.5 Hz, 2H, *H*-g), 8.05 (d, ^3J = 8.5 Hz, 2H, *H*-f), 7.97 (d, ^3J = 8.9 Hz, 2H, *H*-c), 7.85 (d, ^3J = 8.9 Hz, 2H, *H*-b), 2.92 (s, br, 4H, *H*-k), 2.12 (s, 3H, *H*-m) ppm.
^{13}C{^{1}H} NMR (151 MHz, DMSO- d_6) δ = 170.31 (*C*-j), 169.05 (*C*-l), 161.33 (*C*-i), 155.84 (*C*-a), 147.44 (*C*-d), 143.57 (*C*-a), 131.59 (*C*-g), 125.63 (*C*-h), 124.50 (*C*-c), 123.08 (*C*-f), 119.15 (*C*-b), 25.59 (*C*-k), 24.25 (*C*-m) ppm.
IR (ATR): $\tilde{\nu}$ = 3559 (w), 1757 (m), 1732 (m), 1688 (m), 1529 (s), 1446 (m), 1311 (m), 1300 (m), 1235 (m), 1208 (s), 998.3 (m), 861 (s), 848 (m), 739 (m) cm^{-1}.
HRMS (EI, 70 eV) *m/z* (%): $[M]^+$ calcd for $[C_{19}H_{16}N_4O_5]^+$ 380.11152; found 380.11201 (15), 134.2 (100).
Mp: 274 °C.
R_f: 0.15 (*n*-hexane/ethyl acetate 1:1).

2,5-Dioxopyrrolidin-1-yl (*E*)-4-((4-nitrophenyl)diazenyl)benzoate (**3g**)

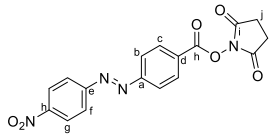

Compound **3c** was synthesized according to general procedure 2a from (*E*)-1-(4-nitrophenyl)-2-(4-iodophenyl)diazene (**1g**) (77.4 mg, 200 µmol, 2.00 equiv). The product **3g** was obtained after crystallization from *n*-hexane/DCM (3:1) at -21 °C as an orange solid (73.1 mg, 198 µmol, 99%).

^{1}H NMR (600 MHz, $CDCl_3$) δ = 8.42 (d, ^3J = 8.5 Hz, 2H, *H*-g), 8.33 (d, ^3J = 8.1 Hz, 2H, *H*-c), 8.11 (d, ^3J = 8.5 Hz, 2H, *H*-f), 8.08 (d, ^3J = 8.1 Hz, 2H, *H*-b), 2.95 (s, br, 4H, *H*-j) ppm.
^{13}C{^{1}H} NMR (151 MHz, $CDCl_3$) δ = 169.2 (*C*-i), 161.3 (*C*-h), 155.7 (*C*-a), 155.4 (*C*-e), 149.5 (*C*-h), 132.0 (*C*-c), 128.0 (*C*-d), 125.0 (*C*-g), 124.1 (*C*-f), 123.7 (*C*-b), 25.9 (*C*-j) ppm.
IR (ATR): $\tilde{\nu}$ = 3080 (w), 1767 (m), 1761 (s), 1606 (m), 1530 (s), 1431 (m), 1407(m), 1346 (s), 1322 (m), 1259 (m), 1237 (m), 1199 (s), 1110 (m), 1076 (s), 1023 (m), 1007 (s), 870 (s), 854 (m), 816 (m), 764 (m), 752 (m) cm^{-1}.
HRMS (EI, 70 eV) *m/z* (%): $[M]^+$ calcd for $[C_{17}H_{12}N_4O_6]^+$ 368.07514; found 368.07562 (4), 254.2 (100).
Mp: 245 °C.
R_f: 0.59 (*n*-hexane/DCM 1:1).

2,5-Dioxopyrrolidin-1-yl (*E*)-4-((4-(allyloxy)phenyl)diazenyl)benzoate (**3h**)

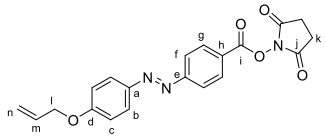

Compound **3h** was synthesized according to general procedure 1a from (*E*)-1-(4-(allyloxy)phenyl)-2-(4-iodophenyl)diazene (**1h**) (72.8 mg, 200 µmol, 2.00 equiv). The compound was purified by column chromatography on silica (eluent: gradient *n*-hexane/ethyl acetate 1:0 → 0:1) yielding **3h** as an orange powder (45.3 mg, 119 µmol, 60%).

^{1}H NMR (600 MHz, $CDCl_3$) δ = 8.27 (d, ^3J = 8.6 Hz, 2H, *H*-g), 7.97 (d, ^3J = 8.6 Hz, 4H, *H*-f/b), 7.05 (d, ^3J = 8.9 Hz, 2H, *H*-c), 6.09 (m, 1H, *H*-m), 5.46 (d, ^2J = 10.5 Hz, 1H, *H*-n), 5.35 (d, ^2J = 10.5 Hz, 1H, *H*-n), 4.65 (d, ^3J = 5.0 Hz, 2H, *H*-l), 2.93 (s, 4H, *H*-k) ppm.
^{13}C{^{1}H} NMR (151 MHz, $CDCl_3$) δ = 169.32 (*C*-j), 162.17 (*C*-d), 161.62 (*C*-i), 157.04 (*C*-e), 148.03 (*C*-a), 132.69 (*C*-m), 131.87 (*C*-g), 126.02 (*C*-h), 125.60 (*C*-f/b), 122.92 (*C*-f/b), 118.41 (*C*-n), 115.27 (*C*-c), 69.26 (*C*-l), 24.35 (*C*-k).
IR (ATR): $\tilde{\nu}$ = 2921 (w), 2851 (w), 1768 (w), 1731 (m), 1600 (m), 1499 (m), 1371 (w), 1204 (s), 1070 (s), 1016 (m), 992 (s), 861 (m), 812 (w), 760 (w), 723 (w), 687 (w) cm^{-1}.
HRMS (EI, 70 eV) *m/z* (%): $[M]^+$ calcd for $[C_{20}H_{17}N_3O_5]^+$ 379.11627; found 379.11643 (20), 133.1 (100)
Mp: - (decomposition).
R_f: 0.35 (*n*-hexane/ethyl acetate 1:1).

2,5-Dioxopyrrolidin-1-yl (*E*)-4-((4-((9-hydroxynonyl)oxy)phenyl)diazenyl)benzoate (**3i**)

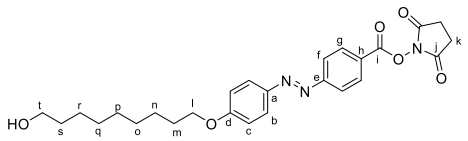

Compound **3i** was synthesized according to general procedure 1a from (*E*)-9-(4-((4-iodophenyl)diazenyl)phenoxy)nonan-1-ol (**1i**) (93.2 mg, 200 µmol, 2.00 equiv). The compound was purified by column chromatography on silica (eluent: gradient *n*-hexane/ethyl acetate 1:0 → 0:1) yielding **3i** as an yellow solid (76.3 mg, 158 µmol, 79%).

^{1}H NMR (600 MHz, $CDCl_3$) δ = 8.27 (d, ^3J = 6.6 Hz, 2H, *H*-g), 7.96 (dd, ^3J = 8.9, 6.6 Hz, 4H, *H*-f/b), 7.02 (d, ^3J = 8.9 Hz, 2H, *H*-c), 4.06 (t, ^3J = 6.5 Hz, 2H, *H*-l), 3.65 (t, ^3J = 6.6 Hz, 2H, *H*-t), 2.93 (s, 4H, *H*-k), 1.87 – 1.79 (m, 2H, *H*-m), 1.60 – 1.52 (m, 2H, *H*-s), 1.51 – 1.48 (m, 2H, *H*-n), 1.41 – 1.30 (m, 8H, *H*-o/p/r/q), 1.23 (s, 1H, O*H*-t) ppm.
^{13}C{^{1}H} NMR (151 MHz, $CDCl_3$) δ = 169.12 (*C*-j), 162.63 (*C*-d), 161.42 (*C*-i), 156.42 (*C*-e), 146.77 (*C*-a), 131.65 (*C*-g), 125.72 (*C*-h), 125.42 (*C*-f/b), 122.68 (*C*-f/b), 115.65 (*C*-c), 68.38 (*C*-l), 63.00(*C*-t), 32.71 (*C*-s), 29.43 (*C*-o/p/r/q), 29.28 (*C*-o/p/r/q), 29.22 (*C*-o/p/r/q), 29.07 (*C*-m), 25.92 (*C*-o/p/r/q), 25.66 (*C*-n), 25.64 (*C*-k) ppm.
IR (ATR): $\tilde{\nu}$ = 3523 (w), 2921 (w), 2850 (w), 1797 (m), 1773 (s), 1715 (s), 1600 (w), 1500 (m), 1381 (w), 1296 (m), 1255 (m), 1210 (s), 1138 (m), 1107 (m), 1075 (s), 1050 (s), 1016(s), 988 (s), 863 (m), 843 (s), 814 (m), 723 (m), 688 (w) cm^{-1}.

HRMS (EI, 70 eV) *m/z* (%): $[M]^+$ calcd for $[C_{26}H_{31}N_3O_6]^+$ 481.22074; found 481.22050 (5), 55.1 (100).
Mp: 156 °C.
R$_f$: 0.15 (*n*-hexane/ethyl acetate 1:1).

2,5-Dioxopyrrolidin-1-yl (*E*)-4-((2,6-dimethyl-4-(nonyloxy)phenyl)diazenyl)-3,5-dimethylbenzoate (**3j**)

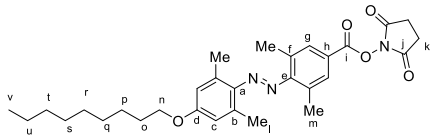

Compound **3j** was synthesized according to general procedure 2a from (*E*)-1-(2,6-dimethyl-4-(nonyloxy)phenyl)-2-(4-iodo-2,6-dimethylphenyl)diazene (**1j**) (92.8 mg, 200 µmol, 2.00 equiv). The compound was purified by column chromatography on silica (eluent: gradient *n*-hexane/ethyl acetate 1:0 → 0:1) yielding **3j** as a red powder (97.0 mg, 186 µmol, 94%).

The NMR yield was obtained according to general procedure 1a with the difference that **1j** (46.4 mg, 100 µmol, 1.00 equiv), $Pd(OAc)_2$ (675 µg, 3.00 µmol, 3 mol%), Xantphos (1.45 mg, 2.50 µmol, 2.5 mol%), 2,5-dioxopyrrolidin-1-yl formate (**2**) (28.6 mg, 200 µmol, 2.00 equiv), 1,3,5-trimethoxybenzene (16.8 mg, 100 µmol) and triethyl amine (22.2 mg, 220 µmol, 1.10 equiv) were used.

^{1}H NMR (600 MHz, $CDCl_3$) δ = 7.91 (s, 2H, *H*-g), 6.70 (s, 2H, *H*-c), 4.03 (t, ^3J = 6.5 Hz, 2H, *H*-n), 2.92 (s, 4H, *H*-k), 2.55 (s, 6H, *H*-l), 2.34 (s, 6H, *H*-m), 1.85 – 1.77 (m, 2H, *H*-o), 1.53 – 1.43 (m, 2H, *H*-p), 1.40 – 1.25 (m, 10H, *H*-q,r,s,t,u), 0.92 – 0.86 (m, 3H, *H*-v).
^{13}C{^{1}H} NMR (151 MHz, $CDCl_3$) δ = 169.32 (*C*-j), 161.72 (*C*-i), 160.34 (*C*-d), 157.55 (*C*-e), 143.83 (*C*-a), 136.72 (*C*-b), 131.32 (*C*-g), 130.41 (*C*-f), 122.77 (*C*-h), 115.31 (*C*-c), 68.13 (*C*-n), 31.90 (*C*-q,r,s,t,u), 29.55 (*C*-q,r,s,t,u), 29.38 (*C*-q,r,s,t,u), 29.28 (*C*-q,r,s,t,u), 29.21 (*C*-o), 26.02 (*C*-p), 25.71 (*C*-k), 22.69 (*C*-q,r,s,t,u), 21.38 (*C*-m), 19.09 (*C*-l), 14.13 (*C*-v).
IR (ATR): $\tilde{\nu}$ = 2922 (m), 2848 (m), 1761 (s), 1732(s), 1599 (m), 1489 (w), 1465 (w), 1431 (w), 1356 (w), 1313 (m), 1297 (m), 1248 (m), 1187 (s), 1161 (s), 1139 (s), 1077 (s), 1058 (s), 1044 (m), 994 (w), 911 (s), 903(s), 868 (m), 854 (m), 827 (w), 806 (w), 689 (w) cm^{-1}.
HRMS (EI, 70 eV) *m/z* (%): $[M]^+$ calcd for $[C_{30}H_{39}N_3O_5]^+$ 521.28842; found 521.28660 (10), 69.1 (100).
Mp: 78 °C.
R$_f$: 0.45 (*n*-hexane/ethyl acetate 1:1).

2,5-Dioxopyrrolidin-1-yl (*E*)-4-((2,7-bis(4-(hexyloxy)phenoxy)naphthalen-1-yl)diazenyl)-3,5-dimethylbenzoate (**3k**)

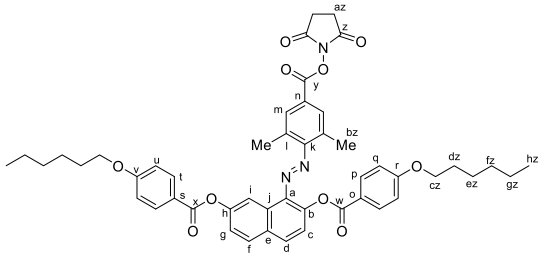

Compound **3k** was synthesized according to general procedure 1a from (*E*)-1-(2,7-bis(4-(hexyloxy)phenoxy)naphthalen-1-yl)-2-(4-iodo-2,6-dimethylphenyl)diazene (**1k**) (154 mg, 200 µmol, 2.00 equiv). The compound was purified by column chromatography on silica (eluent: gradient *n*-hexane/ethyl acetate 1:0 → 0:1) yielding **3k** as a red powder (125 mg, 148 µmol, 74%).

^{1}H NMR (600 MHz, $CDCl_3$) δ = 8.53 (d, ^4J = 2.3 Hz, 1H, *H*-i), 8.16 (d, ^3J = 8.8 Hz, 2H, *H*-t), 8.06 – 8.03 (m, 3H, *H*-p/c), 8.01 (d, ^3J = 8.9 Hz, 1H, *H*-g), 7.81 (s, 2H, *H*-m), 7.49 (dd, ^3J = 8.9, ^4J = 2.3 Hz, 1H, *H*-f), 7.44 (d, ^3J = 8.8 Hz, 1H, *H*-d), 6.97 (d, ^3J = 8.8 Hz, 2H, *H*-u), 6.91 (d, ^3J = 8.8 Hz, 2H, *H*-q), 4.03 (dt, ^2J = 13.3, ^3J = 6.7 Hz, 4H, *H*-cz), 2.90 (s, 4H, *H*-az), 2.24 (s, 6H, *H*-bz), 1.80 (dt, ^2J = 13.3, ^3J = 6.7 Hz, 4H, *H*-dz), 1.55 – 1.44 (m, 4H, *H*-ez), 1.38 - 1.32 (m, 8H, *H*-fz/gz), 0.93 – 0.90 (m, 6H, *H*-hz) ppm.
^{13}C{^{1}H} NMR (151 MHz, $CDCl_3$) δ = 169.35 (*C*-z), 165.11 (*C*-x), 165.08 (*C*-w), 163.81 (*C*-s), 163.75 (*C*-o), 161.68 (*C*-y), 157.03 (*C*-k), 151.06 (*C*-b), 140.03 (*C*-e), 137.81 (*C*-j), 132.53 (*C*-t), 132.45 (*C*-p), 131.33 (*C*-m), 131.20 (*C*-f), 131.01 (*C*-a), 130.53 (*C*-h), 129.67 (*C*-g), 123.74 (*C*-c), 123.03 (*C*-d), 122.40 (*C*-n), 121.40 (*C*-v), 121.17 (*C*-r), 115.84 (*C*-i), 114.47 (*C*-u/q), 68.48 (*C*-cz), 68.45 (*C*-cz), 31.71 (*C-fz/gz)*, 31.69 (*C-fz/gz)*, 29.22 (*C*-dz), 29.20 (*C*-dz), 25.80 (*C*-az, *C*ez), 22.73(*C-fz/gz)*, 18.74 (*C*-bz), 14.17 (*C*-hz) ppm.
IR (ATR): $\tilde{\nu}$ = 2929 (w), 1774 (w), 1735 (s), 1604 (m), 1577 (w), 1511 (w), 1456 (w), 1420 (w), 1367 (w), 1293 (w), 1247 (s), 1202 (s), 1161 (s), 1063 (s), 1017 (s), 1007 (m), 995 (w), 919 (w), 890 (m), 874 (w), 846 (m), 759 (w), 749 (w), 689 (w) cm^{-1}.
HRMS (ESI): *m/z* = $[M + Na]^+$ calcd for $[C_{49}H_{51}IN_3O_{10} + Na]^+$ 864.34619, found 864.34667.
Mp: 80 °C.
R$_f$: 0.45 (*n*-hexane/ethyl acetate 1:1).

2,5-Dioxopyrrolidin-1-yl (*E*)-4-((4-bromophenyl)diazenyl)benzoate (**3l**)

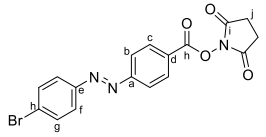

Compound **3l** was synthesized according to general procedure 2a from (*E*)-1-(4-bromophenyl)-2-(4-iodophenyl)diazene (**1l**) (77.4 mg, 200 µmol, 2.00 equiv). The product was obtained after crystallization from *n*-hexane/DCM (3:1) at -21 °C as an orange solid (76.3 mg, 190 µmol, 95%).

^{1}H NMR (600 MHz, $CDCl_3$) δ = 8.30 (d, ^3J = 8.3 Hz, 2H, *H*-c), 8.01 (d, ^3J = 8.3 Hz, 2H, *H*-b), 7.85 (d, ^3J = 8.8 Hz, 2H, *H*-f), 7.69 (d, ^3J = 8.8 Hz, 2H, *H*-g), 2.94 (s, br, 4H, *H*-j) ppm.
^{13}C{^{1}H} NMR (151 MHz, $CDCl_3$) δ = 169.3 (*C*-i), 161.5 (*C*-h), 156.1 (*C*-a), 151.3 (*C*-e), 132.7 (*C*-g), 131.9 (*C*-c), 127.0 (*C*-d), 126.9 (*C*-h), 124.9 (*C*-f), 123.3 (*C*-b), 25.9 (*C*-j) ppm.
IR (ATR): $\tilde{\nu}$ = 2987 (w), 2359 (w), 1790 (w), 1770 (m), 1722 (s), 1601 (m), 1571 (m), 1478 (m), 1426 (m), 1426 (m), 1368 (m), 1260 (m), 1231 (m), 1206 (s), 1144 (m), 1074 (s), 1016 (m), 995 (s), 859 (m), 838 (m), 819 (m), 759 (m), 706 (m) cm^{-1}.
HRMS (EI, 70 eV) *m/z* (%): $[M]^+$ calcd for $[C_{17}H_{12}BrN_3O_4]^+$ 401.00057; found 401.00131 (7), 76.1 (100).
Mp: 285 °C**.**
R$_f$: 0.65 (*n*-hexane/DCM 1:1).

2,5-Dioxopyrrolidin-1-yl (*E*)-4-((3-bromophenyl)diazenyl)benzoate (**3m**)

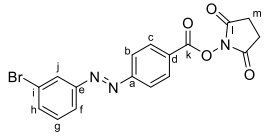

Compound **3m** was synthesized according to general procedure 2a from (*E*)-1-(3-bromophenyl)-2-(4-iodophenyl)diazene (**1m**) (77.4 mg, 200 µmol, 2.00 equiv). The product was obtained after crystallization from *n*-hexane/DCM (3:1) at -21 °C as an orange solid (76.9 mg, 198 µmol, 99%).

^{1}H NMR (600 MHz, $CDCl_3$) δ = 8.31 (d, ^3J = 8.5 Hz, 2H, *H*-c), 8.11 (at, ^4J = 1.9 Hz, 1H, *H*-j), 8.02 (d, ^3J = 8.5 Hz, 2H, *H*-b), 7.94 (ddt, ^3J = 7.9 Hz, ^4J = 1.9 Hz, ^4J = 0.9 Hz, 1H, *H*-f/h), 7.66 (ddt, ^3J = 7.9 Hz, ^4J = 1.9 Hz, ^4J = 0.9 Hz, 1H, *H*-f/h), 7.44 (t, ^3J = 7.9 Hz, 1H, *H*-g), 2.94 (s, br, 4H, *H*-m) ppm.
^{13}C{^{1}H} NMR (151 MHz, $CDCl_3$) δ = 169.2 (*C*-l), 161.5 (*C*-k), 155.9 (*C*-a), 153.4 (*C*-e), 134.8 (*C*-h), 131.9 (*C*-c), 130.8 (*C*-g), 127.2 (*C*-d), 125.1 (*C*-j), 123.7 (*C*-f), 123.4 (*C*-i), 123.4 (*C*-b), 25.9 (*C*-m) ppm.
IR (ATR): $\tilde{\nu}$ = 2937 (w), 1769 (m), 1729 (s), 1598 (m), 1568 (m), 1455 (w), 1435 (m), 1409 (m), 1353 (m), 1257 (m), 1237 (m), 1196 (s), 1143 (m), 1071 (s), 1017 (m), 994 (s), 892 (m), 862 (s), 853 (s), 808 (m), 796 (s), 760 (m), 742 (m) cm^{-1}.
HRMS (EI, 70 eV) *m/z* (%): $[M]^+$ calcd for $[C_{17}H_{12}BrN_3O_4]^+$ 401.00057; found 401.00120 (7), 76.1 (100).
Mp: 192 °C**.**
R$_f$: 0.65 (*n*-hexane/DCM 1:1).

2,5-Dioxopyrrolidin-1-yl (*E*)-4-((2-bromophenyl)diazenyl)benzoate (**3n**)

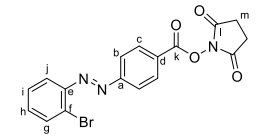

Compound **3n** was synthesized according to general procedure 2a from (*E*)-1-(2-bromophenyl)-2-(4-iodophenyl)diazene (**1n**) (77.4 mg, 200 µmol, 2.00 equiv). The product was obtained after crystallization from *n*-hexane/DCM (3:1) at -21 °C as a red solid (71.6 mg, 178 µmol, 89%).

^{1}H NMR (600 MHz, $CDCl_3$) δ = 8.31 (d, ^3J = 8.5 Hz, 2H, *H*-c), 8.07 (d, ^3J = 8.5 Hz, 2H, *H*-b), 7.80 (dd, ^3J = 7.9 Hz, ^4J = 1.7 Hz, 1H, *H*-g), 7.73 (dd, ^3J = 7.9 Hz, ^4J = 1.7 Hz, 1H, *H*-j), 7.42 (td, ^3J = 7.9 Hz, ^4J = 1.7 Hz, 1H, *H*-i), 7.38 (td, ^3J = 7.9 Hz, ^4J = 1.7 Hz, 1H, *H*-h), 2.94 (s, br, 4H, *H*-m) ppm.

^{13}C{^{1}H} NMR (151 MHz, $CDCl_3$) δ = 169.2 (*C*-l), 161.5 (*C*-k), 156.1 (*C*-a), 149.6 (*C*-e), 134.2 (*C*-g), 133.2 (*C*-h), 131.9 (*C*-c), 128.2 (*C*-i), 127.2 (*C*-d), 127.1 (*C*-f), 123.7 (*C*-b), 117.8 (*C*-j), 25.9 (*C*-m) ppm.
IR (ATR): $\tilde{\nu}$ = 2957 (W), 2359 (w), 1769 (m), 1731 (s), 1600 (m), 1458 (w), 1422 (m), 1407 (m), 1359 (m), 1255 (m), 1235 (m), 1199 (s), 1066 (s), 1045 (m), 997 (s), 859 (m), 849 (m), 807 (m), 780 (m), 761 (m), 716 (m) cm^{-1}.
HRMS (EI, 70 eV) *m/z* (%): $[M]^+$ calcd for $[C_{17}H_{12}BrN_3O_4]^+$ 401.00057; found 401.00125 (9), 76.1 (100).
Mp: 173 °C**.**
R$_f$: 0.65 (*n*-hexane/DCM 1:1).

Bis(2,5-dioxopyrrolidin-1-yl)4,4´-(diazene-1,2-diyl)(*E*)-dibenzoate[5](**5a**)

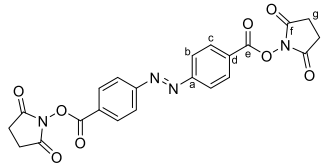

Compound **5a** was synthesized according to general procedure 2b from (*E*)-1,2-bis(4-iodophenyl)diazene (**4a**) (43.4 mg, 200 µmol). The product was obtained after crystallization from *n*-hexane/DCM (3:1) as a red solid (42.0 mg, 194 µmol, 97%, Lit.:[4] 94%[4]).

^{1}H NMR (600 MHz, $CDCl_3$) δ = 8.33 (d, ^3J = 8.5 Hz, 2H, *H*-c), 8.08 (d, ^3J = 8.1 Hz, 2H, *H*-b), 2.94 (s, br, 4H, *H*-g) ppm.
^{13}C{^{1}H} NMR (151 MHz, $CDCl_3$) δ = 169.2 (*C*-f), 161.4 (*C*-e), 155.9 (*C*-a), 132.0 (*C*-c), 127.7 (*C*-d), 123.6 (*C*- b), 25.9 (*C*-g) ppm.
IR (ATR): $\tilde{\nu}$ = 2923 (w), 1770 (m), 1732 (s), 1600 (m), 1426 (w), 1414 (m), 1365 (m), 1310 (m), 1256 (m), 1236 (m), 1201 (s), 1066 (s), 1046 (m), 1015 (m), 987 (s), 977 (s), 873 (s), 843 (m), 809 (m), 767 (m), 727 (m) cm^{-1}.
HRMS (EI, 70 eV) *m/z* (%): $[M]^+$ calcd for $[C_{22}H_{16}N_4O_8]^+$ 464.09626; found 464.09599 (9), 349.9 (100).
Mp: 276 °C Lit.:[4] >250 °C).
R$_f$ = 0.65 (*n*-hexane/DCM 1:1).

Bis(2,5-dioxopyrrolidin-1-yl) 4,4'-(diazene-1,2-diyl)(*E*)-bis(3,5-dimethoxybenzoate) (**5b**)

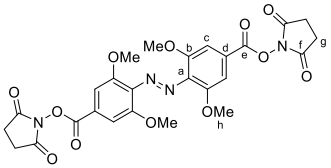

Compound **5b** was synthesized according to general procedure 1b from (*E*)-1,2-bis(4-iodo-2,6-dimethoxyphenyl)diazene[5] (**4b**) (54.4 mg, 100 µmol, 1.00 equiv). The compound was purified by column chromatography on silica (eluent: gradient *n*-hexane/ethyl acetate 1:0 → 0:1) yielding **5b** as a red powder (47.1 mg, 90.5 µmol, 91%).

[4] In this report, the product was prepared by coupling of the corresponding carboxylic acid with NHS using EDC and DMAP.
[5] 90% purity

^{1}H NMR (600 MHz, DMSO-d_6) δ = 7.45 (s, 4H, *H*-c), 3.93 (s, 12H, *H*-h), 2.94 (s, 4H, *H*-g) ppm.
^{13}C{^{1}H} NMR (151 MHz, DMSO-d_6) δ = 169.2 (*C*-f), 161.5 (*C*-e), 151.9 (*C*-a), 138.3 (*C*-b), 125.7 (*C*-d), 107.4 (*C*-c), 57.0 (*C*-h), 25.9 (*C*-g) ppm.
IR (ATR): $\tilde{\nu}$ = 2956 (w), 1732 (s), 1574 (m), 1455 (m), 1408 (m), 1360 (m), 1325 (m), 1231 (m), 1195 (m), 1120 (s), 1071 (s), 1016 (m), 993 (w), 894 (m), 853 (m), 833 (w), 808 (w), 771 (w), 741 (w) cm^{-1}.
HRMS (EI, 70 eV) *m/z* (%): $[M]^+$ calcd for $[C_{26}H_{24}N_4O_{12}]^+$ 584.13852; found 584.13941 (13), 149.1 (100).
Mp: 212 °C.
R$_f$: 0.50 (ethyl acetate).

Bis(2,5-dioxopyrrolidin-1-yl) 4,4'-(diazene-1,2-diyl)(*E*)-bis(3,5-dimethylbenzoate) (**5c**)

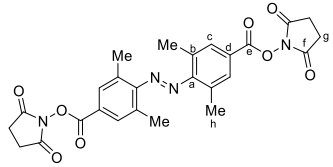

Compound **5c** was synthesized according to general procedure 1b from (*E*)-1,2-bis(4-iodo-2,6-dimethylphenyl)diazene (**4c**) (49.0 mg, 100 µmol, 1.00 equiv). The compound was purified by column chromatography on silica (eluent: gradient *n*-hexane/ethyl acetate 1:0 → 0:1) yielding **5c** as a red powder (47.1 mg, 90.5 µmol, 91%).

^{1}H NMR (600 MHz, $CDCl_3$) δ = 7.98 (s, 4 H, *H*-c), 2.95 (s, 8 H, *H*-g), 2.46 (s, 12 H, *H*-h) ppm.
^{13}C{^{1}H} NMR (151 MHz, $CDCl_3$) δ = 169.3 (*C*-f), 161.6 (*C*-e), 155.7 (*C*-a), 131.8 (*C*-c), 131.7 (*C*-b), 124.8 (*C*-d), 25.7 (*C*-g), 19.4 (*C*-h) ppm.
IR (ATR): $\tilde{\nu}$ = 3429 (m), 3351 (m), 3078 (w), 2926 (w), 2863 (w), 1614 (s), 1567 (m), 1481 (s), 1404 (s), 1309 (s), 1290 (s), 1270 (s), 1191 (m), 1163 (m), 1121 (m), 1069 (m), 933 (m), 884 (m), 862 (m), 812 (s), 780 (m), 748 (m), 733 (m) cm^{-1}.
HRMS (APCI): *m/z* = $[M+H]^+$ calcd for $[C_{26}H_{24}N_4O_8 + H]^+$ 521.166669; found 521.16629.
Mp: 175 °C.
R$_f$: 0.30 (DCM/ethyl acetate 1:1).

Bis(2,5-dioxopyrrolidin-1-yl) 4,4'-(diazene-1,2-diyl)(*E*)-bis(3,5-difluorobenzoate) (**5d**)

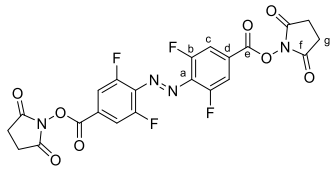

(*E*)-1,2-Bis(2,6-difluoro-4-iodophenyl)diazene (**4d**) (171 mg, 0.500 mmol, 1.00 equiv), *N*-hydroxysuccinimide (**7**) (253 mg, 2.20 mmol, 4.40 equiv) and 4-dimethylaminopyridine (DMAP) (12.5 mg, 100 µmol, 0.20 equiv) were dissolved in DMF (10 mL) at 21 °C. After 10 min of stirring, 1-ethyl-3-(3-dimethylaminopropyl)carbodiimide (EDCI) (310 mg, 11.1 mmol, 3.00 equiv) was added and the solution was stirred at 21 °C for 16 h under a nitrogen atmosphere. The mixture was diluted with DCM (100 mL) and washed with hydrochloric acid (0.1 M, 100 mL). The aqueous phase was extracted DCM (2 × 50 mL). The combined organic phases were dried over sodium sulphate and purified by column

chromatography on silica (eluent: gradient *n*-hexane/ethyl acetate 0:1 → 1:1). **5d** was obtained as an orange solid after crystallisation from THF/*n*-hexane (110 mg, 205 µmol, 41%).

^{1}H NMR (600 MHz, DMSO-d_6) δ = 8.11 (d, ^3J = 8.6 Hz, 4H, *H*-c), 2.93 (s, 8H, *H*-g) ppm.
^{13}C{^{1}H} NMR (151 MHz, DMSO-d_6) δ = 172.25 (*C*-e), 170.4 (*C*-f), 155.00 (d, ^1J = 264.3 Hz, *C*-b), 134.9 (*C*-a), 128.6 (*C*-d), 115.9 (d, ^2J = 24 Hz, *C*-c), 25.59 (*C*-g) ppm.
^{19}F NMR (565 MHz, DMSO-d_6) δ = -118.20 (s, *F*-b)
IR (ATR): $\tilde{\nu}$ = 3092 (w), 1804 (w), 1774 (w), 1731 (s), 1580 (m), 1431 (m), 1327 (m), 1200 (s), 1165 (s), 1072 (s), 1038 (s), 904 (m), 826 (w), 764 (w), 741 (s) cm^{-1}.
HRMS (EI, 70 eV) *m/z* (%): $[M]^+$ calcd for $[C_{22}H_{12}F_4N_4O_8]^+$ 536.05858; found 536.05884 (16), 140.1 (100).
Mp: 296 °C.
R$_f$: 0.60 (ethyl acetate).

2,5-Dioxopyrrolidin-1-yl (Z)-11,12-dihydrodibenzo[c,g][1,2]diazocine-2-carboxylate (**8a**)

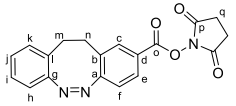

Compound **8a** was synthesized according to general procedure 2a from (*Z*)-2-iodo-11,12-dihydrodibenzo[c,g][1,2]-diazocine (**7a**) (43.4 mg, 200 µmol) in dry DMSO. The product was obtained after crystallization from *n*-hexane/DCM (3:1) as a yellow solid (69.9 mg, 198 µmol, 99%).

^{1}H NMR (600 MHz, $CDCl_3$) δ = 7.89 (dd, ^3J = 8.2 Hz, ^4J = 1.8 Hz, 1H, *H*-e), 7.78 (d, ^4J = 1.8 Hz, 1H, *H*-c), 7.17 (t, ^3J = 7.5 Hz, 1H, *H*-i), 7.06 (t, ^3J = 7.5 Hz, 1H, *H*-j), 6.99 (d, ^3J = 7.5 Hz, 1H, *H*-k), 6.93 (d, ^3J = 8.2 Hz, 1H, *H*-f), 6.85 (d, ^3J = 7.5 Hz, 1H, *H*-h), 3.07 – 2.77 (m, 8H, *H*-m/n/q) ppm.
^{13}C{^{1}H} NMR (151 MHz, $CDCl_3$) δ = 169.3 (*C*-p), 161.2 (*C*-o), 160.8 (*C*-a), 155.5 (*C*-g), 132.4 (*C*-c), 130.2 (*C*-k), 129.7 (*C*-b), 129.5 (*C*-e), 128.0 (*C*-j), 127.3 (*C*-l), 127.2 (*C*-i), 123.6 (*C*-d), 119.3 (*C*-f), 118.7 (*C*-h), 31.6 (*C*-n), 31.5 (*C*-m), 25.8 (*C*-q) ppm.
IR (ATR): $\tilde{\nu}$ = 2921 (w), 2851 (w), 2359 (w), 1769 (m), 1733 (s), 1601 (w), 1417 (m), 1358 (m), 1282 (m), 1236 (m), 1196 (s), 1064 (s), 1036 (m), 914 (m), 874 (m), 765 (m), 742 (s) cm^{-1}.
HRMS (EI, 70 eV) *m/z* (%): $[M]^+$ calcd for $[C_{19}H_{15}N_3O_4]^+$ 349.10571; found 349.10536 (7), 178.1 (100).
Mp: 207 °C.
R$_f$: 0.46 (*n*-hexane/DCM 1:1).

Bis(2,5-dioxopyrrolidin-1-yl) (*Z*)-11,12-dihydrodibenzo[c,g][1,2]diazocine-2,9-dicarboxylate (**8b**)

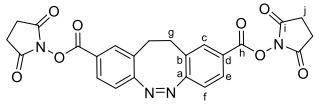

Compound **8b** was synthesized according to general procedure 2b from (*Z*)-2,9-diiodo-11,12-dihydrodibenzo[c,g][1,2]-diazocine (**7b**) (43.4 mg, 200 µmol) in dry DMSO. The product was obtained after crystallization from *n*-hexane/DCM (3:1) as a yellow solid (47.8 mg, 196 µmol, 98%).

^{1}H NMR (600 MHz, $CDCl_3$) δ = 7.95 (d, ^3J = 8.2 Hz, 2H, *H*-e), 7.82 (s, 2H, *H*-c), 7.00 (d, ^3J = 8.2 Hz, 2H, *H*-f), 3.12 – 2.91 (m, 4H, *H*-g), 2.88 (s, br, 8H, *H*-j) ppm.
^{13}C{^{1}H} NMR (151 MHz, $CDCl_3$) δ = 169.1 (*C*-i), 161.0 (*C*-h), 160.1 (*C*-a), 132.8 (*C*-c), 129.9 (*C*-e), 128.5 (*C*-b), 124.5 (*C*-d), 119.4 (*C*-f), 31.4 (*C*-g), 25.8 (*C*-j) ppm.
IR (ATR): $\tilde{\nu}$ = 2990 (w), 2359 (w), 1769 (m), 1732 (s), 1602 (m), 1482 (w), 1425 (m), 1366 (m), 1202 (s), 1069 (s), 1029 (m), 986 (m), 911 (m), 813 (m), 740 (s) cm^{-1}.
HRMS (ESI) *m/z*: [M + Na]$^+$ calcd for [$C_{24}H_{18}N_4O_8$ + Na]$^+$ 513.10168; found 513.10105.
Mp: 187 °C.
R$_f$: 0.61 (ethyl acetate).

Di-*tert*-butyl 2,2'-((4,4'-(diazene-1,2-diyl)bis(benzoyl))bis(azanediyl))(*E*)-dipropionate (**10a**)

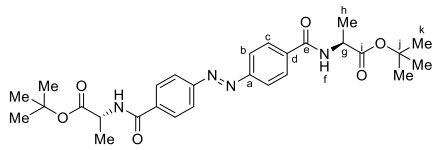

Triethyl amine (153 µL, 1.10 mmol, 2.20 equiv) was added to a solution of L-alanine *tert*-butyl ester hydrochloride (**9**) (200 mg, 1.10 mmol, 2.20 equiv) in dry DMF (10 mL). A solution of bis(2,5-dioxopyrrolidin-1-yl) 4,4'-(diazene-1,2-diyl)(*E*)-dibenzoate (**5a**) (232 mg, 500 µmol, 1.00 equiv) in dry DMF (7 mL) was added and the resulting mixture was stirred at 21 °C for 16 h. Water (100 mL) and ethyl acetate (15 mL) were added and the mixture was washed with brine (3 × 50 mL). The combined organic phases were dried over $MgSO_4$, filtered and the solvent removed under reduced pressure yielding the product as an orange-red solid (257 mg, 490 mmol, 98%).

^{1}H NMR (600 MHz, $CDCl_3$) δ = 8.01 – 7.95 (m, 8H, *H*-b/c), 6.89 (d, ^3J = 7.1 Hz, 2H, *H*-f), 4.70 (p, ^3J = 7.1 Hz, 2H, *H*-g), 1.52 (d, ^3J = 7.1 Hz, 6H, *H*-h), 1.51 (s, 18H, *H*-k) ppm.
^{13}C{^{1}H} NMR (151 MHz, $CDCl_3$) δ = 172.6 (*C*-i), 166.0 (*C*-e), 154.3 (*C*-a), 136.5 (*C*-d), 128.2 (*C*-c), 123.3 (*C*-b), 82.6 (*C*-j), 49.4 (*C*-g), 28.2 (*C*-k), 19.0 (*C*-h) ppm.
IR (ATR): $\tilde{\nu}$ = 3320 (br), 2979 (w), 2359 (w), 1731 (m), 1634 (s), 1529 (s), 1490 (m), 1454 (m), 1368 (m), 1343 (m), 1306 (m), 1271 (m), 1335 (m), 1153 (s), 1046 (m), 1012 (m), 942 (w), 893 (w), 861 (s), 848 (m), 779 (m), 737 (m), 708 (m) cm^{-1}.
HRMS (ESI) *m/z*: [M + Na]$^+$ calcd for [$C_{28}H_{36}N_4O_6$ + Na]$^+$ 547.25271; found 547.25271.
Mp: 187 °C.
R$_f$ = 0.70 (*n*-hexane/DCM 1:1).

Di-*tert*-butyl 2,2'-((11,12-dihydrodibenzo[c,g][1,2]diazocine-2,9-dicarbonyl)bis(azanediyl))(*Z*)-dipropionate (**10b**)

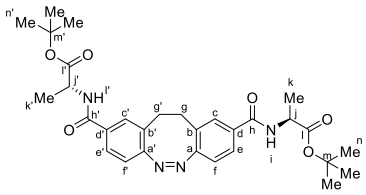

Triethyl amine (22.9 µL, 164 µmol, 2.20 equiv) was added to a solution of L-alanine *tert*-butyl ester hydrochloride (**9**) (29.8 mg, 164 µmol, 2.20 equiv) in dry DMF (2 mL). A solution of bis(2,5-dioxopyrrolidin-1-yl) 4,4'-(diazene-1,2-diyl)(*E*)-dibenzoate (**8b**) (36.5 mg, 74.4 µmol, 1.00 equiv) in dry DMF (1 mL) was added and the resulting mixture was stirred at 21 °C for 16 h. Water (30 mL) and ethyl acetate (15 mL) were added and the mixture was washed with brine (3 × 50 mL). The combined organic phases were dried over $MgSO_4$, filtered and the solvent removed under reduced pressure yielding the product as a yellow solid (33.2 mg, 60.2 µmol, 81%).

^{1}H NMR (600 MHz, $CDCl_3$) δ = 7.55 (dd, ^3J = 8.2 Hz, ^4J = 1.8 Hz, 1H, *H*-e), 7.48 (dd, ^3J = 8.2 Hz, ^4J = 1.8 Hz, 1H, *H*-e'), 7.44 (ad, ^4J = 1.8 Hz, 1H, *H*-c), 7.38 (ad, ^4J = 1.8 Hz, 1H, *H*-c'), 6.87 (d, ^3J = 8.2 Hz, 1H, *H*-f), 6.84 (d, ^3J = 8.2 Hz, 1H, *H*-f'), 4.57 (dp, ^3J = 19.0 Hz, 7.1 Hz, 2H, *H*-j/j'), 3.04 – 2.73 (m, 4H, *H*-g/g'), 1.48 (s, 9H, *H*-n), 1.47 (s, 9H, *H*-n') 1.43 (d, ^3J = 7.1 Hz, 3H, *H*-k), 1.38 (d, ^3J = 7.1 Hz, 3H, *H*-k') ppm.
3.04 – 2.73 (m, 4H, *H*-g/g'), 3.63 (s, br, 4H, *H*-h), 2.69 (s, 4H, *H*-g) ppm.
^{13}C{^{1}H} NMR (151 MHz, $CDCl_3$) δ = 172.8 (*C*-l), 172.6 (*C*-l'), 165.8 (*C*-h), 165.8 (*C*-h'), 157.8 (*C*-a), 157.8 (*C*-a'), 133.3 (*C*-b), 133.0 (*C*-b'), 129.2 (*C*-c), 129.2 (*C*-c'), 128.4 (*C*-d), 128.4 (*C*-d'), 126.1 (*C*-e), 125.8 (*C*-e'), 119.0 (*C*-f), 118.9 (*C*-f'), 82.5 (*C*-m), 82.4 (*C*-m'), 49.2 (*C*-j), 49.2 (*C*-j'), 31.6 (*C*-g), 31.4 (*C*-g'), 28.1 (*C*-n), 28.0 (*C*-n'), 18.8 (*C*-k), 18.7 (*C*-k') ppm.
IR (ATR): $\tilde{\nu}$ = 3306 (br), 2978 (w), 2359 (w), 1722 (m), 1641 (s), 1530 (s), 1480 (m), 1451 (m), 1368 (m), 1347 (m), 1227 (m), 1147 (s), 908 (m), 847 (m), 728 (m) cm^{-1}.
HRMS (ESI) *m/z*: [M + Na]$^+$ calcd for [$C_{30}H_{38}N_4O_6$ + Na]$^+$ 573.26836; found 573.26779.
Mp: 115 °C .
R$_f$ = 0.49 (*n*-hexane/DCM 1:1).

Determination of the ^{1}H NMR Yields

Reaction controls by ^{1}H NMR spectroscopy were performed using 1,3,5-trimethoxybenzene as internal standard. The molar amount of the corresponding product was calculated according to equation (1).

$$n_P = n_{IS} \times r_{P/IS} = n_{IS} \times \frac{integral_P/N_P}{integral_{IS}/N_{IS}} \quad (1)$$

In each reaction, 100 µmol of the standard was used and the integral of the three aromatic protons of the internal standard at 6.09 ppm was assigned to a value of one.

If DMSO was used as a solvent, no internal standard was used as DMSO could not be removed without an aqueous workup. If an internal standard was used, this would lead to a larger error in the procedure.

Table S3. Determination of the ^{1}H NMR Yield.

Product	Peak$_P$ [ppm]	Integral$_P$/N$_P$	n$_P$ [µmol]	Yield [%]
2,5-Dioxopyrrolidin-1-yl (*E*)-4-(phenyldiazenyl)benzoate (**3a**)	8.29	1.33/2	200	>95
2,5-Dioxopyrrolidin-1-yl (*E*)-3-(phenyldiazenyl)benzoate (**3b**)	8.23	1.31/2	197	>95
2,5-Dioxopyrrolidin-1-yl (*E*)-2-(phenyldiazenyl)benzoate (**3c**)	No conversion visible			
2,5-Dioxopyrrolidin-1-yl (*E*)-4-((4-hydroxyphenyl)diazenyl)benzoate (**3d**)	6.99	1.26/2	189	95
2,5-Dioxopyrrolidin-1-yl (*E*)-4-((4-aminophenyl)diazenyl)benzoate (**3e**)	6.71	1.26/2	189	95
2,5-Dioxopyrrolidin-1-yl (*E*)-4-((4-acetamidophenyl)diazenyl)benzoate (**3f**)	8.31	1.27/2	191	>95
2,5-Dioxopyrrolidin-1-yl (*E*)-4-((4-(allyloxy)phenyl)diazenyl)benzoate (**3h**)	8.26	0.91/2	137	69
2,5-Dioxopyrrolidin-1-yl (*E*)-4-((4-((9-hydroxynonyl)oxy)phenyl)diazenyl)benzoate (**3i**)	8.27	1.20/2	180	90
2,5-Dioxopyrrolidin-1-yl (*E*)-4-((2,6-dimethyl-4-(nonyloxy)phenyl)diazenyl)-3,5-dimethylbenzoate (**3j**)	7.90	0.63/4	95	95
2,5-Dioxopyrrolidin-1-yl (*E*)-4-((2,7-bis(4-(hexyloxy)phenoxy)naphthalen-1-yl)diazenyl)-3,5-dimethylbenzoate (**3k**)	7.80	1.26/4	189	95
2,5-Dioxopyrrolidin-1-yl (*E*)-4-((4-bromophenyl)diazenyl)benzoate (**3l**)	8.30	1.32/2	198	>95
2,5-Dioxopyrrolidin-1-yl (*E*)-4-((3-bromophenyl)diazenyl)benzoate (**3m**)	8.31	1.32/2	198	>95
2,5-Dioxopyrrolidin-1-yl (*E*)-4-((2-bromophenyl)diazenyl)benzoate (**3n**)	8.31	1.20/2	180	90
Bis(2,5-dioxopyrrolidin-1-yl) 4,4'-(diazene-1,2-diyl)(*E*)-dibenzoate (**5a**)	8.07	1.30/4	97.5	>95
Bis(2,5-dioxopyrrolidin-1-yl) 4,4'-(diazene-1,2-diyl)(*E*)-bis(3,5-dimethylbenzoate) (**5b**)	8.00	1.35/4	101	>95

The influence of the ligand was investigated using bis(2,5-dioxopyrrolidin-1-yl) 4,4'-(diazene-1,2-diyl)(*E*)-dibenzoate (**5a**) as model reaction.

Table S4: Screening of ligands.

Ligand	Peak [ppm]	integral$_P$/N$_P$	n$_P$ [µmol]	Yield [%]
1,1'-Bis(diphenylphosphino)ferrocene	8.07	0.06/4	4.50	5
2,2′-Bis(diphenylphosphino)-1,1'-binaphthyl	8.07	0.02/4	1.50	2
Di-(1-adamantyl)-*n*-butylphosphine	8.07	0.10/4	7.5	8
Tri-*tert*-butylphosphine	8.07	0.03/4	2.25	2
Xantphos	8.07	1.30/4	97.5	>95

N-Hydroxysuccinimidyl formate[5] (**2**)

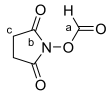

This reaction was not performed under inert conditions.

Acetic anhydride (77.0 mL, 800 µmol, 8.00 equiv) was cooled to 0 °C. Formic acid (38.0 mL, 1.00 mol, 10.0 equiv) was added over the course of 10 min and the solution was stirred at 23 °C for 2 h. 1-Hydroxypyrrolidine-2,5-dione (11.7 g, 100 µmol, 1.00 equiv) was added and the reaction mixture was stirred for further 14 h. Afterwards, the solvent was removed *in vacuo* and the resulting solid dried under reduced pressure at 8×10^{-3} mbar several hours to afford **2**[6] as a colorless solid (14.4 g, 1.00 mol, 100%, Lit.:[5] 99%).

^{1}H NMR (600 MHz, $CDCl_3$) δ = 8.18 (s, 1H, *H*-a), 2.86 (s, 4H, *H*-c) ppm.
^{13}C{^{1}H} NMR (151 MHz, $CDCl_3$) δ = 168.6 (*C*-a), 155.1 (*C*-b), 25.7 (*C*-c) ppm.
HRMS (ESI) *m/z*: $[M + Na]^+$ calcd for $[C_5H_5NO_4 + Na]^+$ 166.01108; found 166.01100.
IR (ATR): $\tilde{\nu}$ = 3002 (m), 2956 (w), 1698 (s), 1209 (m), 646 (m) cm^{-1}.
Mp: 177 °C.

(*E*)-1-(4-Iodophenyl)-2-phenyldiazene[6] (**1a**)

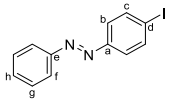

This reaction was not performed under inert conditions.

A solution of 4-iodoaniline (1.10 g, 5.00 mmol, 1.00 equiv) and nitrosobenzene (696 mg, 6.50 mmol, 1.30 equiv) in acetic acid (25 mL) was stirred for 16 h at 25 °C. The solvent was evaporated yielding **1a** as an orange solid (1.54 g, 5.00 mmol, >99%, Lit.:[6] 91%).

^{1}H NMR (600 MHz, $CDCl_3$) δ = 7.92 (d, ^3J = 7.1 Hz, 2H, *H*-f), 7.87 (d,^3J = 8.4 Hz, 2H, *H*-c), 7.66 (d, ^3J = 8.4 Hz, 2H, *H*-b), 7.54 – 7.48 (m, 3H, *H*-g/h) ppm.
^{13}C{^{1}H} NMR (151 MHz, $CDCl_3$) δ = 152.6 (*C*-e), 152.1 (*C*-a), 138.5 (*C*-c), 131.5 (*C*-h), 129.3 (*C*-g), 124.6 (*C*-b), 123.1 (*C*-f), 97.8 (*C*-d) ppm.
IR (ATR): $\tilde{\nu}$ = 3038 (br), 2357 (w), 2107 (w), 1809 (br), 1668 (w), 1563 (m), 1473 (s), 1438 (m), 1391 (m), 1293 (m), 1100 (m), 1049 (m), 998 (s), 915 (m), 838 (s), 768 (s), 701 (m) cm^{-1}.
HRMS (EI, 70 eV) *m/z* (%): $[M]^+$ calcd for $[C_{12}H_9N_2I]^+$ 307.98050; found 307.98043 (56), 77.0 (100).
Mp: 105 °C (Lit.:[6] 105 °C).
R_f = 0.75 (*n*-hexane/DCM 3:1).

[6] The product was stored under dry conditions and a nitrogen atmosphere.

(*E*)-1-(3-Iodophenyl)-2-phenyldiazene[6] (**1b**)

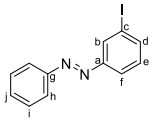

This reaction was not performed under inert conditions.

A solution of 3-iodoaniline (5.48 g, 25.0 mmol, 1.00 equiv) and nitrosobenzene (3.48 g, 32.5 mmol, 1.30 equiv) in acetic acid (150 mL) was stirred for 16 h at 25 °C. The solvent was evaporated yielding **1b** as an orange solid (7.47 g, 24.2 mmol, 97%, Lit.:[6] 96%).

^{1}H NMR (600 MHz, $CDCl_3$) δ = 8.25 (at, ^4J = 1.8 Hz, 1H, *H*-b), 7.94 – 7.90 (m, 3H, *H*-f/h), 7.80 (ddd, ^3J = 7.9 Hz, ^4J = 1.4 Hz, 1.0 Hz, 1H, *H*-d), 7.55 – 7.48 (m, 3H, *H*-i/j), 7.27 (t, ^3J = 7.9 Hz, 1H, *H*-e) ppm.
^{13}C{^{1}H} NMR (151 MHz, $CDCl_3$) δ = 153.5 (*C*-a), 152.5 (*C*-g), 140.0 (*C*-d), 131.6 (*C*-j), 130.8 (*C*-e), 130.7 (*C*-b), 129.3 (*C*-i), 123.7 (*C*-f), 123.2 (*C*-h), 94.7 (*C*-c) ppm.
IR (ATR): $\tilde{\nu}$ = 3056 (w), 1828 (br), 1560 (w), 1451 (m), 1403 (m), 1302 (w), 1203 (m), 1148 (m), 1086 (w), 1070 (w), 1051 (w), 1018 (m), 992 (w), 914 (m), 880 (m), 833 (w), 792 (s), 761 (s) cm^{-1}.
HRMS (EI, 70 eV) *m/z* (%): $[M]^+$ calcd for $[C_{12}H_9N_2I]^+$ 307.98050; found 307.98052 (57), 77.0 (100).
Mp: 71 °C (Lit.:[6] 67 °C).
R_f: 0.75 (*n*-hexane/DCM 3:1).

(*E*)-1-(2-Iodophenyl)-2-phenyldiazene[6] (**1c**)

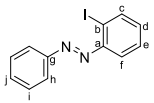

This reaction was not performed under inert conditions.

A solution of 2-iodoaniline (14.2 g, 65.0 mmol, 1.00 equiv) and nitrosobenzene (9.05 g, 84.5 mmol, 1.30 equiv) in acetic acid (400 mL) was stirred for 16 h at 40 °C. The solvent was removed under reduced pressure and the residue crystallized from methanol at -21 °C yielding **1c** as an orange solid (7.47 g, 24.2 mmol, 28%, Lit.:[6] 25%).

^{1}H NMR (600 MHz, $CDCl_3$) δ = 8.04 (dd, ^3J = 7.9 Hz, ^4J = 1.3 Hz, 1H, *H*-c), 8.01 (d, ^3J = 8.2 Hz, 2H, *H*-h), 7.64 (dd, ^3J = 8.0 Hz, ^4J = 1.6 Hz, 1H, *H*-f), 7.57 – 7.49 (m, 3H, *H*-i/j), 7.43 (ddd, ^3J = 7.9 Hz, 7.2 Hz, ^4J = 1.3 Hz, 1H, *H*-e), 7.17 (ddd, ^3J = 7.9 Hz, 7.2 Hz, ^4J = 1.6 Hz, 1H, *H*-d) ppm.
^{13}C{^{1}H} NMR (151 MHz, $CDCl_3$) δ = 152.5 (*C*-g), 151.5 (*C*-a), 140.0 (*C*-c), 132.3 (*C*-d), 131.7 (*C*-j), 129.3 (*C*-i), 129.1 (*C*-e), 123.7 (*C*-h), 117.5 (*C*-f), 102.6 (*C*-b) ppm.
IR (ATR): $\tilde{\nu}$ = 3055 (w), 1887 (br), 1572 (w), 1562 (m), 1489 (w), 1446 (m), 1419 (w), 1303 (w), 1249 (w), 1220 (w), 1142 (m), 1015 (s), 999 (w), 948 (w), 920 (w), 771 (s), 708 (s) cm^{-1}.
HRMS (EI, 70 eV) *m/z* (%): $[M]^+$ calcd for $[C_{12}H_9N_2I]^+$ 307.98050; found 307.98052 (72), 77.0 (100).
Mp: 61 °C (Lit.:[6] 59 °C).
R_f: 0.70 (*n*-hexane/DCM 3:1).

(*E*)-4-((4-Iodophenyl)diazenyl)phenol[7] (**1d**)

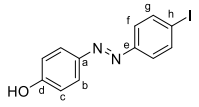

This reaction was not performed under inert conditions.

4-Iodoaniline (2.00 g, 9.13 mmol, 1.20 equiv) was dissolved in a mixture of acetone:water (1:1, 25 mL) and cooled to 0 °C. Subsequently, conc. HCl (1.15 mL, 1.50 equiv) was slowly added to the solution over the course of 10 min and left to stir for another 10 min. Sodium nitrite (735 mg, 10.6 mmol, 1.40 equiv) dissolved in water (6 mL) was added slowly over the course of 3 min and the reaction mixture was stirred for 30 min. Meanwhile, a second mixture with phenol (716 mg, 7.61 mmol, 1.00 equiv), Na_2CO_3 (1.61 g, 15.2 mmol, 2.00 equiv) and NaOH (1.22 g, 30.4 mmol, 4.00 equiv) dissolved in acetone/water (1:1, 25 mL) was cooled to 0 °C. The first prepared solution was slowly added to the solution containing the phenol over the course of 5 min. The resulting mixture was stirred for 12 h while slowly warmed to 21 °C. Subsequently, the mixture was diluted with a HCl solution (1 M, 30 mL). The precipitate that formed was removed by filtration and washed with water (2 × 10 mL). The precipitate was crystallized from MeOH at -21 °C to give **1d** as a yellow solid (2.39 g, 7.38 mmol, 97%, Lit.:[7]81%).

^{1}H NMR (600 MHz, $CDCl_3$) δ = 7.87 (d, ^3J = 8.9 Hz, 2H, *H*-g), 7.84 (d, ^3J = 8.7 Hz, 2H, *H*-c), 7.61 (d, ^3J = 8.7 Hz, 2H, *H*-b), 6.94 (d, ^3J = 8.9 Hz, 2H, *H*-f), 5.11 (s, 1H, O*H*-d) ppm.
^{13}C{^{1}H} NMR (125 MHz, $CDCl_3$) δ = 158.41 (*C*-d), 151.99 (*C*-e), 147.06 (*C*-a), 138.27 (*C*-g), 125.16 (*C*-c), 124.24 (*C*-b), 115.86 (*C*-f), 96.82 (*C*-h) ppm.
HRMS (EI, 70 eV) *m/z* (%): $[M]^+$ calcd for $[C_{12}H_9IN_2O]^+$ 323.97541; found 323.97570 (45), 93.0 (100).
IR: $\tilde{\nu}$ = 3024 (b), 1590 (s), 1562 (w), 1466 (s), 1438 (m), 1298 (s), 1240 (m), 1152 (s), 1140 (s), 1101 (m), 1051 (w), 1002 (w), 829 (s), 724 (s), 704 (m) cm^{-1}.
Mp: 168 °C.
R$_f$: 0.50 (*n*-hexane/ethyl acetate 4:1).

(*E*)-4-((4-Iodophenyl)diazenyl)aniline (**1e**)

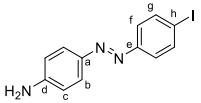

To (*E*)-*N*-(4-((4-Iodophenyl)diazenyl)phenyl)acetamide (365 mg, 1.00 mmol, 1.00 equiv.) was added MeOH (15 mL) and HCl (3 M, 75 mL). The suspension was stirred for 18 h at 85 °C, resulting in a clear red solution. The mixture was neutralized with a saturated aqueous $NaHCO_3$ solution and the precipitate was filtered. The precipitate was washed with water (2 × 20 mL) and the product was crystalized from EtOH at -21 °C to obtain **1e** as a red solid (280 mg, 0.866 mmol, 87%).

^{1}H NMR (600 MHz, DMSO-d_6) δ = 7.87 (d, ^3J = 8.2 Hz, 2H, *H*-g), 7.67 (d, ^3J = 8.4 Hz, 2H, *H*-c), 7.53 (d, ^3J = 8.2 Hz, 2H. *H*-f), 6.67 (d, ^3J = 8.4 Hz, 2H, *H*-b), 6.20 (s, 2H, NH_2-d) ppm.
^{13}C{^{1}H} NMR (151 MHz, DMSO-d_6) δ = 153.74 (*C*-a/e), 152.32 (*C*-a/e), 143.13 (*C*-d), 138.54 (*C*-g), 125.94 (*C*-c), 124.15 (*C*-f), 113.8(*C*-b), 96.20 (*C*-h) ppm.

IR (ATR): $\tilde{\nu}$ = 3446 (m), 3319 (m), 3205 (m), 2667 (w), 1893 (w), 1628 (m), 1593 (s), 1504 (m), 1473 (w), 1416 (m), 1385 (s), 1304 (s), 1230 (w), 1186 (m), 1153 (m), 1138 (s), 1119 (s), 1094 (w), 1004 (w), 943 (w), 829 (s), 722 (s), 699 (w) cm^{-1}.
HRMS (EI, 70 eV) *m/z* (%): $[M]^+$ calcd for $[C_{12}H_{10}IN_3]^+$ 322.99140; found 322.99152 (10), 92.1 (100).
Mp: 162 °C.
R$_f$: 0.40 (*n*-hexane/ethyl acetate 1:1).

(*E*)-*N*-(4-((4-Iodophenyl)diazenyl)phenyl)acetamide (**1f**)

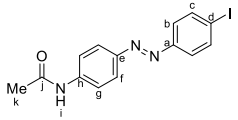

4-Aminoacetanilide (2.40 g, 16.0 mmol, 1.00 equiv) was dissolved in water (200 mL). Oxone® (19.7 g, 32 mmol, 2.00 equiv) was dissolved in water (100 mL) and added to the solution. The mixture was stirred for five minutes, while a green solid precipitated. The precipitate was filtered and the filter cake was extracted with ethyl acetate. The organic phase was dried over $MgSO_4$ and filtered. The solvent was removed and NMR analysis revealed that the nitroso compound was obtained in a high purity and a yield of 850 mg (5.18 mmol, 32%).

This product was used without further purification. 4-Nitrosoacetaniliden (820 mg, 5.00 mmol, 1.00 equiv) was dissolved in acetic acid (100 mL). To this solution, 4-iodoaniline (1.10 g, 5.00 mmol, 1.00 equiv) was added and the mixture was stirred for 1 d at 22 °C. The solvent was removed *in vacuo* and the crude product filtered through a short plug of silica (eluent: DCM). The solvent was removed and the crude product was crystallized in MeOH at -21 °C to yield **1f** as an orange solid (1.25 g, 3.42 mmol, 68%).

^{1}H NMR (600 MHz, DMSO-d_6) δ = 10.32 (s, 1H, N*H*-j), 7.95 (d, ^3J = 8.4 Hz, 2H, *H*-g), 7.88 (d, ^3J = 8.4 Hz, 2H, *H*-f), 7.80 (d, ^3J = 8.7 Hz, 2H, *H*-b), 7.63 (d, ^3J = 8.7 Hz, 2H, *H*-c), 2.10 (s, 3H, *H*-k) ppm.
^{13}C{^{1}H} NMR (151 MHz, DMSO-d_6) δ = 168.9 (*C*-j), 151.4 (*C*-h), 147.3 (*C*-*e*), 142.8 (*C*-a), 138.4 (*C*-g), 124.2 (*C*-f), 123.9 (*C*-b), 119.1 (*C*-c), 98.2 (*C*-d), 24.2 (*C*-k) ppm.
IR (ATR): $\tilde{\nu}$ = 3247 (w), 1658 (m), 1589 (m), 1520 (m), 1495 (m), 1473 (m), 1403 (w), 1367 (m), 1298 (m), 1264 (m), 1156 (w), 1142 (w), 1097 (w), 1037 (w), 1013 (w), 1001 (m), 835 (s), 728 (s), 701 (w) cm^{-1}.
HRMS (EI, 70 eV) *m/z* (%): $[M]^+$ calcd for $[C_{14}H_{12}IN_3O]^+$ 365.00196; found 365.00248 (25), 134.2 (100).
Mp: 230 °C.
R$_f$: 0.15 (*n*-hexane/ethyl acetate 1:1).

(*E*)-1-(4-Iodophenyl)-2-(4-nitrophenyl)diazene[8] (**1g**)

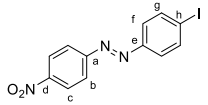

This reaction was not performed under inert conditions.

4-Amino-nitrophenol (20.0 g, 145 mmol, 1.00 equiv) was dissolved in DCM (60 mL). Oxone® (178 g, 190 mmol, 2.00 equiv) was dissolved in water (750 mL) and added to the solution. The biphasic mixture was stirred vigorously for 12 h. The phases were separated and the organic phase was dried over

$MgSO_4$ and filtered to yield 16.8 g crude product with a 60% conversion to the desired nitroso compound. This product was used without further purification.

4-Nitro-nitrosophenol (telescoped from the above reaction, 10.1 g, 66.1 mmol, 1.00 equiv) was dissolved in acetic acid (200 mL). To this solution, 4-iodoaniline (15.9 g, 72.7 mmol, 1.10 equiv) was added and the mixture was stirred for 3 d at 85 °C. The solvent was removed *in vacuo* and the crude product was crystallized two times from MeOH at -21 °C to yield **1g** 15.8 g (44.7 mmol, 68%, Lit.:[8] 51%).

^{1}H NMR (600 MHz, $CDCl_3$) δ = 8.39 (d, ^3J = 9.1 Hz, 2H, *H*-g), 8.04 (d, ^3J = 9.1 Hz, 2H, *H*-f), 7.92 (d, ^3J = 8.7 Hz, 2H, *H*-c), 7.70 (d, ^3J = 8.7 Hz, 2H, *H*-b) ppm.
^{13}C{^{1}H} NMR (125 MHz, $CDCl_3$) δ = 155.46 (*C*-h), 151.63 (*C*-e), 148.89 (*C*-a), 138.65 (*C*-c), 124.85 (*C*-b), 124.78 (*C*-g), 123.55 (*C*-h), 99.68 (*C*-d) ppm.
IR: $\tilde{\nu}$ = 1604 (m), 1514 (s), 1451 (m), 1338 (s), 1324 (m), 1139 (m), 1104 (w), 1048 (m), 1004 (m), 856 (s), 830 (s), 818 (m), 751 (s), 704 (s), 682 (m) cm^{-1}.
HRMS (EI, 70 eV) *m/z* (%): $[M]^+$ calcd for $[C_{12}H_8IN_3O_2]^+$ 352.96558; found 352.96538 (40, 76.0 (100).
Mp: 240 °C.
R_f: 0.40 (*n*-hexane/ethyl acetate 1:1).

(*E*)-1-(4-(Allyloxy)phenyl)-2-(4-iodophenyl)diazene[9] (**1h**)

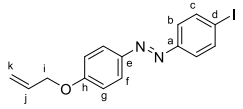

1d (1.62 g, 5.00 mmol, 1.00 equiv) and potassium carbonate (829 mg, 6.00 mmol, 1.10 equiv) were dissolved in anhydrous DMF (20 mL) under nitrogen. The solution was heated to 50 °C. Allyl bromide (1.21 g, 10.0 mmol, 2.00 equiv) in 20 mL DMF were added dropwise. The mixture was stirred at 50 °C for 17 h. After adding ethyl acetate (100 mL), the solution was washed with water (100 mL), brine (100 mL) and dried over $MgSO_4$. After filtration, the solvent was removed by evaporation under reduced pressure. The crude product was filtered through a short plug of silica and further purified by crystallization in methanol to give **1h** as a yellow solid (1.29 g, 3.55 mmol, 71% Lit.:[9] 88%).

^{1}H NMR (600 MHz, $CDCl_3$) δ = 7.90 (d, *J* = 8.9 Hz, 2H, *H*-g), 7.84 (d, *J* = 8.7 Hz, 2H, *H*-b), 7.61 (d, *J* = 8.7 Hz, 2H, *H*-c), 7.02 (d, *J* = 8.9 Hz, 2H, *H*-f), 6.12 – 6.04 (m, 1H, *H*-j), 5.45 (d, *J* = 17.3 Hz, 1H, *H*-k), 5.33 (d, *J* = 10.5 Hz, 1H, *H*-k), 4.63 (d, *J* = 6.6 Hz, 2H, *H*-i).
^{13}C{^{1}H} NMR (151 MHz, $CDCl_3$) δ 161.50 (C-h), 152.23 (C-a), 147.04 (*C*-e), 138.41 (*C*-b), 132.81 (*C*-j), 125.05 (*C*-g), 124.39 (*C*-c), 118.30 (*C*-k), 115.17 (*C*-f), 96.87 (*C*-d), 69.21 (*C*-i).
IR: $\tilde{\nu}$ = 1600 (s), 1579 (m), 1563 (m), 1492 (m), 1473 (w), 1426 (w), 1391 (w), 1362 (w), 1296 (w), 1239 (m), 1152 (m), 1141 (m), 1016 (m), 1016 (m), 993 (s), 930 (m), 838 (s), 826 (s), 727 (m), 705 (m) cm^{-1}.
HRMS (EI, 70 eV) *m/z* (%): $[M]^+$ calcd for $[C_{15}H_{13}N_2OI]^+$ 364.00671; found 364.00660 (60), 133.1 (100).
Mp: 148 °C.
R_f: 0.65 (*n*-hexane/ethyl acetate 1:1).

(*E*)-9-(4-((4-Iodophenyl)diazenyl)phenoxy)nonan-1-ol (**1i**)

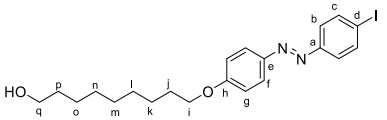

This reaction was not performed under inert conditions.

A mixture of **1d** (6.00 g, 18.5 mmol, 1.00 equiv) and 9-bromo-1-nonanol (4.95 g, 22.2 mmol, 1.20 equiv) was dissolved in acetone (100 mL). Potassium iodide (100 mg, 602 µmol, 3 mol%) and potassium carbonate (5.11 g, 37.0 mmol, 2.00 equiv) was added to the solution. The resulting solution was heated to reflux at 60 °C for 5 h. After the reaction mixture was cooled to 24 °C, water (300 mL) was added to the mixture. A precipitate was formed, which was collected by filtration. The aqueous solution was extracted with DCM (3 × 20 mL). Both the precipitate and the extract were combined and dried *in vacuo*. The resulting crude product was purified by column chromatography (gradient *n*-pentane → DCM) to give **1i** as a yellow solid (3.40 g, 7.29 mmol, 57%).

^{1}H NMR (600 MHz, $CDCl_3$) δ = 7.90 (d, ^3J = 9.0 Hz, 2H, *H*-g), 7.83 (d, ^3J = 8.7 Hz, 2H, *H*-c), 7.61 (d, ^3J = 8.7 Hz, 2H, *H*-b), 6.99 (d, ^3J = 9.0 Hz, 2H, *H*-f), 4.04 (t, ^3J = 6.5 Hz, 2H, *H*-i), 3.65 (t, ^3J = 6.6 Hz, 2H, *H*-q), 1.86-1.77 (m, 2H, *H*-j), 1.58 (p, ^3J = 6.6 Hz, 2H, *H*-p), 1.48 (m, 2H, C2-*H*-k), 1.35 (m, 8H, *H*-l,m,n,o) ppm.
^{13}C{^{1}H} NMR (125 MHz, $CDCl_3$) δ = 162.00 (*C*-h), 152.10 (*C*-e), 146.67 (*C*-d)), 138.23 (*C*-c), 124.92 (*C*-g), 124.20 (*C*-b), 114.76 (*C*-f)), 96.59 (*C*-d), 68.37 (*C*-i), 63.07 (*C*-q), 32.78 (*C*-p), 29.50 (*C*-m), 29.34 (*C*-n), 29.29 (*C*-j), 29.16 (*C*-l), 25.99 (*C*-k), 25.72 (*C*-o) ppm.
IR: $\tilde{\nu}$ = 3298 (b), 2917 (m), 2849 (m), 1602 (s), 1582 (m), 1500 (w), 1471 (w), 1297 (s), 1251 (m), 1143 (s), 1107 (m), 1020 (m), 843 (s), 829 (s), 721 (m), 705 (w) cm^{-1}.
HRMS (EI, 70 eV) *m/z* (%): $[M]^+$ calcd for $[C_{21}H_{27}IN_2O_2]^+$ 466.11118; found 466.11064 (10), 55.0 (100).
Mp: 133 °C.
R_f: 0.50 (*n*-pentane: DCM 1:1).

(*E*)-4-((4-Iodo-2,6-dimethylphenyl)diazenyl)-3,5-dimethylphenol (**S1**)

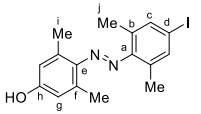

This reaction was not performed under inert conditions.

2,6-Dimethyl-4-nitroaniline (500 mg, 3.01 mmol, 1.00 equiv) and K_2CO_3 (410 mg, 3.01 mmol, 1.00 equiv) were dissolved in water (10 mL). $NaNO_2$ (205 mg, 3.01 mmol, 1.00 equiv) dissolved in water (10 mL) was added dropwise over the course of 1 min. The mixture was cooled to 0 °C and HCl (4 M, 10 mL) was slowly added dropwise over the course of 10 min forming white crystals. The dispersion was stirred for 1 h at 0 °C. The mixture was slowly added dropwise over the course of 10 min to a second solution of 3,5-dimethylphenol (400 mg, 3.27 mmol, 1.08 eq) and NaOH (5 wt%, 10 mL), which was cooled to 0 °C in beforehand. The resulting dispersion was stirred for another 21 h while warming up to 23 °C. The mixture was diluted with HCl (1 M, 20 mL). The precipitate was removed by filtration and washed with water (2 x 10 mL). The residue was crystallized in MeOH at -20 °C to yield **S1** as a dark red solid. (410 mg, 1.34 mmol, 45%).

^{1}H NMR (600 MHz, $CDCl_3$) δ = 7.52 (s, 2 H, *H*-c), 6.65 (s, 2 H, O*H*-g), 2.50 (s, 6 H, *H*-i), 2.35 (s, 6 H, *H*-j) ppm.
^{13}C{^{1}H} NMR (151 MHz, $CDCl_3$) δ = 156.2 (*C*-h), 151.5 (*C*-a), 144.6 (*C*-e), 137.9 (*C*-c), 136.0 (*C*-b), 132.9 (*C*-f), 116.1 (*C*-g), 93.1 (*C*-d), 21.0 (*C*-i), 19.4 (*C*-j) ppm.
IR: $\tilde{\nu}$ = 3418 (m) 2956 (w), 1609 (m), 1507 (s), 1466 (m), 1376 (s), 1337 (s), 1302 (s), 1217 (m), 1148 (s), 1099 (w), 941 (m), 895 (m), 800 (w), 746 (s) cm^{-1}.
HRMS (ESI): *m/z* = [M + Na]$^+$ calcd for [$C_{16}H_{17}N_3O_3$+ Na]$^+$ 322.11621, found 322.11633.
Mp: 190 °C.
R$_f$: 0.70 (*n*-hexane/ethyl acetate 4:1).

(*E*)-1-(2,6-Dimethyl-4-(nonyloxy)phenyl)-2-(4-iodo-2,6-dimethylphenyl)diazene (**1j**)

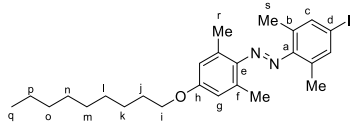

This reaction was not performed under inert conditions.

A mixture of **S1** (1.30 g, 3.42 mmol, 1.00 equiv), K_2CO_3 (886 mg, 6.40 mmol) and 1-bromohexane (2.30 mL, 4.65 mmol, 1.36 equiv) in acetonitrile (20 mL) was stirred at 80 °C. After stirring for 24 h, the solvent was removed. DCM was added and washed with HCl (1 M, 20 mL), water (20 mL), sat. $NaHCO_3$ (20 mL) and brine (20 mL). The organic phase was dried over $MgSO_4$ and filtered. The solvent was removed in vacuo and the residue was purified by column chromatography to afford **1j** as a red oil, which solidified after several hours. (1.02 g, 2.13 mmol, 62%).

^{1}H NMR (600 MHz, $CDCl_3$) δ = 7.49 (s, 2H, *H*-c), 6.68 (s, 2H, *H*-g), 4.01 (t, ^3J = 6.6 Hz, 2H *H*-i), 2.50 (s, 6H, *H*-r), 2.33 (s, 6H, *H*-s), 1.83 – 1.78 (m, 2H, *H*-j), 1.47 (p, ^3J = 7.5, 7.1 Hz, 2H, *H*-k), 1.39 – 1.25 (m, 12H, *H*-l-p), 0.90 (d, ^3J = 7.2 Hz, 3H, *H*-q) ppm.
^{13}C{^{1}H} NMR (151 MHz, $CDCl_3$) δ = 159.79 (*C*-h), 151.73 (*C*-a), 144.41 (*C*-e), 138.00 (*C*-c), 135.88 (*C*-f), 133.02 (*C*-*b*), 115.33 (*C*-g), 93.11 (*C*-d), 68.21 (*C*-i), 32.03 (*C*-l-p), 29.69 (*C*-l-p), 29.53 (*C*-l-p), 29.42 (*C*-l-p), 29.38 (*C*-j), 26.17(*C*-k), 22.83 (*C*-l-p), 21.39 (*C*-r), 19.47 (*C*-s), 14.27 (*C*-q) ppm
IR (ATR): $\tilde{\nu}$ = 2966 (s), 2935 (s), 2921 (m), 2850 (w), 1599 (m), 1588 (w), 1487 (w), 1487 (m), 1462 (m), 1454 (s), 1375 (w), 1311 (s), 1245 (w), 1168 (m), 1147 (s), 1127 (m), 1064 (s), 1036 (m), 877 (m), 863 (s), 854 (s), 825 (m), 779 (w), 747 (m), 730 (w) cm^{-1}.
HRMS (EI, 70 eV) *m/z* (%): [M]$^+$ calcd for [$C_{25}H_{35}N_2OI$]$^+$ 506.17886; found 506.17900 (10), 43.1 (100).
Mp: 66 °C.
R$_f$: 0.70 (*n*-hexane/ethyl acetate 1:1).

(*E*)-1-((4-Iodo-2,6-dimethylphenyl)diazenyl)naphthalene-2,7-diol (**S2**)

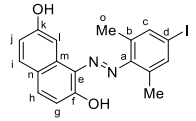

This reaction was not performed under inert conditions.

4-Iodo-2,5-dimethylanilin (2.47 g, 10 mmol, 1.00 equiv) and K_2CO_3 (1.26 g, 10.00 mmol, 1.00 equiv) were dissolved in water (10 mL). $NaNO_2$ (680 mg, 10.0 mmol, 1.00 equiv) dissolved in water (10 mL)

was added dropwise. The mixture was cooled to 0 °C under constant stirring and HCl (4 M, 10 mL) was added dropwise. The mixture was stirred for 1h and was then added dropwise to a mixture of 2,7-dihydroxynaphthalene (1.60 g, 10.0 mmol, 1.00 equiv) and 15 wt% NaOH solution (10 mL). The reaction was stirred for a further 3 h while warming up to 21 °C. The mixture was diluted with HCl (1 M, 50 mL). The precipitate was removed by filtration and washed with water (2 × 10 mL). The residue was crystallized from ethanol/water (5:1) at -21 °C to yield **S2** as a dark red solid (3.49 g, 8.70 mmol, 87%).

^{1}H NMR (600 MHz, DMSO-d_6) δ = 10.14 (s, 2H, O*H*-f/k), 7.83 (d, ^3J = 9.3 Hz, 1H, *H*-j), 7.66 (s, 2H, *H*-c), 7.66 (s, 1H, H-l), 7.63 (d, 1H, ^3J = 8.5 Hz, *H*-g), 6.91 (dd, ^3J = 8.5, ^4J = 2.4 Hz, 1H, *H*-h), 6.67 (d, ^3J = 9.3 Hz, 1H, *H*-i), 2.51 (s, 9H, *H*-o) ppm.
^{13}C{^{1}H} NMR (151 MHz, DMSO-d_6) δ = 169.88 (*C*-k), 158.80 (*C*-f), 141.20 (*C*-a), 140.27 (*C*-j), 138.09 (*C*-c), 135.18 (*C*-e), 132.01 (*C*-b), 130.98 (*C*-g), 130.03 (*C*-m), 121.33 (*C*-n), 120.12 (*C*-i), 115.71 (*C*-h), 105.15 (*C*-l), 92.64 (*C*-d), 19.47 (*C*-o) ppm.
IR (ATR): $\tilde{\nu}$ = 3137 (br), 1621 (m), 1548 (m), 1506 (s), 1479 (s), 1460 (s), 1418 (m), 1356 (w), 1331 (s), 1271 (m), 1242 (m), 1216 (m), 1198 (m), 1163 (m), 1141 (w), 1019 (w), 946 (w), 888 (m), 875 (m), 833 (s), 813 (m) cm^{-1}.
HRMS (EI): *m/z* = [M]$^+$ calcd for [$C_{18}H_{15}IN_2O_2$]$^+$ 418.01728, found 418.01727 (30), 159.1 (100).
Mp: 232 °C.
R$_f$: 0.50 (*n*-hexane/ethyl acetate 1:1).

(*E*)-1-((4-Iodo-2,6-dimethylphenyl)diazenyl)naphthalene-2,7-diyl bis(4-(hexyloxy)benzoate) (**1k**)

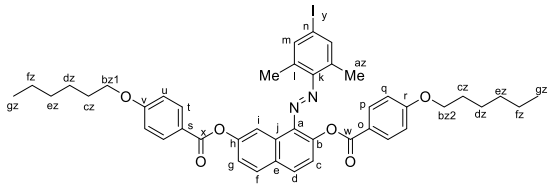

4-Hexyloxybenzoic acid (571 mg, 3.00 mmol, 3.00 equiv), **S2** (418 mg, 1.00 mmol, 1.00 equiv) and DMAP (122 mg, 1.00 mmol, 1.00 equiv) were dissolved in dry DCM (15 mL). Afterwards DCC (1.03 g, 5.00 mmol, 5.00 equiv) was added portion-wise. The mixture was stirred for 16 h. The resulting suspension was filtered, washed with a saturated $NaHCO_3$ solution (30 mL), water (30 mL), brine (30 mL). The organic phase was dried over $MgSO_4$, filtered and the solvent was removed under reduced pressure. The product was purified by column chromatography (eluent: DCM/*n*-hexane 1:1) to yield **1k** as a red solid (637 mg, 720 µmol, 72%).

^{1}H NMR (600 MHz, $CDCl_3$) δ = 8.46 (d, ^4J = 2.3 Hz, 1H, *H*-i), 8.16 (d, ^3J = 8.9 Hz, 2H, *H*-t), 8.04 (d, ^3J = 8.9 Hz, 2H, *H*-p), 7.99 (t, ^3J = 8.8 Hz, 2H, *H*-f/d), 7.46 (dd, ^3J = 8.8, 2.3 Hz, 1H, *H*-g), 7.41 (d, ^3J = 8.8 Hz, 1H, *H*-c), 7.39 (s, 2H, *H*-m), 6.07 (d, ^3J = 8.9 Hz, 2H, *H*-u), 6.90 (d, ^3J = 8.9 Hz, 2H, *H*-q), 4.05 (t, ^3J = 6.5 Hz, 2H, *H*-bz1) 4.02 (t, ^3J = 6.6 Hz, 2H, *H*-bz2), 2.22 (s, 6H, *H*-az), 1.82 (dd, ^2J = 14.8, ^3J = 6.6 Hz, 4H, *H*-cz), 1.52-1.43 (m, 4H, *H*-dz), 1.40-1.31 (m, 8H, *H*-ez/fz), 0.94 – 0.90 (m, 6H, *H*-gz) ppm.
^{13}C{^{1}H} NMR (151 MHz, $CDCl_3$) δ = 165.13 (*C*-x), 165.09 (*C*-w), 163.78 (*C*-s), 163.65 (*C*-o), 151.40 (*C*-k), 150.80 (*C*-b), 139.82 (*C*-e), 138.49 (*C*-j), 138.02 (*C*-m), 133.79 (*C*-l), 132.50 (*C*-p+t), 131.40 (*C*-f), 130.62 (*C*-d), 130.54 (*C*-h), 129.58 (*C*-a), 123.01 (*C*-c), 122.19 (*C*-g), 121.48 (*C*-v), 121.38 (*C*-r), 115.97 (*C*-i), 114.47 (*C*-u), 114.39 (*C*-q), 94.85 (*C*-n), 68.49 (*C*-bz1), 68.45 (*C*-bz2), 31.70 (*C*-fz/ez), 29.21 (*C*-cz), 25.81 (*C*-dz), 24.85 (*C*-ez), 22.74 (*C*-fz/ez), 19.10 (*C*-az), 14.18 (*C*-gz) ppm.

IR (ATR): $\tilde{\nu}$ = 2924 (m), 1721 (s), 1604 (s), 1563 (m), 1512 (m), 1469 (m), 1421 (w), 1249 (s), 1201 (s), 1217 (s), 1201 (m), 1162 (s), 1067 (s), 1006 (m), 934 (m), 916 (m), 899 (w), 875 (m), 848 (w), 759 (s), 690 (m) cm^{-1}.
HRMS (ESI): *m/z* = $[M+Na]^+$ calcd for $[C_{44}H_{47}IN_2O_6+Na]^+$ 849.23669, found 849.23711.
Mp: 232 °C.
R$_f$: 0.50 (*n*-hexane/ethyl acetate 1:1).

(*E*)-1-(4-Bromophenyl)-2-(4-iodophenyl)diazene[10] (**1l**)

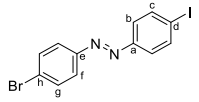

This reaction was not performed under inert conditions.

4-Bromoaniline (3.70 g, 21.5 mmol, 1.00 equiv) was dissolved in DCM (75 mL). To this solution, Oxone® (26.4 g, 43.0 mmol, 2.00 equiv) dissolved in water (300 mL) was added. The solution was stirred under a nitrogen atmosphere at 25 °C for 2 h. The color of the solution turned to green as the corresponding nitrosoarene formed. The layers were separated and the aqueous layer was extracted with DCM (3 × 100 mL). The combined organic layers were washed with HCl (1 M, 150 mL), saturated sodium hydrogen carbonate solution (150 mL), water (150 mL) and brine (150 mL). The organic phase was dried over $MgSO_4$ and filtered. The solvent was removed under reduced pressure. The obtained crude 1-bromo-4-nitrosobenzene (4.00 g, 21.5 mmol, 1.00 equiv) was dissolved in acetic acid (100 mL) and 4-iodoaniline was added (4.71 g, 21.5 mmol, 1.00 equiv). The resulting mixture was stirred at 25 °C for 14 h. The precipitate was separated by filtration and washed with acetic acid (100 mL). The residue was crystallized from methanol at -21 °C yielding **1l** as an orange solid (6.63 g, 17.1 mmol, 80%, Lit.:[10] 86%).

^{1}H NMR (600 MHz, $CDCl_3$) δ = 7.87 (d, ^3J = 8.6 Hz, 2H, *H*-c), 7.79 (d, ^3J = 8.7 Hz, 2H, *H*-f), 7.65 (d, ^3J = 8.7 Hz, 2H, *H*-g), 7.64 (d, ^3J = 8.6 Hz, 2H, *H*-b) ppm.
^{13}C{^{1}H} NMR (151 MHz, $CDCl_3$) δ = 151.9 (*C*-a), 151.3 (*C*-e), 138.6 (*C*-c), 132.6 (*C*-b), 126.0 (*C*-h), 124.7 (*C*-g), 124.6 (*C*-f), 98.3 (*C*-d) ppm.
IR (ATR): $\tilde{\nu}$ = 2355 (w), 2093 (br), 1904 (w), 1652 (w), 1563 (m), 1470 (m), 1395 (m), 1280 (w), 1222 (w), 1143 (w), 1095 (m), 1061 (m), 1001 (s), 831 (s), 773 (s), 709 (s) cm^{-1}.
HRMS (EI, 70 eV) *m/z* (%): $[M]^+$ calcd for $[C_{12}H_8BrIN_2]^+$ 385.89101; found 385.89136 (45), 76.0 (100).
Mp: 205 °C (Lit.:[6] 201 °C).
R$_f$: 0.75 (*n*-hexane/DCM 3:1).

(*E*)-1-(3-Bromophenyl)-2-(4-iodophenyl)diazene (**1m**)

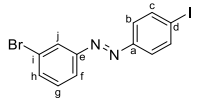

This reaction was not performed under inert conditions.

3-Bromoaniline (6.00 g, 35.0 mmol, 1.00 equiv) was dissolved in DCM (75 mL). To this solution, Oxone® (43.1 g, 75.0 mmol, 2.00 equiv) dissolved in water (300 mL) was added. The solution was stirred under a nitrogen atmosphere at 25 °C for 6 h. The color of the solution turned to green as the corresponding nitrosoarene formed. The layers were separated and the aqueous layer was extracted with DCM (3 ×

100 mL). The combined organic layers were washed with HCl (1 M, 150 mL), saturated sodium hydrogen carbonate solution (150 mL), water (150 mL) and brine (150 mL). The organic phase was dried over $MgSO_4$ and filtered. The solvent was removed under reduced pressure. The obtained crude 1-bromo-3-nitrosobenzene (6.51 g, 35.0 mmol, 1.00 equiv) was dissolved in acetic acid (100 mL) and 4-iodoaniline was added (7.67 g, 35.0 mmol, 1.00 equiv). The resulting mixture was stirred at 25 °C for 16 h. The precipitate was separated by filtration and washed with acetic acid (100 mL). The residue was crystallized from methanol at -21 °C yielding **1m** as an orange solid (9.65 g, 24.9 mmol, 72%).

^{1}H NMR (600 MHz, $CDCl_3$) δ = 8.05 (at, ^4J = 1.9 Hz, 1H, *H*-j), 7.88 – 7.86 (m, 3H, *H*-c/h), 7.65 (d, ^3J = 8.6 Hz, 2H, *H*-b), 7.61 (ddd, ^3J = 7.9 Hz, ^4J = 1.9 Hz, 1.0 Hz, 1H, *H*-f), 7.41 (t, ^3J = 7.9 Hz, 1H, *H*-g) ppm.
^{13}C{^{1}H} NMR (151 MHz, $CDCl_3$) δ = 153.5 (*C*-e), 151.8 (*C*-a), 138.6 (*C*-c), 134.1 (*C*-f), 130.7 (*C*-g), 124.8 (*C*-j), 124.8 (*C*-b), 123.3 (*C*-h), 123.3 (*C*-i), 98.6 (*C*-d) ppm.
IR (ATR): $\tilde{\nu}$ = 2990 (w), 2356 (w), 2120 (w), 1893 (w), 1652 (w), 1563 (m), 1465 (m), 1446 (m), 1409 (m), 1387 (m), 1297 (m), 1209 (w), 1170 (m), 1147 (m), 1089 (m), 1050 (m), 1000 (s), 921 (m), 879 (m), 833 (s), 819 (s), 790 (s), 775 (m), 710 (s), 703 (s) cm^{-1}.
HRMS (EI, 70 eV) *m/z* (%): $[M]^+$ calcd for $[C_{12}H_8BrIN_2]^+$ 385.89101; found 385.89122 (14), 76.0 (100).
Mp: 129 °C.
R$_f$: 0.75 (*n*-hexane/DCM 3:1).

(*E*)-1-(2-Bromophenyl)-2-(4-iodophenyl)diazene (**1n**)

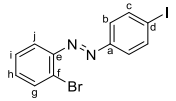

This reaction was not performed under inert conditions.

2-Bromoaniline (12.0 g, 70.0 mmol, 1.00 equiv) was dissolved in DCM (150 mL). To this solution, Oxone® (86.1 g, 140 mmol, 2.00 equiv) dissolved in water (300 mL) was added. The solution was stirred under a nitrogen atmosphere at 25 °C for 24 h. The color of the solution turned to green as the corresponding nitrosoarene formed. The layers were separated and the aqueous layer was extracted with DCM (3 × 100 mL). The combined organic layers were washed with HCl (1 M, 150 mL), saturated sodium hydrogen carbonate solution (150 mL), water (150 mL) and brine (150 mL). The organic phase was dried over $MgSO_4$ and filtered. The solvent was removed under reduced pressure. The obtained crude 1-bromo-2-nitrosobenzene (13.0 g, 70.0 mmol, 1.00 equiv) was dissolved in acetic acid (200 mL) and 4-iodoaniline was added (15.3 g, 70.0 mmol, 1.00 equiv). The resulting mixture was stirred at 25 °C for 16 h. The precipitate was separated by filtration and washed with acetic acid (100 mL). The residue was crystallized from methanol at -21 °C yielding **1n** as an orange solid (19.6 g, 50.6 mmol, 72%).

^{1}H NMR (600 MHz, $CDCl_3$) δ = 7.88 (d, ^3J = 8.6 Hz, 2H, *H*-c), 7.76 (dd, ^3J = 7.9 Hz, ^4J = 1.4 Hz, 1H, *H*-g), 7.70 (d, ^3J = 8.6 Hz, 2H, *H*-b), 7.68 (dd, ^3J = 7.9 Hz, ^4J = 1.7 Hz, 1H, *H*-j), 7.39 (td, ^3J = 7.2 Hz, ^4J = 1.4 Hz, 1H, *H*-i), 7.33 (td, ^3J = 7.2 Hz, ^4J = 1.7 Hz, 1H, *H*-h) ppm.
^{13}C{^{1}H} NMR (151 MHz, $CDCl_3$) δ = 152.1 (*C*-a), 149.6 (*C*-e), 138.6 (*C*-c), 134.0 (*C*-g), 132.4 (*C*-h), 128.2 (*C*-i), 126.2 (*C*-f), 125.1 (*C*-b), 117.9 (*C*-j), 98.7 (*C*-d) ppm.
IR (ATR): $\tilde{\nu}$ = 2356 (w), 2121 (w), 1821 (w), 1660 (w), 1576 (w), 1564 (m), 1475 (w), 1456 (m), 1422 (m), 1392 (w), 1225 (w), 1044 (m), 1024 (s), 1003 (s), 953 (m), 831 (s), 759 (s), 717 (s), 702 (m) cm^{-1}.
HRMS (EI, 70 eV) *m/z* (%): $[M]^+$ calcd for $[C_{12}H_8BrIN_2]^+$ 385.89101; found 385.89146 (36), 76.0 (100).
Mp: 93 °C.
R$_f$: 0.75 (*n*-hexane/DCM 3:1).

(*E*)-1,2-Bis(4-iodophenyl)diazene[11] (**4a**)

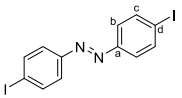

This reaction was not performed under inert conditions.

A solution of 4-iodoaniline (10.0 g, 45.7 mmol, 1.00 equiv) and manganese dioxide (70.0 g, 805 mmol, 17.6 equiv) in toluene (700 mL) was stirred for 3 h at 120 °C. The warm reaction mixture was filtered through a short plug of silica and washed with toluene (400 mL). The solvent was removed under reduced pressure yielding **4a** as a red solid (9.43 g, 21.7 mmol, %, Lit.:[11] 61%[7]).

^{1}H NMR (600 MHz, $CDCl_3$) δ = 7.87 (d, ^3J = 8.7 Hz, 4H, *H*-c), 7.64 (d,^3J = 8.7 Hz, 4H, *H*-b) ppm.
^{13}C{^{1}H} NMR (151 MHz, $CDCl_3$) δ = 151.8 (*C*-a), 138.6 (*C*-c), 124.7 (*C*-b), 98.3 (*C*-d) ppm.
IR (ATR): $\tilde{\nu}$ = 3067 (w), 2359 (w), 2111 (w), 1640 (w), 1574 (m), 1560 (m), 1470 (m), 1393 (m), 1296 (m), 1279 (m), 1096 (m), 1051 (m), 1002 (m), 834 (s), 810 (s), 774 (m), 713 (s) cm^{-1}.
HRMS (APCI) *m/z*: $[M + H]^+$ calcd for $[C_{12}H_8N_2I_2 + H]^+$ 434.88497; found 434.88462.
Mp: 244 °C (Lit.:[11] 210 °C).
R_f = 0.75 (*n*-hexane/DCM 3:1).

4-Iodo-2,6-dimethylaniline[12] (**S3**)

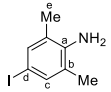

This reaction was not performed under inert conditions.

2,6-Dimethylaniline (31.5 mL, 31.0 g, 212 mmol, 1.00 equiv) was added to diethyl ether (200 mL). Iodine (59.2 g, 233 mmol, 1.10 equiv) and a sat. $NaHCO_3$ solution (600 mL) were added. The resulting biphasic mixture was stirred vigorously. After 5 h, the reaction mixture was diluted with a saturated sodium thiosulfate solution (300 mL). The phases were separated and the aqueous phase was extracted with diethyl ether (2 × 100 mL). The combined organic phases were washed with water (200 mL), dried over $MgSO_4$ and filtered. The solvent was evaporated yielding **S3** as a brown oil, which solidified upon standing at 20 °C (49.7 g, 201 mmol, 95%, Lit.:[12] 99%).

^{1}H NMR (600 MHz, CDCl3) δ = 7.24 (s, 2 H, *H*-c), 3.58 (s, 2 H, NH_2-a), 2.13 (s, 6 H, *H*-e) ppm.
^{13}C{^{1}H} NMR (151 MHz, CDCl3) δ = 142.6 (*C*-a), 136.5 (*C*-c), 124.1 (*C*-b), 79.1 (*C*-d), 17.3 (*C*-e) ppm.
IR: $\tilde{\nu}$ = 3402 (m), 3199 (m), 1625 (m), 1582 (s), 1270 (m), 1222 (w), 1034 (w), 857 (s), 730 (s) cm^{-1}.
HRMS (EI, 70 eV) *m/z* (%): $[M]^+$ calcd for $[C_8H_{10}IN]^+$ 246.98525; found 246.98532 (100).
Mp: 48°C.

[7] In this report, the product was obtained by oxidation using copper chloride.

(*E*)-1,2-Bis(4-iodo-2,6-dimethylphenyl)diazene[13] (**4b**)

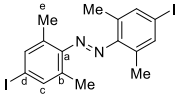

This reaction was not performed under inert conditions.

4-Iodo-2,6-dimethylaniline (**S3**) (3.00 g, 12.1 mmol, 1.00 equiv) was dissolved in toluene (300 mL). MnO_2 (26.3 g, 302 mmol, 25.0 equiv) was added and the solution was heated up to 130 °C for 3 h while vigorously stirring. After allowing the solution to cool to ambient temperature, it was filtered through a pad consisting of a layer of Celite® followed by silica. This assembly was washed with HCl (1 M, 20 mL), sat. sodium hydrogen carbonate (100 mL) and brine (100 mL). The organic phase was dried over $MgSO_4$, filtered and the solvent was evaporated. The crude product was purified by column chromatography (eluent: cyclohexane) yielding **4b** as an orange solid (593 mg, 1.21 mmol, 22%, Lit.:[13] 20%).

^{1}H NMR (500 MHz, CDCl3) δ = 7.52 (s, 4 H, *H*-c), 2.36 (s, 12 H, H-e) ppm.
^{13}C{1H} NMR (151 MHz, CDCl3) δ = 150.6 (*C*-a), 138.2 (*C*-b), 133.6 (*C*-c), 94.7 (*C*-d), 19.5 (*C*-e) ppm.
IR: $\tilde{\nu}$ = 2964 (w), 1616 (w), 1553 (m), 1435 (m), 1398 (w), 1244 (m), 1184 (w), 1033 (w), 880 (s), 864 (s), 843 (s) cm^{-1}.
HRMS (APCI): *m/z* = $[M + H]^+$ calcd for $[C_{16}H_{16}I_2N_2 + H]^+$ 490.94757, found 490.94704.
Mp: 130°C.
R_f: 0.40 (cyclohexane).

4-Bromo-2,6-dimethoxyaniline[14] (**S4**)

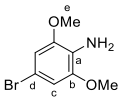

This reaction was not performed under inert conditions.

A solution of bromine (1.00 mL, 3.12 g, 1.95 mmol, 1.00 equiv) in chloroform (50 mL) was added to a solution of 2,6-dimethoxyaniline (3.06 g, 2.00 mmol, 1.03 equiv) in chloroform (50 mL) at 0°C over the course of 1 h. Afterwards, the solution was warmed up to 21 °C and stirred for additional 14 h. Then, NaOH (2 M) was added to adjust the pH to 11. The water phase was extracted with ethyl acetate (3 × 100 mL). The combined organic phases were washed with water (100 mL), brine (100 mL), dried over $MgSO_4$ and filtered. The crude product was purified by column chromatography (eluent: *n*-hexane/DCM 95:5) to yield **S4** as a colorless solid (3.66 g, 1.58 mmol, 79%, Lit.:[14] 77%)

^{1}H NMR (600 MHz, $CDCl_3$) δ = 6.65 (s, 2H, *H*-c), 3.83 (s, 6H, *H*-e), 3.77 (s, 2H, NH_2-a) ppm.
^{213}C{^{1}H} NMR (151 MHz, $CDCl_3$) δ = 147.8 (*C*-a), 124.7 (*C*-b), 108.8 (*C*-d), 107.8 (*C*-c), 56.2 (*C*-e) ppm.
IR (ATR): $\tilde{\nu}$ = 3369 (w), 2926 (w), 1732 (w), 1604 (m), 1503 (m), 1450 (s), 1375 (m), 1297 (s), 1202 (m), 1184 (m), 1155 (s), 1054 (s), 848 (s), 811 (m), 797 (w) cm^{-1}.
HRMS (EI, 70 eV) *m/z* (%): $[M]^+$ calcd for $[C_8H_{10}NO_2Br]^+$ 230.98894; found 230.98907 (95), 233.0 (100).
Mp: 74°C (Lit: [14] 75-76°C).
R_f = 0.45 (*n*-hexane: ethyl acetate 1:1).

(*E*)-1,2-Bis(4-bromo-2,6-dimethoxyphenyl)diazene[15] (**S5**)

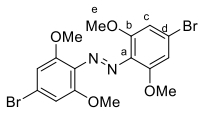

This reaction was not performed under inert conditions.

4-Bromo-2,6-dimethoxylaniline (**S4**) (2.32 g, 10.0 mmol, 1.00 equiv) was dissolved in toluene (100 mL). MnO_2 (10.9 g, 125 mmol, 12.0 equiv) was added and the solution was heated up to 130 °C for 3 h while vigorously stirring. After allowing the solution to cool to ambient temperature, it was filtered through a pad consisting of a layer of Celite® followed by silica. This assembly was washed with HCl (1 M, 20 mL), sat. sodium hydrogen carbonate (20 mL) and brine (20 mL). The organic phase was dried over $MgSO_4$, filtered and the solvent was evaporated. The crude product was purified by column chromatography (eluent: DCM) to obtain **S5** as an orange solid (1.20 g, 2.61 mmol, 52%, Lit.:[15] 20%).

^{1}H NMR (600 MHz, $CDCl_3$) δ = 6.82 (s, 4H, *H*-c), 3.84 (s, 12H, *H*-e); *Z*-Isomer: 6.60 (s, 4H, *H*-c), 3.66 (s, 12H, *H*-e) ppm.
^{13}C{^{1}H} NMR (151 MHz, $CDCl_3$) δ = 152.90 (*C*-a), 133.22 (*C*-b), 123.05 (*C*-c), 109.00 (*C*-c), 56.94 (*C*-e) ppm.
IR (ATR): $\tilde{\nu}$ = 2924 (w), 1731 (w), 1603 (s), 1564 (m), 1514 (w), 1471 (m), 1450 (m), 1398 (m), 1230 (s), 1157 (w), 1117 (s), 1015 (w), 848 (m), 830 (m), 801 (m), 757 (m). cm^{-1}.
HRMS (EI, 70 eV) *m/z* (%): $[M]^+$ calcd for $[C_{16}H_{16}N_2O_4Br_2]^+$ 457.94713; found 457.94716 (20), 243.0 (100).
Mp: 211°C.
R$_f$ = 0.50 (*n*-hexane/ethyl acetate 1:1).

(*E*)-1,2-Bis(4-iodo-2,6-dimethoxyphenyl)diazene (**4c**)

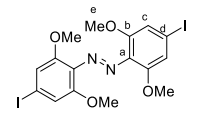

A vial was charged with 4,4´-dibromo-2,2´,6,6´-tetrakis(methoxy)-azobenzene (**S5**) (230 mg, 500 µmol, 2.00 equiv), copper iodide (9.52 mg, 50.0 µmol, 5.00 mol%) and sodium iodide (300 mg, 2.00 mmol, 4.00 equiv). *N,N´*-dimethylethylenediamine (10.8 µL, 0.100 mmol, 10.0 mol%) and dry dioxane (6 mL) were added. The reaction mixture was stirred at 110 °C for 48 h. After cooling down to 21 °C, the suspension was diluted with an aqueous sodium hydrogen carbonate solution (2 M, 50 mL), poured into water (200 mL), and extracted with DCM (3 × 150 mL). The combined organic phases were washed with hydrochloric acid (1 M, 100 mL) and brine (100 mL). After drying over $MgSO_4$ and filtration, the solvent was removed under reduced pressure. The product **4c** was obtained in 90% purity with 10% mono-brominated species left. (260 mg, 469 mmol, 94%).

^{1}H NMR (600 MHz, $CDCl_3$) δ = 7.00 (s, 4H, *H*-c), 3.83 (s, 12H, *H*-e) ppm.
^{13}C{^{1}H} NMR (151 MHz, $CDCl_3$) δ = 152.61 (*C*-a), 134.02 (*C*-b), 115.08 (*C*-c), 94.05 (*C*-d), 56.97 (*C*-e) ppm.
IR (ATR): $\tilde{\nu}$ = 2933 (w), 1558 (s), 1449 (m), 1395 (s), 1230 (s), 1158 (w), 1115 (s), 1018 (w), 828 (s), 803 (m), 742 (w) cm^{-1}.

HRMS (EI, 70 eV) *m/z* (%): $[M]^+$ calcd for $[C_{16}H_{16}I_2N_2O_4]^+$ 553.91940; found 553.91926 (25), 248.0 (100).
Mp: 265°C.
R$_f$ = 0.65 (*n*-hexane/ethyl acetate 1:1).

4-Iodo-2,6-difluoro-aniline[16] (**S6**)

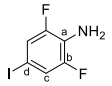

This reaction was not performed under inert conditions.

A solution of *N*-iodosuccinimide (4.95 g, 22.0 mmol, 1.10 equiv) in DMF (25 mL) was added dropwise to a solution of 2,6-difluoroaniline (2.15 g, 20.0 mmol, 1.00 equiv) and *p*-toluenesulfonic acid (760 mg, 4.00 mmol, 20 mol%) in DMF (35 mL) at 5 °C. The mixture was stirred for 2.5 h at 21 °C, diluted with ethyl acetate (250 mL), and thoroughly washed with brine (4 × 150 mL). The phases were separated. The organic phase was dried over $MgSO_4$, filtered, and concentrated under reduced pressure to give **S6** as a light brown solid (5.10 g, 19.8 mmol, 99%, Lit.:[16] 99%).

^{1}H NMR (600 MHz, $CDCl_3$) δ = 7.46 (d, ^3J = 8.0 Hz, 2H, *H*-c), 3.76 (s, 2H, NH_2-a) ppm.
^{13}C{^{1}H} NMR (151 MHz, $CDCl_3$) δ = 151.92 (dd, ^1J = 245.4 Hz, ^4J = 8.1 Hz, *C*-b), 124.3 (t, ^2J = 16.2 Hz, *C*-a), 120.5 – 120.0 (m, *C*-c), 74.28 (t, ^3J = 10.0 Hz, *C*-d) ppm.
^{19}F NMR (565 MHz, $CDCl_3$) δ -119.4 (d, ^3J = 9.2 Hz, *F*-b) ppm.
IR (ATR): $\tilde{\nu}$ = 3458 (m), 3373 (m), 1631 (s), 1593 (m), 1578 (w), 1497 (s), 1416 (s), 1288 (s), 1202 (w), 1152 (s), 1123 (w), 984 (w), 951 (s), 860 (m), 836 (s), 746 (m) cm^{-1}.
HRMS (EI, 70 eV) *m/z* (%): $[M]^+$ calcd for $[C_6H_4INF_4]^+$ 254.93498; found 254.93498 (100), 128.1 (95).
Mp: 81°C.
R$_f$ = 0.70 (*n*-hexane/ethyl acetate 1:1).

(*E*)-1,2-bis(2,6-difluoro-4-iodophenyl)diazene[17] (**4d**)

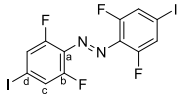

This reaction was not performed under inert conditions.

To a solution of 4-iodo-2,6-difluoroaniline (**S6**) (637 mg, 2.50 mmol, 1.00 equiv) in DCM (40 mL) was added 1,8-diazabicyclo[5.4.0]undec-7-ene (761 mg, 5.00 mmol, 2.00 equiv). The solution was stirred at 21 °C for 5 min before being cooled down to -78 °C. *N*-Chlorosuccinimide (668 mg, 5.00 mmol, 2.00 equiv) was added to the reaction mixture. The orange solution was stirred for 30 min at -78 °C, and a saturated $NaHCO_3$ solution (50 mL) was added. The layers were separated. The organic layer was washed with water (50 mL) and HCl (1 M, 50 mL). The combined organic layers were dried over $MgSO_4$, filtered and concentrated under reduced pressure. The residue was purified by silica gel flash chromatography (eluent: gradient *n*-hexane/ethyl acetate 1:0 → 1:1). **4d** was obtained as a red solid (474 mg, 937 µmol, 75%, Lit.:[17] 63%).

^{1}H NMR (600 MHz, $CDCl_3$) δ = 7.46 (d, ^3J = 8.0 Hz, 4H, *H*-c) ppm.
^{13}C{^{1}H} NMR (151 MHz, $CDCl_3$) δ = 155.00 (dd, ^1J = 267.2 Hz, ^4J = 4.4 Hz, *C*-d), 131.5 (t, ^2J = 9.3 Hz, *C*-a), 122.7 (dd, ^2J = 22.6, ^4J = 3.9 Hz, *C*-c), 94.9 (t, ^3J = 10.4 Hz, *C*-d) ppm.
^{19}F NMR (565 MHz, $CDCl_3$) δ = -119.44 (d, ^4J = 9.2 Hz, *F*-b) ppm.

IR (ATR): $\tilde{\nu}$ = 1595 (s), 1566 (s), 1445 (w), 1412 (s), 1289 (w), 1203 (m), 1046 (s), 866 (m), 855 (m), 838 (s), 747 (m) cm^{-1}.
HRMS (EI, 70 eV) *m/z* (%): $[M]^+$ calcd for $[C_{12}H_4F_4I_2N_2]^+$ 505.83946; found 505.83960 (12), 112.1 (100).
Mp: 201°C.
R_f = 0.50 (*n*-hexane/ethyl acetate 1:1).

4-Bromo-2,6-difluoroaniline[18] (**S7**)

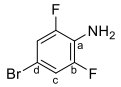

This reaction was not performed under inert conditions.

To a solution of 2,6-difluoroaniline (12.9 g, 100 mmol, 1.00 equiv) in acetonitrile (200 mL) was added a solution of *N*-bromosuccinimide (17.8 g, 100 mmol, 1.00 equiv) in acetonitrile (100 mL) at 0°C dropwise over a duration of 1h. The mixture was stirred overnight while warming up to 21 °C, and then diluted with water (800 mL). The product was extracted with ethyl acetate (3 × 100 mL). The combined organic phases were dried over $MgSO_4$, filtered, and concentrated under reduced pressure. The crude residue was purified by column chromatography over silica gel (eluent: *n*-hexane/DCM, 4:1) to yield **S7** as a colorless solid (17.2 g, 99.0 mmol, 99%, Lit.:[18] 99%).

^{1}H NMR (600 MHz, $CDCl_3$) δ = 7.02 (d, ^3J = 7.8 Hz, 2H, *H*-c), 3.73 (s, 2H, NH_2-a) ppm.
^{13}C{^{1}H} NMR (151 MHz, $CDCl_3$) δ = 151.76 (dd, ^1J = 244.2, ^4J = 8.7 Hz, *C*-b), 123.52 (t, ^2J = 16.1 Hz, *C*-a), 115.17 – 114.21 (m, *C*-c), 107.09 (t, ^3J = 11.6 Hz, *C*-d) ppm.
^{19}F NMR (565 MHz, $CDCl_3$) δ -130.69 (d, ^4J = 6.3 Hz, *F*-b) ppm.
Mp: 66 °C.
R_f: 0.42 (*n*-hexane/DCM 4:1).

4-Amino-3,5-difluorobenzonitrile[19] (**S8**)

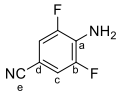

A mixture of copper(I) cyanide (29.3 g, 325 mmol, 1.70 equiv) and 4-bromo-2,6-difluoroaniline (**S7**) (39.5 g, 190 mmol, 1.00 equiv) in *N*-methyl-2-pyrrolidone (120 mL) was stirred under a nitrogen atmosphere at 204 °C for 4 h. After cooling to 30 °C, the resulting mixture was poured into aqueous ammonia until a white precipitate was formed. The suspension was extracted with toluene (5 × 100 mL). The combined organic phases were washed with water (100 mL), brine (100 mL), dried over $MgSO_4$ and filtered. The solvent was removed *in vacuo*. The crude product was dissolved in DCM and purified by column chromatography (eluent: DCM/hexane 1:1). **S8** was obtained as a colorless solid (20.5 g, 133 mmol, 70%, Lit.:[19] 87%).

^{1}H NMR (600 MHz, $CDCl_3$) δ =7.14 (dd, ^3J = 6.0, ^4J = 2.3 Hz, 2H, *H*-c), 4.27 (s, 2H, NH_2-a) ppm.
^{13}C{^{1}H} NMR (151 MHz, $CDCl_3$) δ 150.66 (dd, ^1J = 243.5 Hz, ^4J = 9.1 Hz, *C*-b), 129.75 (t, ^2J = 15.7 Hz, *C*-a), 118.05 (t, ^5J = 3.4 Hz, *C*-e), 115.60 (dd, ^2J = 17.5, ^4J = 7.1 Hz, *C*-c), 98.47 (t, ^3J = 11.1 Hz, *C*-d) ppm.
^{19}F NMR (565 MHz, $CDCl_3$) δ = -130.76 (dd, ^4J = 6.1 Hz, ^6J = 2.2 Hz, *F*-b) ppm.
IR (ATR): $\tilde{\nu}$ = 3376 (w), 3313 (w), 2224 (m), 1650 (w), 1608 (w), 1587 (m), 1523 (m), 1443 (s), 1338 (m), 1163 (s), 977 (s), 875 (s), 862 (m), 727 (s) cm^{-1}.
HRMS (EI, 70 eV) *m/z* (%): $[M]^+$ calcd for $[C_7H_4N_2F_2]^+$ 154.03371; found 154.03383 (100).

Mp: 112 °C.
R_f: 0.40 (*n*-hexane/DCM 1:2).

4-Amino-3,5-difluorobenzoic acid[20] (**S9**)

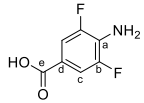

This reaction was not performed under inert conditions.

A mixture of 4-amino-3,5-difluorobenzonitrile (**S8**) (5.00 g, 32,4 mmol, 1.00 equiv) was dissolved in a 25 wt% solution of KOH in water (100 mL). The mixture was heated up to 110 °C for 19 h. After cooling down to 21 °C, the aqueous phase was acidified to pH = 2 with HCl (2 M) and extracted with ethyl acetate (2 × 100 mL). The combined organic extracts were washed with water (75 mL), brine (75 mL), dried over $MgSO_4$ and filtered. The solvent was removed under reduced pressure to obtain **S9** as a slightly yellowish solid (4.99 g, 28.8 mmol, 89%, Lit.:[20] 87%).

^{1}H NMR (600 MHz, DMSO-d_6) δ = δ 7.39 (dd, ^3J = 7.2 Hz, ^4J = 2.4 Hz, 2H, *H*-c), 6.04 (s, 2H, NH_2-a) ppm.
^{13}C{^{1}H} NMR (151 MHz, DMSO-d_6) δ = 166.12 (*C*-e), 149.80 (dd, ^1J = 239.6, ^4J = 9.5 Hz, *C*-b), 130.61 (t, ^2J = 16.7 Hz, *C*-a), 112.31 (dd, ^2J = 15.8 Hz, ^4J = 5.9 Hz, *C*-c), 59.83 (*C*-d) ppm.
^{19}F NMR (565 MHz, DMSO-d_6) δ -131.62 (d, ^4J = 7.2 Hz, *F*-b) ppm.
IR (ATR): $\tilde{\nu}$ = 3397 (w), 1683 (m), 1628 (s), 1587 (m), 1538 (w), 1454 (m), 1422 (s), 1341 (s), 1277 (s), 1243 (m), 1145 (m), 1082 (w), 953 (m), 889 (m), 765 (s), 719 (s) cm^{-1}.
HRMS (EI, 70 eV) *m/z* (%): $[M]^+$ calcd for $[C_7H_5NO_2F_2]^+$ 173.02829; found 173.02830 (75), 156.1 (100).
Mp: 171 °C.
R_f: 0.90 (ethyl acetate).

Ethyl 4-amino-3,5-difluorobenzoate[20] (**S10**)

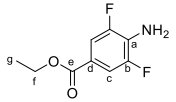

This reaction was not performed under inert conditions.

S9 (2.42 g, 14.0 mmol) was dissolved in EtOH (50 mL) and H_2SO_4 (1 mL), and refluxed for 5 h. The mixture was neutralized (pH = 7) with a saturated $NaHCO_3$ solution and extracted with DCM (3 × 50 mL). The combined organic phases were dried over $MgSO_4$, filtered, and concentrated under reduced pressure to yield **S10** as a pale brown solid (2.74 g, 13.6 mmol, 97%, Lit.:[20] 94%.)

^{1}H NMR (600 MHz, $CDCl_3$) δ = 7.53 (dd, *J* = 7.1, 2.2 Hz, 2H, *H*-c), 4.33 (q, ^3J = 7.1 Hz, 2H, *H*-f), 4.13 (s, 2H, NH_2-a), 1.36 (t, ^3J = 7.1 Hz, 3H, *H*-g) ppm.
^{13}C{^{1}H} NMR (151 MHz, $CDCl_3$) δ = 165.30 (t, ^5J = 3.5 Hz, *C*-e), 150.80 (dd, ^1J = 240.8 Hz, ^4J = 7.9 Hz, *C*-b), 128.92 (t, ^3J = 16.1 Hz, *C*-a), 118.72 (t, ^4J = 8.2 Hz, *C*-d), 113.13 – 112.08 (m, *C*-c), 61.20 (*C*-f), 14.45 (*C*-g) ppm.
^{19}F NMR (565 MHz, $CDCl_3$) δ -132.93 (dd, ^4J = 7.2 Hz, ^6J = 2.3 Hz, *F*-b) ppm.
IR (ATR): $\tilde{\nu}$ = 3505 (w), 3368 (m), 1697 (s), 1629 (s), 1585 (m), 1531 (m), 1477 (w), 1444 (m), 1397 (m), 1370 (m), 1339 (s), 1270 (s), 1222 (s), 1133 (m), 1089 (s), 1027 (s), 946 (s), 881 (m), 760 (m) cm^{-1}.
HRMS (EI, 70 eV) *m/z* (%): $[M]^+$ calcd for $[C_9H_9NO_2F_2]^+$ 201.0599; found 201.05932 (15), 156.1 (100).
R_f: 0.30 (*n*-hexane/DCM 1:1).

(*E*)-4,4'-(Diazene-1,2-diyl)bis(3,5-difluorobenzoic acid)[17] (**S11**)

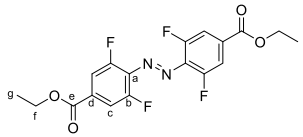

This reaction was not performed under inert conditions.

To a solution of 4-iodo-2,6-difluoroaniline (**S10**) (637 mg, 2.50 mmol, 1.00 equiv) in DCM (40 mL) was added 1,8-diazabicyclo[5.4.0]undec-7-ene (761 mg, 5.00 mmol, 2.00 equiv). The solution was stirred at 21 °C for 5 min before being cooled down to -78 °C. *N*-Chlorosuccinimide (668 mg, 5.00 mmol, 2.00 equiv) was added to the reaction mixture. The orange solution was stirred for 30 min at -78 °C, and a saturated $NaHCO_3$ solution (50 mL) was added. The layers were separated. The organic layer was washed with water (50 mL) and HCl (1 M, 50 mL). The combined organic layers were dried over $MgSO_4$, filtered and concentrated under reduced pressure. The residue was purified by silica gel flash chromatography (eluent: gradient *n*-hexane/DCM 1:0 → 1:1) to obtain **S11** as a red solid (402 mg, 1.01 mmol, 81%, Lit.:[17] 62%).

^{1}H NMR (600 MHz, $CDCl_3$) δ = 7.75 (d, ^3J = 8.9 Hz, 4H, *H*-c), 4.43 (q, ^3J = 7.1 Hz, 4H, *H*-f), 1.43 (t, ^3J = 7.1 Hz, 6H, *H*-g) ppm.
^{13}C{^{1}H} NMR (151 MHz, $CDCl_3$) δ = 163.84 (*C*-e), 155.17 (dd, ^1J = 262.6 Hz, ^4J = 3.8 Hz, *C*-b) ,134.31 (t, ^3J = 10.1 Hz, *C*-a), 133.89 (t, ^4J = 9.2 Hz, *C*-d), 114.07 (dd, ^2J = 21.7, ^4J = 3.9 Hz, *C*-c), 62.34 (*C*-f), 14.36 (*C*-g) ppm.
^{19}F NMR (565 MHz, $CDCl_3$) δ = -120.06 (d, ^4J = 10.4 Hz, *F*-b) ppm.
IR (ATR): $\tilde{\nu}$ = 1721 (m), 1573 (m), 1434 (m), 1369 (s), 1330 (m), 1238 (m), 1192 (m), 1089 (w), 1052 (s), 1017 (s), 886 (s), 767 (s), 752 (s) cm^{-1}.
HRMS (EI, 70 eV) *m/z* (%): $[M]^+$ calcd for $[C_{18}H_{14}N_2O_4F_2]^+$ 398.08842; found 398.08876 (15), 101.1 (100).
Mp: 147°C.
R_f: 0.35 (*n*-hexane/DCM 1:1).

(*E*)-4,4'-(Diazene-1,2-diyl)bis(3,5-difluorobenzoic acid)[20] (**6**)

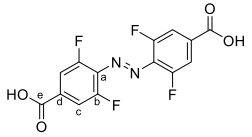

This reaction was not performed under inert conditions.

Diethyl 4,4'-(diazene-1,2-diyl)-bis(3,5-difluorobenzoate) (**S11**) (1.19 g, 3.00 mmol, 1.00 equiv) was dissolved in THF (40 mL) and KOH (673 mg, 12.0 mmol, 4.00 equiv) dissolved in H_2O (40 mL) was added. The reaction mixture was stirred for 1 h at 21 °C and acidified with HCl (1 M) until a precipitate formed. The precipitate was filtered and dried in a vacuum oven at 50°C to yield the desired product **6** (924 mg, 2.70 mmol, 90 %, Lit.:[20] 94%) as a pink solid.

^{1}H NMR (600 MHz, DMSO-d_6) δ = 7.80 (d, ^3J = 9.3 Hz, 4H, *H*-c) ppm.
^{13}C{^{1}H} NMR (151 MHz, DMSO-d_6) δ = 164.64 (*C*-e), 154.35 (dd, ^1J = 260.9 Hz, ^4J = 3.8 Hz, *C*-b), 135.46 (t, ^3J = 9.3 HZ, *C*-d), 133.00 (t, ^2J = 10.3 Hz, *C*-a), 113.97 (dd, ^2J = 21.3 Hz, ^4J = 3.6 Hz, *C*-c) ppm.

^{19}F NMR (565 MHz, DMSO-d_6) δ = -120.06 (d, ^4J = 10.4 Hz, *F*-b) ppm.
IR (ATR): $\tilde{\nu}$ = 2871 (br), 1693 (s), 1577 (s), 1481 (m), 1436 (m), 1414 (m), 1259 (s), 1195 (m), 1054 (s), 893 (s), 879 (m), 773 (s), 729 (m) cm^{-1}.
HRMS (EI, 70 eV) *m/z* (%): $[M]^+$ calcd for $[C_{14}H_6N_2O_4F_4]^+$ 342.02582; found 342.02604 (5), 101.1 (100).
Mp: >300 °C.

2-(2-(2-Aminophenethyl)phenyl)isoindoline-1,3-dione[21] (**S12**)

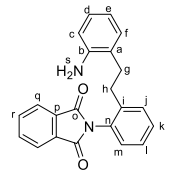

This reaction was not performed under inert conditions.

Phthalic anhydride (2.22 g, 15.0 mmol, 1.00 equiv) and 2,2'-ethylenedianiline (3.18 g, 15.0 mmol, 1.00 equiv) were dissolved in acetic acid (60 mL). The mixture was vigorously stirred for 3 h at 118 °C. After cooling down to 25 °C, water (40 mL) was added and the formed precipitate was filtered. The precipitate was recrystallized from ethanol at 78 °C. The solids were discarded and the filtrate was concentrated. The residue was re-dissolved in DCM (20 mL) and washed with water (20 mL). The aqueous phase was extracted with DCM (3 × 20 mL). Hydrogen chloride (1 M, 20 mL) was added to the combined organic layers. The obtained thick slurry was stirred for 1 h at 0 °C. The precipitate was filtered, washed with water (20 mL) and suspended in DCM (20 mL). An aqueous solution of sodium carbonate was added (2 M, 20 mL). The mixture was stirred for 1 h at 25 °C, until everything was fully dissolved. An aqueous solution of sodium hydroxide (2 M, 20 mL) was added and the phases were separated. The organic phase was dried over $MgSO_4$, filtered and concentrated yielding the product **S12** as yellow solid (1.40 g, 4.09 mmol, 41%, Lit.:[21] 52%).

^{1}H NMR (600 MHz, $CDCl_3$) δ = 7.99 – 7.92 (m, 2H, *H*-q), 7.84 – 7.78 (m, 2H, *H*-r), 7.46 – 7.33 (m, 3H, *H*-k/l/m), 7.21 (dd, ^3J = 7.5 Hz, ^4J = 1.7 Hz, 1H, *H*-j), 6.98 (ddt, ^3J = 8.2 Hz, ^4J = 4.2 Hz, 1.7 Hz, 2H, *H*-d/f), 6.66 (td (^3J = 7.5 Hz, ^4J = 1.2 Hz, 1H, *H*-e), 6.56 (dd, ^3J = 8.2 Hz, ^4J = 1.2 Hz, 1H, *H*-c), 3.54 (s, br, 2H, *H*-s), 2.84 – 2.72 (m, 4H, *H*-g/h) ppm.
^{13}C{^{1}H} NMR (151 MHz, $CDCl_3$) δ = 168.1 (*C*-o), 144.5 (*C*-b), 140.4 (*C*-n), 134.6 (*C*-r), 132.1 (*C*-p), 130.5 (*C*-l), 129.8 (*C*-i), 129.7 (*C*-k), 129.4 (*C*-f), 127.5 (*C*-m), 127.4 (*C*-d), 125.5 (*C*-l), 124.1 (*C*-a), 124.0 (*C*-q), 118.8 (*C*-e), 115.7 (*C*-c), 32.3 (*C*-g), 31.2 (*C*-h) ppm.
IR (ATR): $\tilde{\nu}$ = 3346 (w, br), 2937 (w), 2359 (w), 1708 (s), 1605 (m), 1492 (m), 1466 (m), 1454 (m), 1378 (s), 1220 (m), 1161 (m), 1109 (m), 1082 (m), 1003 (m), 888 (m), 765 (s), 724 (s) cm^{-1}.
HRMS (EI, 70 eV) *m/z* (%): $[M]^+$ calcd for $[C_{22}H_{18}N_2O_2]^+$ 342.13628; found 342.13649 (6), 106.1 (100).
Mp: 134 °C.
R_f = 0.70 (*n*-hexane/DCM 1:1).

2-(2-Aminophenethyl)-4-iodoaniline[21] (**S13**)

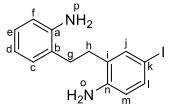

This reaction was not performed under inert conditions.

N-Iodosuccinimide (1.11 g, 7.46 mmol, 1.00 equiv) was added in one portion to a solution of 2-(2-(2-aminophenethyl)phenyl)isoindoline-1,3-dione (**S12**) (2.55 g, 7.46 mmol, 1.00 equiv) in DMSO (50 mL). After stirring the mixture for 3 h at 23 °C, brine (50 mL) was added and the mixture was extracted with DCM (3 × 30 mL). The combined organic layers were washed with water (50 mL) and brine (3 × 50 mL). The solution was filtered over a short plug of silica and the solvent removed under reduced pressure. The crude iodination product (2.61 g, 5.57 mmol) was dissolved in THF (30 mL) and hydrazine monohydrate (1.67 mL, 33.4 mmol, 6.00 equiv) was added. The mixture was stirred at 64 °C for 2 h. After cooling to 23 °C, the mixture was filtered. The solids were washed with THF (60 mL) and discarded. Water (30 mL) was added to the filtrate. The THF was removed under reduced pressure and the residue was extracted with diethyl ether (3 × 30 mL). The combined organic layers were washed with brine (30 mL), dried over $MgSO_4$ and filtered. The solvent was removed under reduced pressure. The residue was dissolved in DCM (5 mL) and precipitated with *n*-hexane (5 mL) yielding **S13** as a brownish-yellow solid (1.51 g, 4.47 mmol, 60%, Lit.:[21] 93%).

^{1}H NMR (600 MHz, $CDCl_3$) δ = 7.36 (ad, ^4J = 2.1 Hz, 1H, *H*-j), 7.30 (dd, ^3J = 8.3 Hz, ^4J = 2.1 Hz, 1H, *H*-l), 7.10 – 7.01 (m, 2H, *H*-c/e), 6.75 (td, ^3J = 7.4 Hz, ^4J = 1.2 Hz, 1H, *H*-d), 6.69 (dd, ^3J = 7.9 Hz, ^4J = 1.2 Hz, 1H, *H*-f), 6.44 (d,^3J = 8.3 Hz, 1H, *H*-m), 3.60 (s, br, 4H, *H*-o/p), 2.80 – 2.70 (m, 4H, *H*-g/h) ppm.
^{13}C{^{1}H} NMR (151 MHz, $CDCl_3$) δ = 144.3 (*C*-a), 144.3 (*C*-n), 138.0 (*C*-j), 136.0 (*C*-l), 129.7 (*C*-c), 129.1 (*C*-i), 127.6 (*C*-e), 126.0 (*C*-b), 119.3 (*C*-d), 118.0 (*C*-m), 116.1 (*C*-f), 80.2 (*C*-k), 31.1 (*C*-g), 30.7 (*C*-h) ppm.
IR (ATR): $\tilde{\nu}$ = 3353 (w, br), 3021 (w), 2927 (w), 2867 (w), 1715 (m), 1616 (s), 1494 (s), 1448 (s), 1368 (m), 1263 (s), 1159 (m), 1055 (m), 858 (m), 749 (s) cm^{-1}.
HRMS (ESI) *m/z*: $[M + H]^+$ calcd for $[C_{14}H_{15}IN_2 + H]^+$ 339.03527; found 339.03462.
Mp: 131 °C.
R_f = 0.57 (*n*-hexane/DCM 1:1).

(*Z*)-2-Iodo-11,12-dihydrodibenzo[c,g][1,2]diazocine[21] (**7a**)

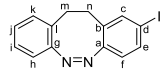

This reaction was not performed under inert conditions.

A freshly prepared solution of *meta*-chloroperoxybenzoic acid (1.44 g, 8.34 mmol, 70%, 2.00 equiv) in acetic acid (50 mL) was added over the course of 2 h under rapid stirring to a solution of 2,2'-(ethane-1,2-diyl)bis(4-iodoaniline) (**S13**) (988 mg, 2.92 mmol, 1.00 equiv) in acetic acid (100 mL) and DCM (300 mL). After the complete addition, the mixture was stirred for a further 1 h at 25 °C. The solvent was removed under reduced pressure. The crude product was purified by column chromatography on silica gel (eluent: cyclohexane) to afford **7a** as a yellow solid (680 mg, 2.04 mmol, 70%, Lit.: [21] 75%).

^{1}H NMR (600 MHz, $CDCl_3$) δ = 7.44 (dd, ^3J = 8.3 Hz, ^4J = 1.8 Hz, 1H, *H*-e), 7.34 (d, ^4J = 1.8 Hz, 1H, *H*-c), 7.16 (dd, ^3J = 7.6 Hz, ^4J = 1.4 Hz, 1H, *H*-i), 7.05 (dd, ^3J = 7.6 Hz, ^4J = 1.4 Hz, 1H, *H*-j), 7.00 (dd, ^3J = 7.6 Hz, ^4J = 1.4 Hz, 1H, *H*-k), 6.83 (dd, ^3J = 7.6 Hz, ^4J = 1.4 Hz, 1H, *H*-h), 6.58 (d,^3J = 8.3 Hz, 1H, *H*-f), 3.06 – 2.62 (m, 4H, *H*-m/n) ppm.
^{13}C{^{1}H} NMR (151 MHz, $CDCl_3$) δ = 155.5 (*C*-g), 155.0 (*C*-a), 138.4 (*C*-c), 135.8 (*C*-e), 130.7 (*C*-b), 129.9 (*C*-k), 127.6 (*C*-l), 127.5 (*C*-j), 127.1 (*C*-i), 120.9 (*C*-f), 118.9 (*C*-h), 91.9 (*C*-d)z, 31.6 (*C*-m), 31.5 (*C*-n) ppm.
IR (ATR): $\tilde{\nu}$ = 2923 (w, br), 2359 (w), 1737 (s), 1605 (m), 1511 (m), 1453 (w), 1248 (s), 1200 (s), 1163 (s), 1062 (s), 891 (m), 848 (m), 760 (m), 751 (m) cm^{-1}.
HRMS (EI, 70 eV) *m/z* (%): $[M]^+$ calcd for $[C_{14}H_{11}IN_2]^+$ 333.99615; found 333.99606 (7), 178.1 (100).
Mp: 131 °C.
R_f = 0.60 (*n*-hexane/DCM 3:1).

2,2'-(Ethane-1,2-diyl)bis(4-iodoaniline)[21] (**S14**)

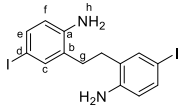

This reaction was not performed under inert conditions.

N-Iodosuccinimide (21.7 g, 96.6 mmol, 2.05 equiv) was added in three portions over 10 min to a solution of 2,2'-ethylenedianiline (10.0 g, 47.1 mmol, 1.00 equiv) in DMSO (125 mL) at 25 °C. After stirring the mixture for 23 h at 25 °C, DCM (100 mL) and water (100 mL) were added. The phases were separated, and the organic layer was washed with an aqueous solution of sodium hydrogen carbonate (2 M, 2 × 100 mL), water (100 mL) and brine (100 mL). The organic phase was dried over $MgSO_4$, filtered and the solvent removed under reduced pressure. **S14** was obtained as a red-brown solid (21.2 g, 45.7 mmol, 97%, Lit.:[21] 87%).

^{1}H NMR (600 MHz, $CDCl_3$) δ = 7.34 – 7.30 (m, 4H, *H*-e/f), 6.48 – 6.44 (m, 2H, *H*-c), 3.64 (s, br, 4H, *H*-h), 2.69 (s, 4H, *H*-g) ppm.
^{13}C{^{1}H} NMR (151 MHz, $CDCl_3$) δ = 144.2 (*C*-a), 138.0 (*C*-f), 136.2 (*C*-e), 128.6 (*C*-b), 118.1 (*C*-c), 80.3 (*C*-d), 30.6 (*C*-g) ppm.
IR (ATR): $\tilde{\nu}$ = 3397 (m, br), 3317 (m), 3219 (w), 2882 (w), 2359 (w), 1626 (m), 1562 (w), 1486 (s), 1470 (m), 1436 (m), 1398 (m), 1297 (s), 1268 (s), 1142 (m), 1096 (m), 1052 (m), 1002 (m), 931 (m), 868 (m), 834 (m), 809 (s), 709 (s) cm^{-1}.
HRMS (EI, 70 eV) *m/z* (%): $[M]^+$ calcd for $[C_{14}H_{14}I_2N_2]^+$ 463.92410; found 463.92397 (78), 232.0 (100).
Mp: 165 °C.
R_f = 0.57 (*n*-hexane/DCM 1:1).

(*Z*)-2,9-Diiodo-11,12-dihydrodibenzo[c,g][1,2]diazocine[21] (**7b**)

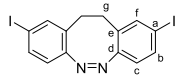

This reaction was not performed under inert conditions.

A freshly prepared solution of *meta*-chloroperoxybenzoic acid (1.75 g, 10.1 mmol, 71%, 2.00 equiv) in acetic acid (125 mL) was added over the course of 3 h under rapid stirring to a solution of 2,2'-(ethane-1,2-diyl)bis(4-iodoaniline) (**S14**) (1.67 g, 3.60 mmol, 1.00 equiv) in acetic acid (100 mL) and DCM (300 mL). After the complete addition, the mixture was stirred for a further 1 h at 25 °C. The solvent was removed under reduced pressure. The crude product was purified by column chromatography on

silica gel (eluent: cyclohexane/DCM 1:4) to afford **7b** as a yellow solid (1.23 g, 2.66 mmol, 71%, Lit.:[21] 72%).

^{1}H NMR (600 MHz, $CDCl_3$) δ = 7.48 (dd, ^3J = 8.3 Hz, ^4J = 1.8 Hz, 2H, *H*-b), 7.36 (d, ^4J = 1.8 Hz, 2H, *H*-f), 6.59 (d,^3J = 8.3 Hz, 2H, *H*-c), 2.97 – 2.62 (m, 4H, *H*-g) ppm.
^{13}C{^{1}H} NMR (151 MHz, $CDCl_3$) δ = 154.9 (*C*-d), 138.6 (*C*-f), 136.1 (*C*-b), 130.1 (*C*-e), 120.9 (*C*-c), 92.4 (*C*-a), 31.3 (*C*-g) ppm.
IR (ATR): $\tilde{\nu}$ = 2921 (w), 2358 (w), 1575 (m), 1533 (w), 1467 (m), 1383 (w), 1280 (w), 1156 (m), 1097 (m), 1052 (w), 1002 (m), 979 (w), 959 (w), 918 (w), 891 (m), 878 (m), 801 (s), 714 (m) cm^{-1}.
HRMS (EI, 70 eV) *m/z* (%): $[M]^+$ calcd for $[C_{14}H_{10}I_2N_2]^+$ 459.89280; found 459.89287 (49), 178.1 (100).
Mp: 173 °C.
R_f = 0.60 (*n*-hexane/DCM 3:1).

References

1. *The ACS Style Guide: Effective Communication of Scientific Information*, 3rd ed.; Coghill, A.M., Garson, L.R., Eds.; American Chemical Society: Washington, DC, 2006.
2. Keiper, S.; Vyle, J.S. Reversible Photocontrol of Deoxyribozyme-Catalyzed RNA Cleavage under Multiple-Turnover Conditions. *Angew. Chem. Int. Ed.* **2006**, *45*, 3306-3309, doi:10.1002/anie.200600164.
3. Zhou, M.; Haldar, S.; Franses, J.; Kim, J.-M.; Thompson, D.H. Synthesis and Self-assembly Properties of Acylated Cyclodextrins and Nitrilotriacetic Acid (NTA)-modified Inclusion Ligands for Interfacial Protein Crystallization. *Supramol. Chem.* **2006**, *17*, 101-111, doi:10.1080/10610270412331329005.
4. Liu, D.; Xie, Y.; Shao, H.; Jiang, X. Using Azobenzene-Embedded Self-Assembled Monolayers to Photochemically Control Cell Adhesion Reversibly. *Angew. Chem. Int. Ed.* **2009**, *48*, 4406-4408, doi:10.1002/anie.200901130.
5. Barré, A.; Ţînţaş, M.-L.; Alix, F.; Gembus, V.; Papamicaël, C.; Levacher, V. Palladium-Catalyzed Carbonylation of (Hetero)Aryl, Alkenyl and Allyl Halides by Means of N-Hydroxysuccinimidyl Formate as CO Surrogate. *J. Org. Chem.* **2015**, *80*, 6537-6544, doi:10.1021/acs.joc.5b01119.
6. Strueben, J.; Lipfert, M.; Springer, J.O.; Gould, C.A.; Gates, P.J.; Sönnichsen, F.D.; Staubitz, A. High-Yield Lithiation of Azobenzenes by Tin-Lithium Exchange. *Chem. Eur. J.* **2015**, *21*, 11165-11173, doi:10.1002/chem.201500003.
7. Tiwari, V.K.; Kumar, A.; Schmidt, R.R. Disaccharide-Containing Macrocycles by Click Chemistry and Intramolecular GIycosylation. *Eur. J. Org. Chem.* **2012**, 2945-2956, doi:10.1002/ejoc.201101815.
8. Yu, B.-C.; Shirai, Y.; Tour, J.M. Syntheses of New Functionalized Azobenzenes for Potential Molecular Electronic Devices. *Tetrahedron* **2006**, *62*, 10303-10310, doi:10.1016/j.tet.2006.08.069.
9. Rasheed, O.K.; Raftery, J.; Quayle, P. A New Benzannulation Reaction of Azoaromatics. *Synlett* **2015**, *26*, 2806-2810.
10. Nguyen, T.-T.-T.; Turp, D.; Wang, D.; Nolscher, B.; Laquai, F.; Mullen, K. A Fluorescent, Shape-Persistent Dendritic Host with Photoswitchable Guest Encapsulation and Intramolecular Energy Transfer. *J. Am. Chem. Soc.* **2011**, *133*, 11194-11204, doi:10.1021/ja2022398.
11. Strueben, J.; Gates, P.J.; Staubitz, A. Tin-Functionalized Azobenzenes as Nucleophiles in Stille Cross-Coupling Reactions. *J. Org. Chem.* **2014**, *79*, 1719-1728, doi:10.1021/jo402598u.
12. Brown, D.G.; Schauer, P.A.; Borau-Garcia, J.; Fancy, B.R.; Berlinguette, C.P. Stabilization of Ruthenium Sensitizers to TiO2 Surfaces through Cooperative Anchoring Groups. *J. Am. Chem. Soc.* **2013**, *135*, 1692-1695, doi:10.1021/ja310965h.
13. Abboud, M.; Sayari, A. Novel Family of Periodic Mesoporous Organosilicas Containing Azobenzene within the Pore Walls. *Microporous Mesoporous Mater.* **2017**, *249*, 157-164, doi:10.1016/j.micromeso.2017.04.061.
14. Broser, W.; Harrer, W. Synthesen, spektroskopische Charakterisierung, Gleichgewichts- und kinetische Messungen an m-methoxylierten Parafuchsinen. *Z. Naturforsch., B: J. Chem. Sci.* **1969**, *24*, 542-547, doi:doi:10.1515/znb-1969-0514.
15. Samanta, S.; Beharry, A.A.; Sadovski, O.; McCormick, T.M.; Babalhavaeji, A.; Tropepe, V.; Woolley, G.A. Photoswitching Azo Compounds in Vivo with Red Light. *J. Am. Chem. Soc.* **2013**, *135*, 9777-9784, doi:10.1021/ja402220t.
16. Bléger, D.; Schwarz, J.; Brouwer, A.M.; Hecht, S. o-Fluoroazobenzenes as Readily Synthesized Photoswitches Offering Nearly Quantitative Two-Way Isomerization with Visible Light. *J. Am. Chem. Soc.* **2012**, *134*, 20597-20600, doi:10.1021/ja310323y.
17. Antoine John, A.; Lin, Q. Synthesis of Azobenzenes Using N-Chlorosuccinimide and 1,8-Diazabicyclo[5.4.0]undec-7-ene (DBU). *J. Org. Chem.* **2017**, *82*, 9873-9876, doi:10.1021/acs.joc.7b01530.
18. Moreno, J.; Gerecke, M.; Grubert, L.; Kovalenko, S.A.; Hecht, S. Sensitized Two-NIR-Photon *Z*→*E* Isomerization of a Visible-Light-Addressable Bistable Azobenzene Derivative. *Angew. Chem. Int. Ed.* **2016**, *55*, 1544-1547, doi:10.1002/anie.201509111.
19. Cigl, M.; Bubnov, A.; Kašpar, M.; Hampl, F.; Hamplová, V.; Pacherová, O.; Svoboda, J. Photosensitive Chiral Self-Assembling Materials: Significant Effects of Small Lateral Substituents. *J. Mater. Chem. C* **2016**, *4*, 5326-5333, doi:10.1039/C6TC01103A.
20. Heinrich, B.; Bouazoune, K.; Wojcik, M.; Bakowsky, U.; Vázquez, O. ortho-Fluoroazobenzene Derivatives as DNA Intercalators for Photocontrol of DNA and Nucleosome Binding by Visible Light. *Org. Biomol. Chem.* **2019**, *17*, 1827-1833, doi:10.1039/C8OB02343C.
21. Maier, M.S.; Hüll, K.; Reynders, M.; Matsuura, B.S.; Leippe, P.; Ko, T.; Schäffer, L.; Trauner, D. Oxidative Approach Enables Efficient Access to Cyclic Azobenzenes. *J. Am. Chem. Soc.* **2019**, *141*, 17295-17304, doi:10.1021/jacs.9b08794.

^{1}H, $^{13}C\{^{1}H\}$ and ^{19}F NMR Spectra of the Purified Compounds

2,5-Dioxopyrrolidin-1-yl (*E*)-4-(phenyldiazenyl)benzoate (**3a**)

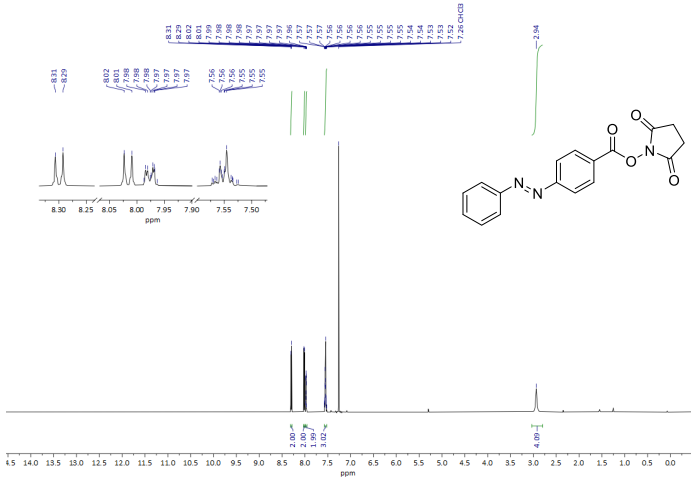

Figure S1: ^{1}H NMR spectrum of **3a** in $CDCl_3$.

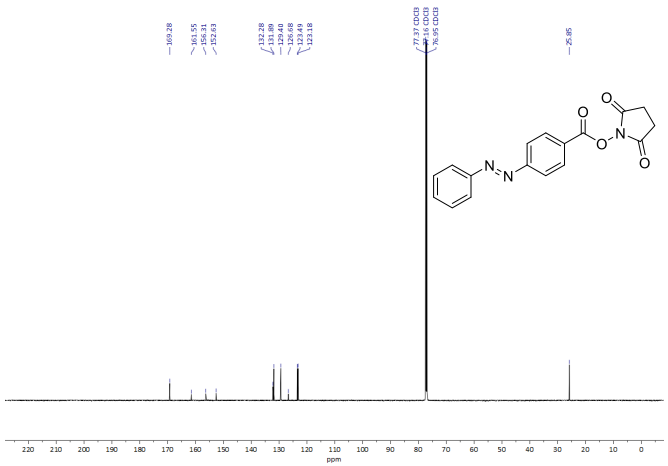

Figure S2: $^{13}C\{^{1}H\}$ NMR spectrum of **3a** in $CDCl_3$.

2,5-Dioxopyrrolidin-1-yl (*E*)-3-(phenyldiazenyl)benzoate (**3b**)

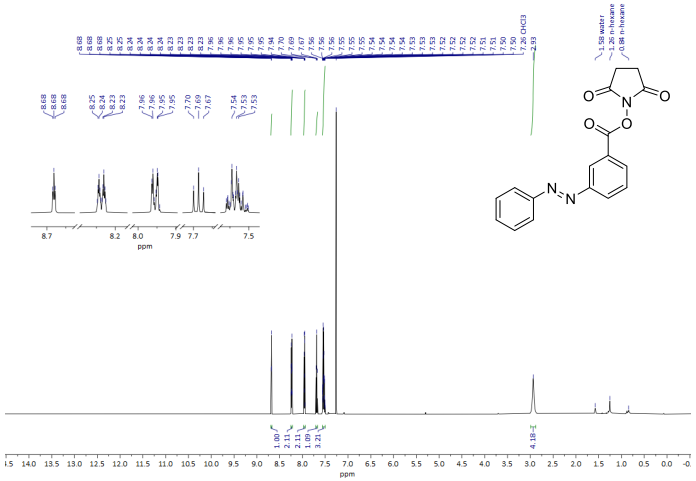

Figure S3: ^{1}H NMR spectrum of **3b** in $CDCl_3$.

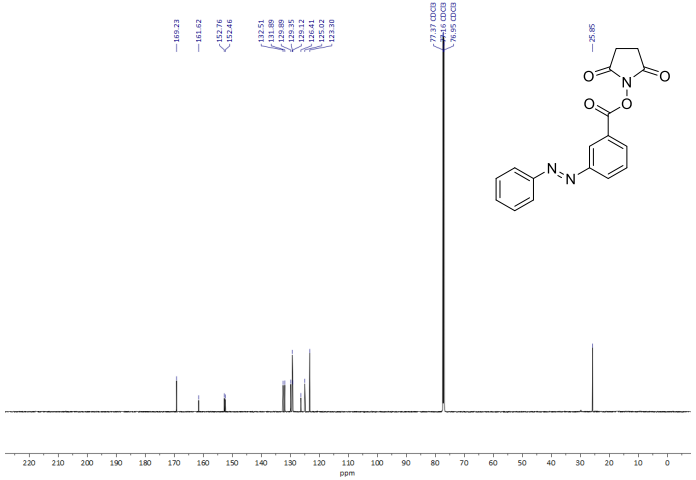

Figure S4: $^{13}C\{^{1}H\}$ NMR spectrum of **3b** in $CDCl_3$.

2,5-Dioxopyrrolidin-1-yl (*E*)-4-((4-aminophenyl)diazenyl)benzoate (**3e**)

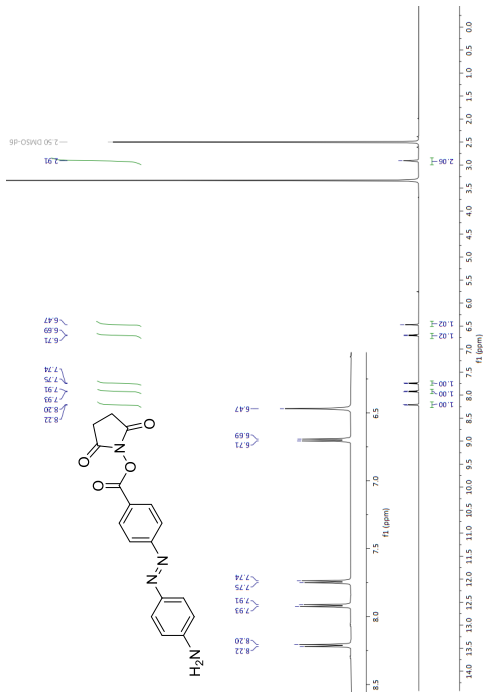

Figure S7: ^{1}H NMR spectrum of **3e** in DMSO-d_6.

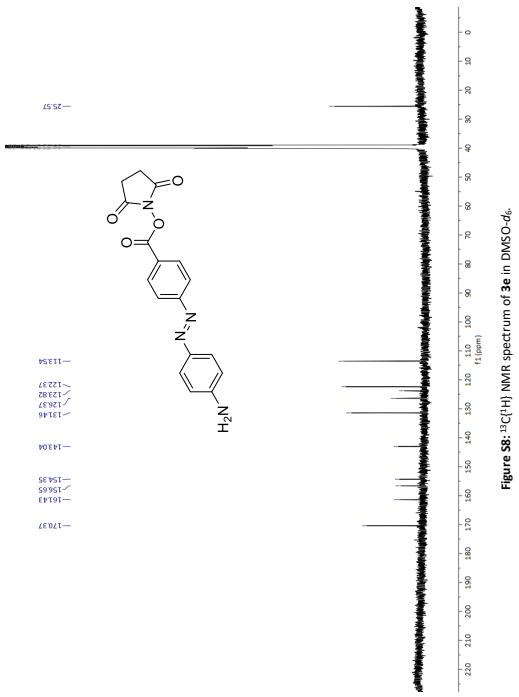

Figure S8: ^{13}C{^{1}H} NMR spectrum of **3e** in DMSO-d_6.

2,5-Dioxopyrrolidin-1-yl (*E*)-4-((4-hydroxyphenyl)diazenyl)benzoate (**3d**)

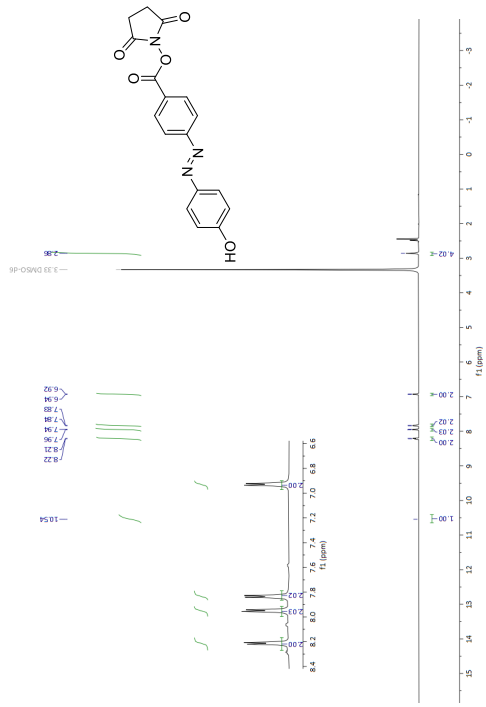

Figure S5: ^{1}H NMR spectrum of **3d** in DMSO-d_6.

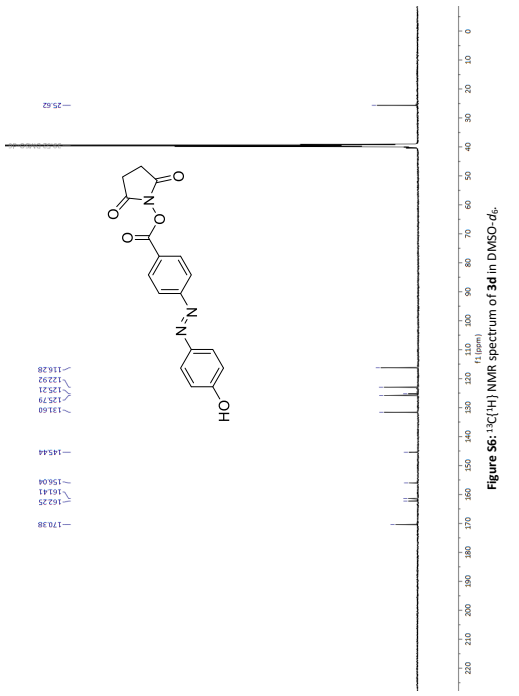

Figure S6: ^{13}C{^{1}H} NMR spectrum of **3d** in DMSO-d_6.

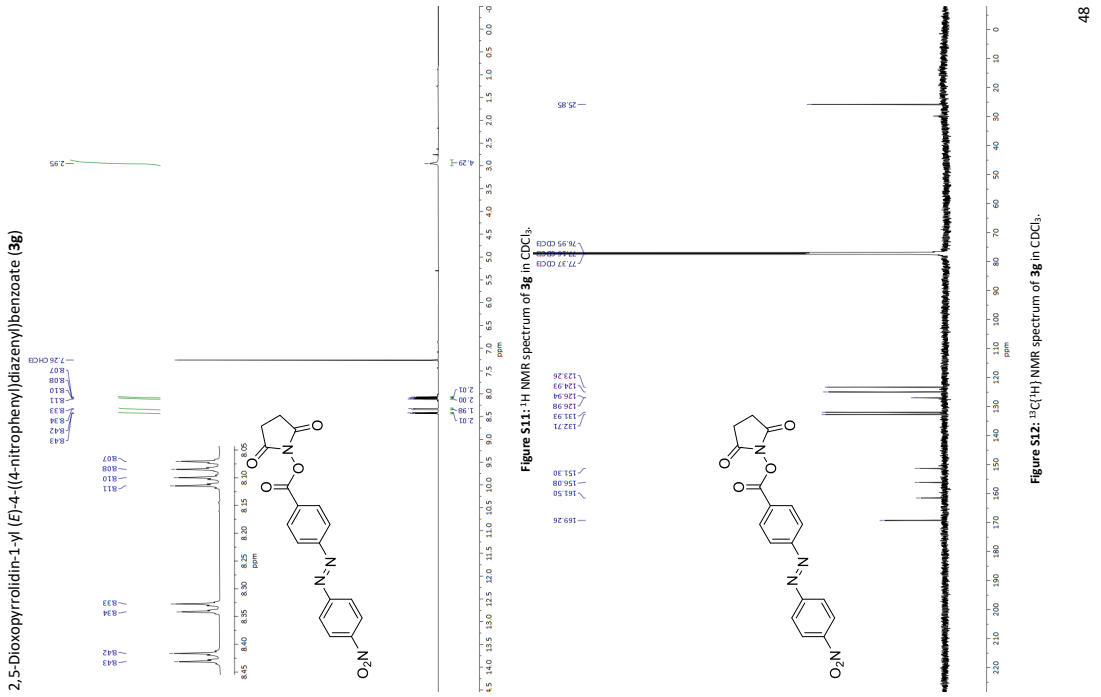

Figure S11: ^{1}H NMR spectrum of **3g** in $CDCl_3$.

Figure S12: $^{13}C\{^1H\}$ NMR spectrum of **3g** in $CDCl_3$.

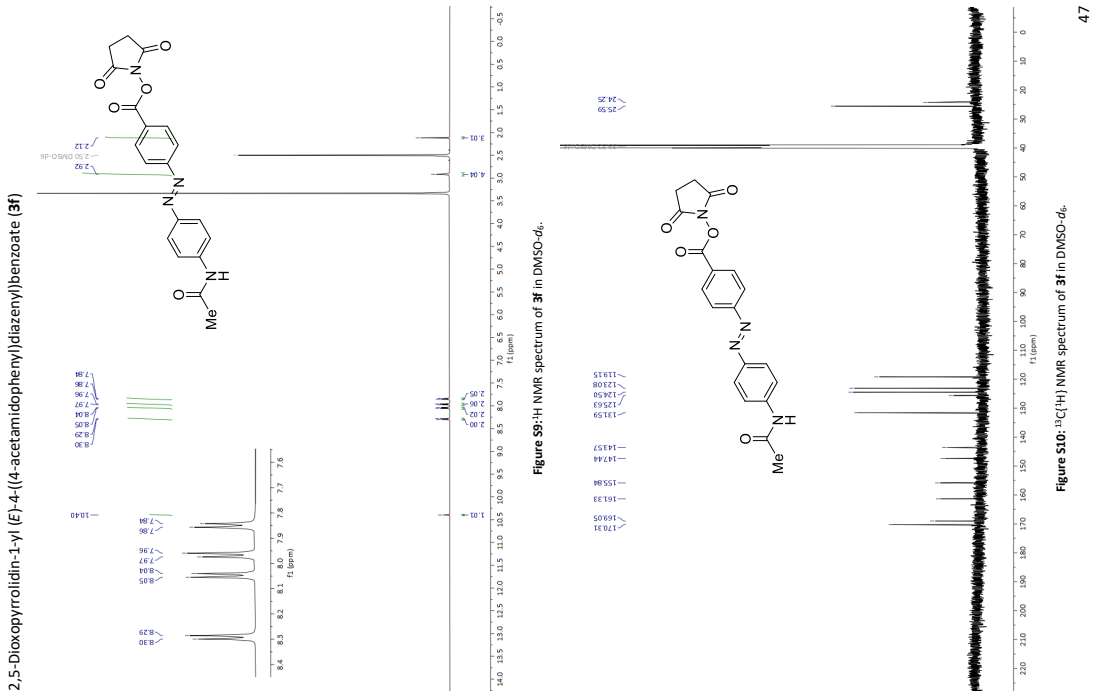

Figure S9: ^{1}H NMR spectrum of **3f** in DMSO-d_6.

Figure S10: $^{13}C\{^1H\}$ NMR spectrum of **3f** in DMSO-d_6.

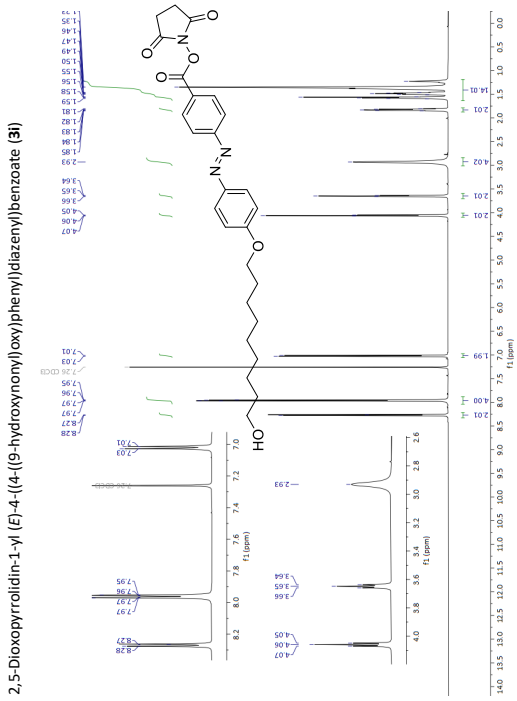

2,5-Dioxopyrrolidin-1-yl (*E*)-4-((4-((9-hydroxynonyl)oxy)phenyl)diazenyl)benzoate (**3i**)

Figure S15: ^{1}H NMR spectrum of **3i** in $CDCl_3$.

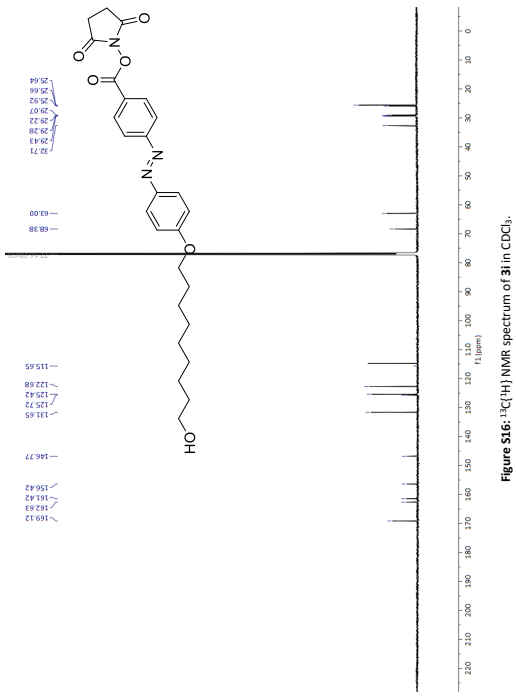

Figure S16: $^{13}C\{^1H\}$ NMR spectrum of **3i** in $CDCl_3$.

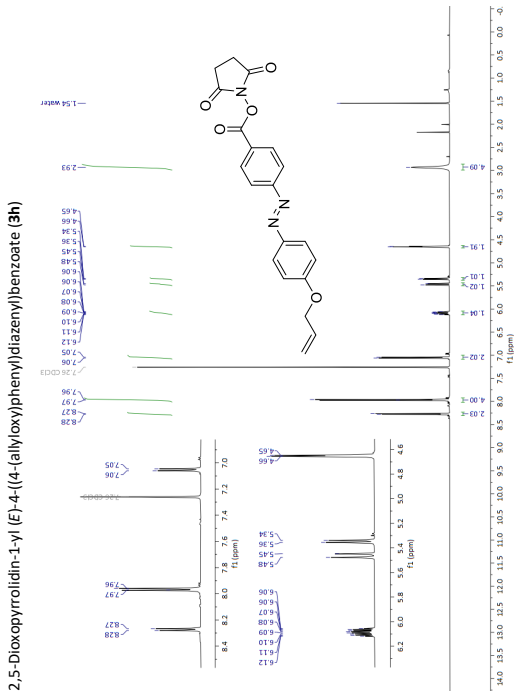

2,5-Dioxopyrrolidin-1-yl (*E*)-4-((4-(allyloxy)phenyl)diazenyl)benzoate (**3h**)

Figure S13: ^{1}H NMR spectrum of **3h** in $CDCl_3$.

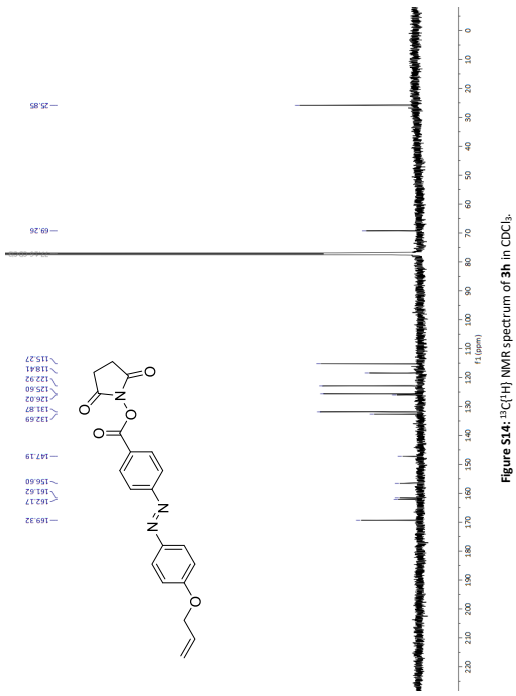

Figure S14: $^{13}C\{^1H\}$ NMR spectrum of **3h** in $CDCl_3$.

2,5-Dioxopyrrolidin-1-yl (*E*)-4-((2,7-bis(4-(hexyloxy)phenoxy)naphthalen-1-yl)diazenyl)-3,5-dimethylbenzoate (**3k**)

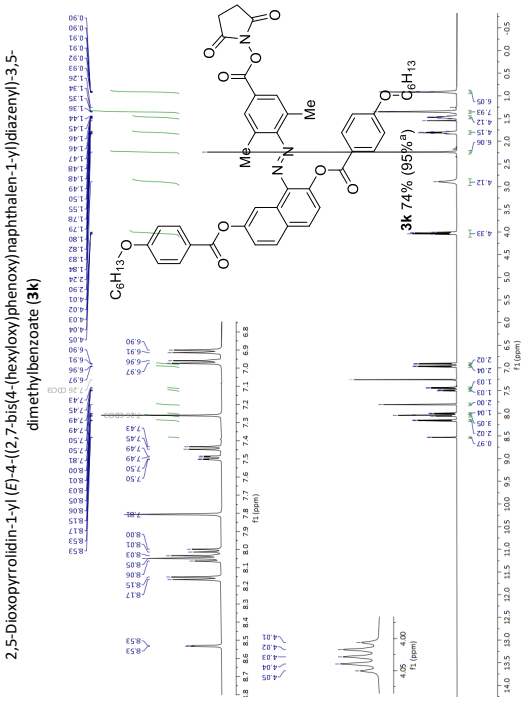

Figure S19: ^{1}H NMR spectrum of **3k** in $CDCl_3$.

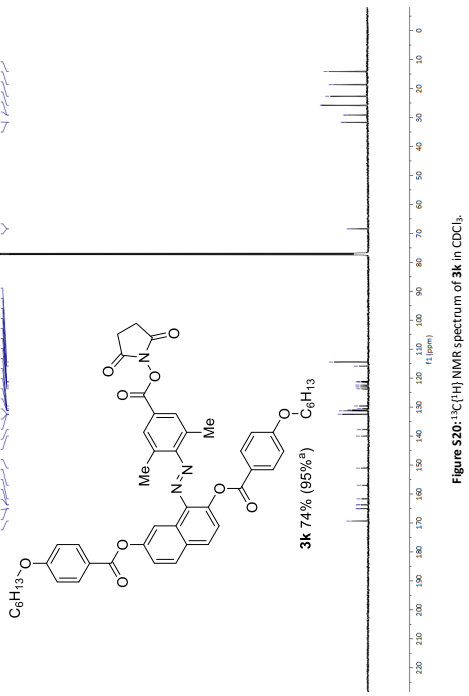

Figure S20: $^{13}C\{^1H\}$ NMR spectrum of **3k** in $CDCl_3$.

2,5-Dioxopyrrolidin-1-yl (*E*)-4-((2,6-dimethyl-4-(nonyloxy)phenyl)diazenyl)-3,5-dimethylbenzoate (**3j**)

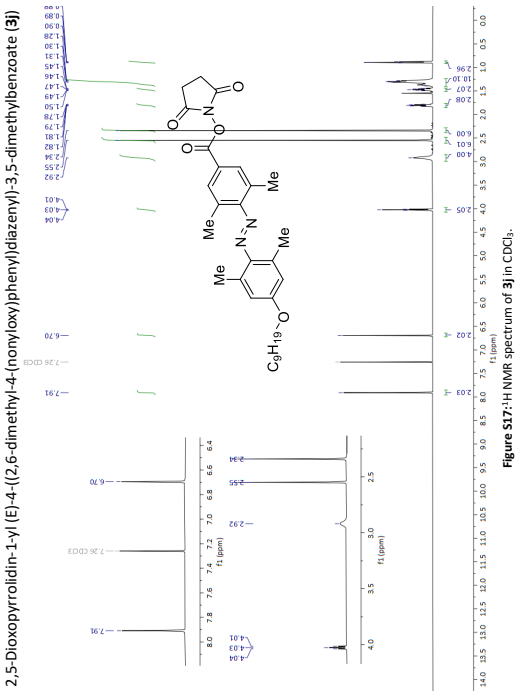

Figure S17: ^{1}H NMR spectrum of **3j** in $CDCl_3$.

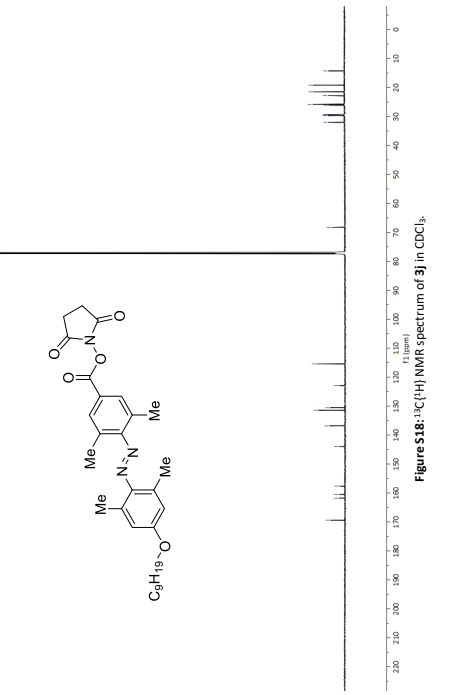

Figure S18: $^{13}C\{^1H\}$ NMR spectrum of **3j** in $CDCl_3$.

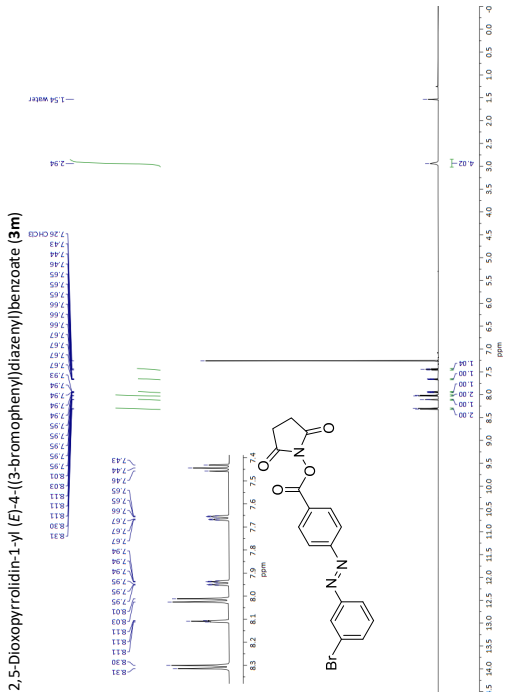

Figure S21: ^{1}H NMR spectrum of **3l** in $CDCl_3$.

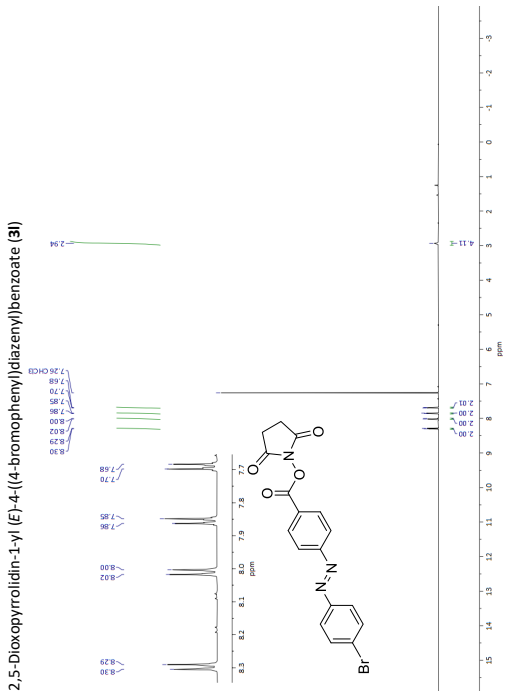

Figure S23: ^{1}H NMR spectrum of **3m** in $CDCl_3$.

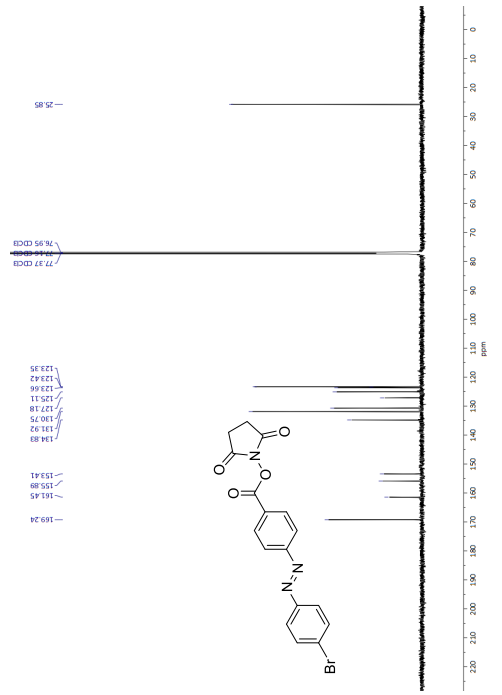

Figure S22: ^{13}C{^{1}H} NMR spectrum of **3l** in $CDCl_3$.

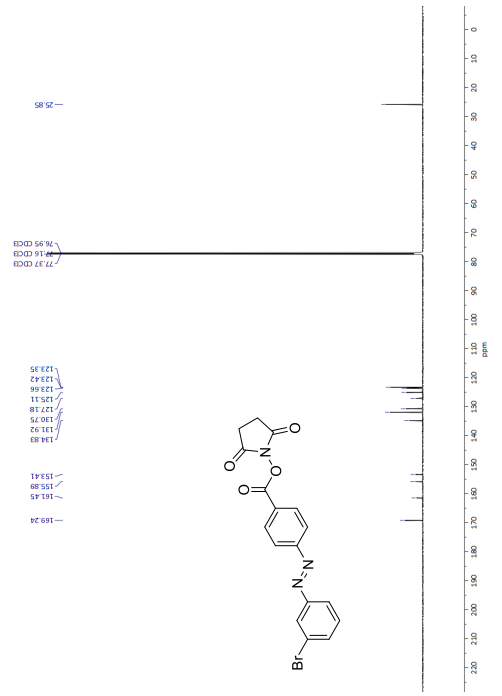

Figure S24: ^{13}C{^{1}H} NMR spectrum of **3m** in $CDCl_3$.

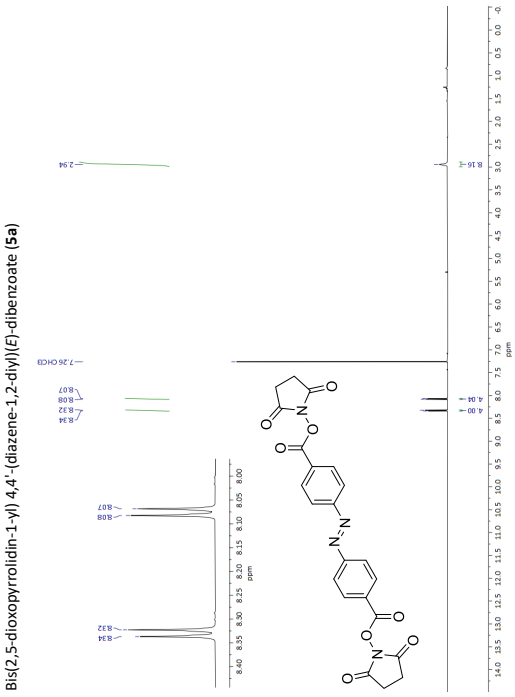

Figure S27: ^{1}H NMR spectrum of **5a** in $CDCl_3$.

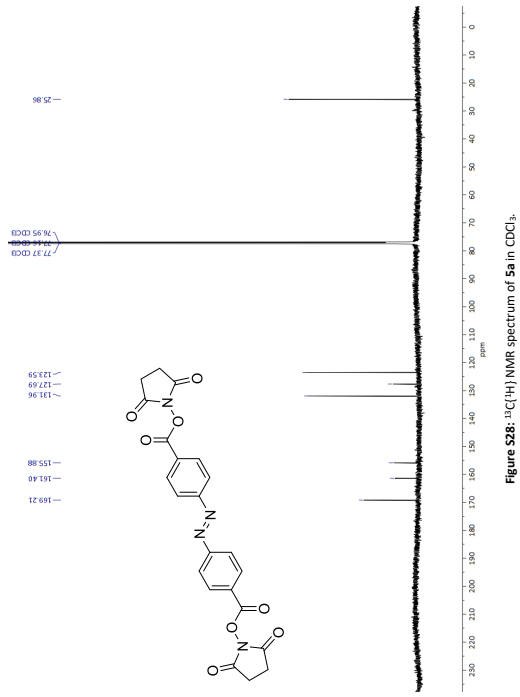

Figure S28: $^{13}C\{^1H\}$ NMR spectrum of **5a** in $CDCl_3$.

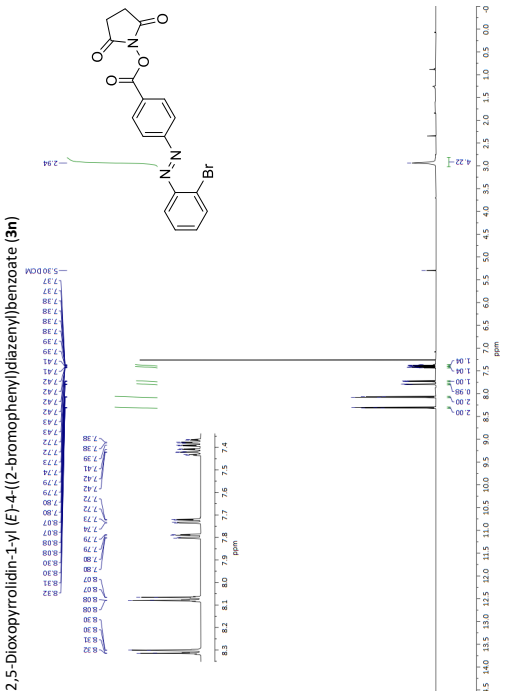

Figure S25: ^{1}H NMR spectrum of **3n** in $CDCl_3$.

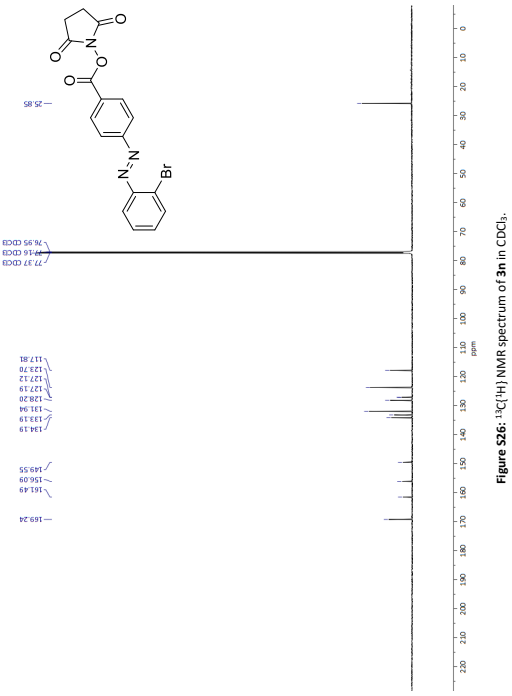

Figure S26: $^{13}C\{^1H\}$ NMR spectrum of **3n** in $CDCl_3$.

Bis(2,5-dioxopyrrolidin-1-yl) 4,4'-(diazene-1,2-diyl)(*E*)-bis(3,5-dimethylbenzoate) **(5b)**

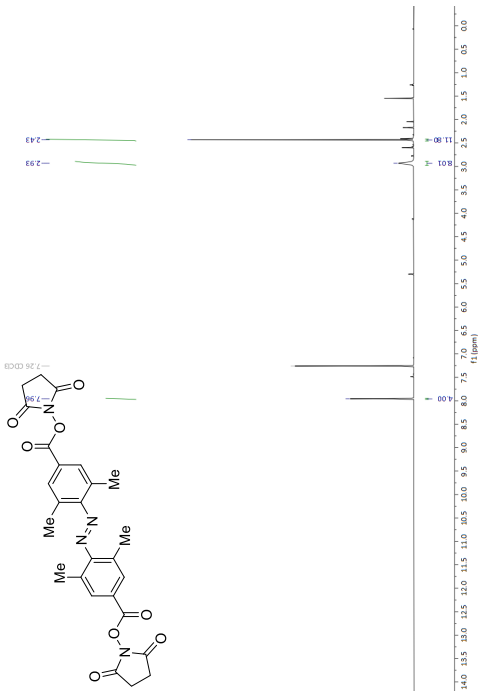

Figure S29: ^{1}H NMR spectrum of **5b** in $CDCl_3$.

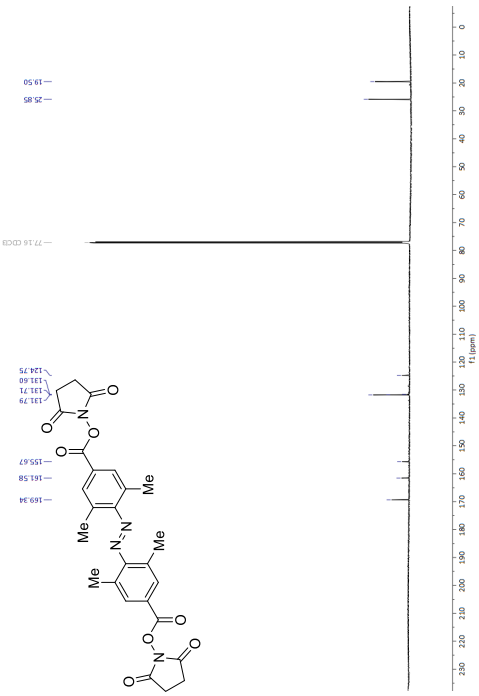

Figure S30: ^{1}H NMR spectrum of **5b** in $CDCl_3$.

Bis(2,5-dioxopyrrolidin-1-yl) 4,4'-(diazene-1,2-diyl)(*E*)-bis(3,5-dimethoxybenzoate) **(5c)**

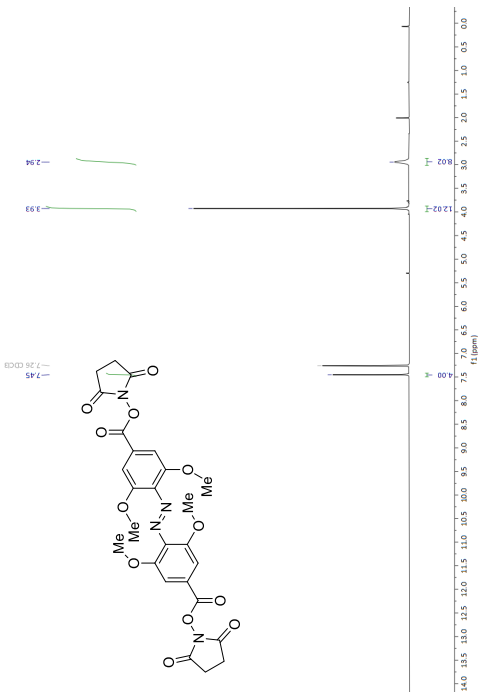

Figure S31: ^{1}H NMR spectrum of **5c** in $CDCl_3$.

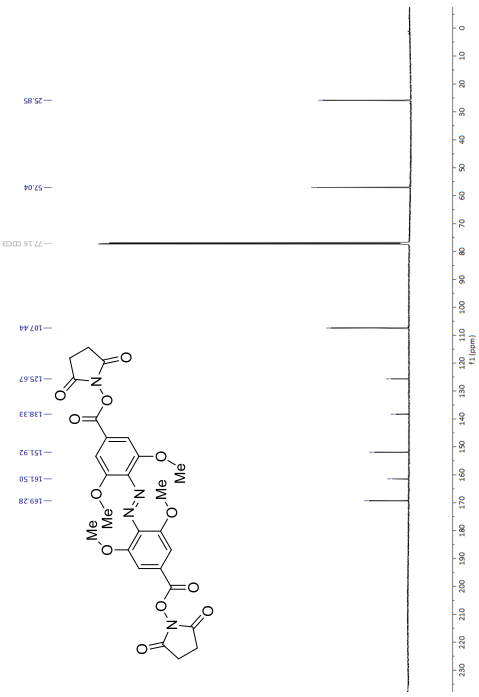

Figure S32: $^{13}C\{^1H\}$ NMR spectrum of **5c** in $CDCl_3$.

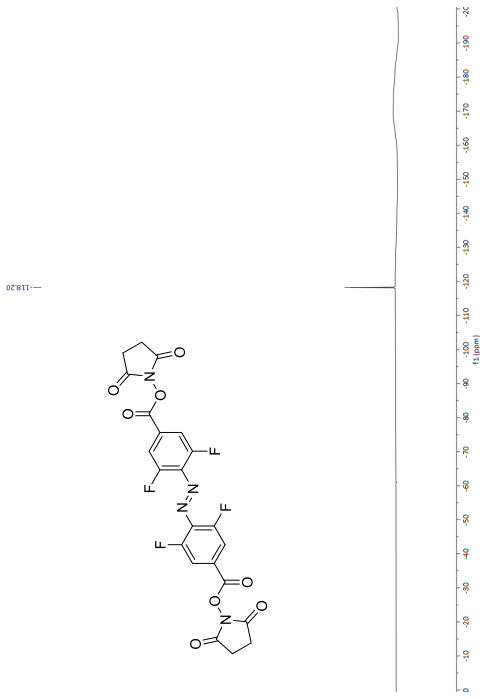

Figure S35: ^{19}F NMR spectrum of **5d** in DMSO-d_6.

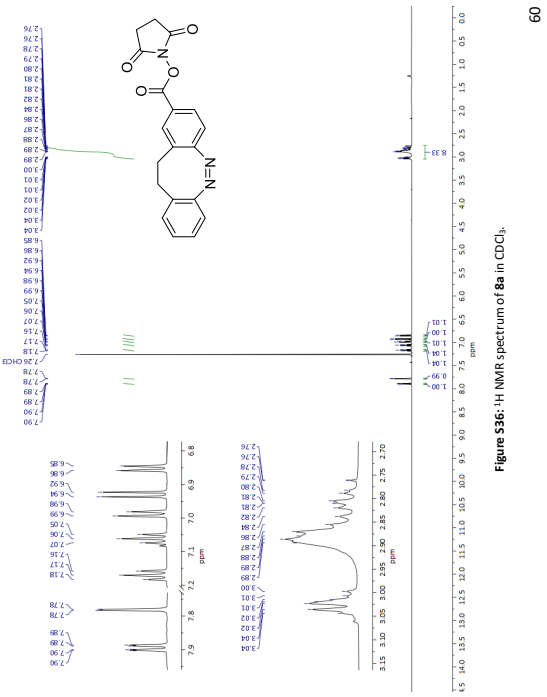

2,5-Dioxopyrrolidin-1-yl (Z)-11,12-dihydrodibenzo[c,g][1,2]diazocine-2-carboxylate (**8a**)

Figure S36: ^{1}H NMR spectrum of **8a** in $CDCl_3$.

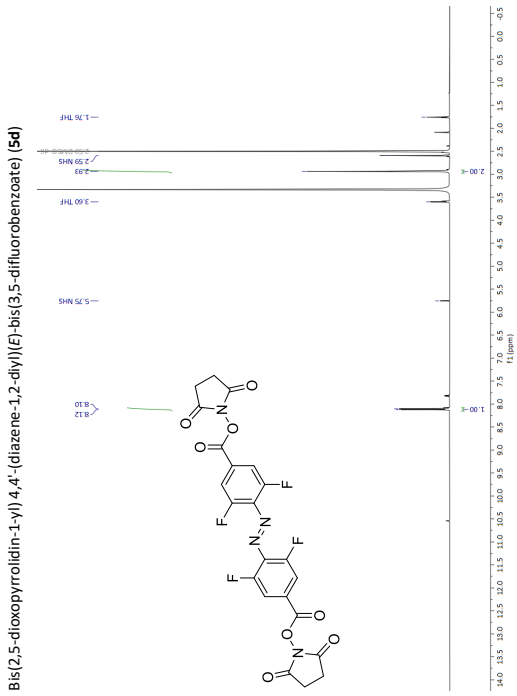

Bis(2,5-dioxopyrrolidin-1-yl) 4,4'-(diazene-1,2-diyl)(*E*)-bis(3,5-difluorobenzoate) (**5d**)

Figure S33: ^{1}H NMR spectrum of **5d** in DMSO-d_6.

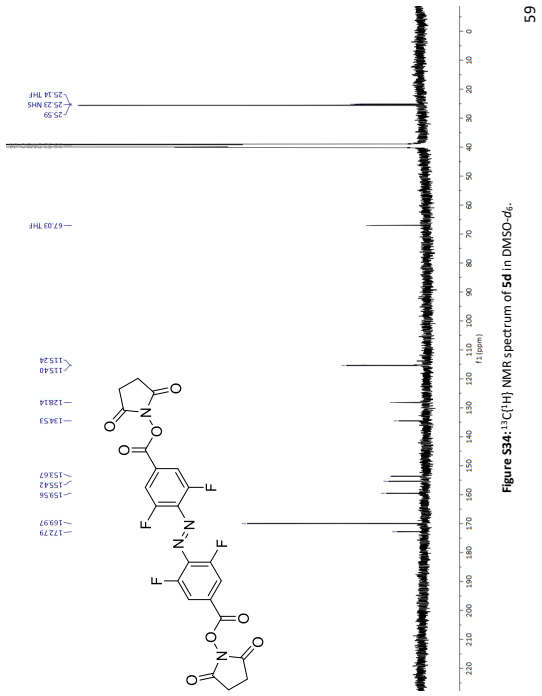

Figure S34: ^{13}C{^{1}H} NMR spectrum of **5d** in DMSO-d_6.

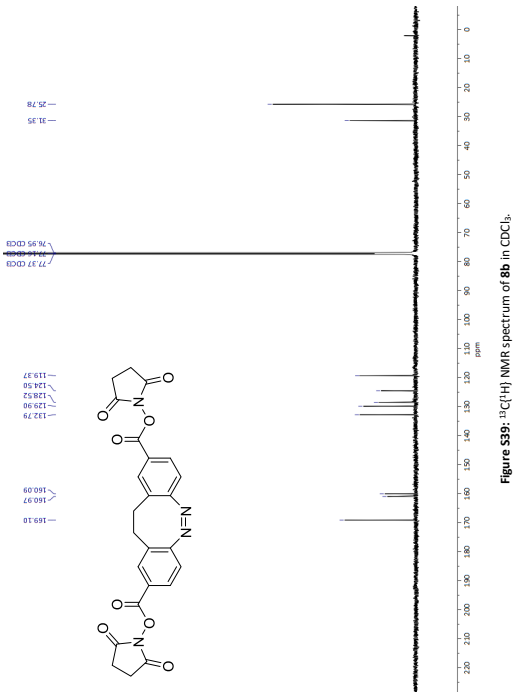

Figure S39: $^{13}C\{^1H\}$ NMR spectrum of **8b** in $CDCl_3$.

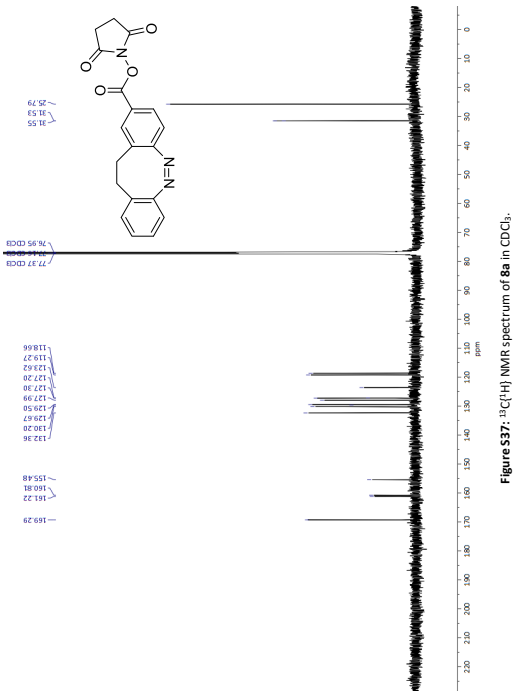

Figure S37: $^{13}C\{^1H\}$ NMR spectrum of **8a** in $CDCl_3$.

Bis(2,5-dioxopyrrolidin-1-yl) (*Z*)-11,12-dihydrodibenzo[c,g][1,2]diazocine-2,9-dicarboxylate (**8b**)

61

Di-tert-butyl 2,2'-((4,4'-(diazene-1,2-diyl)bis(benzoyl))bis(azanediyl))(*E*)-dipropionate (**10a**)

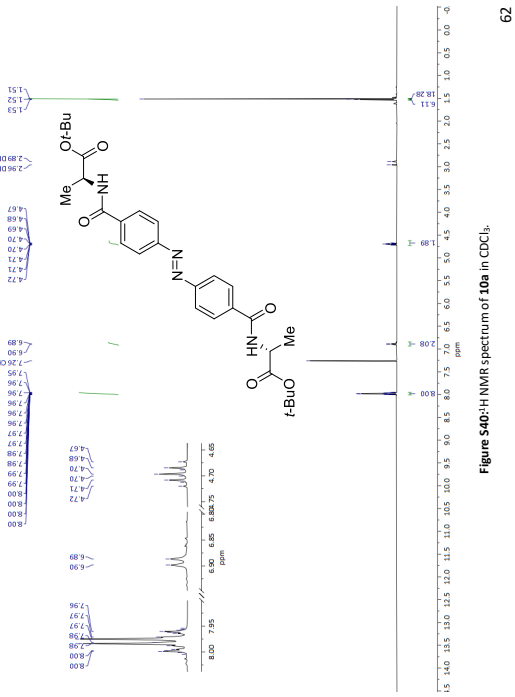

Figure S40: ^1H NMR spectrum of **10a** in $CDCl_3$.

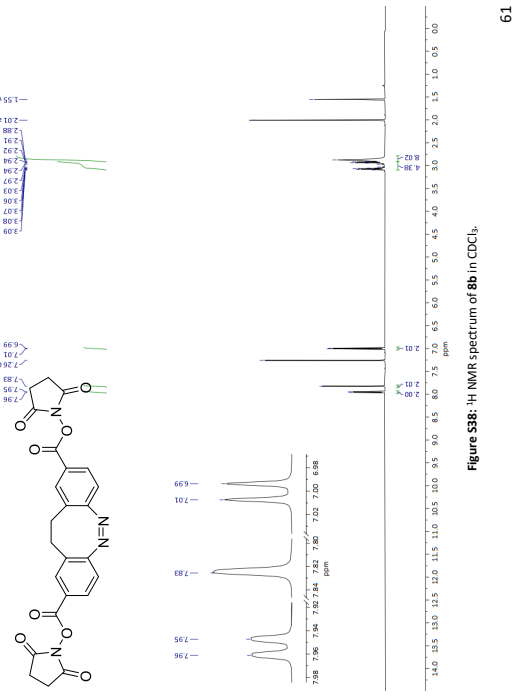

Figure S38: ^1H NMR spectrum of **8b** in $CDCl_3$.

62

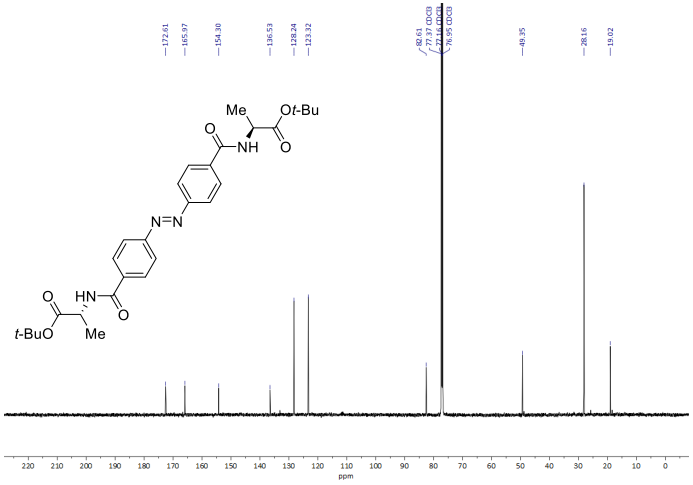

Figure S41: $^{13}C\{^{1}H\}$ NMR spectrum of **10a** in $CDCl_3$.

Di-tert-butyl 2,2'-((11,12-dihydrodibenzo[c,g][1,2]diazocine-2,9-dicarbonyl)bis(azane-diyl))(*Z*)-dipropionate (**10b**)

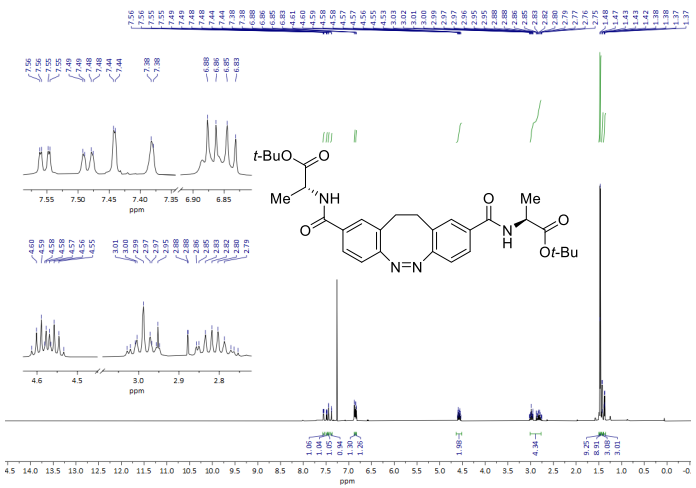

Figure S42: ^{1}H NMR spectrum of **10b** in $CDCl_3$.

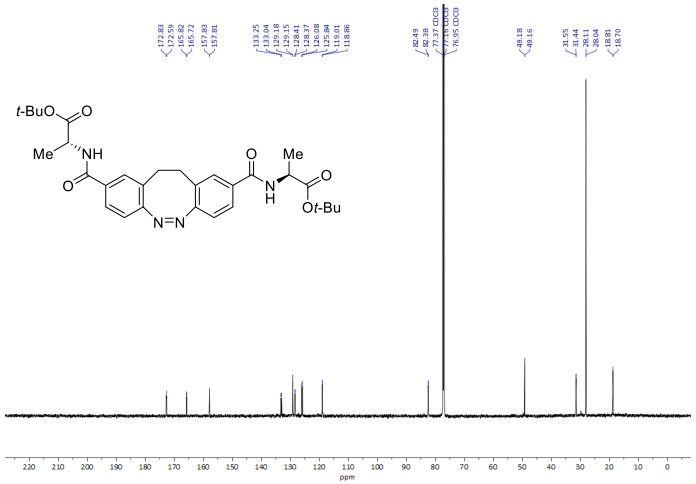

Figure S43: $^{13}C\{^{1}H\}$ NMR spectrum of **10b** in $CDCl_3$.

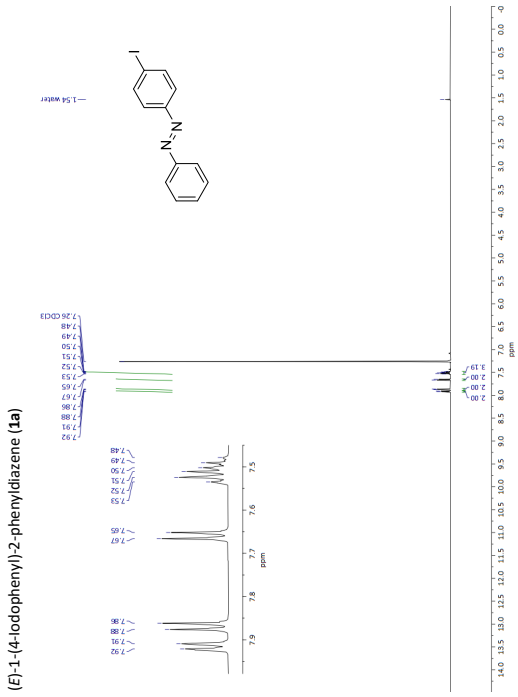

Figure S46: ^{1}H NMR spectrum of **1a** in $CDCl_3$.

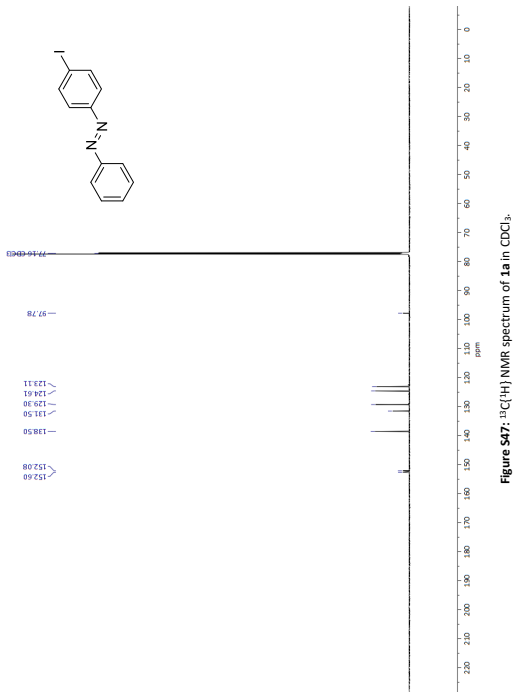

Figure S47: $^{13}C\{^1H\}$ NMR spectrum of **1a** in $CDCl_3$.

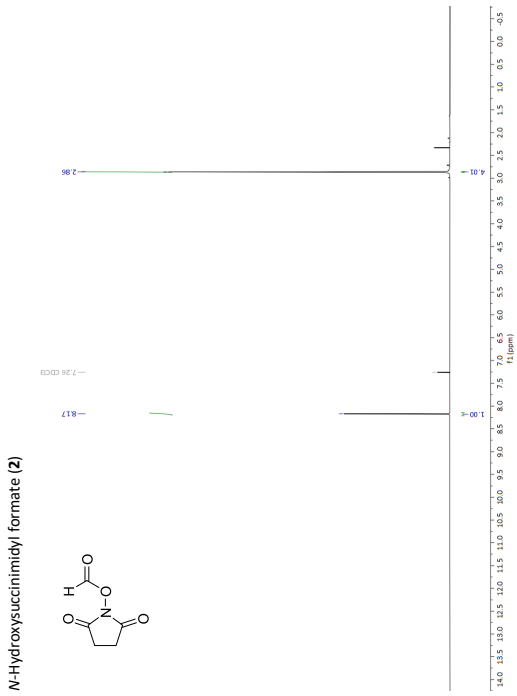

Figure S44: ^{1}H NMR spectrum of **2** in $CDCl_3$.

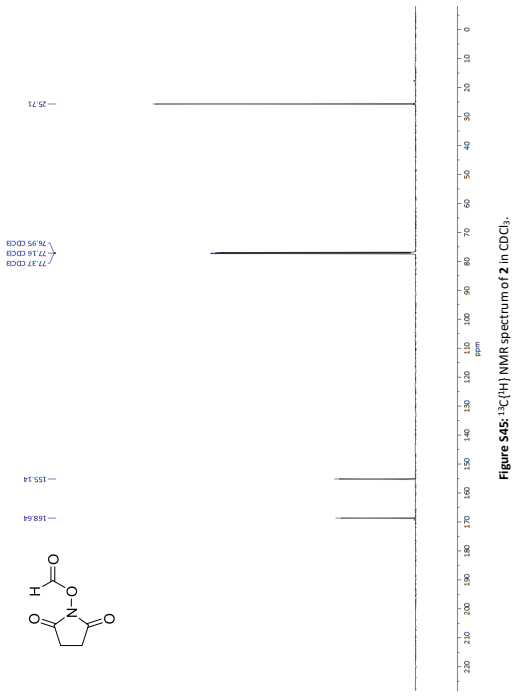

Figure S45: $^{13}C\{^1H\}$ NMR spectrum of **2** in $CDCl_3$.

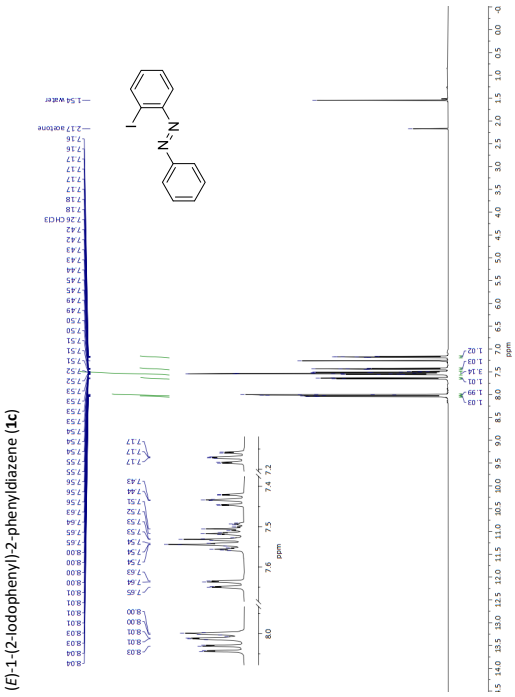

(*E*)-1-(2-Iodophenyl)-2-phenyldiazene (**1c**)

Figure S50: ^{1}H NMR spectrum of **1c** in $CDCl_3$.

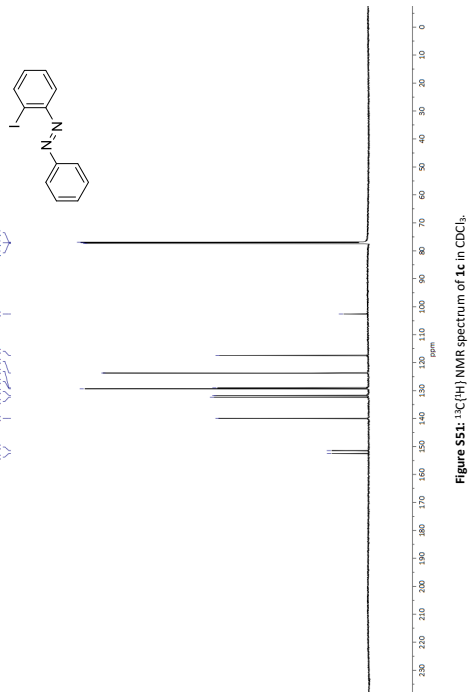

Figure S51: $^{13}C\{^1H\}$ NMR spectrum of **1c** in $CDCl_3$.

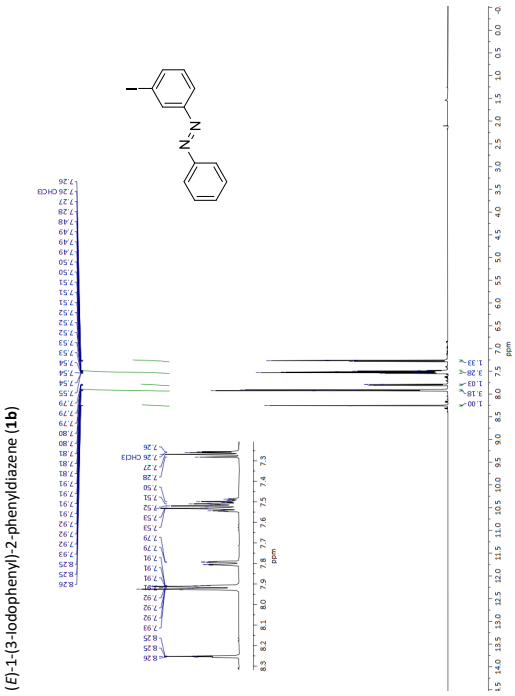

(*E*)-1-(3-Iodophenyl)-2-phenyldiazene (**1b**)

Figure S48: ^{1}H NMR spectrum of **1b** in $CDCl_3$.

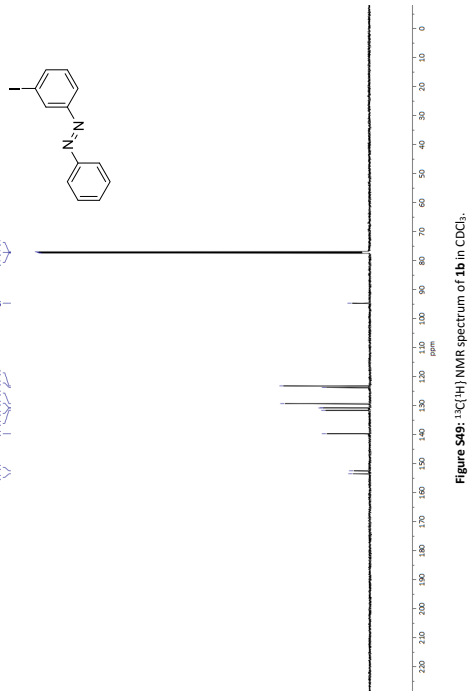

Figure S49: $^{13}C\{^1H\}$ NMR spectrum of **1b** in $CDCl_3$.

(*E*)-4-((4-Iodophenyl)diazenyl)aniline (**1e**)

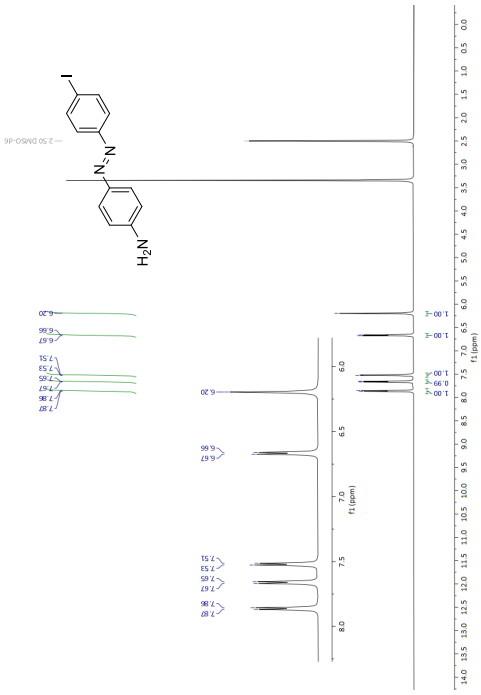

Figure S54: ^{1}H NMR spectrum of **1e** in DMSO-d_6.

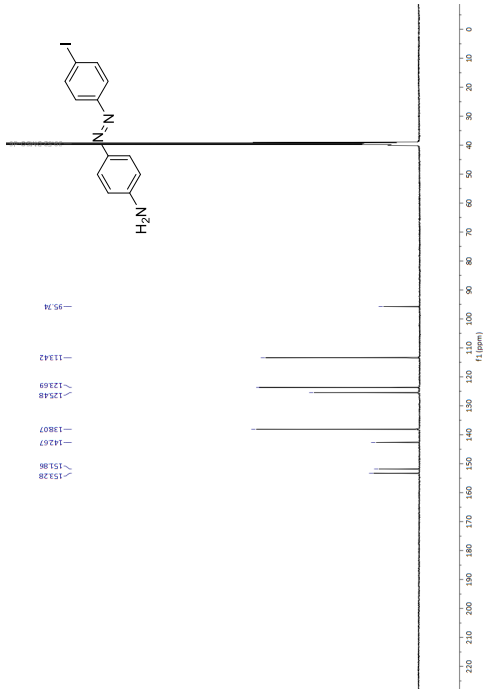

Figure S55: ^{13}C{^{1}H} NMR spectrum of **1e** in DMSO-d_6.

(*E*)-4-((4-Iodophenyl)diazenyl)phenol (**1d**)

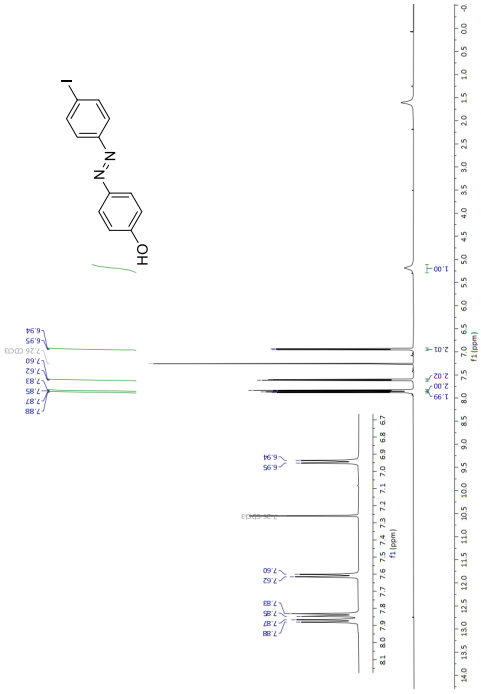

Figure S52: ^{1}H NMR spectrum of **1d** in $CDCl_3$.

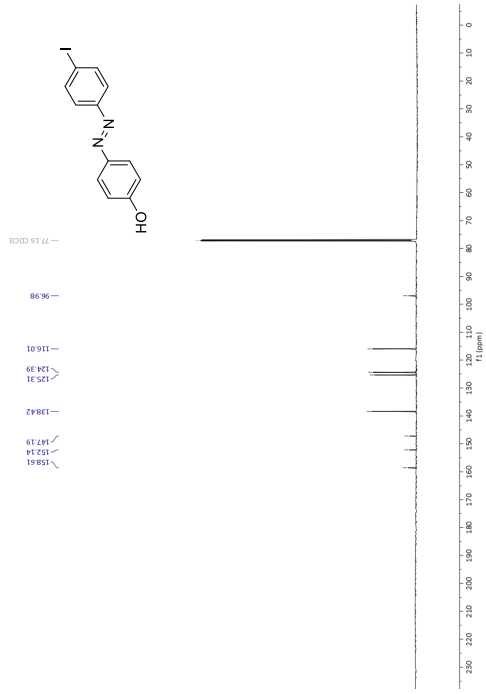

Figure S53: ^{13}C{^{1}H} NMR spectrum of **1d** in $CDCl_3$.

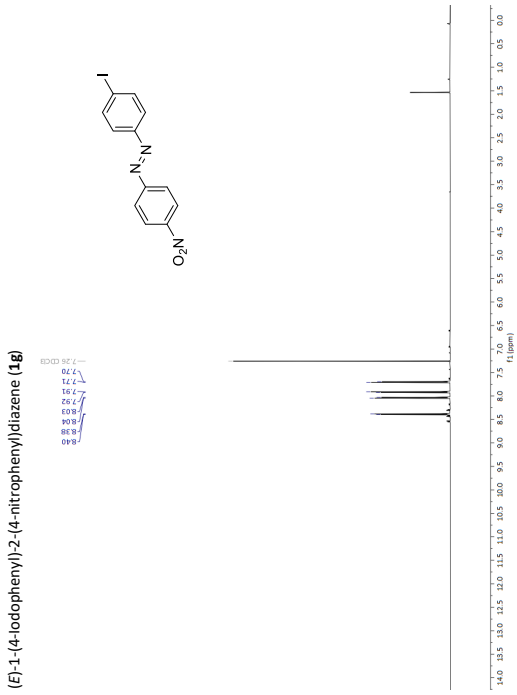

(*E*)-1-(4-Iodophenyl)-2-(4-nitrophenyl)diazene (**1g**)

Figure SS8: ^{1}H NMR spectrum of **1g** in $CDCl_3$.

Figure SS9: $^{13}C\{^1H\}$ NMR spectrum of **1g** in $CDCl_3$.

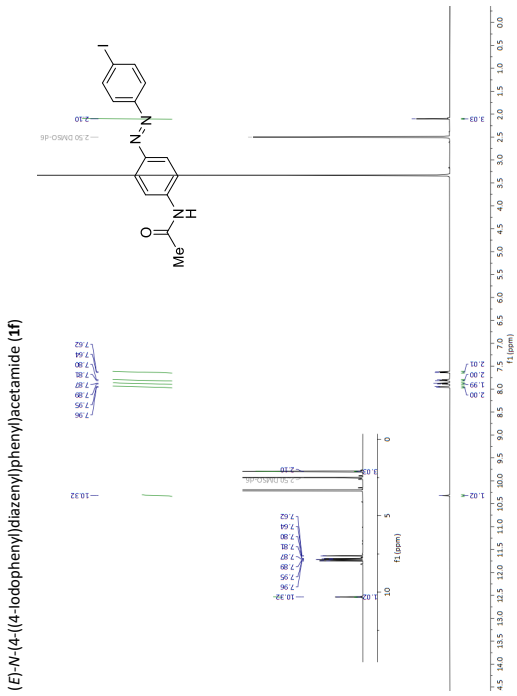

(*E*)-*N*-(4-((4-Iodophenyl)diazenyl)phenyl)acetamide (**1f**)

Figure SS6: ^{1}H NMR spectrum of **1f** in DMSO-d_6.

Figure SS7: $^{13}C\{^1H\}$ NMR spectrum of **1f** in DMSO-d_6.

(*E*)-1-(4-(Allyloxy)phenyl)-2-(4-iodophenyl)diazene (**1h**)

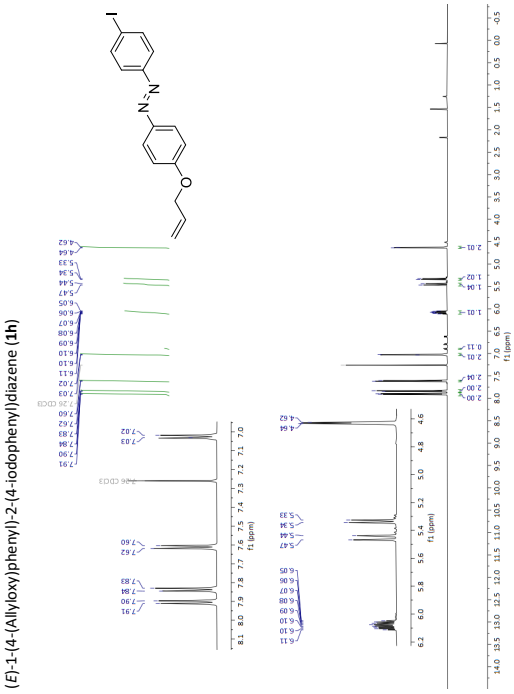

Figure S60: ^{1}H NMR spectrum of **1h** in $CDCl_3$.

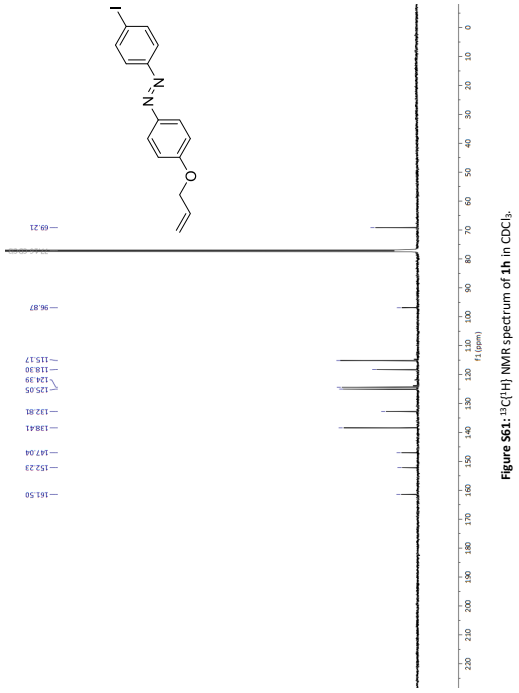

Figure S61: $^{13}C\{^1H\}$ NMR spectrum of **1h** in $CDCl_3$.

(*E*)-9-(4-((4-Iodophenyl)diazenyl)phenoxy)nonan-1-ol (**1i**)

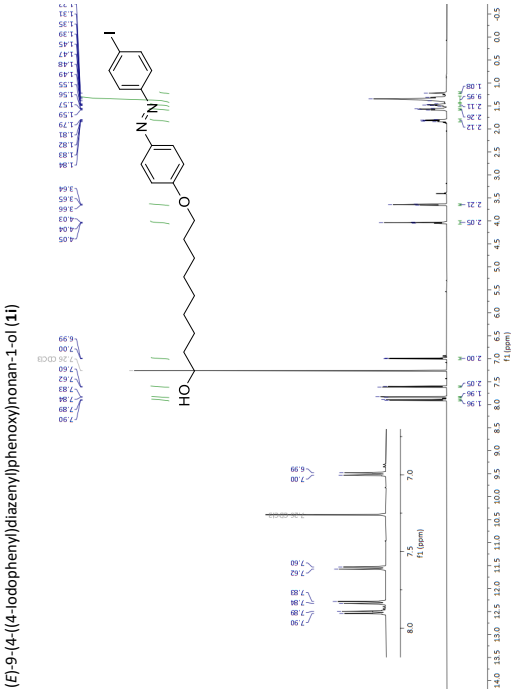

Figure S62: ^{1}H NMR spectrum of **1i** in $CDCl_3$.

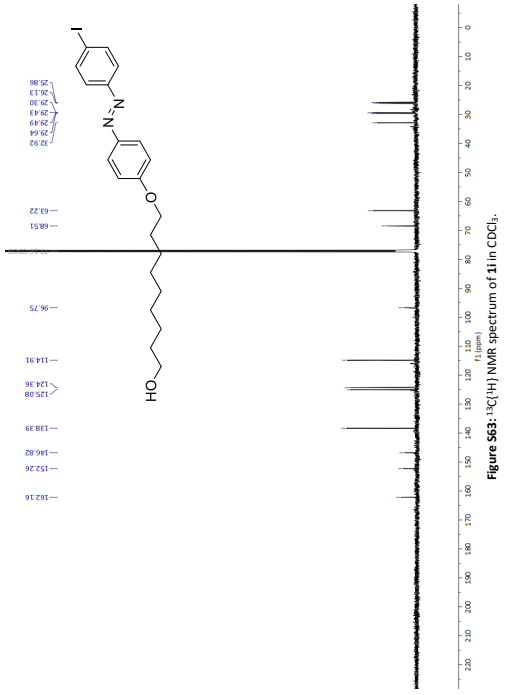

Figure S63: $^{13}C\{^1H\}$ NMR spectrum of **1i** in $CDCl_3$.

(*E*)-4-((4-Iodo-2,6-dimethylphenyl)diazenyl)-3,5-dimethylphenol (**S1**)

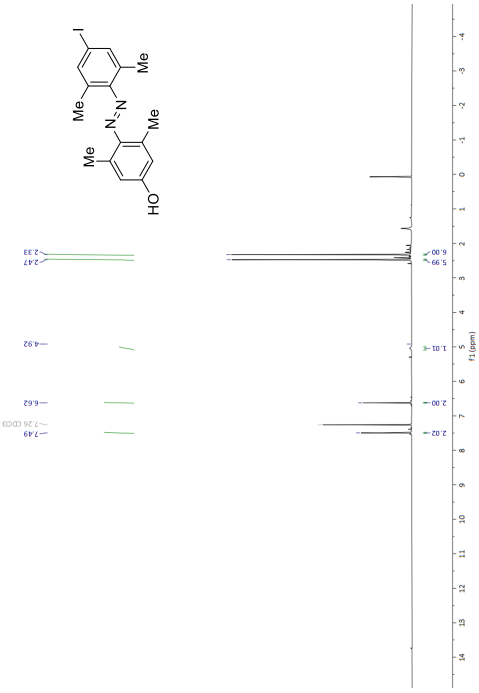

Figure S64: ^{1}H NMR spectrum of **S1** in $CDCl_3$.

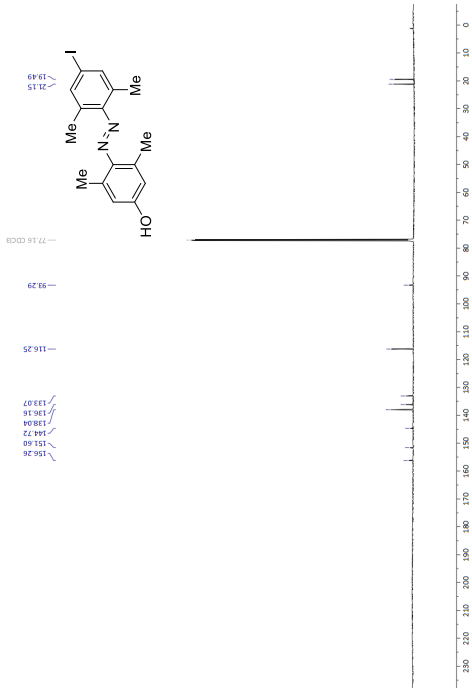

Figure S65: $^{13}C\{^1H\}$ NMR spectrum of **S1** in $CDCl_3$.

75

(*E*)-1-(2,6-Dimethyl-4-(nonyloxy)phenyl)-2-(4-iodo-2,6-dimethylphenyl)diazene (**1j**)

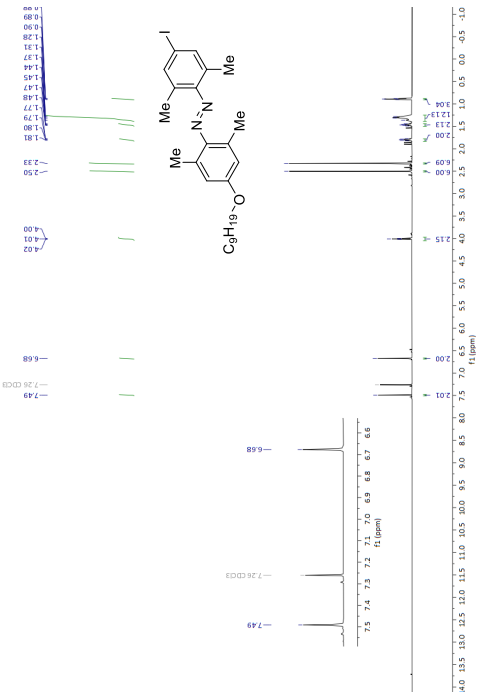

Figure S66: ^{1}H NMR spectrum of **1j** in $CDCl_3$.

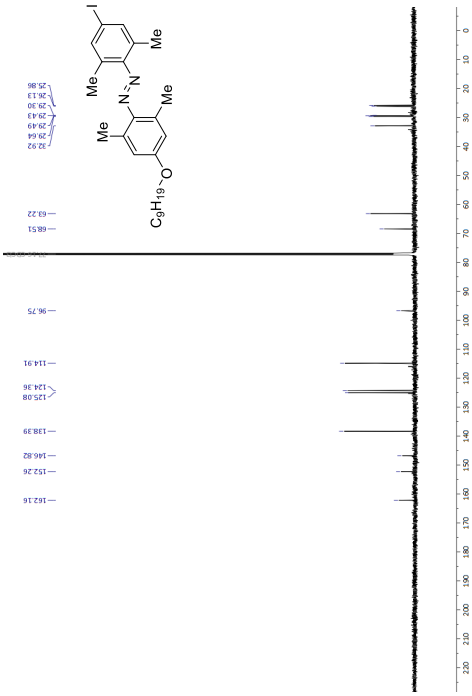

Figure S67: $^{13}C\{^1H\}$ NMR spectrum of **1j** in $CDCl_3$.

76

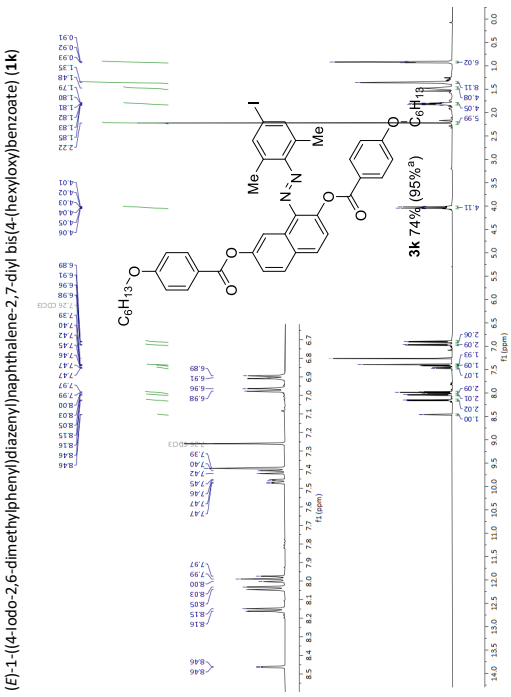

Figure S70: ^{1}H NMR spectrum of **1k** in $CDCl_3$.

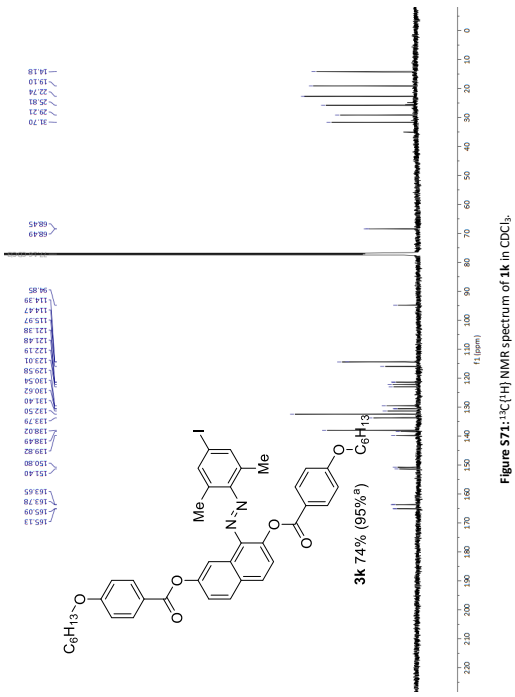

Figure S71: $^{13}C\{^1H\}$ NMR spectrum of **1k** in $CDCl_3$.

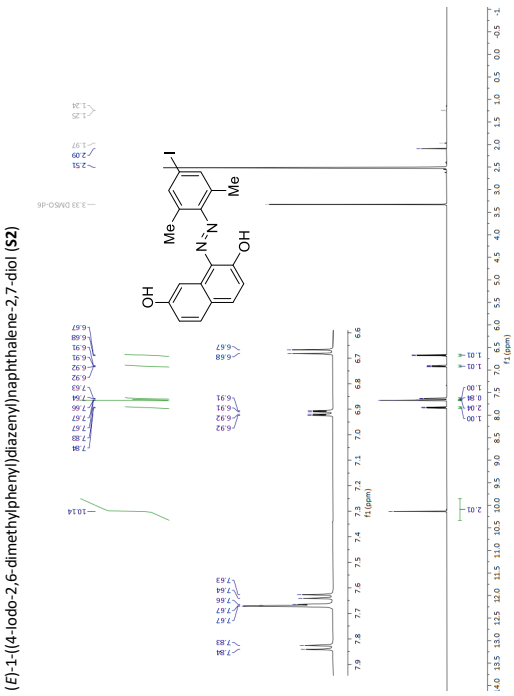

Figure S68: ^{1}H NMR spectrum of **S2** in DMSO-d_6.

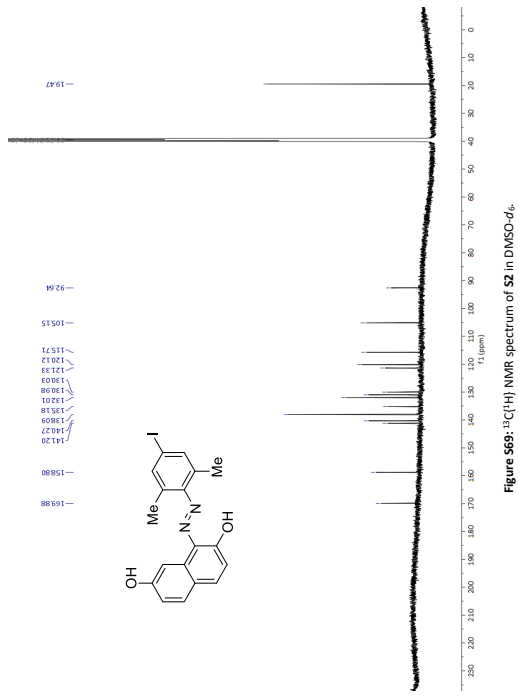

Figure S69: $^{13}C\{^1H\}$ NMR spectrum of **S2** in DMSO-d_6.

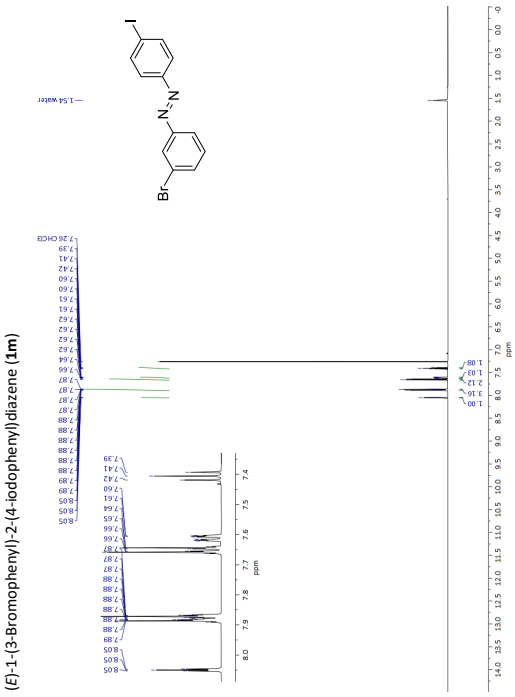

Figure S72: ^{1}H NMR spectrum of **1l** in $CDCl_3$.

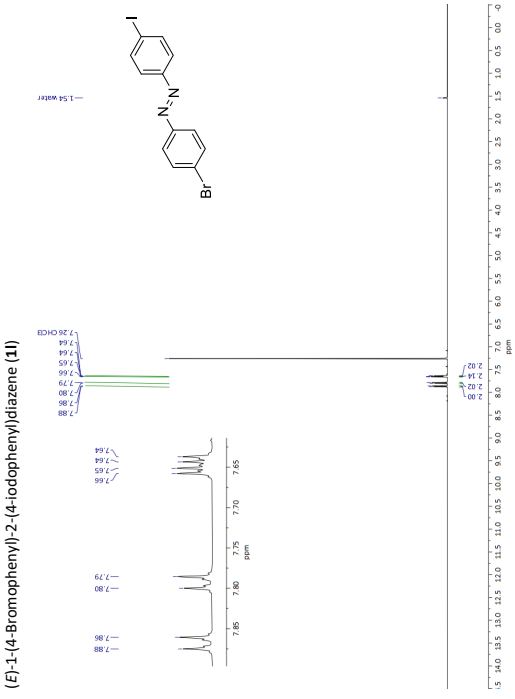

Figure S73: $^{13}C\{^1H\}$ NMR spectrum of **1l** in $CDCl_3$.

Figure S74: ^{1}H NMR spectrum of **1m** in $CDCl_3$.

Figure S75: $^{13}C\{^1H\}$ NMR spectrum of **1m** in $CDCl_3$.

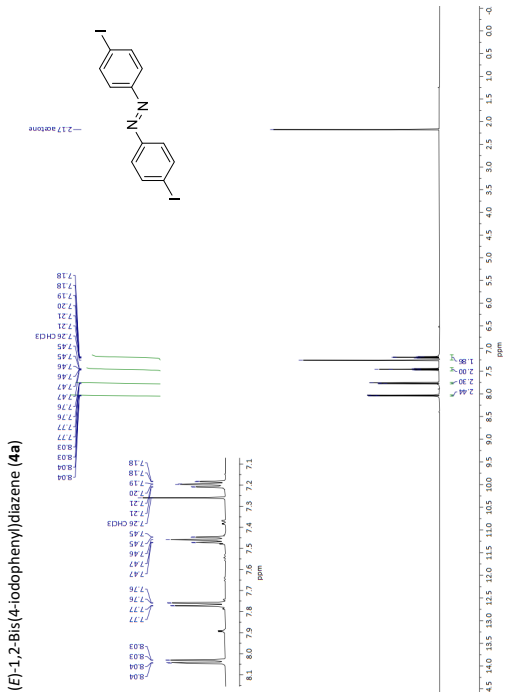

Figure S78: ^{1}H NMR spectrum of **4a** in $CDCl_3$.

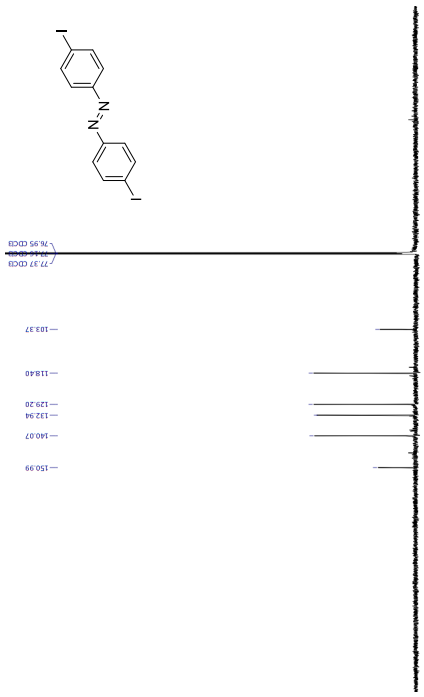

Figure S79: $^{13}C\{^1H\}$ NMR spectrum of **4a** in $CDCl_3$.

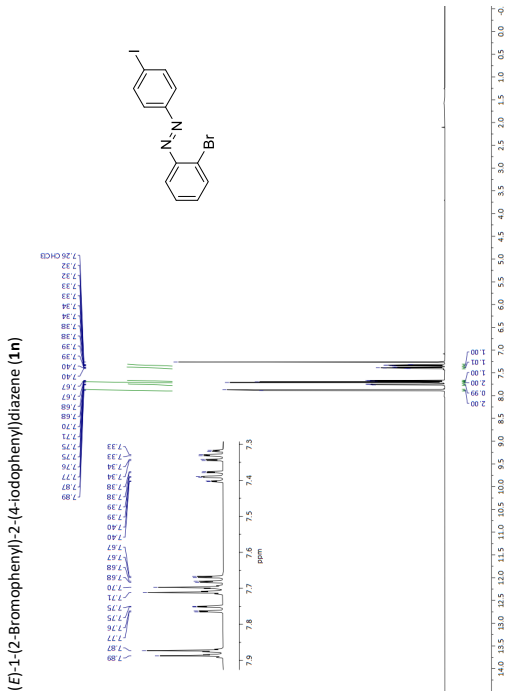

Figure S76: ^{1}H NMR spectrum of **1n** in $CDCl_3$.

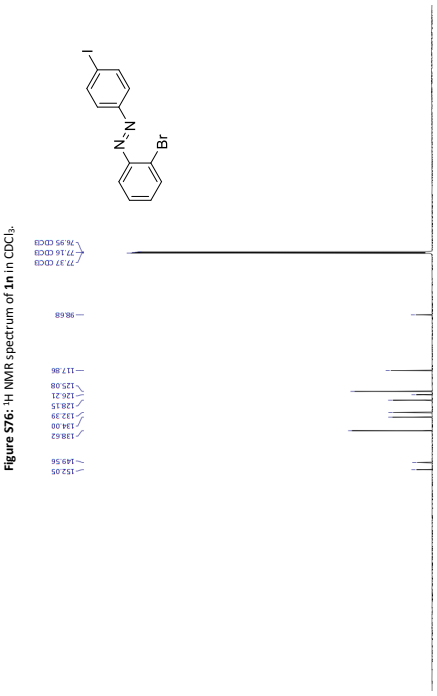

Figure S77: $^{13}C\{^1H\}$ NMR spectrum of **1n** in $CDCl_3$.

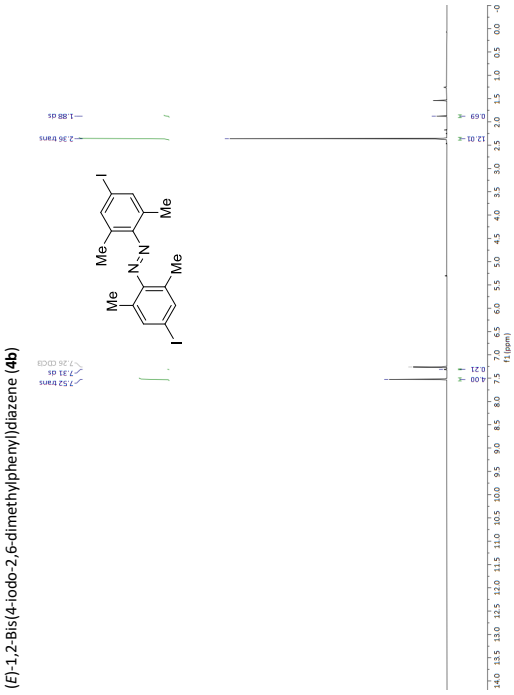

Figure S82: ^{1}H NMR spectrum of **4b** in $CDCl_3$.

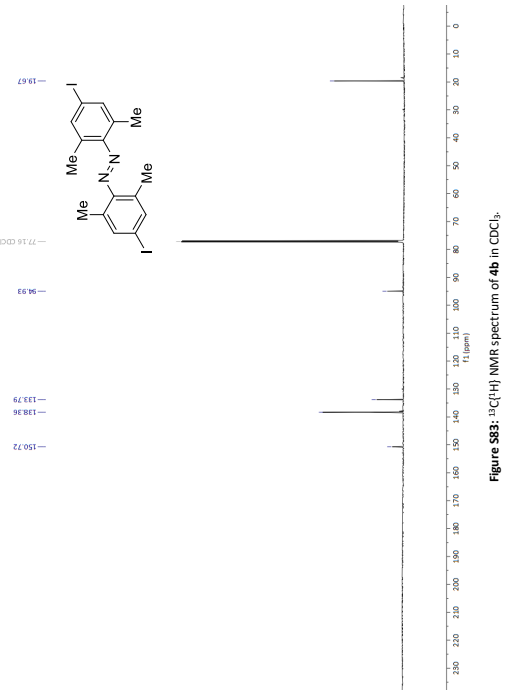

Figure S83: $^{13}C\{^1H\}$ NMR spectrum of **4b** in $CDCl_3$.

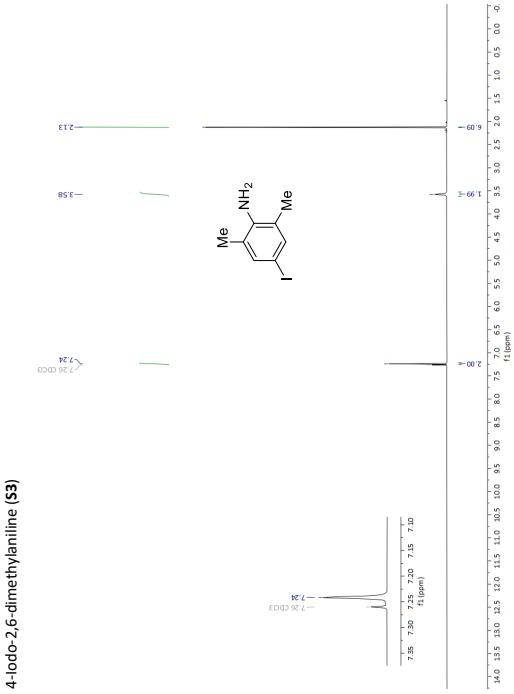

Figure S80: ^{1}H NMR spectrum of **S3** in $CDCl_3$.

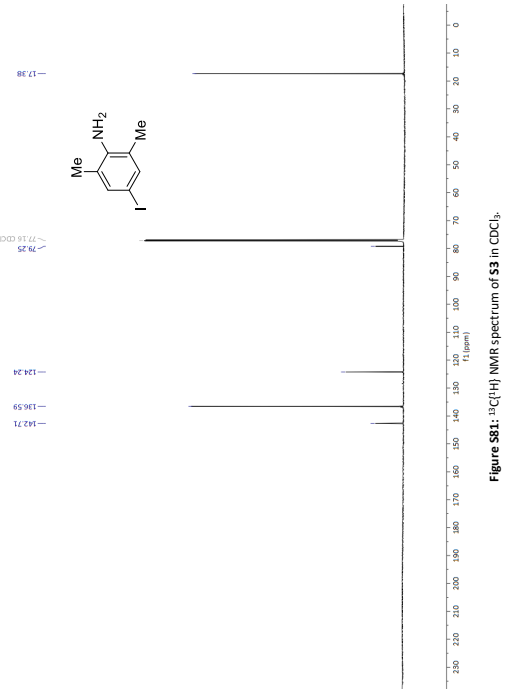

Figure S81: $^{13}C\{^1H\}$ NMR spectrum of **S3** in $CDCl_3$.

4-Bromo-2,6-dimethoxyaniline (**S4**)

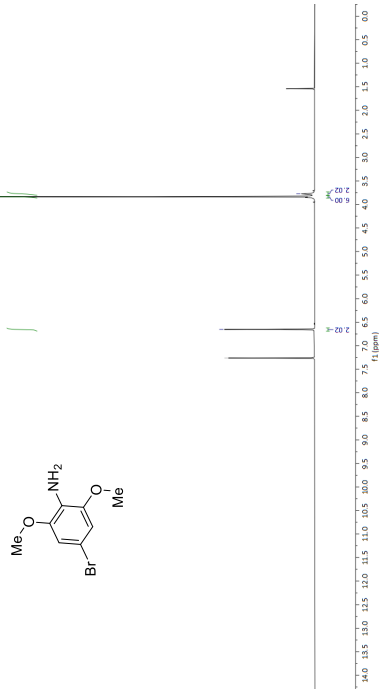

Figure S84: ^{1}H NMR spectrum of **S4** in $CDCl_3$.

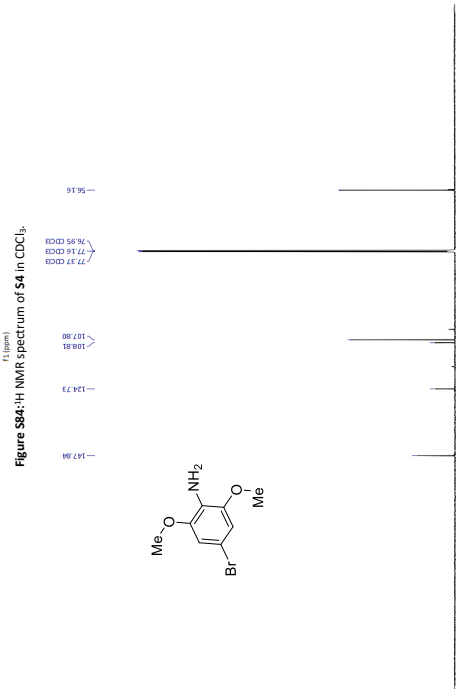

Figure S85: ^{13}C NMR spectrum of **S4** in $CDCl_3$.

85

(*E*)-1,2-Bis(4-bromo-2,6-dimethoxyphenyl)diazene (**S5**)

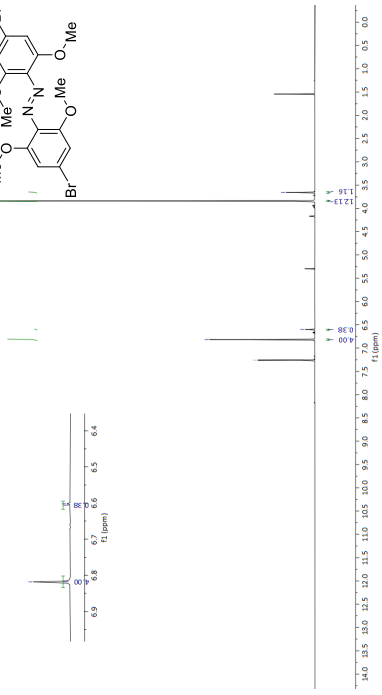

Figure S86: ^{1}H NMR spectrum of **S5** in $CDCl_3$.

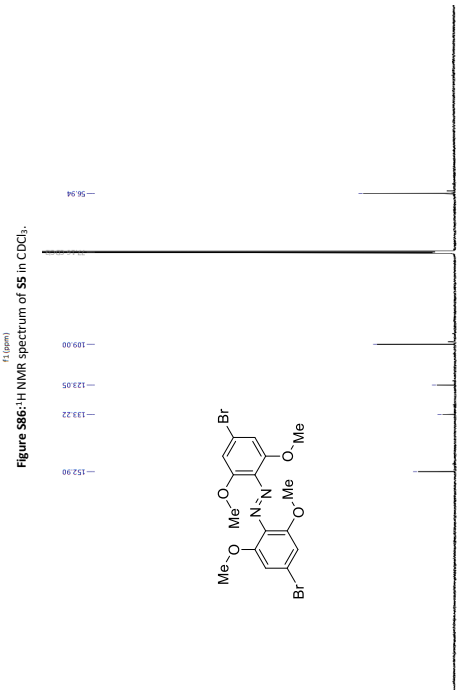

Figure S87: ^{13}C{^{1}H} NMR spectrum of **S5** in $CDCl_3$.

86

(*E*)-1,2-Bis(4-iodo-2,6-dimethoxyphenyl)diazene (**4c**)

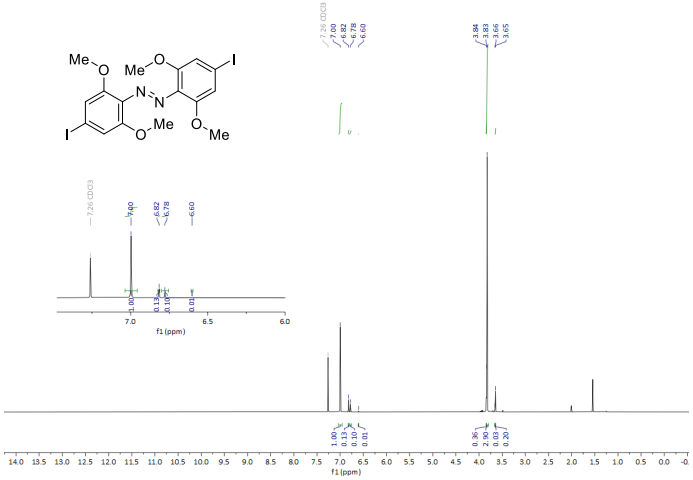

Figure S88: ^{1}H NMR spectrum of **4c** in $CDCl_3$.

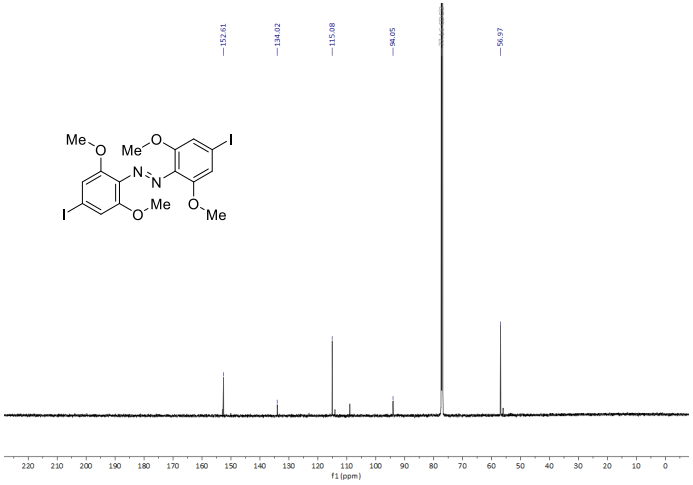

Figure S89: $^{13}C\{^{1}H\}$ NMR spectrum of **4c** in $CDCl_3$.

4-Iodo-2,6-difluoro-aniline (**S6**)

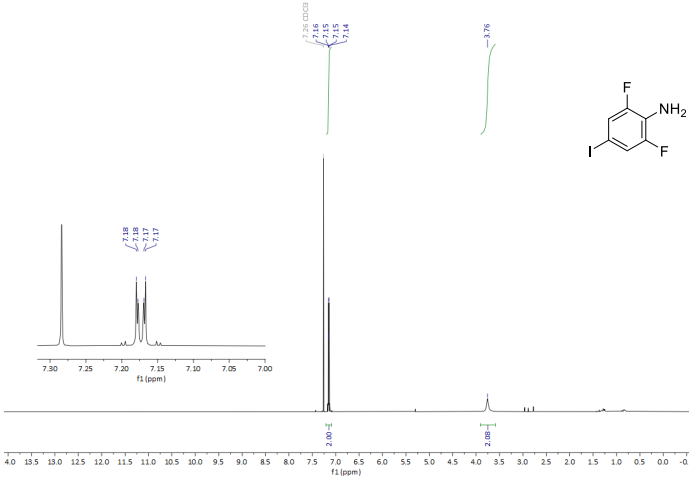

Figure S90: ^{1}H NMR spectrum of **S6** in $CDCl_3$.

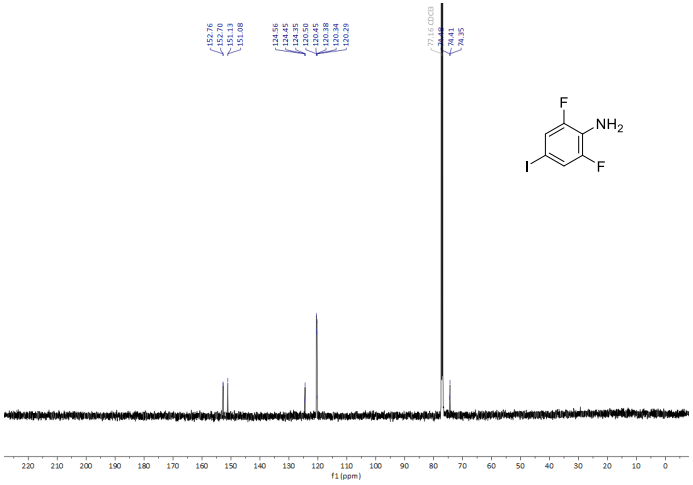

Figure S91: $^{13}C\{^{1}H\}$ NMR spectrum of **S6** in $CDCl_3$.

Figure S94: $^{13}C\{^1H\}$ NMR spectrum of **4d** in $CDCl_3$.

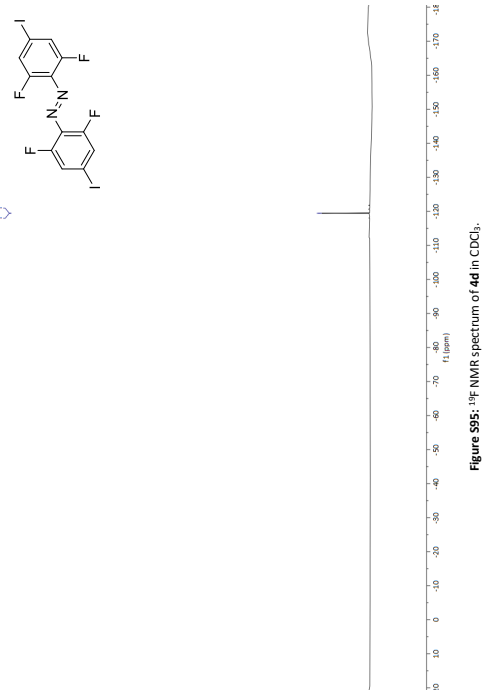

Figure S95: ^{19}F NMR spectrum of **4d** in $CDCl_3$.

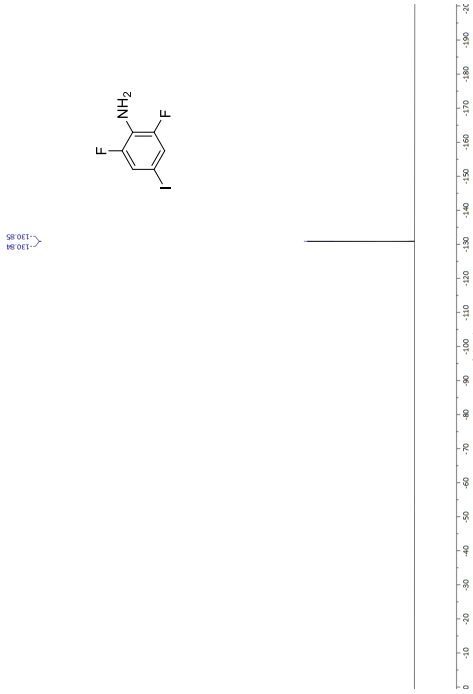

Figure S92: ^{19}F NMR spectrum of **S6** in $CDCl_3$.

(*E*)-1,2-bis(2,6-difluoro-4-iodophenyl)diazene (**4d**)

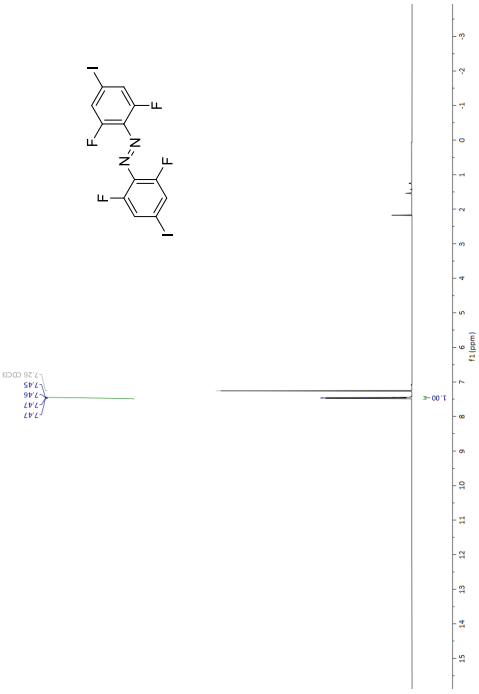

Figure S93: ^1H NMR spectrum of **4d** in $CDCl_3$.

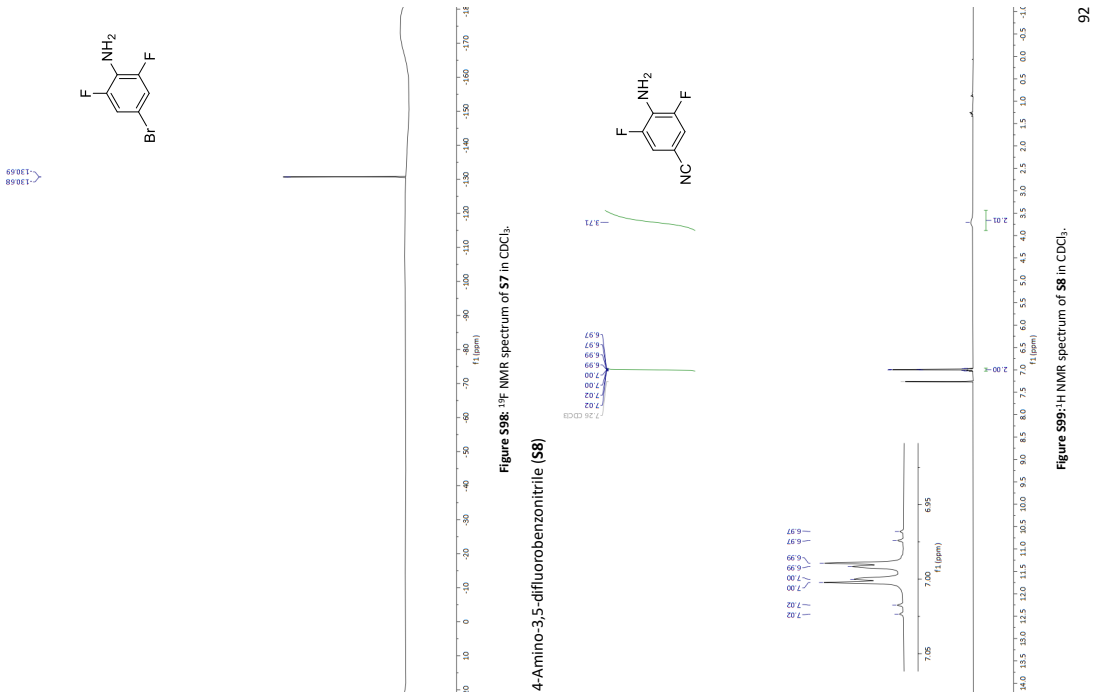

Figure S98: ^{19}F NMR spectrum of **S7** in $CDCl_3$.

Figure S99: ^{1}H NMR spectrum of **S8** in $CDCl_3$.

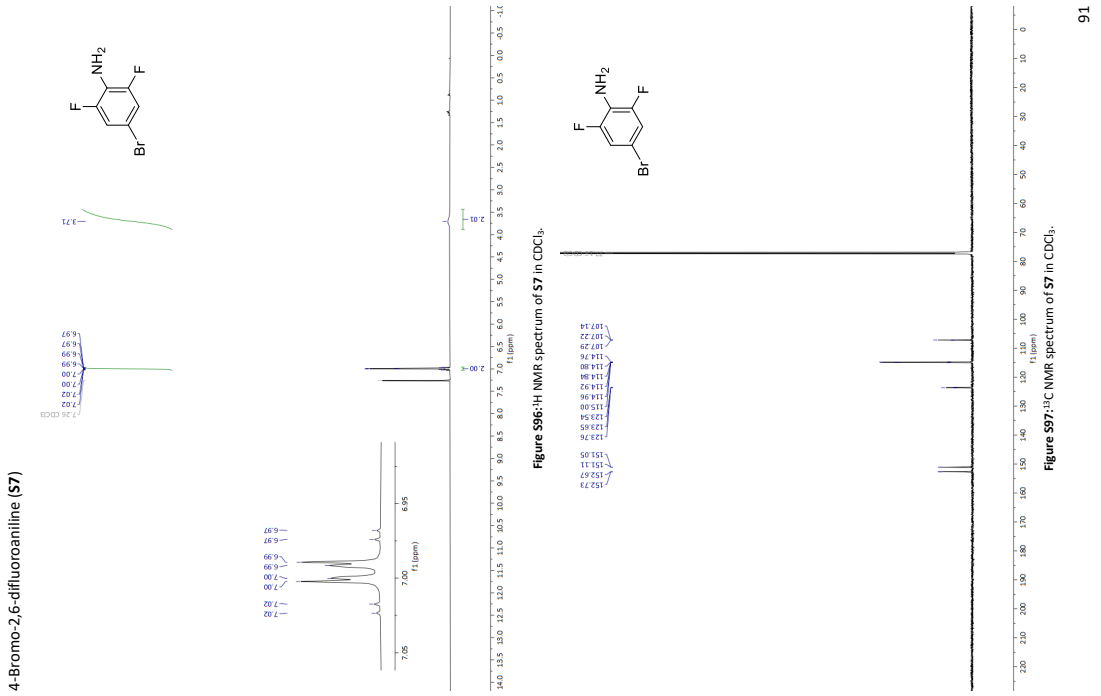

Figure S96: ^{1}H NMR spectrum of **S7** in $CDCl_3$.

Figure S97: ^{13}C NMR spectrum of **S7** in $CDCl_3$.

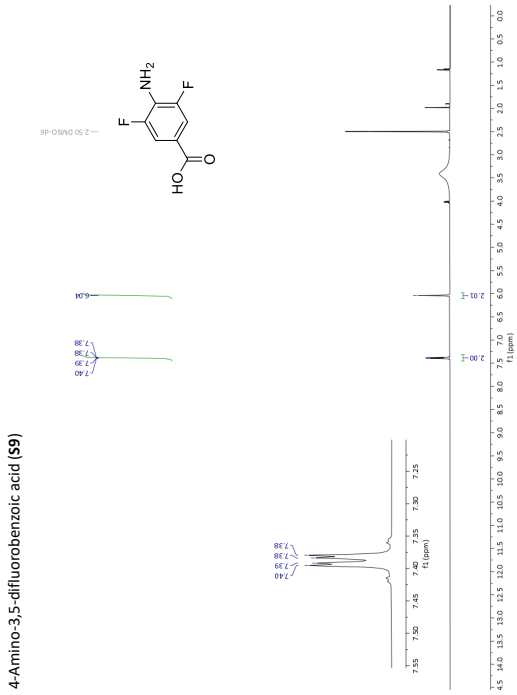

Figure S102: ^{1}H NMR spectrum of **S9** in DMSO-d_6.

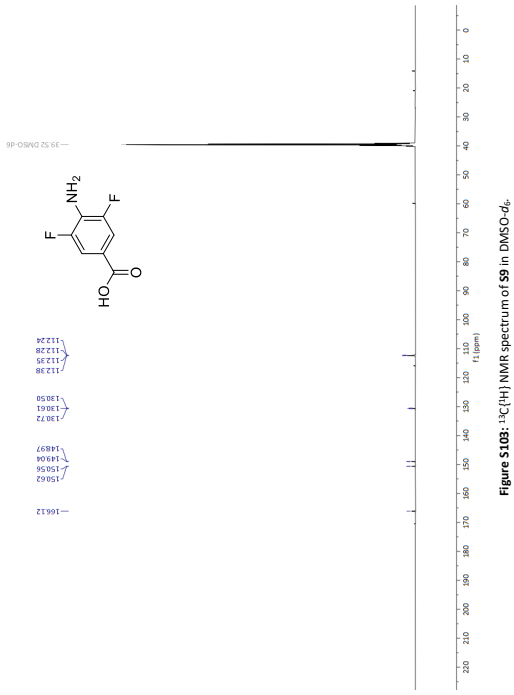

Figure S103: ^{13}C{^{1}H} NMR spectrum of **S9** in DMSO-d_6.

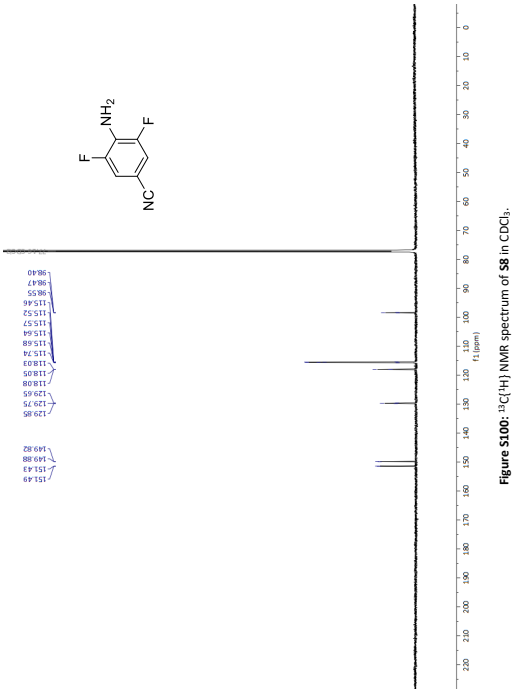

Figure S100: ^{13}C{^{1}H} NMR spectrum of **S8** in $CDCl_3$.

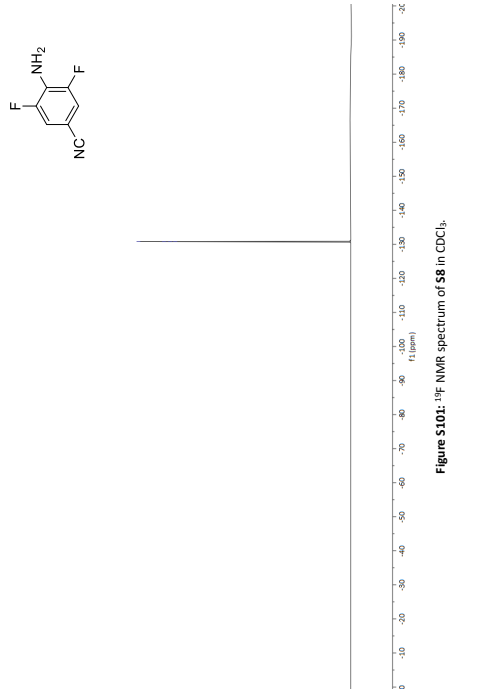

Figure S101: ^{19}F NMR spectrum of **S8** in $CDCl_3$.

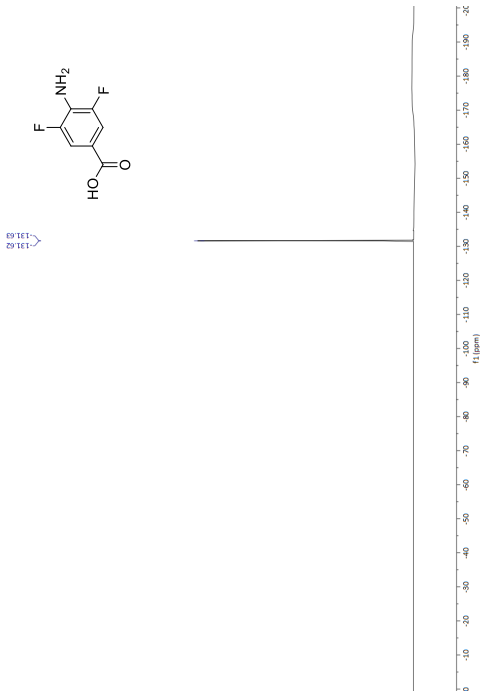

Ethyl 4-amino-3,5-difluorobenzoate (**S10**)

Figure S105: ^{1}H NMR spectrum of **S10** in $CDCl_3$.

Figure S104: ^{19}F NMR spectrum of **S9** in DMSO-d_6.

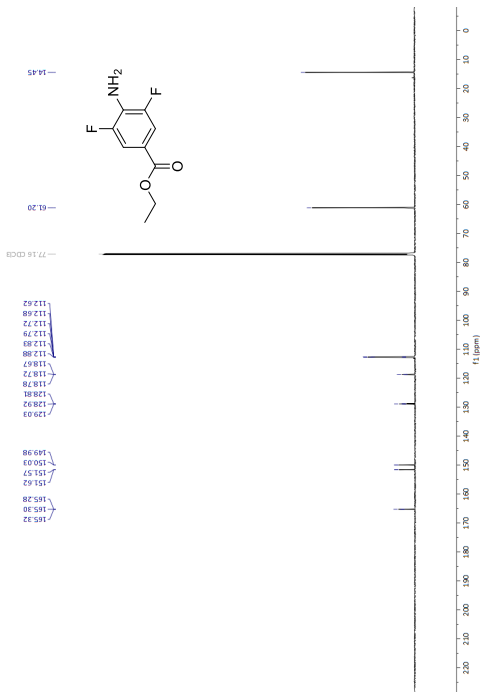

Figure S106: ^{13}C{^{1}H} NMR spectrum of **S10** in $CDCl_3$.

Figure S107: ^{19}F NMR spectrum of **S10** in $CDCl_3$.

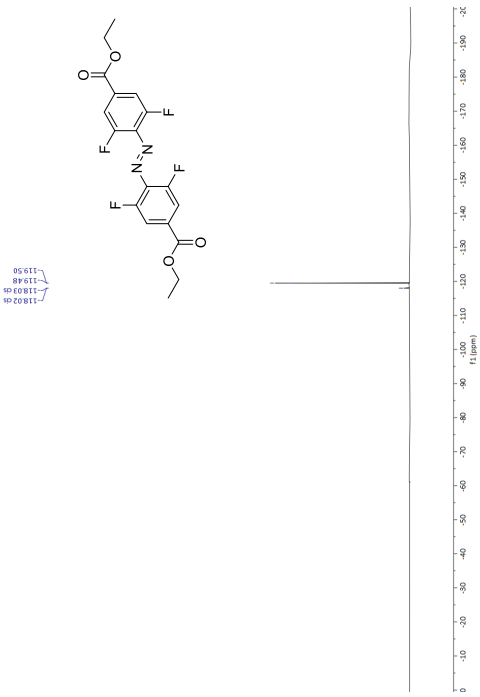

Figure S110: ^{19}F NMR spectrum of **S11** in $CDCl_3$.

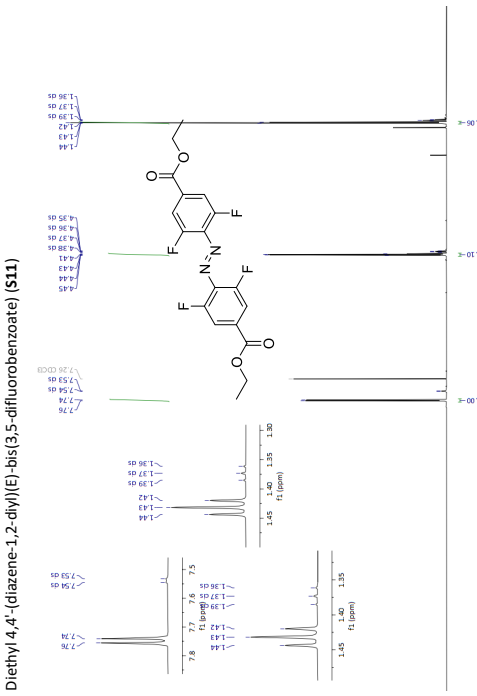

Figure S108: ^1H NMR spectrum of **S11** in $CDCl_3$.

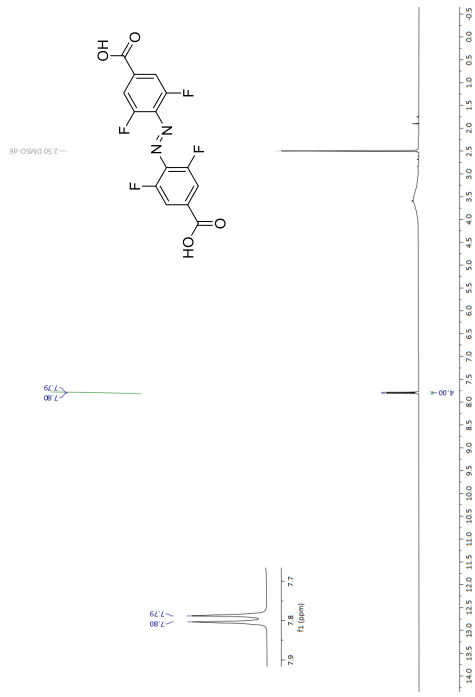

Figure S111: ^1H NMR spectrum of **6** in DMSO-d_6.

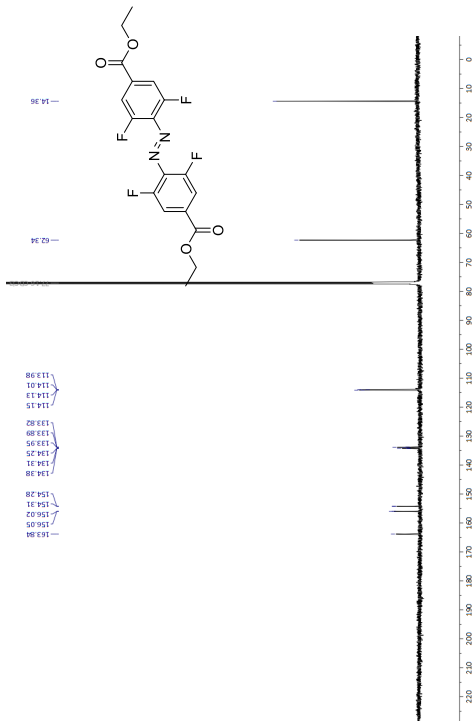

Figure S109: $^{13}C\{^1H\}$ NMR spectrum of **S11** in $CDCl_3$.

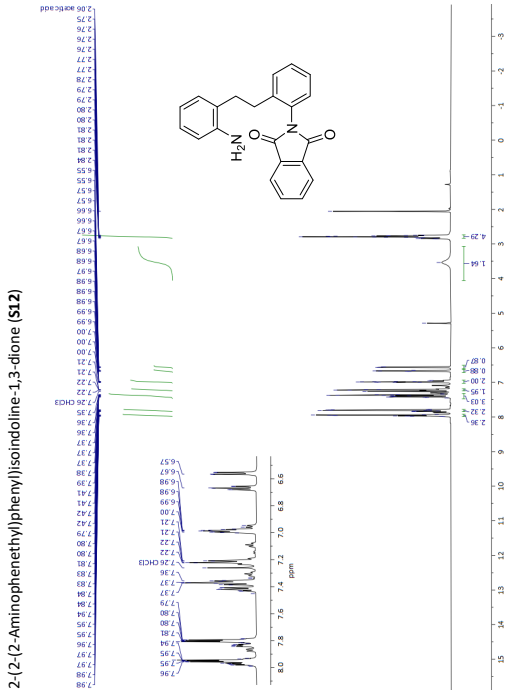

2-(2-(2-Aminophenethyl)phenyl)isoindoline-1,3-dione (**S12**)

Figure S114: ^{1}H NMR spectrum of **S12** in $CDCl_3$.

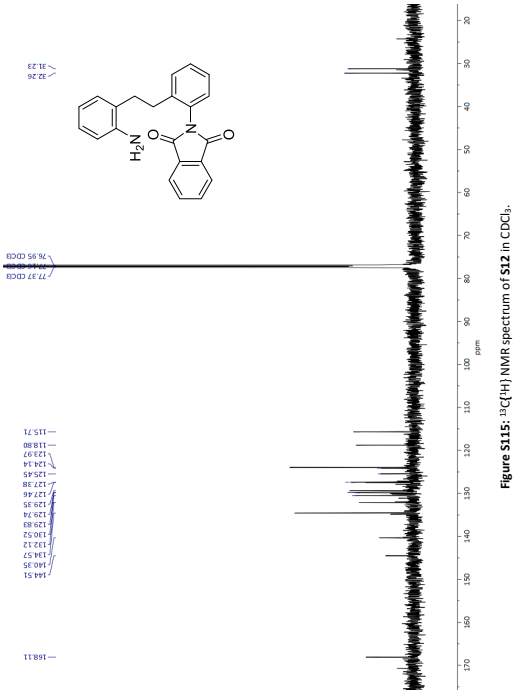

Figure S115: $^{13}C\{^1H\}$ NMR spectrum of **S12** in $CDCl_3$.

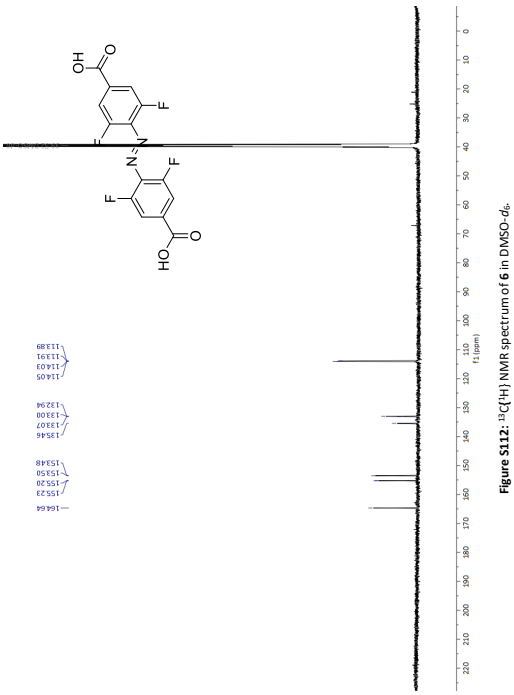

Figure S112: $^{13}C\{^1H\}$ NMR spectrum of **6** in DMSO-d_6.

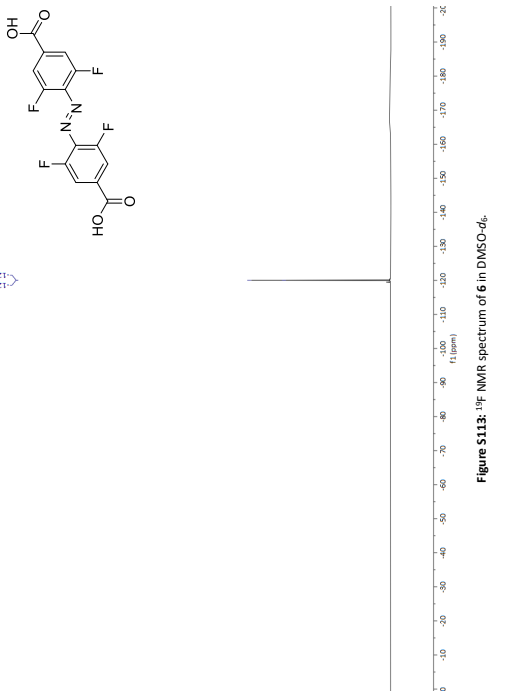

Figure S113: ^{19}F NMR spectrum of **6** in DMSO-d_6.

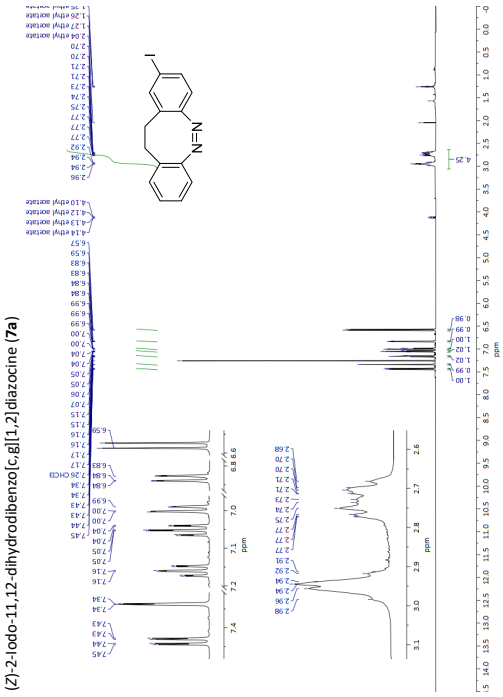

(*Z*)-2-Iodo-11,12-dihydrodibenzo[*c*,*g*][1,2]diazocine (**7a**)

Figure S118: ^{1}H NMR spectrum of **7a** in $CDCl_3$.

Figure S119: $^{13}C\{^{1}H\}$ NMR spectrum of **7a** in $CDCl_3$.

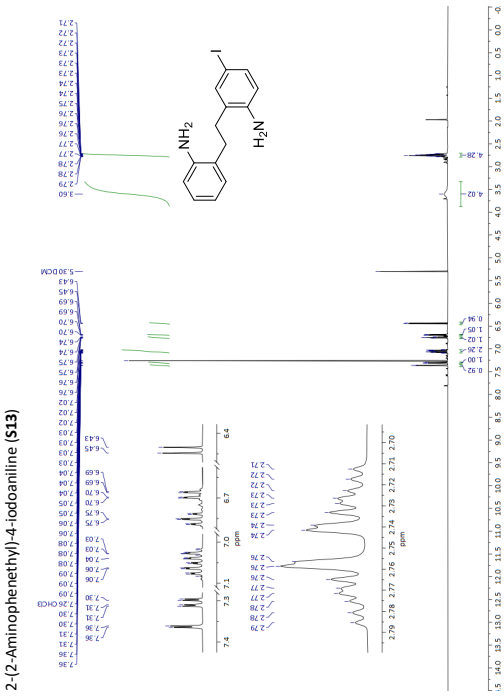

2-(2-Aminophenethyl)-4-iodoaniline (**S13**)

Figure S116: ^{1}H NMR spectrum of **S13** in $CDCl_3$.

Figure S117: $^{13}C\{^{1}H\}$ NMR spectrum of **S13** in $CDCl_3$.

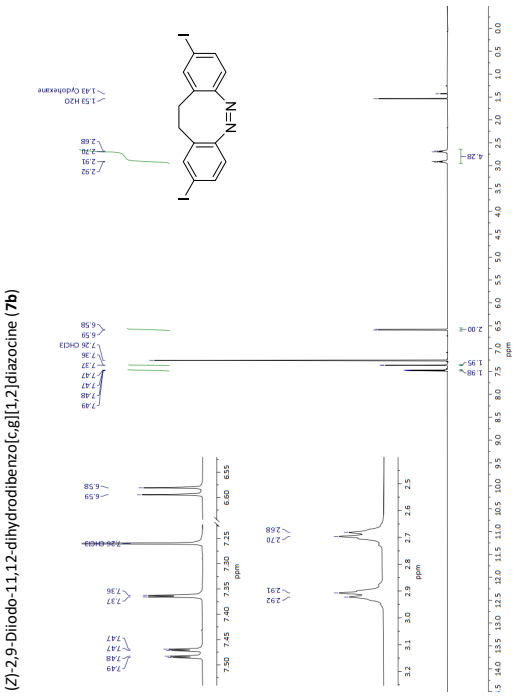

(Z)-2,9-Diiodo-11,12-dihydrodibenzo[c,g][1,2]diazocine (**7b**)

Figure S122: ^{1}H NMR spectrum of **7b** in $CDCl_3$.

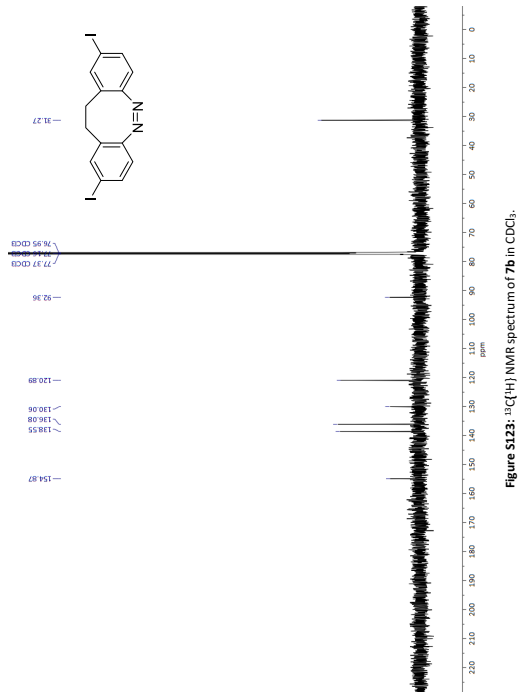

Figure S123: $^{13}C\{^{1}H\}$ NMR spectrum of **7b** in $CDCl_3$.

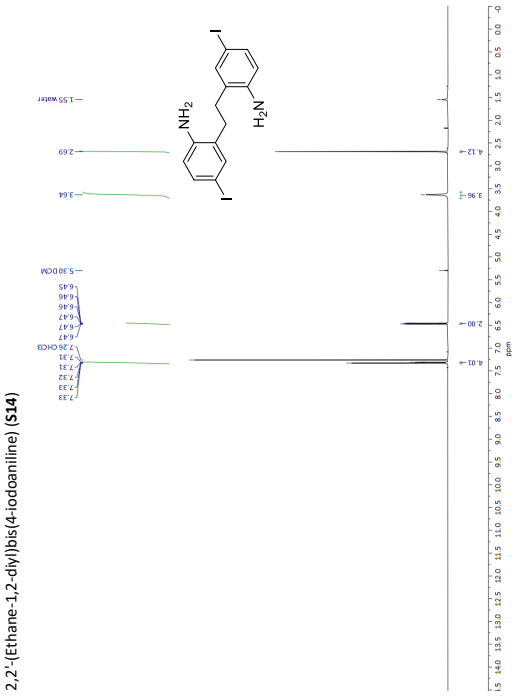

2,2'-(Ethane-1,2-diyl)bis(4-iodoaniline) (**S14**)

Figure S120: ^{1}H NMR spectrum of **S14** in $CDCl_3$.

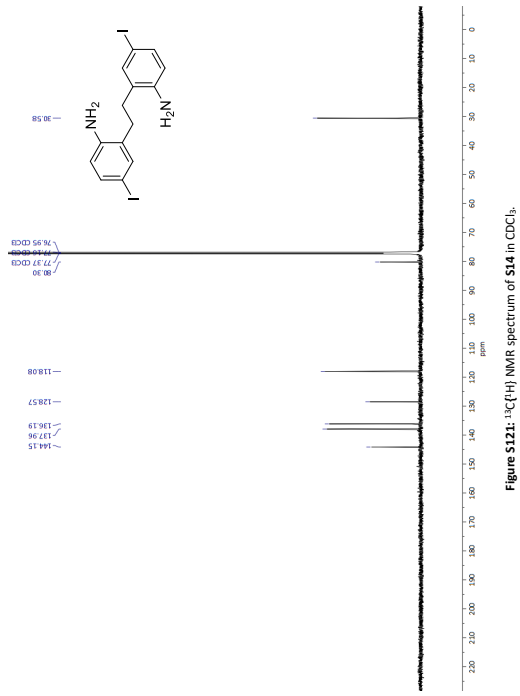

Figure S121: $^{13}C\{^{1}H\}$ NMR spectrum of **S14** in $CDCl_3$.

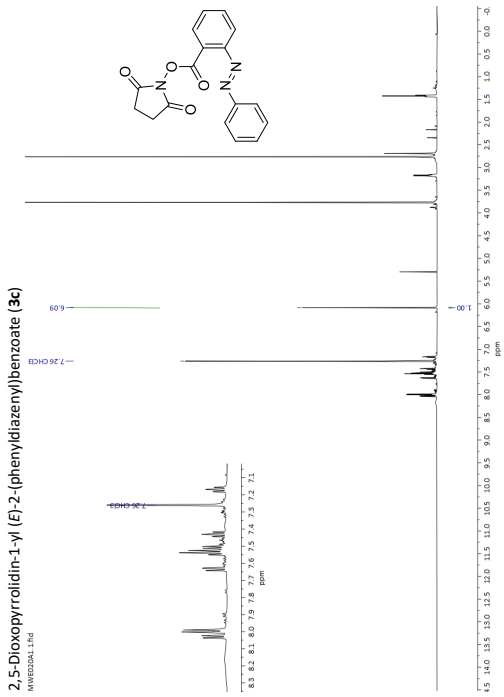

Figure S126: Crude ^{1}H NMR spectrum of **3c** in $CDCl_3$.

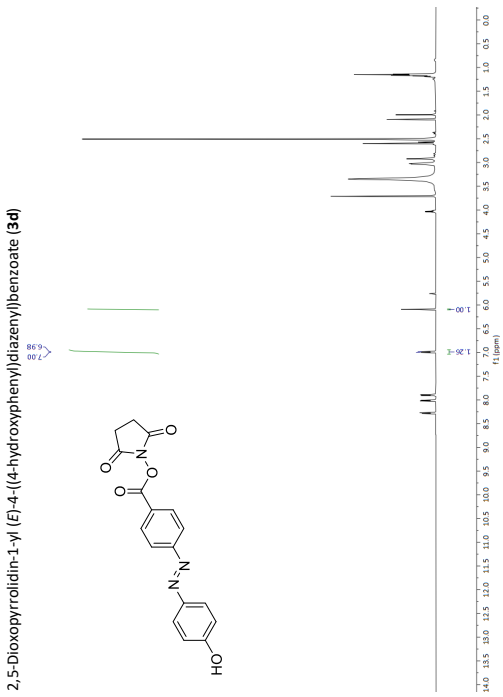

Figure S127: Crude ^{1}H NMR spectrum of **3d** in DMSO-d_6.

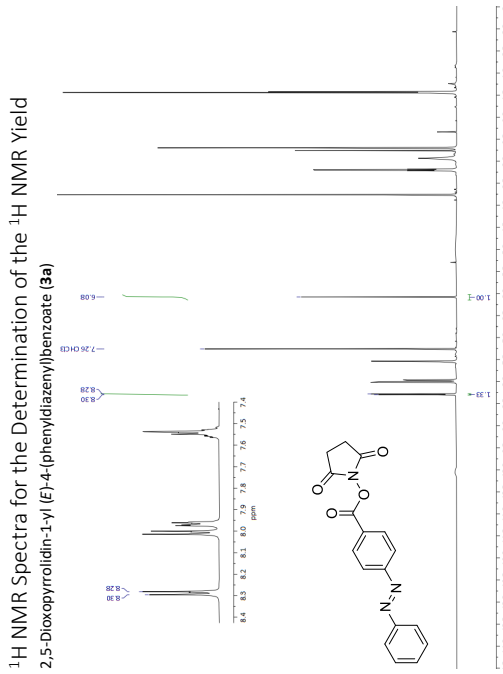

Figure S124: Crude ^{1}H NMR spectrum of **3a** in $CDCl_3$.

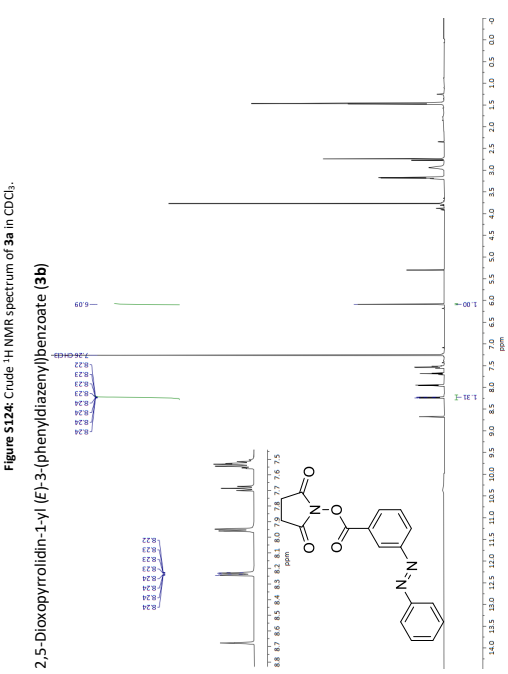

Figure S125: Crude ^{1}H NMR spectrum of **3b** in $CDCl_3$.

2,5-Dioxopyrrolidin-1-yl (*E*)-4-((4-aminophenyl)diazenyl)benzoate (**3e**)

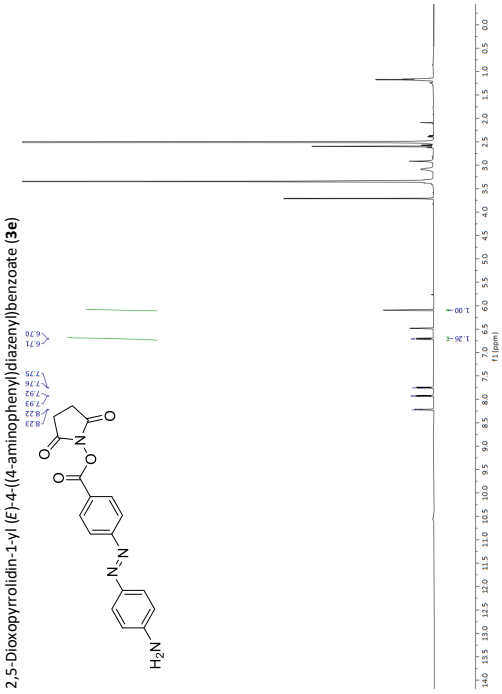

Figure S128: Crude ^{1}H NMR spectrum of **3e** in $CDCl_3$.

2,5-Dioxopyrrolidin-1-yl (*E*)-4-((4-acetamidophenyl)diazenyl)benzoate (**3f**)

Figure S129: Crude ^{1}H NMR spectrum of **3f** in $CDCl_3$.

2,5-Dioxopyrrolidin-1-yl (*E*)-4-((4-(allyloxy)phenyl)diazenyl)benzoate (**3h**)

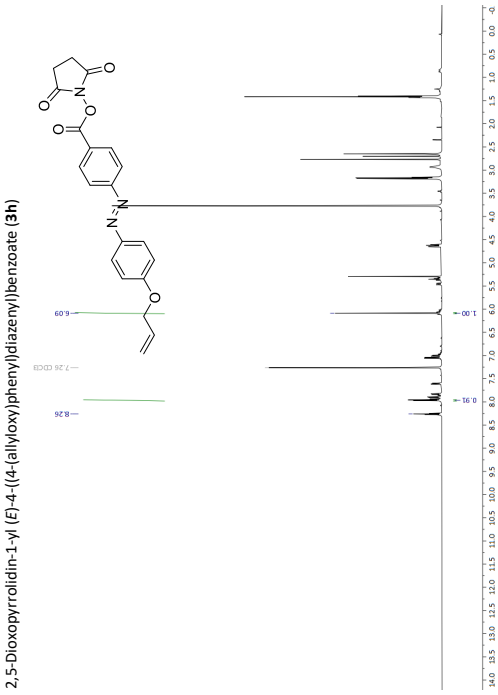

Figure S130: Crude ^{1}H NMR spectrum of **3h** in $CDCl_3$.

2,5-Dioxopyrrolidin-1-yl (*E*)-4-((4-((9-hydroxynonyl)oxy)phenyl)diazenyl)benzoate (**3i**)

Figure S131: Crude ^{1}H NMR spectrum of **3h** in $CDCl_3$.

2,5-Dioxopyrrolidin-1-yl (*E*)-4-((2,6-dimethyl-4-(nonyloxy)phenyl)diazenyl)-3,5-dimethylbenzoate (**3j**)

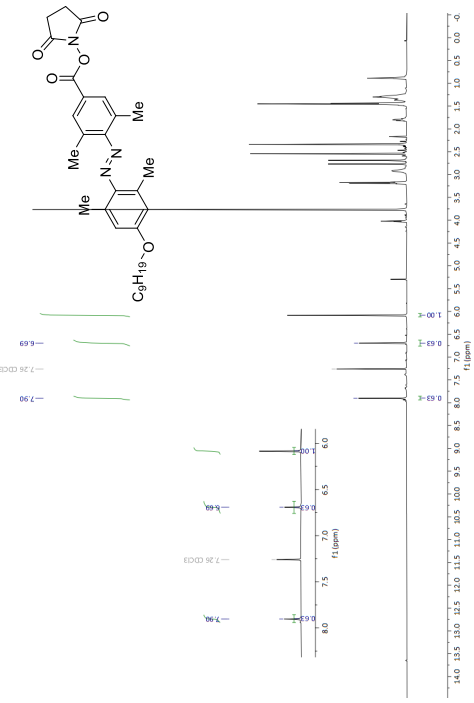

Figure S132: Crude ^{1}H NMR spectrum of **3j** in $CDCl_3$.

2,5-Dioxopyrrolidin-1-yl (*E*)-4-((2,7-bis(4-(hexyloxy)phenoxy)naphthalen-1-yl)diazenyl)-3,5-dimethylbenzoate (**3k**)

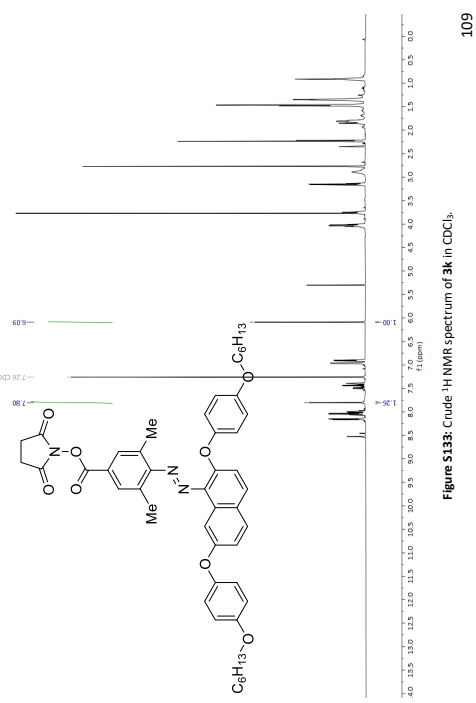

Figure S133: Crude ^{1}H NMR spectrum of **3k** in $CDCl_3$.

2,5-Dioxopyrrolidin-1-yl (*E*)-4-((4-bromophenyl)diazenyl)benzoate (**3l**)

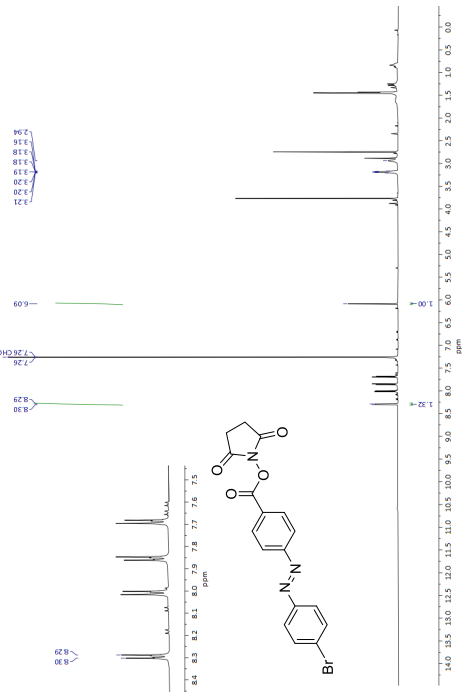

Figure S134: Crude ^{1}H NMR spectrum of **3l** in $CDCl_3$.

2,5-Dioxopyrrolidin-1-yl (*E*)-4-((3-bromophenyl)diazenyl)benzoate (**3m**)

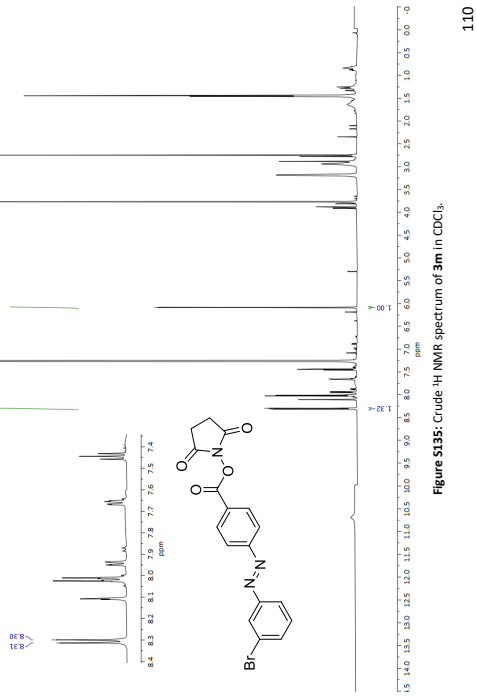

Figure S135: Crude ^{1}H NMR spectrum of **3m** in $CDCl_3$.

2,5-Dioxopyrrolidin-1-yl (*E*)-4-((4-bromophenyl)diazenyl)benzoate (**3n**)

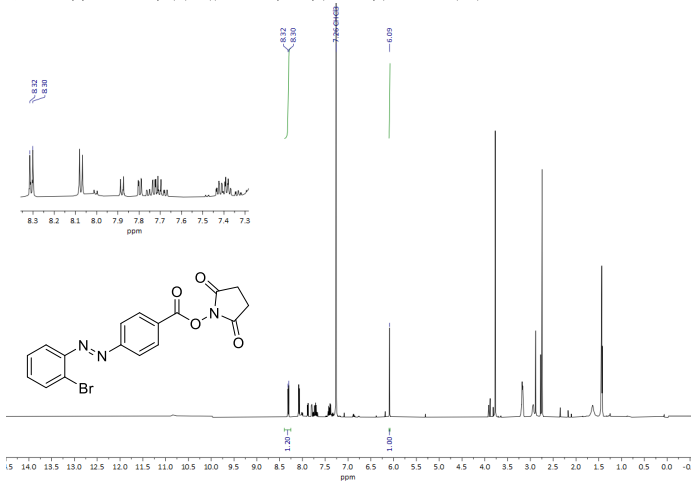

Figure S136: Crude ^{1}H NMR spectrum of **3n** in $CDCl_3$.

Bis(2,5-dioxopyrrolidin-1-yl) 4,4'-(diazene-1,2-diyl)(*E*)-dibenzoate (**5a**)

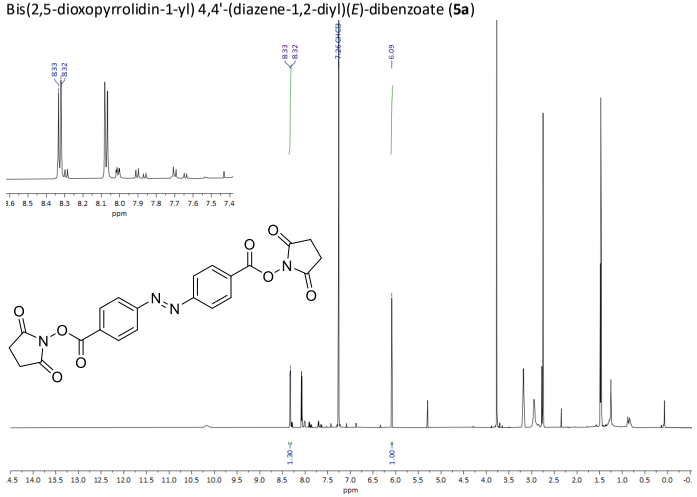

Figure S137: Crude ^{1}H NMR spectrum of **5a** in $CDCl_3$.

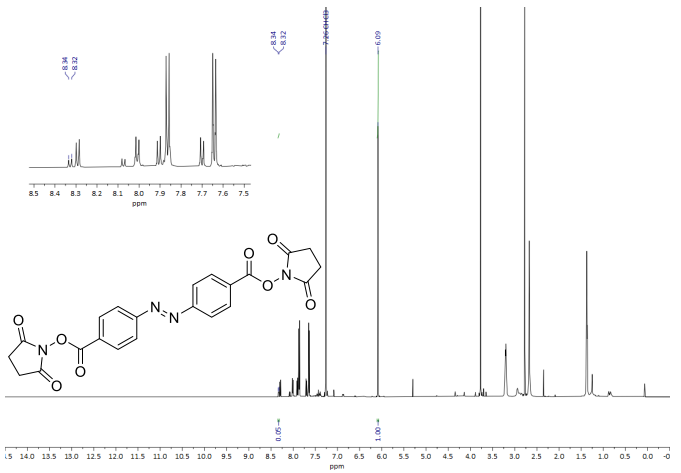

Figure S138: Crude ^{1}H NMR spectrum of **5a** in $CDCl_3$ using 1,1'-bis(diphenylphosphino)ferrocene as ligand.

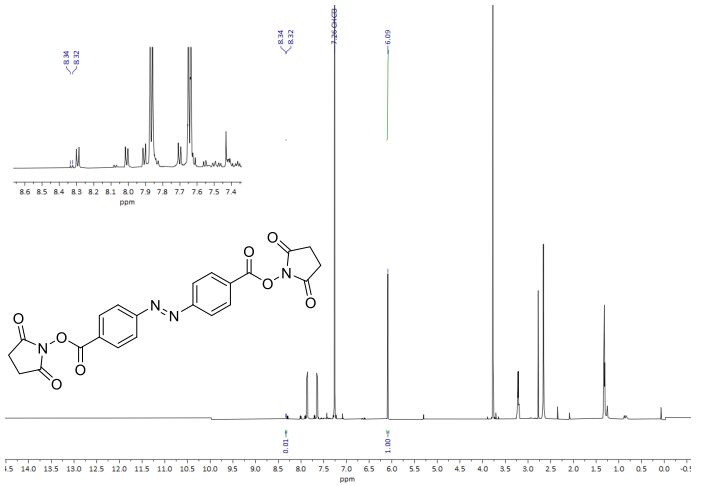

Figure S139: Crude ^{1}H NMR spectrum of **5a** in $CDCl_3$ using 2,2'-bis(diphenylphosphino)-1,1'-binaphthyl as ligand.

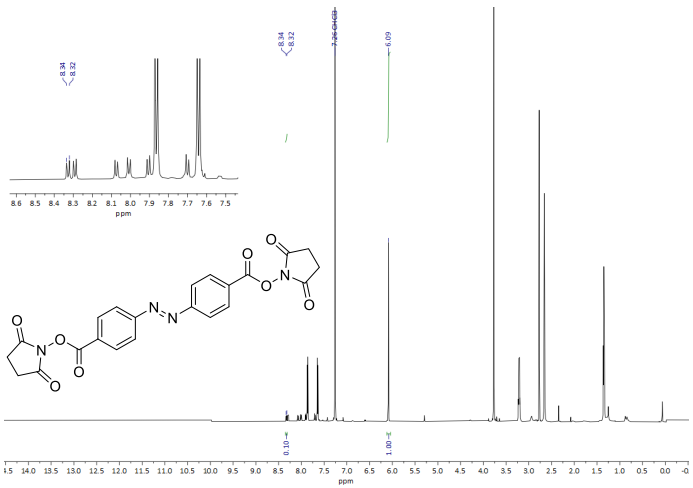

Figure S140: Crude ^{1}H NMR spectrum of **5a** in $CDCl_3$ using di-(1-adamantyl)-*n*-butylphosphine as ligand.

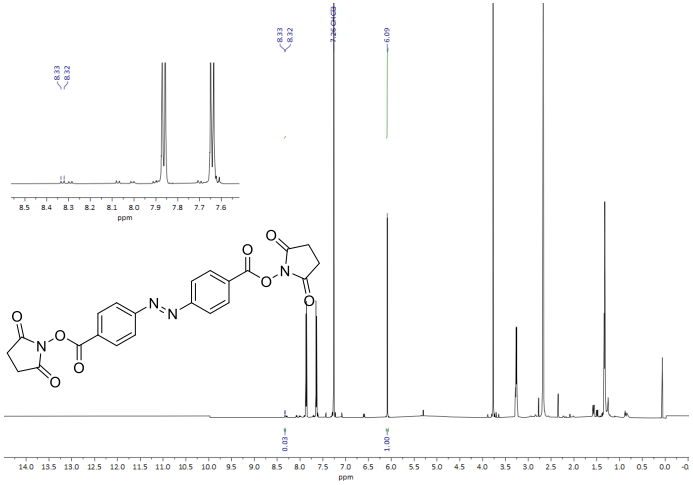

Figure S141: Crude ^{1}H NMR spectrum of **5a** in $CDCl_3$ using tri-*tert*-butylphosphine as ligand.

Bis(2,5-dioxopyrrolidin-1-yl) 4,4'-(diazene-1,2-diyl)(*E*)-bis(3,5-dimethylbenzoate) (**5b**)

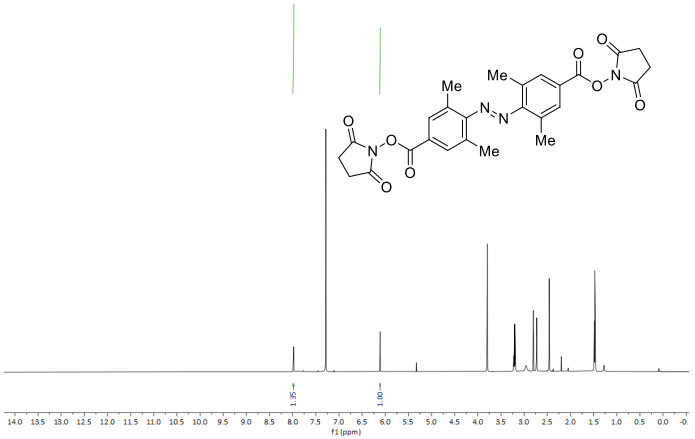

Figure S142: Crude ^{1}H NMR spectrum of **5b** in $CDCl_3$.

5.2 *ortho*-Functionalization of Azobenzenes via Hypervalent Iodine Reagents

Electronic Supplementary Material (ESI) for Chemical Communications.

Ortho-Functionalization of Azobenzenes *via* Hypervalent Iodine Reagents

Ester Maria Di Tommaso, Melanie Walther, Anne Staubitz* and Berit Olofsson*

Table of Contents

1 General Experimental Procedures 1
2 Synthesis of *ortho*-Iodoazobenzenes 1 3
3 Synthesis of *ortho*-Azobenzene-Derived Diaryliodonium Salts 3 7
3.1 Optimization Studies 7
3.2 General Procedures 10
3.3 Analytical Data 12
3.4 Scope Limitations 14
3.5 Anion Exchange with the Diaryliodonium Salt 3a 15
4 X-ray Diffraction Crystal Structure of Diaryliodonium Salt 3a 16
5 Computational details 21
5.1 Cartesian Coordinates and Energies 22
6 Investigation of the Switching Behaviour of 1a and 3a 24
6.1 ^{1}H NMR Analysis 25
6.2 UV/vis Measurements 28
7 Transition Metal-Free Arylations 32
7.1 Arylation with Oxygen Nucleophiles 32
7.2 Arylation of Sulfur Nucleophiles 37
7.3 Arylation of Carbon Nucleophiles 38
7.4 Arylation of Nitrogen Nucleophiles 38
7.5 Comparison with Literature Methods for Synthesis of Products 4-7 and 12-14 42
8 References 45
9 ^{1}H- and ^{13}C-NMR Spectra 47

1 General Experimental Procedures

Chemicals

*m*CPBA (<77 wt.%) was purchased from Sigma-Aldrich and dried under high vacuum at rt for 3 h, which was found important for the reproducibility of the reactions. The weight percent active oxidant was then determined by iodometric titration[1] and varied between 84-88% in different batches.
Unless otherwise stated, all other chemicals were purchased from commercial suppliers and used as received.

Solvents

CH_2Cl_2, TFE, Et_2O, EtOH, MeOH, cyclohexane and acetic acid were used as received. Toluene, THF, acetonitrile, and EtOAc were dried using a VAC-purification system and degassed for 30 minutes by bubbling argon through a long needle before all reactions. Anhydrous 1,4-dioxane was purchased from Acros Organics in an AcroSeal™ bottle with molecular sieves. For the reproducibility of the reactions, the purity of TFE was found crucial.

Purification and Analysis

TLC analysis was performed on pre-coated silica gel 60 F254 plates using UV light. The crude products were purified by flash column chromatography using 40-60 µm 60A silica gel as stationary phase or using automated flash system Teledyne ISCO CombiFlash Rf 200 with RediSep Rf columns.

Melting points were measured using either a STUART SMP3 and are reported uncorrected, or a Büchi Melting Point M-560 and are reported corrected. The melting point measurements refer to the solidified materials as the result of the given experimental procedures, no additional recrystallization was done.

NMR spectra were recorded on 400 MHz Bruker AVANCE II or 600 MHz Bruker Avance Neo 600 with a BBO probe at 298 K, using $CDCl_3$, DMSO-d_6, or MeOH-d_4 as solvents. Chemical shifts are given in ppm relative to the residual peak of $CDCl_3$ (^{1}H NMR δ 7.26, $^{13}C\{^{1}H\}$ NMR 77.16), DMSO-d_6 (^{1}H NMR δ 2.50, $^{13}C\{^{1}H\}$ NMR 39.52) or MeOH-d_4 (^{1}H NMR δ 3.31, $^{13}C\{^{1}H\}$ NMR 49.00) with multiplicity (s=singlet, ad= apparent doublet, d=doublet, dd=doublet of doublets, ddd= doublet of doublet of doublets, t=triplet, q=quartet, m=multiplet), integration and coupling constants (Hz). Complete analytical data is given for compounds that are novel or not fully characterized in the literature; ^{1}H NMR spectra and $^{13}C\{^{1}H\}$ NMR spectra are given for literature reported compounds.

High-resolution mass analyses were obtained using a Bruker microTOF ESI. High-resolution EI mass spectra were recorded on a Finnigan MAT 95XL double-focusing mass spectrometer at an ionization energy of 70 eV. Samples were measured by a direct inlet method with a source temperature of 200 C. High-resolution APCI mass spectra were measured by a direct inlet method on a Bruker Impact II mass spectrometer.

Single crystals were measured on a Bruker APEX-II CCD diffractometer. The crystal was kept at 100 K during data collection. Using Olex2,[2] the structure was solved with the XT[3] structure solution program using Intrinsic Phasing and refined with the SHELXL[4] refinement package using Least Squares minimisation.

UV light illuminations were carried out using an array of three Seoul CUD4AF1B LEDs (340 nm with an optical performance of 55mW each), assembled by Sahlmann Photochemical Solutions. Illuminations with visible light were carried out using one Luxeon LXML-PX01 LED (450 nm with an optical performance of 900mW), assembled by Sahlmann Photochemical solutions. The distance between LED and sample was 1 cm.

UV spectra were recorded at 25 °C with a resolution of 0.5 nm using a UV-2700 spectrometer from Shimadzu with a double monochromator in $CHCl_3$ (spectroscopy grade). High precision quartz cuvettes with a light path length of 10 mm from Hellma Analytics were used. For analyzing the photostationary equilibrium *via* ^{1}H NMR spectroscopy, quartz NMR tubes from Deutero were used.

2 Synthesis of *ortho*-Iodoazobenzenes 1

(*E*)-1-(2-Iodophenyl)-2-phenyldiazene (1a)

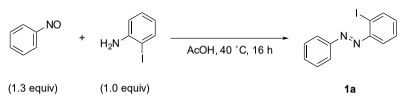

Following a reported procedure,[5] a solution of 2-iodoaniline (1.0 equiv, 65.0 mmol, 14.2 g) and nitrosobenzene (1.3 equiv, 84.5 mmol, 9.05 g) in acetic acid (400 mL) was stirred for 16 h at 40 °C. The solvent was evaporated, and the residue crystallized from MeOH at 65 °C to yield azobenzene **1a** as a red solid (8.32 g, 27.0 mmol, 42%).

Mp: 63 °C. ^{1}H-NMR (600 MHz, $CDCl_3$) δ 8.04 (dd, *J* = 7.9, 1.3 Hz, 1H), 8.02 – 7.99 (m, 2H), 7.64 (dd, *J* = 8.0, 1.6 Hz, 1H), 7.56 – 7.49 (m, 3H), 7.43 (ddd, *J* = 8.0, 7.2, 1.3 Hz, 1H), 7.17 (ddd, *J* = 7.9, 7.2, 1.6 Hz, 1H). ^{13}C-NMR (151 MHz, $CDCl_3$) δ 152.5, 151.5, 140.0, 132.3, 131.7, 129.3, 129.1, 123.7, 117.5, 102.6. HRMS(ESI) m/z: calcd. for $C_{12}H_9IN_2^+$ $[M]^+$ 307.9805; found 307.9805 (71), 77.0 (100). Analytical data were in accordance with those previously reported.[5]

(*E*)-1-(4-Bromophenyl)-2-(2-iodophenyl)diazene (1b)

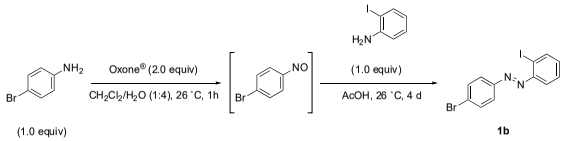

Following a reported procedure,[5] 4-bromoaniline (1.0 equiv, 12.0 g, 70.0 mmol) was dissolved in CH_2Cl_2 (150 mL). Oxone® (2.0 equiv, 86.1 g, 150 mmol) dissolved in water (600 mL) was added to this solution. The reaction mixture was stirred for 3 h at 26 °C under a nitrogen atmosphere, upon which the colour of the solution turned to green. After separation of the layers, the aqueous layer was extracted with DCM (3 × 200 mL). The combined organic layers were washed with 1 N HCl (300 mL), saturated $NaHCO_3$ solution (300 mL), water (300 mL), brine (300 mL) and dried over magnesium sulfate. The organic phase was filtered and concentrated under reduced pressure yielding the corresponding labile nitroso-arene, which was submitted to the next condensation step without further purification. The nitroso-arene (1.0 equiv, 11.9 g, 64.0 mmol) and 2-iodoaniline (1.0 equiv, 14.0 g, 64.0 mmol) were dissolved in acetic acid (200 mL) and stirred for 4 d at 26 °C. The formed precipitate was separated by filtration. The collected solid was washed with acetic acid (100 mL) and dried under reduced pressure to yield azobenzene **1b** as an orange solid (15.3 g, 39.4 mmol, 62%).

Mp: 116 °C. ^{1}H-NMR (600 MHz, $CDCl_3$) δ 8.04 (dd, *J* = 7.9, 1.3 Hz, 1H), 7.87 (d, *J* = 8.8 Hz, 2H), 7.67 (d, *J* = 8.8 Hz, 2H), 7.64 (dd, *J* = 8.0, 1.6 Hz, 1H), 7.43 (ddd, *J* = 8.0, 7.2, 1.3 Hz, 1H), 7.18 (ddd, *J* = 7.9, 7.2, 1.6 Hz, 1H). ^{13}C-NMR (151 MHz, $CDCl_3$) δ 151.3, 151.2, 140.1, 132.7, 132.6, 129.1, 126.3, 125.1, 117.4, 103.0. HRMS(ESI) m/z: calcd. for $C_{12}H_8BrIN_2^+$ $[M]^+$ 385.8910; found 385.8914 (44), 76.0 (100). Analytical data were in accordance with those previously reported.[6]

(*E*)-1-(2-Iodophenyl)-2-(*p*-tolyl)diazene (1c)

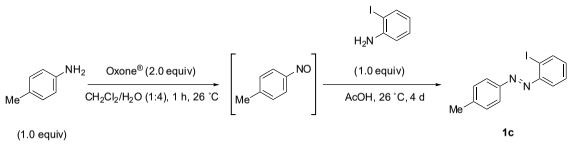

(1.0 equiv) **1c**

Following a reported procedure,[5] *p*-toluidine (1.0 equiv, 3.75 g, 35.0 mmol) was dissolved in CH_2Cl_2 (75 mL). Oxone® (2.0 equiv, 43.1 g, 70.0 mmol) dissolved in water (300 mL) was added to this solution. The reaction mixture was stirred for 1 h at 26 °C under a nitrogen atmosphere, upon which the colour of the solution turned to green. The layers were separated, and the organic phase was concentrated under reduced pressure yielding the corresponding labile nitroso-arene, which was submitted to the next condensation step without further purification. The nitroso-arene (1.0 equiv, 1.14 g, 9.41 mmol) and 2-iodoaniline (1.0 equiv, 2.06 g, 9.41 mmol) were dissolved in acetic acid (200 mL) and stirred for 15 h at 85 °C. After cooling down, the solvent was removed under reduced pressure and the residue was purified by column chromatography on silica (eluent: cyclohexane) to yield azobenzene **1c** as a red solid (906 mg, 2.81 mmol, 30%).

Mp: 80 °C. ^{1}H-NMR (600 MHz, $CDCl_3$) δ 8.02 (dd, *J* = 7.9, 1.3 Hz, 1H), 7.91 (d, *J* = 8.3 Hz, 2H), 7.63 (dd, *J* = 8.0, 1.6 Hz, 1H), 7.42 (ddd, *J* = 8.0, 7.2, 1.3 Hz, 1H), 7.33 (d, *J* = 8.3 Hz, 2H), 7.15 (ddd, *J* = 7.9, 7.2, 1.6 Hz, 1H), 2.45 (s, 3H). ^{13}C-NMR (151 MHz, $CDCl_3$) δ 151.5, 150.7, 142.4, 139.9, 132.0, 130.0, 129.0, 123.7, 117.5, 102.4, 21.7. HRMS(ESI) m/z: calcd. for $C_{13}H_{11}IN_2^+$ $[M]^+$ 321.9961; found 321.9963 (33), 91.0 (100). Analytical data were in accordance with those previously reported.[5]

(*E*)-1-(2-Iodo-4-methylphenyl)-2-phenyldiazene (1d)

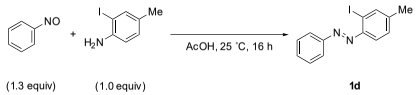

(1.3 equiv) (1.0 equiv) **1d**

Following a reported procedure,[5] A solution of 2-iodo-4-methylaniline (1.0 equiv, 25.0 mmol, 6.23 g) and nitrosobenzene (1.3 equiv, 32.5 mmol, 3.48 g) in acetic acid (400 mL) was stirred for 16 h at 25 °C. The solvent was evaporated, and the residue recrystallized from MeOH at 65 °C to yield azobenzene **1d** as a red solid (7.02 g, 20.8 mmol, 83%).

Mp: 56 °C. ^{1}H-NMR (600 MHz, $CDCl_3$) δ 8.00 – 7.96 (m, 2H), 7.87 (ad, *J* = 1.0 Hz, 1H), 7.57 (d, *J* = 8.2 Hz, 1H), 7.55 – 7.51 (m, 2H), 7.50 – 7.47 (m, 1H), 7.23 (dd, *J* = 8.2, 1.0 Hz, 1H), 2.39 (s, 3H). ^{13}C-NMR (151 MHz, $CDCl_3$) δ 152.5, 149.4, 143.3, 140.3, 131.4, 129.9, 129.3, 123.6, 117.0, 103.4, 21.0. HRMS(ESI) m/z: calcd. for $C_{13}H_{11}IN_2^+$ $[M]^+$ 307.9805; found 321.9963 (67), 77.0 (100). Analytical data were in accordance with those previously reported.[7]

(*E*)-1,2-Bis(2-iodophenyl)diazene (1e)

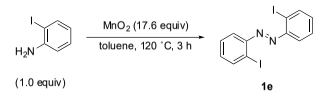

(1.0 equiv) **1e**

Following a reported procedure,[8] a solution of 2-iodoaniline (1.0 equiv, 45.7 mmol, 10.0 g) and activated manganese dioxide (17.6 equiv, 805 mmol, 70.0 g) in toluene (400 mL) was stirred for 3 h at 120 °C. The warm reaction mixture was filtered through silica and washed with toluene (400 mL). The solvent was evaporated yield azobenzene **1e** as a red solid (7.77 g, 17.9 mmol, 78%).

Mp: 141 °C. ^{1}H-NMR (600 MHz, $CDCl_3$) δ 8.04 (dd, *J* = 7.9, 1.3 Hz, 2H), 7.77 (dd, *J* = 8.0, 1.6 Hz, 2H), 7.46 (ddd, *J* = 8.0, 7.3, 1.3 Hz, 2H), 7.20 (ddd, *J* = 7.9, 7.3, 1.6 Hz, 2H). ^{13}C-NMR(151 MHz, $CDCl_3$) δ 151.0, 140.1, 132.9, 129.2, 118.4, 103.4 HRMS(APCI) m/z: calcd. for $[C_{12}H_8I_2N_2 + H]^+$ $[M + H]^+$ 434.8849; found 434.8845 (100). Analytical data were in accordance with those previously reported.[8]

(*E*)-1-(2-Iodophenyl)-2-(4-iodophenyl)diazene (1f)

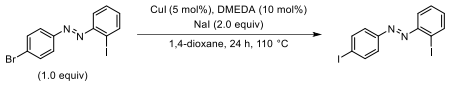

(1.0 equiv) **1b** **1f**

Under inert conditions, azobenzene **1b** (1.0 equiv, 38.8 mg, 100 µmol), copper iodide (5 mol%, 1.0 mg, 5.25 µmol), sodium iodide (2.0 equiv, 30.0 mg, 200 µmol) and *N,N'*-dimethylethylenediamine (10 mol%, 1.08 µL, 10.0 µmol) were dissolved in dry 1,4-dioxane (1 mL) in a high pressure tube. The reaction mixture was stirred for 24 h at 110 °C. The resulting suspension was allowed to reach 22 °C, diluted with $NaHCO_3$ solution (10 mL), poured into water (10 mL), and extracted with dichloromethane (3 × 15 mL). The combined organic phases were dried over magnesium sulfate, filtered and concentrated yielding azobenzene **1f** as an orange solid (38.3 mg, 88.2 µmol) in 88% yield.

Mp: 114 °C. ^{1}H NMR (600 MHz, $CDCl_3$) δ 8.03 (dd, *J* = 7.9, 1.3 Hz, 1H), 7.89 (d, *J* = 8.6 Hz, 2H), 7.72 (d, *J* = 8.6 Hz, 2H), 7.63 (dd, *J* = 8.0, 1.6 Hz, 1H), 7.43 (ddd, *J* = 8.0, 7.2, 1.3 Hz, 1H), 7.18 (ddd, *J* = 7.9, 7.2, 1.6 Hz, 1H). ^{13}C NMR (151 MHz, $CDCl_3$) δ 151.7, 151.2, 140.1, 138.6, 132.7, 129.1, 125.2, 117.4, 103.0, 98.7. HRMS(EI) m/z: calcd. for $C_{12}H_8I_2N_2^+$ $[M]^+$ 433.8771; found 433.8776. Analytical data were in accordance with those previously reported.[9]

(*E*)-1-(2,6-Diiodophenyl)-2-(4-methoxyphenyl)diazene (1g)

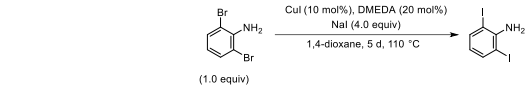

Under inert conditions, 2,6-dibromoaniline (1.0 equiv, 3.76 g, 15.0 mmol), copper iodide (10 mol%, 286 mg, 1.50 mmol), sodium iodide (4.0 equiv, 8.99 g, 60.0 mmol) and *N,N'*-dimethylethylenediamine (20 mol%, 323 µL, 3.00 mmol) were dissolved in dry 1,4-dioxane (75 mL) in a high pressure tube. The reaction mixture was stirred for 5 d at 110 °C. The resulting suspension was allowed to reach 22 °C, diluted with $NaHCO_3$ solution (50 mL), poured into water (50 mL), and extracted with dichloromethane (3 × 100 mL). The combined organic phases were dried over magnesium sulfate, filtered and concentrated yielding the product as a beige solid (5.04 g, 14.6 mol) in 98% yield.

Mp: 121 °C. ^{1}H NMR (600 MHz, $CDCl_3$) δ 7.62 (d, *J* = 7.8 Hz, 2H), 6.16 (t, *J* = 7.8 Hz, 1H), 4.61 (s, br, 2H). ^{13}C NMR (151 MHz, $CDCl_3$) δ 146.2, 139.5, 121.4, 81.7. HRMS(EI) m/z: calcd. for $C_6H_5I_2N^+$ $[M]^+$ 344.8506; found 344.8503.

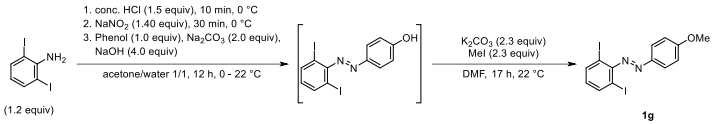

2,6-Diiodoaniline (1.2 equiv, 1.62 g, 4.70 mmol) was dissolved in a mixture of acetone/water (1:1, 20 mL) and cooled to 0 °C. Subsequently, conc. HCl (1.5 equiv, 5.88 mmol, 488 µL) was added dropwise to the solution and left to stir for another 10 min. Sodium nitrite (1.4 equiv, 37.8 mg, 5.48 mmol) dissolved in water (4 mL) was added dropwise and the reaction mixture was stirred for 30 min. Meanwhile, phenol (1.0 equiv, 369 mg, 3.91 mmol), Na_2CO_3 (2.0 equiv, 830 mg, 7.82 mmol) and NaOH (4.0 equiv, 626 mg, 15.7 mmol) were dissolved in acetone/water (1:1, 20 mL) and the obtained solution was cooled to 0 °C. The first prepared solution was slowly added to the solution containing the phenol over the course of 5 min. The resulting mixture was stirred for 12 h while slowly warmed to 21 °C. Subsequently, the mixture was diluted with an aqueous HCl solution (1 N, 30 mL) and extracted with ethyl acetate (3 × 30 mL). The combined organic phases were dried over magnesium sulfate, filtered and concentrated under reduced pressure. The obtained crude azobenzene (1.0 equiv, 1.76 g, 3.91 mmol), potassium carbonate (2.3 equiv, 1.24 g, 8.99 mmol) and iodomethane (2.3 equiv, 1.28 g, 560 µL, 8.99 mmol) were dissolved in DMF (10 mL) and stirred at 25 °C for 21 h. Water (100 mL) was added and the mixture was extracted with ethyl acetate (3 × 100 mL). The combined organic phases were washed with an aqueous HCl solution (1 N, 100 mL), an aqueous $NaHCO_3$ solution (1 N, 100 mL), brine (100 mL), dried over magnesium sulfate and filtered. The solvent was removed under reduced pressure and the residue was purified by recrystallization from MeOH at 78 °C yielding azobenzene **1g** as a red solid (1.79 g, 3.80 mmol) in 97% yield.

Mp: 98 °C. ^{1}H NMR (600 MHz, $CDCl_3$) δ 8.02 (d, *J* = 9.0 Hz, 2H), 7.92 (d, *J* = 7.9 Hz, 2H), 7.07 (d, *J* = 9.0 Hz, 2H), 6.71 (t, *J* = 7.9 Hz, 1H), 3.92 (s, 3H). ^{13}C NMR (151 MHz, $CDCl_3$) δ 163.4, 153.7, 145.7, 140.2, 130.2, 125.6, 114.6, 88.0, 55.9. HRMS(EI) m/z: calcd. for $C_{13}H_{10}I_2N_2O^+$ $[M]^+$ 463.8877; found 463.8875.

3 Synthesis of *ortho*-Azobenzene-Derived Diaryliodonium Salts 3

3.1 Optimization Studies

Initial screening of suitable conditions for the synthesis of diaryliodonium salts **3** from *ortho*-iodoazobenzene **1a** was performed. Our standard one-pot method[10] with *m*CPBA and triflic acid failed in delivering the diaryliodonium triflate **3a'**, as shown in **Scheme S1a**. Increasing the equivalents of TfOH (to 15 equiv) did not provide the desired product. In addition, our one-pot procedure[11] with arylboronic acid using $BF_3{\cdot}OEt_2$ failed, and product **3a''** could not be obtained (**Scheme S1b**). In both one-pot procedures, the unreacted *ortho*-iodoazobenzene **1a** and its decomposition to the unsubstituted azobenzene was detected by ^{1}H NMR spectroscopy of the crude mixture. Increasing the amount of triflic acid from 1.0 equiv to 15.0 equiv led to further decomposition: A black mixture was obtained and many side products were observed by ^{1}H NMR spectroscopy.

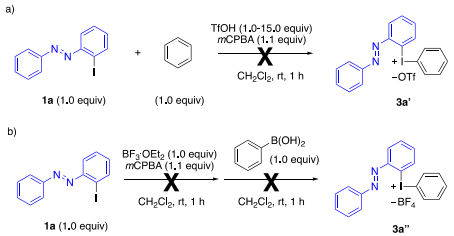

Scheme S1. One-pot synthesis from *ortho*-iodoazobenzene **1a** with a) benzene, TfOH and *m*CPBA; b) $BF_3{\cdot}OEt_2$, *m*CPBA, and arylboronic acid.

Further investigations focused on stepwise synthesis of reagents **3** through isolation of the corresponding Koser's reagents **21**.[12] Under literature conditions,[12-13] compound **21a** could be obtained in 68% yield (**Table S1**, entry 1). When TFE was used as the co-solvent, the product could not be detected (entry 2). Repeating the reaction at 0.5 mmol scale, product **21a** was isolated in 64% yield (entry 3), and further increased scale resulted in excellent yields of **21a** (entries 4, 5). Moreover, the reaction was performed with *p*-bromo-substituted azobenzene **1b** and product **21b** could be obtained in good yield of 88% (entry 6).

Table S1. Reaction conditions used for the synthesis of Koser's reagent **21**. [a] Isolated yield.

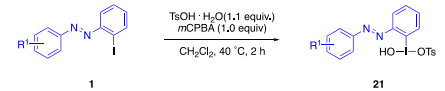

Entry	*n* (mmol)	R^1	Solvent	*T* (°C)	*t* (h)	Yield (%)[a]
1	0.30	H	CH_2Cl_2 (0.2 M)	40	2	**21a** 68
2	0.20	H	CH_2Cl_2/TFE (1:1)	40	2	-
3	0.50	H	CH_2Cl_2 (0.2 M)	40	2	**21a** 64
4	1.00	H	CH_2Cl_2 (0.2 M)	40	2	**21a** 92
5	2.00	H	CH_2Cl_2 (0.2 M)	40	2	**21a** 98
6	1.00	*p*-Br	CH_2Cl_2 (0.2 M)	40	2	**21b** 88

A small optimization was performed for the second step, where anisole (**2a**) was added to the Koser's reagent **21a**. With the idea of performing a sequential one-pot procedure, CH_2Cl_2 was used as the solvent of the reaction, which provided product **3a** in 67% yield (**Table S2**, entry 1). Next, TFE was added as the co-solvent in a ratio of 1:1 with CH_2Cl_2 and **3a** was obtained in good yield of 83% yield (entry 2). The diaryliodonium salt **3a** could also be obtained in 85% yield on a larger scale (entry 3). In entry 4, the product was isolated in lower yield (55%) compared to entry 3. We noticed a loss of product **3a** during the precipitation, and a detailed procedure for this step is described in **Section 3.2**. Finally, these conditions worked well in the case of *p*-bromo-substituted reagent **21b** delivering product **3b** in 90% yield (entry 5).

Table S2. Reaction conditions used for the synthesis of diaryliodonium salt **3**. [a] Isolated yield.

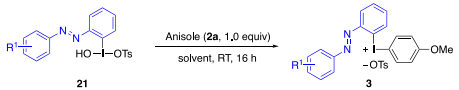

21 3

Entry	*n* (mmol)	R^1	Solvent	*T* (°C)	*t* (h)	Yield (%)[a]
1	0.10	H	CH_2Cl_2	rt	16	**3a** 67
2	0.30	H	CH_2Cl_2/TFE (1:1)	rt	16	**3a** 83
3	1.80	H	CH_2Cl_2/TFE (1:1)	rt	16	**3a** 85
4	1.80	H	CH_2Cl_2/TFE (1:1)	rt	16	**3a** 55
5	0.60	*p*-Br	CH_2Cl_2/TFE (1:1)	rt	16	**3b** 90

Finally, a sequential one-pot procedure was developed,[12-14] with in situ formation of Koser's reagent **21** followed by addition of the arene **2a**. Surprisingly, salt **3a** could be isolated in 84% yield (**Table S3**, entry 1) as described in **Section 3.2**. To prove the strength of the sequential one-pot procedure, reactions were also performed on a large scale (2.0 and 3.2 mmol scale, entry 2 and 3), and the product **3a** could be successfully isolated in good yields of 89% and 77% respectively. The sequential one-pot procedure was also successful in case of EWG and EDG substituents. Indeed, on a larger scale, salt **3b** having *para*-bromine substituent was obtained in 71% yield and 84% yield (entry 4 and 5). Even salt **3d** could be isolated in good yield of 76% (entry 6), and 88% yield was obtained when the reaction scale was increased to 1.0 mmol scale (entry 7).

Table S3. A sequential one-pot procedure for the synthesis of diaryliodonium salt **3**. [a] Isolated yield.

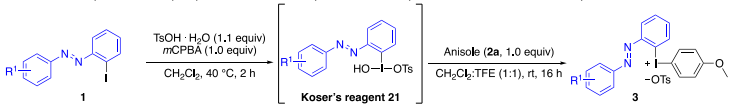

1 3

Entry	*n* (mmol)	R^1	Yield (%)[a]
1	1.00	H	**3a** 84
2	2.00	H	**3a** 89
3	3.20	H	**3a** 77
4	0.20	*p*-Br	**3b** 71
5	1.00	*p*-Br	**3b** 84
6	0.30	*p*-Me	**3c** 76
7	1.00	*p*-Me	**3c** 88

The efficiency of the sequential one-pot transformation was compared with the stepwise synthesis as depicted in **Scheme S2**. The stepwise synthesis *via* isolation of the Koser's reagent **21a** before adding the anisole **2a** yielded the diaryliodonium salt **3a** in a 78% overall yield. Therefore, the sequential one-pot procedure was used instead.

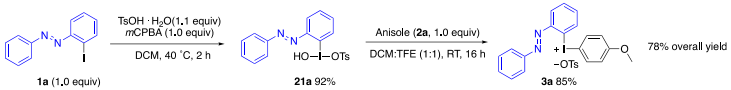

1a (1.0 equiv) **21a** 92% **3a** 85%

Scheme S2. Comparison of the sequential one-pot procedure with the stepwise synthesis.

Different dummy arenes, such as 1,3,5-trimethylbenzene (mesitylene, **2b**), 1,3,5-trimethoxybenzene (**2c**) and benzene (**2d**), were employed under the optimized condition in the sequential one-pot procedure (**Table S4**). When mesitylene was used, the diaryliodonium salt **3e** could only be obtained in 33% yield (entry 2). All attempts were in vain to get product **3e** in better yield even when solvents, temperature, and reaction time were changed. To the contrary, the reaction with **2c** delivered the product in good yield (entry 3). Finally, when benzene was used in the reaction, product **2d** could not be obtained but the corresponding Koser's reagent was isolated (entry 4). Different conditions were tried, e. g. mixture of solvents, prolongated reaction time and elevated temperature. However, in all cases, the Koser's reagent was obtained as the only product.

Table S4. A sequential one-pot procedure for synthesizing diaryliodonium salt **3** with different dummies. [a] Isolated yield.

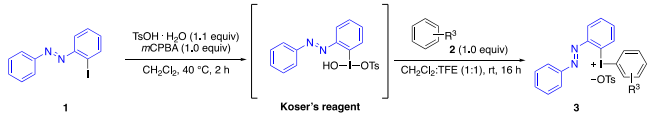

1 3

Entry	Scale (mmol)	arene 2	Yield (%)[a]
1	1.0	anisole (**2a**)	**3a** 84
2	1.0	mesitylene (**2b**)	**3e** 33
3	0.2	1,3,5-trimethoxybenzene (**2c**)	**3f** 76
4	0.2	benzene (**2d**)	-

3.2 General Procedures

General Procedure for the Synthesis of Koser's Reagents 21

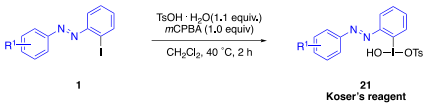

1 — 21 Koser's reagent

Following a reported procedure,[12] iodoazobenzene **1** (1.0 equiv, 1.0 mmol) was dissolved in CH_2Cl_2 0.2 M (5 mL) following by the addition of *m*CPBA (88%, 1.0 equiv, 1.0 mmol) and TsOH·H_2O (1.1 equiv, 1.1 mmol). The reaction mixture was stirred at 40 °C for 2 h. The solvent was removed under reduced pressure, and diethyl ether (5 mL) was added to the residue and stirred for 30 minutes. The solid was filtrated and washed with diethyl ether (5 mL) to obtain the pure compound **21**.

General One-Pot Procedure for the Synthesis of Diaryliodonium Salts 3

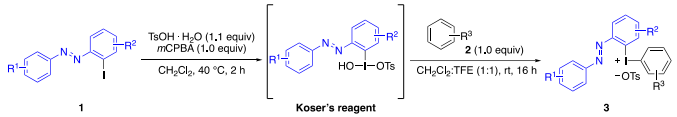

1 — Koser's reagent — 3

*m*CPBA (1.0 equiv, 1.0 mmol) was added to the iodoazobenzene **1a** (1.0 equiv, 1.0 mmol) in CH_2Cl_2 (0.2 M, 5 mL), followed by the addition of TsOH·H_2O (1.1 equiv, 1.1 mmol) and the temperature was raised to 40 °C for 2 h. After cooling to rt, the solvent was evaporated *in vacuo*. The resulting mixture was then dissolved in a mixture of CH_2Cl_2/TFE (1:1, 0.2M) followed by the addition of the arene (1.0 mmol). The reaction was stirred for 16 h at rt, and the solvent was removed after this time. Et_2O (10 mL) was added, and the mixture was left in the -18 °C 16 h prior to filtration. *NB: It is essential to leave the mixture in the freezer due to its initial solid-oil form* (see **Figures S1-S2**). The precipitate was filtered and washed with Et_2O (3 x 20 mL). After drying the solid under vacuum, product **3** was obtained in analytically pure form and retained the *E*-configuration, which was fully characterized by NMR analysis (**Section 3.3**) and the configuration was confirmed by X-ray diffraction (**Section 4**). Some impurities were found to be challenging to remove through the procedure above, especially in product **3g** (see **Section 3.3**). Recrystallization from ethanol was then found to give the pure product.

In all cases, it is essential to leave the mixture in the freezer 16 h prior to filtration due to the initial solid-oil formation of the precipitate, which might affect the successful precipitation of the salt. Therefore, detailed pictures of the procedure of the synthesis of salt **3a** (2.00 mmol scale) are reported in **Figure S1**. After 16 h, the mixture should result as in **Figure S1-A** where precipitation is observed. After the solvents are removed *in vacuo*, the mixture results in a solid-oil form, as depicted in **Figure S1-B**. Next, 10 mL of diethyl ether was added, as shown in **Figure S1-C,** and it was stored in the freezer with a glass stopper for 16 h.

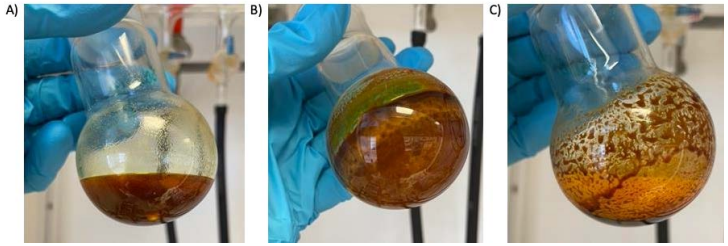

Figure S1. A) Reaction mixture stopped after 16 h; B) Solid-oil form obtained after removing the solvents; C) Addition of diethyl ether to the flask.

After this time, the flask is removed from the freezer, and the mixture is now a brown-yellow solid, as shown in **Figure S2-D**. Using a spatula, the solid is scratched and precipitates as in **Figure S2-E**. Finally, the solid is filtered, washed with diethyl ether (20 mL), and collected in a 20 mL vial with a cap (**Figure S2-F**). The salt must be stored in the dark and in the freezer to avoid decomposition of the salt due to exposure to light.

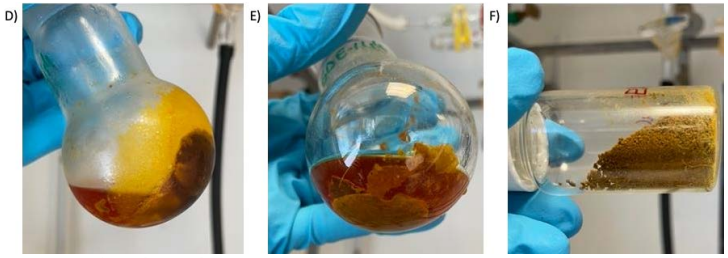

Figure S2. D) Solid formed after storing in the freezer for 16 h; E) The salt precipitation after scratching; F) Salt collected into a 20 mL vial.

3.3 Analytical Data

(*E*)-Hydroxy(2-(phenyldiazenyl)phenyl)-λ³-iodaneyl 4-methylbenzenesulfonate (21a)

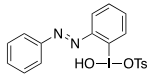

Prepared according to the general procedure, product **21a** was obtained as a yellow solid (994 mg, 2.00 mmol, 98%). Mp: 151 °C. ^{1}H-NMR (400 MHz, MeOD-d_4): δ 8.83 (dd, *J* = 7.6, 1.5 Hz, 1H), 8.23 – 8.02 (m, 5H), 7.86 – 7.78 (m, 1H), 7.77 – 7.66 (m, 4H), 7.26 – 7.17 (m, 2H), 2.36 (s, 3H). ^{13}C-NMR (101 MHz, MeOD-d_4) δ 151.2, 148.2, 143.6, 141.6, 138.6, 136.8, 136.4, 134.0, 131.9, 129.8, 129.1, 127.0, 124.9, 111.4, 21.3. HRMS(ESI) m/z: calcd. for $C_{12}H_{10}IN_2O$ [M-TsO$^-$]$^+$ 324.9838; found 324.9840.

(*E*)-(2-((4-Bromophenyl)diazenyl)phenyl)(hydroxy)-λ³-iodaneyl 4-methylbenzenesulfonate (21b)

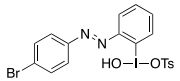

Prepared according to the reported procedure, product **21b** was obtained as a yellow solid (508 mg, 1.00 mmol, 88%). Mp: 161 °C. ^{1}H-NMR (400 MHz, DMSO-d_6): δ 10.03 (s, 1H), 8.80 (d, *J* = 7.7 Hz, 1H), 8.18 – 7.93 (m, 7H), 7.47 (d, *J* = 7.8 Hz, 2H), 7.10 (d, *J* = 7.7 Hz, 2H), 2.28 (s, 3H). ^{13}C-NMR (101 MHz, DMSO-d_6) δ 149.1, 145.9, 145.7, 137.6, 137.0, 135.1, 133.6, 132.5, 128.7, 128.1, 127.6, 125.5, 125.3, 112.0, 20.8. HRMS(ESI) m/z: calcd. for $C_{12}H_9BrIN_2O$ [M-TsO$^-$]$^+$ 402.8943; found 402.8949.

(*E*)-(4-Methoxyphenyl)(2-(phenyldiazenyl)phenyl)iodonium tosylate (3a)

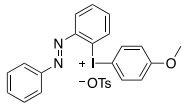

Prepared according to the general one-pot procedure, product **3a** was obtained as a yellow solid (495 mg, 0.84 mmol, 84%). Mp: 151 °C. ^{1}H-NMR (400 MHz, $CDCl_3$): δ 8.34 (dd, *J* = 7.8, 1.5 Hz, 1H), 8.28 – 8.22 (m, 2H), 7.97 – 7.90 (m, 2H), 7.73 (td, *J* = 7.5, 1.1 Hz, 1H), 7.67 – 7.61 (m, 2H), 7.60 – 7.48 (m, 3H), 7.41 (td, *J* = 8.9, 1.6 Hz, 1H), 7.05 (d, *J* = 7.9 Hz, 2H), 7.01 – 6.94 (m, 3H), 3.87 (s, 3H), 2.31 (s, 3H). ^{13}C-NMR (101 MHz, $CDCl_3$): δ 163.2, 149.1, 147.9, 143.1, 139.3, 139.2, 134.3, 134.0, 134.0, 131.7, 130.8, 130.2, 128.6, 126.2, 124.2, 118.0, 103.6, 102.7, 55.8, 21.4. HRMS(ESI) m/z: calcd. for $C_{19}H_{16}IN_2O$ [M-TsO$^-$]$^+$ 415.0302; found 415.0309.

(*E*)-(4-Methoxyphenyl)(2-(4-bromophenyldiazenyl)phenyl)iodonium tosylate (3b)

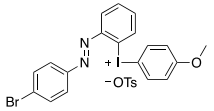

Prepared according to the general one-pot procedure obtained as a yellow solid (562 mg, 0.84 mmol, 84%). Mp: 167 °C. ^{1}H-NMR (400 MHz, $CDCl_3$): δ 8.33 (dd, *J* = 7.8, 1.6 Hz, 1H), 8.18 – 8.11 (m, 2H), 7.98 – 7.91 (m, 2H), 7.74 (td, *J* = 7.6, 1.2 Hz, 1H), 7.69 – 7.59 (m, 4H), 7.43 (ddd, *J* = 8.1, 7.3, 1.6 Hz, 1H), 7.11 – 7.04 (m, 2H), 7.04 – 6.97 (m, 3H), 3.89 (s, 3H), 2.34 (s, 3H).^{13}C-NMR (101 MHz,): δ 163.3, 148.0, 148.1, 139.6, 139.3, 134.5, 133.9, 133.5, 131.8, 130.8, 129.2, 128.7, 126.2, 125.6, 118.1, 104.1, 102.4, 55.8, 21.5. HRMS(ESI) m/z: calcd. for $C_{19}H_{15}BrIN_2O$ [M-TsO$^-$]$^+$ 492.9407; found 492.9400.

(*E*)-(4-Methoxyphenyl)(2-(*p*-tolyldiazenyl)phenyl)iodonium tosylate (3c)

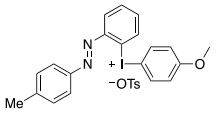

Prepared according to the general one-pot procedure obtained as a yellow solid (529 mg, 0.88 mmol, 88%). Mp: 163 °C. ^{1}H-NMR (400 MHz, $CDCl_3$): δ 8.31 (dd, *J* = 7.8, 1.6 Hz, 1H), 8.20 – 8.12 (m, 2H), 7.98 – 7.90 (m, 2H), 7.72 (d, *J* = 1.2 Hz, 1H), 7.67 (d, *J* = 7.9 Hz, 2H), 7.43 – 7.35 (m, 1H), 7.32 (d, *J* = 8.1 Hz, 2H), 7.07 (d, *J* = 7.9 Hz, 2H), 7.02 – 6.94 (m, 3H), 3.89 (s, 3H), 2.44 (s, 3H), 2.32 (s, 3H).^{13}C-NMR (101 MHz,): δ 163.2, 148.0, 147.2, 145.5, 143.2, 139.3, 139.2, 133.9, 133.7, 131.6, 130.9, 130.6, 128.6, 126.3, 124.3, 117.9, 103.4, 102.9, 55.8, 22.0, 21.4. HRMS(ESI) m/z: calcd. for $C_{20}H_{18}IN_2O$ [M-TsO$^-$]$^+$ 429.0458; found 429.0448.

(*E*)-(4-Methoxyphenyl)(5-methyl-2-(phenyldiazenyl)phenyl)iodonium tosylate (3d)

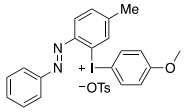

Prepared according to the general one-pot procedure obtained as slightly brown solid (93.6 mg, 0.16 mmol, 49%). Mp: 170 °C. ^{1}H-NMR (400 MHz, $CDCl_3$) δ 8.22 (d, *J* = 7.7 Hz, 3H), 7.94 (d, *J* = 8.5 Hz, 2H), 7.64 (d, *J* = 7.8 Hz, 3H), 7.54 (dd, *J* = 11.8, 7.2 Hz, 4H), 7.02 (dd, *J* = 23.8, 8.2 Hz, 5H), 6.75 (s, 1H), 3.88 (s, 3H), 2.31 (d, *J* = 3.6 Hz, 6H). ^{13}C NMR (101 MHz, $CDCl_3$) δ 163.2, 149.1, 146.1, 146.1, 142.6, 139.6, 139.3, 133.7, 133.7, 132.4, 131.1, 130.1, 128.6, 126.3, 124.0, 117.9, 103.3, 102.6, 55.8, 22.0, 21.4. HRMS(ESI) m/z: calcd. for $C_{20}H_{18}IN_2O$ [M-TsO$^-$]$^+$ 429.0458; found 429.0448.

(*E*)-Mesityl(2-(phenyldiazenyl)phenyl)iodonium tosylate (3e)

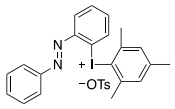

Prepared according to the general one-pot procedure obtained as a brown solid (200 mg, 0.33 mmol, 33%). Mp: 159 °C. ^{1}H-NMR (400 MHz, $CDCl_3$) δ 8.37 – 8.29 (m, 3H), 7.73 (t, *J* = 7.6 Hz, 1H), 7.62 – 7.52 (m, 5H), 7.37 (td, *J* = 7.8, 1.6 Hz, 1H), 7.08 (s, 2H), 7.02 (d, *J* = 7.8 Hz, 2H), 6.81 (d, *J* = 8.0 Hz, 1H), 2.55 (s, 6H), 2.40 (s, 3H), 2.31 (s, 3H). ^{13}C-NMR (101 MHz, $CDCl_3$) δ 149.5, 148.4, 144.2, 143.4, 143.3, 139.0, 134.4, 134.0, 133.6, 131.7, 130.2, 130.0, 129.4, 128.4, 126.1, 124.3, 120.2, 102.3, 26.8, 21.4. HRMS(ESI) m/z: calcd. for $C_{21}H_{20}I_2N_2$ [M-TsO$^-$]$^+$ 427.0660; found 427.0650.

(*E*)-(2,4,6-Trimethoxyphenyl)(2-(phenyldiazenyl)phenyl)iodonium tosylate (3f)

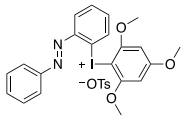

Prepared according to general one-pot procedure obtained as a green solid (108 mg, 0.17 mmol, 76%). Mp: 184 °C. ^{1}H-NMR (400 MHz, $CDCl_3$) δ 8.39 – 8.29 (m, 3H), 7.72 (td, *J* = 7.5, 1.2 Hz, 1H), 7.69 – 7.64 (m, 2H), 7.59 – 7.50 (m, 3H), 7.39 (td, *J* = 7.7, 1.6 Hz, 1H), 7.07 – 7.00 (m, 3H), 6.21 (s, 2H) 3.91 (s, 3H), 3.79 (s, 6H), 2.31 (s, 3H). ^{13}C-NMR (101 MHz, $CDCl_3$) δ 167.5, 161.6, 149.1, 148.4, 143.4, 139.1, 134.7, 134.1, 133.8, 131.3, 130.1, 129.9, 128.5, 126.3, 124.3, 101.5, 91.8, 85.0, 57.1, 56.1, 21.4. HRMS(ESI) m/z: calcd. for $C_{21}H_{20}I_2N_2O_3$ [M-TsO$^-$]$^+$ 475.0513; found 475.0508.

(*E*)-bis(4-Methoxyphenyl)(diazene-1,2-diylbis(2,1-phenylene))iodonium tosylate (3g)

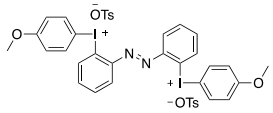

Prepared according to the general one-pot procedure. In this case, increased equivalents of *m*CPBA (2.0 equiv), tosic acid (2.2 equiv), and anisole (2.0 equiv) were necessary to obtain salt **3g** as an orange solid (168 mg, 0.17 mmol, 56 %). ^{1}H-NMR (400 MHz, MeOD-d_4) δ 8.31 (dd, J = 7.9, 1.5 Hz, 2H), 8.08 – 8.00 (m, 4H), 7.99 – 7.91 (m, 4H), 7.77 (td, J = 8.4, 1.5 Hz, 2H), 7.68 – 7.61 (m, 4H), 7.22 – 7.15 (m, 4H), 7.09 – 7.01 (m, 4H), 3.86 (s, 6H), 2.35 (s, 6H). ^{13}C-NMR (101 MHz, MeOD-d_4) δ 165.0, 148.2, 143.6, 141.6, 139.7, 137.5, 135.7, 134.7, 129.8, 126.9, 125.5, 119.2, 116.9, 102.9, 56.5, 21.3. HRMS(ESI) m/z: calcd. for $C_{26}H_{22}I_2N_2O_2Na^+$ [M-TsO$^-$]$^+$ 693.9561; found 693.9626.

3.4 Scope Limitations

Other diiodinated azobenzenes were also evaluated in the diaryliodonium salt synthesis. Limitations were observed for the diiodinated substrates shown below. With the first substrate, we could not observe formation of any iodine(III) compound. The *ortho*- and *para*-diiodinated azobenzene was successfully oxidized to the corresponding Koser's reagent, which could be detected in HRMS and precipitated together with another product, where only one anisyl group had been incorporated. However, it was not possible to fully convert the mixture of these products into the targeted diaryliodonium salt despite evaluation of various reaction conditions.

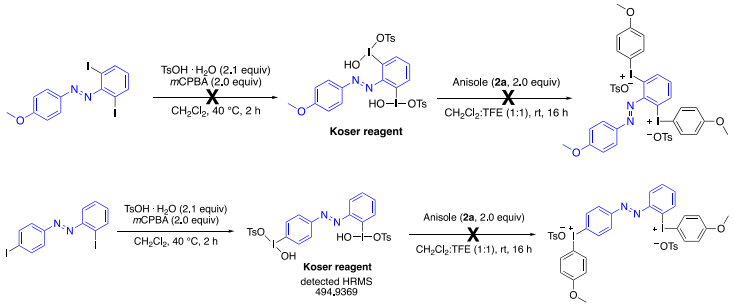

3.5 Anion Exchange with the Diaryliodonium Salt 3a

The nature of the counterion has been shown to play an essential role in many reactions employing diaryliodonium salts.[15] We therefore investigated the possibility of an anion exchange from tosylate to triflate (**Scheme S3**). To our delight, adding 1.0 equiv of TfOH allowed the facile isolation of **3a'** in 63% yield (**Method 1**). Furthermore, salt **3a'** was obtained in 88% yield upon performing a work-up with 25 equiv of NaOTf after isolation of **3a** (**Method 2**).

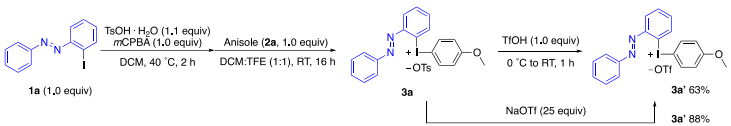

Scheme S3. Anion exchange using *in situ* exchange and work-up methods.

Method 1 – *in situ* with TfOH

After following the general procedure for the synthesis of salt **3a**, an *in situ* anion exchange was performed after full conversion to **3a**. The solvent was removed, and salt **3a** (97 mg, 0.32 mmol) was dissolved in CH_2Cl_2 (1 mL) and cooled to 0 °C. Triflic acid (28 µL, 1.0 equiv) was added, and the mixture was allowed to warm to rt and stirred for 1 h. The solvent was then removed, and Et_2O (5 mL) was added, and the mixture was kept in the freezer overnight prior filtration. After filtration and drying under vacuum, product **3a'** was obtained as a green solid (112 mg, 63% yield). The anion exchange was confirmed by NMR analysis.

Method 2 – work-up with NaOTf

Diaryliodonium salt **3a** (100 mg, 0.32 mmol) was dissolved in CH_2Cl_2 (15 mL) and extracted with NaOTf (1.4 g, 25 equiv) dissolved in H_2O (15 mL). The organic layer was concentrated without drying. Et_2O (10 mL) was added, and the mixture was stirred at rt for 30 min to precipitate a solid. The solid was filtrated and washed with Et_2O and dried *in vacuo* to give triflate salt **3a'** as an orange solid (162 mg, 88% yield). The anion exchange was confirmed by NMR analysis.

Analytical data for diaryliodonium salt 3a'

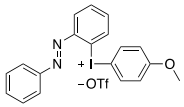

Mp: 156 °C. ^{1}H-NMR (400 MHz, $CDCl_3$) 8.38 (dd, J = 7.8, 1.6 Hz, 1H), 8.21 (dd, J = 7.5, 2.3 Hz, 2H), 7.93 (d, J = 8.8 Hz, 2H), 7.79 (t, J = 7.5 Hz, 1H), 7.67 – 7.55 (m, 4H), 7.52 – 7.44 (m, 1H), 7.10 – 7.02 (m, 2H), 6.99 (d, J = 8.1 Hz, 1H), 3.88 (s, 3H). ^{13}C-NMR (101 MHz, $CDCl_3$) δ 163.7, 148.9, 147.1, 139.4, 134.9, 134.7, 134.4, 132.2, 130.3, 130.2, 124.1, 120.7 (q, J = 353.1 Hz, $CF_3SO_3^-$), 118.4, 100.9, 100.8, 55.9. ^{19}F-NMR (377 MHz, $CDCl_3$) δ −78.2. HRMS(ESI) m/z: calcd. for $C_{19}H_{16}IN_2O$ [M-TfO$^-$]$^+$ 415.0302; found 415.0309.

4 X-ray Diffraction Crystal Structure of Diaryliodonium Salt 3a

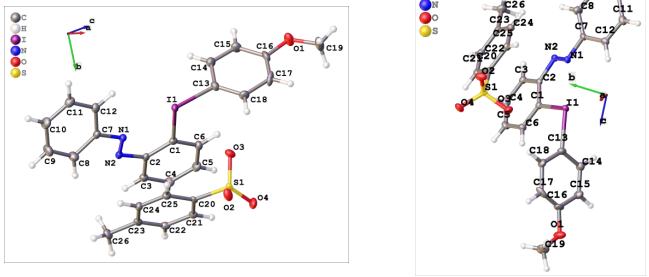

Figure S3. Crystal structure of diaryliodonium salt **3a**.

Single crystals of **3a** were grown by dissolving a small amount (ca. 5 mg) of the compound in CH_2Cl_2 (ca. 200 µL) in a snap cap sample vial. The solution was cautiously overlaid with *n*-hexane (ca. 1 mL) to prevent mixing of the solvents. Subsequently, the solvents were allowed to evaporate slowly at 25 °C by leaving the vial open for 7 d. CCDC Deposition Number: 2215795.

Table S5. Crystal data and structure refinement for **3a.**

Empirical formula	$C_{26}H_{23}IN_2O_4S$
Formula weight	586.42
Temperature/K	100.0
Crystal system	monoclinic
Space group	$P2_1/n$
a/Å	9.8892(4)
b/Å	16.7789(11)
c/Å	14.1591(7)
α/°	90
β/°	98.131(2)
γ/°	90
Volume/Å^3	2325.8(2)
Z	4
ρ_{calc}g/cm^3	1.675
µ/mm^{-1}	1.504
F(000)	1176.0
Crystal size/mm^3	0.4 × 0.02 × 0.02
Radiation	MoKα (λ = 0.71073)
2Θ range for data collection/°	4.726 to 56.642
Index ranges	-13 ≤ h ≤ 12, -22 ≤ k ≤ 22, -18 ≤ l ≤ 18
Reflections collected	73815
Independent reflections	5789 [R_{int} = 0.0475, R_{sigma} = 0.0207]
Data/restraints/parameters	5789/0/308
Goodness-of-fit on F^2	1.108
Final R indexes [I>=2σ (I)]	R_1 = 0.0319, wR_2 = 0.0647
Final R indexes [all data]	R_1 = 0.0407, wR_2 = 0.0676
Largest diff. peak/hole / e Å^{-3}	2.02/-0.78

Table S6. Fractional Atomic Coordinates (×10^4) and Equivalent Isotropic Displacement Parameters (Å^2×10^3) for **3a**. U_{eq} is defined as 1/3 of the trace of the orthogonalised U_{IJ} tensor.

Atom	*x*	*y*	*z*	U(eq)
I1	2922.3(2)	5007.2(2)	5337.2(2)	12.72(5)
S1	5820.8(7)	7120.4(4)	5041.7(5)	13.45(13)
N2	255(2)	5972.5(13)	4197.8(16)	14.0(4)
O3	5797(2)	6300.6(12)	5415.3(15)	20.4(4)
N1	1091(2)	5485.4(13)	3936.3(16)	13.8(4)
O2	6686(2)	7190.7(14)	4293.7(14)	22.4(4)
O1	5471(2)	4067.5(15)	9460.6(16)	28.9(5)
O4	6089(2)	7709.0(13)	5794.7(15)	23.8(5)
C3	-219(3)	6823.3(16)	5459.6(19)	15.0(5)
C1	1736(3)	5952.5(15)	5785.5(19)	12.5(5)
C7	785(3)	5196.1(16)	2985.5(19)	15.2(5)
C2	622(3)	6234.1(15)	5155.2(18)	12.4(5)
C12	1332(3)	4461.2(17)	2797(2)	16.7(5)
C14	3205(3)	4176.7(18)	7230(2)	19.7(6)
C5	1206(3)	6866.2(17)	6987(2)	18.4(6)
C13	3874(3)	4727.6(18)	6728(2)	18.1(6)
C25	3696(3)	6998.0(16)	3567.1(19)	14.5(5)
C16	5026(3)	4319.9(18)	8548(2)	21.6(6)
C22	1945(3)	7947.6(16)	4453.6(19)	15.7(5)
C11	995(3)	4120.2(18)	1899(2)	19.9(6)
C6	2036(3)	6264.3(17)	6698.1(19)	16.5(5)
C23	1506(3)	7651.9(16)	3541.3(19)	15.0(5)
C21	3248(3)	7777.3(16)	4922.1(18)	14.1(5)
C15	3765(3)	3979.9(18)	8152(2)	21.6(6)
C10	154(3)	4516.6(19)	1196(2)	23.6(6)
C18	5103(3)	5070.7(18)	7115(2)	20.1(6)
C20	4129(3)	7306.3(15)	4476.6(18)	11.8(5)
C24	2392(3)	7171.6(16)	3106.1(19)	15.3(5)
C17	5686(3)	4836(2)	8062(2)	24.8(7)
C4	82(3)	7135.6(17)	6372(2)	19.0(6)
C19	6813(3)	4303(2)	9870(3)	35.0(8)
C9	-315(3)	5271(2)	1370(2)	25.8(7)
C8	-1(3)	5618.4(19)	2261(2)	22.3(6)
C26	93(3)	7845.4(19)	3040(2)	20.9(6)

Table S7. Anisotropic Displacement Parameters (Å^2×10^3) for **3a**. The Anisotropic displacement factor exponent takes the form: -2π^2[h^{2}a*^{2}U_{11}+2hka*b*U_{12}+...].

Atom	U_{11}	U_{22}	U_{33}	U_{23}	U_{13}	U_{12}
I1	10.52(8)	14.40(8)	12.72(8)	-1.01(7)	-0.16(5)	0.26(7)
S1	12.6(3)	15.4(3)	11.5(3)	1.7(2)	-1.1(2)	0.4(2)
N2	14.4(11)	13.5(11)	13.5(11)	-0.2(8)	-0.2(9)	-2.8(9)
O3	19.8(10)	17.7(10)	23.1(10)	6.6(8)	1.1(8)	3.7(8)
N1	14.9(11)	12.2(10)	13.6(10)	-0.9(8)	-0.4(8)	-0.7(9)
O2	13.2(9)	35.3(12)	18.7(10)	4.6(9)	2.5(8)	-0.8(9)
O1	24.4(12)	40.9(14)	20.2(11)	10.9(10)	-1.4(9)	-5.0(10)

Table S7. Anisotropic Displacement Parameters ($Å^2 \times 10^3$) for **3a**. The Anisotropic displacement factor exponent takes the form: $-2\pi^2[h^2a^{*2}U_{11}+2hka^*b^*U_{12}+...]$.

Atom	U_{11}	U_{22}	U_{33}	U_{23}	U_{13}	U_{12}
O4	25.2(11)	23.4(11)	19.9(10)	-6.0(9)	-7.2(8)	-0.4(9)
C3	14.5(13)	14.8(12)	15.9(13)	1.7(10)	3.2(10)	-0.2(10)
C1	11.4(12)	12.4(12)	14.3(12)	0.2(10)	3.5(10)	-0.8(9)
C7	16.8(13)	15.2(13)	13.1(12)	-1.4(9)	0.7(10)	-3.7(10)
C2	12.5(12)	12.8(12)	11.8(11)	0.5(9)	1.8(9)	-3.2(10)
C12	13.4(13)	19.6(13)	17.1(13)	-0.4(11)	2.4(10)	-1.2(11)
C14	16.1(13)	20.3(14)	22.2(14)	1.0(11)	1.3(11)	-1.1(11)
C5	22.3(14)	20.5(14)	13.0(12)	-4.4(10)	4.4(11)	-2.3(11)
C13	18.2(14)	20.1(13)	15.0(13)	2.1(10)	-0.6(11)	2.4(11)
C25	13.6(12)	14.4(12)	15.8(12)	-0.7(10)	2.8(10)	0.7(10)
C16	23.3(15)	24.7(15)	14.5(13)	1.8(11)	-5.4(11)	8.3(12)
C22	17.3(13)	13.5(12)	17.2(13)	2.3(10)	6.1(10)	1.3(10)
C11	19.5(14)	20.8(14)	20.5(14)	-5.4(11)	7.3(11)	-2.8(11)
C6	16.4(13)	18.8(13)	13.7(12)	0.3(10)	-0.1(10)	-0.8(11)
C23	13.2(13)	14.7(12)	17.3(13)	4.5(10)	2.5(10)	-0.9(10)
C21	18.4(13)	13.0(12)	11.3(12)	1.7(10)	3.5(10)	-0.8(10)
C15	19.3(14)	23.7(15)	22.2(14)	6.5(12)	3.9(11)	-3.4(12)
C10	30.8(17)	26.0(16)	13.8(13)	-5.3(12)	2.2(12)	-2.3(13)
C18	20.1(13)	19.0(14)	21.4(13)	4.6(12)	3.8(11)	-4.5(12)
C20	13.0(12)	11.5(12)	10.5(11)	5.1(9)	0.5(9)	-0.2(9)
C24	15.6(13)	15.9(13)	13.7(12)	-0.5(10)	-0.3(10)	-1.8(10)
C17	9.9(12)	40.2(19)	23.5(14)	-15.2(13)	-0.2(11)	-3.7(12)
C4	19.9(14)	18.4(13)	20.1(14)	-3.3(11)	7.9(11)	1.6(11)
C19	20.9(16)	47(2)	33.2(18)	10.6(16)	-10.2(14)	-4.9(15)
C9	30.2(17)	30.5(16)	15.2(13)	0.4(12)	-2.1(12)	7.1(13)
C8	26.0(16)	20.0(14)	20.6(14)	-0.7(11)	2.1(12)	6.4(12)
C26	14.9(13)	24.0(15)	22.9(14)	3.4(12)	-0.5(11)	4.4(11)

Table S8. Bond Lengths for **3a**.

Atom	Atom	Length/Å	Atom	Atom	Length/Å
I1	C1	2.122(3)	C14	C13	1.389(4)
I1	C13	2.111(3)	C14	C15	1.385(4)
S1	O3	1.475(2)	C5	C6	1.399(4)
S1	O2	1.457(2)	C5	C4	1.388(4)
S1	O4	1.450(2)	C13	C18	1.386(4)
S1	C20	1.777(3)	C25	C20	1.398(4)
N2	N1	1.255(3)	C25	C24	1.392(4)
N2	C2	1.422(3)	C16	C15	1.413(4)
N1	C7	1.423(3)	C16	C17	1.333(5)
O1	C16	1.372(3)	C22	C23	1.395(4)
O1	C19	1.427(4)	C22	C21	1.392(4)
C3	C2	1.399(4)	C11	C10	1.374(4)
C3	C4	1.387(4)	C23	C24	1.396(4)
C1	C2	1.398(4)	C23	C26	1.510(4)
C1	C6	1.387(4)	C21	C20	1.392(4)
C7	C12	1.387(4)	C10	C9	1.383(4)
C7	C8	1.390(4)	C18	C17	1.438(4)
C12	C11	1.392(4)	C9	C8	1.384(4)

Table S9. Bond Angles for **3a**.

Atom	Atom	Atom	Angle/˚	Atom	Atom	Atom	Angle/˚
C13	I1	C1	94.56(11)	C18	C13	I1	121.8(2)
O3	S1	C20	105.27(12)	C18	C13	C14	121.9(3)
O2	S1	O3	112.14(13)	C24	C25	C20	119.8(2)
O2	S1	C20	105.70(12)	O1	C16	C15	113.3(3)
O4	S1	O3	112.45(13)	C17	C16	O1	124.9(3)
O4	S1	O2	114.48(14)	C17	C16	C15	121.8(3)
O4	S1	C20	105.90(13)	C21	C22	C23	121.0(3)
N1	N2	C2	113.1(2)	C10	C11	C12	120.3(3)
N2	N1	C7	116.1(2)	C1	C6	C5	119.2(3)
C16	O1	C19	116.9(3)	C22	C23	C24	118.8(2)
C4	C3	C2	119.7(3)	C22	C23	C26	120.4(3)
C2	C1	I1	118.72(19)	C24	C23	C26	120.9(3)
C6	C1	I1	120.4(2)	C20	C21	C22	119.8(2)
C6	C1	C2	120.8(2)	C14	C15	C16	119.4(3)
C12	C7	N1	116.6(2)	C11	C10	C9	119.9(3)
C12	C7	C8	120.3(3)	C13	C18	C17	117.9(3)
C8	C7	N1	123.1(3)	C25	C20	S1	119.7(2)
C3	C2	N2	115.4(2)	C21	C20	S1	120.4(2)
C1	C2	N2	125.2(2)	C21	C20	C25	119.9(2)
C1	C2	C3	119.4(2)	C25	C24	C23	120.8(2)
C7	C12	C11	119.4(3)	C16	C17	C18	119.9(3)
C15	C14	C13	119.1(3)	C3	C4	C5	120.6(3)
C4	C5	C6	120.2(3)	C10	C9	C8	120.7(3)
C14	C13	I1	116.3(2)	C9	C8	C7	119.2(3)

Table S10. Torsion Angles for **3a**.

A	B	C	D	Angle/˚	A	B	C	D	Angle/˚
I1	C1	C2	N2	-4.3(3)	C13	C18	C17	C16	-1.8(5)
I1	C1	C2	C3	176.13(19)	C22	C23	C24	C25	-0.8(4)
I1	C1	C6	C5	-177.6(2)	C22	C21	C20	S1	177.1(2)
I1	C13	C18	C17	-179.1(2)	C22	C21	C20	C25	-0.9(4)
N2	N1	C7	C12	-155.3(2)	C11	C10	C9	C8	-3.1(5)
N2	N1	C7	C8	25.7(4)	C6	C1	C2	N2	177.9(2)
O3	S1	C20	C25	-78.7(2)	C6	C1	C2	C3	-1.7(4)
O3	S1	C20	C21	103.3(2)	C6	C5	C4	C3	-1.2(4)
N1	N2	C2	C3	175.4(2)	C23	C22	C21	C20	0.1(4)
N1	N2	C2	C1	-4.2(4)	C21	C22	C23	C24	0.7(4)
N1	C7	C12	C11	175.6(2)	C21	C22	C23	C26	-179.7(3)
N1	C7	C8	C9	-176.2(3)	C15	C14	C13	I1	-178.8(2)
O2	S1	C20	C25	40.1(2)	C15	C14	C13	C18	1.7(5)
O2	S1	C20	C21	-137.9(2)	C15	C16	C17	C18	1.1(5)
O1	C16	C15	C14	-179.3(3)	C10	C9	C8	C7	-0.6(5)
O1	C16	C17	C18	-178.6(3)	C20	C25	C24	C23	0.0(4)
O4	S1	C20	C25	162.0(2)	C24	C25	C20	S1	-177.2(2)
O4	S1	C20	C21	-16.0(2)	C24	C25	C20	C21	0.8(4)
C7	C12	C11	C10	1.6(4)	C17	C16	C15	C14	1.0(5)
C2	N2	N1	C7	179.8(2)	C4	C3	C2	N2	-177.9(2)

Table S10. Torsion Angles for **3a**.

A	B	C	D	Angle/°	A	B	C	D	Angle/°
C2	C3	C4	C5	-0.3(4)	C4	C3	C2	C1	1.7(4)
C2	C1	C6	C5	0.2(4)	C4	C5	C6	C1	1.2(4)
C12	C7	C8	C9	4.8(5)	C19	O1	C16	C15	172.4(3)
C12	C11	C10	C9	2.6(5)	C19	O1	C16	C17	-7.9(5)
C14	C13	C18	C17	0.4(5)	C8	C7	C12	C11	-5.3(4)
C13	C14	C15	C16	-2.3(5)	C26	C23	C24	C25	179.6(3)

Table S11. Hydrogen Atom Coordinates (Å×10^4) and Isotropic Displacement Parameters (Å^2×10^3) for **3a**.

Atom	*x*	*y*	*z*	U(eq)
H3	-993.39	7008.61	5043.19	18
H12	1931.78	4193.06	3277.71	20
H14	2375.56	3938.48	6944.56	24
H5	1412.82	7091.07	7606.79	22
H25	4290.94	6670.74	3264.32	17
H22	1347.46	8269.87	4759.93	19
H11	1347.14	3610.91	1770.29	24
H6	2796.73	6071.43	7121.8	20
H21	3533.78	7981.9	5543.84	17
H15	3306.28	3619.58	8515.97	26
H10	-103.97	4272.57	592.04	28
H18	5546.88	5449.25	6765.01	24
H24	2101.02	6960.95	2488.01	18
H17	6540.42	5048.38	8341.51	30
H4	-487.23	7537.53	6578.09	23
H19A	7056.32	4036.98	10486.56	52
H19B	6837.82	4881.71	9962.4	52
H19C	7465.34	4151.4	9441.09	52
H9	-858.21	5554.47	873.33	31
H8	-318.45	6138.96	2376.05	27
H26A	-164.03	8383.24	3217.58	31
H26B	-562.78	7459.25	3228.44	31
H26C	88.49	7819.25	2347.94	31

5 Computational details

The Gaussian16 package[16] was employed and the functional Minnesota M06-2X[17] was used for all calculations presented in this work. Geometry optimizations were performed with def2-SVP basis set for all atoms. Energy corrections were applied to the optimized structures performing a single-point calculation using M06-2X with a larger basis set consisting of def2-TZVP for all atoms.

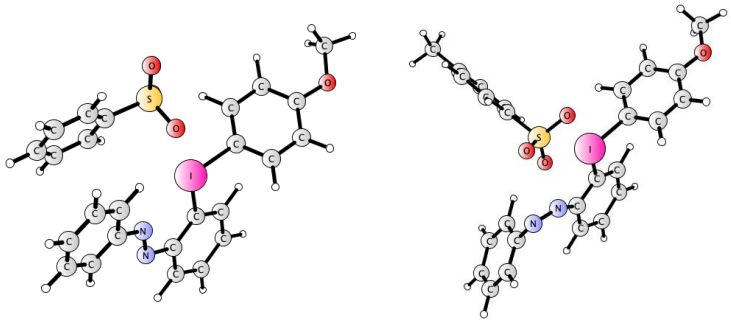

(*E*)-Salt **3a** (*Z*)-Salt **3a**

Table S12. Calculated absolute energies and energy corrections.

	M06-2X (def2-SVP) Electronic Energy (hartree)	M06-2X (def2-SVP) Free Energy correction	M06-2X (def2-TZVP) Electronic Energy (hartree)
(*E*)-Salt (3a)	-2108.8629649	0.373716	-2110.6567429
(Z)-Salt (3a)	-2108.8393281	0.374018	-2110.6336596

5.1 Cartesian Coordinates and Energies

Energies are given in Hartree
Sum of electronic and zero-point energies = $\varepsilon_0 + \varepsilon_{ZPE}$
Sum of electronic and thermal energies = $\varepsilon_0 + E_{tot}$
Sum of electronic and thermal enthalpies = $\varepsilon_0 + H_{corr}$
Sum of electronic and thermal free energies = $\varepsilon_0 + G_{corr}$

(*E*)-Salt **3a**

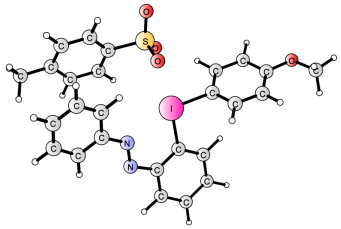

$\varepsilon_0 + \varepsilon_{ZPE}$ = -2108.422055
$\varepsilon_0 + E_{tot}$ = -2108.390465
$\varepsilon_0 + H_{corr}$ = -2108.389521
$\varepsilon_0 + G_{corr}$ = -2108.489249

C	-4.24845869	2.17076307	0.70817134
C	-2.93614622	1.72455813	0.66573633
C	-2.58028293	0.78983660	-0.31104242
C	-3.50057747	0.32815965	-1.24647897
C	-4.82102702	0.77359738	-1.19427599
C	-5.19908555	1.69853873	-0.21070440
H	-4.56696905	2.90758426	1.44563883
H	-2.17859127	2.12912384	1.34167657
H	-3.20603682	-0.38491354	-2.01910312
H	-5.53498028	0.40605980	-1.92929296
I	-0.58756148	0.11189777	-0.43406386
O	-6.44316694	2.18946483	-0.08234416
C	-1.03087922	-1.88443991	0.21179025
C	-2.29820306	-2.23691779	0.66402031
C	0.00446986	-2.84321202	0.23038106
C	-2.54880446	-3.53543306	1.11535652
H	-3.10220593	-1.49954580	0.67454524
C	-0.26379457	-4.14048121	0.68130872
C	-1.53467685	-4.49091726	1.12096408
H	-3.54854342	-3.79284391	1.46755264
H	0.56207342	-4.85254351	0.67514322
H	-1.73270504	-5.50373921	1.47242124
N	1.34129794	-2.61104307	-0.17426870
O	0.04763200	1.92341100	-0.90436700
S	0.45023600	2.76041400	0.29164000
O	-0.28666500	2.31080900	1.48931700
O	0.45873900	4.18434400	-0.00124400
C	2.15427900	2.28751700	0.59808300
C	3.17915000	2.96453400	-0.05628800
C	2.43956000	1.22774300	1.45806200
C	4.49849100	2.55736100	0.13722300
H	2.92848600	3.81258800	-0.69608100
C	3.76102600	0.82619200	1.63602600
H	1.62009000	0.74407100	1.99355800
C	4.80859200	1.47948300	0.97474400
H	5.30663600	3.08691400	-0.37346800
H	3.98760500	-0.00893200	2.30382100
C	6.23214900	1.03098300	1.17589900
H	6.31928800	-0.05820400	1.04870800
H	6.90869500	1.51672300	0.46006800
H	6.58292400	1.27508000	2.19027800
C	-7.42946216	1.78430270	-0.99732750
H	-8.34924506	2.30863327	-0.71798681
H	-7.15613815	2.05800068	-2.02925566
H	-7.60349051	0.69697330	-0.94586937
N	1.56264341	-1.45376703	-0.55291910
C	2.86385260	-1.11183168	-0.98129180
C	2.99875885	0.13984171	-1.59434746
C	3.97044854	-1.95211130	-0.79917630
C	4.25100996	0.53992063	-2.05396717
H	2.13359985	0.80254765	-1.69550143
C	5.21661260	-1.53166551	-1.24596204
H	3.82967467	-2.91479280	-0.30846092
C	5.35635432	-0.29167279	-1.87938113
H	4.36108161	1.51212315	-2.53430767
H	6.08789864	-2.17320455	-1.10585059
H	6.33855518	0.02894608	-2.23082319

(*Z*)-Salt **3a**

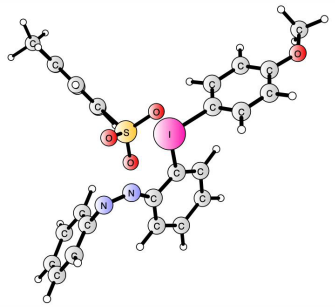

$\varepsilon_0 + \varepsilon_{ZPE}$ = -2108.398912
$\varepsilon_0 + E_{tot}$ = -2108.367980
$\varepsilon_0 + H_{corr}$ = -2108.367036
$\varepsilon_0 + G_{corr}$ = -2108.465310

I	-1.30302100	-1.26435800	-1.33094100
C	-0.41591300	-1.67842600	0.54730900
C	-1.00074700	-1.32620000	1.74561100
C	0.84408500	-2.25506900	0.42084800
C	-0.30822000	-1.67500000	2.90438500
H	-1.94932200	-0.79108900	1.78303800
C	1.50120700	-2.63249500	1.59951600
C	0.91555600	-2.34061600	2.82665700
H	-0.73121600	-1.41868400	3.87593600
H	2.46633700	-3.13366600	1.55752300
H	1.43749700	-2.61874600	3.74255800
N	1.20324700	-2.48935000	-0.94127600
N	2.33452600	-2.63873200	-1.39910400
C	3.52079400	-2.45808300	-0.62952400
C	4.48475600	-3.46652800	-0.70391200
C	3.76190300	-1.27440200	0.07691900
C	5.67662700	-3.32518800	0.00333300
H	4.28058200	-4.35293900	-1.30589200
C	4.97018700	-1.13711900	0.75337300
H	3.00566000	-0.48864700	0.09880400
C	5.92041900	-2.16066600	0.73245500
H	6.42372500	-4.11946300	-0.02946300
H	5.16013600	-0.21813600	1.30941500
H	6.86002900	-2.04465600	1.27465200
C	-3.19060200	-0.69573300	-0.61064700
C	-3.38335300	0.61907600	-0.19607100
C	-4.22491000	-1.63809100	-0.58188700
C	-4.64513100	1.00221400	0.26044100
H	-2.54201100	1.31802300	-0.18572400
C	-5.47493400	-1.24848500	-0.13138400
H	-4.05713500	-2.66602500	-0.90592400
C	-5.69470400	0.07454400	0.29142600
H	-4.79014300	2.02867700	0.59288100
H	-6.30902100	-1.94896500	-0.09180800
O	-6.93684900	0.35774600	0.71174600
C	-7.22224700	1.66384800	1.15194400
H	-7.06301400	2.40032800	0.34826600
H	-8.27742600	1.67013000	1.44371300
H	-6.60305800	1.93707600	2.02119700
O	1.24550900	0.47004100	-0.94151200
S	0.87226500	1.21988600	0.28635200
O	1.51768800	0.70676100	1.50688200
O	-0.59900800	1.37390300	0.41244400
C	1.51014400	2.87393400	0.04994100
C	1.83938200	3.64403900	1.16316500
C	1.63141100	3.39303600	-1.23493800
C	2.28129700	4.95120400	0.98138400
H	1.75580200	3.19988600	2.15630000
C	2.07688200	4.70296600	-1.40321000
H	1.38994900	2.75640200	-2.08738900
C	2.40610100	5.50047400	-0.30168100
H	2.54053000	5.55991300	1.85118700
H	2.17599700	5.11456600	-2.41040900
C	2.91633300	6.90620000	-0.48556700
H	4.01240100	6.94041700	-0.38614000
H	2.65957600	7.29715000	-1.47898100
H	2.49693900	7.58360100	0.27135000

6 Investigation of the Switching Behaviour of 1a and 3a

The influence of the hypervalent iodine moiety on the photo-switching behavior of the azobenzene was examined by ^{1}H NMR and UV/vis spectroscopy in $CDCl_3$ and $CHCl_3$, respectively. The diaryliodonium salt **3a** and the corresponding azobenzene **1a** were compared. Under ambient conditions, both molecules existed exclusively in the *E*-isomer. However, both molecules could be converted upon irradiation with UV light of 340 nm to the corresponding Z-isomer, which could be switched back to the *E*-isomer upon irradiation with visible light of 450 nm. The exact *E*/*Z*-ratio was determined by ^{1}H NMR spectroscopy. After 10 min of irradiation with 340 nm, the hypervalent azobenzene **3a** was switched by 71%, whereas the *Z*-isomer of the normal azobenzene **1a** was only obtained in 31% suggesting a faster *E*/*Z*-isomerization of the hypervalent azobenzene **3a**. Longer irradiation led to a higher *E*/*Z*-conversion (*E*/*Z*-ratio 32/68 for **1a** and 17/83 for **3a**). However, the hypervalent azobenzene **3a** started to decompose under such a long irradiation time, which is probably due to the high energy of the UV lamp and the sensitivity of iodine towards it. Free tosic acid became visible in the ^{1}H NMR spectrum (see **Figure S6**).

Upon irradiation with 450 nm, **1a** and **3a** re-isomerized to the corresponding *E*-isomer. For both molecules, the back-switching occurred faster than the *E*-*Z*-isomerization but a full conversion to the *E*-isomer could not be obtained. Again, **3a** switched faster than **1a**. The PSS450 of **3a** was obtained after irradiation with 450 nm for 1 min (*E*/*Z*-ratio: 72/28) and for **1a** after 2 min (*E*/*Z*-ratio: 90/10). However, this was in contrast to the UV/vis measurements. Here, the PSS340 and PSS450 of **1a** could be reached faster (PSS340: irradiation for 10 min; PSS450: irradiation for 1 min) and complete re-isomerization was possible. This is attributed to the concentration differences of NMR and absorption spectroscopy. The resistance against photo-bleaching was tested by reversible irradiation of **1a** and **3a** with UV and visible light. Both molecules showed no significant decomposition in the absorption spectra over five switching cycles. The incorporation of the hypervalent moiety had almost no influence on the absorption maxima of the azobenzene switch: **1a** showed the $\pi\pi^*$ transition at 325 nm and the weaker $n\pi^*$ transition at 434 nm; the hypervalent azobenzene **3a** at 338 nm ($\pi\pi^*$) and 436 nm ($n\pi^*$). However, the half-life time was significantly decreased by the incorporation of the hypervalent iodine bond: Whereas for **1a** a half-life time of 124.6 h was determined, for **3a** it was only 5.83 h, which we attributed to the strong electron acceptor character of the iodine(III) moiety. The thermal re-isomerization of azobenzene is a first order reaction. In the end, an equilibrium is reached where the equilibrium constant can be determined by the Van't Hoff equation. For the isomers of azobenzene the energy difference is ~ 40 kJ/mol leading to a rate constant of k = 0.984. In the case of our hypervalent azobenzene derivative, the energy difference between (*Z*)- and (*E*)-isomer is ~ 62.9 kJ/mol leading to a rate constant of k = 0.975. Hence, the concentration of the (*Z*)-isomer is negligible and the thermal re-isomerization should proceed completely.

6.1 ^{1}H NMR Analysis

To determine the ratio between *E* and *Z* isomer, ^{1}H NMR spectra of **1a** and **3a** in $CDCl_3$ were recorded without irradiation (ambient conditions) and after irradiation of the sample with 340 nm (PSS340) and 450 nm (PSS450), respectively. The sample concentration was approx. 3 mg/mL. For the analysis of the composition, the integral of two aromatic doublets were determined and set to one.

1-(2-Iodophenyl)-2-phenyldiazene (1a)

For the analysis of the composition, the doublets at 8.00 ppm (*E* isomer) and at 7.87 ppm (*Z* isomer) were chosen (**Table S13**).

Table S13. *E*/*Z* Ratio of **1a**.

Conditions	*E* isomer [%]	*Z* isomer [%]
No irradiation	100	0
340 nm 1 min	92	8
340 nm 2 min	90	10
340 nm 5 min	81	19
340 nm 10 min	69	31
340 nm 30 min	32	68
450 nm 1 min	90	10
450 nm 2 min	90	10
450 nm 5 min	90	10

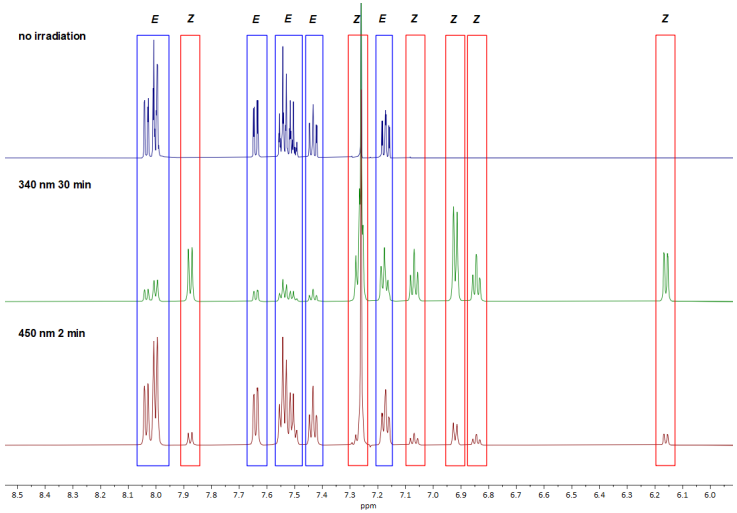

Figure S4. ^{1}H NMR spectra of **1a** in $CDCl_3$ under ambient conditions (top), PSS340 (middle) and PSS450 (bottom).

(4-Methoxyphenyl)(2-(phenyldiazenyl)phenyl)iodonium tosylate (3a)

For the analysis of the composition, the doublets at 8.27 ppm (*E* isomer) and at 8.05 ppm (*Z* isomer) were chosen (**Table S14**).

Table S14. *E*/*Z* Ratio of **3a**.

Conditions	*E* isomer [%]	*Z* isomer [%]
No irradiation	100	0
340 nm 1 min	78	22
340 nm 2 min	66	34
340 nm 5 min	53	47
340 nm 10 min	29	71
340 nm 30 min	17	83
450 nm 1 min	72	28
450 nm 2 min	72	28
450 nm 5 min	72	28

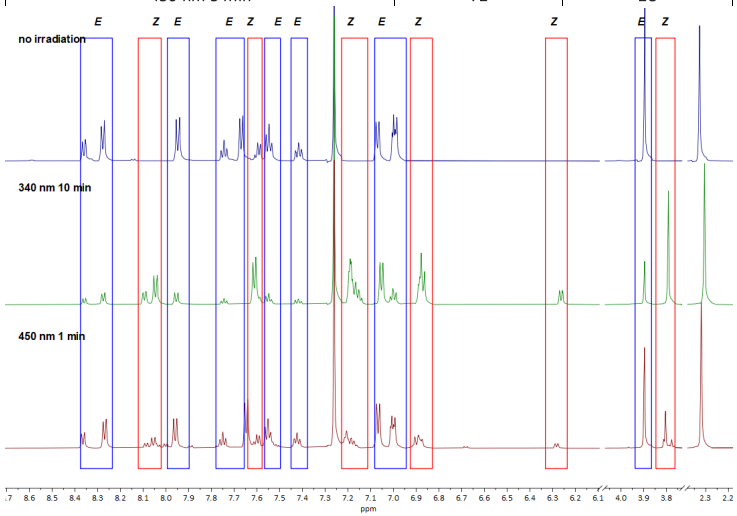

Figure S5. ^{1}H NMR spectra of **3a** in $CDCl_3$ under ambient conditions (top), PSS340 (middle) and PSS450 (bottom).

Upon irradiation with 340 nm for 30 min, the *Z* isomer was further enriched. However, decomposition of **3a** started to occur and free tosic acid became visible in the ^{1}H NMR spectrum, e.g. the broad singlet at 2.71 ppm (**Figure S6**).

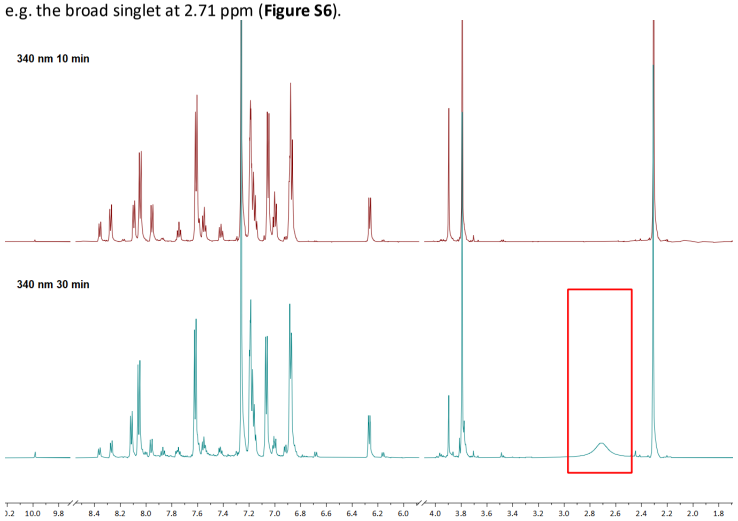

Figure S6. Comparison of ^{1}H NMR spectra of **3a** in $CDCl_3$ after irradiation with 340 nm for 10 min (top) and 30 min (bottom).

6.2 UV/vis Measurements

The sample concentration for the UV/vis measurements was approx. 0.1 µmol/mL. The samples were measured in $CHCl_3$.

1-(2-Iodophenyl)-2-phenyldiazene (1a)

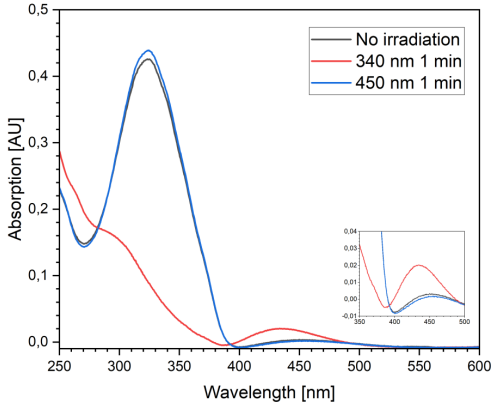

Figure S7. Absorption spectra of the **1a** without irradiation (black), of the PSS340 after irradiation for 1 min (red), and of the PSS450 after irradiation for 1 min (blue).

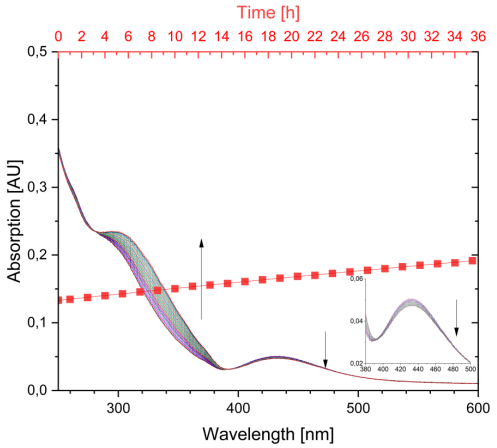

Figure S8. Thermal relaxation of **1a** after irradiation with 340 nm for 1min. The spectra were recorded with a delay of 30 min over the course of 36 h. Arrows indicate the change of absorption over time. The time profile of the thermal relaxation of the ππ* band (325 nm) is shown as red rectangles. This was used to determine the half-life time *via* an exponential fit to be 124.6 h.

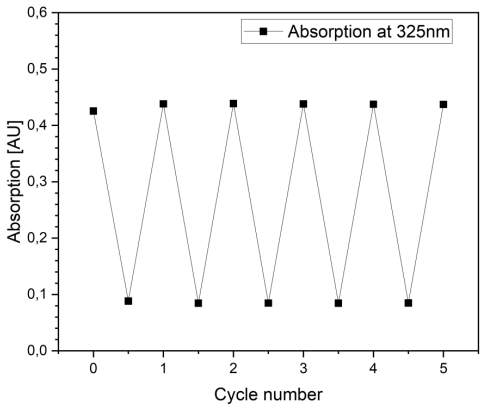

Figure S9. The stability of **1a** against photo-bleaching was tested by alternating switching between PSS340 and PSS450 in five cycles.

(4-Methoxyphenyl)(2-(phenyldiazenyl)phenyl)iodonium tosylate (3a)

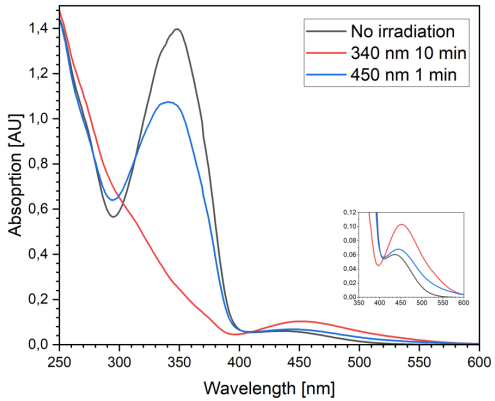

Figure S10. Absorption spectra of the **3a** without irradiation (black), of the PSS340 after irradiation for 10 min (red), and of the PSS450 after irradiation for 1 min (blue).

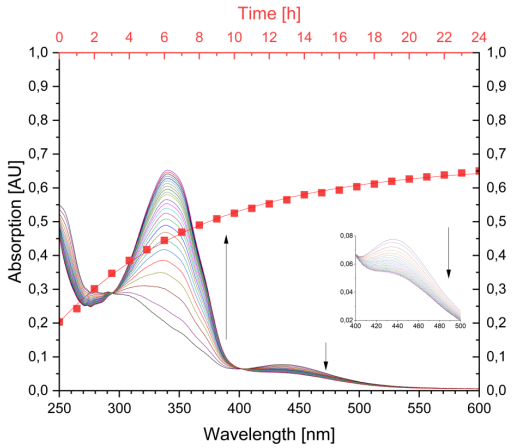

Figure S11. Thermal relaxation of **3a** after irradiation with 340 nm for 10min. The spectra were recorded with a delay of 60 min over the course of 24 h. Arrows indicate the change of absorption over time. The time profile of the thermal relaxation of the ππ* band (338 nm) is shown as red rectangles. This was used to determine the half-life time *via* an exponential fit to be 5.83 h.

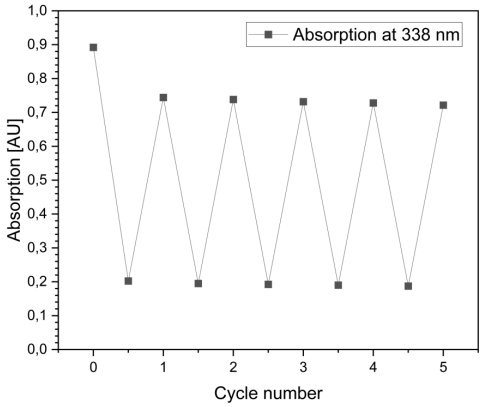

Figure S12. The stability of 3**a** against photo-bleaching was tested by alternating switching between PSS340 and PSS450 in five cycles.

7 Transition Metal-Free Arylations

7.1 Arylation with Oxygen Nucleophiles

(*E*)-1-(2-Phenoxyphenyl)-2-phenyldiazene (4)

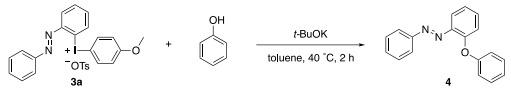

Following a reported procedure,[18] to a suspension of *t*-BuOK (1.2 equiv, 0.24 mmol, 27 mg) in anhydrous toluene (2.0 mL) was added phenol (1.2 equiv, 0.24 mmol, 22 mg) at 0 °C and the reaction was left to stir at this temperature for 15 min. Diaryliodonium salt **3a** (1.0 equiv, 0.20 mmol, 117 mg) was added in one portion, and the reaction was stirred at 40 °C for 2 h. The reaction was then quenched with H_2O at 0 °C, the organic phase was separated and the water phase was extracted with CH_2Cl_2 (3 × 10 mL). The combined organic phases were dried with Na_2SO_4, filtered and concentrated *in vacuo*. The crude material was purified by flash chromatography (silica, 1% of Et_2O in *n*-pentane) to give diaryl ether **4** as a red oil (0.15 mmol, 41 mg, 75% yield).

^{1}H NMR (400 MHz, $CDCl_3$) δ 7.78 (dd, *J* = 8.0, 1.7 Hz, 1H), 7.75 – 7.69 (m, 2H), 7.48 – 7.39 (m, 4H), 7.36 – 7.28 (m, 2H), 7.23 (ddd, *J* = 8.3, 7.2, 1.3 Hz, 1H), 7.17 (dd, *J* = 8.1, 1.3 Hz, 1H), 7.10 – 7.02 (m, 3H). ^{13}C{^{1}H} NMR (101 MHz, $CDCl_3$) δ 158.9, 154.6, 153.1, 144.3, 132.5, 131.2, 129.8, 129.1, 124.4, 123.2, 123.0, 121.5, 118.3, 117.5. HRMS(ESI) *m/z*: calcd. for $C_{18}H_{14}N_2ONa^+$ [M+Na]$^+$ 297.0998; found 297.0980. Analytical data were in accordance with those previously reported.[19]

(*E*)-2-(Phenyldiazenyl)phenyl benzoate (5)

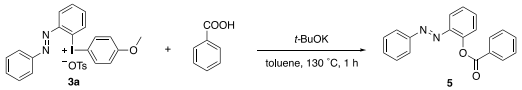

Following a reported procedure,[18] *t*-BuOK (1.2 equiv, 0.24 mmol, 27 mg) was dissolved in anhydrous toluene (2 mL). Benzoic acid (1.2 equiv, 0.24 mmol, 29 mg) and salt **3a** (1.0 equiv, 0.20 mmol, 117 mg) were added sequentially as solids. The flask was then heated to reflux in an oil bath for 1 h. The reaction mixture was diluted with CH_2Cl_2 (3 × 5 mL), washed with water (4 mL) and brine (4 mL), dried over magnesium sulfate and concentrated *in vacuo*. The crude material was purified by column chromatography (silica, 1% Et_2O in *n*-pentane) to yield aryl ester **5** as a red solid (0.16 mmol, 48 mg, 79% yield).

^{1}H NMR (400 MHz, $CDCl_3$) δ 8.31 – 8.24 (m, 2H), 7.89 (dd, *J* = 8.5, 1.6 Hz, 1H), 7.75 – 7.63 (m, 3H), 7.59 – 7.50 (m, 3H), 7.44 – 7.32 (m, 5H). ^{13}C{^{1}H} NMR (101 MHz, $CDCl_3$) δ 165.6, 152.8, 149.4, 144.1, 133.7, 132.2, 131.4, 130.5, 129.6, 129.1, 128.8, 126.7, 123.7, 123.2, 118.0. HRMS(ESI) *m/z*: calcd. for $C_{19}H_{14}N_2O_2Na^+$ [M+Na]$^+$ 325.0947; found 325.0941. Analytical data were in accordance with those previously reported.[20]

(*E*)-2-(Phenyldiazenyl)phenyl acetate (6)

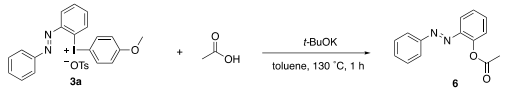

Following a reported procedure,[18] *t*-BuOK (1.2 equiv, 0.24 mmol, 27 mg) was dissolved in anhydrous toluene (2 mL). Acetic acid (1.2 equiv, 0.24 mmol, 14 µL) and salt **3a** (1.0 equiv, 0.20 mmol, 117 mg) were added sequentially as solids. The reaction was then refluxed in an oil bath for 1 h. The mixture was allowed to cool down to rt and diluted with CH_2Cl_2 (3 × 5 mL), washed with water (4 mL) and brine (4 mL), dried over magnesium sulfate and concentrated *in vacuo*. The crude material was purified by column chromatography (silica, 1% Et_2O in *n*-pentane) to yield aryl ester **6** as a red solid (0.14 mmol, 33 mg, 70% yield).

^{1}H NMR (400 MHz, $CDCl_3$) δ 7.89 – 7.84 (m, 2H), 7.82 (dd, *J* = 8.0, 1.6 Hz, 1H), 7.55 – 7.47 (m, 4H), 7.35 (ddd, *J* = 8.1, 7.3, 1.4 Hz, 1H), 7.26 – 7.23 (m, 1H), 2.40 (s, 3H). ^{13}C{^{1}H} NMR (101 MHz, $CDCl_3$) δ 169.7, 152.9, 149.1, 144.1, 132.2, 131.5, 129.2, 126.7, 123.5, 123.1, 117.8, 20.9. Analytical data were in accordance with those previously reported.[21]

(*E*)-2-(Phenyldiazenyl)phenol (7)

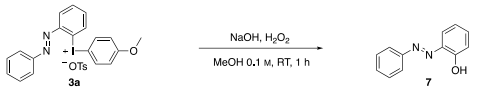

Following a reported procedure,[22] sodium hydroxide (2.0 equiv, 0.40 mmol, 16 mg) was added to a microwave vial, followed by the addition of methanol (1.0 mL). Hydrogen peroxide (2.1 equiv, 0.42 mmol, 20 µL) was added followed by diaryliodonium salt **3a** (1.0 equiv, 0.2 mmol, 117 mg). Additional methanol (1.0 mL) was added, and the reaction was stirred at rt for 1 h. The reaction was quenched with the addition of sat. $NH_4Cl_{(aq)}$ and extracted with EtOAc (3 × 10 mL). The organic phases were washed with brine, dried over magnesium sulfate and concentrated *in vacuo*. The crude was purified using flash chromatography (silica, silica, 1% Et_2O in *n*-pentane) to provide 2-hydroxyazobenzene **7** as a red solid (0.08 mmol, 15 mg, 38% yield) .

^{1}H NMR (400 MHz, $CDCl_3$) δ 12.92 (s, 1H), 7.96 (dd, *J* = 7.9, 1.7 Hz, 1H), 7.92 – 7.85 (m, 2H), 7.58 – 7.46 (m, 3H), 7.36 (ddd, *J* = 8.5, 7.2, 1.7 Hz, 1H), 7.12 – 7.01 (m, 2H). ^{13}C{^{1}H} NMR (101 MHz, $CDCl_3$) δ 152.9, 150.7, 137.5, 133.4, 133.4, 131.3, 129.5, 122.4, 120.1, 118.4. Analytical data were in accordance with those previously reported.[21]

Synthesis of 2-Hydroxyazobenzene (7) by Hydrolysis

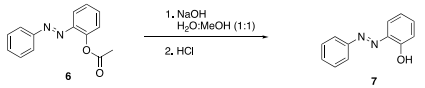

Following a reported procedure,[21] compound **6** (1.0 equiv, 0.14 mmol, 34 mg) and NaOH (10 equiv, 1.40 mmol, 56 mg) were added in a 5 mL vial followed by addition of 2 mL H_2O/MeOH (1:1). The reaction mixture was stirred vigorously at rt for 2 h. After this time, $HCl_{(aq)}$ (15 equiv, 2.10 mmol, 0.18 mL) was added to the mixture, and the reaction was stirred for additional 30 min. The orange product formed was filtered to obtain **7** (0.11 mmol, 23 mg, 81% yield).

^{1}H NMR (400 MHz, $CDCl_3$) δ 12.92 (s, 1H), 7.96 (dd, *J* = 7.9, 1.7 Hz, 1H), 7.92 – 7.85 (m, 2H), 7.58 – 7.46 (m, 3H), 7.36 (ddd, *J* = 8.5, 7.2, 1.7 Hz, 1H), 7.12 – 7.01 (m, 2H). $^{13}C\{^1H\}$ NMR (101 MHz, $CDCl_3$) δ 152.9, 150.7, 137.5, 133.4, 133.4, 131.3, 129.5, 122.4, 120.1, 118.4. Analytical data were in accordance with those previously reported.[21]

(*E*)-1,2-bis(2-Phenoxyphenyl)diazene (14)

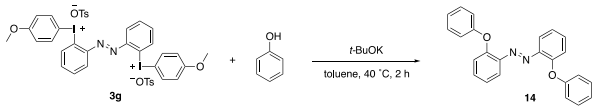

Following a reported procedure,[18] to a suspension of *t*-BuOK (2.1 equiv, 0.21 mmol, 24 mg) in anhydrous toluene (1.0 mL) was added phenol (2.1 equiv, 0.21 mmol, 20 mg) at 0 °C and the reaction was left to stir at this temperature for 15 min. Diaryliodonium salt **3g** (1.0 equiv, 0.10 mmol, 98 mg) was added in one portion and the reaction was stirred at 40 °C. After quenching with H_2O at 0 °C, the organic phase was separated, and the water phase was extracted with CH_2Cl_2 (3 × 10 mL). The combined organic phases were dried over Na_2SO_4, filtered, and concentrated *in vacuo*. The crude material was purified by flash chromatography (silica, 1% of Et_2O in *n*-pentane) to give diaryl ether **14** as a red oil (0.06 mmol, 21 mg, 57% yield).

^{1}H NMR (400 MHz, $CDCl_3$) δ 7.42 – 7.27 (m, 8H), 7.14 – 6.99 (m, 10H). $^{13}C\{^1H\}$ NMR (101 MHz, $CDCl_3$) δ 158.9, 154.6, 144.6, 132.5, 129.8, 124.3, 122.9, 121.3, 118.3, 117.8. HRMS(ESI) *m/z*: calcd. for $C_{24}H_{18}N_2O_2Na^+$ [M+Na]$^+$ 389.1260; found 389.1260. Analytical data were in accordance with those previously reported.[23]

Arylation of Estrone to give (8*R*,9*S*,13*S*,14*S*)-13-Methyl-3-(2-((*E*)-phenyldiazenyl)phenoxy)-6,7,8,9,11,12,13,14,15,16-decahydro-17*H*-cyclopenta[*a*]phenanthren-17-one (15)

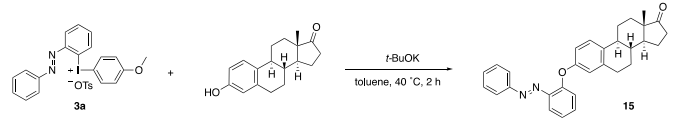

Following a reported procedure,[18] to a suspension of *t*-BuOK (1.2 equiv, 0.24 mmol, 27 mg) in anhydrous toluene (2.0 mL) was added estrone (1.2 equiv, 0.24 mmol, 65 mg) at 0 °C and the reaction was left to stir at this temperature for 15 min. Diaryliodonium salt **3a** (1.0 equiv, 0.20 mmol, 117 mg) was added in one portion, and the reaction was stirred at 40 °C. The reaction was then quenched with H_2O at 0 °C, the organic phase was separated, and the water phase was extracted with CH_2Cl_2 (3 × 10 mL). The combined organic phases were dried over sodium sulfate, filtered, and

concentrated *in vacuo*. The crude material was purified by flash chromatography (silica, 1% of Et_2O in *n*-pentane) to give diaryl ether **15** as a red sticky oil (0.12 mmol, 54 mg, 60% yield).

^{1}H NMR (400 MHz, $CDCl_3$) δ 7.80 – 7.73 (m, 2H), 7.47 – 7.39 (m, 3H), 7.25 – 7.17 (m, 2H), 7.14 (dd, *J* = 8.2, 1.3 Hz, 1H), 6.86 (dd, *J* = 8.5, 2.7 Hz, 1H), 6.81 (d, *J* = 2.7 Hz, 1H), 2.92 – 2.79 (m, 2H), 2.55 – 2.45 (m, 1H), 2.44 – 2.34 (m, 1H), 2.32 – 2.22 (m, 1H), 2.20 – 1.89 (m, 4H), 1.69 – 1.35 (m, 6H), 0.92 (s, 3H). $^{13}C\{^1H\}$ NMR (101 MHz, $CDCl_3$) δ 220.9, 156.5, 154.9, 153.1, 144.2, 138.3, 134.6, 132.4, 131.1, 129.0, 126.7, 123.9, 123.2, 121.1, 118.6, 117.4, 116.0, 50.6, 48.1, 44.2, 38.4, 36.0, 31.7, 29.6, 26.6, 26.0, 21.7, 14.0. HRMS(ESI) *m/z*: calcd. for $C_{30}H_{30}N_2O_2Na^+$ [M+Na]$^+$473.2199; found 473.2183.

Arylation of a Protected Ribose to give (*E*)-1-(2-(((4*R*,6*R*)-6-methoxy-2,2-dimethyltetrahydrofuro[3,4-*d*][1,3]dioxol-4-yl)methoxy)phenyl)-2-phenyldiazene (16)

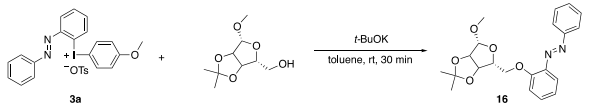

Following a reported procedure,[24] the protected ribose (1.0 equiv, 0.2 mmol, 41 mg) was stirred in a 5 mL screw-cap vial in toluene (2 mL) for 3 min. After this time, the mixture of salt **3a** (1.5 equiv, 0.30 mmol, 176 mg) and *t*-BuOK (1.5 equiv, 0.30 mmol, 34 mg) were added portion-wise under air. The reaction mixture was stirred for 30 min. The mixture was transferred to a round-bottom flask with EtOAc (3 x 5 mL), and celite was added. Then, the solvents were removed under reduced pressure and the residue was purified by column chromatography (silica, petroleum ether/EtOAc 4/1) to afford product **16** as a red oil (0.09 mmol, 34 mg, 44% yield).

^{1}H NMR (400 MHz, $CDCl_3$) δ 7.98 – 7.91 (m, 2H), 7.68 (dd, *J* = 8.0, 1.7 Hz, 1H), 7.55 – 7.38 (m, 4H), 7.13 (dd, *J* = 8.3, 1.3 Hz, 1H), 7.07 (ddd, *J* = 8.3, 7.3, 1.2 Hz, 1H), 5.02 (s, 1H), 4.94 (dd, *J* = 5.9, 1.0 Hz, 1H), 4.69 – 4.62 (m, 2H), 4.30 (dd, *J* = 9.8, 5.8 Hz, 1H), 4.20 (dd, *J* = 9.8, 8.7 Hz, 1H), 3.32 (s, 3H), 1.52 (s, 3H), 1.33 (s, 3H). $^{13}C\{^1H\}$ NMR (101 MHz, $CDCl_3$) δ 156.3, 153.2, 143.2, 132.4, 131.0, 129.2, 123.2, 122.1, 117.3, 116.6, 112.6, 109.7, 85.3, 84.6, 82.3, 71.3, 55.0, 26.6, 25.1. HRMS(ESI) *m/z*: calcd. for $C_{12}H_{24}N_2O_5Na^+$ [M+Na]$^+$407.1577; found 407.1576.

Protection of Cholic Acid (20)

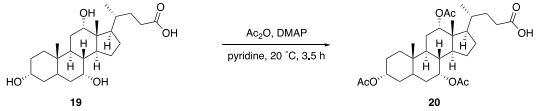

Following a reported procedure,[25] to a suspension of cholic acid **19** (1.0 equiv, 4.90 mmol, 2.0 g) in acetic anhydride (4 mL), pyridine (6 mL) and 4-methylaminopyridine (DMAP) (0.6 equiv, 2.94 mmol, 359 mg) were added. The reaction mixture was stirred at 20 °C for 3.5 h and after this time, the solvent was removed under reduced pressure. The mixture was diluted with diethyl ether (40 mL) and washed with a solution of HCl 1 M (3 x 30 mL), sat. $NaHCO_3$(aq) (2 x 30 mL) and brine (30 mL). The organic phase was dried over sodium sulfate, filtrated and concentrated under reduced pressure to obtain the protected cholic acid **20** as a colourless solid (4.64 mmol, 2.5 g, 95%).

^{1}H NMR (400 MHz, $CDCl_3$) δ 5.09 (m, 1H), 4.91 (m, 1H), 4.57 (m, 1H), 2.14 (s, 3H), 2.08 (s, 3H), 2.04 (s, 3H), 0.91 (s, 3H), 0.85 (s, 3H), 0.73 (s, 3H). Analytical data were in accordance with those previously reported.[25]

Arylation of the Protected Cholic Acid to give (3*R*,7*R*,8*R*,9*S*,10*S*,12*S*,13*R*,14*S*,17*R*)-10,13-Dimethyl-17-((*R*)-5-oxo-5-(2-((*E*)-phenyldiazenyl)phenoxy)pentan-2-yl)hexadecahydro-1*H*-cyclopenta[*a*]phenanthrene-3,7,12-triyl triacetate (17)

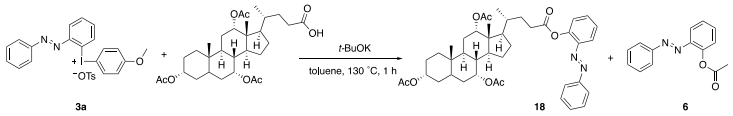

3a 18 6

Following a reported procedure,[18] *t*-BuOK (1.2 equiv, 0.24 mmol, 27 mg) was dissolved in anhydrous toluene (2 mL). Protected cholic acid (1.2 equiv, 0.24 mmol, 128 mg) and salt **3a** (1.0 equiv, 0.20 mmol, 117 mg) were added sequentially. The mixture was refluxed in an oil bath for 1 h. and after cooling down diluted with CH_2Cl_2 (3 × 5 mL), washed with water (4 mL) and brine (4 mL), dried over $MgSO_4$ and concentrated *in vacuo*. The crude material was purified by column chromatography (silica, 1% Et_2O in *n*-pentane) to yield aryl ester **17** (0.09 mmol, 66 mg, 46%) as a red solid. In addition, the side-product **6** (0.04 mmol, 9 mg, 20%) was isolated as a red solid.

^{1}H NMR (400 MHz, $CDCl_3$) δ 7.87 – 7.82 (m, 2H), 7.80 (dd, *J* = 8.1, 1.6 Hz, 1H), 7.53 – 7.45 (m, 4H), 7.34 (td, *J* = 7.4, 1.4 Hz, 1H), 7.22 (dd, *J* = 8.1, 1.4 Hz, 1H), 5.10 (t, *J* = 3.0 Hz, 1H), 4.94 – 4.87 (m, 1H), 4.63 – 4.52 (m, 1H), 2.77 – 2.66 (m, 1H), 2.63 – 2.51 (m, 1H), 2.14 (s, 3H), 2.08 (s, 3H), 2.04 (s, 3H), 2.01 – 1.19 (m, 22H), 1.17 – 1.00 (m, 3H), 0.92 (s, 3H), 0.70 (s, 3H). ^{13}C{^{1}H} NMR (101 MHz, $CDCl_3$) δ 172.7, 170.7,170.6, 170.5, 152.9, 149.2, 144.1, 132.2, 131.5, 129.2, 126.6, 123.4, 123.1, 117.6, 75.5, 74.2, 70.8, 47.6, 45.2, 43.6, 41.1, 37.9, 34.8, 34.8, 34.7, 34.5, 31.4, 31.0, 30.9, 29.0, 27.4, 27.0, 25.7, 23.0, 22.7, 21.7, 21.6, 21.6, 17.7, 12.3. HRMS(ESI) *m/z*: calcd. for $C_{42}H_{54}N_2O_8Na^+$ [M+Na]$^+$ 737.3772; found 737.3771.

Analytical data for product **6**
^{1}H NMR (400 MHz, $CDCl_3$) δ 7.89 – 7.84 (m, 2H), 7.82 (dd, *J* = 8.0, 1.6 Hz, 1H), 7.55 – 7.47 (m, 4H), 7.35 (ddd, *J* = 8.1, 7.3, 1.4 Hz, 1H), 7.26 – 7.23 (m, 1H), 2.40 (s, 3H). ^{13}C{^{1}H} NMR (101 MHz, $CDCl_3$) δ 169.7, 152.9, 149.1, 144.1, 132.2, 131.5, 129.2, 126.7, 123.5, 123.1, 117.8, 20.9. Analytical data were in accordance with those previously reported.[21]

Arylation of Oleic Acid to give 2-((*E*)-Phenyldiazenyl)phenyl (*E*)-octadec-9-enoate (18)

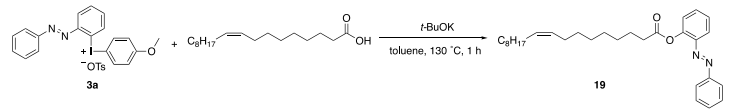

3a 19

Following a reported procedure,[18] *t*-BuOK (1.2 equiv, 0.24 mmol, 27 mg) was dissolved in anhydrous toluene (2 mL). Oleic acid (1.2 equiv, 0.24 mmol, 76 µL) and salt **3a** (1.0 equiv, 0.20 mmol, 117 mg) were added sequentially. The reaction mixture was refluxed in an oil bath for 1 h and after

cooling down to rt diluted with CH_2Cl_2 (3 × 5 mL), washed with water (4 mL) and brine (4 mL), dried over $MgSO_4$ and concentrated *in vacuo*. The crude material was purified by column chromatography (silica, 1% Et_2O in *n*-pentane) to yield aryl ester **18** as a red oil (0.07 mmol, 34 mg, 37% yield).

^{1}H NMR (400 MHz, $CDCl_3$) δ 7.89 – 7.83 (m, 2H), 7.80 (dd, *J* = 8.1, 1.6 Hz, 1H), 7.53 – 7.45 (m, 3H), 7.34 (ddd, *J* = 8.5, 7.3, 1.4 Hz, 1H), 7.24 (dd, *J* = 8.1, 1.3 Hz, 1H), 5.43 – 5.29 (m, 2H), 2.67 (t, *J* = 7.5 Hz, 2H), 2.02 (m, 4H), 1.81 (p, *J* = 7.5 Hz, 2H), 1.48 – 1.20 (m, 22H), 0.94 – 0.83 (m, 3H). ^{13}C{^{1}H} NMR (101 MHz, $CDCl_3$) δ 172.4, 153.0, 149.2, 144.3, 132.1, 131.4, 130.2, 129.9, 129.2, 128.6, 126.6, 123.6, 123.2, 117.6, 34.3, 32.0, 29.9, 29.9, 29.7, 29.5, 29.4, 29.2, 27.3, 25.2, 22.8, 14.3. HRMS(ESI) *m/z*: calcd. for $C_{30}H_{42}N_2O_2Na^+$ [M+Na]$^+$ 485.3138; found 485.3134.

7.2 Arylation of Sulfur Nucleophiles

(*E*)-2-((2-(Phenyldiazenyl)phenyl)thio)benzo[*d*]thiazole (8)

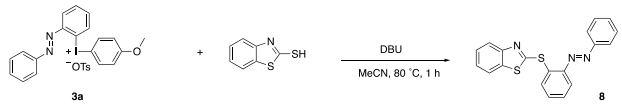

3a 8

Following a reported procedure,[26] a microwave vial was charged with mercaptothiazole (1.0 equiv, 0.20 mmol, 33 mg) and diaryliodonium salt **3a** (1.1 equiv, 0.22 mmol, 129 mg) caped and evacuated/backfilled with argon three times. Anhydrous acetonitrile (2.0 mL) was added followed by 1,8-diazabicyclo 5.4.0 undec-7-ene (DBU, 1.1 equiv, 0.22 mmol, 33 µL). The reaction was stirred for 1 h at 80 °C. After the reaction was cooled down to rt, a small amount of silica was added. Volatiles were removed *in vacuo* and the on silica absorbed crude loaded onto a silica column., The product was purified by column chromatography (silica, 1% Et_2O in *n*-pentane) to obtain the product **8** as a red oil (0.19 mmol, 65 mg, 93% yield).

^{1}H NMR (400 MHz, $CDCl_3$) δ 7.95 (dt, *J* = 8.2, 0.9 Hz, 1H), 7.91 – 7.86 (m, 2H), 7.84 (dd, *J* = 7.9, 1.6 Hz, 1H), 7.79 (dd, *J* = 7.6, 1.5 Hz, 1H), 7.68 (dt, *J* = 7.5, 0.8 Hz, 1H), 7.57 – 7.39 (m, 6H), 7.30 (ddd, *J* = 8.2, 7.2, 1.2 Hz, 1H). ^{13}C{^{1}H} NMR (101 MHz, $CDCl_3$) δ 167.2, 153.8, 152.7, 151.8, 136.4, 134.4, 132.4, 131.8, 131.8, 130.3, 129.3, 126.3, 124.9, 123.5, 122.5, 121.1, 118.2. HRMS(ESI) *m/z*: calcd. for $C_{19}H_{13}N_3S_2Na^+$ [M+Na]$^+$ 370.0443; found 370.0433.

2-((*E*)-Phenyldiazenyl)phenyl (*Z*)-*N*-benzylbenzimidothioate (9)

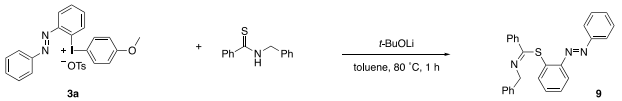

3a 9

Following a reported procedure,[27] thioamide (1.0 equiv, 0.20 mmol, 45 mg), the diaryliodonium salt **3a** (1.1 equiv, 0.22 mmol, 129 mg) and *t*-BuOLi (1.1 equiv, 0.22 mmol, 18 mg) were weighed into an oven dried 4 mL microwave vial. The reaction was sealed with a metal cap, evacuated, and backfilled with argon three times. The solids were dissolved in degassed anhydrous toluene (1 mL) under argon and the mixture was stirred at 80 °C for 1 h. The reaction mixture was purified by

column chromatography (silica, 10% Et_2O in *n*-pentane) to obtain product **9** as a red oil (0.04 mmol, 17 mg, 21% yield).

^{1}H NMR (400 MHz, $CDCl_3$) δ 7.94 – 7.88 (m, 2H), 7.65 – 7.58 (m, 2H), 7.58 – 7.37 (m, 9H), 7.35 – 7.31 (m, 1H), 7.28 – 7.24 (m, 2H), 7.22 – 7.17 (m, 1H), 7.17 – 7.10 (m, 2H), 5.15 (s, 2H). ^{13}C{^{1}H} NMR (101 MHz, $CDCl_3$) δ 162.1, 152.7, 150.8, 139.9, 138.5, 134.7, 133.6, 131.6, 131.1, 129.8, 129.2, 129.2, 128.6, 128.5, 128.1, 127.9, 126.9, 123.5, 117.1, 59.0. HRMS(ESI) *m/z*: calcd. for $C_{26}H_{21}N_3SNa^+$ $[M+Na]^+$ 408.1529; 408.1524.

7.3 Arylation of Carbon Nucleophiles

Ethyl-(*E*)-2-nitro-2-(2-(phenyldiazenyl)phenyl)propanoate (10)

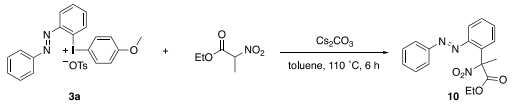

Following a reported procedure,[28] ethyl-2-nitropropanoate (1.0 equiv, 0.20 mmol, 29 mg), and Cs_2CO_3 (1.2 equiv, 0.24 mmol, 78 mg) were added to an oven-dry microwave vial. Anhydrous toluene (1.5 mL) was added to the vial at 0 °C and the solution was stirred at rt for 10 min. Diaryliodonium salt **3a** (1.0 equiv, 0.20 mmol, 117 mg) was then added to the reaction mixture at rt open to air. The reaction mixture was stirred at rt for 1 h followed by 6 h at 110 °C. After cooling to rt, the reaction mixture was quenched with brine (4 mL) and extracted CH_2Cl_2 (3 × 5 mL), washed with water (4 mL) and brine (4 mL), dried over $MgSO_4$ and concentrated *in vacuo*. The crude was purified by flash column chromatography (silica, 1% Et_2O in pentane) to afford the propanoate **10** as a red oil (0.09 mmol, 29 mg, 45% yield).

^{1}H NMR (400 MHz, $CDCl_3$) δ 7.93 – 7.89 (m, 1H), 7.84 – 7.78 (m, 2H), 7.57 – 7.47 (m, 5H), 7.40 – 7.36 (m, 1H), 4.22 (q, *J* = 7.1 Hz, 2H), 2.36 (s, 3H), 1.16 (t, *J* = 7.1 Hz, 3H). ^{13}C{^{1}H} NMR (101 MHz, $CDCl_3$) δ 167.5, 152.6, 148.9, 135.5, 131.9, 131.4, 130.4, 129.4, 126.8, 123.9, 116.2, 95.4, 63.2, 25.8, 13.9. HRMS(ESI) *m/z*: calcd. for $C_{17}H_{17}N_3O_4Na^+$ $[M+Na]^+$ 350.1111; found 350.1109.

7.4 Arylation of Nitrogen Nucleophiles

(*E*)-2-(Phenyldiazenyl)-*N*-(3-phenylpropyl)aniline (11)

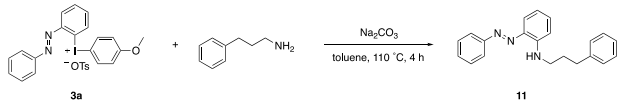

Following a reported procedure,[29] diaryliodonium salt **3a** (1.00 equiv, 200 µmol, 113 mg) and Na_2CO_3 (1.1 equiv, 0.22 mmol, 23 mg) were added to an oven-dried microwave vial and sealed with a cap. The vial was evacuated and backfilled with argon three times. Freshly distilled 3-phenylpropan-1-amine (1.1 equiv, 0.22 mmol, 31 µL) was added, followed by the addition of anhydrous and degassed toluene (1 mL). The mixture was stirred at 110 °C for 4 h and after

completion of the reaction, the mixture was diluted with CH_2Cl_2 (3 × 5 mL), washed with water (4 mL) and brine (4 mL), dried over magnesium sulfate and concentrated *in vacuo*. The crude material was purified by column chromatography (silica, 1% Et_2O in pentane) to yield the aniline product **11** as a red oil (0.04 mmol, 14 mg, 22% yield).

^{1}H NMR (400 MHz, $CDCl_3$) δ 9.03 (s, 1H), 7.87 (dd, *J* = 8.0, 1.7 Hz, 1H), 7.84 – 7.79 (m, 2H), 7.53 – 7.46 (m, 2H), 7.43 – 7.36 (m, 1H), 7.34 – 7.27 (m, 3H), 7.25 – 7.18 (m, 3H), 6.82 – 6.71 (m, 2H), 3.36 – 3.28 (m, 2H), 2.85 – 2.77 (m, 2H), 2.13 – 2.02 (m, 2H). ^{13}C{^{1}H} NMR (101 MHz, $CDCl_3$) δ 153.0, 143.4, 141.5, 136.2, 132.8, 132.0, 129.7, 129.2, 128.6, 128.6, 126.2, 122.0, 115.7, 111.9, 42.0, 33.5, 30.8. HRMS(ESI) *m/z*: calcd. for $C_{21}H_{21}N_3Na^+$ $[M+Na]^+$ 338.1628; found 338.1624.

(*E*)-*N*-Phenyl-*N*-(2-(phenyldiazenyl)phenyl)acetamide (12)

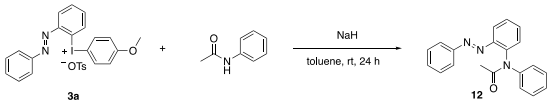

Following a reported procedure,[30] acetanilide (1.0 equiv, 0.20 mmol, 27 mg), diaryliodonium salt **3a** (1.5 equiv, 0.30 mmol, 176 mg) and NaH (60%, 1.5 equiv, 0.30 mmol, 12 mg) were added to a dry 5 mL microwave vial, which was capped. The vial was evacuated and backfilled with nitrogen three times. Stirring was started and anhydrous toluene (4 mL) added. *NB: Gas evolved.* The solution was stirred at ambient temperature for 24 h. *NB: It is important that the stirring is vigorous*. The reaction mixture was diluted with CH_2Cl_2 (3 × 5 mL), washed with water (4 mL) and brine (4 mL), dried over magnesium sulfate and concentrated *in vacuo*. The crude was purified by column chromatography (silica, 1% Et_2O in pentane) to yield product **12** as a red oil (0.16 mmol, 50 mg, 79% yield).

^{1}H NMR (500 MHz, $CDCl_3$, 298 K) δ 7.94 – 7.88 (m, 2H, rotamer A), 7.83 (dd, *J* = 8.0, 1.6 Hz, 1H, rotamer B), 7.54 – 7.47 (m, 4H), 7.46 – 7.39 (m, 2H), 7.38 – 7.28 (m, 5H), 7.19 (t, *J* = 7.2 Hz, 1H), 2.12 (s, 3H, rotamer B), 2.05 (s, 3H, rotamer A). ^{13}C{^{1}H} NMR (126 MHz, $CDCl_3$) δ 171.0, 153.1, 142.4, 132.2, 131.8, 130.0, 129.4, 129.2, 128.9, 128.6, 128.3, 127.3, 126.6, 123.4, 117.4, 30.6, 23.6. HRMS(ESI) *m/z*: calcd. for $C_{20}H_{17}N_3ONa^+$ $[M+Na]^+$ 338.1264; found 338.1262. The product is previously reported,[31] but comparison of the NMR data is complicated by the the restricted rotation around the C-N bond causing tertiary amides to exist as rotamers. For this compound, the presence of rotamers caused the peaks broadening at ambient temperature. Therefore, the ^{1}H- and ^{13}C-NMR were recorded at 263 K, 298 K and 323 K in both $CDCl_3$ and DMSO-d_6. In the spectra, peaks of the methyl group are consistent with varying degrees of restricted rotation of the amide group. When the ^{1}H-NMR spectra were recorded in $CDCl_3$, the two rotamers were established to be in a 1:7 ratio (**Figure S3**). Instead, it was established that these peaks coalesce when recording the ^{1}H (**Figure S3**, above) and ^{13}C NMR spectra (**Figure S3**, below), going from 263 K to 323 K in DMSO-d_6.

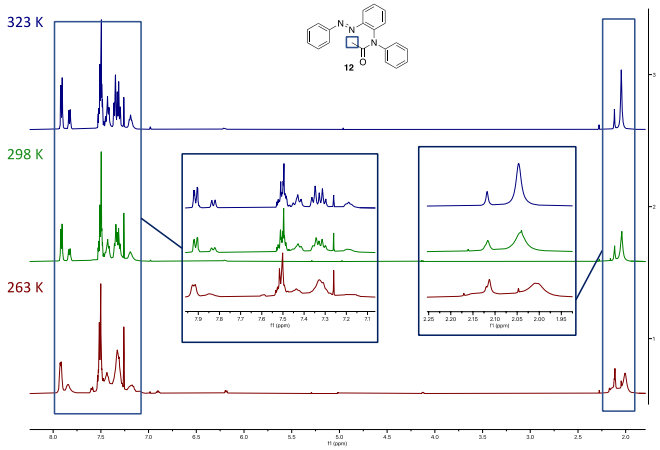

Figure S13. ^{1}H NMR spectra of amide **11** from 263 K to 323 K in $CDCl_3$.

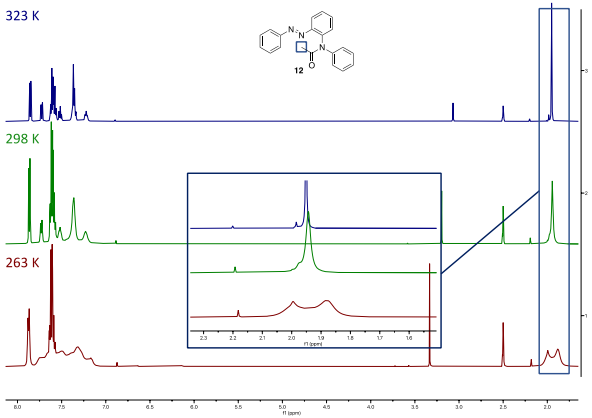

Figure S14. ^{1}H NMR spectra of amide **11** from 263 K to 323 K in DMSO-d_6.

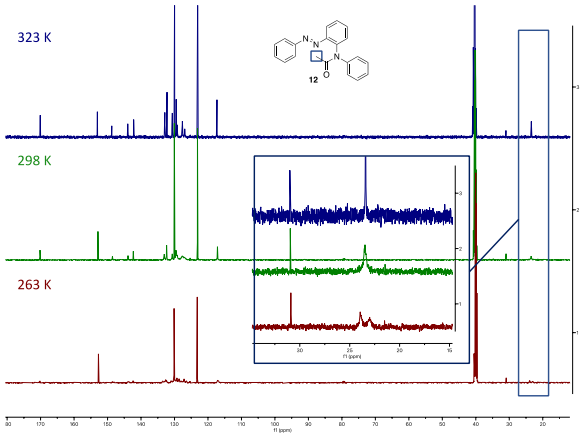

Figure S15. ^{13}C NMR spectra of amide **11** from 263 K to 323 K in DMSO-d_6.

(*E*)-1-(2-Nitrophenyl)-2-phenyldiazene (13)

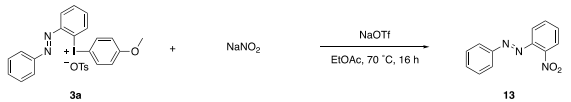

Following a reported procedure,[32] diaryliodonium salt **3a** (1.0 equiv, 0.20 mmol, 117 mg), sodium nitrite (1.1 equiv, 0.22 mmol, 15 mg) and sodium triflate (1.0 equiv, 0.20 mmol, 34 mg) were added to a microwave vial followed by EtOAc (1 mL). The vial was capped, and the solution was stirred at 70 °C for 16 h. The solvent was evaporated, and the crude was loaded onto silica and purified by flash chromatography (silica, 1% of Et_2O in *n*-pentane) to yield product **13** as a red oil (0.13 mmol, 29 mg, 63% yield).

^{1}H NMR (400 MHz, $CDCl_3$) δ 8.00 – 7.93 (m, 3H), 7.74 – 7.67 (m, 2H), 7.63 – 7.53 (m, 4H). $^{13}C\{^{1}H\}$ NMR (101 MHz, $CDCl_3$) δ 152.6, 147.6, 145.6, 133.2, 132.5, 130.6, 129.4, 124.2, 123.8, 118.6. HRMS(ESI) *m/z*: calcd for $C_{12}H_9N_3O_2Na^+$ $[M+Na]^+$ 250.0587; found 250.0590. Analytical data were in accordance with those previously reported.[33]

7.5 Comparison with Literature Methods for Synthesis of Products 4-7 and 12-14

To evaluate the efficiency of the presented methodology, a comparison with reported routs to the know products **4-7** and **12-14** are given below.

Product 4: Previously obtained through an oxidative coupling from the corresponding aniline (a Mills reaction), no yield was reported (**Scheme S4**).[19] In a similar manner, the product was later obtained in 48% yield.[23] Yield with our method: 75% from **3a**.

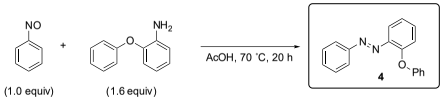

Scheme S4. Synthesis of product **4**.

Product 5: Previously obtained in 82% yield through a Pd-catalyzed *ortho*-functionalization of azoarenes (**Scheme S5**).[20] Yield with our method: 79% from **3a**.

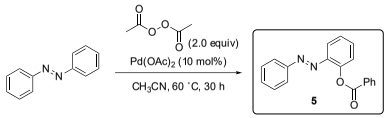

Scheme S5. Synthesis of product **5**.

Product 6: Previously synthesized *via* a Pd-catalyzed C-H acetoxylation of azobenzene with (diacetoxyiodo)benzene to give **6** in excellent yield using expensive hexafluoroisopropanol (HFIP) as solvent (**Scheme S6a**).[21] The synthesis of product **6** was also attempted *via* Pd-catalyzed *ortho*-functionalization of azoarenes with acylperoxides used in the synthesis of **5** (above) but the product could not be detected (**Scheme S6b**).[20] Yield with our method: 70% from **3a**.

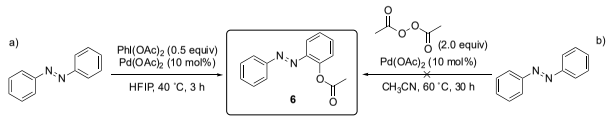

Scheme S6. Methodologies for the synthesis of product **6**.

Product 7: Several methods are reported for the synthesis of product **7**. Despite the traditional approach of a Mills reaction,[34] it was obtained in 42% yield as side product in a reaction with iodoazobenzene and stoichiometric amount of copper salt (**Scheme S7a**).[35] Alternatively, it could be obtained by hydrolysis of product **5**, formed through Pd-catalyzed detailed above (75% from azobenzene over two steps) (**Scheme S7b**).[20] Moreover, a Pd-catalyzed hydroxylation of azoarenes delivered **7** in 61% yield upon heating to 80 °C for prolonged time (**Scheme S7c**).[36] Finally, a Pd-catalyzed oxidation using excess PIFA in the toxic solvent DCE gave **7** in 81% (**Scheme S7d**).[37] Yield with our method: 81% from **6** (57% over two steps from **3a**); 38% directly from **3a**.

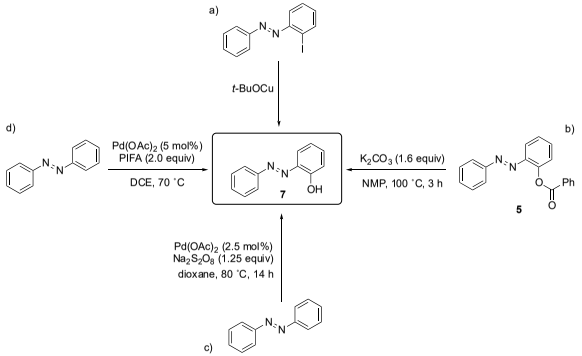

Scheme S7. Methodologies for the synthesis of product **7**.

Product 12: A copper(II)-catalyzed dehydrogenation amidation of azoarenes was used to synthetize the azobenzene amide **12** in 56% yield.[31] The protocol required extended heating to 120 °C in toxic benzene, in a pressurized reaction vessel (bp of benzene = 80 °C) (**Scheme S8**). Yield with our method: 79% from **3a**.

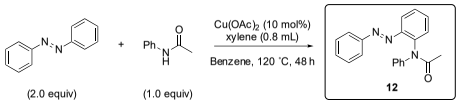

Scheme S8. Cu(II)-catalyzed amidation to obtain product **12**.

Product 13: Previously obtained in 72% yield *via* a Pd-catalyzed C-H functionalization of azobenzene in presence of tetrabutyl ammonium bromide (TBAB) upon heating to 80 °C in chlorobenzene for 24 h (**Scheme S9**)[33] or by traditional Mills reaction in 77-81% yield.[38] Yield with our method: 63% from **3a**.

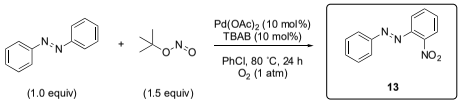

Scheme S9. Pd-catalyzed nitration to obtain product **13**.

Product 14: Previously obtained in only 8% yield through an oxidative coupling from the corresponding aniline (**Scheme S10**).[23] Yield with our method: 57% from **3h**.

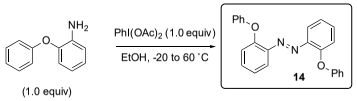

Scheme S10. Pd-catalyzed nitration to obtain product **14**.

In summary, a range of Pd-catalyzed methods have previously been reported to reach target products **5-7** and **13**, whereas Cu-catalysis was employed to reach product **12**. Finally, metal-free oxidative couplings from pre-functionalized anilines have been employed to obtain products **4**, **7**, **13** and **14** in differing yields.

The majority of the methods require a transition metal catalyst, prolonged heating and/or a toxic solvent. Furthermore, nitroso compounds are not always stable. While our methodology cannot always compete in terms of yield, it is a mild and transition metal-free method to reach the target products, as well as several novel structures with a variety of O, S, and N-functional groups.

8 References

[1] B. S. A. I. F. Vogel, A. J. Hannaford, V. Rogers, P. W. G. Smith, A. R. Tatchell, *Vogel's Textbook of Practical Organic Chemistry, 4th ed.*, **1978**.

[2] O. V. Dolomanov, L. J. Bourhis, R. J. Gildea, J. A. K. Howard, H. Puschmann, *J. Appl. Cryst.* **2009**, *42*, 339-341.

[3] G. M. Sheldrick, *Acta Cryst.* **2015**, *A71*, 3-8.

[4] G. M. Sheldrick, *Acta Cryst.* **2015**, *C71*, 3-8.

[5] J. Strueben, M. Lipfert, J. O. Springer, C. A. Gould, P. J. Gates, F. D. Sonnichsen, A. Staubitz, *Chem. Eur. J* **2015**, *21*, 11165-11173.

[6] W.-S. Yong, S. Park, H. Yun, P. H. Lee, *Adv. Synth. Catal.* **2016**, *358*, 1958-1967.

[7] L. D. Shirtcliff, T. J. R. Weakley, M. M. Haley, F. Köhler, R. Herges, *J. Org. Chem.* **2004**, *69*, 6979-6985.

[8] J. Hoffmann, T. J. Kuczmera, E. Lork, A. Staubitz, *Molecules* **2019**, *24*.

[9] A. Sadatnabi, N. Mohamadighader, D. Nematollahi, *Org. Lett.* **2021**, *23*, 6488-6493.

[10] (a) M. Zhu, N. Jalalian, B. Olofsson, *Synlett* **2008**, *2008*, 592-596.(b) M. Bielawski, M. Zhu, B. Olofsson, *Adv. Synth. Catal.* **2007**, *349*, 2610-2618.(c) M. Bielawski, B. Olofsson, *Chem. Commun.* **2007**, 2521-2523.

[11] M. Bielawski, D. Aili, B. Olofsson, *J. Org. Chem* **2008**, *73*, 4602-4607.

[12] E. A. Merritt, V. M. T. Carneiro, L. F. Silva, B. Olofsson, *J. Org. Chem.* **2010**, *75*, 7416-7419.

[13] E. Lindstedt, M. Reitti, B. Olofsson, *J. Org. Chem.* **2017**, *82*, 11909-11914.

[14] T. L. Seidl, S. K. Sundalam, B. McCullough, D. R. Stuart, *J. Org. Chem.* **2016**, *81*, 1998-2009.

[15] L. Qin, B. Hu, K. D. Neumann, E. J. Linstad, K. McCauley, J. Veness, J. J. Kempinger, S. G. DiMagno, *Eur. J. Org. Chem.* **2015**, *2015*, 5919-5924.

[16] M. J. Frisch, G. W. Trucks, H. B. Schlegel, G. E. Scuseria, M. A. Robb, J. R. Cheeseman, G. Scalmani, V. Barone, G. A. Petersson, H. Nakatsuji, X. Li, M. Caricato, A. V. Marenich, J. Bloino, B. G. Janesko, R. Gomperts, B. Mennucci, H. P. Hratchian, J. V. Ortiz, A. F. Izmaylov, J. L. Sonnenberg, Williams, F. Ding, F. Lipparini, F. Egidi, J. Goings, B. Peng, A. Petrone, T. Henderson, D. Ranasinghe, V. G. Zakrzewski, J. Gao, N. Rega, G. Zheng, W. Liang, M. Hada, M. Ehara, K. Toyota, R. Fukuda, J. Hasegawa, M. Ishida, T. Nakajima, Y. Honda, O. Kitao, H. Nakai, T. Vreven, K. Throssell, J. A. Montgomery Jr., J. E. Peralta, F. Ogliaro, M. J. Bearpark, J. J. Heyd, E. N. Brothers, K. N. Kudin, V. N. Staroverov, T. A. Keith, R. Kobayashi, J. Normand, K. Raghavachari, A. P. Rendell, J. C. Burant, S. S. Iyengar, J. Tomasi, M. Cossi, J. M. Millam, M. Klene, C. Adamo, R. Cammi, J. W. Ochterski, R. L. Martin, K. Morokuma, O. Farkas, J. B. Foresman, D. J. Fox, Wallingford, CT, **2016**.

[17] Y. Zhao, D. G. Truhlar, *Theor. Chem. Acc.* **2008**, *120*, 215-241.

[18] N. Jalalian, T. B. Petersen, B. Olofsson, *Chem. Eur. J.* **2012**, *18*, 14140-14149.

[19] Z. Wang, Z. Yin, F. Zhu, Y. Li, X.-F. Wu, *ChemCatChem* **2017**, *9*, 3637-3640.

[20] C. Qian, D. Lin, Y. Deng, X.-Q. Zhang, H. Jiang, G. Miao, X. Tang, W. Zeng, *Org. Biomol. Chem.* **2014**, *12*, 5866-5875.

[21] X. Fu, Z. Wei, C. Xia, C. Shen, J. Xu, Y. Yang, K. Wang, P. Zhang, *Catalysis Letters* **2017**, *147*, 400-406.

[22] M. Reitti, R. Gurubrahamam, M. Walther, E. Lindstedt, B. Olofsson, *Org. Lett.* **2018**, *20*, 1785-1788.

[23] S. Mehrparvar, Z. N. Scheller, C. Wölper, G. Haberhauer, *J. Am. Chem. Soc.* **2021**, *143*, 19856-19864.

[24] G. L. Tolnai, U. J. Nilsson, B. Olofsson, *Angew. Chem. Int. Ed.* **2016**, *55*, 11226-11230.

[25] R. Thakare, H. Gao, R. E. Kosa, Y.-A. Bi, M. V. S. Varma, M. A. Cerny, R. Sharma, M. Kuhn, B. Huang, Y. Liu, A. Yu, G. S. Walker, M. Niosi, L. Tremaine, Y. Alnouti, A. D. Rodrigues, *Drug Metab. Dispos.* **2017**, *45*, 721-733.
[26] S. Sarkar, N. Wojciechowska, A. A. Rajkiewicz, M. Kalek, *Eur. J. Org. Chem.* **2022**, *2022*, e202101408.
[27] P. Villo, G. Kervefors, B. Olofsson, *Chem. Commun.* **2018**, *54*, 8810-8813.
[28] C. Dey, E. Lindstedt, B. Olofsson, *Org. Lett.* **2015**, *17*, 4554-4557.
[29] N. Purkait, G. Kervefors, E. Linde, B. Olofsson, *Angew. Chem. Int. Ed.* **2018**, *57*, 11427-11431.
[30] F. Tinnis, E. Stridfeldt, H. Lundberg, H. Adolfsson, B. Olofsson, *Org. Lett.* **2015**, *17*, 2688-2691.
[31] G. Li, X. Chen, X. Lv, C. Jia, P. Gao, Y. Wang, S. Yang, *Science China Chemistry* **2018**, *61*, 660-663.
[32] M. Reitti, P. Villo, B. Olofsson, *Angew. Chem. Int. Ed.* **2016**, *55*, 8928-8932.
[33] Y.-F. Liang, X. Li, X. Wang, Y. Yan, P. Feng, N. Jiao, *ACS Catal.* **2015**, *5*, 1956-1963.
[34] (a) S. Steinwand, T. Halbritter, D. Rastadter, J. M. Ortiz-Sanchez, I. Burghardt, A. Heckel, J. Wachtveitl, *Chem. Eur. J.* **2015**, *21*, 15720-15731. (b) R. Bosma, N. C. Dijon, Y. Zheng, H. Schihada, N. J. Hauwert, S. Shi, M. Arimont, R. Riemens, H. Custers, A. van de Stolpe, H. F. Vischer, M. Wijtmans, N. D. Holliday, D. W. D. Kuster, R. Leurs, *iScience* **2022**, *25*, 104882.
[35] P. V. Roling, *J. Org. Chem.* **1975**, *40*, 2421-2425.
[36] K. Seth, M. Nautiyal, P. Purohit, N. Parikh, A. K. Chakraborti, *Chem. Commun.* **2015**, *51*, 191-194.
[37] T. H. L. Nguyen, N. Gigant, S. Delarue-Cochin, D. Joseph, *J. Org. Chem.* **2016**, *81*, 1850-1857.
[38] (a) H. Wettach, F. Pasker, S. Höger, *Macromolecules* **2008**, *41*, 9513-9515.(b) T. V. Nykaza, T. S. Harrison, A. Ghosh, R. A. Putnik, A. T. Radosevich, *J. Am. Chem. Soc.* **2017**, *139*, 6839-6842.(c) T. Wirtanen, E. Rodrigo, S. R. Waldvogel, *Chem. Eur. J.* **2020**, *26*, 5592-5597.

9 ^{1}H- and ^{13}C-NMR Spectra

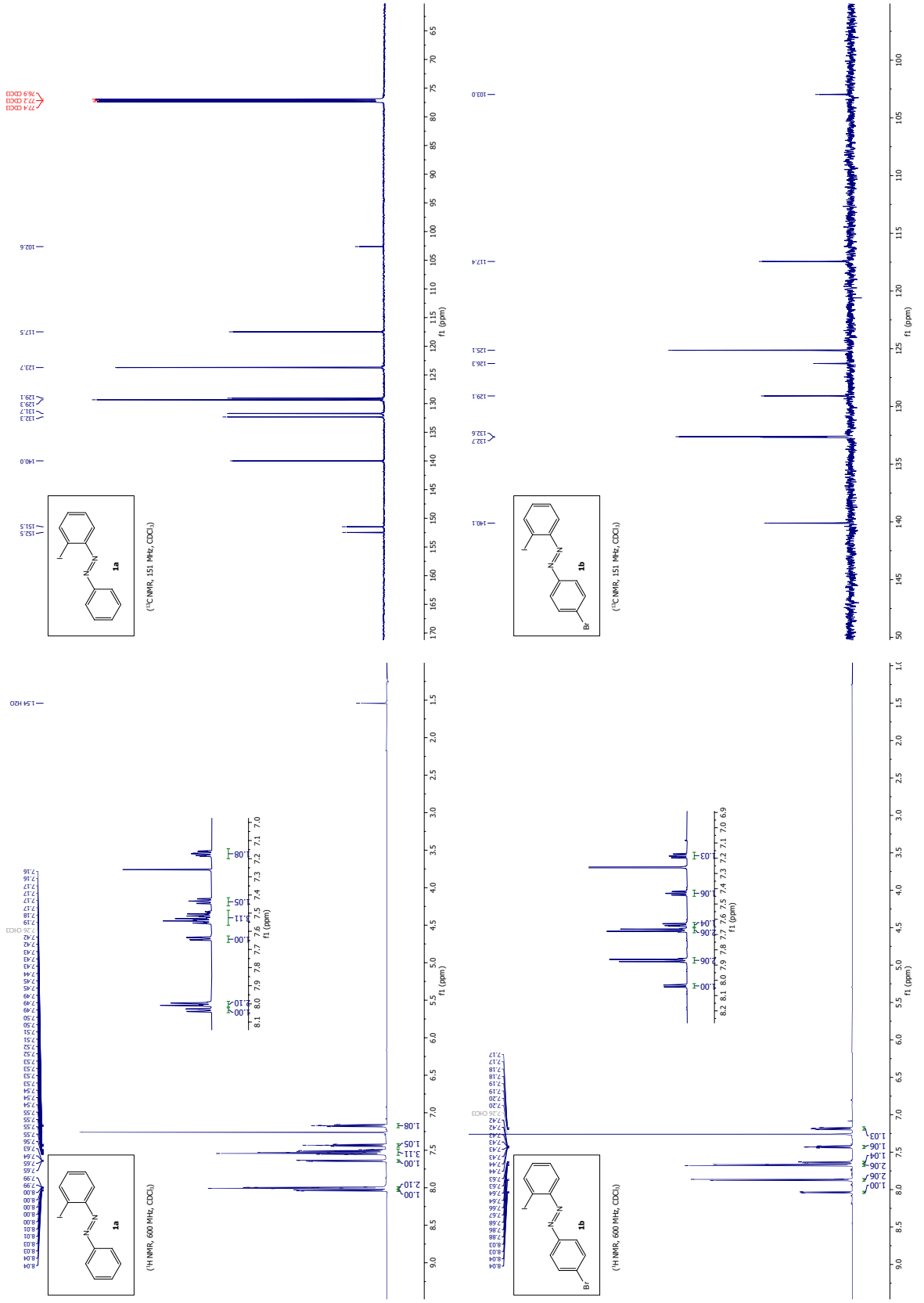
1a
1b
Br
(^{13}C NMR, 151 MHz, $CDCl_3$)
(^{1}H NMR, 600 MHz, $CDCl_3$)
f1 (ppm)

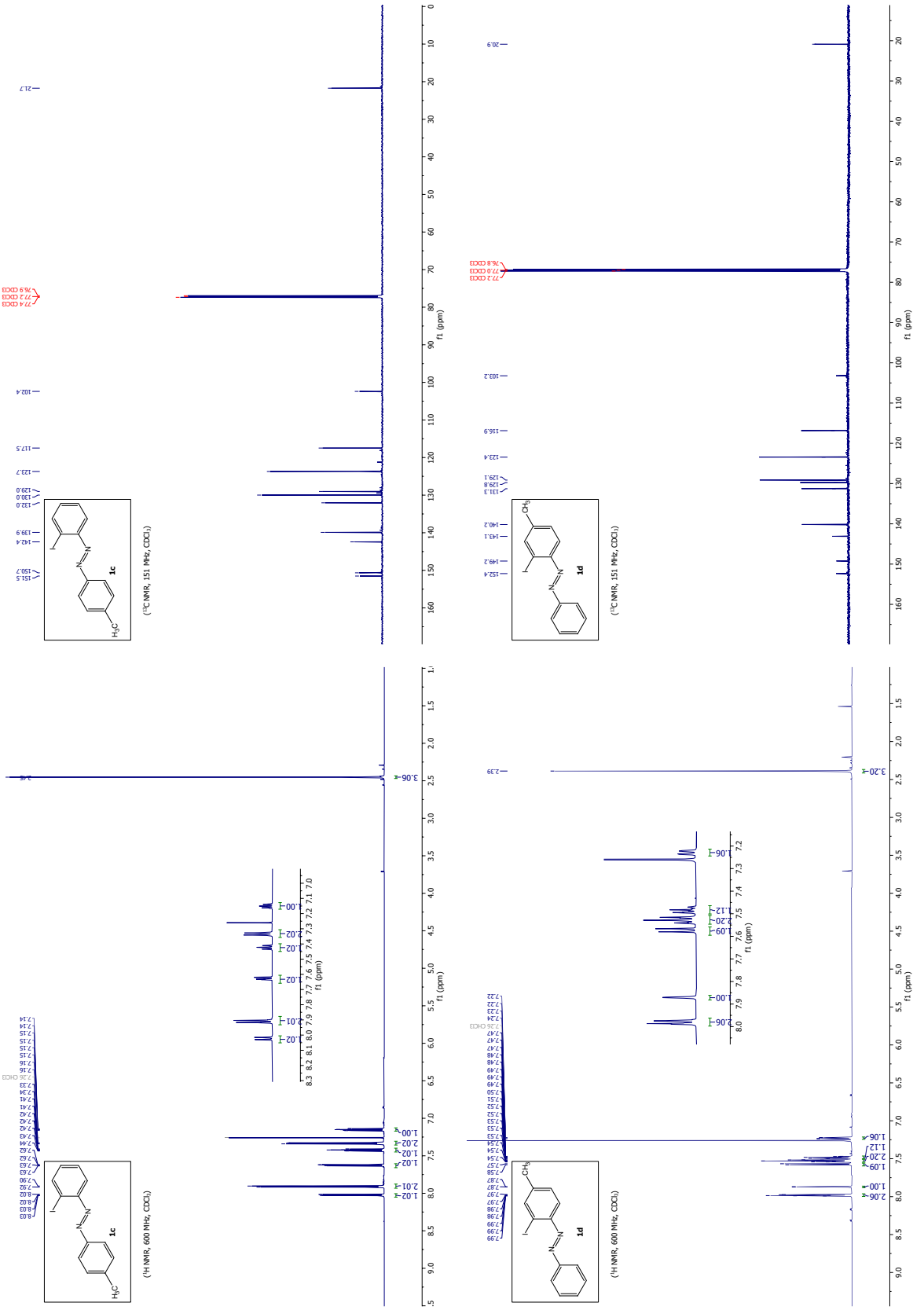
1c
(^{13}C NMR, 151 MHz, $CDCl_3$)
1d
(^{13}C NMR, 151 MHz, $CDCl_3$)
1c
(^{1}H NMR, 600 MHz, $CDCl_3$)
1d
(^{1}H NMR, 600 MHz, $CDCl_3$)
f1 (ppm)

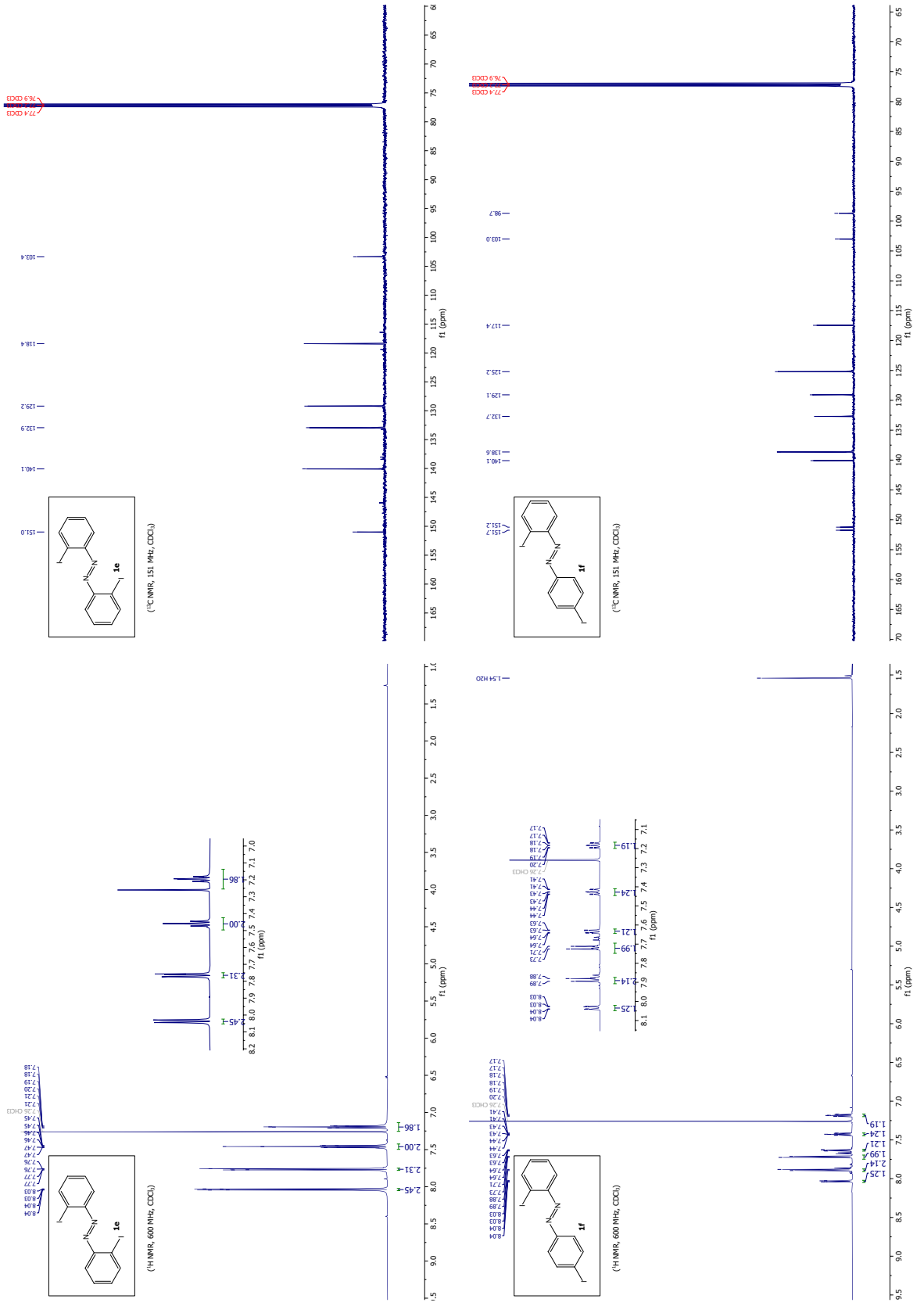
1e
(^{13}C NMR, 151 MHz, $CDCl_3$)
1f
(^{13}C NMR, 151 MHz, $CDCl_3$)
1e
(^{1}H NMR, 600 MHz, $CDCl_3$)
1f
(^{1}H NMR, 600 MHz, $CDCl_3$)
f1 (ppm)

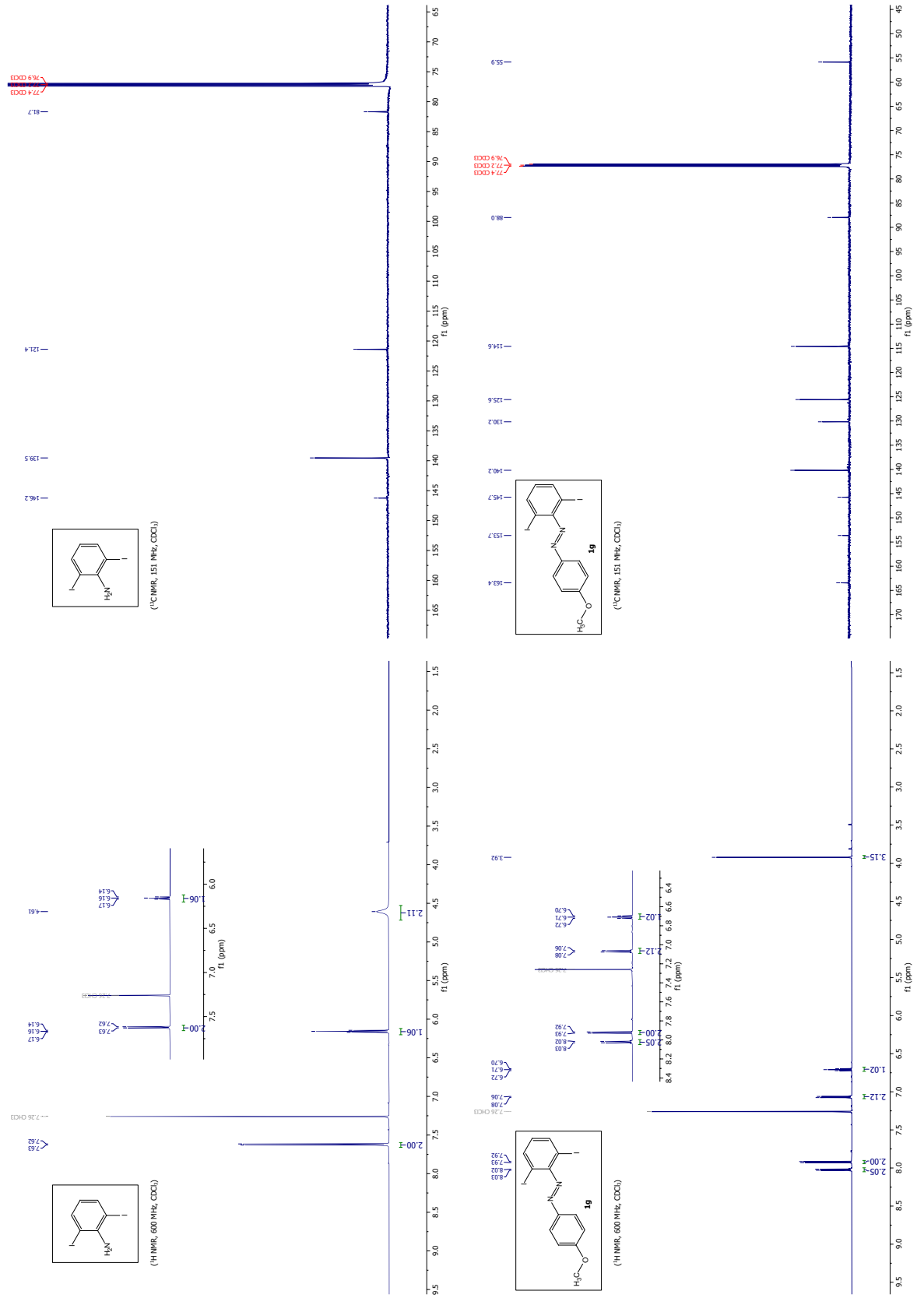
(^{13}C NMR, 151 MHz, $CDCl_3$)
(^{1}H NMR, 600 MHz, $CDCl_3$)
1g

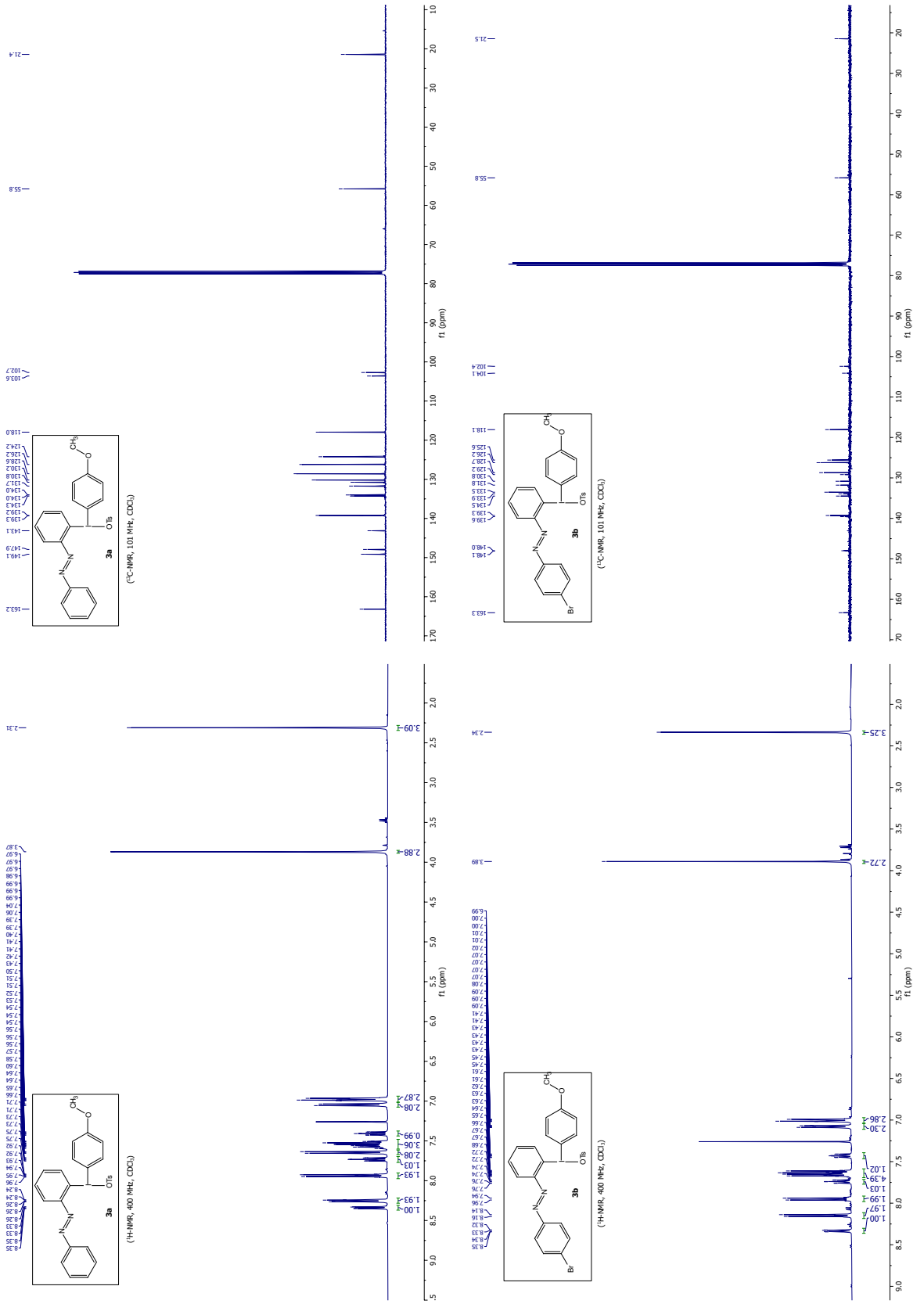
3a
OTs
(¹H-NMR, 400 MHz, CDCl₃)
3b
Br
(¹H-NMR, 400 MHz, CDCl₃)
(¹³C-NMR, 101 MHz, CDCl₃)
(¹³C-NMR, 101 MHz, CDCl₃)
f1 (ppm)

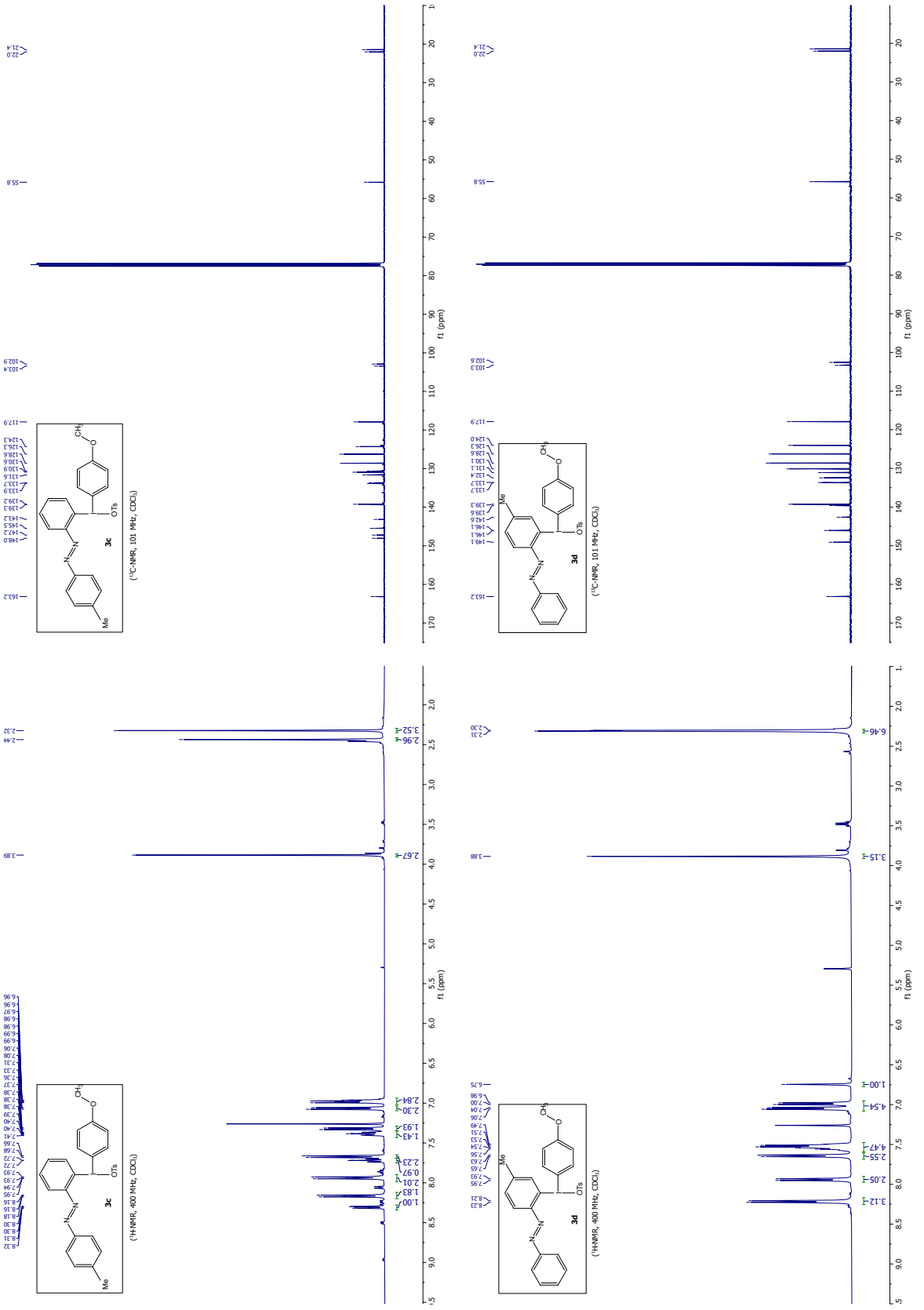
3c
(^{1}H-NMR, 400 MHz, CDCl$_3$)
(^{13}C-NMR, 101 MHz, CDCl$_3$)
3d
(^{1}H-NMR, 400 MHz, CDCl$_3$)
(^{13}C-NMR, 101 MHz, CDCl$_3$)
f1 (ppm)

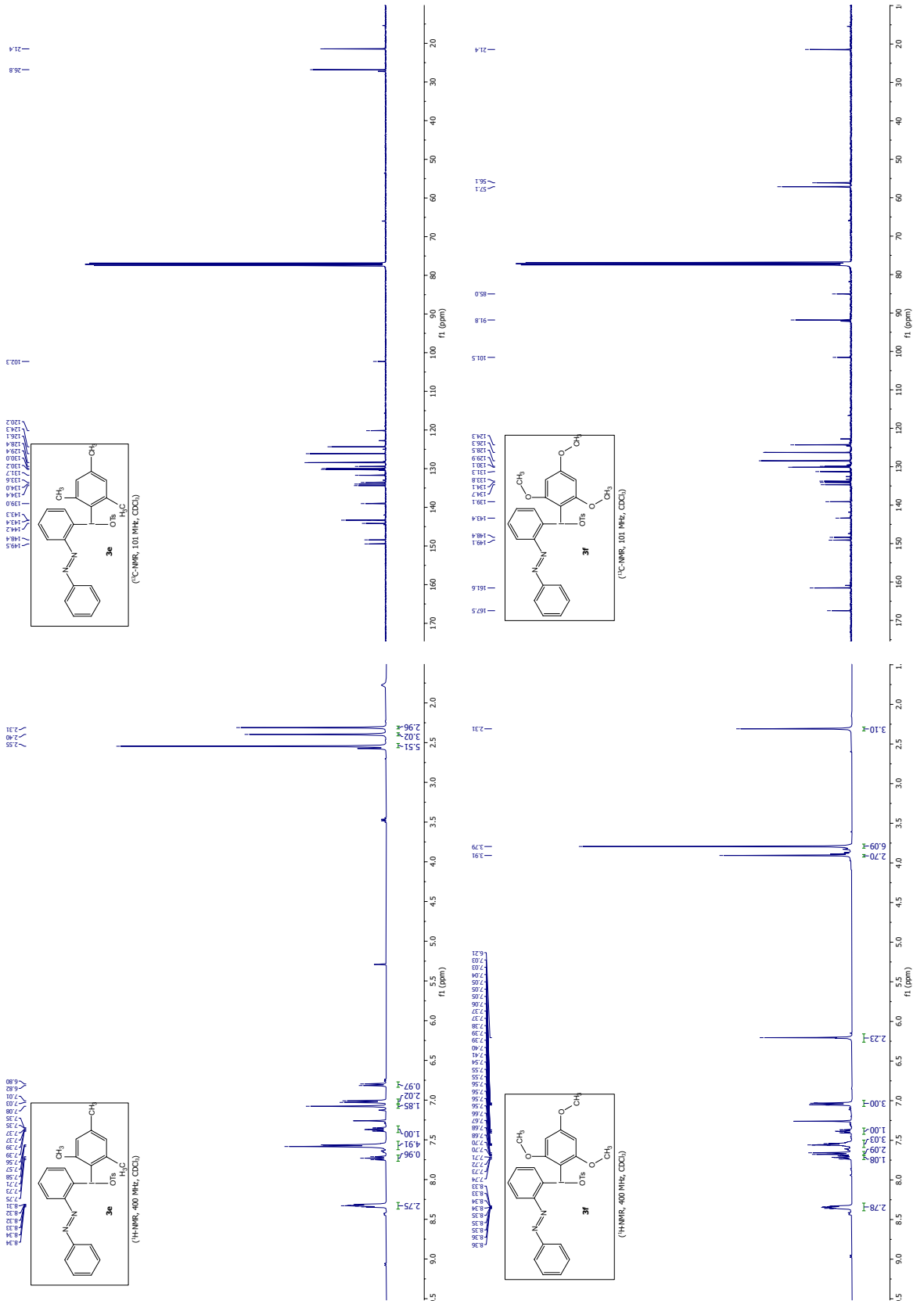
3e
(^{13}C-NMR, 101 MHz, CDCl$_3$)
3e
(^{1}H-NMR, 400 MHz, CDCl$_3$)
3f
(^{13}C-NMR, 101 MHz, CDCl$_3$)
3f
(^{1}H-NMR, 400 MHz, CDCl$_3$)
f1 (ppm)

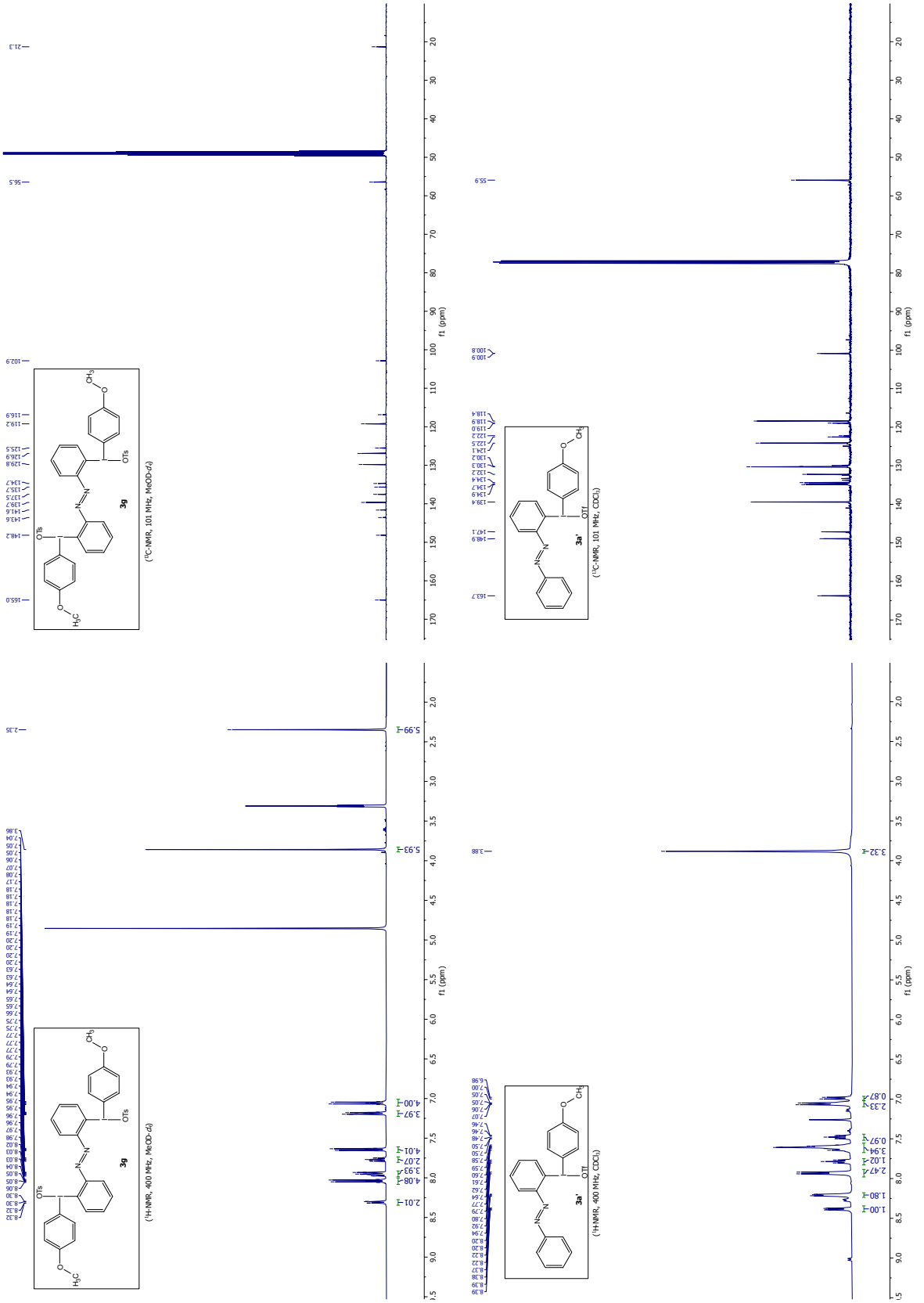
3g
(¹³C-NMR, 101 MHz, MeOD-d4)
3g
(¹H-NMR, 400 MHz, MeOD-d4)
3a'
(¹³C-NMR, 101 MHz, CDCl3)
3a'
(¹H-NMR, 400 MHz, CDCl3)
f1 (ppm)

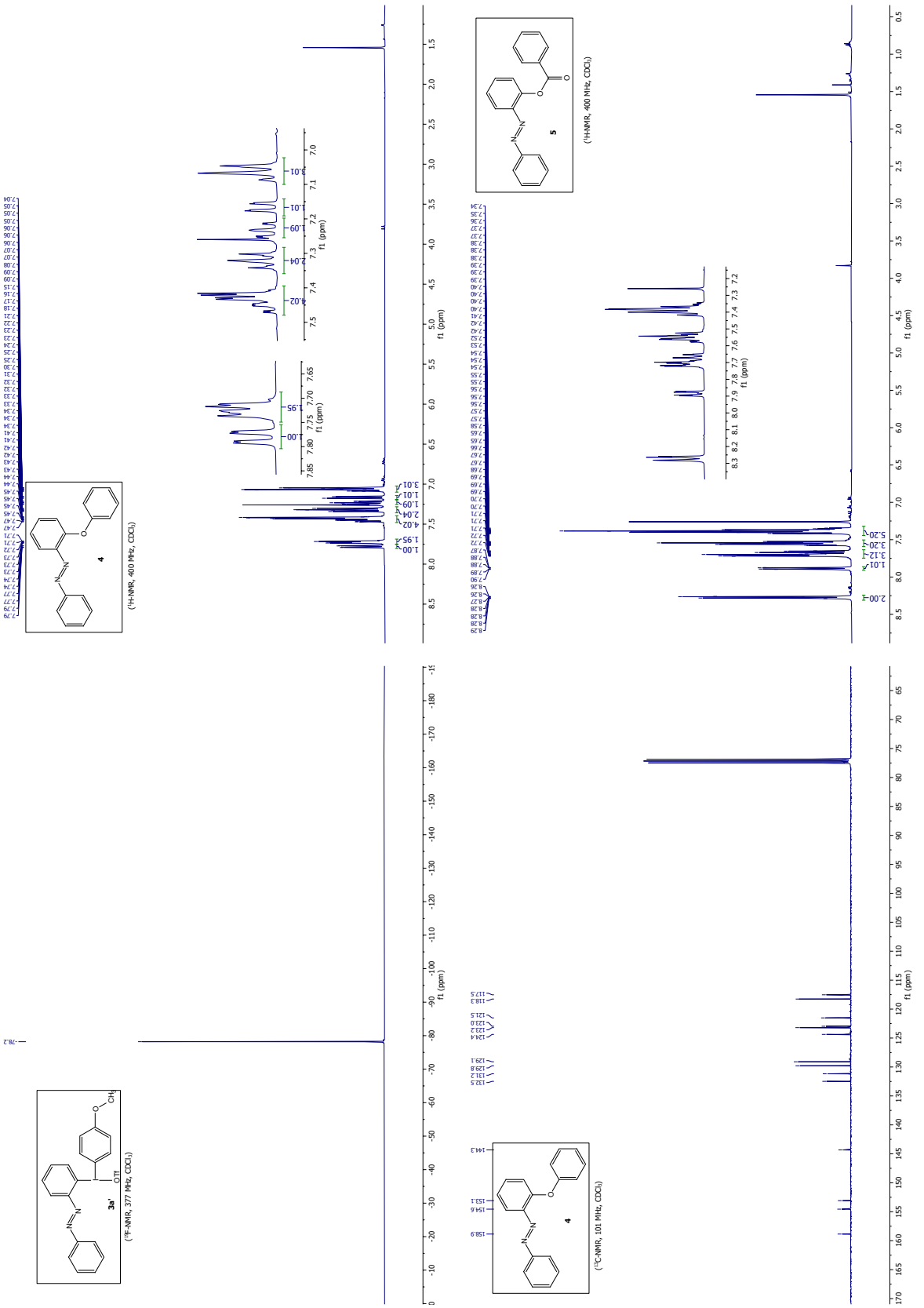
(¹H-NMR, 400 MHz, CDCl₃)
4
(¹H-NMR, 400 MHz, CDCl₃)
5
(¹⁹F-NMR, 377 MHz, CDCl₃)
3a'
(¹³C-NMR, 101 MHz, CDCl₃)
4
f1 (ppm)

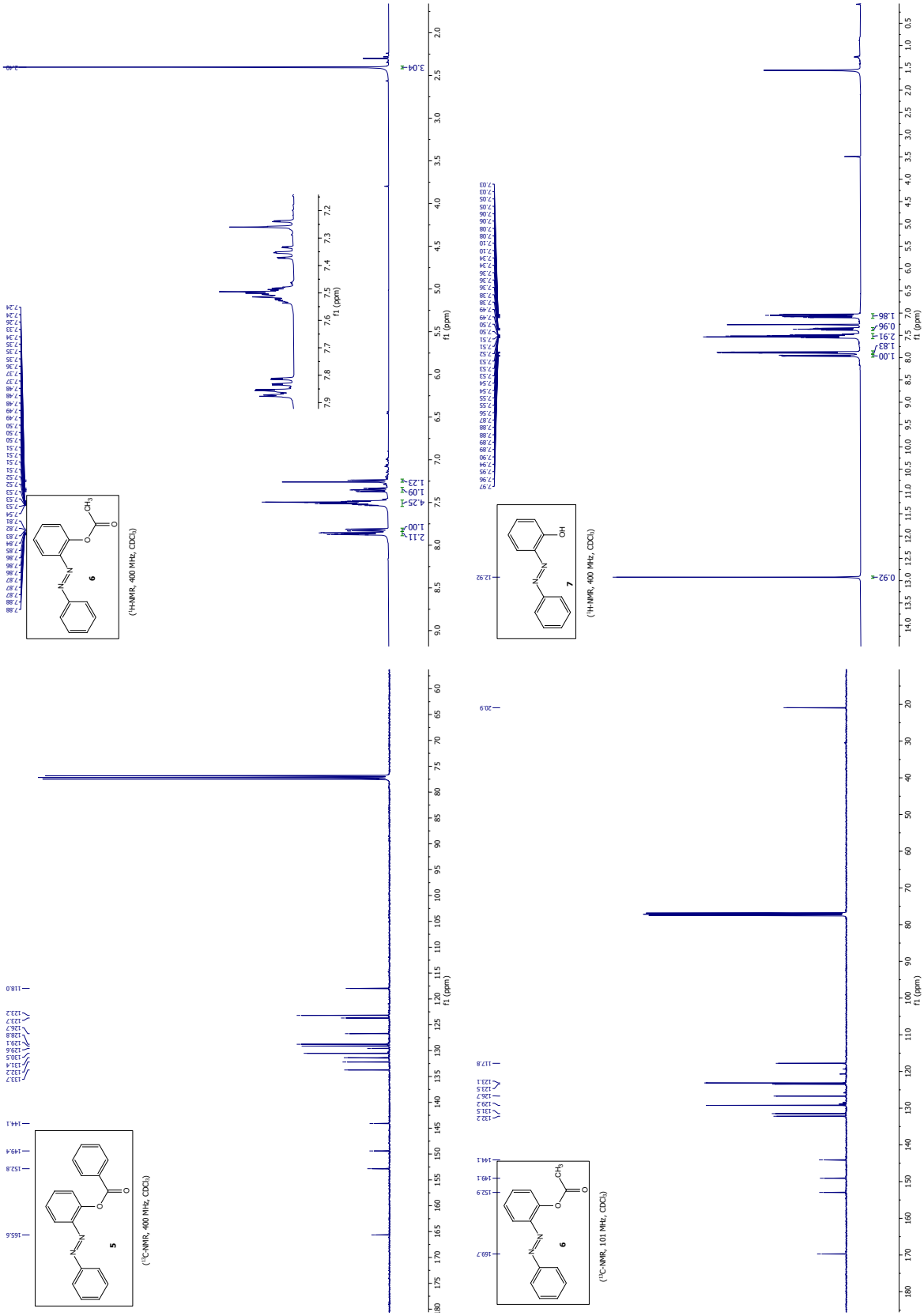
(¹H-NMR, 400 MHz, CDCl₃)
(¹³C-NMR, 400 MHz, CDCl₃)
(¹H-NMR, 400 MHz, CDCl₃)
(¹³C-NMR, 101 MHz, CDCl₃)
f1 (ppm)

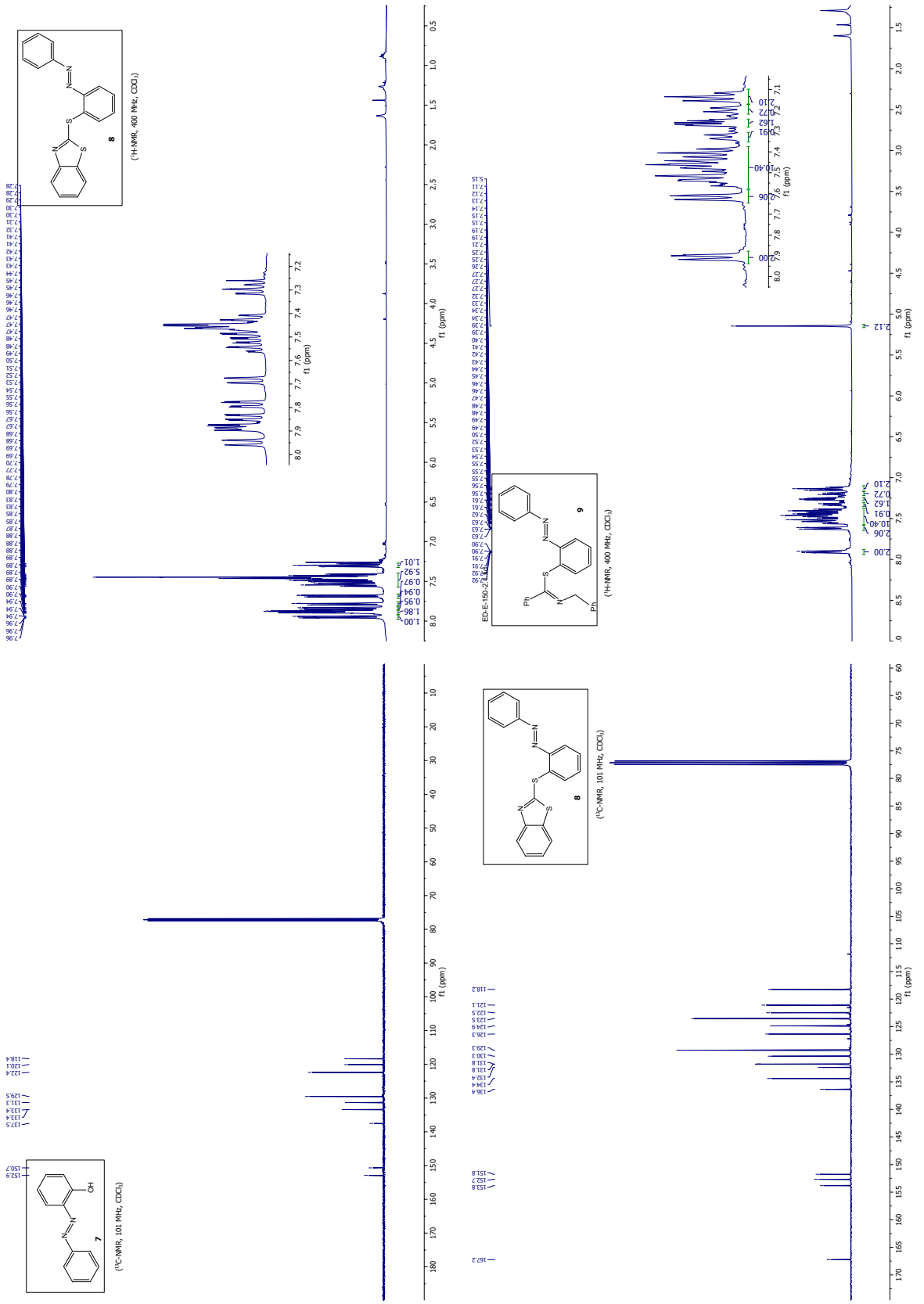
(^{1}H-NMR, 400 MHz, CDCl$_3$)
8
(^{1}H-NMR, 400 MHz, CDCl$_3$)
9
(^{13}C-NMR, 101 MHz, CDCl$_3$)
8
(^{13}C-NMR, 101 MHz, CDCl$_3$)
7
f1 (ppm)

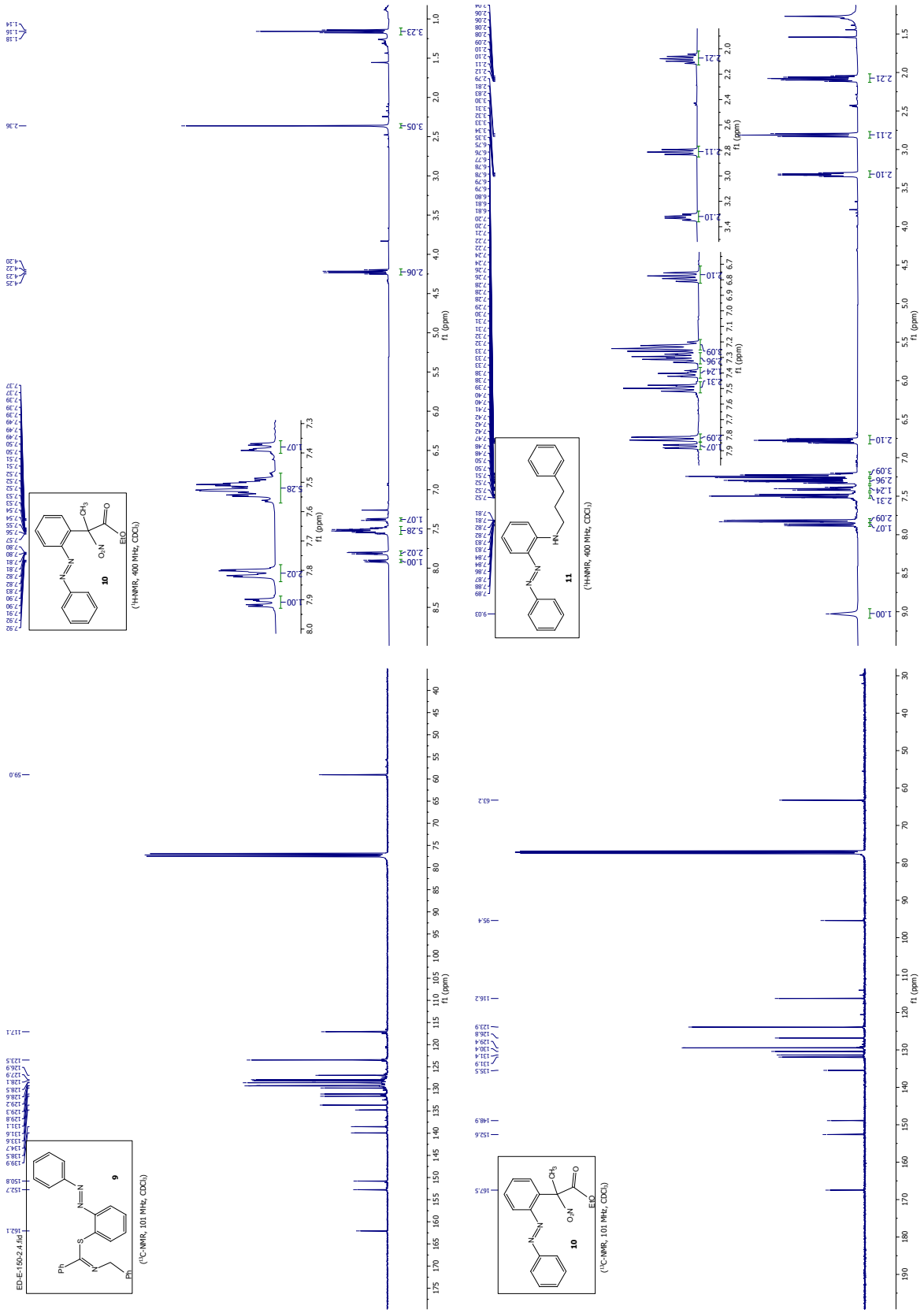
(¹H-NMR, 400 MHz, CDCl₃)
(¹³C-NMR, 101 MHz, CDCl₃)
f1 (ppm)

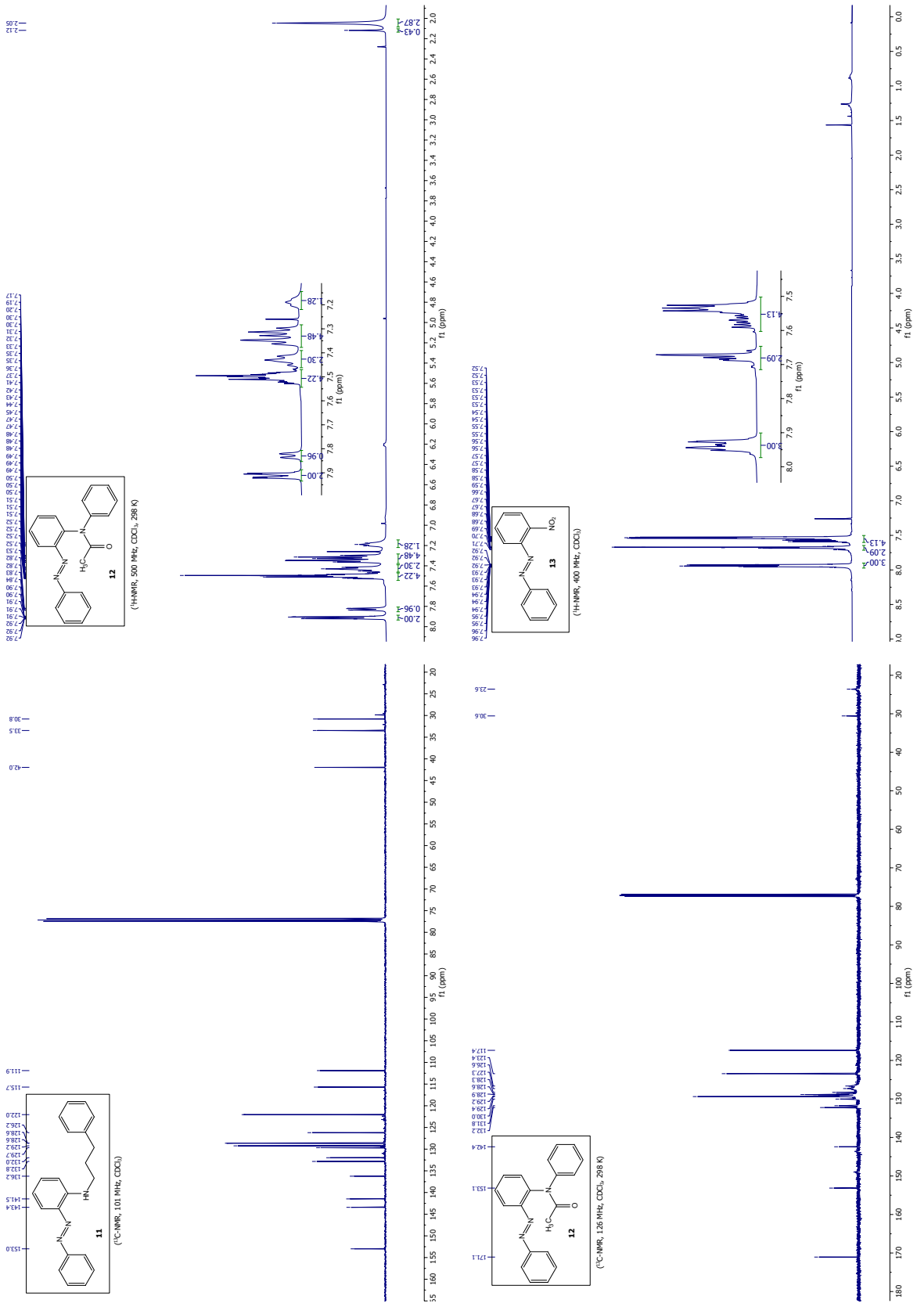
(¹H-NMR, 500 MHz, CDCl₃, 298 K)
12
(¹H-NMR, 400 MHz, CDCl₃)
13
(¹³C-NMR, 101 MHz, CDCl₃)
11
(¹³C-NMR, 126 MHz, CDCl₃, 298 K)
12
f1 (ppm)

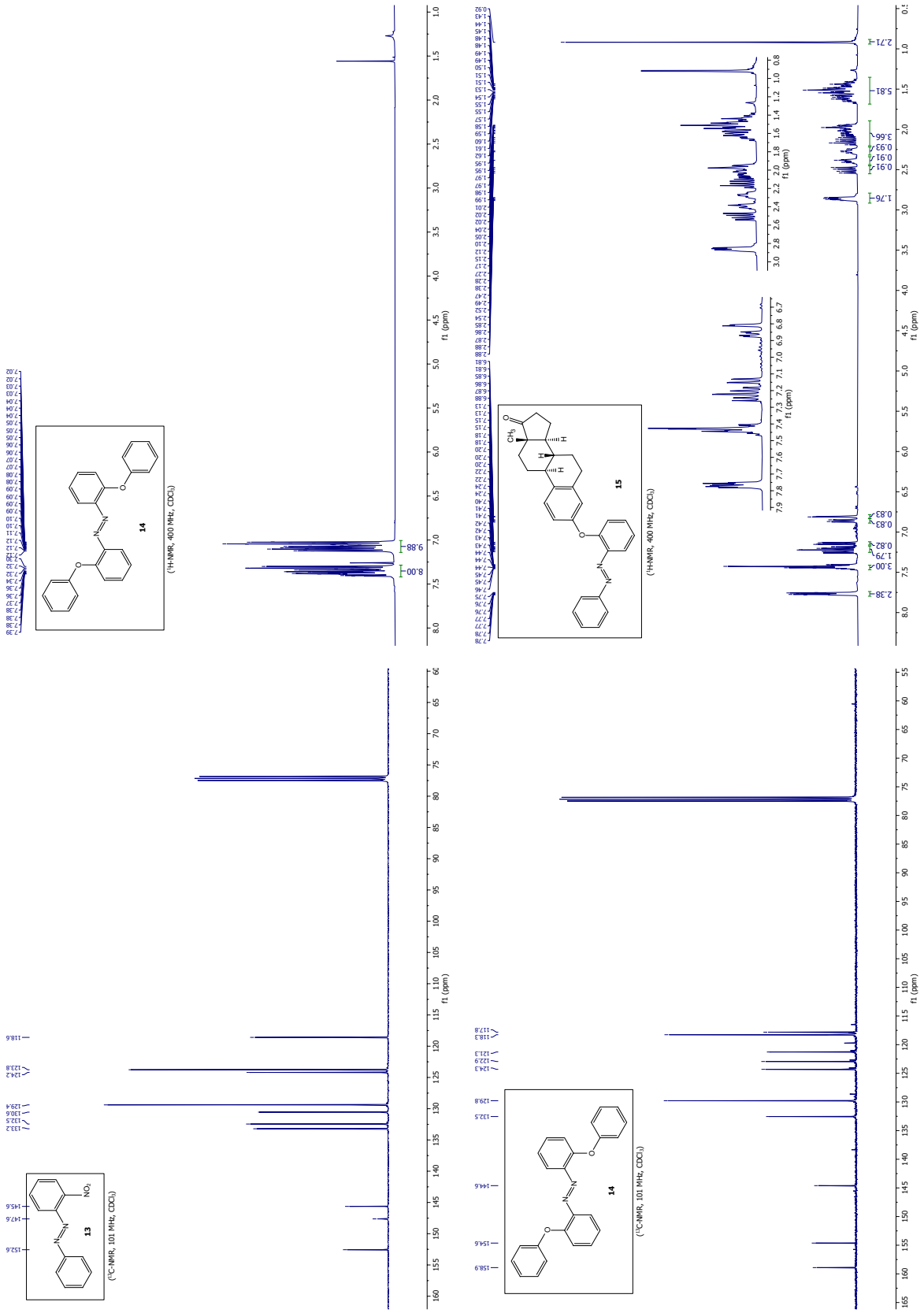
13
14
15
(^{1}H-NMR, 400 MHz, CDCl$_3$)
(^{13}C-NMR, 101 MHz, CDCl$_3$)
f1 (ppm)

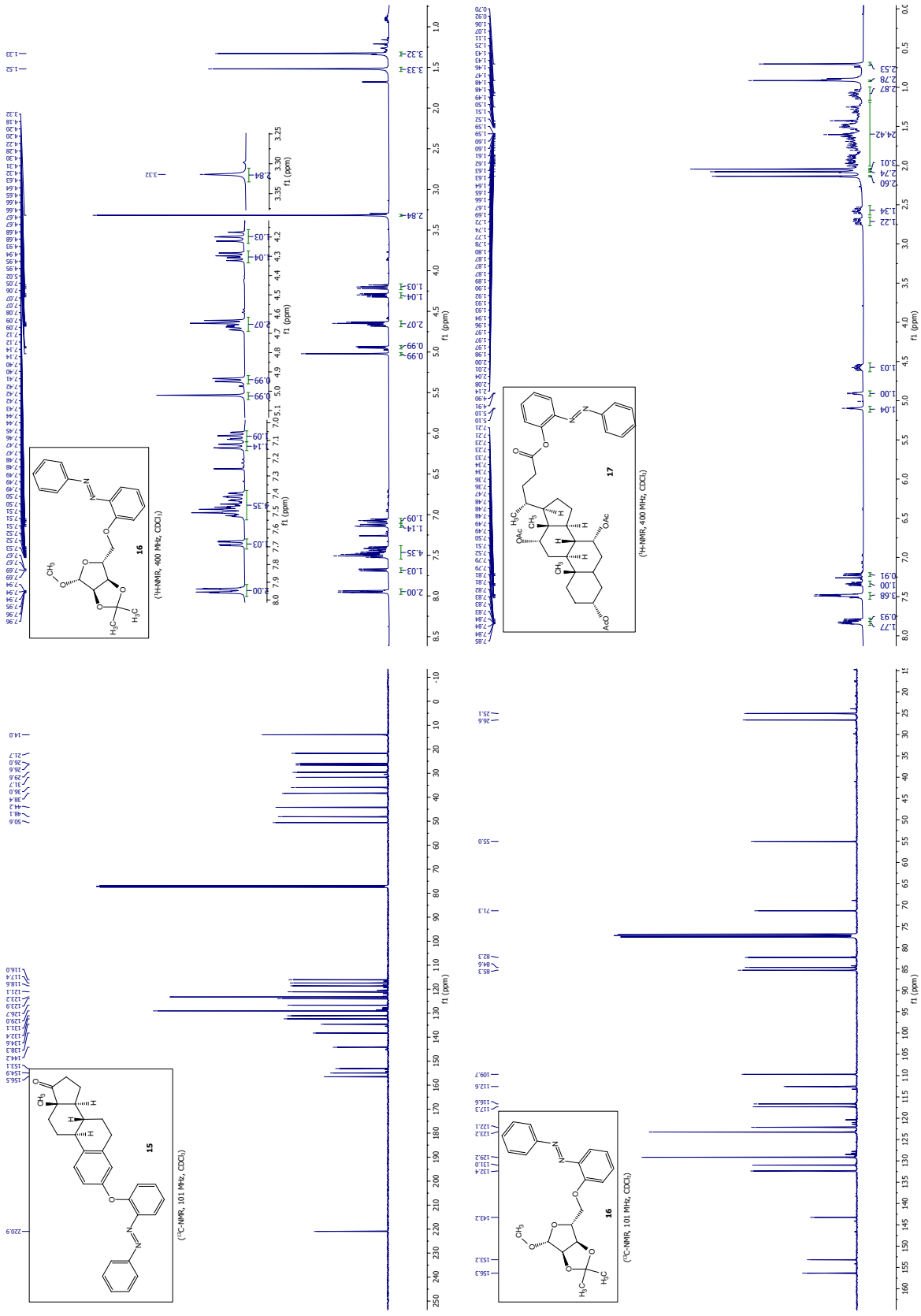
16
(¹H-NMR, 400 MHz, CDCl₃)
17
(¹H-NMR, 400 MHz, CDCl₃)
15
(¹³C-NMR, 101 MHz, CDCl₃)
16
(¹³C-NMR, 101 MHz, CDCl₃)
f1 (ppm)

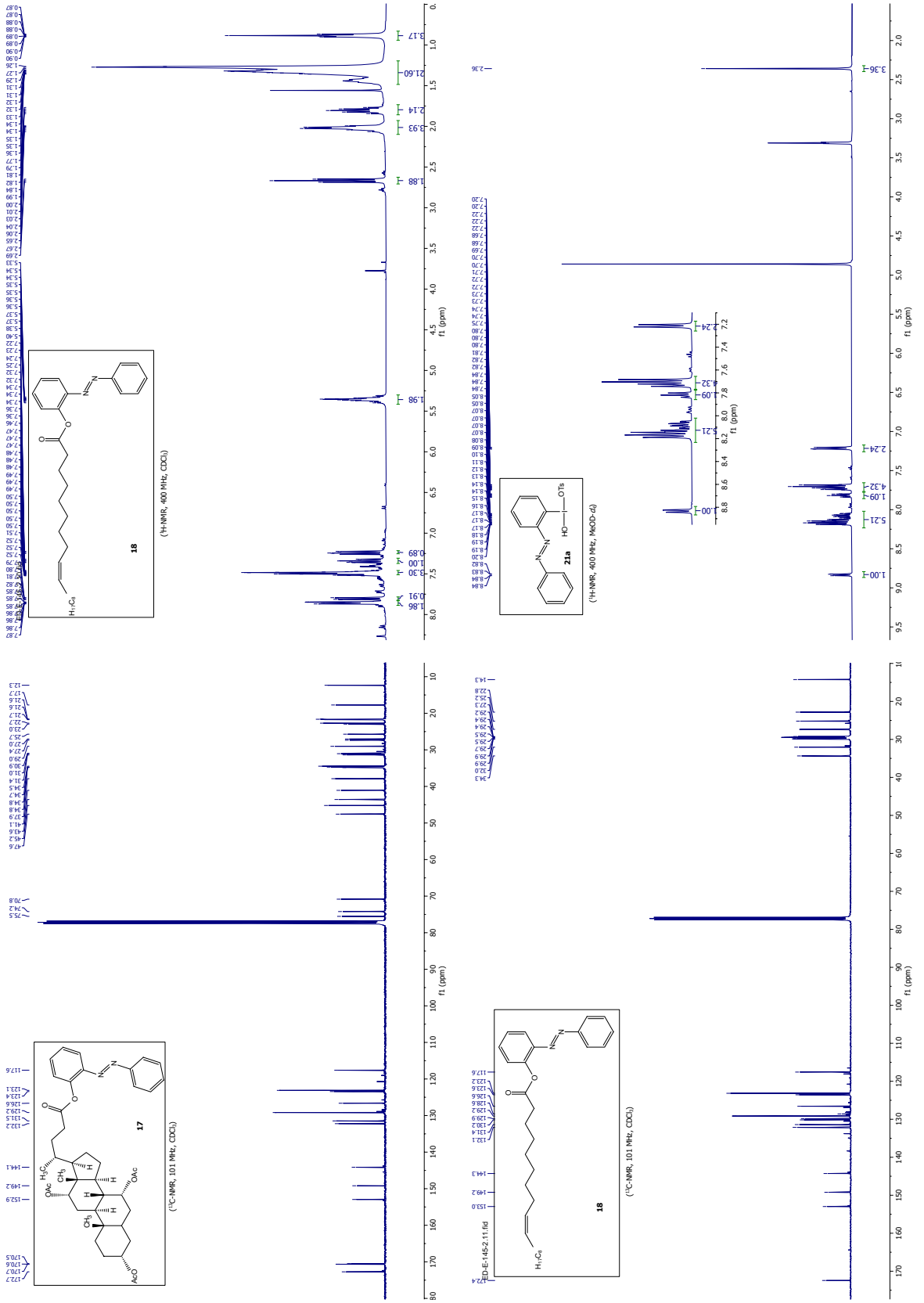
18
(¹H-NMR, 400 MHz, CDCl₃)
21a
(¹H-NMR, 400 MHz, MeOD-d₄)
17
(¹³C-NMR, 101 MHz, CDCl₃)
18
(¹³C-NMR, 101 MHz, CDCl₃)
f1 (ppm)

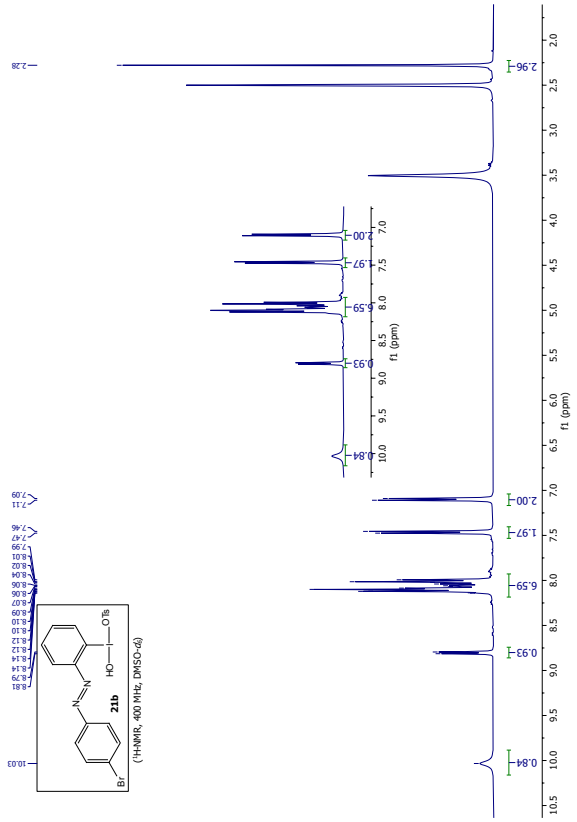
21b
(¹H-NMR, 400 MHz, DMSO-d6)
f1 (ppm)

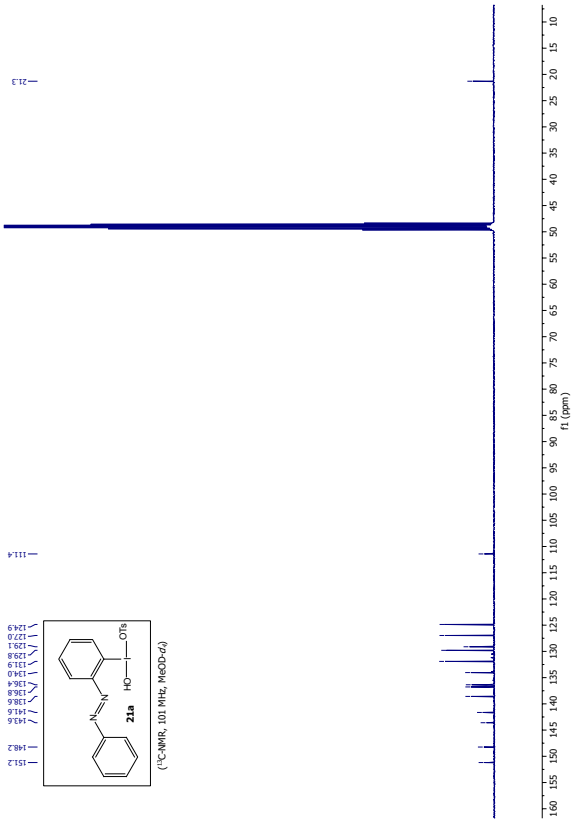
21a
(¹³C-NMR, 101 MHz, MeOD-d4)
f1 (ppm)

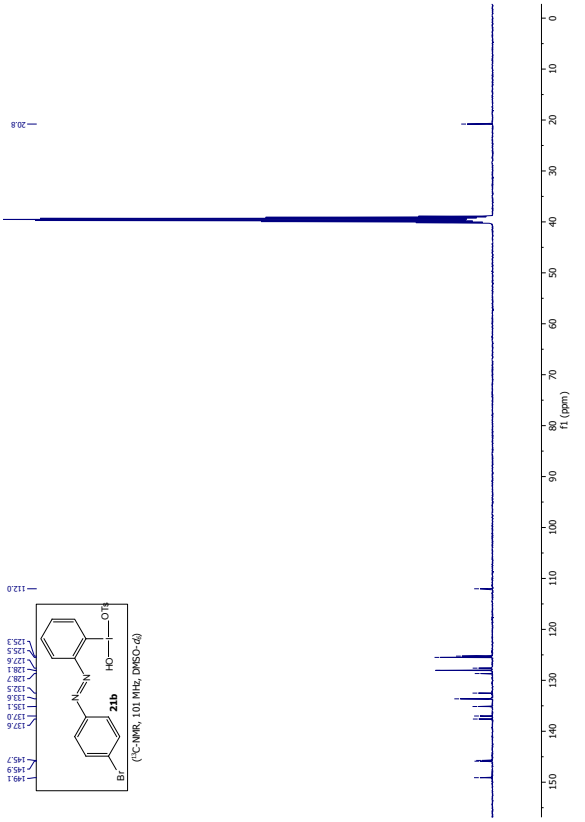
21b
(¹³C-NMR, 101 MHz, DMSO-d6)
f1 (ppm)

5.3 Stille vs. Suzuki - Cross-Coupling for the Functionalization of Diazocines

Supporting Information
for

Stille vs. Suzuki – Cross-Coupling for the Functionalization of Diazocines

M. Walther [1,2,†], Waldemar Kipke [1,2,†], R. Renken [1] and Anne Staubitz [1,2,*]

[1] University of Bremen, Institute for Analytical and Organic Chemistry, Leobener Straße 7, D-28359 Bremen, Germany

[2] University of Bremen, MAPEX Center for Materials and Processes, Bibliothekstraße 1, D-28359 Bremen, Germany

* Correspondence: staubitz@uni-bremen.de; Tel.: +49421/21863210

† Both authors contributed equally to this work.

Table of Contents

General Information 3
Reagents 4
Solvents 5
Syntheses 6
Syntheses of iodinated precursors 6
2,2'-(Ethane-1,2-diyl)bis(4-iodoaniline)[3] 6
(*Z*)-2,9-Diiodo-11,12-dihydrodibenzo[*c*,*g*][1,2]diazocine[3] (**1**) 6
5-Iodo-2-(4-iodo-2-nitrophenethyl)aniline[4] 7
6,6'-(Ethane-1,2-diyl)bis(3-iodoaniline) 7
(*Z*)-3,8-Diiodo-11,12-dihydrodibenzo[*c*,*g*][1,2]diazocine (**2**) 8
General Procedure for the Stille-Kelly Cross-Coupling Reaction 9
(*Z*)-2,9-Bis(trimethylstannyl)-11,12-dihydrodibenzo[*c*,*g*][1,2]diazocine (**3**) 9
(*Z*)-3,8-Bis(trimethylstannyl)-11,12-dihydrodibenzo[*c*,*g*][1,2]diazocine (**4**) 9
Optimization of the Miyaura Borylation 10
General Procedure for the Miyaura Borylation 10
(*Z*)-2,9-Bis(4,4,5,5-tetramethyl-1,3,2-dioxaborolan-2-yl)-11,12-dihydrodibenzo[*c*,*g*][1,2]diazocine (**5**) 11
2,9-Bis(4,4,5,5-tetramethyl-1,3,2-dioxaborolan-2-yl)-5,6,11,12-tetrahydrodibenzo[c,g][1,2]diazocine 11
(*Z*)-3,8-Bis(4,4,5,5-tetramethyl-1,3,2-dioxaborolan-2-yl)-11,12-dihydrodibenzo[*c*,*g*][1,2]diazocine (**6**) 12
Optimization for the Stille Cross-Coupling Reaction 13
General Procedure for the Stille Cross-Coupling Reaction 14
Optimization and General Procedure for the Suzuki Cross-Coupling Reaction 15
(*Z*)-2,9-Di-*p*-tolyl-11,12-dihydrodibenzo[*c*,*g*][1,2]diazocine (**7**) 16
(*Z*)-2,9-Bis(4-isopropylphenyl)-11,12-dihydrodibenzo[*c*,*g*][1,2]diazocine (**8**) 16
(*Z*)-2,9-Bis(3-isopropylphenyl)-11,12-dihydrodibenzo[*c*,*g*][1,2]diazocine (**9**) 17
(*Z*)-2,9-Bis(2-isopropylphenyl)-11,12-dihydrodibenzo[*c*,*g*][1,2]diazocine (**10**) 18
(*Z*)-2,9-Dimesityl-11,12-dihydrodibenzo[*c*,*g*][1,2]diazocine (**11**) 18
(*Z*)-2,9-Bis(4-methoxyphenyl)-11,12-dihydrodibenzo[*c*,*g*][1,2]diazocine (**12**) 19
(*Z*)-4,4'-(11,12-Dihydrodibenzo[*c*,*g*][1,2]diazocine-2,9-diyl)diphenol (**13**) 20
Side Product of the Suzuki Cross-Coupling Reaction (Z)-4-(11,12-dihydrodibenzo-[*c*,*g*][1,2]diazocin-2-yl)phenol (**32**) 20
(*Z*)-4,4'-(11,12-Dihydrodibenzo[*c*,*g*][1,2]diazocine-2,9-diyl)bis(*N*,*N*-dimethylaniline)-diazocine (**14**) 21
(*Z*)-4,4'-(11,12-Dihydrodibenzo[*c*,*g*][1,2]diazocine-2,9-diyl)bis(*N*,*N*-diphenylaniline) (**15**) 21
(*Z*)-4,4'-(11,12-Dihydrodibenzo[*c*,*g*][1,2]diazocine-2,9-diyl)dianiline (**16**) 22
Side Product of the Suzuki Cross-Coupling Reaction (*Z*)-4-(11,12-dihydrodibenzo-[*c*,*g*][1,2]diazocin-2-yl)aniline (**33**) 23
Side Product of the Suzuki Cross-Coupling Reaction (*Z*)-*N*1-(4-(11,12-dihydrodi-benzo[*c*,*g*][1,2]diazocin-2-yl)phenyl)benzene-1,4-diamine (**34**) 23
(*Z*)-2,9-Bis(4-nitrophenyl)-11,12-dihydrodibenzo[*c*,*g*][1,2]diazocine (**17**) 23
(*Z*)-2,9-Bis(3-nitrophenyl)-11,12-dihydrodibenzo[*c*,*g*][1,2]diazocine (**18**) 24
(*Z*)-2,9-Bis(2-nitrophenyl)-11,12-dihydrodibenzo[*c*,*g*][1,2]diazocine (**19**) 24
(*Z*)-2,9-Bis(3,5-bis(trifluoromethyl)phenyl)-11,12-dihydrodibenzo[*c*,*g*][1,2]diazocine (**20**) 25
(*Z*)-4,4'-(11,12-Dihydrodibenzo[*c*,*g*][1,2]diazocine-2,9-diyl)dibenzonitrile (**21**) 26
(*Z*)-1,1'-((11,12-Dihydrodibenzo[*c*,*g*][1,2]diazocine-2,9-diyl)bis(4,1-phenylene))bis-(ethan-1-one) (**22**) 26
Dimethyl 4,4'-(11,12-dihydrodibenzo[*c*,*g*][1,2]diazocine-2,9-diyl)(*Z*)-dibenzoate (**23**) 27
(*Z*)-2,9-Bis(benzo[*d*][1,3]dioxol-5-yl)-11,12-dihydrodibenzo[*c*,*g*][1,2]diazocine (**24**) 28
(*Z*)-2,9-Di(thiophen-2-yl)-11,12-dihydrodibenzo[*c*,*g*][1,2]diazocine (**25**) 28
(*Z*)-2,9-Di(thiophen-3-yl)-11,12-dihydrodibenzo[*c*,*g*][1,2]diazocine (**26**) 29
(*Z*)-5,5'-(11,12-Dihydrodibenzo[*c*,*g*][1,2]diazocine-2,9-diyl)bis(furan-2-carbaldehyde) (**27**) 29
Dimethyl 5,5'-(11,12-dihydrodibenzo[*c*,*g*][1,2]diazocine-2,9-diyl)(*Z*)-bis(furan-2-carboxylate) (**28**) 30
(*Z*)-2,9-Di(pyridin-4-yl)-11,12-dihydrodibenzo[*c*,*g*][1,2]diazocine (**29**) 31
(*Z*)-2,9-Diallyl-11,12-dihydrodibenzo[*c*,*g*][1,2]diazocine (**30**) 32
(*Z*)-3,8-Di-*p*-tolyl-11,12-dihydrodibenzo[*c*,*g*][1,2]diazocine (**35**) 32
(*Z*)-3,8-Bis(4-methoxyphenyl)-11,12-dihydrodibenzo[*c*,*g*][1,2]diazocine (**36**) 33
(*Z*)-3,8-Bis(4-nitrophenyl)-11,12-dihydrodibenzo[*c*,*g*][1,2]diazocine (**37**) 34
References 35
^{1}H, ^{13}C{^{1}H}, ^{11}B, ^{19}F and ^{119}Sn NMR Spectra of the Purified Compounds 36

General Information

For reactions under inert conditions, a nitrogen filled glovebox (Pure Lab^{HE} from Inert, Amesbury, MA USA) and standard Schlenk techniques were used.

Stannylation reactions were performed in high pressure vessels using an Emrys Optimizer (Biotage, Uppsala, Sweden) or a Biotage Initiator+ SP wave (Biotage, Uppsala, Sweden) in the organic synthesis mode.

All glassware was dried in an oven at 200 °C for several hours prior to use. NMR tubes were dried in an oven at 110 °C for several hours prior to use.

NMR spectra were recorded on a Bruker Avance Neo 600 (Bruker BioSpin, Rheinstetten, Germany) (600 MHz (^{1}H), 151 MHz (^{13}C{^{1}H}), 193 MHz (^{11}B{^{1}H}), 565 MHz (^{19}F), 224 MHz (^{119}Sn{^{1}H})) or Bruker DRX 500 (500 MHz (^{1}H), 126 MHz (^{13}C{^{1}H}), 471 MHz (^{19}F)) at 298 K. All ^{1}H NMR and ^{13}C{^{1}H} NMR spectra were referenced to the residual proton signals of the solvent (^{1}H) or the solvent itself (^{13}C{^{1}H}). ^{19}F NMR and ^{119}Sn{^{1}H} NMR spectra were referenced indirectly according to the IUPAC recommendations for the frequency ratio to ^{1}H.[1] The exact assignment of the peaks was performed by two-dimensional NMR spectroscopy such as ^{1}H COSY, ^{13}C{^{1}H} HSQC and ^{1}H/^{13}C{^{1}H} HMBC when possible.

High-resolution EI mass spectra were recorded on a MAT 95XL double-focusing mass spectrometer from Finnigan MAT (Thermo Fisher Scientific, Waltham, MA, USA) at an ionization energy of 70 eV. Samples were measured by a direct inlet method with a source temperature of 200 °C. High-resolution ESI and APCI mass spectra were measured by a direct inlet method on an Impact II mass spectrometer from Bruker Daltonics (Bruker Daltonics, Bremen, Germany). ESI mass spectra were recorded in the positive ion collection mode.

IR spectra were recorded on a Nicolet i510 FT-IR spectrometer from Thermo Fisher Scientific (Thermo Fisher Scientific, Waltham, MA, USA) with a diamond window in an area from 500 – 4000 cm^{-1} with a resolution of 4 cm^{-1}. All samples were measured 16 times against a background scan.

Melting points were recorded on a Büchi Melting Point M-560 (Büchi, Essen, Germany) and are reported corrected.

Thin layer chromatography (TLC) was performed using TLC Silica gel 60 F_{254} from Merck (Merck, Darmstadt, Germany) and compounds were visualized by exposure to UV light at a wavelength of 254 nm. Column chromatography was performed either manually using silica gel 60 (0.015-0.040 mm) from Merck (Merck, Darmstadt, Germany) or by using a PuriFlash 4250 column machine (Interchim, Mannheim, Germany). Silica gel columns of the type CHROMABOND Flash RS 15 SPHERE SiOH 15 µm (Macherey-Nagel, Düren, Germany) and PF-15SiHP-F0040, PF-50SiHP-JP-F0080, PF-50SiHP-JP-F0120 (Interchim, Mannheim, Germany) were used. The sample was applied via dry load with Celite® 503 (Macherey-Nagel, Düren, Germany) as column material. If stated, Celite® 503 (Macherey-Nagel, Düren, Germany) was used as filtration aid.

The use of abbreviations follows the conventions from the ACS Style guide.[2]

Reagents

All chemicals were commercially available and used without purification unless stated otherwise.

Table S1. List of supplier and purity of used chemicals.

Reagent	Supplier	Purity	Comments
(1,1'-Bis(diphenylphosphino)ferrocene)palladium(II) dichloride	Abcr	99.9%	Stored in a glovebox
1-Bromo-2-isopropylbenzene	BLD Pharmatech	99.30%	
1-Bromo-2-nitrobenzene	Apollo	98%	
1-Bromo-3-isopropylbenzene	BLD Pharmatech	95%	
1-Bromo-3-nitrobenzene	TCI	>98%	
1-Bromo-4-isopropylbenzene	BLD Pharmatech	96.35%	
1-Bromo-4-nitrobenzene	Acros Organics	99%	
2,2'-Ethylenedianiline	TCI	>98%	
2-Bromomesitylene	Alfa Aesar	99%	
2-Bromothiophene	Alfa Aesar	98+%	
3,5-Bis-(trifluoromethyl)-bromobenzene	Abcr	98%	
3-Bromothiophene	Alfa Aesar	97%	
4-Bromoacetophenone	Alfa Aesar	98%	
4-Bromoaniline	Sigma Aldrich	97%	
4-Bromoanisole	Abcr	99%	
4-Bromobenzonitrile	Alfa Aesar	98%	
4-Bromo-*N*,*N*-dimethylaniline	BLD Pharmatech	99.97%	
4-Bromophenol	Acros Organics	97%	
(4-Bromophenyl)diphenylamine	BLD Pharmatech	98%	
4-Bromopyridine hydrochloride	BLD Pharmatech	95%	
4-Bromotoluene	Abcr	98%	
4-Iodo-2-nitrotoluene	Apollo	98%	
5-Bromobenzo[d][1,3]dioxole	BLD Pharmatech	98.45%	
5-Bromofuran-2-carbaldehyde	BLD Pharmatech	98%	
Allyl bromide	Acros Organics	99%	Stabilized with 300 ppm propylene oxide
Bis(pinacolato)diboron	Abcr	98%	
Bromine	Acros	99+%	
Carbon	J.T.Baker	90-100%	Activated
Cesium fluoride	Abcr	99%	Stored in a glovebox
2-Dicyclohexylphosphino-2',4',6'-triisopropyl-biphenyl (XPhos)	BLD Pharm	97%	
Hexamethyldistannane	Acros	99%	Stored in a glovebox

Hydrazine monohydrate	Fisher	≥99%	
Iron(III) chloride hexahydrate	Sigma Aldrich	97%	
Magnesium sulfate	VWR		Dried
meta-Chloroperoxybenzoic acid	Acros	70 – 75%[1]	
Methyl 4-bromobenzoate	BLD Pharmatech	97.85%	
Methyl 5-bromofuran-2-carboxylate	BLD Pharmatech	97.88%	
N-Iodosuccinimide	Apollo	98%	Stored in a fridge
Palladium acetate	Carbolution	98%	
Potassium carbonate	Acros Organics	99+%	For analysis, anhydrous
Potassium hydroxide	Honeywell	≥85%	Pellets
Potassium *tert*-butoxide	TCI	≥97.0%	Stored in a glovebox
Sodium chloride	Th. Geyer	min 99.0%	
Sodium hydrogen carbonate	VWR	ACS, Reag. Ph. Eur.	
Sodium sulfate	Merck	≥99.0%	anhydrous

Solvents

All solvents for purification and extraction were used as received. All solvents used for synthesis under inert conditions were dried by a solvent purification system (SPS) from Inert Technologies.

Table S2. List of supplier and purity of used solvents.

Solvent	**Supplier**	**Purity**	**Comments**
1,2-Dimethoxyethane	J&K	99.5%	SuperDry, water ≤ 30 ppm, J&KSeal
1,4-Dioxane	Acros Organics	99.5%	Extra dry, over molecular sieve, stabilized, AcroSeal™
Acetic Acid	Merck	≥99.8%	
Chloroform-d_1	Euroisotop	99.8%	
Cyclohexane	Merck	≥99.5%	
DCM	Merck	≥99.9%	
DMSO	VWR	technical grade	
DMSO	Acros Organics	99.7%	Extra dry, AcroSeal™
DMSO-d_6	Sigma Aldrich	99.9%	
Ethyl acetate	Merck	≥99.5%	
Methanol	VWR	≥99.8%	
Tetrahydrofuran	VWR	HPLC grade	Anhydrous from SPS, stored in a glovebox
Tetrahydrofuran	Fisher Scientific	≥99.8%	
Toluene	Merck	≥99.7%	Anhydrous from SPS, stored in a glovebox
Water		deionized	

[1] The exact concentration was determined by iodometric titration against sodium thiosulfate.

Syntheses

Syntheses of iodinated precursors

2,2'-(Ethane-1,2-diyl)bis(4-iodoaniline)[3]

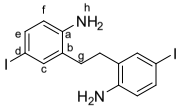

Compound **2*p*** was synthesized according to a literature procedure. The analytical data are consistent with the literature.[3]

^{1}H NMR (600 MHz, $CDCl_3$) δ = 7.34 – 7.30 (m, 4H, *H*-e/f), 6.48 – 6.44 (m, 2H, *H*-c), 3.64 (s, br, 4H, *H*-h), 2.69 (s, 4H, *H*-g) ppm.
^{13}C{^{1}H} NMR (151 MHz, $CDCl_3$) δ = 144.2 (*C*-a), 138.0 (*C*-f), 136.2 (*C*-e), 128.6 (*C*-b), 118.1 (*C*-c), 80.3 (*C*-d), 30.6 (*C*-g) ppm.
IR (ATR): $\tilde{\nu}$ = 3397 (m, br), 3317 (m), 3219 (w), 2882 (w), 2359 (w), 1626 (m), 1562 (w), 1486 (s), 1470 (m), 1436 (m), 1398 (m), 1297 (s), 1268 (s), 1142 (m), 1096 (m), 1052 (m), 1002 (m), 931 (m), 868 (m), 834 (m), 809 (s), 709 (s) cm^{-1}.
HRMS (EI, 70 eV) *m/z* (%): $[M]^+$ calcd for $[C_{14}H_{14}I_2N_2]^+$ 463.92410; found 463.92397, 232.0 (100).
Mp: 165 °C.
R_f = 0.57 (*n*-hexane/DCM 1/1).

(*Z*)-2,9-Diiodo-11,12-dihydrodibenzo[*c*,*g*][1,2]diazocine[3] (**1**)

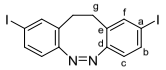

Compound **1** was synthesized according to literature procedure. The analytical data are consistent with the literature.[3]

^{1}H NMR (600 MHz, $CDCl_3$) δ = 7.48 (dd, ^3J = 8.3 Hz, ^4J = 1.8 Hz, 2H, *H*-b), 7.36 (ad, ^4J = 1.8 Hz, 2H, *H*-f), 6.59 (d, ^3J = 8.3 Hz, 2H, *H*-c), 2.97 – 2.62 (m, 4H, *H*-g) ppm.
^{13}C{^{1}H} NMR (151 MHz, $CDCl_3$) δ = 154.9 (*C*-d), 138.5 (*C*-f), 136.1 (*C*-b), 130.1 (*C*-e), 120.9 (*C*-c), 92.4 (*C*-a), 31.3 (*C*-g) ppm.
IR (ATR): $\tilde{\nu}$ = 2921 (w), 2358 (w), 1575 (m), 1533 (w), 1467 (m), 1383 (w), 1280 (w), 1156 (m), 1097 (m), 1052 (w), 1002 (m), 979 (w), 959 (w), 918 (w), 891 (m), 878 (m), 801 (s), 714 (m) cm^{-1}.
HRMS (EI, 70 eV) *m/z* (%): $[M]^+$ calcd for $[C_{14}H_{10}I_2N_2]^+$ 459.89280; found 459.89287, 178.1 (100).
Mp: 173 °C.
R_f = 0.60 (*n*-hexane/DCM 3/1).

5-Iodo-2-(4-iodo-2-nitrophenethyl)aniline[4]

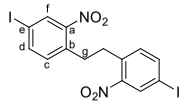

This reaction was not performed under inert conditions.

t-BuOK (5.61 g, 50.0 mmol, 1.00 equiv) was added at 0 °C to a solution of 4-iodo-2-nitrotoluene (13.2 g, 50.0 mmol, 1.00 equiv) in THF (300 mL) and the solution was stirred for 1 min. Then, bromine (2.56 mL, 7.99 g, 50.0 mmol, 1.00 equiv) was added and the mixture was stirred for 10 min at 0 °C. The reaction mixture was poured into ice (1 L). The precipitate was filtered, washed with water (400 mL) and cyclohexane (400 mL) and subsequently dried under reduced pressure yielding **3** as a yellow solid (11.1 g, 21.2 mmol, 85%, Lit.[4]:31%[2]).

^{1}H NMR (600 MHz, $CDCl_3$) δ = 8.28 (ad, ^4J = 1.8 Hz, 2H, *H*-f), 7.86 (dd, ^3J = 8.1 Hz, ^4J = 1.8 Hz, 2H, *H*-d), 7.14 (d, ^3J = 8.1 Hz, 2H, *H*-c), 3.16 (s, 4H, *H*-g) ppm.
^{13}C{^{1}H} NMR (151 MHz, $CDCl_3$) δ = 149.6 (*C*-a), 142.4 (*C*-d), 135.4 (*C*-b), 134.1 (*C*-e), 133.6 (*C*-f), 91.1 (*C*-c), 34.1 (*C*-g) ppm.
IR (ATR): $\tilde{\nu}$ = 3079 (w), 2847 (br, w), 1517 (s), 1471 (m), 1336 (s), 1172 (w), 1130 (w), 1068 (m), 890 (m), 868 (m), 837 (s), 794 (s), 761 (s), 741 (m) cm^{-1}.
HRMS (ESI) *m/z*: $[M + Na]^+$ calcd for $[C_{14}H_{10}I_2N_2O_4 + Na]^+$ 546.86222; found 546.86133.
Mp: 212 °C.
R_f = 0.80 (cyclohexane/DCM 1/3).

6,6'-(Ethane-1,2-diyl)bis(3-iodoaniline)

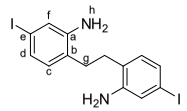

This reaction was not performed under inert conditions.

1,2-Bis(4-iodo-2-nitrophenyl)ethane (**3**) (5.24 g, 10.0 mmol, 1.00 equiv), activated carbon (444 mg, 37.0 mmol, 3.70 equiv) and $FeCl_3 \times 6\ H_2O$ (32.4 mg, 120 µmol, 1.2 mol%) were dissolved in methanol (150 mL) and stirred for 10 min at 65 °C. Hydrazine monohydrate (4.85 mL, 103 mmol, 10.0 equiv) was added and the reaction mixture was stirred for 18 h at 65 °C. After cooling down to 23 °C, the reaction mixture was filtered through Celite®. The solvent was removed under reduced pressure yielding ***2m*** as a pale-yellow solid (3.87 g, 8.35 mmol, 83%, Lit.[5]:48%[3]).

^{1}H NMR (600 MHz, $CDCl_3$) δ = 7.03 (dd, ^3J = 7.9 Hz, ^4J = 1.8 Hz, 2H, *H*-d), 7.01 (ad, ^4J = 1.8 Hz, 2H, *H*-f), 6.71 (d, ^3J = 7.9 Hz, 2H, *H*-c), 3.59 (s, br, 4H, *H*-h), 2.70 (s, 4H, *H*-g) ppm.
^{13}C{^{1}H} NMR (151 MHz, $CDCl_3$) δ = 145.9 (*C*-a), 131.3 (*C*-c), 128.0 (*C*-d), 125.5 (*C*-b), 124.4 (*C*-f), 92.2 (*C*-e), 30.4 (*C*-g) ppm.
IR (ATR): $\tilde{\nu}$ = 3415 (w), 3340 (w), 2882 (br, m), 2118 (br, w), 1866 (br, w), 1613 (m), 1584 (m), 1563 (m), 1485 (s), 1438 (m), 1401 (m), 1265 (m), 1181 (m), 1084 (m), 938 (w), 871 (m), 854 (m), 813 (s), 775 (m) cm^{-1}.

[2] In this report, air was used as oxidant.
[3] In this report, tin(II) chloride hexahydrate was used as reducing agent.

HRMS (EI, 70 eV) *m/z* (%): $[M]^+$ calcd for $[C_{14}H_{14}I_2N_2]^+$ 463.92410; found 463.92399, 231.9 (100).
Mp: 160 °C.
R_f = 0.37 (*n*-hexane/DCM 1/1).

(*Z*)-3,8-Diiodo-11,12-dihydrodibenzo[*c*,*g*][1,2]diazocine (**2**)

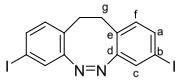

This reaction was not performed under inert conditions.

A freshly prepared solution of *m*CPBA (70%, 2.47 g, 14.3 mmol, 2.00 equiv) in acetic acid (20 mL) was added dropwise over the course of 2 h under rapid stirring to a solution of a 2,2'-ethylenedi(3-iodoaniline) (***2m***) (2.32 g, 5.00 mmol, 1.00 equiv) in acetic acid (30 mL) and DCM (90 mL). After the complete addition of the *m*CPBA solution, the mixture was stirred for further 16 h at 25 °C. Then, the solvent was removed under reduced pressure. The residue was re-dissolved in DCM (50 mL) and washed with an aqueous solution of sodium hydrogen carbonate (2 M, 3 × 50 mL). The combined organic phases were dried over magnesium sulfate, filtered and concentrated under reduced pressure. The crude product was purified via column chromatography on silica (eluent: cyclohexane/DCM 1/3) to afford **2** as a yellow solid (855 mg, 1.86 mmol, 37%, Lit.[5]: 35%).

^{1}H NMR (600 MHz, $CDCl_3$) δ = 7.36 (dd, ^3J = 8.1 Hz, ^4J = 1.8 Hz, 2H, *H*-a), 7.19 (ad, ^4J = 1.8 Hz, 2H, *H*-c), 6.73 (d, ^3J = 8.1 Hz, 2H, *H*-f), 2.94 – 2.66 (m, 4H, *H*-g) ppm.
^{13}C{^{1}H} NMR (151 MHz, $CDCl_3$) δ = 156.1 (*C*-d), 136.5 (*C*-a), 131.6 (*C*-f), 127.7 (*C*-e), 127.6 (*C*-c), 91.4 (*C*-b), 31.3 (*C*-g) ppm.
IR (ATR): $\tilde{\nu}$ = 3037 (w), 1577 (m), 1552 (m), 1462 (m), 1376 (m), 1258 (w), 1158 (w), 1090 (m), 975 (w), 882 (m), 820 (s), 798 (s), 721 (m) cm^{-1}.
HRMS (EI, 70 eV) *m/z* (%): $[M]^+$ calcd for $[C_{14}H_{10}I_2N_2]^+$ 459.89280; found 459.89334, 178.0 (100).
Mp: 184 °C.
R_f = 0.66 (cyclohexane/DCM 1/3).

General Procedure for the Stille-Kelly Cross-Coupling Reaction

Under inert conditions, the corresponding di-iodinated diazocine (345 mg, 750 µmol, 1.00 equiv), hexamethyldistannane (573 mg, 1.75 mmol, 2.33 equiv) and $[Pd(PPh_3)_4]$[6] (34.8 mg, 30.0 µmol, 4 mol%) were dissolved in toluene (2.5 mL) and THF (2.5 mL) in a microwave reaction vessel. The reaction mixture was stirred for 10 min at 150 °C under microwave irradiation and subsequently filtered through Celite®. Then, the solvent and excess hexamethyldistannane were removed under reduced pressure (9.5×10^{-2} mbar, 80 °C). The residue was purified via column chromatography on silica.

(*Z*)-2,9-Bis(trimethylstannyl)-11,12-dihydrodibenzo[*c*,*g*][1,2]diazocine (**3**)

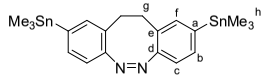

Compound **3** was synthesized according to the general procedure from (*Z*)-2,9-diiodo-11,12-dihydrodibenzo[*c*,*g*][1,2]diazocine (**1**). The product **3** was obtained after purification via column chromatography on silica (eluent: cyclohexane/DCM 1/2) as a yellow solid (326 mg, 612 µmol, 82%). The reaction was repeated on a 3.00 mmol scale yielding **3** in 77% (1.23 g, 2.31 mmol).

^{1}H NMR (600 MHz, $CDCl_3$) δ = 7.26 (d, ^3J = 7.5 Hz, 2H, *H*-b), 7.10 (s, 2H, *H*-f), 6.84 (d, ^3J = 7.5 Hz, 2H, *H*-c), 3.02 – 2.73 (m, 4H, *H*-g), 0.23 (s, 18H, *H*-h) ppm.
^{13}C{^{1}H} NMR (151 MHz, $CDCl_3$) δ = 155.6 (*C*-d), 141.3 (*C*-a), 137.2 (*C*-f), 134.1 (*C*-b), 127.2 (*C*-e), 118.6 (*C*-c), 32.0 (*C*-g), -9.3 (*C*-h) ppm.
^{z119}Sn{^{1}H} NMR (224 MHz, $CDCl_3$) δ = -25.55 ppm.
IR (ATR): $\tilde{\nu}$ = 2987 (w), 2907 (w), 2359 (w), 1703 (w), 1524 (w), 1457 (w), 1429 (w), 1374 (w), 1183 (w), 1068 (w), 948 (w), 922 (w), 891 (w), 833 (w), 763 (s), 711 (m) cm^{-1}.
HRMS (EI, 70 eV) *m/z* (%): $[M]^+$ calcd for $[C_{20}H_{28}N_2{}^{120}Sn_2]^+$ 536.02909; found 536.03099, 490.8 (100).
Mp: 139 °C.
R_f = 0.46 (cyclohexane/DCM 2/1).

(*Z*)-3,8-Bis(trimethylstannyl)-11,12-dihydrodibenzo[*c*,*g*][1,2]diazocine (**4**)

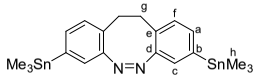

Compound **4** was synthesized according to the general procedure from (*Z*)-3,8-diiodo-11,12-dihydrodibenzo[*c*,*g*][1,2]diazocine (**2**). The product **4** was obtained after purification via column chromatography on silica (eluent: cyclohexane/DCM 1/2) as a yellow solid (281 mg, 527 µmol, 70%).

^{1}H NMR (600 MHz, $CDCl_3$) δ = 7.12 (dd, ^3J = 7.4 Hz, ^4J = 1.0 Hz, 2H, *H*-a), 6.94 (d, ^3J = 7.4 Hz, 2H, *H*-f), 6.94 (ad, ^4J = 1.0 Hz, 2H, *H*-c), 3.01 – 2.69 (m, 4H, *H*-g), 0.22 (s, 18H, *H*-h) ppm.
^{13}C{^{1}H} NMR (151 MHz, $CDCl_3$) δ = 155.4 (*C*-d), 140.6 (*C*-b), 134.5 (*C*-a), 129.1 (*C*-f), 128.1 (*C*-e), 125.9 (*C*-c), 31.9 (*C*-g), -9.4 (*C*-h) ppm.
^{119}Sn{^{1}H} NMR (224 MHz, $CDCl_3$) δ = -23.71 ppm.
IR (ATR): $\tilde{\nu}$ = 2912 (w, br), 1514 (w), 1434 (w), 1366 (w), 1261 (w), 1186 (m), 1073 (m), 984 (w), 954 (w), 922 (w), 887 (m), 858 (w), 820 (m), 799 (m), 764 (s), 714 (s) cm^{-1}.
HRMS (EI, 70 eV) *m/z* (%): $[M]^+$ calcd for $[C_{20}H_{28}N_2{}^{120}Sn_2]^+$ 536.03001; found 536.03073, 490.8 (100).
Mp: 103 °C.
R_f = 0.43 (cyclohexane/DCM 2/1).

Optimization of the Miyaura Borylation

1 **5**

Table S3. Optimization of the Miyaura Borylation of **1**.

Entry	mmol	Base [4 eq]	Catalyst [5mol%]	B_2pin_2 [eq]	Solvent	T [°C]	Time [h]	Yield [%]
1	0.2	KOAc	$Pd(dppf)Cl_2$	3.00	DMSO	100	16	65
2	0.2	KOAc	$Pd(acac)_2$	3.00	DMSO	100	16	26
3	0.2	KOAc	$Pd(PPh_3)_4$	3.00	DMSO	100	16	52
4	0.2	KOAc	$Pd(PPh_3)_4$	3.00	DMSO	100	48	43
5	0.2	*t*-BuOK	$Pd(dppf)Cl_2$	3.00	DMSO	100	16	0
6	0.2	K_3PO_4	$Pd(dppf)Cl_2$	3.00	1,4-Dioxan	100	16	0
7	0.2	K_3PO_4	$Pd(dppf)Cl_2$	3.00	DMSO	100	16	14
8	0.2	K_3PO_4	$Pd(dppf)Cl_2$	3.00	1,4-Dioxan / Water (10:1)	100	16	Traces
9	0.2	KOAc	$Pd(dppf)Cl_2$	3.00	1,4-Dioxan	100	16	Traces
10	0.2	KOAc	$Pd(dppf)Cl_2$	3.00	1,4-Dioxan / Water (10:1)	100	16	10
11	1.0	KOAc	$Pd(dppf)Cl_2$	3.00	DMSO	70	16	27
12	1.0	KOAc	$Pd(dppf)Cl_2$	3.00	DMSO	90	16	63
13	1.0	KOAc	$Pd(dppf)Cl_2$	3.00	DMSO	120	16	13
14	1.0	KOAc	$Pd(dppf)Cl_2$	2.60	DMSO	100	16	66
15	1.0	KOAc	$Pd(dppf)Cl_2$	2.80	DMSO	100	16	70
16	1.0	KOAc	$Pd(dppf)Cl_2$	2.80	DMSO	100	2[4]	91
17	1.0	KOAc	$Pd(dppf)Cl_2$	2.80	DMSO	90	4[4]	86

General Procedure for the Miyaura Borylation

Under inert conditions, the corresponding di-iodinated diazocine (1.00 equiv), $Pd(dppf)Cl_2$ (5 mol%), B_2Pin_2 (2.80 equiv) and KOAc (4.00 equiv) were dissolved in DMSO (10 mL/mmol). The mixture was stirred at 100 °C and the reaction progress was monitored by TLC (cyclohexane/DCM/ethyl acetate 55/40/5). After completion (approx. 2 h), the reaction mixture was diluted with ethyl acetate (20 mL/mmol) and washed with brine (4 × 50 mL/mmol). The organic phase was dried over sodium sulfate, filtered and the solvent removed *in vacuo*. The residue was purified by column chromatography on silica (eluent: cyclohexane/DCM/ethyl acetate 55/40/5) to obtain the corresponding diazocine as a yellow solid.

[4] Stopped after consumption of starting material. Monitored by TLC every 20 minutes.

(*Z*)-2,9-Bis(4,4,5,5-tetramethyl-1,3,2-dioxaborolan-2-yl)-11,12-dihydrodibenzo[*c,g*][1,2]diazocine (**5**)

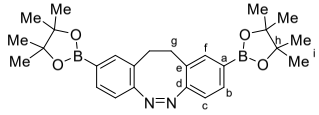

Compound **5** was synthesized according to the general procedure from (*Z*)-3,8-diiodo-11,12-dihydrodibenzo[*c,g*][1,2]diazocine (**1**). The product **5** was obtained after purification via column chromatography on silica (eluent: cyclohexane/DCM/ethyl acetate 55/40/5) as a yellow solid (419 mg, 910 µmol, 91%). The reaction was repeated on a 4.00 mmol scale yielding **5** in 82%.

^{1}H NMR (600 MHz, $CDCl_3$) δ = 7.55 (dd, ^3J = 7.8 Hz, ^4J =1.1 Hz, 2H, *H*-b), 7.40 (d, ^4J = 1.1 Hz, 2H, *H*-f), 6.8 (d, ^3J = 7.8 Hz, 2H, *H*-c), 2.98 - 2.78 (m, 4H, *H*-g), 1.30 (d, ^3J = 5.7 Hz, 24H, *H*-j) ppm.
^{13}C{^{1}H} NMR (151 MHz, $CDCl_3$) δ = 158.0 (*C*-d), 136.6 (*C*-f), 133.3 (*C*-b), 127.3 (*C*-e), 118.1(*C*-c), 84.0 (*C*-h), 31.6 (*C*-g), 25.1 (*C*-i), 25.0 (*C*-i) ppm.[5]
^{11}B{^{1}H}NMR (193 MHz, $CDCl_3$) δ 31.0 ppm.
IR (ATR): $\tilde{\nu}$ = 2977 (w, br), 1605 (w), 1485 (w), 1468 (w), 1408 (w), 1389 (m), 1354 (s), 1327 (m), 1278 (m), 1210 (w), 1166 (w), 1139 (s), 1118 (m), 1108 (s), 1013 (w), 992 (w), 964 (m), 909 (w), 848 (s), 832 (m), 811 (w), 776 (w), 745 (w), 709 (w), 695 (w), 680 (m) cm^{-1}.
HRMS (EI, 70 eV) *m/z* (%): $[M]^+$ calcd for $[C_{26}H_{34}{}^{11}B_2N_2O_4]^+$ 460.27083; found 460.27096, 83.1 (100).
Mp: 275°C.
R$_f$ = 0.60 (cyclohexane/DCM/EA 5/4/1).

2,9-Bis(4,4,5,5-tetramethyl-1,3,2-dioxaborolan-2-yl)-5,6,11,12-tetrahydrodibenzo[c,g][1,2]diazocine

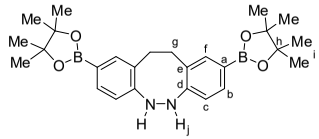

Side product 2,9-Bis(4,4,5,5-tetramethyl-1,3,2-dioxaborolan-2-yl)-5,6,11,12-tetrahydrodibenzo[c,g][1,2]di-azocine was synthesized according to the general procedure from (*Z*)-3,8-diiodo-11,12-dihydrodibenzo[*c,g*][1,2]diazocine (**1**) with longer reaction times of 18 h. The product 2,9-Bis(4,4,5,5-tetramethyl-1,3,2-dioxaborolan-2-yl)-5,6,11,12-tetrahydrodibenzo[c,g][1,2]di-azocine was obtained after purification via column chromatography on silica (eluent: cyclohexane/ethyl acetate 4/1) as a colourless solid (210 mg, 455 µmol, 46%).

^{1}H NMR (600 MHz, $CDCl_3$) δ = 7.59 (d, ^4J = 1.5 Hz, 2H, *H*-f), 7.52 (dd, ^3J = 7.7 Hz, ^3J = 1.5 Hz, 2H, *H*-b), 6.70 (d, ^3J = 7.7 Hz, 2H, *H*-c), 5.63 (s, 2H, *H*-j), 3.20 (s, 4H, *H*-g), 1.33 (s, 24H, *H*-i). ppm.
^{13}C{^{1}H} NMR (151 MHz, $CDCl_3$) δ =149.3 (*C*-d), 137.8 (*C*-f), 133.6 (*C*-b), 132.5 (*C*-e), 122.4 (*C*-a), 116.8 (*C*-c), 83.6 (*C*-h), 31.2 (*C*-g), 25.0 (*C*-i), 24.9 (*C*-i) ppm.
^{11}B{^{1}H}NMR (193 MHz, $CDCl_3$) δ 31.0 ppm.
IR (ATR): $\tilde{\nu}$ = 3356(w), 2976 (w), 2920 (w), 1607 (w), 1577 (w), 1515 (w), 1470 (w), 1442 (w), 1409 (w), 1372 (m), 1349 (m), 1326 (w), 1270 (w), 1240 (w), 1216 (w), 1167(m), 1143 (m), 1131 (m), 1119 (m), 1094 (w), 1008 (w), 966 (w), 952 (w), 925 (w), 905 (w), 855 (w), 823 (w), 767 (w), 742 (w), 697 (m), 681 (m) cm^{-1}.

[5] Due to the quadrupolar relaxation of the boron nucleus *C*-b was not observed.

HRMS (EI, 70 eV) *m/z* (%): $[M]^+$ calcd for $[C_{26}H_{36}{}^{11}B_2N_2O_4]^+$ 462.28612; found 462.28613, 232.1 (100).
Mp: 218°C.
R$_f$ = 0.43 (cyclohexane/ethyl acetate 4/1).

(*Z*)-3,8-Bis(4,4,5,5-tetramethyl-1,3,2-dioxaborolan-2-yl)-11,12-dihydrodibenzo[*c,g*][1,2]diazocine (**6**)

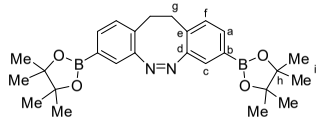

Compound **6** was synthesized according to the general procedure from (*Z*)-3,8-diiodo-11,12-dihydrodibenzo[*c,g*][1,2]diazocine (**2**). The product **6** was obtained after purification via column chromatography on silica (eluent: cyclohexane/DCM/ethyl acetate 55/40/5) as a yellow solid (312 mg, 678 µmol, 68%).

^{1}H NMR (600 MHz, $CDCl_3$) δ = 7.43 (dd, ^3J = 7.5 Hz, ^4J = 1.2 Hz, 2H, *H*-a), 7.29 (ad, ^4J = 1.2 Hz, 2H, *H*-c), 6.98 (d, ^3J = 7.5 Hz, 2H, *H*-f), 3.02 – 2.75 (m, 4H, *H*-g), 1.30 (d, ^3J = 5.8 Hz, 24H, *H*-i) ppm.
^{13}C{^{1}H} NMR (151 MHz, $CDCl_3$) δ = 155.0 (*C*-d), 133.5 (*C*-a), 131.1 (*C*-e), 129.1 (*C*-f), 125.5 (*C*-c), 84.1 (*C*-h), 32.1 (*C*-g), 25.1 (*C*-h), 24.9 (*C*-h) ppm.[6]
^{11}B{^{1}H} NMR (193 MHz, $CDCl_3$) δ = 29.73 ppm.
IR (ATR): $\tilde{\nu}$ = 2981 (w, br), 1606 (w), 1496 (w), 1389 (m), 1357 (s), 1325 (m), 1262 (m), 1262 (w), 1211 (m), 1141 (s), 1122 (m), 1106 (s), 965 (m), 997 (w), 850 (s), 821 (m), 717 (m) cm^{-1}.
HRMS (ESI) *m/z*: $[M + H]^+$ calcd for $[C_{26}H_{35}{}^{11}B_2N_2O_4 + H]^+$ 461.27799; found 461.27800.
Mp: 282 °C.
R$_f$ = 0.38 (cyclohexane/DCM/ethyl acetate 55/40/5).

[6] Due to the quadrupolar relaxation of the boron nucleus *C*-b was not observed.

Optimization for the Stille Cross-Coupling Reaction

The Stille reaction is a well investigated cross-coupling method with many different reported reaction conditions and catalytic systems.[7] Depending on the reaction conditions, the Stille reaction proceeds via a concerted or an open reaction mechanism. The conversion of the reaction can be highly enhanced by the addition of an additive suitable for the specific mechanism. However, this additive can also hinder the reaction if the mechanism proceeds via the other pathway. Hence, the reaction conditions have to be evaluated carefully when applying the Stille reaction.[8] Although there has been a lot of progress in the reaction conditions of the Stille reaction,[7] these benefits have not been exploited to the Stille reaction on diazocines so far, i.e. no additives were used[9] or the combination of the catalytic system with the solvent and additive was not effective.[10]. As our group has a broad expertise in the Stille cross-coupling reaction, we were interested if the coupling of diazocines can be highly enhanced by an efficient combination of the catalytic system. Firstly, we applied the reaction conditions of our established protocol of the Stille reaction for stannylated azobenzenes[11] on the stannylated diazocine **3** (**Table S3**, entry 1). With the addition of CuCl and LiCl, we could obtain the product **12** in 42% yield, which is significantly lower than the yield for the corresponding azobenzene. As the reaction required a high stochiometric amount of the additives and a long reaction time, we envisioned that another catalytic system might be more efficient. Baldwin and co-workers reported a great enhancement of the Stille reaction using a combination of CuI and CsF as additives.[12] This method proceeds under mild conditions as it provides the cross-coupling products in good yields while using a low reaction temperature of only 45 °C.[12] Unfortunately, using these reaction conditions in the Stille reaction of stannylated diazocine **3** with 4-bromotoluene led to no detectable formation of the cross-coupling product **7** (entry 2). By increasing the reaction temperature to 70 °C, the desired coupling product **7** could be obtained in 70% yield (entry 3). A full conversion of stannylated diazocine **3** could not be achieved with this catalytic system and side reactions occurred that could not be further analyzed. To circumvent these side reactions, a different catalytic system was used. Buchwald and co-workers published an efficient protocol for the Stille reaction using $Pd(OAc)_2$/XPhos as catalytic system, CsF as additive and DME as solvent.[13] Compared to the previously used conditions, this method requires lower catalyst loads and fewer additives. Remarkably, they were able to couple stannylated compounds with a wide range of even chlorinated electrophilic compounds, which are less reactive than the commonly used brominated derivatives. However, the Stille reaction of the stannylated diazocine **3** and 4-chlorotoluene led to no detectable formation of the desired coupling product **7** within 4 h (entry 4). Changing the electrophilic compound to the more reactive 4-bromotoluene proved to be successful; the coupling product **7** was obtained in 94% yield (entry 5). Decreasing the amount of catalytic system and additive further, led to no significant decrease in yield (entry 6). As we could also more than double the yield of the coupling between **3** and 4-bromoanisole with these reaction conditions compared to our first attempt (entry 7), these conditions were used to investigate the scope of the Stille reaction of diazocines.

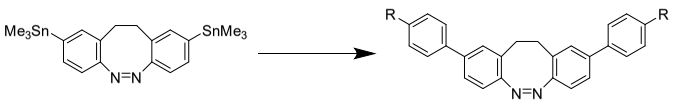

3

Table S4. Optimization of Stille cross-coupling reaction of stannylated diazocine **3**.

Entry	Coupling Partner	Catalytic System	Additives	Solvent	T [°C]	T [h]	Yield [%]
1	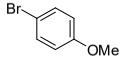 (2.33 equiv)	$Pd(PPh_3)_4$ (4 mol%)	CuCl (6.00 equiv), LiCl (12.0 equiv)	DMF	70	65	43
2	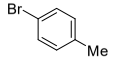 (2.00 equiv)	$PdCl_2$ (4 mol%), P(*t*-Bu_3)(8 mol%)	CuI (8 mol%), CsF (4.00 equiv)	DMF	45	100	--
3	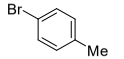 (2.00 equiv)	$PdCl_2$ (4 mol%), P(*t*-Bu_3)(8 mol%)	CuI (8 mol%), CsF (1.80 equiv)	DMF	70	19	70
4	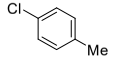 (2.00 equiv)	$Pd(OAc)_2$ (4 mol%), XPhos (4.4 mol%)	CsF (4.00)	DME	80	4	--
5	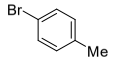 (2.00 equiv)	$Pd(OAc)_2$ (4 mol%), XPhos (4.4 mol%)	CsF (4.00)	DME	80	4	94
6	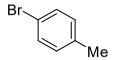 (2.00 equiv)	$Pd(OAc)_2$ (2 mol%), XPhos (2.2 mol%)	CsF (2.00)	DME	80	4	92
7	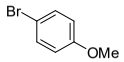 (2.00 equiv)	$Pd(OAc)_2$ (2 mol%), XPhos (2.2 mol%)	CsF (2.00)	DME	80	4	90

General Procedure for the Stille Cross-Coupling Reaction

Under inert conditions, the corresponding di-stannylated diazocine (53.4 mg, 100 µmol, 1.00 equiv), the corresponding brominated coupling partner (200 µmol, 2.00 equiv), $Pd(OAc)_2$ (449 µg, 2.00 µmol, 2 mol%), XPhos (1.05 mg, 2.20 µmol, 2.2 mol%) and CsF (30.4 mg, 200 µmol, 2.00 equiv) were dissolved in dry DME (2 mL) in a pressure reaction vial. The mixture was stirred at 80 °C for 24 h. After cooling to 23 °C, the reaction mixture was filtered through Celite® and the solvent was removed under reduced pressure.

Optimization and General Procedure for the Suzuki Cross-Coupling Reaction

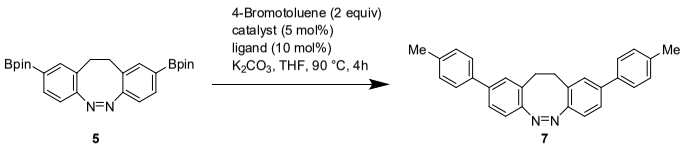

5 7

Table S5. Optimization of Suzuki cross-coupling reaction of borylated diazocine **5**.

Catalyst	Ligand	Yield (%)
$Pd(PPh_3)_4$		35
$Pd(ddpf)_2Cl_2$	-	39
$Pd(OAc)_2$	-	53
$Pd(OAc)_2$	XantPhos	54
$Pd(OAc)_2$	BrettPhos	51
$Pd(OAc)_2$	SPhos	86
$Pd(OAc)_2$	XPhos	91

Under inert conditions, the corresponding di-borylated diazocine **5** (46.0 mg, 100 µmol, 1.00 equiv), $Pd(OAc)_2$ (1.12 mg, 5 µmol, 5 mol%), XPhos (4.77 mg, 10.0 µmol, 10 mol%), K_2CO_3 (69.11 mg, 500 µmol, 5.00 equiv) and the corresponding brominated coupling partner (200 µmol, 2.00 equiv) were dissolved in THF (5 mL) and sealed in a pressure reaction vial. The mixture was stirred at 90 °C for 18 h. After cooling to 23 °C, the reaction mixture was filtered through Celite® and the solvent was removed under reduced pressure.

(*Z*)-2,9-Di-*p*-tolyl-11,12-dihydrodibenzo[*c*,*g*][1,2]diazocine (**7**)

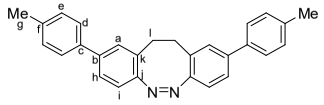

Stille cross-coupling reaction:

Compound **7** was synthesized according to the general procedure from 4-bromotoluene (34.2 mg, 200 µmol) with a reaction time of 4 h. The product **7** was obtained after purification via column chromatography on silica (eluent: cyclohexane/DCM 1/2) as a yellow solid (35.6 mg, 91.6 µmol, 92%).

Suzuki cross-coupling reaction:

Compound **7** was synthesized according to the general procedure from 4-bromotoluene (34.2 mg, 200 µmol). The product **7** was obtained after purification via column chromatography on silica (eluent: cyclohexane/DCM 3/2) as a yellow solid (35.2 mg, 90.6 µmol, 91%).

^{1}H NMR (600 MHz, $CDCl_3$) δ = 7.39 (d, ^3J = 8.3 Hz, 2H, *H*-d), 7.37 (dd, ^3J = 8.1 Hz, ^4J = 1.9 Hz, 2H, *H*-h), 7.21 (ad, ^4J = 1.9 Hz, 2H, *H*-a), 7.18 (d, ^3J = 8.3 Hz, 4H, *H*-e), 6.96 (d, ^3J = 8.1 Hz, 2H, *H*-i), 2.97 (s, 4H, *H*-l), 2.35 (s, 6H, *H*-g) ppm.
^{13}C{^{1}H} NMR (151 MHz, $CDCl_3$) δ = 154.5 (*C*-j), 140.1 (*C*-b), 137.4 (*C*-f), 137.3 (*C*-c), 129.6 (*C*-e), 128.5 (*C*-k), 128.2 (*C*-a), 126.9 (*C*-d), 125.4 (*C*-h), 119.9 (*C*-i), 32.2 (*C*-l), 21.2 (*C*-g) ppm.
IR (ATR): $\tilde{\nu}$ = 2914 (w), 1601 (w), 1515 (m), 1478 (m), 1462 (w), 1389 (w), 1184 (w), 1112 (w), 898 (m), 837 (w), 811 (s), 797 (s), 714 (w) cm^{-1}.
HRMS (EI, 70 eV) *m/z* (%): $[M]^+$ calcd for $[C_{28}H_{24}N_2]^+$ 388.19340; found 388.19379, 360.0 (100).
Mp: 192 °C**.**
R_f: 0.62 (cyclohexane/DCM 1/2), 0.17 (cyclohexane/DCM 3/2)

(*Z*)-2,9-Bis(4-isopropylphenyl)-11,12-dihydrodibenzo[*c*,*g*][1,2]diazocine (**8**)

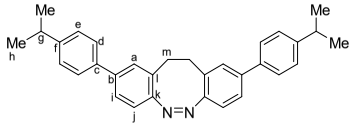

Stille cross-coupling reaction:

Compound **8** was synthesized according to the general procedure from 1-bromo-4-isopropylbenzene (39.8 mg, 200 µmol) with a reaction time of 4 h. The product **8** was obtained after purification via column chromatography on silica (eluent: cyclohexane/ethyl acetate 4/1) as a yellow solid (39.9 mg, 89.7 µmol, 90%).

Suzuki cross-coupling reaction:

Compound **8** was synthesized according to the general procedure from 1-bromo-4-isopropylbenzene (39.8 mg, 200 µmol). The product **8** was obtained after purification via column chromatography on silica (eluent: cyclohexane/DCM 3/2) as a yellow solid (37.4 mg, 84.1 µmol, 84%).

^{1}H NMR (600 MHz, $CDCl_3$) δ = 7.41 (d, ^3J = 8.2 Hz, 4H, *H*-d), 7.37 (dd, ^3J = 8.1 Hz, ^4J = 1.9 Hz, 2H, *H*-i), 7.24 (d, ^3J = 8.2 Hz, 4H, *H*-e), 7.21 (ad, ^4J = 1.9 Hz, 2H, *H*-a), 6.95 (d, ^3J = 8.1 Hz, 2H, *H*-j), 2.96 (s, 4H, *H*-m) , 2.91 (p, ^3J = 6.9 Hz, 2H, *H*-g) , 1.25 (d, ^3J = 6.9 Hz, 12H, *H*-h) ppm.

$^{13}C\{^{1}H\}$ NMR (151 MHz, $CDCl_3$) δ = 154.6 (*C*-k), 148.4 (*C*-f), 140.1 (*C*-b), 137.7 (*C*-c), 128.5 (*C*-l), 128.3 (*C*-a), 127.0 (*C*-d), 127.0 (*C*-e), 125.4 (*C*-i), 119.8 (*C*-j), 33.9 (*C*-g), 32.2 (*C*-m), 24.1 (*C*-h) ppm.
IR (ATR): $\tilde{\nu}$ = 2958 (w), 1906 (w), 1515 (w), 1478 (m), 1458 (w), 1387 (w), 1362 (w), 1302 (w), 1097 (w), 1057 (w), 1017 w), 952 (w), 900 (m), 839 (m), 821 (s), 804 (s), 740 (w), 697 (w) cm^{-1}.
HRMS (EI, 70 eV) *m/z* (%): $[M]^+$ calcd for $[C_{32}H_{32}N_2]^+$ 444.25600; found 444.25554, 401.0 (100).
Mp: 200 °C**.**
R_f: 0.47 (cyclohexane/ethyl acetate 4/1), 0.23 (cyclohexane/DCM 3/2).

(*Z*)-2,9-Bis(3-isopropylphenyl)-11,12-dihydrodibenzo[*c*,*g*][1,2]diazocine (**9**)

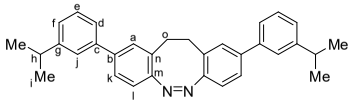

Stille cross-coupling reaction:

Compound **9** was synthesized according to the general procedure from 1-bromo-3-isopropylbenzene (39.8 mg, 200 µmol) with a reaction time of 4 h. The product **9** was obtained after purification via column chromatography on silica (eluent: cyclohexane/ethyl acetate 4/1) as a yellow solid (41.1 mg, 93.1 µmol, 93%).

Suzuki cross-coupling reaction:

Compound **9** was synthesized according to the general procedure from 1-bromo-3-isopropylbenzene (39.8 mg, 200 µmol). The product **9** was obtained after purification via column chromatography on silica (eluent: cyclohexane/DCM 3/2) as a yellow solid (36.5 mg, 82.1 µmol, 82%).

^{1}H NMR (600 MHz, $CDCl_3$) δ = 7.40 (dd, ^{3}J = 8.2 Hz, ^{4}J = 1.9 Hz, 2H, *H*-k), 7.34 (s, 2H, *H*-j), 7.31 (d, ^{3}J = 5.2 Hz, 4H, *H*-d, e), 7.24 (ad, ^{4}J = 1.9 Hz, 2H, *H*-a), 7.20 – 7.16 (m, 2H, *H*-f), 6.97 (d, ^{3}J = 8.2 Hz, 2H, *H*-l), 3.13 – 2.85 (m, 6H, *H*-h, o), 1.26 (d, ^{3}J = 7.0 Hz, 12H, *H*-i) ppm.
$^{13}C\{^{1}H\}$ NMR (151 MHz, $CDCl_3$) δ = 154.7 (*C*-m), 149.6 (*C*-g), 140.4 (*C*-b), 140.2 (*C*-c), 128.9 (*C*-e), 128.5 (*C*-a), 128.5 (*C*-n), 125.7 (*C*-k), 125.7 (*C*-f), 125.3 (*C*-j), 124.6 (*C*-d), 119.8 (*C*-l), 34.4 (*C*-h), 32.2 (*C*-o), 24.2 (*C*-i) ppm.
IR (ATR): $\tilde{\nu}$ = 3022 (w), 2956 (m), 1732 (w), 1600 (m), 1515 (w), 1473 (m), 1460 (m), 1431.7 (w), 1383 (w), 1362 (w), 1330 (w), 1259 (w), 1171 (w), 1097 (w), 1048 (w), 999 (w), 887 (m), 830 (m), 789 (s), 702 (s), 667 (w) cm^{-1}.
HRMS (EI, 70 eV) *m/z* (%): $[M]^+$ calcd for $[C_{32}H_{32}N_2]^+$ 444.25600; found 444.25576, 416.0 (100).
Mp: 101 °C**.**
R_f: 0.52 (cyclohexane/ethyl acetate 4/1), 0.13 (cyclohexane/DCM 3/2).

(*Z*)-2,9-Bis(2-isopropylphenyl)-11,12-dihydrodibenzo[*c*,*g*][1,2]diazocine (**10**)

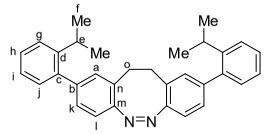

Stille cross-coupling reaction:

Compound **10** was synthesized according to the general procedure from 1-bromo-2-isopropylbenzene (39.8 mg, 200 µmol) using pre-milled $Pd(OAc)_2$/XPhos (1:3 ratio, 16.5 mg, 10.0 µmol, 10 mol%). The reaction mixture was stirred for 3 d at 80 °C. The product **10** was obtained after purification via column chromatography on silica (eluent: cyclohexane/DCM 1/1) as a yellow solid (38.2 mg, 85.8 µmol, 86%).

Suzuki cross-coupling reaction:

Compound **10** was synthesized according to the general procedure from 1-bromo-2-isopropylbenzene (39.8 mg, 200 µmol). The product **10** was obtained after purification via column chromatography on silica (eluent: cyclohexane/DCM 3/2) as a yellow solid (26.8 mg, 60.2 µmol, 60%).

^{1}H NMR (600 MHz, $CDCl_3$) δ 7.34 (dd, ^{3}J = 7.9 Hz, ^{4}J = 1.5 Hz, 2H, *H*-g), 7.31 (ddd, ^{3}J = 7.9 Hz, ^{3}J = 7.4 Hz, ^{4}J = 1.4 Hz, 2H, *H*-h), 7.16 (ddd ^{3}J = 7.4, ^{3}J = 7.3 Hz, ^{4}J = 1.5 Hz, 2H, *H*-i), 7.11 (dd, ^{3}J = 6.2 Hz, ^{4}J = 1.8 Hz, 2H, *H*-k), 7.02 (dd, ^{3}J = 7.3 Hz, ^{4}J = 1.4 Hz 2H, *H*-j), 6.93 (d, ^{4}J = 1.8 Hz 2H, *H*-a), 6.92 (d, ^{3}J = 6.2 Hz, 2H, *H*-l), 3.11 - 2.75 (m, 4H, *H*-o), 2.94 – 2.88 (m, 2H, *H*-e), 1.11 (d, ^{3}J = 8.2 Hz, 12H, *H*-f) ppm.
$^{13}C\{^{1}H\}$ NMR (151 MHz, $CDCl_3$) δ = 154.5 (*C*-k), 146.4 (*C*-d), 141.1 (*C*-b), 140.2 (*C*-c), 130.5 (*C*-a), 129.9 (*C*-j), 128.1 (*C*-n), 128.0 (*C*-g), 127.7 (*C*-k), 125.7 (*C*-h), 125.4 (*C*-i), 118.7 (*C*-l), 32.0 (*C*-o), 29.4 (*C*-e), 24.3 (*C*-f), 24.2 (*C*-f) ppm.
IR (ATR): $\tilde{\nu}$ = 2960 (m, br), 1474 (m), 1345 (w), 1085 (w), 1043 (w), 909 (m), 832 (m), 816 (w), 756 (s), 741 (s) cm^{-1}.
HRMS (EI, 70 eV) *m/z* (%): $[M]^+$ calcd for $[C_{32}H_{32}N_2]^+$ 444.25600; found 444.25363, 444.0 (100).
Mp: 141 °C**.**
R_f: 0.22 (cyclohexane/DCM 1/1), 0.17 (cyclohexane/DCM 3/2).

(*Z*)-2,9-Dimesityl-11,12-dihydrodibenzo[*c*,*g*][1,2]diazocine (**11**)

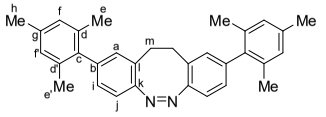

Stille cross-coupling reaction:

Compound **11** was synthesized according to the general procedure from 2-bromomesitylene (39.8 mg, 200 µmol) using pre-milled $Pd(OAc)_2$/XPhos (1:3 ratio, 16.5 mg, 10.0 µmol, 10 mol%). The reaction mixture was stirred for 3 d at 80 °C. The product **11** was obtained after purification via column chromatography on silica (eluent: cyclohexane → DCM) as a yellow solid (25.5 mg, 57.3 µmol, 57%).

Suzuki cross-coupling reaction:

Compound **11** was synthesized according to the general procedure from 2-bromomesitylene (39.8 mg, 200 µmol). The product **11** was obtained after purification via column chromatography on silica (eluent: cyclohexane/DCM 3/2) as a yellow solid (15.7 mg, 35.3 µmol, 35%).

^{1}H NMR (600 MHz, $CDCl_3$) δ = 6.94 – 6.90 (m, 6H, *H*-i, j, f'), 6.85 (ad, ^4J = 2.0 Hz, 2H, *H*-f), 6.76 (ad, ^4J = 1.3 Hz, 2H, *H*-a), 3.13 – 2.71 (m, 4H, *H*-m), 2.29 (s, 6H, *H*-h), 2.03 (s, 6H, *H*-e), 1.64 (s, 6H, *H*-e') ppm.
^{13}C{^{1}H} NMR (151 MHz, $CDCl_3$) δ = 154.4 (*C*-k), 140.1 (*C*-b), 138.2 (*C*-c), 136.9 (*C*-g), 136.1 (*C*-d), 135.9 (*C*-d'), 130.4 (*C*-a), 128.6 (*C*-l), 128.0 (*C*-f), 127.8 (*C*-f', i), 118.9 (*C*-j), 32.0 (*C*-m), 21.1 (*C*-h), 20.9 (*C*-e), 20.5 (*C*-e') ppm.
IR (ATR): $\tilde{\nu}$ = 2917 (w, br), 2109 (w), 1901 (w), 1470 (m), 1435 (m), 1376 (w), 1326 (w), 1095 (m), 1037 (m), 901 (m), 854 (s), 827 (s), 809 (s), 744 (w), 704 (w) cm^{-1}.
HRMS (EI, 70 eV) *m/z* (%): $[M]^+$ calcd for $[C_{32}H_{32}N_2]^+$ 444.25600; found 444.25578, 416.0 (100).
Mp: 217 °C**.**
R_f: 0.33 (cyclohexane/DCM 1/2), 0.26 (cyclohexane/DCM 3/2).

(*Z*)-2,9-Bis(4-methoxyphenyl)-11,12-dihydrodibenzo[*c*,*g*][1,2]diazocine (**12**)

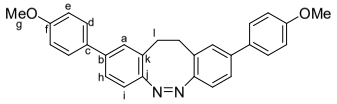

Stille cross-coupling reaction:

Compound **12** was synthesized according to the general procedure from 4-bromoanisole (37.4 mg, 200 µmol) with a reaction time of 4 h. The product **12** was obtained after purification via column chromatography on silica (eluent: cyclohexane/ethyl acetate 3/1) as a yellow solid (37.8 mg, 89.9 µmol, 90%).

Suzuki cross-coupling reaction:

Compound **12** was synthesized according to the general procedure from 4-bromoanisole (37.4 mg, 200 µmol). The product **12** was obtained after purification via column chromatography on silica (eluent: cyclohexane/DCM/ethyl acetate 5/4/1) as a yellow solid (39.8 mg, 94.6 µmol, 95%).

^{1}H NMR (600 MHz, $CDCl_3$) δ = 7.43 (d, ^3J = 8.8 Hz, 4H, *H*-d), 7.34 (dd, ^3J = 8.2 Hz, ^4J = 1.9 Hz, 2H, *H*-h), 7.19 (ad, ^4J = 1.9 Hz, 2H, *H*-a), 6.95 (d, ^3J = 8.2 Hz, 2H, *H*-i), 6.91 (d, ^3J = 8.8 Hz, 4H, *H*-e), 3.82 (s, 6H, *H*-g), 2.96 (s, 4H, *H*-l) ppm.
^{13}C{^{1}H} NMR (151 MHz, $CDCl_3$) δ = 159.4 (*C*-f), 154.3 (*C*-j), 139.7 (*C*-b), 132.7 (*C*-c), 128.5 (*C*-k), 128.1 (*C*-d), 127.9 (*C*-a), 125.1 (*C*-h), 120.0 (*C*-i), 114.3 (*C*-e), 55.5 (*C*-g), 32.2 (*C*-l) ppm.
IR (ATR): $\tilde{\nu}$ = 2923 (w), 2851 (w), 2223 (w), 1887 (w), 1606 (m), 1579 (w), 1513 (m), 1478 (m), 1461 (m), 1451 (m), 1440 (m), 1307 (w), 1289 (w), 1242 (s), 1179 (s), 1110 (m), 1031 (w), 1018 (m), 956 (w), 925 (w), 894 (m), 834 (m), 821 (s), 802 (s), 723 (w) cm^{-1}.
HRMS (EI, 70 eV) *m/z* (%): $[M]^+$ calcd for $[C_{28}H_{24}N_2O_2]^+$ 420.18322; found 420.18361, 392.0 (100).
Mp: 211 °C**.**
R_f: 0.37 (cyclohexane/ethyl acetate 3/1), 0.45 (cyclohexane/DCM/ ethyl acetate 5/4/1).

(*Z*)-4,4'-(11,12-Dihydrodibenzo[*c*,*g*][1,2]diazocine-2,9-diyl)diphenol (**13**)

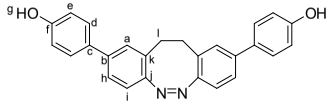

Stille cross-coupling reaction:

Compound **13** was synthesized according to the general procedure from 4-bromophenol (34.6 mg, 200 µmol) using pre-milled $Pd(OAc)_2$/XPhos (1:3 ratio, 16.5 mg, 10.0 µmol, 10 mol%). The reaction mixture was stirred for 3 d at 80 °C. The product **13** was obtained after purification via column chromatography on silica (eluent: DCM → DCM/MeOH 99/1) as a yellow solid (22.0 mg, 56.4 µmol, 56%).

Suzuki cross-coupling reaction:

Compound **13** was synthesized according to the general procedure from 4-bromophenol (34.6 mg, 200 µmol). No product was obtained.

^{1}H NMR (600 MHz, DMSO-d_6) δ = 9.53 (s, 2H, *H*-g), 7.41 (d, ^3J = 8.7 Hz, 4H, *H*-d), 7.40 (dd, ^3J = 8.2 Hz, ^4J = 2.0 Hz, 2H, *H*-h), 7.34 (ad, ^4J = 2.0 Hz, 2H, *H*-a), 6.93 (d, ^3J = 8.2 Hz, 2H, *H*-i), 6.77 (d, ^3J = 8.7 Hz, 4H, *H*-e), 2.93 – 2.86 (m, 4H, *H*-l) ppm.
^{13}C{^{1}H} NMR (151 MHz, DMSO-d_6) δ = 157.3 (*C*-f), 153.6 (*C*-j), 138.8 (*C*-b), 129.6 (*C*-c), 128.4 (*C*-k), 127.6 (*C*-d), 127.1 (*C*-a), 124.2 (*C*-h), 119.5 (*C*-i), 115.7 (*C*-e), 31.2 (*C*-l) ppm.
IR (ATR): $\tilde{\nu}$ = 3352 (br), 2930 (w, br), 1610 (m), 1593 (m), 1516 (s), 1478 (m), 1457 (m), 1380 (m), 1244 (s), 1172 (m), 1106 (w), 1003 (w), 898 (m), 814 (s), 802 (s), 755 (s) cm^{-1}.
HRMS (EI, 70 eV) *m/z* (%): $[M]^+$ calcd for $[C_{26}H_{20}N_2O_2]^+$ 392.15193; found 392.15221, 364.0 (100).
Mp: 190 °C**.**
R_f: 0.07 (DCM).

Side Product of the Suzuki Cross-Coupling Reaction (Z)-4-(11,12-dihydrodibenzo-[*c*,*g*][1,2]diazocin-2-yl)phenol (**32**)

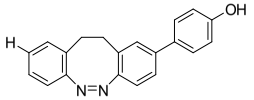

^{1}H NMR (600 MHz, $CDCl_3$) δ = 7.37 (d, ^3J = 8.6 Hz, 1H), 7.33 (d, ^3J = 8.8 Hz, 2H), 7.15 (d, ^4J = 2.0 Hz, 1H), 7.05 – 6.96 (m, 2H), 6.91 – 6.87 (m, 1H), 6.87 – 6.83 (m, 2H), 6.73 (d, ^3J = 8.8 Hz, 2H), 4.87 (s, 1H), 3.12 – 2.92 (m, 2H), 2.91 – 2.72 (m, 2H) ppm.
MS (EI, 70 eV) *m/z* (%): $[M]^+$ calcd for $[C_{20}H_{16}N_2O]^+$ 300.13; found 300 .1 (45), 272.1 (100).

(*Z*)-4,4'-(11,12-Dihydrodibenzo[*c*,*g*][1,2]diazocine-2,9-diyl)bis(*N*,*N*-dimethylaniline)-diazocine (**14**)

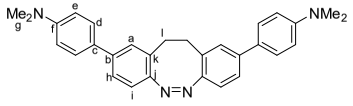

Stille cross-coupling reaction:

Compound **14** was synthesized according to the general procedure from 4-bromo-*N*,*N*-dimethylaniline (40.0 mg, 200 µmol). The product **14** was obtained after purification via column chromatography on silica (eluent: cyclohexane/ethyl acetate 3/1) as a yellow solid (40.6 mg, 90.9 µmol, 91%).

Suzuki cross-coupling reaction:

Compound **14** was synthesized according to the general procedure from 4-bromo-*N*,*N*-dimethylaniline (40.0 mg, 200 µmol). The product **14** was obtained after purification via column chromatography on silica (eluent: cyclohexane/DCM/ethyl acetate 5/4/1) as a yellow solid (13.7 mg, 30.7 µmol, 31%).

^{1}H NMR (600 MHz, $CDCl_3$) δ = 7.40 (d, ^3J = 8.2 Hz, 4H, *H*-d), 7.34 (dd, ^3J = 8.2 Hz, ^4J = 1.9 Hz, 2H, *H*-h), 7.18 (ad, ^4J = 1.9 Hz, 2H, *H*-a), 6.93 (d, ^3J = 8.2 Hz, 2H, *H*-i), 6.73 (d, ^3J = 8.2 Hz, 4H, *H*-e), 3.08 – 2.79 (m, 16H, *H*-g, l) ppm.
^{13}C{^{1}H} NMR (151 MHz, $CDCl_3$) δ = 153.8 (*C*-j), 150.2 (*C*-f), 140.0 (*C*-b), 128.4 (*C*-k), 128.1 (*C*-c), 127.6 (*C*-d), 127.4 (*C*-a), 124.6 (*C*-h), 120.0 (*C*-i), 112.8 (*C*-e), 40.7 (*C*-l), 32.3 (*C*-g) ppm.
IR (ATR): $\tilde{\nu}$ = 2922 (w), 2852 (w), 1888 (w), 1606 (m), 1579 (w), 1513 (m), 1478 (m), 1462 (m), 1451 (m), 1440 (m), 1307 (w), 1242 (s), 1179 (m), 1110 (w), 1031 (m), 1018 (m), 987 (w), 956 (w), 895 (w), 835 (m), 825 (m), 802 (s) cm^{-1}.
HRMS (EI, 70 eV) *m/z* (%): $[M]^+$ calcd for $[C_{30}H_{30}N_4]^+$ 446.24650; found 446.24601, 446.1(100).
Mp: 268 °C**.**
R$_f$: 0.40 (cyclohexane/ethyl acetate 3/1), 0.52(cyclohexane/DCM/ethyl acetate 5/4/1).

(*Z*)-4,4'-(11,12-Dihydrodibenzo[*c*,*g*][1,2]diazocine-2,9-diyl)bis(*N*,*N*-diphenylaniline) (**15**)

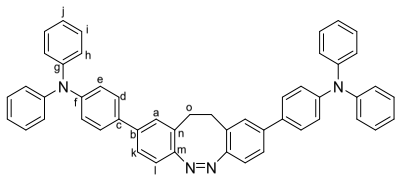

Stille cross-coupling reaction:

Compound **15** was synthesized according to the general procedure from 4-bromodiphenylamine (68.4 mg, 200 µmol). The product **15** was obtained after purification via column chromatography on silica (eluent: DCM) as a yellow solid (59.8 mg, 86.0 µmol, 86%).

Suzuki cross-coupling reaction:

Compound **15** was synthesized according to the general procedure from 4-bromodiphenylamine (68.4 mg, 200 µmol). The product **15** was obtained after purification via column chromatography on silica (eluent: cyclohexane/DCM/ethyl acetate 5/4/1) as a yellow solid (50.4 mg, 72.4 µmol, 72%).

^{1}H NMR (600 MHz, $CDCl_3$) δ = 7.39 – 7.34 (m, 6H, *H*-d/k), 7.26 – 7.23 (m, 8H, *H*-i), 7.20 (ad, ^4J = 1.9 Hz, 2H, *H*-a), 7.11 – 7.06 (m, 12H, *H*-h/e), 7.02 (tt, ^3J = 7.4 Hz, ^4J = 1.2 Hz, 4H, *H*-j), 6.93 (d, ^3J = 8.2 Hz, 2H, *H*-l), 3.10 – 2.80 (m, 4H, *H*-o) ppm.
^{13}C{^{1}H} NMR (151 MHz, $CDCl_3$) δ = 154.5 (*C*-m), 147.7 (*C*-g), 147.5 (*C*-f), 139.5 (*C*-b), 134.0 (*C*-c), 129.4 (*C*-i), 128.6 (*C*-n), 127.8 (*C*-a), 127.7 (*C*-d), 125.0 (*C*-k), 124.5 (*C*-h), 124.0 (*C*-e), 123.1 (*C*-j), 119.8 (*C*-l), 32.2 (*C*-o) ppm.
IR (ATR): $\tilde{\nu}$ = 3033 (br, w), 1589 (s), 1513 (m), 1478 (s), 1325 (m), 1272 (s), 1176 (w), 1075 (w), 1028 (w), 897 (w), 819 (m), 804 (m), 752 (s) cm^{-1}.
HRMS (APCI) *m/z* (%): $[M+H]^+$ calcd for $[C_{50}H_{38}N_4 + H]^+$ 695.31692; found 695.31639, 134.0 (100).
Mp: 134 °C**.**
R$_f$: 0.48 (DCM), 0.62 (cyclohexane/DCM/ethyl acetate 5/4/1).

(*Z*)-4,4'-(11,12-Dihydrodibenzo[*c*,*g*][1,2]diazocine-2,9-diyl)dianiline (**16**)

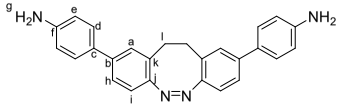

Stille cross-coupling reaction:

Compound **16** was synthesized according to the general procedure from 4-bromoaniline (34.4 mg, 200 µmol) using pre-milled $Pd(OAc)_2$/XPhos (1:3 ratio, 16.5 mg, 10.0 µmol, 10 mol%). The reaction mixture was stirred for 3 d at 80 °C. The product **16** was obtained after purification via column chromatography on silica (eluent: DCM → DCM/MeOH 99/1) as a yellow solid (18.3 mg, 46.9 µmol, 47%).

Suzuki cross-coupling reaction:

Compound **16** was synthesized according to the general procedure from 4-bromoaniline (34.4 mg, 200 µmol). No product was obtained.

^{1}H NMR (600 MHz, $CDCl_3$) δ = 7.33 – 7. 29 (m, 6H, *H*-d, h), 7.16 (ad, ^4J = 1.9 Hz, 2H, *H*-a), 6.92 (d, ^3J = 8.1 Hz, 2H, *H*-i), 6.69 (d, ^3J = 8.1 Hz, 4H, *H*-e), 3.70 (s, br, 4H, *H*-g), 3.09 – 2.76 (m, 4H, *H*- l) ppm.
^{13}C{^{1}H} NMR (151 MHz, $CDCl_3$) δ = 154.0 (*C*-j), 146.1 (*C*-f), 140.0 (*C*-b), 130.5 (*C*-c), 128.4 (*C*-k), 127.9 (*C*-d), 127.5 (*C*-a), 124.7 (*C*-h), 119.9 (*C*-i), 115.5 (*C*-e), 32.2 (*C*-l) ppm.
IR (ATR): $\tilde{\nu}$ = 3348 (br, m), 2926 (br, w), 1601 (s), 1517 (s), 1477 (s), 1432 (w), 1378 (m), 1278 (s), 1182 (m), 1129 (m), 895 (m), 819 (s), 804 (s) cm^{-1}.
HRMS (EI, 70 eV) *m/z* (%): $[M]^+$ calcd for $[C_{26}H_{22}N_4]^+$ 390.18390; found 390.18436, 362.1 (100).
Mp: 144 °C**.**
R$_f$: 0.10 (DCM).

Side Product of the Suzuki Cross-Coupling Reaction (*Z*)-4-(11,12-dihydrodibenzo-[*c*,*g*][1,2]diazocin-2-yl)aniline (**33**)

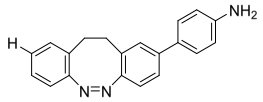

^{1}H NMR (600 MHz, $CDCl_3$) δ = 7.30 (m, 3H), 7.14 (d, ^4J = 2.2 Hz, 2H), 7.06 – 6.98 (m, 2H), 6.90 – 6.85 (m, 2H), 6.70 (d, ^3J = 8.4 Hz, 2H), 3.71 (s, 2H), 3.10 – 2.95 (m, 2H), 2.85 – 2.72 (m, 2H) ppm.
HRMS (EI, 70 eV) *m/z* (%): $[M]^+$ calcd for $[C_{20}H_{17}N_3]^+$ 299.14159; found 299.14170, 271.2 (100).

Side Product of the Suzuki Cross-Coupling Reaction (*Z*)-*N*1-(4-(11,12-dihydrodi-benzo[*c*,*g*][1,2]diazocin-2-yl)phenyl)benzene-1,4-diamine (**34**)

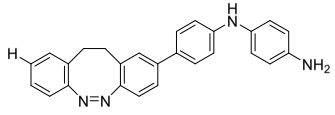

^{1}H NMR (600 MHz, $CDCl_3$) δ = 7.33 (d, ^3J = 8.6 Hz, 2H), 7.31 (dd, ^3J = 8.3 Hz, ^4J = 1.9 Hz, 1H), 7.17 – 7.12 (m, 2H), 7.05 – 6.95 (m, 4H), 6.90 – 6.83 (m, 4H), 6.68 (d, ^3J = 8.5 Hz, 2H), 5.47 (s, 1H), 3.56 (s, 2H), 3.16 – 2.95 (m, 2H), 2.87 – 2.73 (m, 2H) ppm.
MS (EI, 70 eV) *m/z* (%): $[M]^+$ calcd for $[C_{26}H_{22}N_4]^+$ 390.18; found 390.2 (40), 107.0 (100).

(*Z*)-2,9-Bis(4-nitrophenyl)-11,12-dihydrodibenzo[*c*,*g*][1,2]diazocine (**17**)

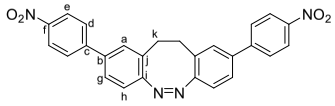

Stille cross-coupling reaction:

Compound **17** was synthesized according to the general procedure from 1-bromo-4-nitrobenzene (40.4 mg, 200 µmol). The product **17** was obtained after purification via column chromatography on silica (eluent: cyclohexane/ethyl acetate 3/1) as a yellow solid (40.1 mg, 89.0 µmol, 89%).

Suzuki cross-coupling reaction:

Compound **17** was synthesized according to the general procedure from 1-bromo-4-nitrobenzene (40.4 mg, 200 µmol). The product **17** was obtained after purification via column chromatography on silica (eluent cyclohexane/DCM/ethyl acetate 5/4/1) as a yellow solid (36.1 mg, 80.1 µmol, 80%).

^{1}H NMR (600 MHz, $CDCl_3$) δ = 8.24 (d, ^3J = 8.7 Hz, 4H, *H*-e), 7.64 (d, ^3J = 8.7 Hz, 4H, *H*-d), 7.45 (dd, ^3J = 8.2 Hz, ^4J = 1.9 Hz, 2H, *H*-g), 7.29 (ad, ^4J = 1.9 Hz, 2H, *H*-a), 7.04 (d, ^3J = 8.2 Hz, 2H, *H*-h), 3.20 – 2.83 (m, 4H, *H*-k) ppm.
^{13}C{^{1}H} NMR (151 MHz, $CDCl_3$) δ = 155.9 (*C*-i), 147.3 (*C*-f), 146.4 (*C*-c), 137.8 (*C*-b), 128.9 (*C*-a), 128.9 (*C*-j), 127.7 (*C*-d), 126.2 (*C*-g), 124.3 (*C*-e), 120.2 (*C*-h), 32.0 (*C*-k) ppm.

IR (ATR): $\tilde{\nu}$ = 2930 (w), 1592 (m), 1509 (s), 1339 (s), 1165 (w), 1110 (m), 1011 (w), 956 (w), 909 (w), 862 (m), 850 (s), 836 (m), 830 (m), 809 (m), 752 (s), 741 (m), 724 (w), 689 (m) cm^{-1}.
HRMS (EI, 70 eV) *m/z* (%): $[M]^+$ calcd for $[C_{26}H_{18}N_4O_4]^+$ 450.13226; found 450.13225, 44.0 (100).
Mp: 225 °C.
R_f: 0.29 (cyclohexane/ethyl acetate 3/1), 0.44 (cyclohexane/DCM/ethyl acetate 5/4/1).

(*Z*)-2,9-Bis(3-nitrophenyl)-11,12-dihydrodibenzo[*c*,*g*][1,2]diazocine (**18**)

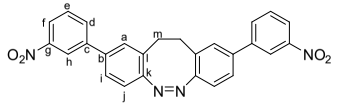

Stille cross-coupling reaction:

Compound **18** was synthesized according to the general procedure from 1-bromo-3-nitrobenzene (40.4 mg, 200 µmol). The product **18** was obtained after purification via column chromatography on silica (eluent: DCM) as a yellow solid (34.5 mg, 85.3 µmol, 85%).

Suzuki cross-coupling reaction:

Compound **18** was synthesized according to the general procedure from 1-bromo-3-nitrobenzene (40.4 mg, 200 µmol). The product **18** was obtained after purification via column chromatography on silica (eluent: cyclohexane/DCM/ethyl acetate 5/4/1) as a yellow solid (39.6 mg, 88.1 µmol, 88%).

^{1}H NMR (600 MHz, $CDCl_3$) δ 8.35 (dd, ^4J = 2.3 Hz, 2.0 Hz, 2H, *H*-h), 8.16 (ddd, ^3J = 8.0 Hz, ^4J = 2.3 Hz, ^4J = 1.0 Hz, 2H, *H*-f), 7.83 (ddd, ^3J = 7.7 Hz, ^4J = 2.0 Hz, ^4J = 1.0 Hz, 2H, *H*-d), 7.56 (dd, ^3J = 8.0 Hz, ^3J = 7.7 Hz, 2H, *H*-e), 7.44 (dd, ^3J = 8.2, ^4J = 2.0 Hz, 2H, *H*-i), 7.30 (d, ^4J = 2.0 Hz, 2H, *H*-a), 7.03 (d, ^3J = 8.2 Hz, 2H, *H*-j), 3.23 – 2.84 (m, 4H, m) ppm.
^{13}C{^{1}H} NMR (151 MHz, $CDCl_3$) δ 155.7 (*C*-k), 148.8 (*C*-g), 141.7 (*C*-b), 137.7 (*C*-c), 133.0 (*C*-d), 129.9 (*C*-e), 129.0 (*C*-l), 128.7 (*C*-a), 125.9 (*C*-i), 122.4 (*C*-f), 121.9 (*C*-h), 120.1 (*C*-j), 32.0 (*C*-m) ppm.
IR (ATR): $\tilde{\nu}$ = 3078 (w), 2924 (br, w), 1523 (s), 1470 (w), 1345 (s), 1103 (w), 1084 (w), 892 (m), 842 (m), 801 (m), 736 (s) cm^{-1}.
HRMS (EI, 70 eV) *m/z* (%): $[M]^+$ calcd for $[C_{26}H_{18}N_4O_4]^+$ 450.13226; found 450.13181, 422.0 (100).
Mp: 150 °C.
R_f: 0.36 (DCM), 0.47 (cyclohexane/DCM/ethyl acetate 5/4/1).

(*Z*)-2,9-Bis(2-nitrophenyl)-11,12-dihydrodibenzo[*c*,*g*][1,2]diazocine (**19**)

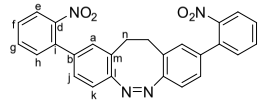

Stille cross-coupling reaction:

Compound **19** was synthesized according to the general procedure from 1-bromo-2-nitrobenzene (40.4 mg, 200 µmol). The product **19** was obtained after purification via column chromatography on silica (eluent: DCM) as a yellow solid (39.7 mg, 88.2 µmol, 88%).

Suzuki cross-coupling reaction:

Compound **19** was synthesized according to the general procedure from 1-bromo-2-nitrobenzene (40.4 mg, 200 µmol). The product **19** was obtained after purification via column chromatography on silica (eluent: cyclohexane/DCM/ethyl acetate 5/4/1) as a yellow solid (31.2 mg, 69.2 µmol, 69%).

^{1}H NMR (600 MHz, $CDCl_3$) δ = 7.82 (dd, ^3J = 8.1 Hz, ^4J = 1.3 Hz, 2H, *H*-e), 7.57 (ddd, ^3J = 7.7 Hz, ^3J = 7.5 Hz, ^4J = 1.3 Hz, 2H, *H*-g), 7.45 (ddd, ^3J = 8.1 Hz, ^3J = 7.5 Hz, ^4J = 1.5 Hz, 2H, *H*-f), 7.38 (dd, ^3J = 7.7 Hz, ^4J = 1.5 Hz, 2H, *H*-h), 7.10 (dd, ^3J = 8.0 Hz, ^4J = 1.9 Hz, 2H, *H*-j), 6.93 (d, ^4J = 1.9 Hz, 2H, *H*-a), 6.88 (d, ^3J = 8.0 Hz, 2H, *H*-k), 3.11 – 2.71 (m, 4H, *H*-n) ppm.
^{13}C{^{1}H} NMR (151 MHz, $CDCl_3$) δ = 155.6 (*C*-l), 149.2 (*C*-d), 136.5 (*C*-b), 135.6 (*C*-i), 132.5 (*C*-g), 132.2 (*C*-h), 129.3 (*C*-a), 128.9 (*C*-m), 128.5 (*C*-f), 126.6 (*C*-j), 124.2 (*C*-e), 119.0 (*C*-k), 31.6 (*C*-n)
IR (ATR): $\tilde{\nu}$ = 2922 (br, w), 1603 (w), 1519 (s), 1468 (m), 1345 (m), 1288 (w), 1085 (m), 899 (m), 781 (s), 750 (s), 732 (m) cm^{-1}.
HRMS (EI, 70 eV) *m/z* (%): $[M]^+$ calcd for $[C_{26}H_{18}N_4O_4]^+$ 450.13226; found 450.13003, 326.2 (100).
Mp: 151 °C**.**
R$_f$: 0.34 (DCM), 0.50 (cyclohexane/DCM/ethyl acetate 5/4/1).

(*Z*)-2,9-Bis(3,5-bis(trifluoromethyl)phenyl)-11,12-dihydrodibenzo[*c*,*g*][1,2]diazocine (**20**)

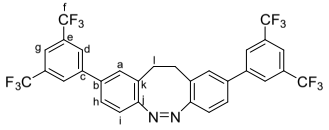

Stille cross-coupling reaction:

Compound **20** was synthesized according to the general procedure from 3,5-bis(trifluoromethyl)-brombenzene (58.6 mg, 200 µmol). The product **20** was obtained after purification via crystallization from DCM/MeOH (*v/v* 1/1) at -21 °C as a yellow solid (56.7 mg, 89.7 µmol, 90%).

Suzuki cross-coupling reaction:

Compound **20** was synthesized according to the general procedure from 3,5-bis(trifluoromethyl)-bromobenzene (58.6 mg, 200 µmol). The product **20** was obtained after purification via column chromatography on silica (eluent: cyclohexane/DCM/ethyl acetate 5/4/1) as a yellow solid (53.1 mg, 84.0 µmol, 84%).

^{1}H NMR (500 MHz, $CDCl_3$) δ = 7.92 – 7.90 (m, 4H, *H*-d), 7.83 – 7.79(m, 2H, *H*-g), 7.44 (dd, ^3J = 8.1 Hz, ^4J = 2.0 Hz, 2H, *H*-h), 7.28 (d, ^4J = 2.0 Hz, 2H, *H*-a), 7.05 (d, ^3J = 8.1 Hz, 2H, *H*-i), 3.23 – 2.90 (m, 4H, *H*-l) ppm.
^{13}C NMR (126 MHz, $CDCl_3$) δ = 155.9 (*C*-j), 142.1 (*C*-c), 137.3 (*C*-b), 132.4 (q, *J* = 33.4 Hz, *C*-e), 129.1 (*C*-k), 128.7 (*C*-a), 127.1 (d, *J* = 3.8 Hz, *C*-d), 126.0 (*C*-h), 124.5 (*C*-f), 122.3 (*C*-f), 121.3 (m, *C*-g) 120.3 (*C*-i), 31.9 (*C*-l) ppm.
^{19}F NMR (471 MHz, $CDCl_3$) δ = -63.4 ppm.
IR (ATR): $\tilde{\nu}$ = 2929 (w), 1465 (w), 1377 (s), 1278 (s), 1158 (m), 1128 (s), 1116 (s), 1056 (m), 893 (m), 882 (m), 845 (m), 825 (m), 805 (m), 776 (w), 708 (m9, 701 (m) cm^{-1}.
HRMS (APCI) *m/z* (%): $[M+H]^+$ calcd for $[C_{30}H_{16}F_{12}N_2 + H]^+$ 633.11946; found 633.11894, 134.0 (100).
Mp: 216 °C**.**
R$_f$: 0.35 (cyclohexane/ethyl acetate 9/1), 0.65 (cyclohexane/DCM/ethyl acetate 5/4/1).

(*Z*)-4,4'-(11,12-Dihydrodibenzo[*c*,*g*][1,2]diazocine-2,9-diyl)dibenzonitrile (**21**)

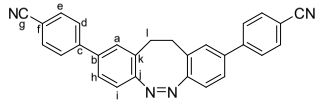

Stille cross-coupling reaction:

Compound **21** was synthesized according to the general procedure from 4-bromobenzonitrile (36.4 mg, 200 µmol) with a reaction time of 4 h. The product **21** was obtained after purification via column chromatography on silica (eluent: cyclohexane/ethyl acetate 3/1) as a yellow solid (36.6 mg, 89.2 µmol, 89%).

Suzuki cross-coupling reaction:

Compound **21** was synthesized according to the general procedure from 4-bromotoluene (34.2 mg, 200 µmol). The product **21** was obtained after purification via column chromatography on silica (eluent: cyclohexane/DCM/ethyl acetate 5/4/1) as a yellow solid (29.6 mg, 72.2 µmol, 72%).

^{1}H NMR (600 MHz, $CDCl_3$) δ = 7.67 (d, ^3J = 8.7 Hz, 4H, *H*-e), 7.58 (d, ^3J = 8.7 Hz, 4H, *H*-d), 7.40 (dd, ^3J = 8.2 Hz, ^4J = 1.9 Hz, 2H, *H*-h), 7.24 (ad, ^4J = 1.9 Hz, 2H, *H*-a), 7.01 (d, ^3J = 8.2 Hz, 2H, *H*-i), 3.41 – 2.62 (m, 4H, *H*-l) ppm.
^{13}C{^{1}H} NMR (151 MHz, $CDCl_3$) δ = 155.7 (*C*-j), 144.4 (*C*-c), 138.2 (*C*-b), 132.7 (*C*-e), 128.9 (*C*-k), 128.7 (*C*-a), 127.6 (*C*-d), 125.9 (*C*-h), 120.1 (*C*-i), 118.9 (*C*-g), 111.4 (*C*-f), 32.0 (*C*-l) ppm.
IR (ATR): $\tilde{\nu}$ = 2894 (w), 1682 (s), 1675 (s), 1601 (m), 1555 (w), 1519 (w), 1478 (w), 1434 (w), 1418 (w), 1391 (w), 1357 (m), 1317 (w), 1272 (m), 1258 (s), 1199 (m), 1199 (w), 1012 (w), 961.3 (m), 925 (w), 900 (m), 893 (m), 851 (w), 836 (m), 817 (s), 800 (s), 754 (w), 726 (w), 691 (w), 659 (w) cm^{-1}.
HRMS (EI, 70 eV) *m/z* (%): $[M]^+$ calcd for $[C_{28}H_{18}N_4]^+$ 410.15260; found 410.15298, 382.0 (100).
Mp: 238 °C**.**
R$_f$: 0.25 (cyclohexane/ethyl acetate 3/1), 0.31(cyclohexane/DCM/ethyl acetate 5/4/1).

(*Z*)-1,1'-((11,12-Dihydrodibenzo[*c*,*g*][1,2]diazocine-2,9-diyl)bis(4,1-phenylene))bis-(ethan-1-one) (**22**)

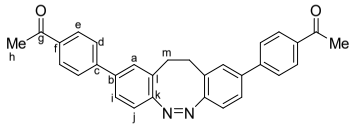

Stille cross-coupling reaction:

Compound **22** was synthesized according to the general procedure from 4-bromoacetophenone (39.8 mg, 200 µmol). The product **22** was obtained after purification via column chromatography on silica (eluent: cyclohexane/DCM 1/1) as a yellow solid (36.5 mg, 82.1 µmol, 82%).

Suzuki cross-coupling reaction:

Compound **22** was synthesized according to the general procedure from 4-bromoacetophenone (39.8 mg, 200 µmol). The product **22** was obtained after purification via column chromatography on silica (eluent: cyclohexane/DCM/ethyl acetate 5/4/1 → 2/2/1) as a yellow solid (26.2 mg, 58.9 µmol, 59%).

^{1}H NMR (600 MHz, $CDCl_3$) δ = 7.97 (d, ^3J = 8.4 Hz, 4H, *H*-e), 7.59 (d, ^3J = 8.4 Hz, 4H, *H*-d), 7.44 (dd, ^3J = 8.2 Hz, ^4J = 1.9 Hz, 2H, *H*-i), 7.29 (ad, ^4J = 1.9 Hz, 2H, *H*-a), 7.01 (d, ^3J = 8.2 Hz, 2H, *H*-j), 3.22 – 2.77 (m, 4H, *H*-m), 2.61 (s, 6H, *H*-h) ppm.
^{13}C{^{1}H} NMR (151 MHz, $CDCl_3$) δ = 197.8 (*C*-g), 155.5 (*C*-k), 144.6 (*C*-c), 138.9 (*C*-b), 136.2 (*C*-f), 129.0 (*C*-e), 128.7 (*C*-l), 128.7 (*C*-a), 127.1 (*C*-d), 125.9 (*C*-i), 120.0 (*C*-j), 32.1 (*C*-m), 26.8 (*C*-h) ppm.
IR (ATR): $\tilde{\nu}$ = 2894 (w), 1682 (s), 1674 (s), 1601 (m), 1556 (w), 1520 (w), 1476 (w), 1460 (w), 1434 (w), 1418 (w), 1390 (w), 1356 (m), 1272 (m), 1258 (s), 1199 (m), 1166 (w), 1120 (w), 1101 (w), 1079 (w), 1023 (w), 1012 (w), 962 (m), 900 (m), 893 (m), 851 (w), 836 (m), 817 (s), 799 (s), 754 (m), 726 (w), 691 (w), 659 (w) cm^{-1}.
HRMS (EI, 70 eV) *m/z* (%): $[M]^+$ calcd for $[C_{30}H_{24}N_2O_2]^+$ 444.18323; found 444.18275, 43.0 (100).
Mp: 189 °C**.**
R$_f$: 0.45 (cyclohexane/ethyl acetate 1/1), 0.29 (cyclohexane/DCM/ethyl acetate 5/4/1)

Dimethyl 4,4'-(11,12-dihydrodibenzo[*c*,*g*][1,2]diazocine-2,9-diyl)(*Z*)-dibenzoate (**23**)

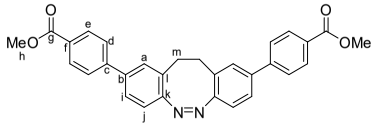

Stille cross-coupling reaction:

Compound **23** was synthesized according to the general procedure from methyl-4-bromobenzoate (43.0 mg, 200 µmol). The product **23** was obtained after purification via crystallization from DCM/*n*-hexane (*v/v* 1/2) at -21 °C as a yellow solid (38.3 mg, 80.2 µmol, 80%).

Suzuki cross-coupling reaction:

Compound **23** was synthesized according to the general procedure from methyl-4-bromobenzoate (43.0 mg, 200 µmol). The product **23** was obtained after purification via column chromatography on silica (eluent: cyclohexane/DCM/ethyl acetate 5/4/1) as a yellow solid (27.7 mg, 58.2 µmol, 58%).

^{1}H NMR (600 MHz, $CDCl_3$) δ = 8.04 (d, ^3J = 8.4 Hz, 4H, *H*-e), 7.56 (d, ^3J = 8.4 Hz, 4H, *H*-d), 7.43 (dd, ^3J = 8.2 Hz, ^4J = 1.9 Hz, 2H, *H*-i), 7.28 (ad, ^4J = 1.9 Hz, 2H, *H*-a), 7.00 (d, ^3J = 8.2 Hz, 2H, *H*-j), 3.91 (s, 6H, *H*-h), 3.12 – 2.88 (m, 4H, *H*-m) ppm.
^{13}C{^{1}H} NMR (151 MHz, $CDCl_3$) δ = 167.0 (*C*-g), 155.4 (*C*-k), 144.4 (*C*-c), 139.0 (*C*-b), 130.2 (*C*-e), 129.2 (*C*-f), 128.7 (*C*-a), 126.9 (*C*-d), 125.9 (*C*-i), 119.9 (*C*-j), 52.3 (*C*-h), 32.1 (*C*-m) ppm.
IR (ATR): $\tilde{\nu}$ = 2944 (br, w), 1711 (s), 1607 (w), 1522 (m), 1430 (m), 1345 (m), 1276 (s), 1183 (m), 1103 (s), 1015 (m), 962 (w), 894 (m), 802 (m), 766 (s), 740 (m) cm^{-1}.
HRMS (EI, 70 eV) *m/z* (%): $[M]^+$ calcd for $[C_{30}H_{24}N_2O_4]^+$ 476.17306; found 476.17340, 58.9 (100).
Mp: 233 °C**.**
R$_f$: 0.37 (cyclohexane/ethyl acetate 3/1), 0.48 (cyclohexane/DCM/ethyl acetate 5/4/1)

(*Z*)-2,9-Bis(benzo[*d*][1,3]dioxol-5-yl)-11,12-dihydrodibenzo[*c*,*g*][1,2]diazocine (**24**)

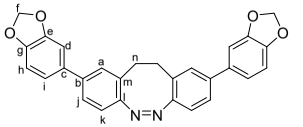

Stille cross-coupling reaction:

Compound **24** was synthesized according to the general procedure from 5-bromobenzo[d][1,3]dioxole (40.2 mg, 200 µmol). The product **24** was obtained after purification via column chromatography on silica (eluent: DCM) as a yellow solid (31.5 mg, 70.3 µmol, 70%).

Suzuki cross-coupling reaction:

Compound **24** was synthesized according to the general procedure from 5-bromobenzo[d][1,3]dioxole (40.2 mg, 200 µmol). The product **24** was obtained after purification via column chromatography on silica (eluent: cyclohexane/DCM/ethyl acetate 5/4/1) as a yellow solid (33.7 mg, 75.1 µmol, 75%).

^{1}H NMR (600 MHz, $CDCl_3$) δ = 7.30 (dd, ^3J = 8.1 Hz, ^4J = 1.9 Hz, 2H, *H*-j), 7.14 (ad, ^4J = 1.9 Hz, 2H, *H*-a), 6.98 – 6.96 (m, 4H, *H*-d/h), 6.93 (d, ^3J = 8.1 Hz, 2H, *H*-k), 6.82 (d, ^3J = 7.7 Hz, ^4J = 0.8 Hz, 2H, *H*-i), 5.96 (s, 4H, *H*-f), 3.12 – 2.78 (m, 4H, *H*-nl) ppm.
^{13}C{^{1}H} NMR (151 MHz, $CDCl_3$) δ = 154.5 (*C*-l), 148.3 (*C*-g), 147.4 (*C*-e), 139.8 (*C*-b), 134.5 (*C*-c), 128.5 (*C*-m), 128.1 (*C*-a), 125.3 (*C*-j), 120.6 (*C*-d), 119.9 (*C*-k), 108.7 (*C*-i), 107.6 (*C*-h), 101.3 (*C*-f), 32.1 (*C*-n) ppm.
IR (ATR): $\tilde{\nu}$ = 2987 (br, w), 1600 (w), 1504 (m), 1472 (s), 1436 (m), 1333 (w), 1256 (w), 1228 (s), 1102 (w), 1032 (s), 931 (s), 907 (m), 856 (m), 838 (m), 796 (s) cm^{-1}.
HRMS (EI, 70 eV) *m/z* (%): $[M]^+$ calcd for $[C_{28}H_{20}N_2O_4]^+$ 448.14176; found 448.14155, 420.0 (100).
Mp: 236 °C**.**
R$_f$: 0.24 (DCM), 0.44 (cyclohexane/DCM/ethyl acetate 5/4/1)

(*Z*)-2,9-Di(thiophen-2-yl)-11,12-dihydrodibenzo[*c*,*g*][1,2]diazocine (**25**)

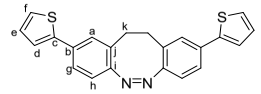

Stille cross-coupling reaction:

Compound **25** was synthesized according to the general procedure from 3-bromothiophene (32.6 mg, 200 µmol). The product **25** was obtained after purification via crystallization from MeOH at -21 °C as a yellow solid (33.7 mg, 90.3 µmol, 90%).

Suzuki cross-coupling reaction:

Compound **25** was synthesized according to the general procedure from 3-bromothiophene (32.6 mg, 200 µmol). The product **25** was obtained after purification via column chromatography on silica (eluent: cyclohexane/DCM/ethyl acetate 5/4/1) as a yellow solid (24.0 mg, 64.3 µmol, 64%).

^{1}H NMR (600 MHz, $CDCl_3$) δ = 7.40 (dd, ^3J = 8.2 Hz, ^4J = 1.9 Hz, 2H, *H*-g), 7.25 (ad, ^4J = 1.9 Hz, 2H, *H*-a), 7.24 – 7.21 (m, 4H, *H*-d, e), 7.04 – 7.00 (m, 2H, *H*-f), 6.90 (d, ^3J = 8.2 Hz, 2H, *H*-h), 3.08 – 2.80 (m, 4H, *H*-k) ppm.
^{13}C{^{1}H} NMR (151 MHz, $CDCl_3$) δ = 154.8 (*C*-i), 143.3 (*C*-c), 133.5 (*C*-b), 128.7 (*C*-j), 128.2 (*C*-f), 127.1 (*C*-a), 125.1 (*C*-e), 124.4 (*C*-g), 123.4 (*C*-d), 119.9 (*C*-h), 31.9 (*C*-k) ppm.
IR (ATR): $\tilde{\nu}$ = 3094 (w, br), 2919 (w, br), 1601 (w), 1507 (w), 1476 (m), 1460 (m), 1425 (w), 1341 (w), 1256 (m), 1218 (w), 1161 (w), 1076 (m), 1049 (m), 894 (m), 854 (m), 826 (s), 802 (s), 701 (s) cm^{-1}.
HRMS (EI, 70 eV) *m/z* (%): $[M]^+$ calcd for $[C_{22}H_{16}N_2S_2]^+$ 372.07494; found 372.07541, 371.9.0 (100).
Mp: 218 °C**.**
R$_f$: 0.26 (cyclohexane/DCM 2/1), 0.55 (cyclohexane/DCM/ethyl acetate 5/4/1).

(*Z*)-2,9-Di(thiophen-3-yl)-11,12-dihydrodibenzo[*c,g*][1,2]diazocine (**26**)

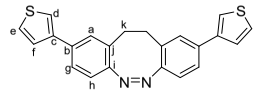

Stille cross-coupling reaction:

Compound **26** was synthesized according to the general procedure from 3-bromothiophene (32.6 mg, 200 µmol). The product **26** was obtained after purification via column chromatography on silica (eluent: cyclohexane/DCM 1/2) as a yellow solid (34.9 mg, 93.6 µmol, 94%).

Suzuki cross-coupling reaction:

Compound **26** was synthesized according to the general procedure from 3-bromothiophene (32.6 mg, 200 µmol). The product **26** was obtained after purification via column chromatography on silica (eluent: cyclohexane/DCM/ethyl acetate 5/4/1)as a yellow solid (24.7 mg, 66.2 µmol, 70%).

^{1}H NMR (500 MHz, $CDCl_3$) δ = 7.39 – 7.35 (m, 4H, *H*-d,g), 7.33 (dd, ^3J = 5.0, ^4J = 3.0 Hz, 2H, *H*-e), 7.28 (dd, ^3J = 5.0, ^4J =1.4 Hz, 2H, *H*-f), 7.23 (d, ^4J = 1.9 Hz, 2H, *H*-a), 6.91 (d, ^3J = 8.1 Hz, 2H, *H*-h), 3.11-2.72(m, 4H) ppm.
^{13}C NMR (126 MHz, $CDCl_3$) δ = 154.5 (*C*-i), 141.2 (*C*-c), 134.7 (*C*-b), 128.5 (*C*-j), 127.5 (*C*-a), 126.3 (*C*-e), 126.0 (*C*-f), 124.8 (*C*-g), 120.4(*C*-d), 119.7 (*C*-h), 31.9 (*C*-k) ppm.
IR (ATR): $\tilde{\nu}$ = 3093 (w, br), 2954 (w, br), 1601 (w), 1504 (w), 1477 (m), 1462 (m), 1426 (w), 1204 (m), 1163 (w), 1086 (m), 1041 (w), 892 (s), 872 (m), 845 (s), 778 (s), 733 (m) cm^{-1}.
HRMS (EI, 70 eV) *m/z* (%): $[M]^+$ calcd for $[C_{22}H_{16}N_2S_2]^+$ 372.07494; found 372.07508, 343.9.0 (100).
Mp: 218 °C**.**
R$_f$: 0.26 (cyclohexane/DCM 2/1), 0.55 (cyclohexane/DCM/ethyl acetate 5/4/1).

(*Z*)-5,5'-(11,12-Dihydrodibenzo[*c,g*][1,2]diazocine-2,9-diyl)bis(furan-2-carbaldehyde) (**27**)

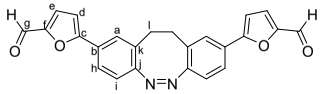

Stille cross-coupling reaction:

Compound **27** was synthesized according to the general procedure from 5-bromofuran-2-carbaldehyde (35.0 mg, 200 µmol). The product **27** was obtained after purification via column chromatography on silica (eluent: DCM → DCM/MeOH 95/5) as a yellow solid (36.1 mg, 91.1 µmol, 91%).

Suzuki cross-coupling reaction:

Compound **27** was synthesized according to the general procedure from 5-bromofuran-2-carbaldehyde (35.0 mg, 200 µmol). The product **27** was obtained after purification via column chromatography on silica (eluent: DCM → DCM/MeOH 95/5) as a yellow solid (15.5 mg, 39.0 µmol, 39%).

^{1}H NMR (600 MHz, $CDCl_3$) δ = 9.59 (s, 2H, *H*-g), 7.57 (dd, ^3J = 8.2 Hz, ^4J = 1.8 Hz, 2H, *H*-h), 7.50 (ad, ^4J = 1.8 Hz, 2H, *H*-a), 7.25 (d, ^3J = 3.7 Hz, 2H, *H*-e), 6.93 (d, ^3J = 8.2 Hz, 2H, *H*-i), 6.75 (d, ^3J = 3.7 Hz, 2H, *H*-d), 3.08 – 2.88 (m, 4H, *H*-l) ppm.
^{13}C{^{1}H} NMR (151 MHz, $CDCl_3$) δ = 177.3 (*C*-g), 158.4 (*C*-c), 156.5 (*C*-j), 152.2 (*C*-f), 141.0 (*C*-e), 129.1 (*C*-b), 128.2 (*C*-k), 126.8 (*C*-a), 124.2 (*C*-h), 119.6 (*C*-i), 108.1 (*C*-d), 31.6 (*C*-l) ppm.
IR (ATR): $\tilde{\nu}$ = 3111 (w, br), 2926 (w, br), 1634 (s), 1515 (s), 1463 (s), 1408 (m), 1385 (w), 1255 (m), 1026 (s), 966 (m), 898 (m), 795 (s), 766 (s), 754 (s) cm^{-1}.
HRMS (EI, 70 eV) *m/z* (%): $[M]^+$ calcd for $[C_{24}H_{16}N_2O_4]^+$ 396.11046; found 396.11059, 44.0 (100).
Mp: 125 °C**.**
R$_f$: 0.36 (DCM/MeOH 95/5).

Dimethyl 5,5'-(11,12-dihydrodibenzo[*c,g*][1,2]diazocine-2,9-diyl)(*Z*)-bis(furan-2-carboxylate) (**28**)

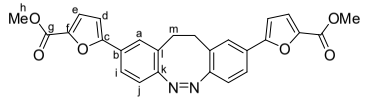

Stille cross-coupling reaction:

Compound **28** was synthesized according to the general procedure from methyl 5-bromofuran-2-carboxylate (41.0 mg, 200 µmol). The product **28** was obtained after purification via column chromatography on silica (eluent: DCM → DCM/MeOH 95/5) as a yellow solid (36.4 mg, 79.8 µmol, 80%).

Suzuki cross-coupling reaction:

Compound **28** was synthesized according to the general procedure from methyl 5-bromofuran-2-carboxylate (41.0 mg, 200 µmol). The product **28** was obtained after purification via column chromatography on silica (eluent: DCM → DCM/MeOH 95/5) as a yellow solid (26.1 mg, 57.2 µmol, 57%).

^{1}H NMR (600 MHz, $CDCl_3$) δ = 7.52 (dd, ^3J = 8.2 Hz, ^4J = 1.8 Hz, 2H, *H*-i), 7.45 (ad, ^4J = 1.8 Hz, 2H, *H*-a), 7.18 (d, ^3J = 3.6 Hz, 2H, *H*-e), 6.90 (d, ^3J = 8.2 Hz, 2H, *H*-j), 6.64 (d, ^3J = 3.6 Hz, 2H, *H*-d), 3.89 (s, 6H, *H*-h), 3.05 – 2.89 (m, 4H, *H*-m) ppm.
^{13}C{^{1}H} NMR (151 MHz, $CDCl_3$) δ = 159.2 (*C*-g), 156.6 (*C*-f), 156.0 (*C*-k), 143.8 (*C*-c), 129.0 (*C*-b), 128.6 (*C*-l), 126.2 (*C*-a), 123.6 (*C*-i), 120.1 (*C*-e), 119.6 (*C*-j), 107.3 (*C*-d), 52.1 (*C*-h), 31.6 (*C*-m) ppm.
IR (ATR): $\tilde{\nu}$ = 2948 (w, br), 1708 (s), 1587 (w), 1515 (m), 1465 (m), 1434 (m), 1408 (w), 1364 (w), 1297 (s), 1216 (m), 1190 (m), 1135 (s), 1024 (m), 987 (m), 925 (w), 899 (m), 795 (s), 757 (s) cm^{-1}.
HRMS (EI, 70 eV) *m/z* (%): $[M]^+$ calcd for $[C_{26}H_{20}N_2O_6]^+$ 456.13159; found 456.13126, 44.0 (100).
Mp: 115 °C**.**
R$_f$: 0.43 (DCM/MeOH 95/5).

(*Z*)-2,9-Di(pyridin-4-yl)-11,12-dihydrodibenzo[*c,g*][1,2]diazocine (**29**)

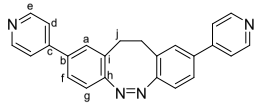

Stille cross-coupling reaction:

Under inert conditions, the di-stannylated diazocine **3** (53.4 mg, 100 µmol, 1.00 equiv), 4-bromopyridine[7] (31.6 mg, 200 µmol, 2.00 equiv), pre-milled $Pd(OAc)_2$/XPhos (1:3 ration, 6.62 mg, 4.00 µmol, 4 mol%) and CsF (30.4 mg, 200 µmol, 2.00 equiv) were dissolved in dry 1,4-dioxane (2 mL) in a pressure reaction vial. The mixture was stirred at 80 °C for 4 d. After cooling to 23 °C, the reaction mixture was filtered through Celite® and the solvent was removed under reduced pressure. The product **29** was obtained after purification via column chromatography on silica (eluent: DCM → DCM/MeOH 95/5) as a yellow solid (35.0 mg, 89.7 µmol, 90%).

Suzuki cross-coupling reaction:

Under inert conditions, the di-borylated diazocine **5** (46.0 mg, 100 µmol, 1.00 equiv), $Pd(OAc)_2$ (1.12 mg, 5 µmol, 5 mol%), XPhos (4.77 mg, 10.0 µmol, 10 mol%), KOH aq (2 M, 1 mL) and 4-bromopyridine (31.6 mg, 200 µmol, 2.00 equiv)) were dissolved in THF (4 mL) and sealed in a pressure reaction vial. The mixture was stirred 90 °C for 18 h. After cooling to 23 °C, the reaction mixture was filtered through Celite® and the solvent was removed under reduced pressure. The product **29** was obtained after purification via column chromatography on silica (eluent: DCM → DCM/MeOH 95/5) as a yellow solid (18.6 mg, 50.1 µmol, 50%).

^{1}H NMR (600 MHz, $CDCl_3$) δ = 8.60 (dd, ^3J = 4.5 Hz, ^4J = 1.6 Hz, 4H, *H*-d), 7.45 (dd, ^3J = 8.2 Hz, ^4J = 1.9 Hz, 2H, *H*-f), 7.40 (dd, ^3J = 4.5 Hz, ^4J = 1.6 Hz, 4H, *H*-e), 7.29 (ad, ^4J = 1.9 Hz, 2H, *H*-a), 7.01 (d, ^3J = 8.2 Hz, 2H, *H*-g), 3.17 – 2.87 (m, 4H, *H*-j) ppm.
^{13}C{^{1}H} NMR (151 MHz, $CDCl_3$) δ = 156.0 (*C*-h), 150.4 (*C*-d), 147.1 (*C*-b), 137.2 (*C*-c), 128.9 (*C*-i), 128.5 (*C*-a), 125.7 (*C*-f), 121.5 (*C*- e), 120.0 (*C*-g), 32.0 (*C*-j) ppm.
IR (ATR): $\tilde{\nu}$ = 3027 (w), 2928 (w, br), 1595 (s), 1542 (w), 1475 (m), 1417 (m), 1395 (m), 1329 (w), 1221 (w), 1171 (w), 1069 (w), 993 (m), 901 (m), 832 (m), 814 (s), 799 (s) cm^{-1}.
HRMS (EI, 70 eV) *m/z* (%): $[M]^+$ calcd for $[C_{24}H_{18}N_4]^+$ 362.15260; found 362.15266, 334.1 (100).
Mp: 112 °C**.**
R$_f$: 0.16 (DCM/MeOH 95/5).

[7] Freshly prepared from 4-bromopyridine hydrochloride.

(*Z*)-2,9-Diallyl-11,12-dihydrodibenzo[*c,g*][1,2]diazocine (**30**)

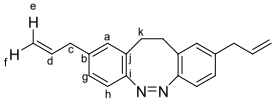

Stille cross-coupling reaction:

Compound **30** was synthesized according to the general procedure from 3-bromoprop-1-ene (24.2mg, 200 µmol). The product **30** was obtained after purification via column chromatography on silica (eluent: DCM) as a yellow oil (16.4 mg, 56.9 µmol, 57%).

Suzuki cross-coupling reaction:

Compound **30** was synthesized according to the general procedure from 3-bromoprop-1-ene (24.2 mg, 200 µmol). The product **30** was obtained after purification via column chromatography on silica (eluent: cyclohexane/DCM 3/2) as a yellow solid (18.1 mg, 62.9 µmol, 63%).

^{1}H NMR (600 MHz, $CDCl_3$) δ = 6.95 (dd, ^3J = 8.0 Hz, ^4J = 1.9 Hz, 2H, *H*-g), 6.80 (d, ^4J = 1.9 Hz, 2H, *H*-a), 6.78 (d, ^3J = 8.0 Hz, 2H, *H*-h), 5.87 (ddt, ^3J = 17.0 Hz, ^3J = 10.0 Hz, ^3J = 6.6 Hz, 2H, *H*-d), 5.03 (dq, ^3J = 10.0 Hz, ^2J = 1.5 Hz, 2H, *H*-f), 4.97 (dq, ^3J = 17.0 Hz, , ^2J = 1.7 Hz, 2H, *H*-e), 3.26 – 3.24 (m, 4H, *H*-c), 3.00 - 2.67 (m, 4H, *H*-k) ppm.
^{13}C{^{1}H} NMR (151 MHz, $CDCl_3$) δ = 153.7 (*C*-i), 138.7 (*C*-b), 137.0 (*C*-d), 129.7 (*C*-a), 128.1 (*C*-j), 126.9 (*C*-g), 119.2 (*C*-h), 116.1 (*C*-e,f), 39.5 (*C*-c), 31.8 (*C*-k) ppm.
IR (ATR): $\tilde{\nu}$ = 3076 (w), 2896 (w, br), 1637 (m), 1604 (m), 1482 (m), 1431 (w), 1288 (w), 1226 (w), 1147 (w), 1090 (w), 993 (s), 911 (s), 823 (s), 802 (s), 747 (m) cm^{-1}.
HRMS (EI, 70 eV) *m/z* (%): $[M]^+$ calcd for $[C_{20}H_{20}N_2]^+$ 288.16210; found 288.16242, 178.1 (100).
R$_f$: 0.38 (DCM), 0.17 (cyclohexane/DCM 3/2).

(*Z*)-3,8-Di-*p*-tolyl-11,12-dihydrodibenzo[*c,g*][1,2]diazocine (**35**)

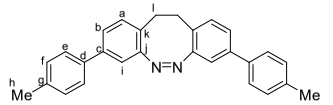

Stille cross-coupling reaction:

Compound **35** was synthesized according to the general procedure from 4-bromotoluene (34.2 mg, 200 µmol). The product **35** was obtained after purification via column chromatography on silica (eluent: DCM) as a yellow solid (32.8 mg, 84.3 µmol, 84%).

Suzuki cross-coupling reaction:

Compound **35** was synthesized according to the general procedure from 4-bromotoluene (34.2 mg, 200 µmol). The product **35** was obtained after purification via column chromatography on silica (eluent: DCM) as a yellow solid (29.9 mg, 77.1 µmol, 77%).

^{1}H NMR (600 MHz, $CDCl_3$) δ = 7.39 (d, ^3J = 8.2 Hz, 4H, *H*-e), 7.25 (dd, ^3J = 7.9 Hz, ^4J = 2.0 Hz, 2H, *H*-b), 7.19 (d, ^3J = 8.2 Hz, 4H, *H*-f), 7.08 (ad, ^4J = 2.0 Hz, 2H, *H*-i), 7.06 (d, ^3J = 7.9 Hz, 2H, *H*-a), 3.11 – 2.78 (m, 4H, *H*-l), 2.35 (s, 6H, *H*-h) ppm.

$^{13}C\{^{1}H\}$ NMR (151 MHz, $CDCl_3$) δ = 155.8 (*C*-j), 139.8 (*C*-c), 137.5 (*C*-g), 137.1 (*C*-d), 130.3 (*C*-a), 129.6 (*C*-f), 126.9 (*C*-e), 126.9 (*C*-k), 125.7 (*C*-b), 117.4 (*C*-i), 31.6 (*C*-l), 21.2 (*C*-h) ppm.
IR (ATR): $\tilde{\nu}$ = 2915 (w, br), 1520 (w), 1486 (m), 1457 (w), 1431 (w), 1383 (w), 1019 (w), 895 (m), 840 (w), 810 (s), 799 (s) cm^{-1}.
HRMS (EI, 70 eV) *m/z* (%): $[M]^+$ calcd for $[C_{28}H_{24}N_2]^+$ 388.19340; found 388.19354, 359.9 (100).
Mp: 187 °C**.**
R_f: 0.74 (DCM).

(*Z*)-3,8-Bis(4-methoxyphenyl)-11,12-dihydrodibenzo[*c*,*g*][1,2]diazocine (**36**)

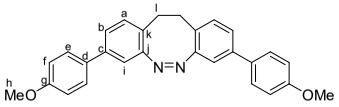

Stille cross-coupling reaction:

Compound **36** was synthesized according to the general procedure from 4-bromoanisole (37.4 mg, 200 µmol). The product **36** was obtained after purification via column chromatography on silica (eluent: DCM) as a yellow solid (29.9 mg, 71.0 µmol, 71%).

Suzuki cross-coupling reaction:

Compound **36** was synthesized according to the general procedure from 4-bromoanisole (37.4 mg, 200 µmol). The product **36** was obtained after purification via column chromatography on silica (eluent: DCM) as a yellow solid (32.8 mg, 78.1 µmol, 78%).

^{1}H NMR (600 MHz, $CDCl_3$) δ = 7.43 (d, ^{3}J = 8.8 Hz, 4H, *H*-e), 7.22 (dd, ^{3}J = 8.0 Hz, ^{4}J = 1.9 Hz, 2H, *H*-b), 7.06 – 7.04 (m, 4H, *H*-a/i), 6.91 (d, ^{3}J = 8.8 Hz, 4H, *H*-f), 3.81 (s, 6H, *H*-h), 3.07 – 2.78 (m, 4H, *H*-l) ppm.
$^{13}C\{^{1}H\}$ NMR (151 MHz, $CDCl_3$) δ = 159.5 (*C*-g), 155.8 (*C*-j), 139.5 (*C*-c), 132.5 (*C*-d), 130.3 (*C*-a), 128.1 (*C*-e), 126.5 (*C*-k), 125.4 (*C*-b), 117.1 (*C*-i), 114.3 (*C*-f), 55.5 (*C*-h), 31.6 (*C*-l) ppm.
IR (ATR): $\tilde{\nu}$ = 3004 (w, br), 2836 (w, br), 1606 (m), 1578 (w), 1520 (m), 1486 (s), 1437 (m), 1294 (m), 1247 (s), 1182 (s), 1116 (w), 1042 (m), 1021 (s), 888 (m), 832 (s), 826 (s), 813 (s), 789 (m) cm^{-1}.
HRMS (EI, 70 eV) *m/z* (%): $[M]^+$ calcd for $[C_{28}H_{24}N_2O_2]^+$ 420.18323; found 420.18355, 391.9 (100).
Mp: 225 °C**.**
R_f: 0.38 (DCM).

(*Z*)-3,8-Bis(4-nitrophenyl)-11,12-dihydrodibenzo[*c*,*g*][1,2]diazocine (**37**)

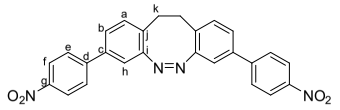

Stille cross-coupling reaction:

Compound **37** was synthesized according to the general procedure from 1-bromo-4-nitrobenzene (40.4 mg, 200 µmol). The product **37** was obtained after purification via column chromatography on silica (eluent: DCM) as a yellow solid (34.3 mg, 76.2 µmol, 76%).

Suzuki cross-coupling reaction:

Compound **37** was synthesized according to the general procedure from 1-bromo-4-nitrobenzene (40.4 mg, 200 µmol). The product **37** was obtained after purification via column chromatography on silica (eluent: DCM) as a yellow solid (37.5 mg, 83.3 µmol, 83%).

^{1}H NMR (600 MHz, $CDCl_3$) δ = 8.24 (d, ^{3}J = 8.9 Hz, 4H, *H*-f), 7.65 (d, ^{3}J = 8.9 Hz, 4H, *H*-e), 7.34 (dd, ^{3}J = 7.9 Hz, ^{4}J = 2.0 Hz, 2H, *H*-b), 7.17 (d, ^{3}J = 7.9 Hz, 2H, *H*-a), 7.16 (ad, ^{4}J = 2.0 Hz, 2H, *H*-h), 3.13 – 2.87 (m, 4H, *H*-k) ppm.
$^{13}C\{^{1}H\}$ NMR (151 MHz, $CDCl_3$) δ = 155.9 (*C*-i), 147.4 (*C*-g), 146.1 (*C*-d), 137.6 (*C*-c), 130.9 (*C*-a), 129.0 (*C*-j), 127.7 (*C*-e), 126.3 (*C*-b), 124.3 (*C*-f), 118.0 (*C*-h), 31.6 (*C*-k) ppm.
IR (ATR): $\tilde{\nu}$ = 2925 (w, br), 1597 (m), 1510 (s), 1479 (m), 1339 (s), 1110 (m), 1014 (w), 981 (w), 933 (w), 895 (m), 855 (s), 839 (s), 820 (s), 809 (s), 752 (s) cm^{-1}.
HRMS (EI, 70 eV) *m/z* (%): $[M]^+$ calcd for $[C_{26}H_{18}N_4O_4]^+$ 450.13226; found 450.13230, 421.8 (100).
Mp: 212 °C**.**
R_f: 0.47 (DCM).

References

1. R. K. Harris, E. D. Becker, S. M. Cabral de Menezes, P. Granger, R. E. Hoffman and K. W. Zilm, *Pure and Applied Chemistry*, 2008, **80**, 59-84.
2. *The ACS Style Guide: Effective Communication of Scientific Information*, American Chemical Society, Washington, DC, 3rd edn., 2006.
3. S. Schultzke, M. Walther and A. Staubitz, *Molecules*, 2021, **26**, 3916.
4. T. Tellkamp, J. Shen, Y. Okamoto and R. Herges, *Eur. J. Org. Chem.*, 2014, DOI: 10.1002/ejoc.201402541, 5456-5461.
5. D. Hugenbusch, M. Lehr, J. S. von Glasenapp, A. J. McConnell and R. Herges, *Angew. Chem. Int. Ed.*, 2023, **62**, e202212571.
6. D. R. Coulson, L. C. Satek and S. O. Grim, in *Inorganic Syntheses*, ed. F. A. Cotton, McGraw-Hill, Inc., 1972, DOI: 10.1002/9780470132449.ch23, pp. 121-124.
7. C. Cordovilla, C. Bartolomé, J. M. Martínez-Ilarduya and P. Espinet, *ACS Catal.*, 2015, **5**, 3040-3053.
8. V. Farina, V. Krishnamurthy and W. J. Scott, *Org. React.*, 1997, **50**, 1-652.
9. (a) L. Heintze, D. Schmidt, T. Rodat, L. Witt, J. Ewert, M. Kriegs, R. Herges and C. Peifer, *Int. J. Mol. Sci.*, 2020, **21**, 8961. (b) Q. Zhu, S. Wang and P. Chen, *Org. Lett.*, 2019, **21**, 4025-4029.
10. (a) E. R. Thapaliya, J. Zhao and G. C. R. Ellis-Davies, *ACS Chem. Neurosci.*, 2019, **10**, 2481-2488. (b) V. Farina, S. Kapadia, B. Krishnan, C. Wang and L. S. Liebeskind, *J. Org. Chem.*, 1994, **59**, 5905-5911.
11. J. Strueben, P. J. Gates and A. Staubitz, *J. Org. Chem.*, 2014, **79**, 1719-1728.
12. S. P. Mee, V. Lee and J. E. Baldwin, *Chem. Eur. J.*, 2005, **11**, 3294-3308.
13. J. R. Naber and S. L. Buchwald, *Adv. Synth. Catal.*, 2008, **350**, 957-961.

^{1}H, $^{13}C\{^{1}H\}$, ^{11}B, ^{19}F and ^{119}Sn NMR Spectra of the Purified Compounds

2,2'-(Ethane-1,2-diyl)bis(4-iodoaniline)

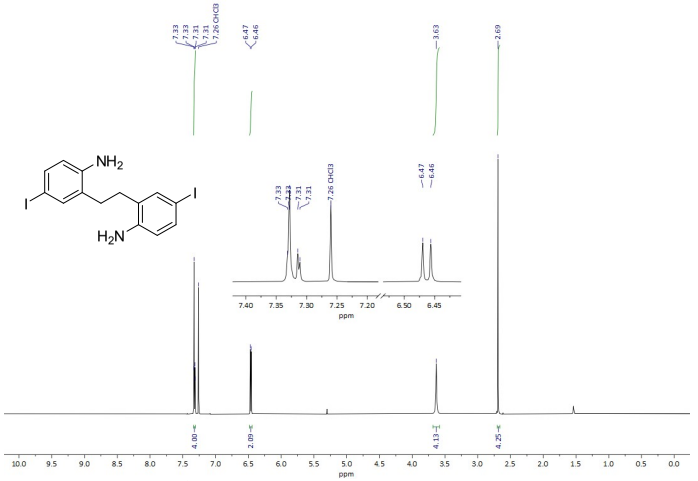

Figure 1: ^{1}H NMR spectrum of2,2'-(ethane-1,2-diyl)bis(4-iodoaniline) in $CDCl_3$.

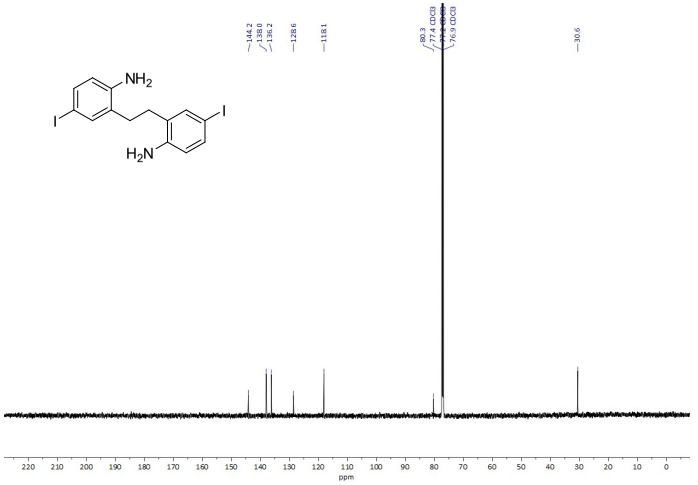

Figure 2: $^{13}C\{^{1}H\}$ NMR spectrum of 2,2'-(ethane-1,2-diyl)bis(4-iodoaniline) in $CDCl_3$.

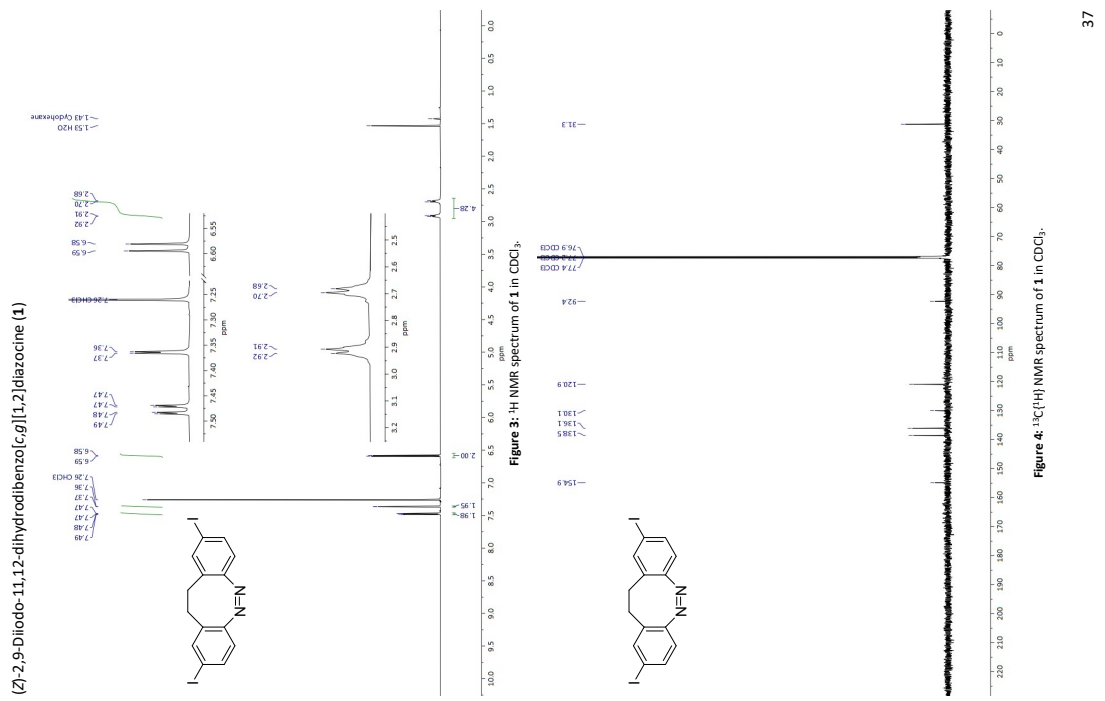

Figure 3: ^{1}H NMR spectrum of **1** in $CDCl_3$.

37

Figure 4: $^{13}C\{^1H\}$ NMR spectrum of **1** in $CDCl_3$.

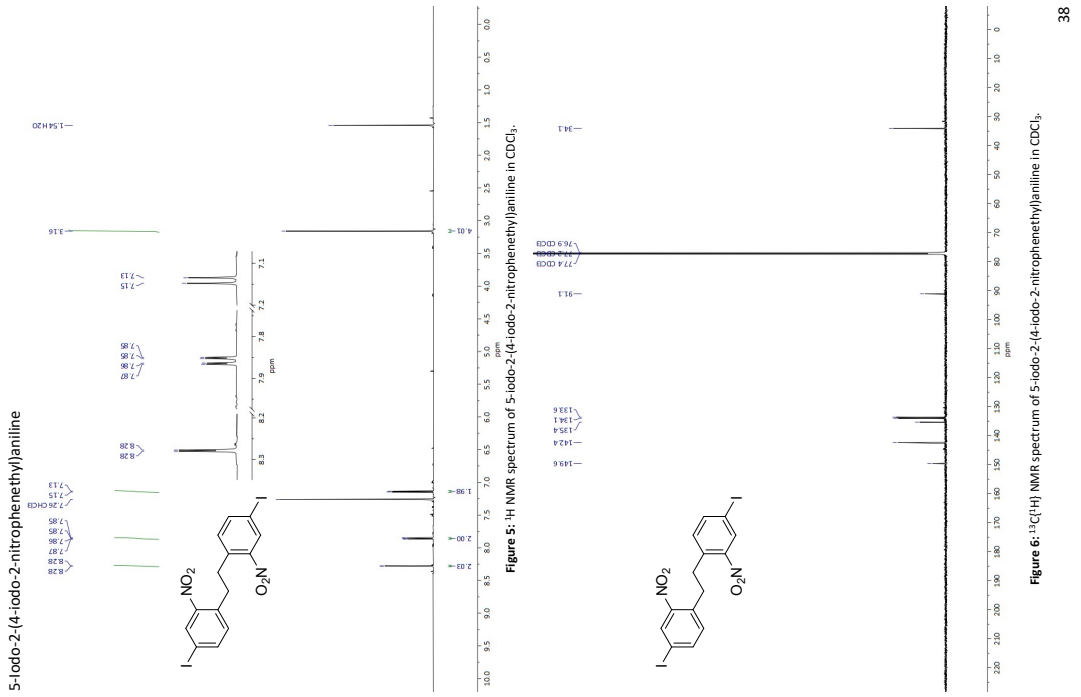

Figure 5: ^{1}H NMR spectrum of 5-iodo-2-(4-iodo-2-nitrophenethyl)aniline in $CDCl_3$.

Figure 6: $^{13}C\{^1H\}$ NMR spectrum of 5-iodo-2-(4-iodo-2-nitrophenethyl)aniline in $CDCl_3$.

38

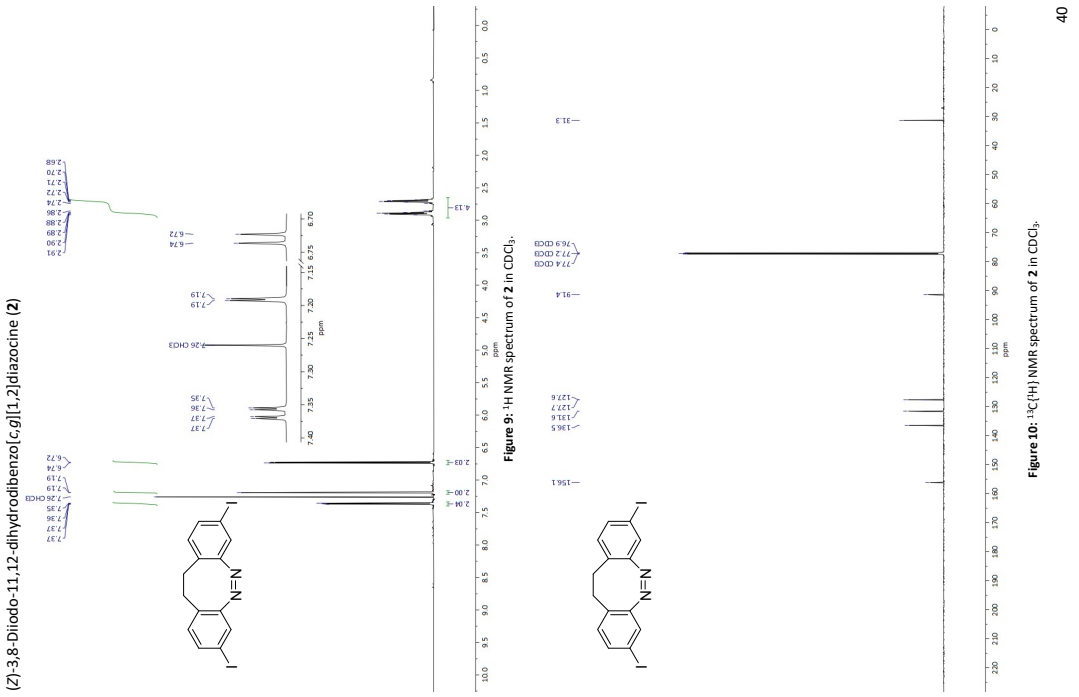

Figure 9: ^{1}H NMR spectrum of **2** in $CDCl_3$.

Figure 10: $^{13}C\{^{1}H\}$ NMR spectrum of **2** in $CDCl_3$.

40

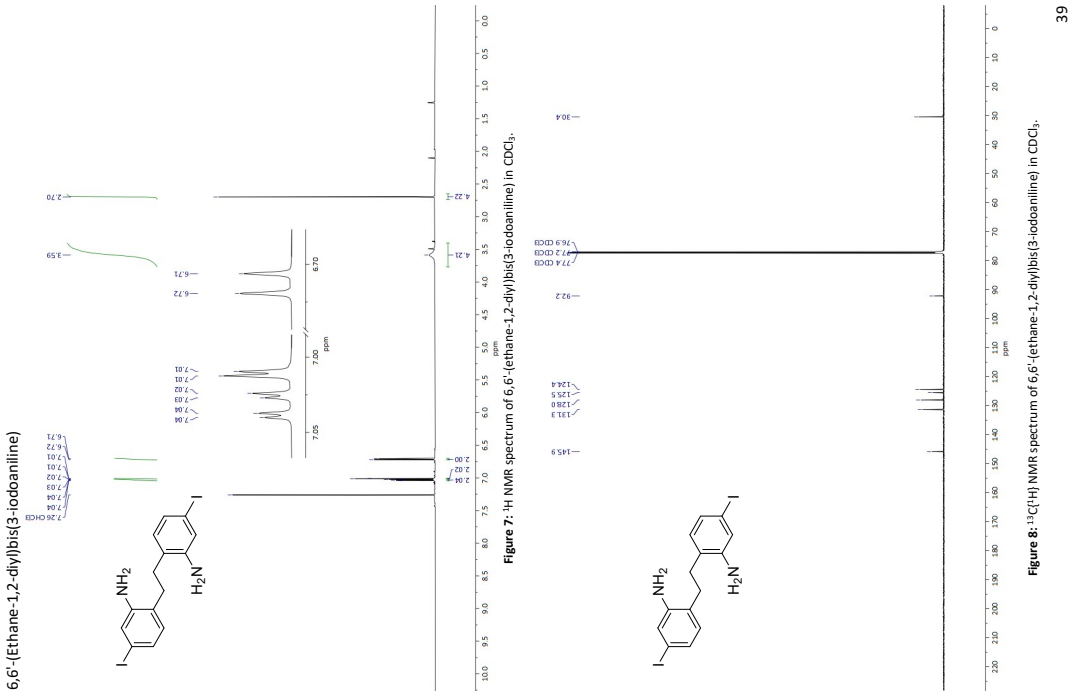

Figure 7: ^{1}H NMR spectrum of 6,6'-(ethane-1,2-diyl)bis(3-iodoaniline) in $CDCl_3$.

Figure 8: $^{13}C\{^{1}H\}$ NMR spectrum of 6,6'-(ethane-1,2-diyl)bis(3-iodoaniline) in $CDCl_3$.

39

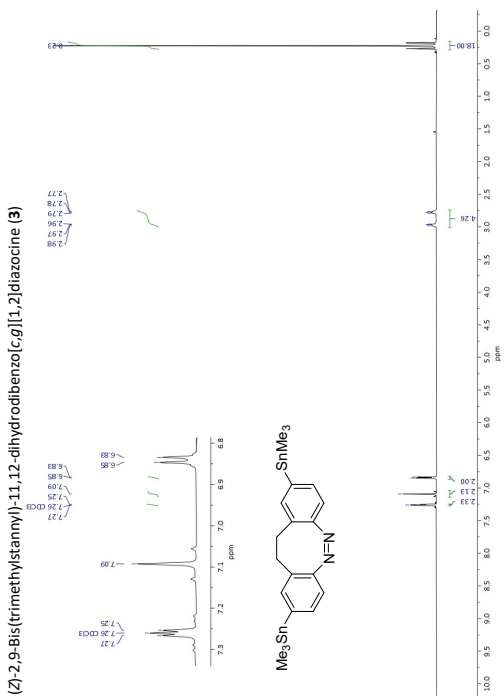

Figure 11: ^{1}H NMR spectrum of **3** in $CDCl_3$.

41

Figure 12: $^{13}C\{^1H\}$ NMR spectrum of **3** in $CDCl_3$.

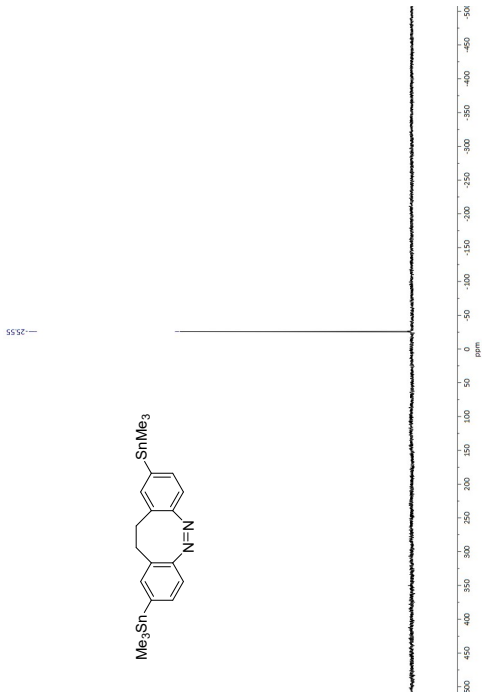

Figure 13: $^{119}Sn\{^1H\}$ NMR spectrum of **3** in $CDCl_3$.

42

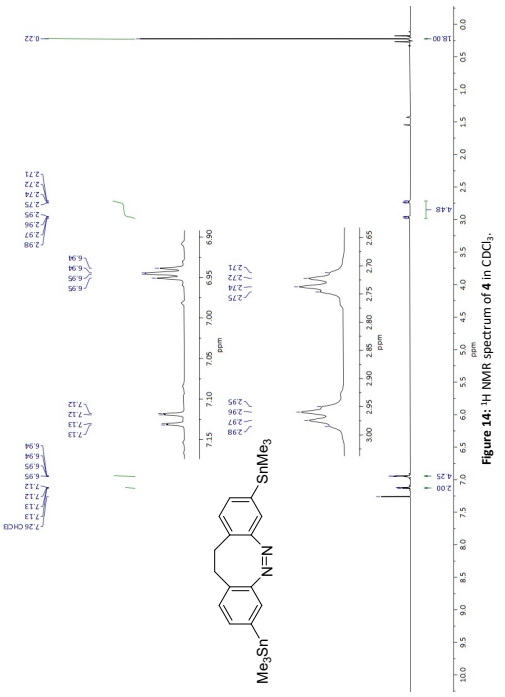

Figure 14: ^{1}H NMR spectrum of **4** in $CDCl_3$.

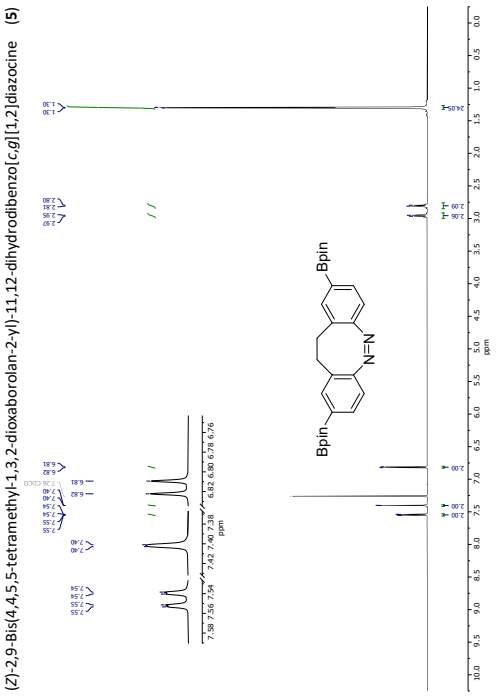

Figure 17: ^{1}H NMR spectrum of **5** in $CDCl_3$.

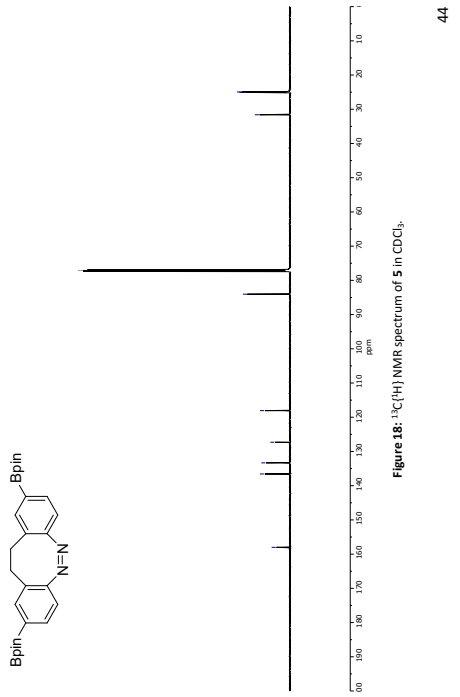

Figure 18: $^{13}C\{^1H\}$ NMR spectrum of **5** in $CDCl_3$.

44

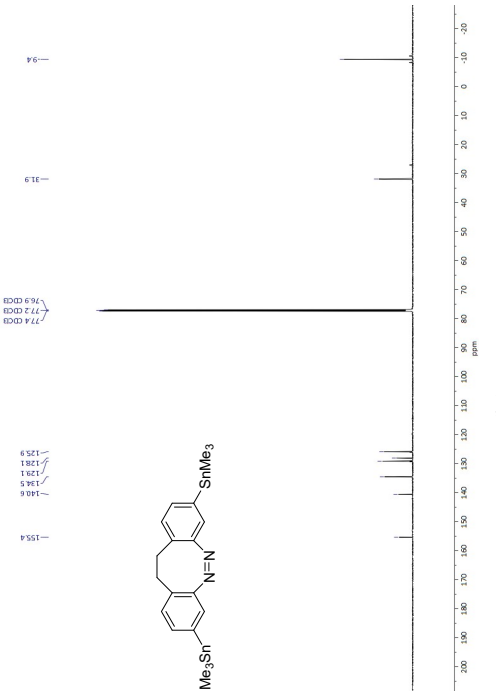

Figure 15: $^{13}C\{^1H\}$ NMR spectrum of **4** in $CDCl_3$.

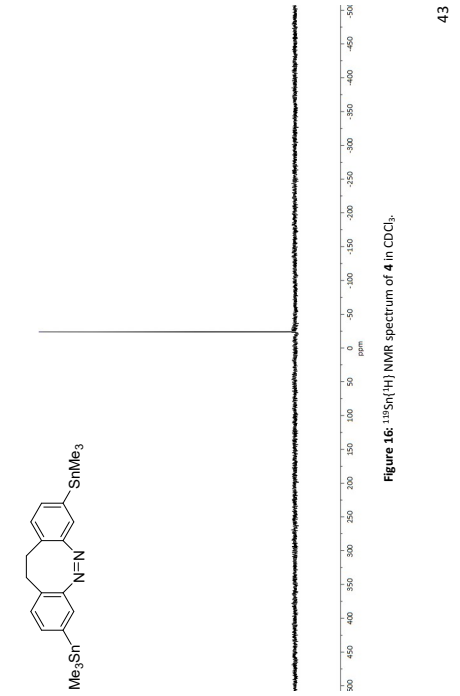

Figure 16: $^{119}Sn\{^1H\}$ NMR spectrum of **4** in $CDCl_3$.

43

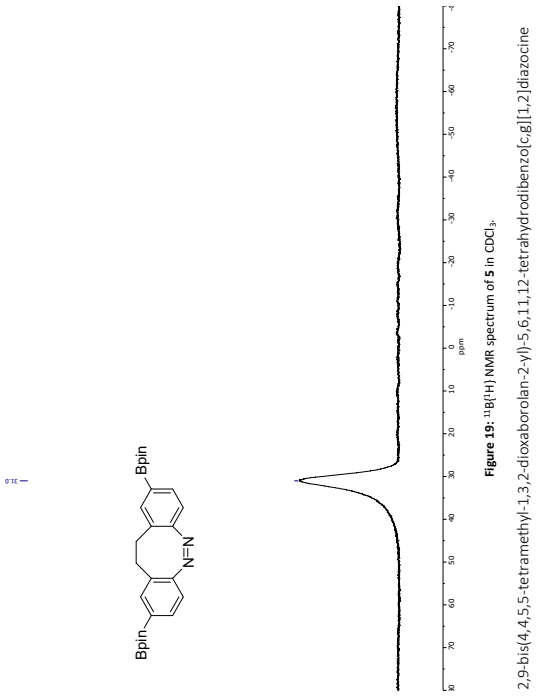

Figure 19: $^{11}B\{^1H\}$ NMR spectrum of **5** in $CDCl_3$.

2,9-bis(4,4,5,5-tetramethyl-1,3,2-dioxaborolan-2-yl)-5,6,11,12-tetrahydrodibenzo[c,g][1,2]diazocine

Figure 20: ^1H NMR spectrum of 2,9-bis(4,4,5,5-tetramethyl-1,3,2-dioxaborolan-2-yl)-5,6,11,12-tetrahydrodibenzo[c,g][1,2]diazocine in $CDCl_3$.

45

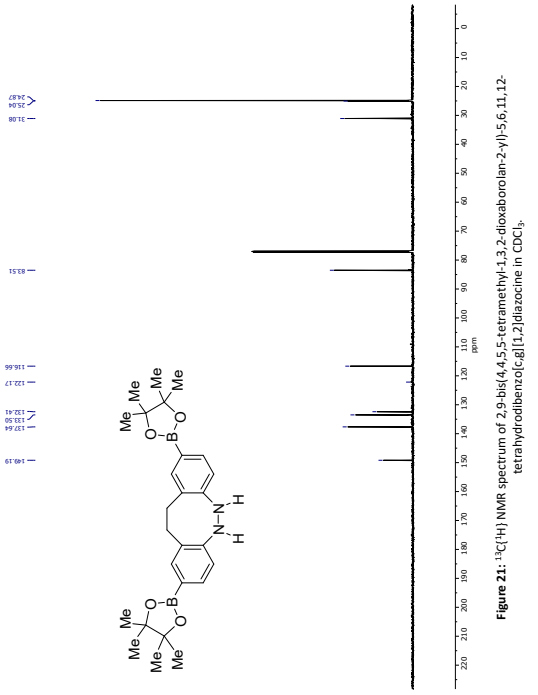

Figure 21: $^{13}C\{^1H\}$ NMR spectrum of 2,9-bis(4,4,5,5-tetramethyl-1,3,2-dioxaborolan-2-yl)-5,6,11,12-tetrahydrodibenzo[c,g][1,2]diazocine in $CDCl_3$.

Figure 22: $^{11}B\{^1H\}$ NMR spectrum of 2,9-bis(4,4,5,5-tetramethyl-1,3,2-dioxaborolan-2-yl)-5,6,11,12-tetrahydrodibenzo[c,g][1,2]diazocine in $CDCl_3$.

46

(*Z*)-3,8-Bis(4,4,5,5-tetramethyl-1,3,2-dioxaborolan-2-yl)-11,12-dihydrodibenzo[*c*,*g*][1,2]diazocine (**6**)

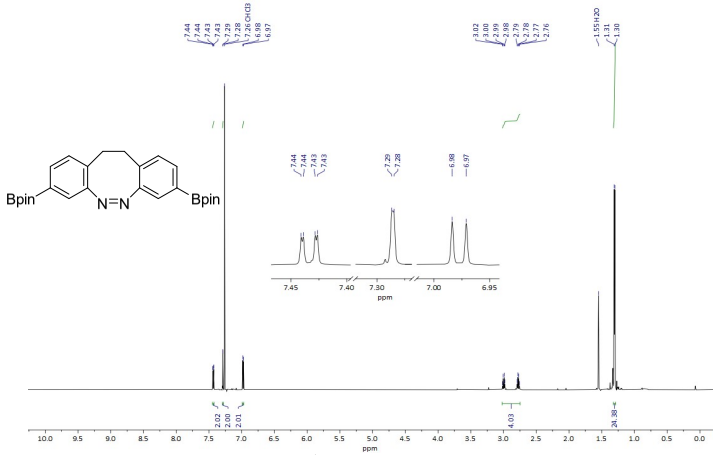

Figure 23: ^{1}H NMR spectrum of **6** in $CDCl_3$.

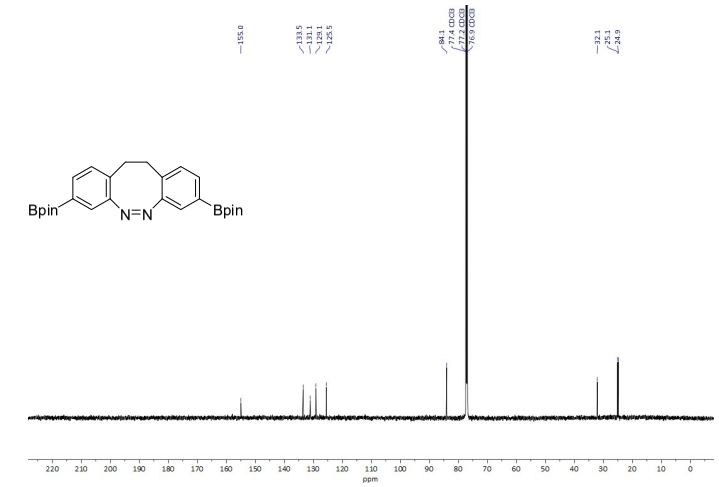

Figure 24: $^{13}C\{^{1}H\}$ NMR spectrum of **6** in $CDCl_3$.

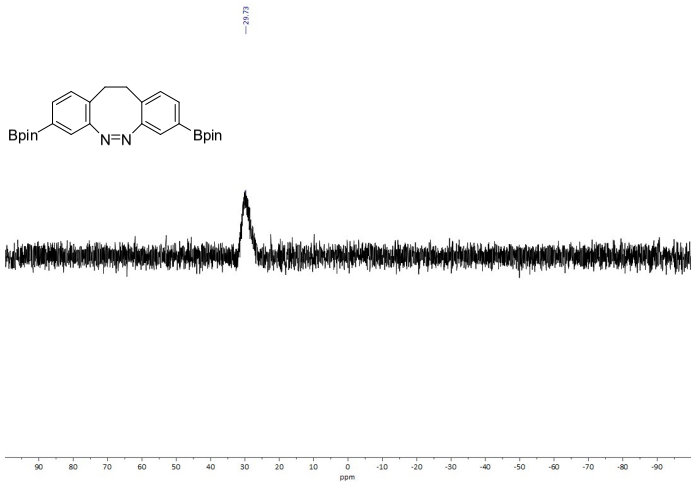

Figure 25: $^{11}B\{^{1}H\}$ NMR spectrum of **6** in $CDCl_3$.

(*Z*)-2,9-Di-*p*-tolyl-11,12-dihydrodibenzo[*c*,*g*][1,2]diazocine (**7**)

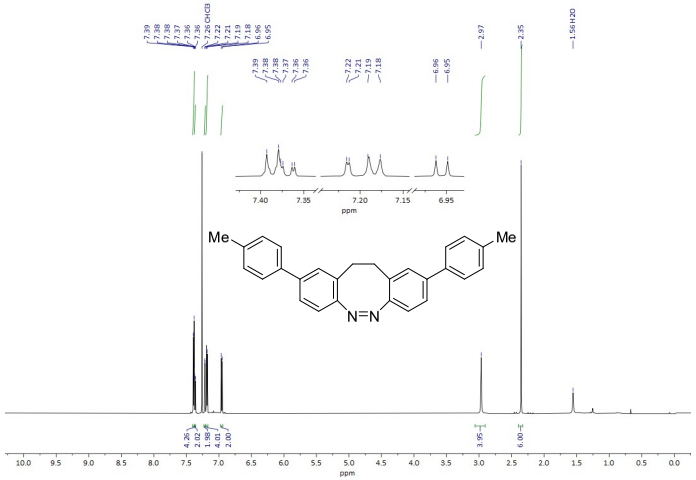

Figure 26: ^{1}H NMR spectrum of **7** in $CDCl_3$.

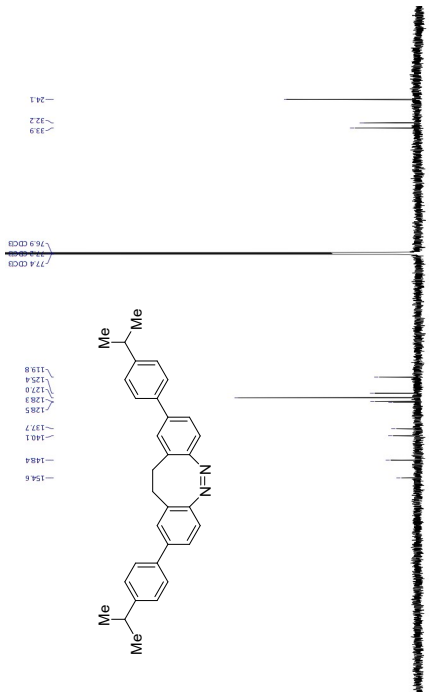

Figure 29: $^{13}C\{^1H\}$ NMR spectrum of **8** in $CDCl_3$.

(*Z*)-2,9-Bis(3-isopropylphenyl)-11,12-dihydrodibenzo[*c,g*][1,2]diazocine (**9**)

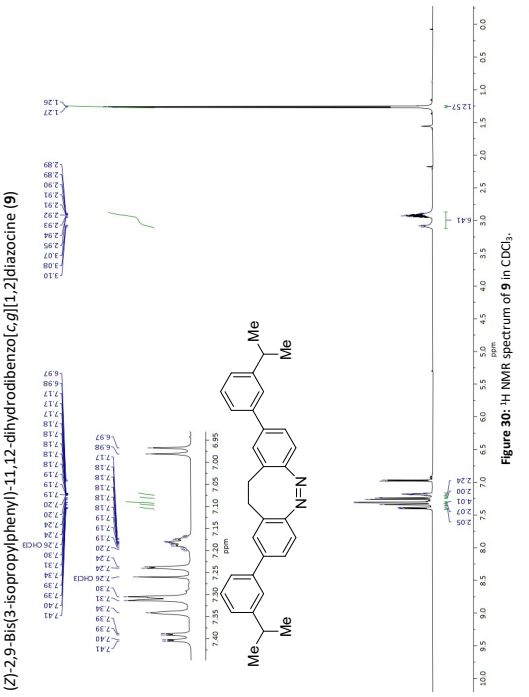

Figure 30: ^1H NMR spectrum of **9** in $CDCl_3$.

50

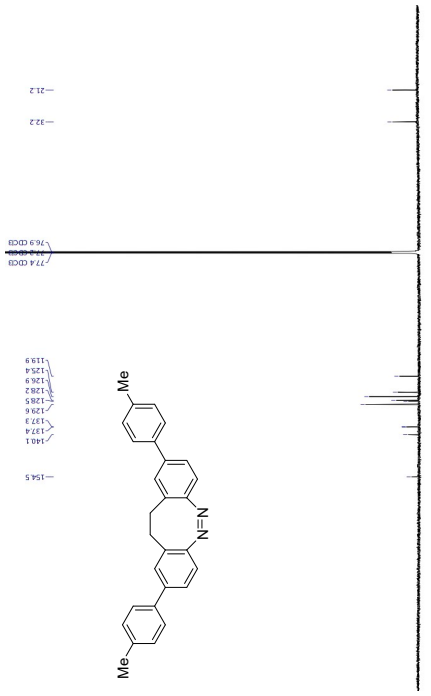

Figure 27: $^{13}C\{^1H\}$ NMR spectrum of **7** in $CDCl_3$.

(*Z*)-2,9-Bis(4-isopropylphenyl)-11,12-dihydrodibenzo[*c,g*][1,2]diazocine (**8**)

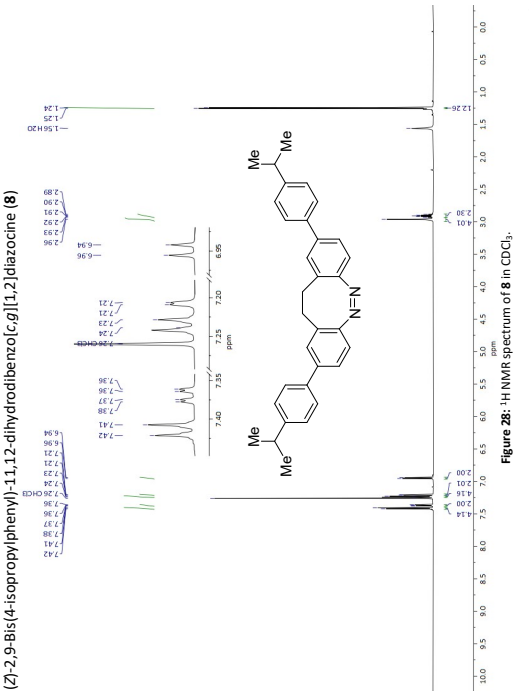

Figure 28: ^1H NMR spectrum of **8** in $CDCl_3$.

49

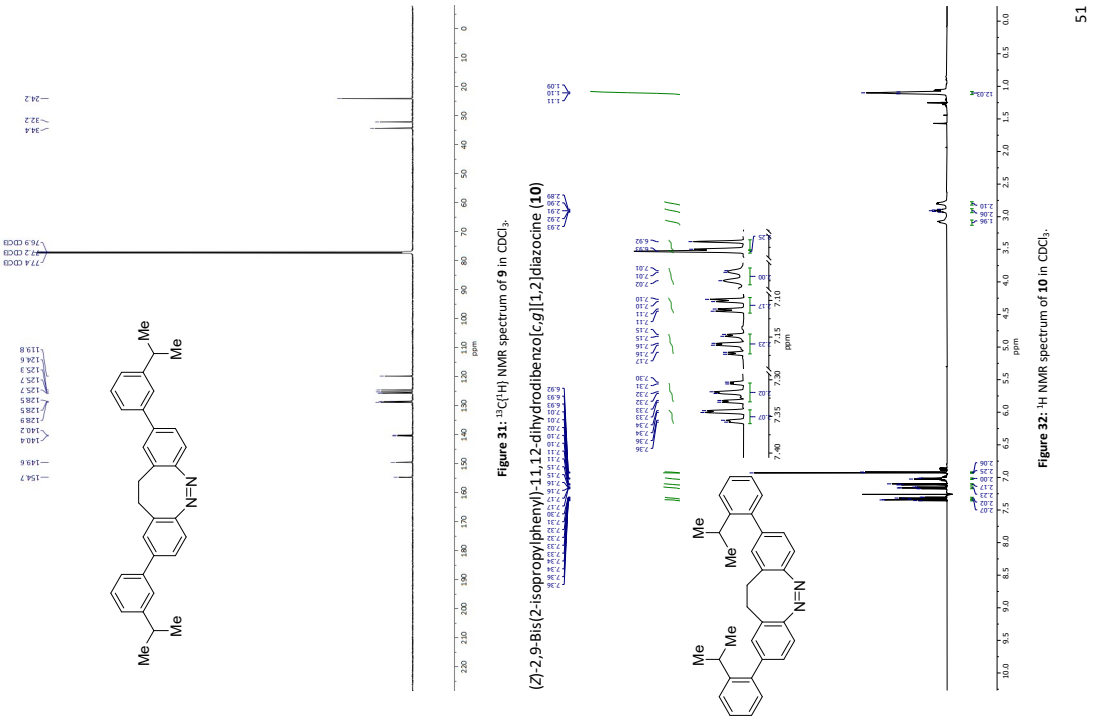

Figure 31: $^{13}C\{^1H\}$ NMR spectrum of **9** in $CDCl_3$.

(*Z*)-2,9-Bis(2-isopropylphenyl)-11,12-dihydrodibenzo[*c*,*g*][1,2]diazocine (**10**)

Figure 32: ^1H NMR spectrum of **10** in $CDCl_3$.

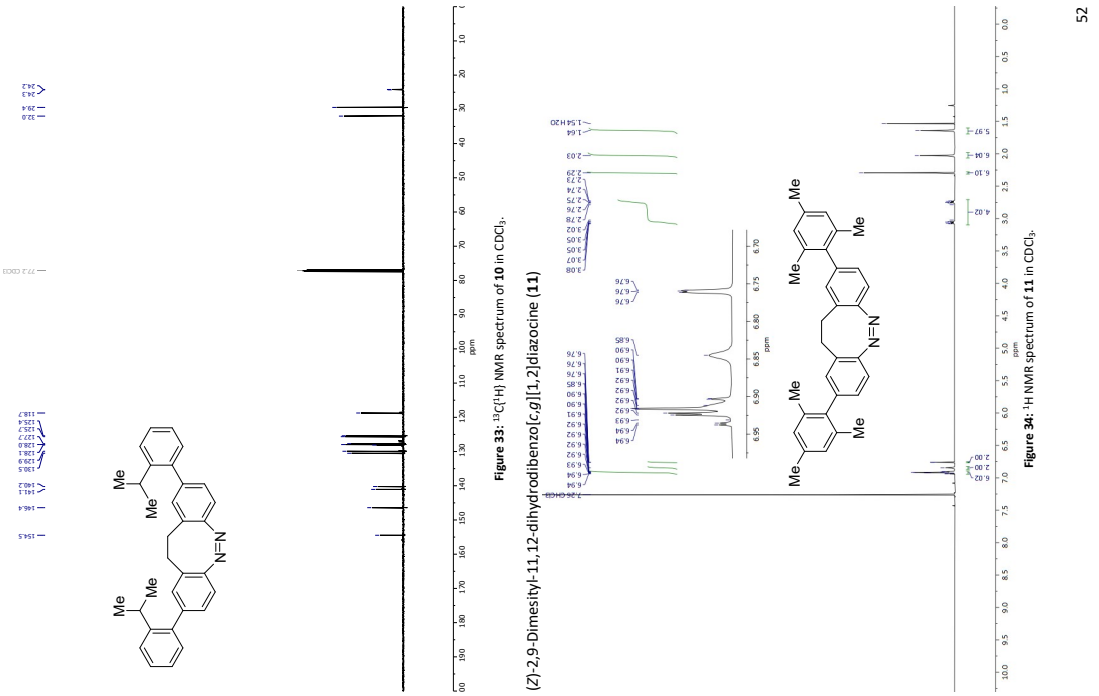

Figure 33: $^{13}C\{^1H\}$ NMR spectrum of **10** in $CDCl_3$.

(*Z*)-2,9-Dimesityl-11,12-dihydrodibenzo[*c*,*g*][1,2]diazocine (**11**)

Figure 34: ^1H NMR spectrum of **11** in $CDCl_3$.

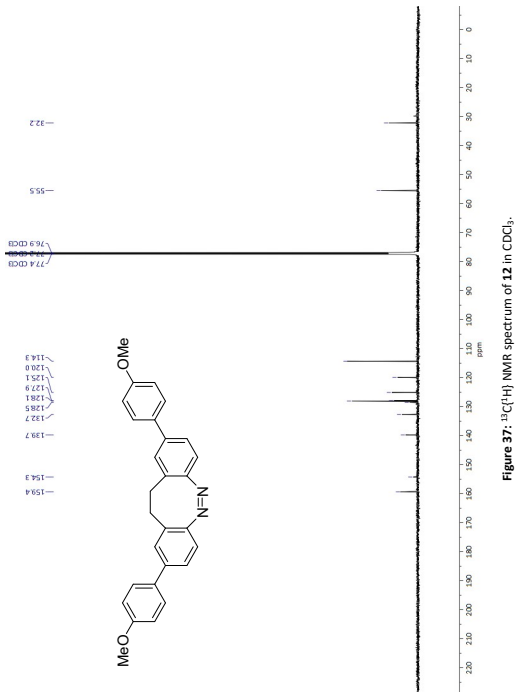

Figure 37: $^{13}C\{^1H\}$ NMR spectrum of **12** in $CDCl_3$.

(*Z*)-4,4'-(11,12-Dihydrodibenzo[*c,g*][1,2]diazocine-2,9-diyl)diphenol (**13**)

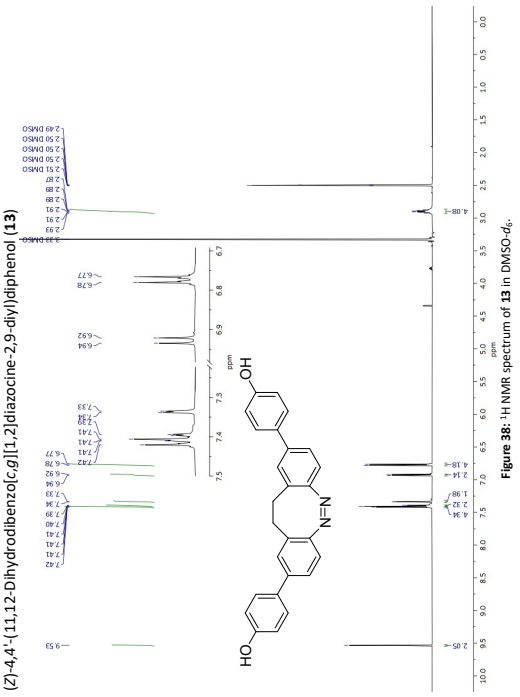

Figure 38: ^1H NMR spectrum of **13** in DMSO-d_6.

54

(*Z*)-2,9-Bis(4-methoxyphenyl)-11,12-dihydrodibenzo[*c,g*][1,2]diazocine (**12**)

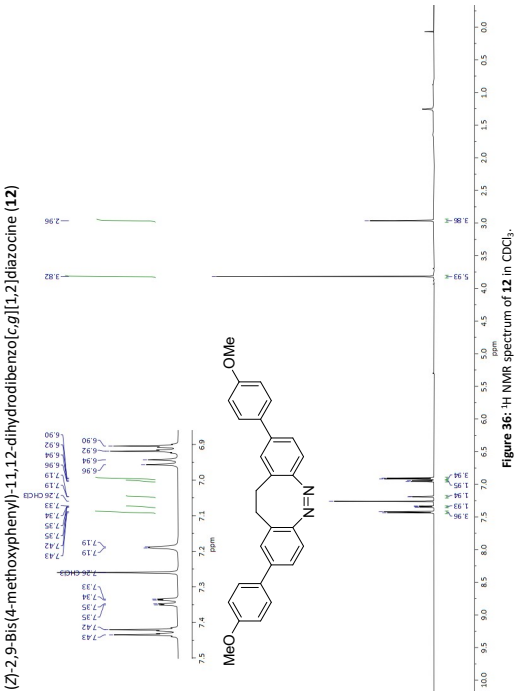

Figure 36: ^1H NMR spectrum of **12** in $CDCl_3$.

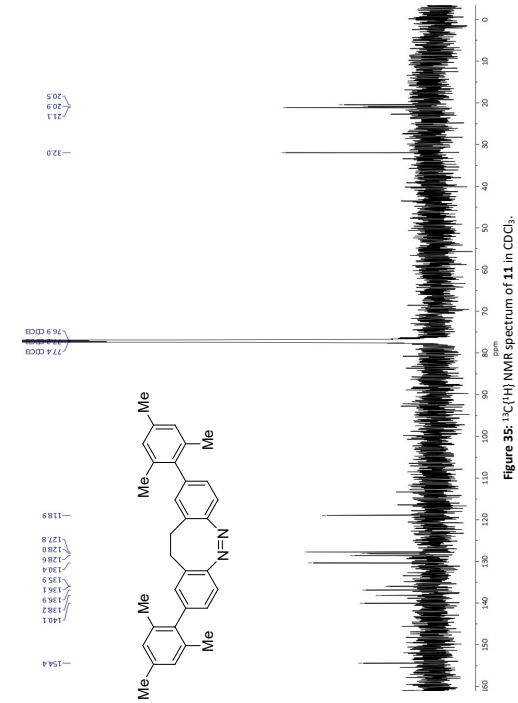

Figure 35: $^{13}C\{^1H\}$ NMR spectrum of **11** in $CDCl_3$.

53

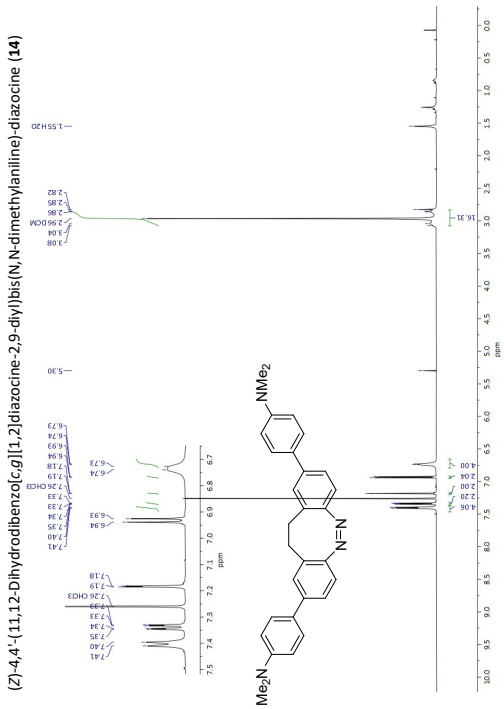

Figure 41: ^{1}H NMR spectrum of **14** in $CDCl_3$.

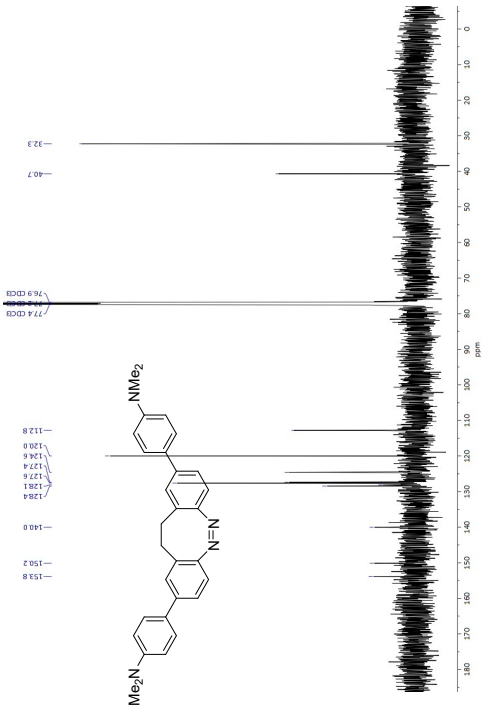

Figure 42: $^{13}C\{^1H\}$ NMR spectrum of **14** in $CDCl_3$.

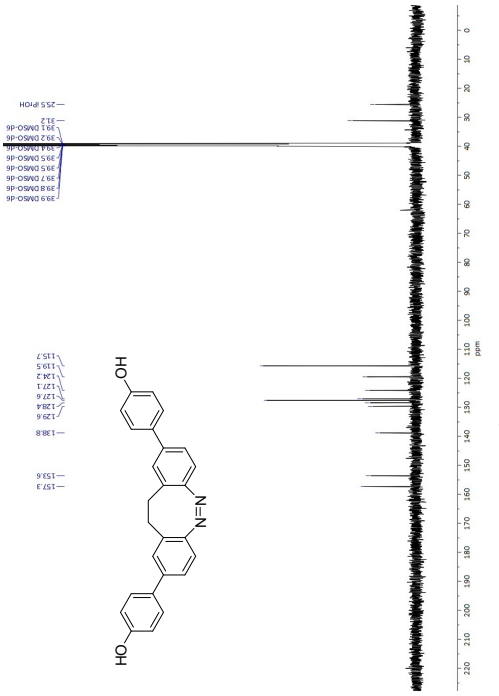

Figure 39: $^{13}C\{^1H\}$ NMR spectrum of **13** in DMSO-d_6.

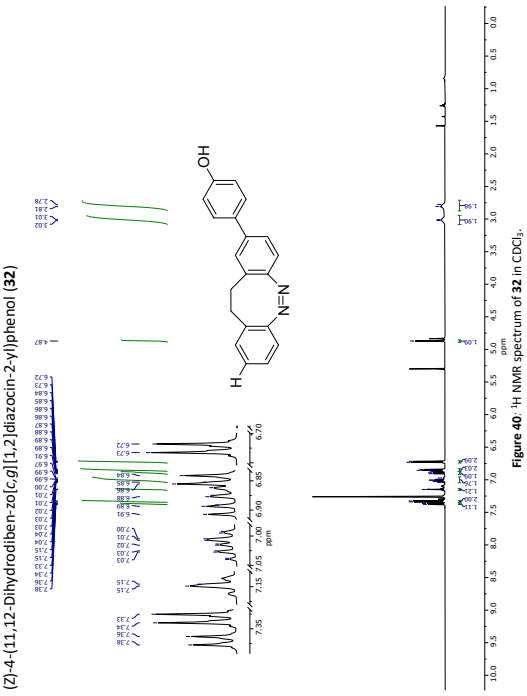

Figure 40: ^{1}H NMR spectrum of **32** in $CDCl_3$.

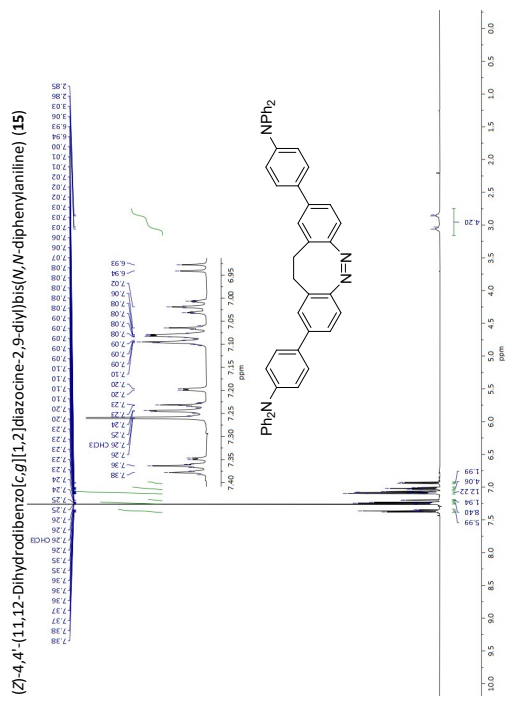

Figure 43: ^{1}H NMR spectrum of **15** in $CDCl_3$.

Figure 44: $^{13}C\{^1H\}$ NMR spectrum of **15** in $CDCl_3$.

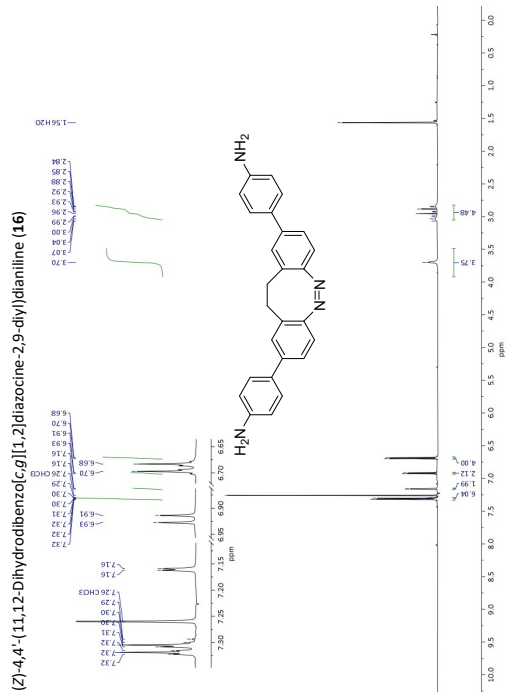

Figure 45: ^{1}H NMR spectrum of **16** in $CDCl_3$.

Figure 46: $^{13}C\{^1H\}$ NMR spectrum of **16** in $CDCl_3$.

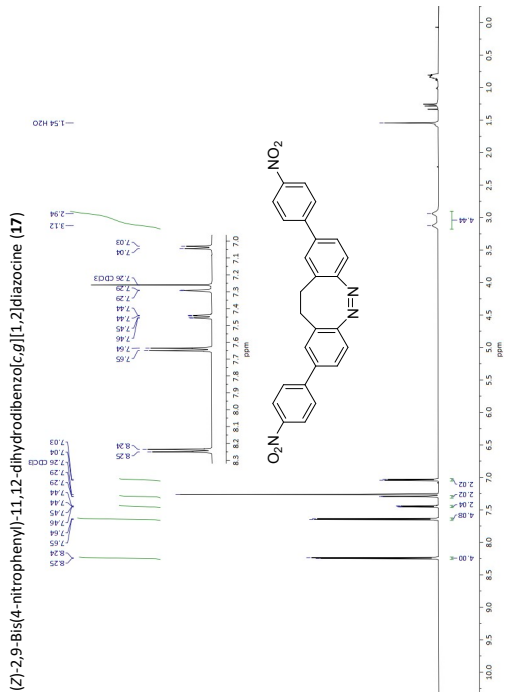

Figure 52: ^{1}H NMR spectrum of **17** in $CDCl_3$.

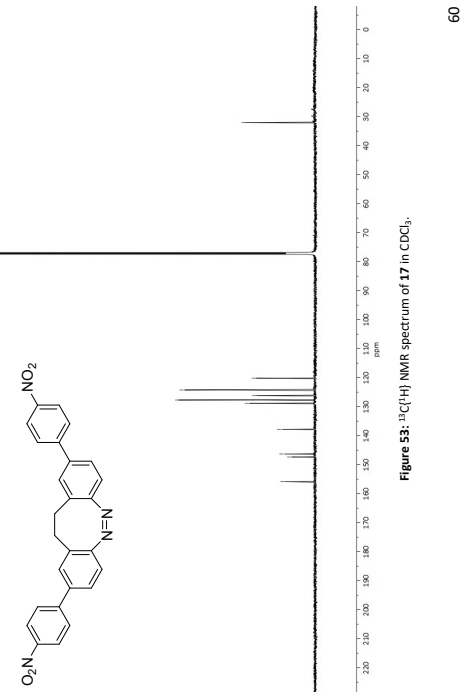

Figure 53: $^{13}C\{^1H\}$ NMR spectrum of **17** in $CDCl_3$.

60

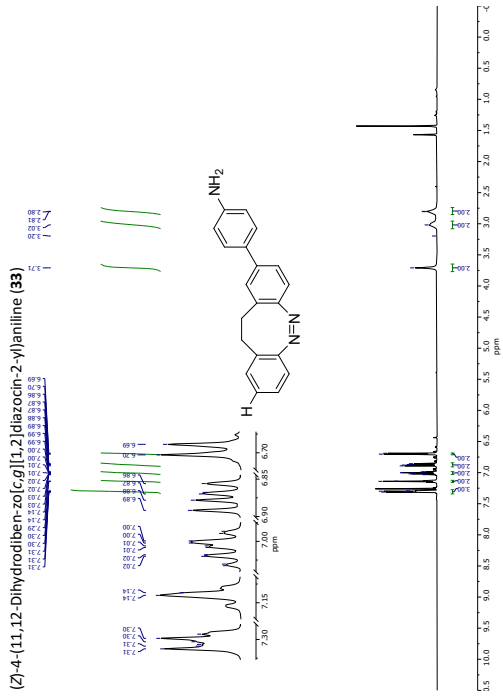

Figure 47: ^{1}H NMR spectrum of **33** in $CDCl_3$.

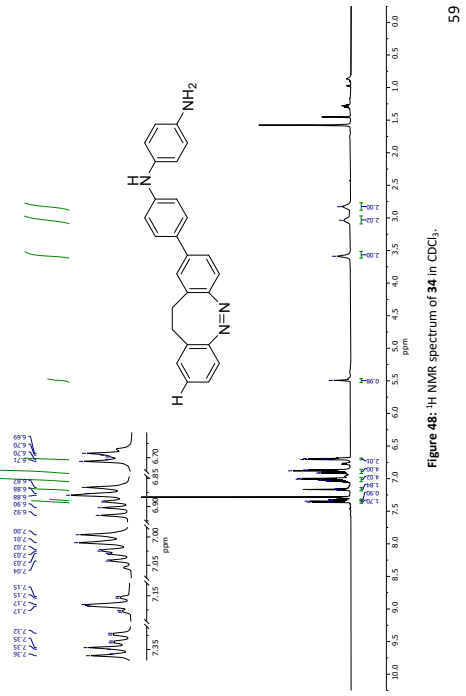

Figure 48: ^{1}H NMR spectrum of **34** in $CDCl_3$.

59

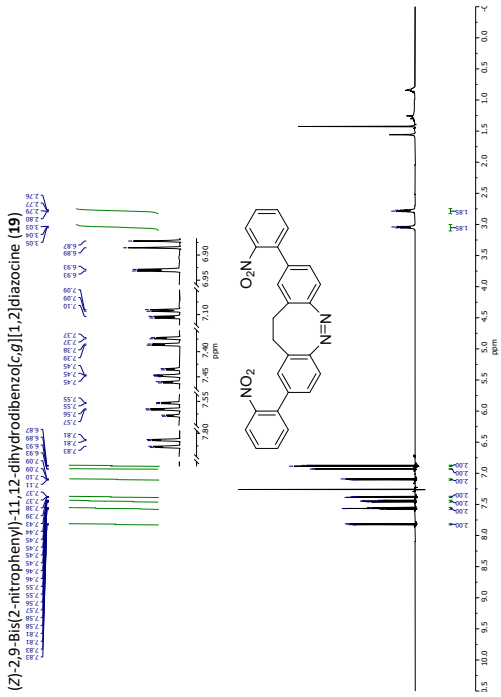

Figure 56: ^{1}H NMR spectrum of **19** in $CDCl_3$.

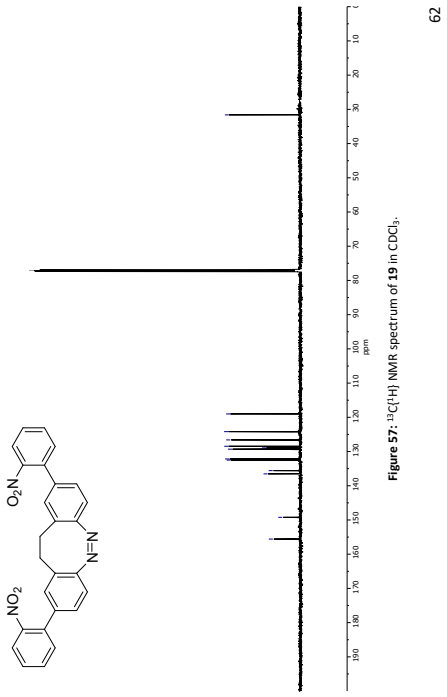

Figure 57: $^{13}C\{^1H\}$ NMR spectrum of **19** in $CDCl_3$.

62

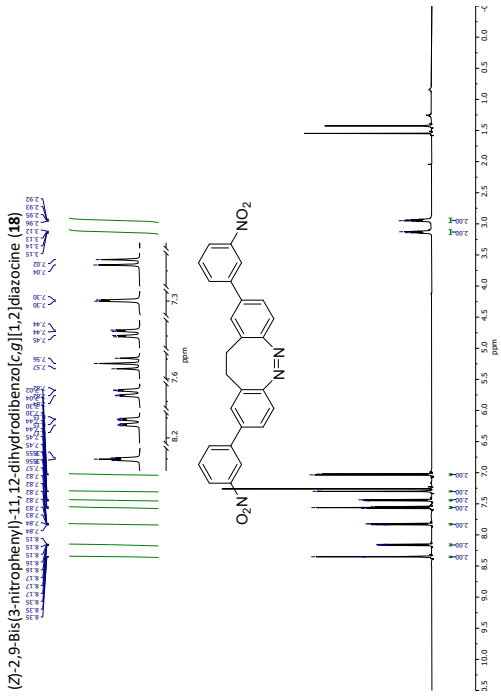

Figure 54: ^{1}H NMR spectrum of **18** in $CDCl_3$.

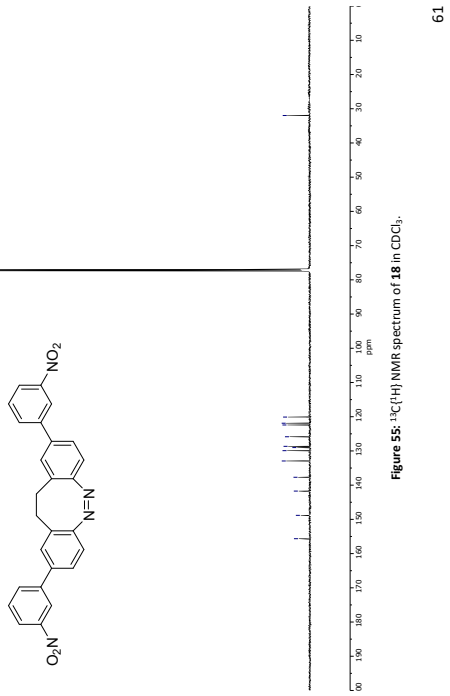

Figure 55: $^{13}C\{^1H\}$ NMR spectrum of **18** in $CDCl_3$.

61

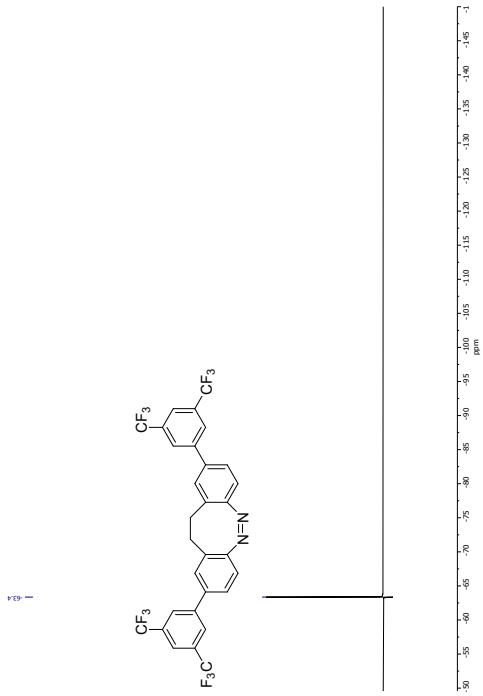

Figure 51: $^{19}F\{^1H\}$ NMR spectrum of **20** in $CDCl_3$.

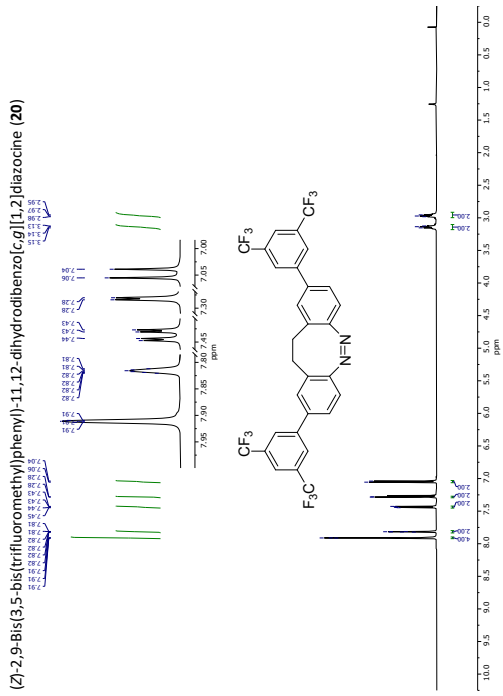

Figure 49: ^1H NMR spectrum of **20** in $CDCl_3$.

Figure 50: $^{13}C\{^1H\}$ NMR spectrum of **20** in $CDCl_3$.

63

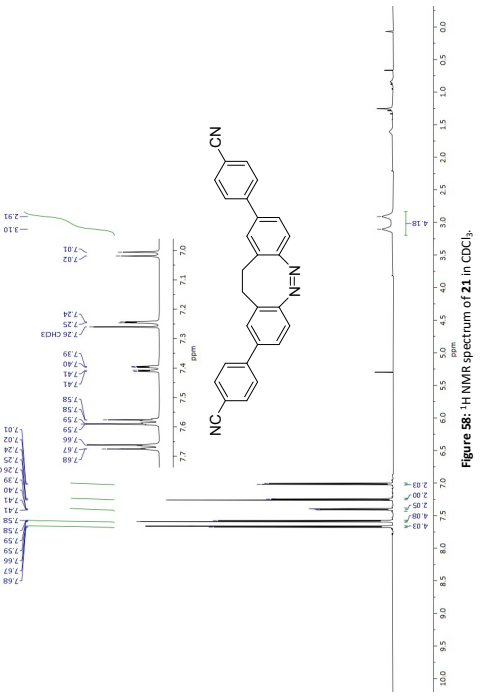

Figure 58: ^1H NMR spectrum of **21** in $CDCl_3$.

64

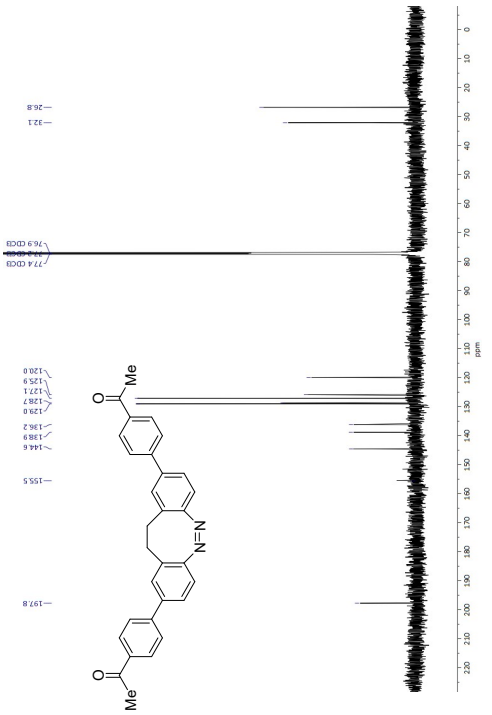

Figure 61: $^{13}C\{^1H\}$ NMR spectrum of **22** in $CDCl_3$.

66

Dimethyl 4,4'-(11,12-dihydrodibenzo[*c,g*][1,2]diazocine-2,9-diyl)(*Z*)-dibenzoate (**23**)

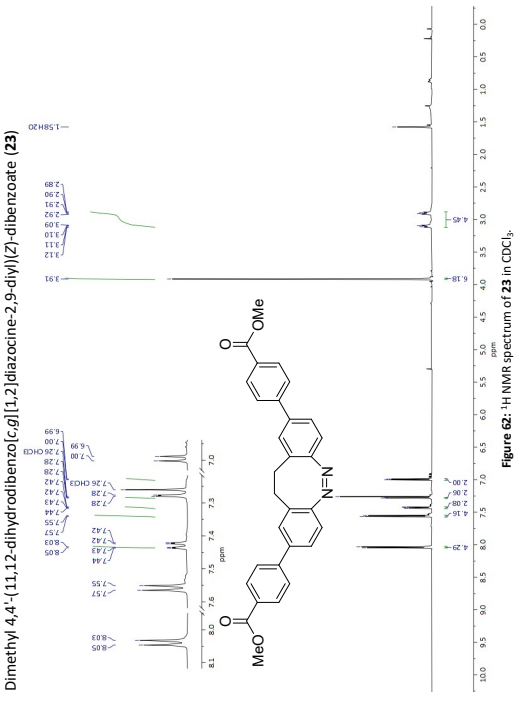

Figure 62: ^1H NMR spectrum of **23** in $CDCl_3$.

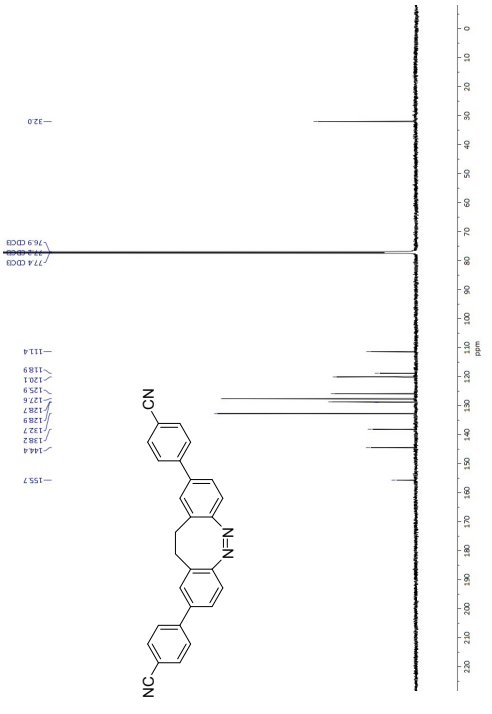

Figure 59: $^{13}C\{^1H\}$ NMR spectrum of **21** in $CDCl_3$.

65

(*Z*)-1,1'-((11,12-Dihydrodibenzo[*c,g*][1,2]diazocine-2,9-diyl)bis(4,1-phenylene))bis-(ethan-1-one) (**22**)

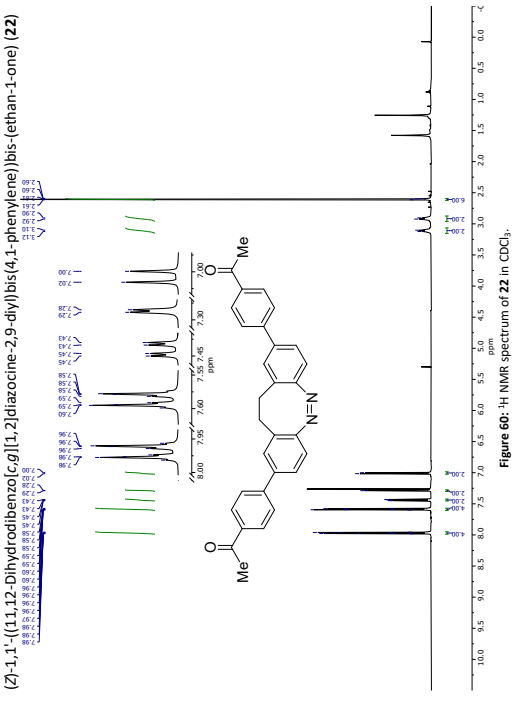

Figure 60: ^1H NMR spectrum of **22** in $CDCl_3$.

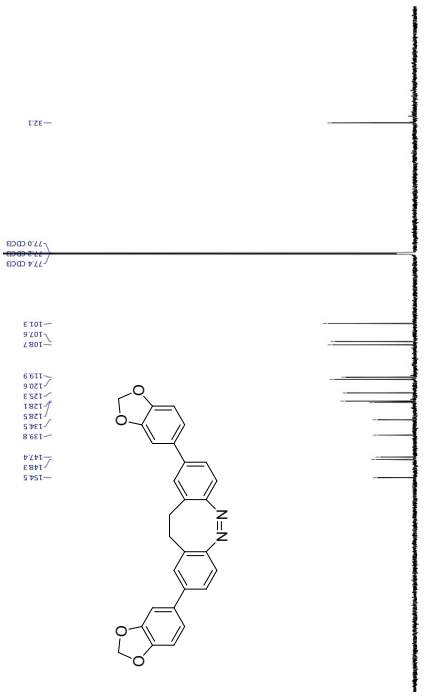

Figure 65: $^{13}C\{^1H\}$ NMR spectrum of **24** in $CDCl_3$.

(Z)-2,9-Di(thiophen-2-yl)-11,12-dihydrodibenzo[*c,g*][1,2]diazocine (**25**)

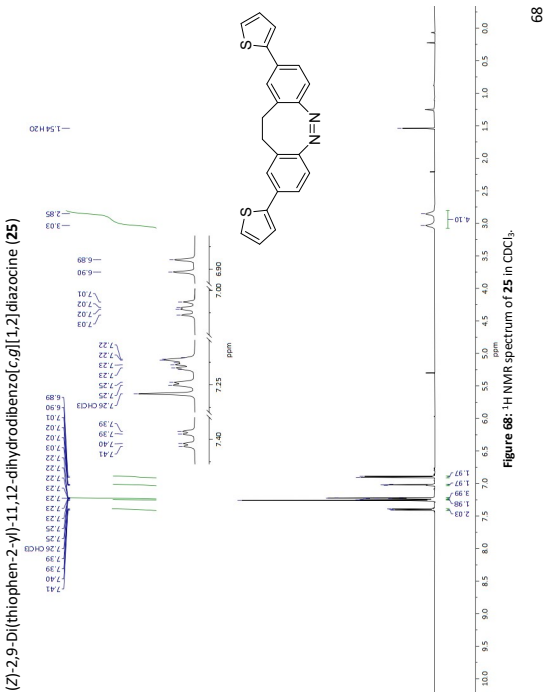

Figure 68: ^1H NMR spectrum of **25** in $CDCl_3$.

68

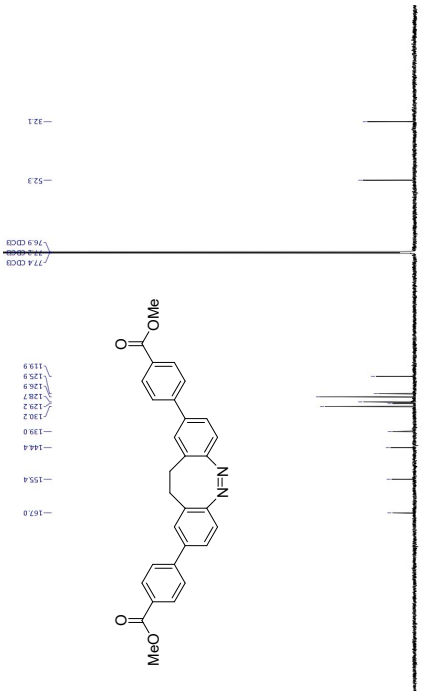

Figure 63: $^{13}C\{^1H\}$ NMR spectrum of **23** in $CDCl_3$.

(Z)-2,9-Bis(benzo[*d*][1,3]dioxol-5-yl)-11,12-dihydrodibenzo[*c,g*][1,2]diazocine (**24**)

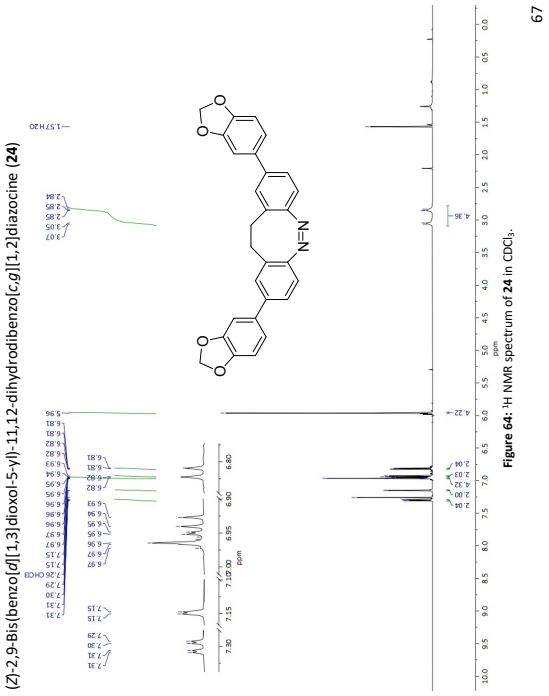

Figure 64: ^1H NMR spectrum of **24** in $CDCl_3$.

67

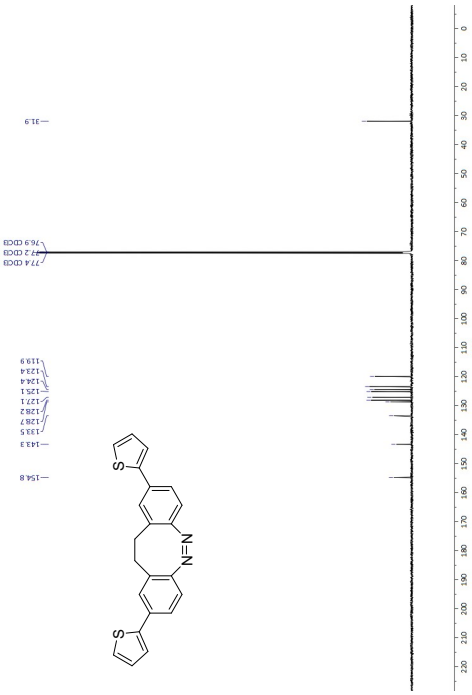

Figure 69: $^{13}C\{^1H\}$ NMR spectrum of **25** in $CDCl_3$.

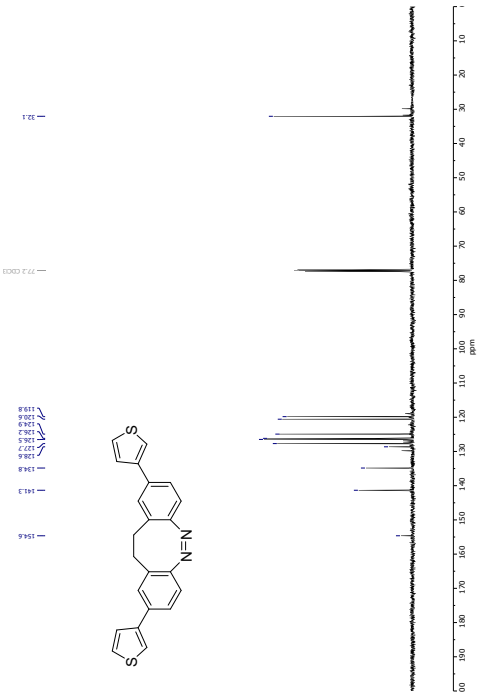

(*Z*)-2,9-Di(thiophen-3-yl)-11,12-dihydrodibenzo[*c*,*g*][1,2]diazocine (**26**)

Figure 70: ^1H NMR spectrum of **26** in $CDCl_3$.

69

Figure 71: $^{13}C\{^1H\}$ NMR spectrum of **26** in $CDCl_3$.

(*Z*)-5,5'-(11,12-Dihydrodibenzo[*c*,*g*][1,2]diazocine-2,9-diyl)bis(furan-2-carbaldehyde) (**27**)

Figure 72: ^1H NMR spectrum of **27** in $CDCl_3$.

70

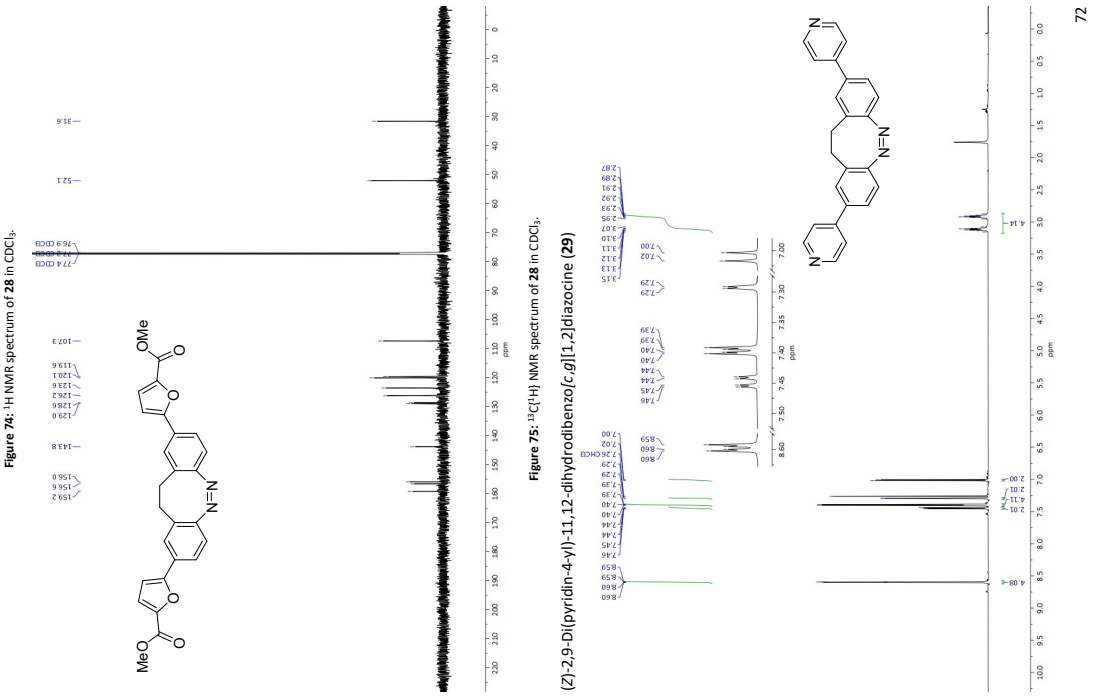

Figure 74: ^{1}H NMR spectrum of **28** in $CDCl_3$.

Figure 75: ^{13}C{^{1}H} NMR spectrum of **28** in $CDCl_3$.

(*Z*)-2,9-Di(pyridin-4-yl)-11,12-dihydrodibenzo[*c,g*][1,2]diazocine (**29**)

72

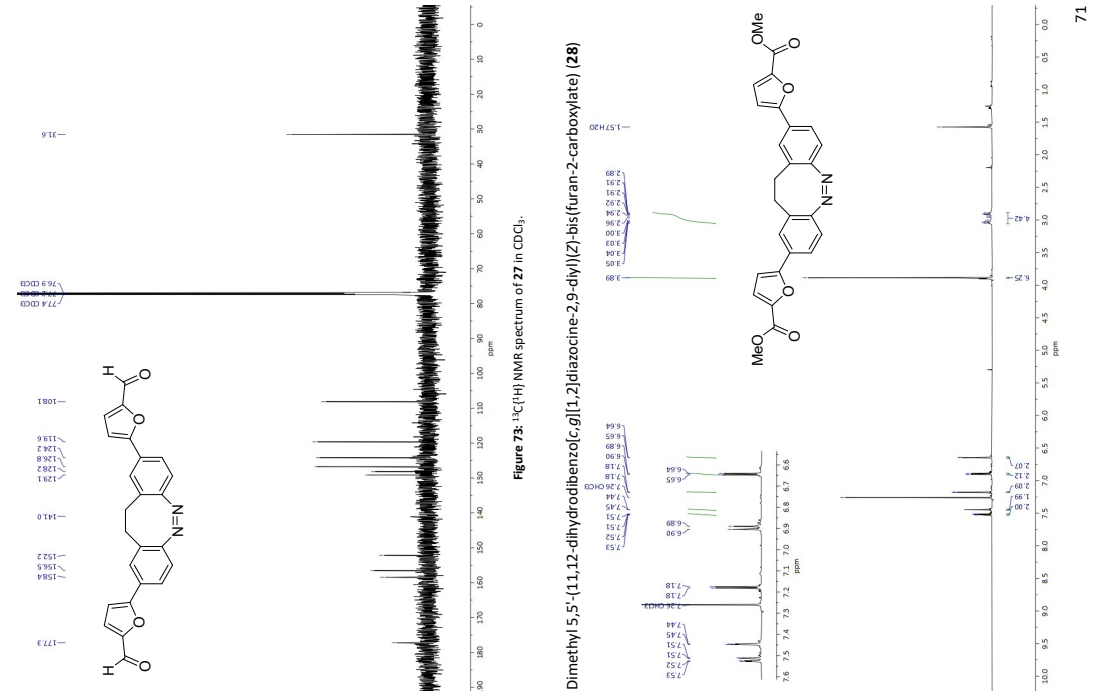

Figure 73: ^{13}C{^{1}H} NMR spectrum of **27** in $CDCl_3$.

Dimethyl 5,5'-(11,12-dihydrodibenzo[*c,g*][1,2]diazocine-2,9-diyl)(*Z*)-bis(furan-2-carboxylate) (**28**)

71

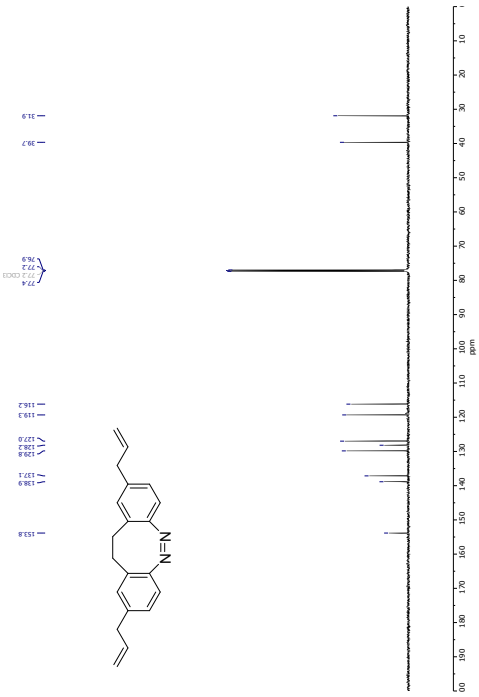

Figure 66: ^{1}H NMR spectrum of **29** in $CDCl_3$.

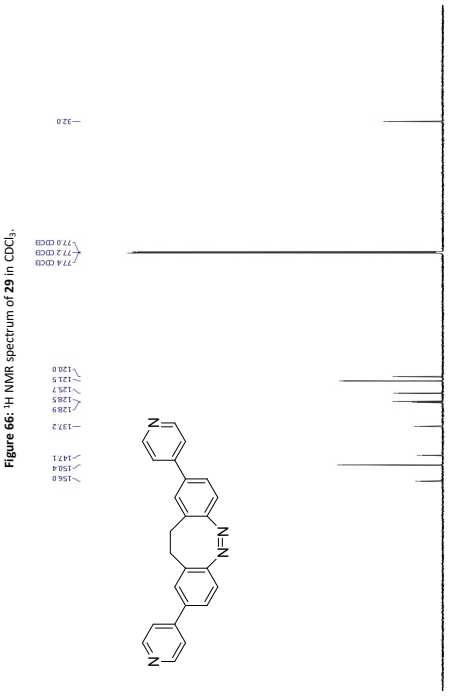

Figure 67: $^{13}C\{^1H\}$ NMR spectrum of **29** in $CDCl_3$.

(*Z*)-2,9-Diallyl-11,12-dihydrodibenzo[*c,g*][1,2]diazocine (**30**)

73

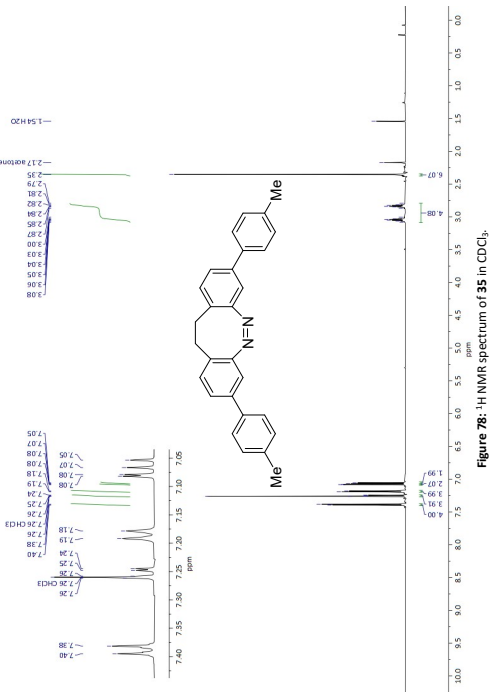

Figure 77: $^{13}C\{^1H\}$ NMR spectrum of **30** in $CDCl_3$.

(*Z*)-3,8-Di-*p*-tolyl-11,12-dihydrodibenzo[*c,g*][1,2]diazocine (**35**)

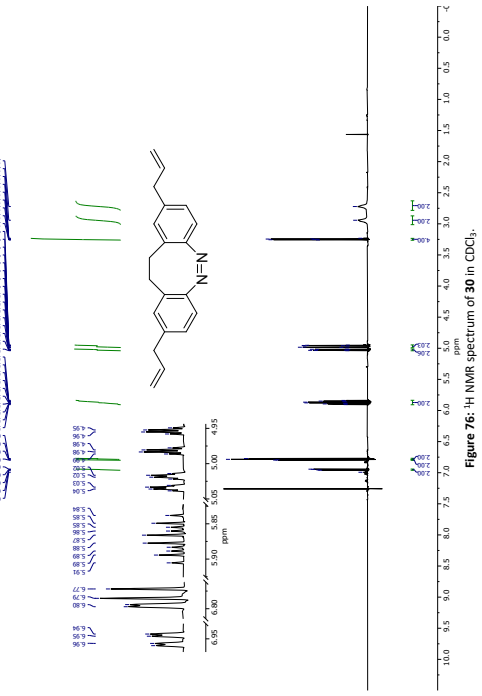

Figure 78: ^{1}H NMR spectrum of **35** in $CDCl_3$.

74

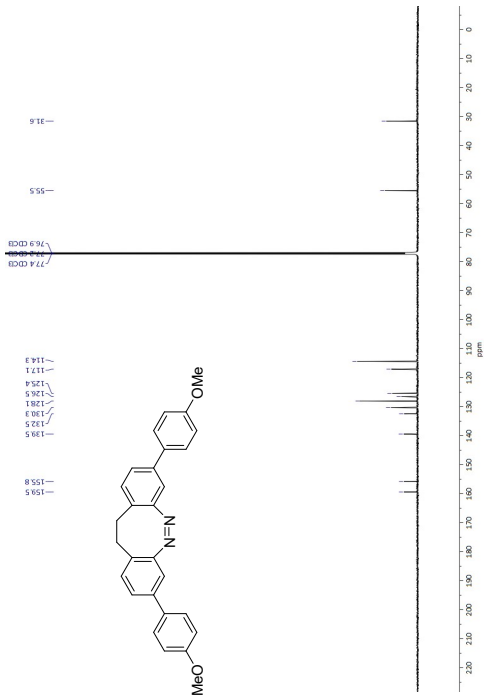

Figure 81: $^{13}C\{^1H\}$ NMR spectrum of **36** in $CDCl_3$.

(*Z*)-3,8-Bis(4-nitrophenyl)-11,12-dihydrodibenzo[*c,g*][1,2]diazocine (**37**)

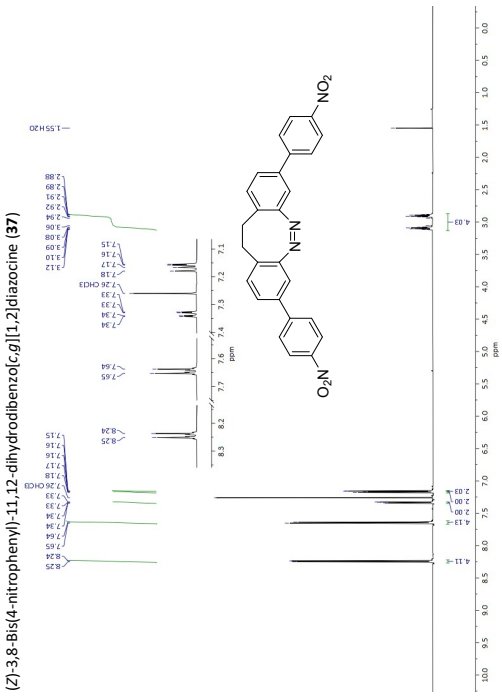

Figure 82: ^1H NMR spectrum of **37** in $CDCl_3$.

76

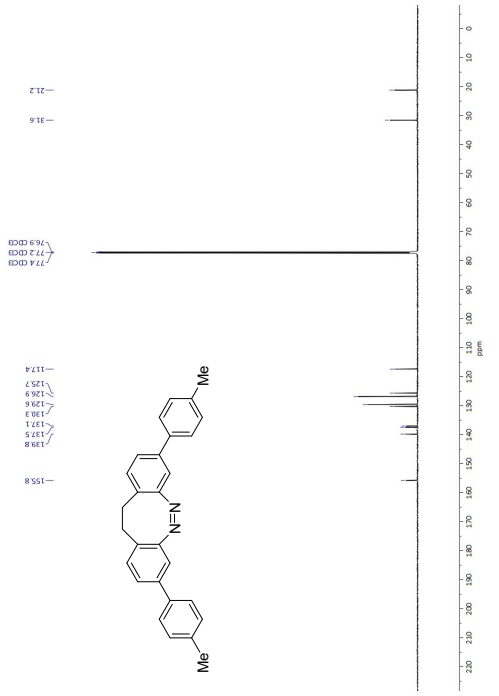

Figure 79: $^{13}C\{^1H\}$ NMR spectrum of **35** in $CDCl_3$.

(*Z*)-3,8-Bis(4-methoxyphenyl)-11,12-dihydrodibenzo[*c,g*][1,2]diazocine (**36**)

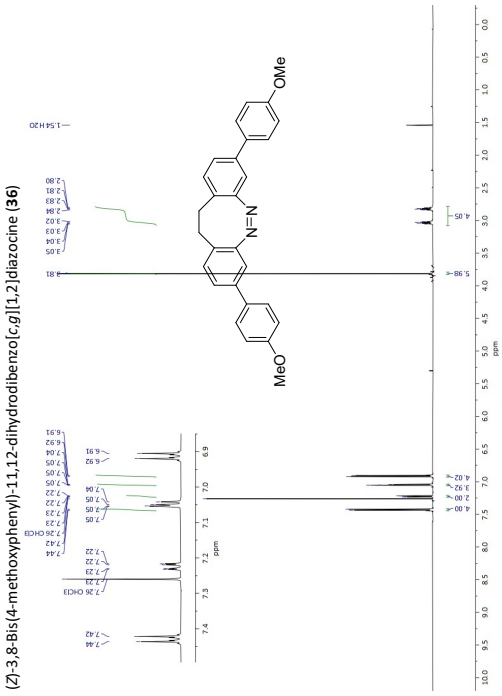

Figure 80: ^1H NMR spectrum of **36** in $CDCl_3$.

75

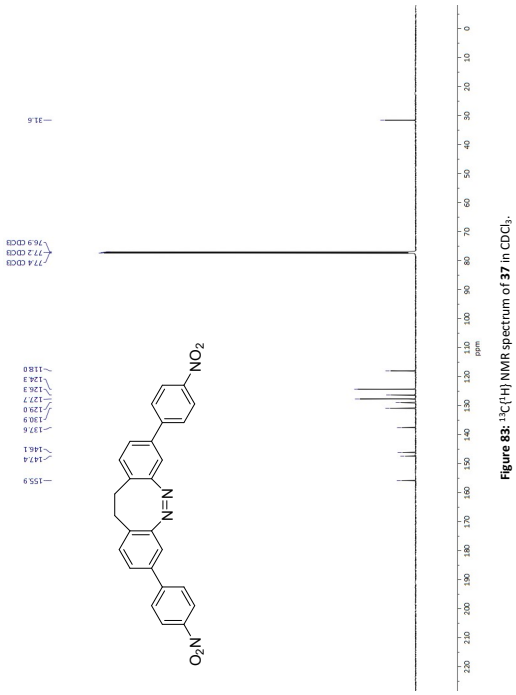

Figure 83: $^{13}C\{^1H\}$ NMR spectrum of **37** in $CDCl_3$.

77

References

[1] *The ACS Style Guide. Effective Communication of Scientific Information*, 3rd edition, (Eds.: A. M. Coghill, L. R. Garson), American Chemical Society, Washington, DC, **2006**.

[2] B. L. Feringa, *J. Org. Chem.* **2007**, *72*, 6635–6652.

[3] E. Moulin, L. Faour, C. C. Carmona-Vargas, N. Giuseppone, *Adv. Mater.* **2020**, *32*, 1906036 (1–26).

[4] D. Dattler, G. Fuks, J. Heiser, E. Moulin, A. Perrot, X. Yao, N. Giuseppone, *Chem. Rev.* **2020**, *120*, 310–433.

[5] *Molecular Switches*, Second, Co, (Eds.: B. L. Feringa, W. R. Browne), Wiley, Weinheim, **2011**.

[6] E. Merino, M. Ribagorda, *Beilstein J. Org. Chem.* **2012**, *8*, 1071–1090.

[7] K. G. Yager, C. J. Barrett, *J. Photochem. Photobiol. A* **2006**, *182*, 250–261.

[8] S. Venkataramani, U. Jana, M. Dommaschk, F. D. Sönnichsen, F. Tuczek, F. Herges, *Science* **2011**, *331*, 445–449.

[9] W. A. Velema, J. P. Van Der Berg, M. J. Hansen, W. Szymanski, A. J. Driessen, B. L. Feringa, *Nat. Chem.* **2013**, *5*, 924–928.

[10] J. B. Trads, K. Hüll, B. S. Matsuura, L. Laprell, T. Fehrentz, N. Görldt, K. A. Kozek, C. D. Weaver, N. Klöcker, D. M. Barber, D. Trauner, *Angew. Chemie - Int. Ed.* **2019**, *58*, 15421–15428.

[11] A. K. Flatt, S. M. Dirk, J. C. Henderson, D. E. Shen, J. Su, M. A. Reed, J. M. Tour, *Tetrahedron* **2003**, *59*, 8555–8570.

[12] A. H. Jaafar, C. Lowe, A. Gee, N. T. Kemp, *ACS Appl. Polym. Mater.* **2023**, *5*, 2367–2373.

[13] D. Kwaria, K. McGehee, S. Liu, Y. Kikkawa, S. Ito, Y. Norikane, *ACS Appl. Opt. Mater.* **2023**, *1*, 633–639.

[14] L. Dong, Y. Chen, F. Zhai, L. Tang, W. Gao, J. Tang, Y. Feng, W. Feng, *J. Mater. Chem. A* **2020**, *8*, 18668–18676.

[15] B. Zhang, Y. Feng, W. Feng, *Nano-Micro Lett.* **2022**, *14*, 1–37.

[16] S. Wu, H. J. Butt, *Macromol. Rapid Commun.* **2020**, *41*, 1900413.

[17] E. Mitscherlich, *Ann. der Phys. und Chemie* **1834**, *108*, 225–227.

[18] G. S. Hartley, *Nature* **1937**, *140*, 281.

[19] S. Benkhaya, S. M'rabet, A. El Harfi, *Heliyon* **2020**, *6*, e03271.

[20] H. M. D. Bandara, S. C. Burdette, *Chem. Soc. Rev.* **2012**, *41*, 1808–1825.

[21] G. S. Hartley, L. F. R. J. W, *J. Chem. Soc.* **1939**, *0*, 531–535.

[22] C. J. Brown, *Acta Cryst.* **1966**, *21*, 146–152.

[23] A. Mostad, C. Rømming, *Acta Chem. Scand.* **1971**, *25*, 3561–3568.

[24] M. Quick, A. L. Dobryakov, M. Gerecke, C. Richter, F. Berndt, I. N. Ioffe, A. A. Granovsky, R. Mahrwald, N. P. Ernsting, S. A. Kovalenko, *J. Phys. Chem. B* **2014**, *118*, 8756–8771.

[25] M. Gao, D. Kwaria, Y. Norikane, Y. Yue, *Nat. Sci.* **2023**, *3*, 1–45.

[26] I. K. Lednev, T. Q. Ye, P. Matousek, M. Towrie, P. Foggi, F. V. Neuwahl, S. Umapathy, R. E. Hester, J. N. Moore, *Chem. Phys. Lett.* **1998**, *290*, 68–74.

[27] I. K. Lednev, T. Q. Ye, L. C. Abbott, R. E. Hester, J. N. Moore, *J. Phys. Chem. A* **1998**, *102*, 9161–9166.

[28] T. Schultz, J. Quenneville, B. Levine, A. Toniolo, T. J. Martinez, S. Lochbrunner, M. Schmitt, J. P. Shaffer, M. Z. Zgierski, A. Stolow, *J. Am. Chem. Soc.* **2003**, *125*, 8098–8099.

[29] H. Rau, E. Lüddecke, *J. Am. Chem. Soc.* **1982**, *104*, 1616–1620.

[30] P. Tavadze, G. Avendaño Franco, P. Ren, X. Wen, Y. Li, J. P. Lewis, *J. Am. Chem. Soc.* **2018**, *140*, 285–290.

[31] C. W. Chang, Y. C. Lu, T. T. Wang, E. W. G. Diau, *J. Am. Chem. Soc.* **2004**, *126*, 10109–10118.

[32] T. Fujino, T. Tahara, *J. Phys. Chem. A* **2000**, *104*, 4203–4210.

[33] I. Conti, M. Garavelli, G. Orlandi, *J. Am. Chem. Soc.* **2008**, *130*, 5216–5230.

[34] R. Siewertsen, J. B. Schönborn, B. Hartke, F. Renth, F. Temps, *Phys. Chem. Chem. Phys.* **2011**, *13*, 1054–1063.

[35] C. Ciminelli, G. Granucci, M. Persico, *J. Chem. Phys.* **2005**, *123*, 174317.

[36] C. Nonnenberg, H. Gaub, I. Frank, *ChemPhysChem* **2006**, *7*, 1455–1461.

[37] C. R. Crecca, A. E. Roitberg, *J. Phys. Chem. A* **2006**, *110*, 8188–8203.

[38] S. Axelrod, E. Shakhnovich, G.-B. Rafael, *ACS Cent. Sci.* **2023**, *9*, 166–176.

[39] J. K. Yu, C. Bannwarth, R. Liang, E. G. Hohenstein, T. J. Martínez, *J. Am. Chem. Soc.* **2020**, *142*, 20680–20690.

[40] A. Nenov, R. Borrego-Varillas, A. Oriana, L. Ganzer, F. Segatta, I. Conti, J. Segarra-Marti, J. Omachi, M. Dapor, S. Taioli, C. Manzoni, S. Mukamel, G. Cerullo, M. Garavelli, *J. Phys. Chem. Lett.* **2018**, *9*, 1534–1541.

[41] E. M. Tan, S. Amirjalayer, S. Smolarek, A. Vdovin, F. Zerbetto, W. J. Buma, *Nat. Commun.* **2015**, *6*, 5860.

[42] J. Casellas, M. J. Bearpark, M. Reguero, *ChemPhysChem* **2016**, *17*, 3068–3079.

[43] A. Cembran, F. Bernardi, M. Garavelli, L. Gagliardi, G. Orlandi, *J. Am. Chem. Soc.* **2004**, *126*, 3234–3243.

[44] K. Veys, D. Escudero, *Acc. Chem. Res.* **2022**, *55*, 2698–2707.

[45] F. Aleotti, L. Soprani, A. Nenov, R. Berardi, A. Arcioni, C. Zannoni, M. Garavelli, *J. Chem. Theory Comput.* **2019**, *15*, 6813–6823.

[46] F. A. Jerca, V. V. Jerca, R. Hoogenboom, *Nat. Rev. Chem.* **2022**, *6*, 51–69.

[47] M. C. Spiridon, F. A. Jerca, V. V. Jerca, D. S. Vasilescu, D. M. Vuluga, *Eur. Polym. J.* **2013**, *49*, 452–463.

[48] V. V. Jerca, F. A. Jerca, I. Rau, A. M. Manea, D. M. Vuluga, F. Kajzar, *Opt. Mater.* **2015**, *48*, 160–164.

[49] F. A. Jerca, V. V. Jerca, D. F. Anghel, G. Stinga, G. Marton, D. S. Vasilescu, D. M. Vuluga, *J. Phys. Chem. C* **2015**, *119*, 10538–10549.

[50] J. Dokić, M. Gothe, J. Wirth, M. V. Peters, J. Schwarz, S. Hecht, P. Saalfrank, *J. Phys. Chem. A* **2009**, *113*, 6763–6773.

[51] M. Reimann, E. Teichmann, S. Hecht, M. Kaupp, *J. Phys. Chem. Lett.* **2022**, *13*, 10882–10888.

[52] Z. Sekkat, W. Knoll, L. Blinov, M. Irie, J. Kumar, P. Rochon, A. Natansohn, V. Churikov, C. Hsu, C. Fiorini, et al., *Photoreactive Organic Thin Films*, Elsevier Science, **2002**.

[53] Y. Ye, J. Pang, X. Zhou, J. Huang, *Comput. Theor. Chem.* **2016**, *1076*, 17–22.

[54] M. Baroncini, J. Groppi, S. Corra, S. Silvi, A. Credi, *Adv. Opt. Mater.* **2019**, *7*, 1900392.

[55] R. Siewertsen, H. Neumann, B. Buchheim-Stehn, R. Herges, C. Näther, F. Renth, F. Temps, *J. Am. Chem. Soc.* **2009**, *131*, 15594–15595.

[56] Y. Norikane, R. Katoh, N. Tamaoki, *Chem. Commun.* **2008**, 1898–1900.

[57] Y. Norikane, *J. Photopolym. Sci. Technol.* **2012**, *25*, 153–158.

[58] M. Matsui, Y. Iwata, T. Kato, K. Shibata, *Dye. Pigment.* **1988**, *9*, 109–117.

[59] E. Merino, *Chem. Soc. Rev.* **2011**, *40*, 3835–3853.

[60] K. H. Pausacker, *J. Chem. Soc.* **1953**, *0*, 1989–1990.

[61] W. Lu, C. Xi, *Tetrahedron Lett.* **2008**, *49*, 4011–4015.

[62] H. Ma, W. Li, J. Wang, G. Xiao, Y. Gong, C. Qi, Y. Feng, X. Li, Z. Bao, W. Cao, Q. Sun, C. Veaceslav, F. Wang, Z. Lei, *Tetrahedron* **2012**, *68*, 8358–8366.

[63] C. Zhang, N. Jiao, *Angew. Chem. Int. Ed.* **2010**, *122*, 6310–6313.

[64] R. F. Nystrom, W. G. Brown, *J. Am. Chem. Soc.* **1948**, *70*, 3738–3740.

[65] S. H. Gund, R. S. Shelkar, J. M. Nagarkar, *RSC Adv.* **2014**, *4*, 42947–42951.

[66] J. Hoffmann, T. J. Kuczmera, E. Lork, A. Staubitz, *Molecules* **2019**, *24*, 303.

[67] C. Glaser, *Liebigs Ann. Chem.* **1867**, *142*, 364–369.

[68] R. Thorwirth, F. Bernhardt, A. Stolle, B. Ondruschka, J. Asghari, *Chem. - A Eur. J.* **2010**, *16*, 13236–13242.

[69] B. Ortiz, P. Villanueva, F. Walls, *Notes J. Org. Chem.* **1972**, *37*, 2748–2750.

[70] A. Grirrane, A. Corma, H. García, *Science* **2008**, *322*, 1661–1664.

[71] M. L. Di Gioia, A. Leggio, I. F. Guarino, V. Leotta, E. Romio, A. Liguori, *Tetrahedron Lett.* **2015**, *56*, 5341–5344.

[72] R. O. Hutchins, D. W. Lamson, L. Rua, C. Milewski, B. Maryanoff, *J. Org. Chem.* **1971**, *36*, 803–806.

[73] K. Pothula, L. Tang, Z. Zha, Z. Wang, *RSC Adv.* **2015**, *5*, 83144–83148.

[74] D. Formenti, F. Ferretti, F. K. Scharnagl, M. Beller, *Chem. Rev.* **2019**, *119*, 2611–2680.

[75] H. Zhu, X. Ke, X. Yang, S. Sarina, H. Liu, *Angew. Chemie - Int. Ed.* **2010**, *49*, 9657–9661.

[76] H. J. Shine, H. Zmuda, H. Kwart, A. G. Horgan, M. Brechbiel, *J. Am. Chem. Soc.* **1982**, *104*, 5181–5184.

[77] K. Haghbeen, E. W. Tan, *J. Org. Chem.* **1998**, *63*, 4503–4505.

[78] J. R. Bourne, C. Hilber, G. Tovstiga, *Chem. Eng. Commun.* **1985**, *37*, 293–314.

[79] K. M. Ibne-Rasa, C. G. Lauro, J. O. Edwards, *J. Am. Chem. Soc.* **1963**, *85*, 1165–1167.

[80] M. H. Davey, V. Y. Lee, R. D. Miller, T. J. Marks, *J. Org. Chem.* **1999**, *64*, 4976–4979.

[81] L. S. Runtsch, D. M. Barber, P. Mayer, M. Groll, D. Trauner, J. Broichhagen, *Beilstein J. Org. Chem.* **2015**, *11*, 1129–1135.

[82] T. Cohen, R. J. Lewarchik, J. Z. Tarinolb, *J. Am. Chem. Soc.* **1974**, *96*, 7753–7760.

[83] R. Reuter, H. A. Wegner, *Beilstein J. Org. Chem.* **2012**, *8*, 877–883.

[84] B. G. Gowenlock, G. B. Richter-Addo, *Chem. Rev.* **2004**, *104*, 3315–3340.

[85] R. J. Tombari, J. R. Tuck, N. Yardeny, P. W. Gingrich, D. J. Tantillo, D. E. Olson, *Org. Biomol. Chem.* **2021**, *19*, 7575–7580.

[86] Y. A. Mikheev, *Russ. J. Phys. Chem. A* **2021**, *95*, 1803–1810.

[87] Y. K. Lim, K. S. Lee, C. G. Cho, *Org. Lett.* **2003**, *5*, 979–982.

[88] Z. Q. Wang, J. X. Yu, S. Q. Bai, B. Liu, C. Y. Wang, J. H. Li, *ACS Omega* **2020**, *5*, 28856–28862.

[89] J. Börgel, T. Ritter, *Chem* **2020**, *6*, 1877–1887.

[90] M. Walther, W. Kipke, S. Schultzke, S. Ghosh, A. Staubitz, *Synthesis* **2021**, *53*, 1213–1228.

[91] D. Barišić, M. Pajić, I. Halasz, D. Babić, M. Ćurić, *Beilstein J. Org. Chem.* **2022**, *18*, 680–687.

[92] P. J. Elder, J. C. Landry, A. F. Cozzolino, A. E. Chapman, I. Vargas-Baca, *J. Organomet. Chem.* **2012**, *716*, 11–18.

[93] Y. Tao, R. Hu, Z. Xie, P. Lin, W. Su, *J. Org. Chem.* **2022**, *87*, 4724–4731.

[94] N. Kano, F. Komatsu, T. Kawashima, *J. Am. Chem. Soc.* **2001**, *123*, 10778–10779.

[95] J. Yoshino, N. Kano, T. Kawashima, *Tetrahedron* **2008**, *64*, 7774–7781.

[96] J. Yoshino, A. Furuta, T. Kambe, H. Itoi, N. Kano, T. Kawashima, Y. Ito, M. Asashima, *Chem. - A Eur. J.* **2010**, *16*, 5026–5035.

[97] A. R. Katritzky, J. Wu, S. V. Verin, *Synthesis* **1995**, 651–653.

[98] T. T. T. Nguyen, A. Boussonnière, E. Banaszak, A. S. Castanet, K. P. P. Nguyen, J. Mortier, *J. Org. Chem.* **2014**, *79*, 2775–2780.

[99] F. A. Garlichs-Zschoche, K. H. Dötz, *Organometallics* **2007**, *26*, 4535–4540.

[100] J. Strueben, M. Lipfert, J.-O. Springer, C. A. Gould, P. J. Gates, F. D. Sönnichsen, A. Staubitz, *Chem. Eur. J.* **2015**, *21*, 11165–11173.

[101] H. Duval, *Bull. Soc. Chim. Fr.* **1910**, *7*, 727–732.

[102] E. Tauer, R. Machinek, *Liebigs Ann.* **1996**, *9*, 1213–1216.

[103] W. Moormann, T. Tellkamp, E. Stadler, F. Röhricht, C. Näther, R. Puttreddy, K. Rissanen, G. Gescheidt, R. Herges, *Angew. Chemie - Int. Ed.* **2020**, *59*, 15081–15086.

[104] T. Matsubara, *Phys. Chem. Chem. Phys.* **2022**, *24*, 17303–17313.

[105] J. Isokuortti, T. Griebenow, J. S. von Glasenapp, T. Raeker, M. A. Filatov, T. Laaksonen, R. Herges, N. A. Durandin, *Chem. Sci.* **2023**, *14*, 9161–9166.

[106] L. Liu, Y. Wang, Q. Fang, *J. Chem. Phys.* **2017**, *146*, 064308.

[107] O. Carstensen, J. Sielk, J. B. Schönborn, G. Granucci, B. Hartke, *J. Chem. Phys.* **2010**, *133*, 124305.

[108] M. Böckmann, N. L. Doltsinis, D. Marx, *J. Chem. Phys.* **2012**, *137*, 22A505.

[109] M. Jun, D. K. Joshi, R. S. Yalagala, J. Vanloon, R. Simionescu, A. J. Lough, H. L. Gordon, H. Yan, *ChemistrySelect* **2018**, *3*, 2697–2701.

[110] M. Hammerich, C. Schütt, C. Stähler, P. Lentes, F. Röhricht, R. Höppner, R. Herges, *J. Am. Chem. Soc.* **2016**, *138*, 13111–13114.

[111] W. Moormann, D. Langbehn, R. Herges, *Synthesis* **2017**, *49*, 3471–3475.

[112] S. Li, N. Eleya, A. Staubitz, *Org. Lett.* **2020**, *22*, 1624–1627.

[113] T. Tellkamp, J. Shen, Y. Okamoto, R. Herges, *European J. Org. Chem.* **2014**, 5456–5461.

[114] R. Löw, T. Rusch, F. Röhricht, O. Magnussen, R. Herges, *Beilstein J. Org. Chem.* **2019**, *15*, 1485–1490.

[115] Q. Zhu, S. Wang, P. Chen, *Org. Lett.* **2019**, *21*, 4025–4029.

[116] J. Wang, J. He, C. Zhi, B. Luo, X. Li, Y. Pan, X. Cao, H. Gu, *RSC Adv.* **2014**, *4*, 16607–16611.

[117] M. S. Maier, K. Hüll, M. Reynders, B. S. Matsuura, P. Leippe, T. Ko, L. Schäffer, D. Trauner, *J. Am. Chem. Soc.* **2019**, *141*, 17295–17304.

[118] M. Reynders, A. Chaikuad, B. T. Berger, K. Bauer, P. Koch, S. Laufer, S. Knapp, D. Trauner, *Angew. Chemie - Int. Ed.* **2021**, *60*, 20178–20183.

[119] S. Samanta, C. Qin, A. J. Lough, G. A. Woolley, *Angew. Chemie* **2012**, *124*, 6558–6561.

[120] S. Li, G. Han, W. Zhang, *Macromolecules* **2018**, *51*, 4290–4297.

[121] L. Heintze, D. Schmidt, T. Rodat, L. Witt, J. Ewert, M. Kriegs, R. Herges, C. Peifer, *Int. J. Mol. Sci.* **2020**, *21*, 1–23.

[122] C. Deo, N. Bogliotti, R. Métivier, P. Retailleau, J. Xie, *Chem. - A Eur. J.* **2016**, *22*, 9092–9096.

[123] F. Klockmann, C. Fangmann, E. Zender, T. Schanz, C. Catapano, A. Terfort, *ACS Omega* **2021**, *6*, 18434–18441.

[124] T. Zheng, J. Fu, Q. Xiong, X. Shen, B. Li, X. Zhao, Z. Yu, *Chem. Commun.* **2023**, *59*, 1201–1204.

[125] P. Lentes, J. Rudtke, T. Griebenow, R. Herges, *Beilstein J. Org. Chem.* **2021**, *17*, 1503–1508.

[126] W. Moormann, D. Langbehn, R. Herges, *Beilstein J. Org. Chem.* **2019**, *15*, 727–732.

[127] G. Cabré, A. Garrido-Charles, À. González-Lafont, W. Moormann, D. Langbehn, D. Egea, J. M. Lluch, R. Herges, R. Alibés, F. Busqué, P. Gorostiza, J. Hernando, *Org. Lett.* **2019**, *21*, 3780–3784.

[128] J. Ewert, L. Heintze, M. Jordà-Redondo, J. S. Von Glasenapp, S. Nonell, G. Bucher, C. Peifer, R. Herges, *J. Am. Chem. Soc.* **2022**, *144*, 15059–15071.

[129] A. Nagaki, Y. Tsuchihashi, S. Haraki, J. ichi Yoshida, *Org. Biomol. Chem.* **2015**, *13*, 7140–7145.

[130] M. S. Maier, K. Hüll, M. Reynders, B. S. Matsuura, P. Leippe, T. Ko, L. Schäffer, D. Trauner, *J. Am. Chem. Soc.* **2019**, *141*, 17295–17304.

[131] H. Sell, C. Näther, R. Herges, *Beilstein J. Org. Chem.* **2013**, *9*, 1–7.

[132] M. A. Smith, B. Weinstein, F. D. Greene, *J. Org. Chem.* **1980**, *45*, 4597–4602.

[133] M. Schehr, D. Hugenbusch, T. Moje, C. Näther, R. Herges, *Beilstein J. Org. Chem.* **2018**, *14*, 2799–2804.

[136] P. Lentes, P. Fruhwirt, H. Freimuth, W. Moormann, F. Kruse, G. Gescheidt, R. Herges, *J. Org. Chem.* **2021**, *86*, 4355–4360.

[137] X. Shen, C. Zhang, F. Lan, Z. Su, Y. Zheng, T. Zheng, Q. Xiong, X. Xie, G. Du, X. Zhao, C. Hu, P. Deng, Z. Yu, *Angew. Chemie - Int. Ed.* **2022**, *61*, 1–9.

[138] M. Schehr, C. Ianes, J. Weisner, L. Heintze, M. P. Müller, C. Pichlo, J. Charl, E. Brunstein, J. Ewert, M. Lehr, U. Baumann, D. Rauh, U. Knippschild, C. Peifer, R. Herges, *Photochem. Photobiol. Sci.* **2019**, *18*, 1398–1407.

[134] N. Uchida, Y. Ryu, Y. Takagi, K. Yoshizawa, K. Suzuki, Y. Anraku, I. Ajioka, N. Shimokawa, M. Takagi, N. Hoshino, T. Akutagawa, T. Matsubara, T. Sato, Y. Higuchi, H. Ito, M. Morita, T. Muraoka, *J. Am. Chem. Soc.* **2023**, *145*, 6210–6220.

[135] P. Lentes, E. Stadler, F. Röhricht, A. Brahms, J. Gröbner, F. D. Sönnichsen, G. Gescheidt, R. Herges, *J. Am. Chem. Soc.* **2019**, *141*, 13592–13600.

[139] J. Deng, X. Wu, G. Guo, X. Zhao, Z. Yu, *Org. Biomol. Chem.* **2020**, *18*, 5602–5607.

[140] E. R. Thapaliya, J. Zhao, G. C. Ellis-Davies, *ACS Chem. Neurosci.* **2019**, *10*, 2481–2488.

[141] H. Lee, J. Tessarolo, D. Langbehn, A. Baksi, R. Herges, G. H. Clever, *J. Am. Chem. Soc.* **2022**, *144*, 3099–3105.

[142] W. Fang, Y. Feng, J. Gao, H. Wang, J. Ge, Q. Yang, W. Feng, *Molecules* **2022**, *27*, 3296.

[143] T. Ko, M. M. Oliveira, J. M. Alapin, J. Morstein, E. Klann, D. Trauner, *J. Am. Chem. Soc.* **2022**, *144*, 21494–21501.

[144] D. Hugenbusch, M. Lehr, J. S. von Glasenapp, A. J. McConnell, R. Herges, *Angew. Chemie - Int. Ed.* **2023**, *62*, 1–5.

[145] F. Eljabu, J. Dhruval, H. Yan, *Bioorganic Med. Chem. Lett.* **2015**, *25*, 5594–5596.

[146] D. K. Joshi, M. J. Mitchell, D. Bruce, A. J. Lough, H. Yan, *Tetrahedron* **2012**, *68*, 8670–8676.

[147] M. Reynders, D. Trauner, *Methods Mol. Biol.* **2021**, *2365*, 315–329.

[148] S. Li, R. Colaco, A. Staubitz, *ACS Appl. Polym. Mater.* **2022**, *4*, 6825–6833.

[149] S. Li, K. Bamberg, Y. Lu, F. D. Sönnichsen, A. Staubitz, *Polymers (Basel).* **2023**, *15*, 1306.

[150] M. H. Burk, S. Schröder, W. Moormann, D. Langbehn, T. Strunskus, S. Rehders, R. Herges, F. Faupel, *Macromolecules* **2020**, *53*, 1164–1170.

[151] M. H. Burk, D. Langbehn, G. Hernández Rodríguez, W. Reichstein, J. Drewes, S. Schröder, S. Rehders, T. Strunskus, R. Herges, F. Faupel, *ACS Appl. Polym. Mater.* **2021**, *3*, 1445–1456.

[152] Y. Luo, G. D. Prestwich, *Bioconjug. Chem.* **2001**, *12*, 1085–1088.

[153] J. Nicolas, E. Khoshdel, D. M. Haddleton, *Chem. Commun.* **2007**, 1722–1724.

[154] N. Stephanopoulos, M. B. Francis, *Nat. Chem. Biol.* **2011**, *7*, 876–884.

[155] A. Sigen, Q. Xu, D. Zhou, Y. Gao, J. M. Vasquez, U. Greiser, W. Wang, W. Liu, W. Wang, *Polym. Chem.* **2017**, *8*, 1283–1287.

[156] O. Koniev, A. Wagner, *Chem. Soc. Rev.* **2015**, *44*, 5495–5551.

[157] G. W. Anderson, J. E. Zimmerman, F. M. Callahan, *J. Am. Chem. Soc.* **1964**, *86*, 1839–1842.

[158] G. W. Anderson, F. M. Callahan, J. E. Zimmerman, *J. Am. Chem. Soc.* **1967**, *89*, 178.

[159] G. Anderson, J. Zimmerman, F. Callahan, *J. Am. Chem. Soc.* **1963**, *85*, 3039.

[160] X. Li, Y. Gao, Y. Kuang, B. Xu, *Chem. Commun.* **2010**, *46*, 5364–5366.

[161] S. K. Rastogi, H. E. Anderson, J. Lamas, S. Barret, T. Cantu, S. Zauscher, W. J. Brittain, T. Betancourt, *ACS Appl. Mater. Interfaces* **2018**, *10*, 30071–30080.

[162] G. Han, H. Zhang, J. Chen, Q. Sun, Y. Zhang, H. Zhang, *New J. Chem.* **2015**, *39*, 1410–1420.

[163] X. Pang, B. Xu, X. Qing, J. Wei, Y. Yu, *Macromol. Rapid Commun.* **2018**, *39*, 1–7.

[164] A. Barré, M. L. Ţînţaś, V. Levacher, C. Papamicaël, V. Gembus, *Synth.* **2017**, *49*, 472–483.

[165] N. Patel, M. C. Davies, M. Hartshorne, R. J. Heaton, C. J. Roberts, S. J. Tendler, P. M. Williams, *Langmuir* **1997**, *13*, 6485–6490.

[166] N. Zhan, G. Palui, J. P. Merkl, H. Mattoussi, *J. Am. Chem. Soc.* **2016**, *138*, 3190–3201.

[167] A. K. Ghosh, T. T. Doung, S. P. McKee, W. J. Thompson, *Tetrahedron Lett.* **1992**, *33*, 2781–2784.

[168] A. Schulze, A. Giannis, *Adv. Synth. Catal.* **2004**, *346*, 252–256.

[169] A. Barré, M. L. Tîntaş, F. Alix, V. Gembus, C. Papamicaël, V. Levacher, *J. Org. Chem.* **2015**, *80*, 6537–6544.

[170] T. Ueda, H. Konishi, K. Manabe, *Org. Lett.* **2012**, *14*, 5370–5373.

[171] B. Tan, N. Toda, C. F. Barbas, *Angew. Chemie - Int. Ed.* **2012**, *51*, 12538–12541.

[172] T. Wirth, *Angew. Chem. Int. Ed.* **2005**, *44*, 3656–3665.

[173] E. A. Merritt, B. Olofsson, *Angew. Chem. Int. Ed. Engl.* **2009**, *48*, 9052–9070.

[174] P. J. Stang, *J. Org. Chem.* **2003**, *68*, 2997–3008.

[175] R. E. Rundle, *J. Am. Chem. Soc.* **1963**, *85*, 112–113.

[176] M. Ochiai in *Hypervalent Iodine Chem. Mod. Dev. Org. Synth. Top. Curr. Chem. Vol. 224*, (Ed.: T. Wirth), Springer-Verlag, Berlin Heidelberg, **2003**, pp. 5–68.

[177] P. J. Stang, V. V. Zhdankin, *Chem. Rev.* **1966**, *96*, 1123–1178.

[178] C. Hartmann, V. Meyer, *Ber. Dtsch. Chem. Ges.* **1894**, *27*, 426–432.

[179] M. Bielawski, M. Zhu, B. Olofsson, *Adv. Synth. Catal.* **2007**, *349*, 2610–2618.

[180] M. Zhu, N. Jalalian, B. Olofsson, *Synlett* **2008**, *4*, 592–596.

[181] M. Bielawski, D. Aili, B. Olofsson, *J. Org. Chem.* **2008**, *73*, 4602–4607.

[182] M. Ochiai, Y. Kitagawa, M. Toyonari, *Arkivoc* **2003**, *vi*, 43–48.

[183] J. I. Seeman, *Chem. Rev.* **1983**, *83*, 83–134.

[184] J. Malmgren, S. Santoro, N. Jalalian, F. Himo, B. Olofsson, *Chem. Eur. J.* **2013**, *19*, 10334–10342.

[185] H. Pinto de Magalhães, H. P. Lüthi, A. Togni, *Org. Lett.* **2012**, *14*, 3830–3833.

[186] J.-H. Chun, S. Lu, Y.-S. Lee, V. W. Pike, *J. Org. Chem.* **2010**, *75*, 3332–3338.

[187] F. M. Beringer, R. A. Falk, *J. Chem. Soc.* **1964**, 4442–4451.

[188] Y.-S. Lee, J.-H. Chun, M. Hodošček, V. W. Pike, *Chem. Eur. J.* **2017**, *23*, 4353–4363.

[189] K. M. Lancer, G. H. Wiegand, *J. Org. Chem.* **1976**, *41*, 3360–3364.

[190] T. B. Petersen, R. Khan, B. Olofsson, *Org. Lett.* **2011**, *13*, 3462–3465.

[191] N. Jalalian, T. B. Petersen, B. Olofsson, *Chem. Eur. J.* **2012**, *18*, 14140–14149.

[192] E. Lindstedt, R. Ghosh, B. Olofsson, *Org. Lett.* **2013**, *15*, 6070–6073.

[193] R. Ghosh, E. Lindstedt, N. Jalalian, B. Olofsson, *ChemistryOpen* **2014**, *3*, 54–57.

[194] E. Lindstedt, E. Stridfeldt, B. Olofsson, *Org. Lett.* **2016**, *18*, 4234–4237.

[195] R. Ghosh, B. Olofsson, *Org. Lett.* **2014**, *16*, 1830–1832.

[196] N. Takeda, O. Miyata, T. Naito, *Eur. J. Org. Chem.* **2007**, 1491–1509.

[197] R. Ghosh, E. Stridfeldt, B. Olofsson, *Chem. Eur. J.* **2014**, *20*, 8888–8892.

[198] F. Tinnis, E. Stridfeldt, H. Lundberg, H. Adolfsson, B. Olofsson, *Org. Lett.* **2015**, *17*, 2688–2691.

[199] F. Guo, L. Wang, P. Wang, J. Yu, J. Han, *Asian J. Org. Chem.* **2012**, *1*, 218–221.

[200] L. Ackermann, M. Dellacqua, S. Fenner, R. Vicente, R. Sandmann, *Org. Lett.* **2011**, *13*, 2358–2360.

[201] F. M. Beringer, S. A. Galton, *J. Org. Chem.* **1963**, *28*, 3417–3421.

[202] C. H. Oh, J. S. Kim, H. H. Jung, *J. Org. Chem.* **1999**, *64*, 1338–1340.

[203] M. Ochiai, Y. Kitagawa, N. Takayama, Y. Takaoka, M. Shiro, *J. Am. Chem. Soc.* **1999**, *121*, 9233–9234.

[204] L. Joucla, L. Djakovitch, *Adv. Synth. Catal.* **2009**, *351*, 673–714.

[205] Y. Zhu, M. Bauer, J. Ploog, L. Ackermann, *Chem. Eur. J.* **2014**, *20*, 13099–13102.

[206] S. Sarkar, N. Wojciechowska, A. A. Rajkiewicz, M. Kalek, *European J. Org. Chem.* **2022**, e202101408.

[207] P. Villo, G. Kervefors, B. Olofsson, *Chem. Commun.* **2018**, *54*, 8810–8813.

[208] T. G. Johnson, A. Sadeghi-Kelishadi, M. J. Langton, *J. Am. Chem. Soc.* **2022**, *144*, 10455–10461.

Permissions to Reprint

The permissions to reprint were obtained from the publishers and are attached hereafter.

M. Gao, D. Kwaria, Y. Norikane, Y. Yue, *Nat. Sci.* 2023, 3, 1–45.

Figure 1.1 is part of the following publication: M. Gao, D. Kwaria, Y. Norikane, Y. Yue, *Nat. Sci.* **2023**, 3, 1–45.[25] This is an open access article under the terms of the Creative Commons Attribution License, which permits use, distribution and reproduction in any medium, provided the work is properly cited (`https://creativecommons.org/licenses/by/4.0/`).

F. A. Jerca, et al., *Nat. Chem. Rev.* 2022, *6*, 51–69.

Figure 1.2 was adapted with permission from F. A. Jerca, V. V. Jerca, R. Hoogenboom, *Nat. Chem. Rev.* **2022**, *6*, 51–69.[46] The numbering has been modified to concur with the numbering used in this thesis. No other alterations have been made.

SPRINGER NATURE LICENSE
TERMS AND CONDITIONS

Sep 18, 2023

This Agreement between Universität Bremen -- Melanie Walther ("You") and Springer Nature ("Springer Nature") consists of your license details and the terms and conditions provided by Springer Nature and Copyright Clearance Center.

License Number	5632000398970
License date	Sep 18, 2023
Licensed Content Publisher	Springer Nature
Licensed Content Publication	Nature Reviews Chemistry
Licensed Content Title	Advances and opportunities in the exciting world of azobenzenes
Licensed Content Author	Florica Adriana Jerca et al
Licensed Content Date	Nov 18, 2021
Type of Use	Thesis/Dissertation
Requestor type	academic/university or research institute
Format	print and electronic
Portion	figures/tables/illustrations
Number of figures/tables/illustrations	1
Would you like a high resolution image with your order?	no
Will you be translating?	no
Circulation/distribution	1 - 29
Author of this Springer Nature content	no
Title	Modification of Azobenzene Based Switches
Institution name	University of Bremen
Expected presentation date	Sep 2023
Order reference number	Permission-Photoisomerization-Azobenzene
Portions	Figure 2 Photoisomerization mechanism of azobenzene
Requestor Location	Universität Bremen Leobener Straße 7 NW2 Bremen, 28359 Germany Attn: Universität Bremen
Billing Type	Invoice
Billing Address	Universität Bremen Leobener Straße 7 NW2 Bremen, Germany 28359 Attn: Universität Bremen
Total	**0.00 EUR**
Terms and Conditions	

Springer Nature Customer Service Centre GmbH Terms and Conditions
The following terms and conditions ("Terms and Conditions") together with the terms specified in your [RightsLink] constitute the License ("License") between you as Licensee and Springer Nature Customer Service Centre GmbH as

R. Siewertsen, et al., *J. Am. Chem. Soc.* 2009, *131*, 15594–15595.

Figure 1.3 was adapted with permission from R. Siewertsen, H. Neumann, B. Buchheim-Stehn, R. Herges, C. Nähter, F. Renth, F. Temps, *J. Am. Chem. Soc.* **2009**, *131*, 15594–15595.[55] The numbering has been modified to concur with the numbering used in this thesis. No other alterations have been made.